ISSN 1007-9327 (print)
ISSN 2219-2840 (online)

World Journal of *Gastroenterology*

World J Gastroenterol 2019 September 7; 25(33): 4796-5016

Published by Baishideng Publishing Group Inc

World Journal of Gastroenterology

Contents

Weekly Volume 25 Number 33 September 7, 2019

Contents

World Journal of Gastroenterology

Volume 25 Number 33 September 7, 2019

ABOUT COVER

Editorial board member of *World Journal of Gastroenterology*, Amedeo Lonardo, MD, Doctor, Senior Lecturer, Department of Biomedical, Metabolic and Neural Sciences, University of Modena and Reggio Emilia, Modena 41126, Italy

AIMS AND SCOPE

World Journal of Gastroenterology (*World J Gastroenterol*, *WJG*, print ISSN 1007-9327, online ISSN 2219-2840, DOI: 10.3748) is a peer-reviewed open access journal. The *WJG* Editorial Board consists of 701 experts in gastroenterology and hepatology from 58 countries.

The primary task of *WJG* is to rapidly publish high-quality original articles, reviews, and commentaries in the fields of gastroenterology, hepatology, gastrointestinal endoscopy, gastrointestinal surgery, hepatobiliary surgery, gastrointestinal oncology, gastrointestinal radiation oncology, *etc*. The *WJG* is dedicated to become an influential and prestigious journal in gastroenterology and hepatology, to promote the development of above disciplines, and to improve the diagnostic and therapeutic skill and expertise of clinicians.

INDEXING/ABSTRACTING

The *WJG* is now indexed in Current Contents®/Clinical Medicine, Science Citation Index Expanded (also known as SciSearch®), Journal Citation Reports®, Index Medicus, MEDLINE, PubMed, PubMed Central, and Scopus. The 2019 edition of Journal Citation Report® cites the 2018 impact factor for *WJG* as 3.411 (5-year impact factor: 3.579), ranking *WJG* as 35th among 84 journals in gastroenterology and hepatology (quartile in category Q2). CiteScore (2018): 3.43.

RESPONSIBLE EDITORS FOR THIS ISSUE

Responsible Electronic Editor: *Yu-Jie Ma*

Proofing Production Department Director: *Yun-Xiaojian Wu*

NAME OF JOURNAL
World Journal of Gastroenterology

ISSN
ISSN 1007-9327 (print) ISSN 2219-2840 (online)

LAUNCH DATE
October 1, 1995

FREQUENCY
Weekly

EDITORS-IN-CHIEF
Subrata Ghosh, Andrzej S Tarnawski

EDITORIAL BOARD MEMBERS
http://www.wjgnet.com/1007-9327/editorialboard.htm

EDITORIAL OFFICE
Ze-Mao Gong, Director

PUBLICATION DATE
September 7, 2019

INSTRUCTIONS TO AUTHORS
https://www.wjgnet.com/bpg/gerinfo/204

GUIDELINES FOR ETHICS DOCUMENTS
https://www.wjgnet.com/bpg/GerInfo/287

GUIDELINES FOR NON-NATIVE SPEAKERS OF ENGLISH
https://www.wjgnet.com/bpg/gerinfo/240

PUBLICATION MISCONDUCT
https://www.wjgnet.com/bpg/gerinfo/208

ARTICLE PROCESSING CHARGE
https://www.wjgnet.com/bpg/gerinfo/242

STEPS FOR SUBMITTING MANUSCRIPTS
https://www.wjgnet.com/bpg/GerInfo/239

ONLINE SUBMISSION
https://www.f6publishing.com

World Journal of Gastroenterology

Submit a Manuscript: https://www.f6publishing.com

World J Gastroenterol 2019 September 7; 25(33): 4796-4804

DOI: 10.3748/wjg.v25.i33.4796

ISSN 1007-9327 (print) ISSN 2219-2840 (online)

EDITORIAL

Role of NLRP3 inflammasome in inflammatory bowel diseases

Evanthia Tourkochristou, Ioanna Aggeletopoulou, Christos Konstantakis, Christos Triantos

ORCID number: Evanthia Tourkochristou (0000-0003-1586-6854); Ioanna Aggeletopoulou (0000-0003-4489-1485); Christos Konstantakis (0000-0001-5834-9182); Christos Triantos (0000-0003-3094-8209).

Author contributions: Tourkochristou E, Aggeletopoulou I and Konstantakis C were responsible for the literature review and analysis; Tourkochristou E and Aggeletopoulou I were responsible for drafting the manuscript and interpreting the data; Triantos C was responsible for the revision of the manuscript for important intellectual content; all authors provided final approval for the version to be submitted.

Conflict-of-interest statement: Not related to this article.

Manuscript source: Invited manuscript

Received: May 30, 2019
Peer-review started: May 30, 2019

Evanthia Tourkochristou, Ioanna Aggeletopoulou, Christos Konstantakis, Christos Triantos, Division of Gastroenterology, Department of Internal Medicine, Medical School, University of Patras, Patras 26504, Greece

Corresponding author: Christos Triantos, PhD, Assistant Professor in Internal Medicine and Gastroenterology, Division of Gastroenterology, Department of Internal Medicine, Medical School, University of Patras, D. Stamatopoulou 4, Patras 26504, Greece. chtriantos@upatras.gr
Telephone: +30-261-6972894651
Fax: +30-261-0625382

Abstract

Inflammasomes are multiprotein intracellular complexes which are responsible for the activation of inflammatory responses. Among various subtypes of inflammasomes, NLRP3 has been a subject of intensive investigation. NLRP3 is considered to be a sensor of microbial and other danger signals and plays a crucial role in mucosal immune responses, promoting the maturation of proinflammatory cytokines interleukin 1β (IL-1β) and IL-18. NLRP3 inflammasome has been associated with a variety of inflammatory and autoimmune conditions, including inflammatory bowel diseases (IBD). The role of NLRP3 in IBD is not yet fully elucidated as it seems to demonstrate both pathogenic and protective effects. Studies have shown a relationship between genetic variants and mutations in NLRP3 gene with IBD pathogenesis. A complex interaction between the NLRP3 inflammasome and the mucosal immune response has been reported. Activation of the inflammasome is a key function mediated by the innate immune response and in parallel the signaling through IL-1β and IL-18 is implicated in adaptive immunity. Further research is needed to delineate the precise mechanisms of NLRP3 function in regulating immune responses. Targeting NLRP3 inflammasome and its downstream signaling will provide new insights into the development of future therapeutic strategies.

Key words: NLRP3 inflammasome; Inflammatory bowel diseases; Mucosal immune system; Interleukin 1β; Interleukin 18; NLRP3 gene polymorphisms

Core tip: NLRP3 inflammasome plays a major role in inflammatory bowel diseases (IBD) pathogenesis through its contribution to chronic inflammatory processes. Abnormal activation of NLRP3 inflammasome has been observed in inflamed tissue of IBD murine models and patients, highlighting its possible pathogenic role in the disease. However, protective effects of NLRP3 function have also been recorded. The pathogenic

First decision: July 21, 2019
Revised: July 30, 2019
Accepted: August 7, 2019
Article in press: August 7, 2019
Published online: September 7, 2019

P-Reviewer: Aldrich MB, Cheng TH, Rangel-Corona R, Schietroma M
S-Editor: Yan JP
L-Editor: A
E-Editor: Ma YJ

NLRP3 inflammasome activity in mucosal immune system may be implicated in the aberrant immune responses and in the disruption of intestinal homeostasis that characterizes IBD. Targeting NLRP3 inflammasome and its downstream signaling will provide new insights into the development of future therapeutic strategies.

Citation: Tourkochristou E, Aggeletopoulou I, Konstantakis C, Triantos C. Role of NLRP3 inflammasome in inflammatory bowel diseases. *World J Gastroenterol* 2019; 25(33): 4796-4804
URL: https://www.wjgnet.com/1007-9327/full/v25/i33/4796.htm
DOI: https://dx.doi.org/10.3748/wjg.v25.i33.4796

INTRODUCTION

The innate immune system is the first-line host defense specified to recognize specific microbial pathogens, named pathogen-associated molecular patterns and damage-associated molecular patterns, and to sense microbial and other danger signals. These functions occur in macrophages, neutrophils, monocytes, dendritic cells (DCs), and epithelial cells through host pattern recognition receptors, such as toll-like receptors and nucleotide-binding domain leucine-rich repeat-containing receptors (NLRs)[1-4]. NLRs play a critical role in innate immune responses and intestinal tissue repair[1].

The NLRP (NOD-like receptor family, pyrin domain-containing) subfamily comprises several subtypes and NLRP3 is one of the best-characterized. The multiprotein complex of NLRP3, called the NLRP3 "inflammasome", consists of three major components—the sensor NLRP3 protein, the adaptor-apoptosis-associated speck-like protein containing a N-terminal PYRIN-PAAD-DAPIN domain and a C-terminal caspase recruitment domain (CARD) (ASC) and the effector protein-caspase-1[5,6]. Activation of NLRP3 occurs when the host is subjected to an exogenous or endogenous stimulus, resulting in the recruitment of ASC and caspase 1. The stimulated NLRP3 interacts with ASC and pro-caspase-1 binds to ASC *via* CARD to assemble into a large cytosolic complex, which triggers activation of caspase-1. Active caspase-1 cleaves the pro-inflammatory cytokines interleukin 1 β (IL-1β) and IL-18 from their precursors to their biologically active forms[7]. These cytokines induce inflammation by promoting the production of proinflammatory cytokines, chemokines and growth factors (Figure 1), as well as recruiting and activating other immune cells. NLRP3 inflammasome has been associated with a variety of inflammatory and autoimmune conditions including inflammatory bowel diseases (IBD)[8,9]. Crohn's disease (CD) and ulcerative colitis (UC) are the main types of IBD. UC is usually limited to the colon and consists of diffuse mucosal inflammation, whereas CD can involve inflammation at any part of the gastrointestinal tract (from mouth to anus)[10,11]. Although the etiology of IBD pathogenesis is not fully elucidated, it has been widely suggested that a genetic-environmental mediated dysregulation of the mucosal immune response is implicated in these diseases. The NLRP3 inflammasome, acting as a sensor of microbial and other danger signals, plays a fundamental role in host defense[12-14]. Recent data have demonstrated the function of NLRP3 inflammasome, not only as a crucial mediator of host defense but also as a critical regulator of intestinal homeostasis[15]. However, the studies on the role of NLRP3 inflammasome in IBD have reported controversial findings.

NLRP3 INFLAMMASOME IN IBD PATHOGENESIS: DATA FROM ANIMAL AND HUMAN STUDIES

Animal studies

The exact role of NLRP3 in IBD is not yet fully elucidated as it seems to demonstrate both pathogenic and protective effects. The study by Bauer *et al*[16] was conducted in two IBD models (dextran sulfate sodium and 2,4,6-trinitrobenzene sulfonic acid induced colitis) and showed that mice with NLRP3 deficiency [NLRP3(-/-)] exhibited attenuated colitis. This result was followed by increased numbers of immunosuppressive $CD103^+$ tolerogenic DCs[16]. An abnormal NLRP3 activation has also been reported to play an important pathogenic role in IBD, in a study using a murine IBD model[17]. In this report, NLRP3 and ASC protein levels were significantly

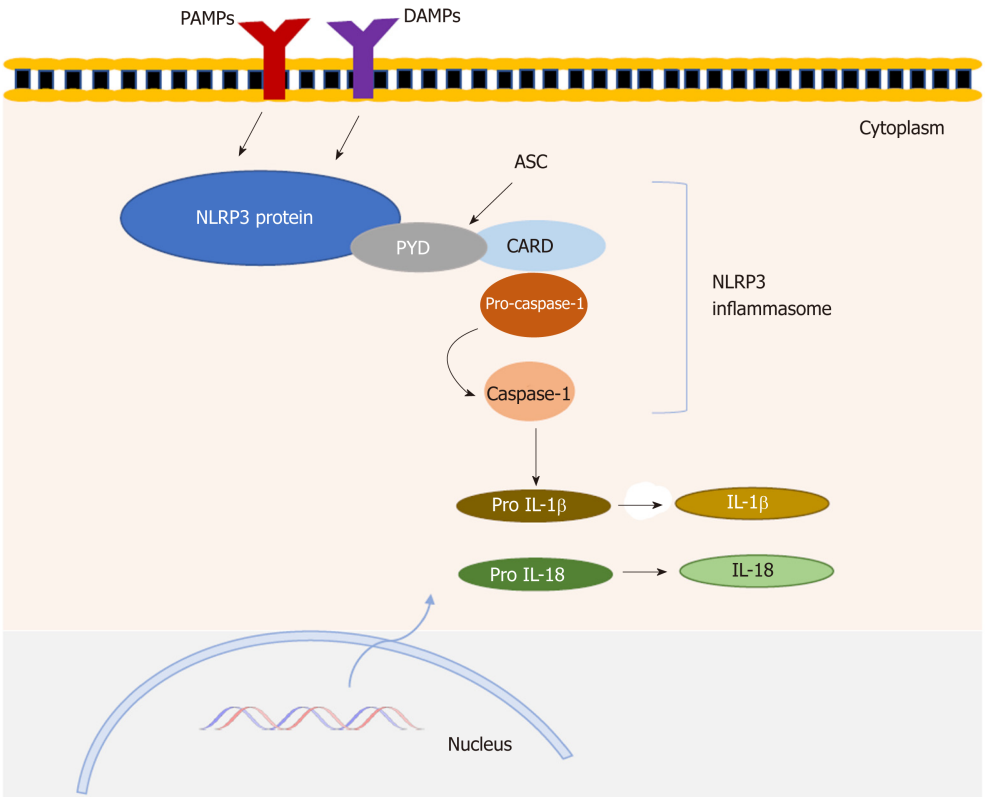

Figure 1 NLRP3 inflammasome structure. NLRP3 inflammasome consists of three major components-the sensor NLRP3 protein, the adaptor-apoptosis-associated speck-like protein (ASC) which contains a N-terminal PYRIN-PAAD-DAPIN domain (PYD) and a C-terminal caspase recruitment domain (CARD) and the effector protein-caspase-1. Activation of NLRP3 occurs when the cell is subjected to pathogen-associated molecular patterns and damage-associated molecular patterns. The stimulated NLRP3 interacts through PYD domain with ASC and pro-caspase-1 binds to ASC *via* CARD to assemble into a large cytosolic complex, which triggers activation of caspase-1. Active caspase-1 cleaves the pro-inflammatory cytokines interleukin 1β (IL-1β) and IL-18 from their precursors to their biologically active forms inducing inflammation. ASC: Adaptor-apoptosis-associated speck-like protein; CARD: C-terminal caspase recruitment domain; PYD: PYRIN-PAAD-DAPIN domain; IL: Interleukin; PAMPs: Pathogen-associated molecular patterns; DAMPs: Damage-associated molecular patterns.

elevated in the colonic mucosa of deficient mice for anti-inflammatory cytokine IL-10 (IL-10-/-) before the onset of colitis compared to the wild type (WT) mice[17]. Other studies using spontaneous colitis mice showed that the inhibition of caspase-1 activity and the selected blockade of NLRP3 complex ameliorated colonic inflammation and were associated with decreased colitis[18,19]. In contrast, a protective role of NLRP3 inflammasome was recorded in studies presenting that mice with NLRP3, ASC or caspase-1 deficiency exhibited more severe experimental colitis and decreased intestinal epithelial integrity[20,21]. The association of NLRP3 deficiency with IBD severity was also highlighted in an oxazolone-induced colitis murine model, mediated by T helper 2 (Th2) cytokines (IL-4, IL-13)[22]. Th2 cytokines, such as IL-4 and IL-13, were increased at mRNA and protein level in NLRP3-/- mice compared to WT mice[22]. NLRP3-/- and caspase 1-/- mice exhibited severe colitis after oxazolone treatment compared to WT mice[22]. Administration of IL-1β or IL-18 prevented progression of colitis in NLRP3-/- mice, but did not affect the severity of colitis in WT mice[22].

Therapeutic strategies targeting NLRP3 activity are used in IBD murine models, highlighting the potent clinical relevance of NLRP3 in the disease. A micro-RNA (miR-223) has been shown to be an important therapeutic target for IBD[23]. It regulates the NLRP3 inflammasome activity, by interfering and inhibiting mRNA expression of NLRP3 gene[23]. Treatment of experimental colitis mice with nanoparticles for overexpression of miR-223 ameliorated colitis symptoms and caused a decrease in protein levels of NLRP3 and IL-1β[23]. The therapeutic potential of the blockade of IL-1β and IL-18 cytokines has also been reported. Experimental colitis mice with genetic and pharmacological deficiency of IL-1β and IL-18 exhibited attenuated colitis[24]. Lastly, in a murine colitis model, suppression of pyroptosis signaling through Cholecalciterol Cholesterol Emulsion was associated with ameliorated disease[25].

Human studies

Human data have demonstrated that the NLRP3 inflammasome activity plays a key part in IBD pathogenesis. Lazaridis *et al*[26], presented that *ex vivo* NLRP3

inflammasome was activated in CD patients whereas in UC patients NLRP3 activation occurred in late disease stage compared to controls. This finding was combined with an *in vitro* increase in IL-1β concentrations in peripheral blood mononuclear cells of CD patients compared to UC patients and controls[26]. A recent study has displayed an upregulation of NLRP3 components in both CD and UC patients as increased mRNA expression of NLRP3, IL-1β, ASC and Caspase-1 was observed in their colonic biopsies; this result was associated with increased disease activity[27]. Inhibition of NLRP3 inflammasome in CD patients resulted in suppressive response of proinflammatory cytokines and chemokines, emphasizing the pathogenic contribution of NLRP3 aberrant activation in the disease[17].

Moreover, IL-1β and IL-18 cytokines have been increased in plasma and colonic mucosa of IBD patients[28,29]. Increased IL-1β secretion from colonic tissues and macrophages in IBD patients has been correlated to the severity of the disease, by promoting chronic intestinal inflammation[27,28]. In a study encompassing children with IBD, the balance between IL-18 cytokine and its natural inhibitor IL-18-binding protein (IL-18BP) has been involved in IBD pathogenesis[30]. Specific microRNAs have been correlated to UC activity based on a high-throughput profiling of blood serum microRNAs of UC patients[31]. A major involvement of microRNAs in IBD development, through interfering NLRP3 activity, has been observed. NLRP3 deficiency in IBD patients, caused by a microRNA, called miR-223, which inhibits NLRP3 gene expression, was associated with active inflammation state in IBD, as increased miR-223 levels were observed in mucosal biopsies[23,32].

Clinical studies which target NLRP3 inflammasome activity are limited[33,34]. Curcumin, an NLRP3 inhibitor acting by interfering the inflammasome-mediated secretion of IL-1β and activation of caspase-1, has been proven to be a potential and safe agent for the treatment of UC[35]. The use of curcumin combined with mesalamine in UC patients was linked to clinical improvement and endoscopic remission[36,37].

The controversial data on the NLRP3 activity in IBD reveal the complicated and probably diverse role of NLRP3 inflammasome in IBD. The NLRP3 activation seems to be a major characteristic in inflamed tissue of IBD murine models and patients, as high expression levels of its components have been observed. Activation of NLRP3 inflammasome constitutes a crucial step in the initiation of inflammatory processes, which results in tissue damage and IBD clinical manifestations development. Thus, NLRP3 pathogenic effect may be due to increased or aberrant activity of the complex. The etiological factors of inflammasome abnormal activity remain to be clarified. Furthermore, the possibility of the NLRP3 inflammasome exerting a protective function during inflammation as a compensatory mechanism of maintaining intestinal homeostasis, should be investigated. Study on molecular regulation of NLRP3 inflammasome activity during inflammation will provide useful knowledge in development of therapeutic approaches in IBD. Activation of NLRP3 inflammasome as well as endpoints of this process (IL-1β, IL-18, pyroptosis) seem to be promising therapeutic options which need further research.

GENETIC STUDIES ON THE ROLE OF NLRP3 INFLAMMASOME IN IBD

Numerous genetic studies have been performed to explain the association of genetic variants in NLRP3 inflammasome with IBD pathogenesis. These data suggest that NLRP3 inflammasome dysregulation may have a prominent role in the pathogenesis of IBD. Genetic variations could be responsible for NLRP3 enhanced or reduced activity, affecting the microenvironment balance and inflammatory state in pathological conditions such as IBD. Mutations or polymorphisms in NLRP3 have been associated with inflammatory diseases[38-40].

Specific single nucleotide polymorphisms (SNPs), which are located in a regulatory region downstream the NLRP3 gene, have been linked to CD susceptibility. These SNPs have been related to hypoproduction of IL-1β and decreased NLRP3 expression[41]. However, a panel study showed no significant associations among SNPs in the regulatory region of NLRP3 and CD pathogenesis[42]. Another SNP analysis in CD and UC patients of Chinese Han population demonstrated an association between two SNPs in NLRP3 gene, with susceptibility to UC but not to CD[43].

A mutation affecting a component of NLRP3 inflammasome could also contribute to susceptibility to IBD. A study in CD patients, who carry a loss-of-function mutation of T60 CARD8, a negative regulator of inflammasome activation, has reported increased NLRP3 inflammasome activity and excessive production of IL-1β and IL-18 by monocytes[44]. This mutation resulted in decreased overall CARD8 function, which

normally regulates negatively NLRP3 activation by inhibiting its oligomerization[44]. A combination of polymorphisms in NLRP3 and CARD8 genes has been linked to high risk of developing CD in men[45].

Nevertheless, hyperactivation of NLRP3 inflammasome has been suggested to be a protective mechanism against colitis in a murine model[46]. Particularly, genetically modified mice carrying the NLRP3 R258W mutation, which induces hyperactivation of NLRP3 inflammasome, were strongly resistant to experimental colitis[46]. This result was due to an excess of local IL-1β production, but not IL-18, which causes the intestinal microbiota to induce local regulatory T cells (Tregs) , maintaining intestinal homeostasis[46].

Mutations or polymorphisms related to NLRP3 inflammasome genes contribute to IBD susceptibility in various ways. It has been reported that an aberrant activity of NLRP3 inflammasome in IBD may be due to a specific genetic background. Further studies, which will elucidate the link among NLRP3 inflammasome associated genes, genetic susceptibility and the molecular function and mechanisms of NLRP3 inflammasome, will provide new insights into the field of IBD pathogenesis.

ROLE OF NLRP3 INFLAMMASOME IN MUCOSAL IMMUNE RESPONSES

There is a complex interaction among the NLRP3 inflammasome, the mucosal immune response and the gut homeostasis. A disrupted inflammasome signaling may result in dysbiosis and increased colonization of pathobionts. Intestinal microbiota plays a crucial role in regulating gut homeostasis[47,48]. Alterations in the microbiota composition initiate aberrant innate immune responses[49]. Microbiota infiltrates into the lamina propria and recruits immune cells which secrete cytokines, chemokines and antimicrobial agents promoting inflammation[49]. NLRP3 inflammasome may also lead to death of innate cells such as macrophages and DCs by triggering a caspace-1-dependent form of cell death, called pyroptosis[50]. Thus, NLRP3 inflammasome can have a dual role in IBD pathogenesis, related to initiation and maintenance of inflammation. Firstly, a disrupted NLRP3 signaling may alter the colonization of intestinal microbiota, causing dysbiosis, a crucial condition for IBD development. Secondly, NLRP3 inflammasome through pyroptosis may promote a vicious circle of inflammation, leading to tissue destruction due to consecutive release of cellular debris, which will reactivate immune cells.

Aberrant Th cell responses play a major role in IBD pathogenesis. In particular, chronic inflammation in CD has been associated with Th1 immune responses. High levels of Th1 cytokines and high expression of transcription factors and cytokine receptors that promote Th1 cell development, have been reported[51]. Moreover, it has been noted that dysfunction of immunosuppressive Th cells, such as Tregs and Th3 cells, may constitute a pathogenic factor for CD. Th17 cells have an important role in IBD, and especially in CD, by stimulating intestinal inflammation and regulating the integrity of epithelial cell barrier[52]. By contrast, UC is considered to be a Th2 driven disease, as inflamed tissue in UC patients expresses high levels of Th2-associated cytokines[53,54].

NLRP3 protein, which is crucial for NLRP3 inflammasome formation, has been proven to be a key regulator in Th2 differentiation. Bruchard *et al*[55] supported that NLRP3 expression in naïve CD4+ T cells induced a Th2 immune profile in a mouse model. NLRP3 protein can act as a transcriptional factor, regulating the expression of genes associated with the Th2 cells, independently of the inflammasome[55]. IL-1β, which is produced as a result of activation of NLRP3 inflammasome, has been found to contribute to differentiation of Th lymphocytes, such as Th17 and Th1 derived from Th17 cells *in vitro* and *in vivo*[56], and to enhance the antigen-driven expansion of naive and memory T cells[57].

The mechanism, by which NLRP3 inflammasome links innate to adaptive immunity in IBD, has not been elucidated. Mak'Anyengo *et al*[58], using a T cell transfer murine colitis model, examined the role of the NLRP3 inflammasome in DCs' differentiation, T cell polarization and intestinal inflammation. Intestinal DCs have a significant involvement in antigen presentation, T cell activity and Tregs differentiation. Specifically, intestinal $CD103^+$ DCs have immunosuppressive function and promote Tregs activity[59,60]. Mak'Anyengo *et al*[58] showed that NLRP3 inflammasome-driven cytokine release of IL-1β led to the induction of Th17 inflammatory immune response[58]. NLRP3-deficient mice with decreased IL-1β levels were protected from colitis due to accumulation of $CD103^+$ DCs. This study suggested that NLRP3 inflammasome acts as a checkpoint regulator of IL-1β and IL-18 in the intestine, controlling the secretion of DC-expanding cytokines by T cells *in vitro* and *in*

vivo[58].

NLRP3 inflammasome activation results in the maturation of proinflammatory cytokines IL-1β and IL-18. IL-1β has a multifunctional role in immune responses, inducing cytokine production, enhancing T cell activation and antigen recognition, and directing innate immune cells to the site of infection[61,62]. Increased levels of IL-1β have been recorded in IBD patients and mice models and have been associated with severity of disease[28]. IL-1β signaling is required for the development of acute inflammation in both T cell–independent and T cell–mediated colitis[28]. The pathogenic activity of IL-1β in IBD has been shown to induce the accumulation of IL-17A producing cells and Th17 inflammatory responses. However, the dominant role of IL-1β in IBD development has not been fully determined[28,63]. IL-1β signaling induces activation of nuclear factor kappa light chain enhancer of activated B cells (NF-κB) and mitogen-activated protein kinase signaling cascades which results in the transcriptional activation of genes encoding cytokines, chemokines and a variety of pro-inflammatory mediators[64,65].

IL-18 is another cytokine which belongs to the IL-1 family of cytokines. Constant expression of IL-18 has been proposed to be important for the maintenance of epithelial integrity. IL-18 can promote barrier function in the intestine, controlling the outgrowth of colitogenic bacteria[66]. The role of IL-18 in immune responses has also been noted. It induces interferon gamma (IFN-γ) production by natural killer and T cells in the presence of IL-12, whereas in the absence of IL-12, IL-18 promotes Th2 responses by inducing IL-4 production[67]. Although increased plasma levels of free IL-18 have been reported in CD patients[29], an immunomodulatory activity of this cytokine has been demonstrated in chronic inflammation in IBD[68]. An *in vitro* analysis of cells isolated from CD lesions showed that IL-18 affects IFN-γ and IL-10 production and apoptosis. T cells isolated from inflamed tissue of CD patients in the presence of IL-18 had increased IFN-γ and decreased IL-10 production compared to controls[68]. Inhibition of IL-18 with recombinant human IL-18 binding protein (rhIL-18BPa) in experimental colitis model was associated with reduced apoptosis of lamina propria CD4+ T cells[68]. Protective function of IL-18 in IBD has been suggested in a T-cell driven colitis model[69]. IL-18R1 receptor expression on CD4+ T cells seems to be crucial for suppression of IL-17 production and Th17 differentiation. In addition, during intestinal inflammation, IL-18/IL-18R1 signaling has been shown to play a key role in Tregs function, by promoting expression of their effector molecules[69].

PERSPECTIVE

NLRP3 inflammasome is probably a key point in inflammatory processes that characterize IBD. The differential role of the inflammasome in IBD is supported by controversial findings about its protective and pathogenic activity; NLRP3 inflammasome has either pathogenic activity, the etiological factors of which have not been elucidated, or it acquires a protective function during the disease, being a compensatory mechanism. Further animal and human studies are needed to examine these hypotheses. Specific genetic background may be responsible for the aberrant activity of NLRP3 inflammasome in IBD. Investigation of the link between genetic susceptibility of NLRP3 inflammasome associated genes and molecular regulation of NLRP3 inflammasome, is of particular importance. NLRP3 inflammasome acts as a potent regulator of mucosal immune responses and intestinal homeostasis due to its association with innate and adaptive immunity. Targeting activation of NLRP3 inflammasome and the related endpoints (IL-1β, IL-18, pyroptosis) will provide new insights into the development of novel therapeutic options in IBD.

REFERENCES

1 **Prossomariti A**, Sokol H, Ricciardiello L. Nucleotide-Binding Domain Leucine-Rich Repeat Containing Proteins and Intestinal Microbiota: Pivotal Players in Colitis and Colitis-Associated Cancer Development. *Front Immunol* 2018; **9**: 1039 [PMID: 29868004 DOI: 10.3389/fimmu.2018.01039]

2 **De Nardo D**, De Nardo CM, Latz E. New insights into mechanisms controlling the NLRP3 inflammasome and its role in lung disease. *Am J Pathol* 2014; **184**: 42-54 [PMID: 24183846 DOI: 10.1016/j.ajpath.2013.09.007]

3 **Liston A**, Masters SL. Homeostasis-altering molecular processes as mechanisms of inflammasome activation. *Nat Rev Immunol* 2017; **17**: 208-214 [PMID: 28163301 DOI: 10.1038/nri.2016.151]

4 **Próchnicki T**, Latz E. Inflammasomes on the Crossroads of Innate Immune Recognition and Metabolic Control. *Cell Metab* 2017; **26**: 71-93 [PMID: 28683296 DOI: 10.1016/j.cmet.2017.06.018]

5 **Hauenstein AV**, Zhang L, Wu H. The hierarchical structural architecture of inflammasomes, supramolecular inflammatory machines. *Curr Opin Struct Biol* 2015; **31**: 75-83 [PMID: 25881155 DOI: 10.1016/j.sbi.2015.03.014]

6 **Martinon F**, Burns K, Tschopp J. The inflammasome: A molecular platform triggering activation of inflammatory caspases and processing of proIL-beta. *Mol Cell* 2002; **10**: 417-426 [PMID: 12191486 DOI: 10.1016/S1097-2765(02)00599-3]

7 **Próchnicki T**, Mangan MS, Latz E. Recent insights into the molecular mechanisms of the NLRP3 inflammasome activation. *F1000Res* 2016; **5**: pii: F1000 Faculty Rev-1469 [PMID: 27508077 DOI: 10.12688/f1000research.8614.1]

8 **Benetti E**, Chiazza F, Patel NS, Collino M. The NLRP3 Inflammasome as a novel player of the intercellular crosstalk in metabolic disorders. *Mediators Inflamm* 2013; **2013**: 678627 [PMID: 23843683 DOI: 10.1155/2013/678627]

9 **Hutton HL**, Ooi JD, Holdsworth SR, Kitching AR. The NLRP3 inflammasome in kidney disease and autoimmunity. *Nephrology (Carlton)* 2016; **21**: 736-744 [PMID: 27011059 DOI: 10.1111/nep.12785]

10 **Zhang YZ**, Li YY. Inflammatory bowel disease: Pathogenesis. *World J Gastroenterol* 2014; **20**: 91-99 [PMID: 24415861 DOI: 10.3748/wjg.v20.i1.91]

11 **Ungar B**, Kopylov U. Advances in the development of new biologics in inflammatory bowel disease. *Ann Gastroenterol* 2016; **29**: 243-248 [PMID: 27366024 DOI: 10.20524/aog.2016.0027]

12 **Kummer JA**, Broekhuizen R, Everett H, Agostini L, Kuijk L, Martinon F, van Bruggen R, Tschopp J. Inflammasome components NALP 1 and 3 show distinct but separate expression profiles in human tissues suggesting a site-specific role in the inflammatory response. *J Histochem Cytochem* 2007; **55**: 443-452 [PMID: 17164409 DOI: 10.1369/jhc.6A7101.2006]

13 **Lei-Leston AC**, Murphy AG, Maloy KJ. Epithelial Cell Inflammasomes in Intestinal Immunity and Inflammation. *Front Immunol* 2017; **8**: 1168 [PMID: 28979266 DOI: 10.3389/fimmu.2017.01168]

14 **Zhen Y**, Zhang H. NLRP3 Inflammasome and Inflammatory Bowel Disease. *Front Immunol* 2019; **10**: 276 [PMID: 30873162 DOI: 10.3389/fimmu.2019.00276]

15 **Zaki MH**, Lamkanfi M, Kanneganti TD. The Nlrp3 inflammasome: contributions to intestinal homeostasis. *Trends Immunol* 2011; **32**: 171-179 [PMID: 21388882 DOI: 10.1016/j.it.2011.02.002]

16 **Bauer C**, Duewell P, Lehr HA, Endres S, Schnurr M. Protective and aggravating effects of Nlrp3 inflammasome activation in IBD models: Influence of genetic and environmental factors. *Dig Dis* 2012; **30** Suppl 1: 82-90 [PMID: 23075874 DOI: 10.1159/000341681]

17 **Liu L**, Dong Y, Ye M, Jin S, Yang J, Joosse ME, Sun Y, Zhang J, Lazarev M, Brant SR, Safar B, Marohn M, Mezey E, Li X. The Pathogenic Role of NLRP3 Inflammasome Activation in Inflammatory Bowel Diseases of Both Mice and Humans. *J Crohns Colitis* 2017; **11**: 737-750 [PMID: 27993998 DOI: 10.1093/ecco-jcc/jjw219]

18 **Zhang J**, Fu S, Sun S, Li Z, Guo B. Inflammasome activation has an important role in the development of spontaneous colitis. *Mucosal Immunol* 2014; **7**: 1139-1150 [PMID: 24472848 DOI: 10.1038/mi.2014.1]

19 **Perera AP**, Fernando R, Shinde T, Gundamaraju R, Southam B, Sohal SS, Robertson AAB, Schroder K, Kunde D, Eri R. MCC950, a specific small molecule inhibitor of NLRP3 inflammasome attenuates colonic inflammation in spontaneous colitis mice. *Sci Rep* 2018; **8**: 8618 [PMID: 29872077 DOI: 10.1038/s41598-018-26775-w]

20 **Zaki MH**, Boyd KL, Vogel P, Kastan MB, Lamkanfi M, Kanneganti TD. The NLRP3 inflammasome protects against loss of epithelial integrity and mortality during experimental colitis. *Immunity* 2010; **32**: 379-391 [PMID: 20303296 DOI: 10.1016/j.immuni.2010.03.003]

21 **Dupaul-Chicoine J**, Yeretssian G, Doiron K, Bergstrom KS, McIntire CR, LeBlanc PM, Meunier C, Turbide C, Gros P, Beauchemin N, Vallance BA, Saleh M. Control of intestinal homeostasis, colitis, and colitis-associated colorectal cancer by the inflammatory caspases. *Immunity* 2010; **32**: 367-378 [PMID: 20226691 DOI: 10.1016/j.immuni.2010.02.012]

22 **Itani S**, Watanabe T, Nadatani Y, Sugimura N, Shimada S, Takeda S, Otani K, Hosomi S, Nagami Y, Tanaka F, Kamata N, Yamagami H, Tanigawa T, Shiba M, Tominaga K, Fujiwara Y, Arakawa T. NLRP3 inflammasome has a protective effect against oxazolone-induced colitis: A possible role in ulcerative colitis. *Sci Rep* 2016; **6**: 39075 [PMID: 27966619 DOI: 10.1038/srep39075]

23 **Neudecker V**, Haneklaus M, Jensen O, Khailova L, Masterson JC, Tye H, Biette K, Jedlicka P, Brodsky KS, Gerich ME, Mack M, Robertson AAB, Cooper MA, Furuta GT, Dinarello CA, O'Neill LA, Eltzschig HK, Masters SL, McNamee EN. Myeloid-derived miR-223 regulates intestinal inflammation via repression of the NLRP3 inflammasome. *J Exp Med* 2017; **214**: 1737-1752 [PMID: 28487310 DOI: 10.1084/jem.20160462]

24 **Impellizzeri D**, Siracusa R, Cordaro M, Peritore AF, Gugliandolo E, Mancuso G, Midiri A, Di Paola R, Cuzzocrea S. Therapeutic potential of dinitrobenzene sulfonic acid (DNBS)-induced colitis in mice by targeting IL-1β and IL-18. *Biochem Pharmacol* 2018; **155**: 150-161 [PMID: 29963998 DOI: 10.1016/j.bcp.2018.06.029]

25 **Xiong Y**, Lou Y, Su H, Fu Y, Kong J. Cholecalciterol cholesterol emulsion ameliorates experimental colitis via down-regulating the pyroptosis signaling pathway. *Exp Mol Pathol* 2016; **100**: 386-392 [PMID: 26970278 DOI: 10.1016/j.yexmp.2016.03.003]

26 **Lazaridis LD**, Pistiki A, Giamarellos-Bourboulis EJ, Georgitsi M, Damoraki G, Polymeros D, Dimitriadis GD, Triantafyllou K. Activation of NLRP3 Inflammasome in Inflammatory Bowel Disease: Differences Between Crohn's Disease and Ulcerative Colitis. *Dig Dis Sci* 2017; **62**: 2348-2356 [PMID: 28523573 DOI: 10.1007/s10620-017-4609-8]

27 **Ranson N**, Veldhuis M, Mitchell B, Fanning S, Cook AL, Kunde D, Eri R. NLRP3-Dependent and -Independent Processing of Interleukin (IL)-1β in Active Ulcerative Colitis. *Int J Mol Sci* 2018; **20**: pii: E57 [PMID: 30583612 DOI: 10.3390/ijms20010057]

28 **Coccia M**, Harrison OJ, Schiering C, Asquith MJ, Becher B, Powrie F, Maloy KJ. IL-1β mediates chronic intestinal inflammation by promoting the accumulation of IL-17A secreting innate lymphoid cells and CD4(+) Th17 cells. *J Exp Med* 2012; **209**: 1595-1609 [PMID: 22891275 DOI: 10.1084/jem.20111453]

29 **Ludwiczek O**, Kaser A, Novick D, Dinarello CA, Rubinstein M, Tilg H. Elevated systemic levels of free interleukin-18 (IL-18) in patients with Crohn's disease. *Eur Cytokine Netw* 2005; **16**: 27-33 [PMID: 15809203]

30 **Leach ST**, Messina I, Lemberg DA, Novick D, Rubenstein M, Day AS. Local and systemic interleukin-18 and interleukin-18-binding protein in children with inflammatory bowel disease. *Inflamm Bowel Dis* 2008; **14**: 68-74 [PMID: 17879274 DOI: 10.1002/ibd.20272]

31 **Polytarchou C**, Oikonomopoulos A, Mahurkar S, Touroutoglou A, Koukos G, Hommes DW, Iliopoulos D. Assessment of Circulating MicroRNAs for the Diagnosis and Disease Activity Evaluation in Patients with Ulcerative Colitis by Using the Nanostring Technology. *Inflamm Bowel Dis* 2015; **21**: 2533-2539 [PMID: 26313695 DOI: 10.1097/MIB.0000000000000547]

32 **Bauernfeind F**, Rieger A, Schildberg FA, Knolle PA, Schmid-Burgk JL, Hornung V. NLRP3 inflammasome activity is negatively controlled by miR-223. *J Immunol* 2012; **189**: 4175-4181 [PMID: 22984082 DOI: 10.4049/jimmunol.1201516]

33 **Perera AP**, Kunde D, Eri R. NLRP3 Inhibitors as Potential Therapeutic Agents for Treatment of Inflammatory Bowel Disease. *Curr Pharm Des* 2017; **23**: 2321-2327 [PMID: 28155620 DOI: 10.2174/1381612823666170201162414]

34 **Shao BZ**, Wang SL, Pan P, Yao J, Wu K, Li ZS, Bai Y, Linghu EQ. Targeting NLRP3 Inflammasome in Inflammatory Bowel Disease: Putting out the Fire of Inflammation. *Inflammation* 2019; **42**: 1147-1159 [PMID: 30937839 DOI: 10.1007/s10753-019-01008-y]

35 **Gong Z**, Zhou J, Li H, Gao Y, Xu C, Zhao S, Chen Y, Cai W, Wu J. Curcumin suppresses NLRP3 inflammasome activation and protects against LPS-induced septic shock. *Mol Nutr Food Res* 2015; **59**: 2132-2142 [PMID: 26250869 DOI: 10.1002/mnfr.201500316]

36 **Iqbal U**, Anwar H, Quadri AA. Use of Curcumin in Achieving Clinical and Endoscopic Remission in Ulcerative Colitis: A Systematic Review and Meta-analysis. *Am J Med Sci* 2018; **356**: 350-356 [PMID: 30360803 DOI: 10.1016/j.amjms.2018.06.023]

37 **Wang Y**, Tang Q, Duan P, Yang L. Curcumin as a therapeutic agent for blocking NF-κB activation in ulcerative colitis. *Immunopharmacol Immunotoxicol* 2018; **40**: 476-482 [PMID: 30111198 DOI: 10.1080/08923973.2018.1469145]

38 **Jenko B**, Praprotnik S, Tomšic M, Dolžan V. NLRP3 and CARD8 Polymorphisms Influence Higher Disease Activity in Rheumatoid Arthritis. *J Med Biochem* 2016; **35**: 319-323 [PMID: 28356883 DOI: 10.1515/jomb-2016-0008]

39 **Lee YH**, Bae SC. Association between functional NLRP3 polymorphisms and susceptibility to autoimmune and inflammatory diseases: A meta-analysis. *Lupus* 2016; **25**: 1558-1566 [PMID: 27060062 DOI: 10.1177/0961203316644336]

40 **von Herrmann KM**, Salas LA, Martinez EM, Young AL, Howard JM, Feldman MS, Christensen BC, Wilkins OM, Lee SL, Hickey WF, Havrda MC. NLRP3 expression in mesencephalic neurons and characterization of a rare NLRP3 polymorphism associated with decreased risk of Parkinson's disease. *NPJ Parkinsons Dis* 2018; **4**: 24 [PMID: 30131971 DOI: 10.1038/s41531-018-0061-5]

41 **Villani AC**, Lemire M, Fortin G, Louis E, Silverberg MS, Collette C, Baba N, Libioulle C, Belaiche J, Bitton A, Gaudet D, Cohen A, Langelier D, Fortin PR, Wither JE, Sarfati M, Rutgeerts P, Rioux JD, Vermeire S, Hudson TJ, Franchimont D. Common variants in the NLRP3 region contribute to Crohn's disease susceptibility. *Nat Genet* 2009; **41**: 71-76 [PMID: 19098911 DOI: 10.1038/ng.285]

42 **Lewis GJ**, Massey DC, Zhang H, Bredin F, Tremelling M, Lee JC, Berzuini C, Parkes M. Genetic association between NLRP3 variants and Crohn's disease does not replicate in a large UK panel. *Inflamm Bowel Dis* 2011; **17**: 1387-1391 [PMID: 21560198 DOI: 10.1002/ibd.21499]

43 **Zhang HX**, Wang ZT, Lu XX, Wang YG, Zhong J, Liu J. NLRP3 gene is associated with ulcerative colitis (UC), but not Crohn's disease (CD), in Chinese Han population. *Inflamm Res* 2014; **63**: 979-985 [PMID: 25297810 DOI: 10.1007/s00011-014-0774-9]

44 **Mao L**, Kitani A, Similuk M, Oler AJ, Albenberg L, Kelsen J, Aktay A, Quezado M, Yao M, Montgomery-Recht K, Fuss IJ, Strober W. Loss-of-function CARD8 mutation causes NLRP3 inflammasome activation and Crohn's disease. *J Clin Invest* 2018; **128**: 1793-1806 [PMID: 29408806 DOI: 10.1172/JCI98642]

45 **Schoultz I**, Verma D, Halfvarsson J, Törkvist L, Fredrikson M, Sjöqvist U, Lördal M, Tysk C, Lerm M, Söderkvist P, Söderholm JD. Combined polymorphisms in genes encoding the inflammasome components NALP3 and CARD8 confer susceptibility to Crohn's disease in Swedish men. *Am J Gastroenterol* 2009; **104**: 1180-1188 [PMID: 19319132 DOI: 10.1038/ajg.2009.29]

46 **Yao X**, Zhang C, Xing Y, Xue G, Zhang Q, Pan F, Wu G, Hu Y, Guo Q, Lu A, Zhang X, Zhou R, Tian Z, Zeng B, Wei H, Strober W, Zhao L, Meng G. Remodelling of the gut microbiota by hyperactive NLRP3 induces regulatory T cells to maintain homeostasis. *Nat Commun* 2017; **8**: 1896 [PMID: 29196621 DOI: 10.1038/s41467-017-01917-2]

47 **Hirota SA**, Ng J, Lueng A, Khajah M, Parhar K, Li Y, Lam V, Potentier MS, Ng K, Bawa M, McCafferty DM, Rioux KP, Ghosh S, Xavier RJ, Colgan SP, Tschopp J, Muruve D, MacDonald JA, Beck PL. NLRP3 inflammasome plays a key role in the regulation of intestinal homeostasis. *Inflamm Bowel Dis* 2011; **17**: 1359-1372 [PMID: 20872834 DOI: 10.1002/ibd.21478]

48 **Willing B**, Halfvarson J, Dicksved J, Rosenquist M, Järnerot G, Engstrand L, Tysk C, Jansson JK. Twin studies reveal specific imbalances in the mucosa-associated microbiota of patients with ileal Crohn's disease. *Inflamm Bowel Dis* 2009; **15**: 653-660 [PMID: 19023901 DOI: 10.1002/ibd.20783]

49 **Belkaid Y**, Hand TW. Role of the microbiota in immunity and inflammation. *Cell* 2014; **157**: 121-141 [PMID: 24679531 DOI: 10.1016/j.cell.2014.03.011]

50 **Shi J**, Gao W, Shao F. Pyroptosis: Gasdermin-Mediated Programmed Necrotic Cell Death. *Trends Biochem Sci* 2017; **42**: 245-254 [PMID: 27932073 DOI: 10.1016/j.tibs.2016.10.004]

51 **Matsuoka K**, Inoue N, Sato T, Okamoto S, Hisamatsu T, Kishi Y, Sakuraba A, Hitotsumatsu O, Ogata H, Koganei K, Fukushima T, Kanai T, Watanabe M, Ishii H, Hibi T. T-bet upregulation and subsequent interleukin 12 stimulation are essential for induction of Th1 mediated immunopathology in Crohn's disease. *Gut* 2004; **53**: 1303-1308 [PMID: 15306590 DOI: 10.1136/gut.2003.024190]

52 **Li N**, Shi RH. Updated review on immune factors in pathogenesis of Crohn's disease. *World J Gastroenterol* 2018; **24**: 15-22 [PMID: 29358878 DOI: 10.3748/wjg.v24.i1.15]

53 **Heller F**, Florian P, Bojarski C, Richter J, Christ M, Hillenbrand B, Mankertz J, Gitter AH, Bürgel N, Fromm M, Zeitz M, Fuss I, Strober W, Schulzke JD. Interleukin-13 is the key effector Th2 cytokine in ulcerative colitis that affects epithelial tight junctions, apoptosis, and cell restitution. *Gastroenterology* 2005; **129**: 550-564 [PMID: 16083712 DOI: 10.1016/j.gastro.2005.05.002]

54 **Nemeth ZH**, Bogdanovski DA, Barratt-Stopper P, Paglinco SR, Antonioli L, Rolandelli RH. Crohn's Disease and Ulcerative Colitis Show Unique Cytokine Profiles. *Cureus* 2017; **9**: e1177 [PMID: 28533995 DOI: 10.7759/cureus.1177]

55 **Bruchard M**, Rebé C, Derangère V, Togbé D, Ryffel B, Boidot R, Humblin E, Hamman A, Chalmin F, Berger H, Chevriaux A, Limagne E, Apetoh L, Végran F, Ghiringhelli F. The receptor NLRP3 is a transcriptional regulator of TH2 differentiation. *Nat Immunol* 2015; **16**: 859-870 [PMID: 26098997 DOI: 10.1038/ni.3202]

56 **Santarlasci V**, Cosmi L, Maggi L, Liotta F, Annunziato F. IL-1 and T Helper Immune Responses. *Front Immunol* 2013; **4**: 182 [PMID: 23874332 DOI: 10.3389/fimmu.2013.00182]

57 **Vargas TR**, Martin F, Apetoh L. Role of interleukin-1-family cytokines on effector CD4 T cell

differentiation. *World J Immunol* 2017; **7**: 24-31 [DOI: 10.5411/wji.v7.i2.24]
58 **Mak'Anyengo R**, Duewell P, Reichl C, Hörth C, Lehr HA, Fischer S, Clavel T, Denk G, Hohenester S, Kobold S, Endres S, Schnurr M, Bauer C. Nlrp3-dependent IL-1β inhibits CD103+ dendritic cell differentiation in the gut. *JCI Insight* 2018; **3**: pii: 96322 [PMID: 29515025 DOI: 10.1172/jci.insight.96322]
59 **Ruane DT**, Lavelle EC. The role of CD103 dendritic cells in the intestinal mucosal immune system. *Front Immunol* 2011; **2**: 25 [PMID: 22566815 DOI: 10.3389/fimmu.2011.00025]
60 **Lewis KL**, Reizis B. Dendritic cells: Arbiters of immunity and immunological tolerance. *Cold Spring Harb Perspect Biol* 2012; **4**: a007401 [PMID: 22855722 DOI: 10.1101/cshperspect.a007401]
61 **Dinarello CA**. A clinical perspective of IL-1β as the gatekeeper of inflammation. *Eur J Immunol* 2011; **41**: 1203-1217 [PMID: 21523780 DOI: 10.1002/eji.201141550]
62 **van de Veerdonk FL**, Netea MG. New Insights in the Immunobiology of IL-1 Family Members. *Front Immunol* 2013; **4**: 167 [PMID: 23847614 DOI: 10.3389/fimmu.2013.00167]
63 **Mao L**, Kitani A, Strober W, Fuss IJ. The Role of NLRP3 and IL-1β in the Pathogenesis of Inflammatory Bowel Disease. *Front Immunol* 2018; **9**: 2566 [PMID: 30455704 DOI: 10.3389/fimmu.2018.02566]
64 **Kanneganti TD**, Lamkanfi M, Núñez G. Intracellular NOD-like receptors in host defense and disease. *Immunity* 2007; **27**: 549-559 [PMID: 17967410 DOI: 10.1016/j.immuni.2007.10.002]
65 **Palomo J**, Dietrich D, Martin P, Palmer G, Gabay C. The interleukin (IL)-1 cytokine family--Balance between agonists and antagonists in inflammatory diseases. *Cytokine* 2015; **76**: 25-37 [PMID: 26185894 DOI: 10.1016/j.cyto.2015.06.017]
66 **Siegmund B**. Interleukin-18 in intestinal inflammation: Friend and foe? *Immunity* 2010; **32**: 300-302 [PMID: 20346770 DOI: 10.1016/j.immuni.2010.03.010]
67 **Nakanishi K**, Yoshimoto T, Tsutsui H, Okamura H. Interleukin-18 regulates both Th1 and Th2 responses. *Annu Rev Immunol* 2001; **19**: 423-474 [PMID: 11244043 DOI: 10.1146/annurev.immunol.19.1.423]
68 **Maerten P**, Shen C, Colpaert S, Liu Z, Bullens DA, van Assche G, Penninckx F, Geboes K, Vanham G, Rutgeerts P, Ceuppens JL. Involvement of interleukin 18 in Crohn's disease: Evidence from in vitro analysis of human gut inflammatory cells and from experimental colitis models. *Clin Exp Immunol* 2004; **135**: 310-317 [PMID: 14738461 DOI: 10.1111/j.1365-2249.2004.02362.x]
69 **Harrison OJ**, Srinivasan N, Pott J, Schiering C, Krausgruber T, Ilott NE, Maloy KJ. Epithelial-derived IL-18 regulates Th17 cell differentiation and Foxp3 Treg cell function in the intestine. *Mucosal Immunol* 2015; **8**: 1226-1236 [PMID: 25736457 DOI: 10.1038/mi.2015.13]

World Journal of Gastroenterology

Submit a Manuscript: https://www.f6publishing.com

World J Gastroenterol 2019 September 7; 25(33): 4805-4813

DOI: 10.3748/wjg.v25.i33.4805

ISSN 1007-9327 (print) ISSN 2219-2840 (online)

OPINION REVIEW

Gastroesophageal reflux disease, obesity and laparoscopic sleeve gastrectomy: The burning questions

Halim Bou Daher, Ala I Sharara

ORCID number: Halim Bou Daher (0000-0001-8565-705X); Ala I Sharara (0000-0003-0248-9527).

Author contributions: Sharara AI conceived the idea for the manuscript; Bou Daher H and Sharara AI reviewed the literature and drafted the manuscript.

Conflict-of-interest statement: The authors declare no conflict of interests.

Manuscript source: Invited manuscript

Received: February 27, 2019
Peer-review started: February 27, 2019
First decision: April 30, 2019
Revised: August 3, 2019
Accepted: August 19, 2019
Article in press: August 19, 2019
Published online: September 7, 2019

P-Reviewer: Liu F
S-Editor: Yan JP

Halim Bou Daher, Ala I Sharara, Division of Gastroenterology, Department of Internal Medicine, American University of Beirut Medical Center, Beirut 1107 2020, Lebanon

Corresponding author: Ala I Sharara, AGAF, FACG, FRCP, MD, Professor, Division of Gastroenterology, Department of Internal Medicine, American University of Beirut Medical Center, Cairo Street, P.O. Box 11-0236/16-B, Beirut 1107 2020, Lebanon.
ala.sharara@aub.edu.lb
Telephone: +961-1-3500005351

Abstract

Obesity is a global health epidemic with considerable economic burden. Surgical solutions have become increasingly popular following technical advances leading to sustained efficacy and reduced risk. Sleeve gastrectomy accounts for almost half of all bariatric surgeries worldwide but concerns regarding its relationship with gastroesophageal reflux disease (GERD) has been a topic of debate. GERD, including erosive esophagitis, is highly prevalent in the obese population. The role of pre-operative endoscopy in bariatric surgery has been controversial. Two schools of thought exist on the matter, one that believes routine upper endoscopy before bariatric surgery is not warranted in the absence of symptoms and another that believes that symptoms are poor predictors of underlying esophageal pathology. This debate is particularly important considering the evidence for the association of laparoscopic sleeve gastrectomy (LSG) with *de novo* and/or worsening GERD compared to the less popular Roux-en-Y gastric bypass procedure. In this paper, we try to address 3 burning questions regarding the inter-relationship of obesity, GERD, and LSG: (1) What is the prevalence of GERD and erosive esophagitis in obese patients considered for bariatric surgery? (2) Is it necessary to perform an upper endoscopy in obese patients considered for bariatric surgery? And (3) What are the long-term effects of sleeve gastrectomy on GERD and should LSG be done in patients with pre-existing GERD?

Key words: Reflux; Erosive; Acid; Bariatric; Obesity; Gastric bypass; Endoscopy

Core tip: The convenience and ease of sleeve gastrectomy comes at a risk of *de novo* or worsening of pre-existing gastroesophageal reflux disease. Candidates for bariatric surgery should have a thorough evaluation of reflux symptoms as well as esophageal anatomy and pathology. This should be followed by an informed and open discussion with the patient about risks and benefits of different bariatric surgical options leading to

L-Editor: A
E-Editor: Ma YJ

optimal shared decision making.

Citation: Bou Daher H, Sharara AI. Gastroesophageal reflux disease, obesity and laparoscopic sleeve gastrectomy: The burning questions. *World J Gastroenterol* 2019; 25(33): 4805-4813
URL: https://www.wjgnet.com/1007-9327/full/v25/i33/4805.htm
DOI: https://dx.doi.org/10.3748/wjg.v25.i33.4805

INTRODUCTION

Obesity is a modern-day global epidemic with significant health and economic burden. According to the World Health Organization, 650 million adults (13% of all adults) and over 340 million children and adolescents are overweight or obese[1]. In light of the oft-disappointing long-term results of medical and behavioral interventions, an increasingly larger number of obese patients are turning to minimally invasive bariatric surgery. According to the American Society for Metabolic and Bariatric Surgery, approximately 216000 individuals underwent bariatric surgery in 2016 in the United States, a net increase of 36.7% over a five-year period starting in 2011[2]. Laparoscopic sleeve gastrectomy (LSG) is currently the most popular procedure accounting for more than 50% to 60% of bariatric surgeries worldwide[2,3]. Two recent large randomized trials have confirmed that there is no significant difference in excess weight loss between LSG and laparoscopic Roux-en-Y gastric bypass (RYGB) at 5 years of follow-up[4,5]. However, enthusiasm for this relatively simple procedure has been curtailed by concerns of post-operative gastroesophageal reflux disease (GERD), as a result of either persistent or *de novo* reflux[2]. This remains an issue of significant controversy and active debate in clinical practice. At the Fifth International Consensus Conference on LSG, 52.5% of general surgeons and 23.3% of bariatric experts considered GERD a contraindication to LSG[6]. This article will address 3 burning questions concerning the inter-relationship between obesity, GERD, and LSG.

WHAT IS THE PREVALENCE OF GERD AND EROSIVE ESOPHAGITIS IN OBESE PATIENTS CONSIDERED FOR BARIATRIC SURGERY?

Obesity is an important risk factor for GERD and is associated with esophageal complications such as erosive esophagitis (EE), Barrett's esophagus, and esophageal adenocarcinoma[7,8]. GERD has been reported in as many as 62.4% to 73% of bariatric surgery candidates[9,10]. The pathophysiological mechanisms predisposing to GERD in obesity include increased intra-abdominal pressure[11], impaired gastric emptying[12], decreased lower esophageal sphincter (LES) pressure, and higher frequency of transient LES relaxation[13,14]. In addition, a higher prevalence of hiatal hernia has been described in obese individuals[15]. Central obesity, rather than body mass index (BMI), is more closely associated with GERD[7,16]. High-resolution manometry suggests that both intragastric pressure and gastroesophageal pressure gradient correlate primarily with waist circumference[10].

Overweight and obesity (especially abdominal visceral obesity) are also risk factors for EE. EE is associated with higher distal acid exposure time (percentage time with pH < 4) and higher percentage of reflux episodes reaching the proximal esophagus[17]. El-Serag *et al*[7] showed that patients with a BMI > 30 are 2.5 times more likely to have reflux symptoms and EE than those with a normal BMI. A meta-analysis of 6 studies showed that the adjusted risk ratio for EE was 1.76 in patients with BMI > 25 compared to those with BMI < 25[18]. Prospective endoscopic studies in bariatric surgery candidates have documented a high prevalence of EE in obese individuals ranging from 4.2% to 33.9% (Table 1)[9-11,19-25]. Risk factors for EE varied between studies and included increased waist circumference, insulin resistance, and presence of reflux symptoms[11]. It is important to note that the absence of symptoms does not exclude erosive disease. In one study, 12.3% of obese patients with low probability of reflux symptoms (low GERDQ score < 8) had EE[9]. The literature is conclusive on the matter: Obesity is associated with higher prevalence of GERD and erosive esophagitis.

Table 1 Prospective studies on the prevalence of erosive esophagitis in obese patients

Publication	Year	Number of subjects	Prevalence of EE (%)	Comments
Verset *et al*[18]	1997	147	30.6	High incidence of peptic lesions that were mainly asymptomatic
Ortiz *et al*[9]	2006	138	18.8	Sensitivity of heartburn as diagnostic criterion of GERD was 29.3%, with a specificity of 85.7%
				Asymptomatic GER (abnormal esophageal acid exposure and/or EE) more common than symptomatic GER
Csendes *et al*[10]	2007	426	26.3	Out of the 112 EE patients, 77 (68.7%) reported GERD symptoms
Merrouche *et al*[11]	2007	94	6.4	46% of patients had abnormal 24-pH study
Dutta *et al*[19]	2009	101	8.9	6.9% EE in age- and sex-matched non-obese control subjects
Tai *et al*[20]	2010	260	32.3	Increased waist circumference, insulin resistance, and presence of reflux symptoms independent risk factors for EE
Martin-Perez *et al*[21]	2014	88	4.5	Esophageal pH monitoring tests positive in 65% of patients
				Absence of symptoms did not rule out abnormal esophageal function tests
Carabotti *et al*[24]	2015	142	4.2	Majority of endoscopic lesions were asymptomatic
Mora *et al*[23]	2016	196	17.3	Esophageal pH-metry abnormal in 54.2% of patients
				Symptoms not enough to diagnose underlying GERD or EE
Sharara *et al*[24]	2019	242	33.9	Anthropometric data and GERD questionnaires have limited accuracy for EE
				12.3% of patients with low GERDQ (< 8) had EE

GERD: Gastroesophageal reflux disease; EE: Erosive esophagitis.

IS IT NECESSARY TO DO AN UPPER ENDOSCOPY IN OBESE PATIENTS CONSIDERED FOR BARIATRIC SURGERY?

Clinical practice guidelines published in 2013 by the American Association of Clinical Endocrinologists, The Obesity Society, and American Society for Metabolic and Bariatric Surgery recommend preoperative endoscopy only when clinically indicated[26]. This is in line with the Society of American Gastrointestinal and Endoscopic Surgeons (SAGES) 2008 guidelines and the 2014 interdisciplinary European guidelines endorsed by the International Federation for the Surgery of Obesity and Metabolic Disorders-European Chapter and European Association for the Study of Obesity[27]. On the other hand, the 2015 ASGE guidelines recommend that the decision be individualized[28] while the European Association of Endoscopic Surgeons advises that all patients be evaluated by either endoscopy or upper gastrointestinal series prior to their bariatric surgery[29]. In short, the jury is still out on the matter and a consensus between international and national societies seems unlikely. In a recent series of 1555 patients, asymptomatic patients with significant findings on endoscopy

did not require a change in management or surgery[30]. The authors went on to conclude that routine upper endoscopy requires further justifications for asymptomatic patients. On the other hand, several recent studies emphasized the importance of doing an upper endoscopy preoperatively[23-25]. Carabotti *et al*[24] showed that the incidence of endoscopic lesions was the same between patients who reported symptoms and those who did not; the study also concluded that with the current adopted approach to preoperative endoscopy, 87% of EE cases would have been missed. In our experience, we had similar outcomes when we administered the GERD-Q and the Nocturnal GERD Symptom Severity and Impact Questionnaire (N-GSSIQ) to more than 240 consecutive unselected patients scheduled for bariatric surgery. These validated scores were poorly predictive of endoscopically-proven EE in these patients, even when combined with clinical assessment as part of a composite score[9]. As mentioned earlier, the absence of symptoms does not rule out the presence of GERD[9,23]. A recent survey conducted in the United Kingdom showed that 90% of bariatric units perform preoperative upper endoscopy either routinely or selectively[31]. However, there is also no clear consensus on the indications amongst those who do it selectively. This is particularly important in patients considered for LSG given the evidence linking it to worsening GERD and PPI dependence[32-34]. The reason so much debate surrounds the issue is because significant GERD plays a major role in the choice of the bariatric procedure and the presence of per-operative reflux symptoms appears to be associated with post-operative GERD[35]. In the absence of proper randomized trials and dedicated large long-term follow-up studies, the impact of baseline GERD as well as its post-operative risk should be thoroughly discussed with the patient to help guide the choice of the bariatric procedure. We recommend routine upper endoscopy for all patients scheduled to undergo bariatric surgery to assist with this shared decision process.

WHAT ARE THE LONG-TERM EFFECTS OF SLEEVE GASTRECTOMY ON GERD? AND SHOULD LSG BE DONE IN PATIENTS WITH PRE-EXISTING GERD?

Several short-term (less than 2 years) follow-up studies have looked at the effect of sleeve gastrectomy on GERD. Some have shown improvement of GERD symptoms after LSG[36-40] while others reported worsening and *de novo* GERD[41-45]. Few studies have objectively evaluated the presence of pathologic reflux by 24-h multichannel intraluminal impedance pH monitoring at ≥ 12 mo after LSG reporting conflicting results[46-50]. A systematic review and meta-analysis was inconclusive reporting "high heterogeneity among available studies and paradoxical outcomes of objective esophageal function tests"[32]. Recently, two large randomized controlled trials were published comparing the 5-year follow-up outcome of LSG and RYGB[4,5]. The SM-BOSS trial reported 5-year postoperative GERD remission in 25% in the LSG group compared to 60.4% in RYGB (P = 0.002) with *de novo* GERD in 31.6% of LSG patients compared to 10.7% in RYGB patients (P = 0.01). The study also reported that 9% of LSG patients had to undergo conversion to RYGB because of GERD (highest reason for conversion in the study population). The SLEEVEPASS trial reported RYGB conversion in 6% due to reflux (the study excluded patients with "severe gastroesophageal reflux with a large hiatal hernia"). These figures are consistent with previous literature that showed a 5%-10% conversion rate from LSG to RYGB due to GERD[35,51]. A systematic review published in 2016 demonstrated that 8 out of 10 studies showed new onset GERD at long-term follow up after LSG with a range of 10% to 23%[52]. A prospective study by Genco *et al*. of 110 LSG patients followed over a mean of 58 months showed that the incidence of GERD symptoms, EE and PPI intake increased significantly post-operatively. Upward migration of the GEJ Z-line was found in 73.6% of cases on follow-up endoscopy. What was most alarming in this study was the fact that non-dysplastic Barrett's esophagus was newly diagnosed in 17.2% of patients. This finding has been duplicated in another recent small multicenter study from Italy[53].

The lines of evidence supporting that LSG is a refluxogenic procedure are multiple and include the observation of increased intragastric pressure and impedance reflux episodes on high-resolution impedance manometry after LSG[54], significant increase in non-acidic reflux with stasis and acidification in esophagus, and the higher rate of *de novo* reflux in cohort studies and in randomized controlled studies compared to RYGB. In a rat model, LSG was independently associated with histopathologic changes of severe esophagitis compared to high-fat diet fed and to sham-operated rats[55]. The putative pathophysiological mechanisms underlying GERD after LSG are summarized in Table 2[49,56-62]. They include a hypotensive LES, loss of angle of His flap

valve, increased gastroesophageal pressure gradient with intra-thoracic migration of the remnant stomach, reduction in the compliance of the gastric remnant provoking an increase in transient LES relaxations, relative gastric stasis in the proximal remnant and increased emptying from the antrum, stasis and acidification in the esophagus, as well as higher intragastric pressure and increased impedance reflux episodes. Figure 1 showcases some of the endoscopic and radiologic findings of GERD post LSG.

Given the evidence for long-term GERD burden post LSG, the 2015 joint statement by the ASMBS, SAGES and ASGE considered EE as a relative contraindication to the surgery[28]. A recent prospective study showed that the presence of pre-operative GERD symptoms and EE at baseline were independently associated with a higher need of postoperative PPI use at 6 mo after LSG[34]. The totality of the evidence suggests that LSG is associated with an increased incidence of GERD. While some obese patients with mild non-erosive reflux disease may benefit from LSG with resolution of GERD symptoms after weight loss, those with severe reflux and erosive disease appear to have a high probability of persistent GERD. The opportunity to save such patients from persistent gastroesophageal reflux, PPI dependence, and possible revisional surgery should be seized and the available evidence openly discussed with the patient.

CONCLUSION

The popularity of sleeve gastrectomy derives mainly from its relative ease, safety and efficacy. The "Achilles heel" of this procedure appears to be gastroesophageal reflux and its complications. This is an issue of concern particularly for patients with pre-existing GERD or EE. As physicians, we have a duty not to cause harm. We believe that a thorough evaluation of reflux symptoms as well as esophageal anatomy and pathology should be systematically undertaken in all patients considered for bariatric surgery. This should be followed by an informed and open discussion with the patient about risks and benefits of different bariatric surgical options leading to optimal shared decision making.

Table 2 Putative pathophysiological mechanisms of gastroesophageal reflux disease post laparoscopic sleeve gastrectomy

Hypotensive lower esophageal sphincter[48]
Loss of angle of His flap valve[55]
Increased gastro-esophageal pressure gradient and intra-thoracic migration of the remnant stomach[56]
Reduction in the compliance of the gastric remnant provoking an increase in transient lower esophageal sphincter relaxations[57]
Lack of gastric compliance and emptying during the first postoperative year[58]
Relative gastric stasis in the proximal remnant and increased emptying from the antrum (suggested on time-resolved MRI studies)[59]
Excessively large or dilated sleeve retaining increased acid production capacity leading to reflux[60]
Overly narrowed or strictured sleeve resulting in reflux and decreased esophageal acid clearance[61]

MRI: Magnetic resonance imaging.

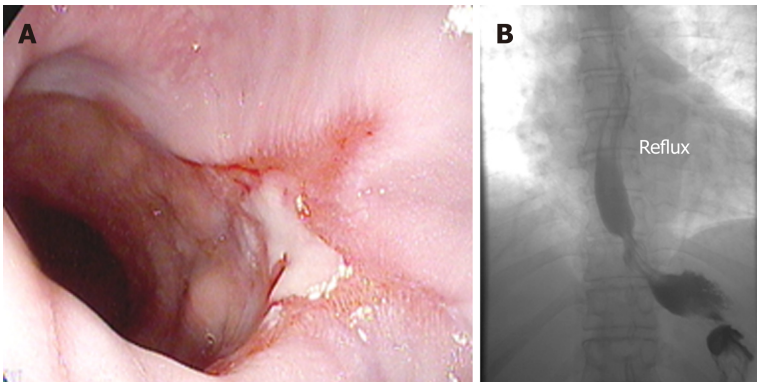

Figure 1 Erosive esophagitis and gastroesophageal reflux. A: Erosive esophagitis in a patient with *de novo* reflux symptoms post laparoscopic sleeve gastrectomy; B: Barium upper gastrointestinal series demonstrating gastroesophageal reflux in a patient post laparoscopic sleeve gastrectomy.

REFERENCES

1 **World Health Organization**. Obesity and overweight. Fact Sheets. 2018; Available from: https://www.who.int/news-room/fact-sheets/detail/obesity-and-overweight
2 **English WJ**, DeMaria EJ, Brethauer SA, Mattar SG, Rosenthal RJ, Morton JM. American Society for Metabolic and Bariatric Surgery estimation of metabolic and bariatric procedures performed in the United States in 2016. *Surg Obes Relat Dis* 2018; **14**: 259-263 [PMID: 29370995 DOI: 10.1016/j.soard.2017.12.013]
3 **Angrisani L**, Santonicola A, Iovino P, Vitiello A, Zundel N, Buchwald H, Scopinaro N. Bariatric Surgery and Endoluminal Procedures: IFSO Worldwide Survey 2014. *Obes Surg* 2017; **27**: 2279-2289 [PMID: 28405878 DOI: 10.1007/s11695-017-2666-x]
4 **Peterli R**, Wölnerhanssen BK, Peters T, Vetter D, Kröll D, Borbély Y, Schultes B, Beglinger C, Drewe J, Schiesser M, Nett P, Bueter M. Effect of Laparoscopic Sleeve Gastrectomy vs Laparoscopic Roux-en-Y Gastric Bypass on Weight Loss in Patients With Morbid Obesity: The SM-BOSS Randomized Clinical Trial. *JAMA* 2018; **319**: 255-265 [PMID: 29340679 DOI: 10.1001/jama.2017.20897]
5 **Salminen P**, Helmiö M, Ovaska J, Juuti A, Leivonen M, Peromaa-Haavisto P, Hurme S, Soinio M, Nuutila P, Victorzon M. Effect of Laparoscopic Sleeve Gastrectomy vs Laparoscopic Roux-en-Y Gastric Bypass on Weight Loss at 5 Years Among Patients With Morbid Obesity: The SLEEVEPASS Randomized Clinical Trial. *JAMA* 2018; **319**: 241-254 [PMID: 29340676 DOI: 10.1001/jama.2017.20313]
6 **Gagner M**, Hutchinson C, Rosenthal R. Fifth International Consensus Conference: Current status of sleeve gastrectomy. *Surg Obes Relat Dis* 2016; **12**: 750-756 [PMID: 27178618 DOI: 10.1016/j.soard.2016.01.022]
7 **El-Serag HB**, Graham DY, Satia JA, Rabeneck L. Obesity is an independent risk factor for GERD symptoms and erosive esophagitis. *Am J Gastroenterol* 2005; **100**: 1243-1250 [PMID: 15929752 DOI: 10.1111/j.1572-0241.2005.41703.x]
8 **El-Serag HB**. Obesity and disease of the esophagus and colon. *Gastroenterol Clin North Am* 2005; **34**: 63-82 [PMID: 15823439 DOI: 10.1016/j.gtc.2004.12.006]
9 **Sharara AI**, Rustom LBO, Bou Daher H, Rimmani HH, Shayto RH, Minhem M, Ichkhanian Y, Aridi H, Al-Abbas A, Shaib Y, Alami R, Safadi B. Prevalence of gastroesophageal reflux and risk factors for erosive esophagitis in obese patients considered for bariatric surgery. *Dig Liver Dis* 2019; **pii**: S1590-8658(19)30550-X [PMID: 31076325 DOI: 10.1016/j.dld.2019.04.010]
10 **Merrouche M**, Sabaté JM, Jouet P, Harnois F, Scaringi S, Coffin B, Msika S. Gastro-esophageal reflux and esophageal motility disorders in morbidly obese patients before and after bariatric surgery. *Obes Surg* 2007; **17**: 894-900 [PMID: 17894148 DOI: 10.1007/s11695-007-9166-3]
11 **Tai CM**, Lee YC, Tu HP, Huang CK, Wu MT, Chang CY, Lee CT, Wu MS, Lin JT, Wang WM. The relationship between visceral adiposity and the risk of erosive esophagitis in severely obese Chinese patients. *Obesity (Silver Spring)* 2010; **18**: 2165-2169 [PMID: 20559298 DOI: 10.1038/oby.2010.143]
12 **Pandolfino JE**, Kwiatek MA, Kahrilas PJ. The pathophysiologic basis for epidemiologic trends in

gastroesophageal reflux disease. *Gastroenterol Clin North Am* 2008; **37**: 827-843, viii [PMID: 19028320 DOI: 10.1016/j.gtc.2008.09.009]
13 **El-Serag HB**, Tran T, Richardson P, Ergun G. Anthropometric correlates of intragastric pressure. *Scand J Gastroenterol* 2006; **41**: 887-891 [PMID: 16803686 DOI: 10.1080/00365520500535402]
14 **El-Serag HB**, Ergun GA, Pandolfino J, Fitzgerald S, Tran T, Kramer JR. Obesity increases oesophageal acid exposure. *Gut* 2007; **56**: 749-755 [PMID: 17127706 DOI: 10.1136/gut.2006.100263]
15 **Wilson LJ**, Ma W, Hirschowitz BI. Association of obesity with hiatal hernia and esophagitis. *Am J Gastroenterol* 1999; **94**: 2840-2844 [PMID: 10520831 DOI: 10.1111/j.1572-0241.1999.01426.x]
16 **Ze EY**, Kim BJ, Kang H, Kim JG. Abdominal Visceral to Subcutaneous Adipose Tissue Ratio Is Associated with Increased Risk of Erosive Esophagitis. *Dig Dis Sci* 2017; **62**: 1265-1271 [PMID: 28281164 DOI: 10.1007/s10620-017-4467-4]
17 **Savarino E**, Tutuian R, Zentilin P, Dulbecco P, Pohl D, Marabotto E, Parodi A, Sammito G, Gemignani L, Bodini G, Savarino V. Characteristics of reflux episodes and symptom association in patients with erosive esophagitis and nonerosive reflux disease: Study using combined impedance-pH off therapy. *Am J Gastroenterol* 2010; **105**: 1053-1061 [PMID: 19997095 DOI: 10.1038/ajg.2009.670]
18 **Hampel H**, Abraham NS, El-Serag HB. Meta-analysis: Obesity and the risk for gastroesophageal reflux disease and its complications. *Ann Intern Med* 2005; **143**: 199-211 [PMID: 16061918 DOI: 10.7326/0003-4819-143-3-200508020-00006]
19 **Ortiz V**, Ponce M, Fernández A, Martínez B, Ponce JL, Garrigues V, Ponce J. Value of heartburn for diagnosing gastroesophageal reflux disease in severely obese patients. *Obesity (Silver Spring)* 2006; **14**: 696-700 [PMID: 16741272 DOI: 10.1038/oby.2006.79]
20 **Csendes A**, Burgos AM, Smok G, Beltran M. Endoscopic and histologic findings of the foregut in 426 patients with morbid obesity. *Obes Surg* 2007; **17**: 28-34 [PMID: 17355765 DOI: 10.1007/s11695-007-9002-9]
21 **Verset D**, Houben JJ, Gay F, Elcheroth J, Bourgeois V, Van Gossum A. The place of upper gastrointestinal tract endoscopy before and after vertical banded gastroplasty for morbid obesity. *Dig Dis Sci* 1997; **42**: 2333-2337 [PMID: 9398814 DOI: 10.1023/A:1018835205458]
22 **Dutta SK**, Arora M, Kireet A, Bashandy H, Gandsas A. Upper gastrointestinal symptoms and associated disorders in morbidly obese patients: A prospective study. *Dig Dis Sci* 2009; **54**: 1243-1246 [PMID: 18975090 DOI: 10.1007/s10620-008-0485-6]
23 **Martín-Pérez J**, Arteaga-González I, Martín-Malagón A, Díaz-Luis H, Casanova-Trujillo C, Carrillo-Pallarés A A. Frequency of abnormal esophageal acid exposure in patients eligible for bariatric surgery. *Surg Obes Relat Dis* 2014; **10**: 1176-1180 [PMID: 25443048 DOI: 10.1016/j.soard.2014.04.011]
24 **Carabotti M**, Avallone M, Cereatti F, Paganini A, Greco F, Scirocco A, Severi C, Silecchia G. Usefulness of Upper Gastrointestinal Symptoms as a Driver to Prescribe Gastroscopy in Obese Patients Candidate to Bariatric Surgery. A Prospective Study. *Obes Surg* 2016; **26**: 1075-1080 [PMID: 26328530 DOI: 10.1007/s11695-015-1861-x]
25 **Mora F**, Cassinello N, Mora M, Bosca M, Minguez M, Ortega J. Esophageal abnormalities in morbidly obese adult patients. *Surg Obes Relat Dis* 2016; **12**: 622-628 [PMID: 26686303 DOI: 10.1016/j.soard.2015.08.002]
26 **Mechanick JI**, Youdim A, Jones DB, Timothy Garvey W, Hurley DL, Molly McMahon M, Heinberg LJ, Kushner R, Adams TD, Shikora S, Dixon JB, Brethauer S. Clinical practice guidelines for the perioperative nutritional, metabolic, and nonsurgical support of the bariatric surgery patient--2013 update: Cosponsored by American Association of Clinical Endocrinologists, the Obesity Society, and American Society for Metabolic & Bariatric Surgery. *Surg Obes Relat Dis* 2013; **9**: 159-191 [PMID: 23537696 DOI: 10.1016/j.soard.2012.12.010]
27 **Fried M**, Yumuk V, Oppert JM, Scopinaro N, Torres A, Weiner R, Yashkov Y, Frühbeck G; International Federation for Surgery of Obesity and Metabolic Disorders-European Chapter (IFSO-EC); European Association for the Study of Obesity (EASO); European Association for the Study of Obesity Obesity Management Task Force (EASO OMTF). Interdisciplinary European guidelines on metabolic and bariatric surgery. *Obes Surg* 2014; **24**: 42-55 [PMID: 24081459 DOI: 10.1007/s11695-013-1079-8]
28 **Evans JA**, Muthusamy VR, Acosta RD, Bruining DH, Chandrasekhara V, Chathadi KV, Eloubeidi MA, Fanelli RD, Faulx AL, Fonkalsrud L, Khashab MA, Lightdale JR, Pasha SF, Saltzman JR, Shaukat A, Wang A, Stefanidis D, Richardson WS, Khothari SN, Cash BD; ASGE Standards of Practice Committee. The role of endoscopy in the bariatric surgery patient. *Surg Obes Relat Dis* 2015; **11**: 507-517 [PMID: 26093766 DOI: 10.1016/j.soard.2015.02.015]
29 **Sauerland S**, Angrisani L, Belachew M, Chevallier JM, Favretti F, Finer N, Fingerhut A, Garcia Caballero M, Guisado Macias JA, Mittermair R, Morino M, Msika S, Rubino F, Tacchino R, Weiner R, Neugebauer EA; European Association for Endoscopic Surgery. Obesity surgery: Evidence-based guidelines of the European Association for Endoscopic Surgery (EAES). *Surg Endosc* 2005; **19**: 200-221 [PMID: 15580436 DOI: 10.1007/s00464-004-9194-1]
30 **Salama A**, Saafan T, El Ansari W, Karam M, Bashah M. Is Routine Preoperative Esophagogastroduodenoscopy Screening Necessary Prior to Laparoscopic Sleeve Gastrectomy? Review of 1555 Cases and Comparison with Current Literature. *Obes Surg* 2018; **28**: 52-60 [PMID: 28685362 DOI: 10.1007/s11695-017-2813-4]
31 **Zanotti D**, Elkalaawy M, Hashemi M, Jenkinson A, Adamo M. Current Status of Preoperative Oesophago-Gastro-Duodenoscopy (OGD) in Bariatric NHS Units-a BOMSS Survey. *Obes Surg* 2016; **26**: 2257-2262 [PMID: 27424002 DOI: 10.1007/s11695-016-2304-z]
32 **Oor JE**, Roks DJ, Ünlü Ç, Hazebroek EJ. Laparoscopic sleeve gastrectomy and gastroesophageal reflux disease: A systematic review and meta-analysis. *Am J Surg* 2016; **211**: 250-267 [PMID: 26341463 DOI: 10.1016/j.amjsurg.2015.05.031]
33 **Felsenreich DM**, Kefurt R, Schermann M, Beckerhinn P, Kristo I, Krebs M, Prager G, Langer FB. Reflux, Sleeve Dilation, and Barrett's Esophagus after Laparoscopic Sleeve Gastrectomy: Long-Term Follow-Up. *Obes Surg* 2017; **27**: 3092-3101 [PMID: 28593484 DOI: 10.1007/s11695-017-2748-9]
34 **Sharara AI**, Rimmani HH, Al Abbas AI, Safadi B, Shayto RH, Aridi H, Shaib Y, R. Erosive esophagitis is prevalent and Predictable by pre-operative gerdq questionnaire in Obese individuals and is associated with the need for Continued ppi use after laparoscopic sleeve Gastrectomy. UEG Week 2017 Oral Presentations. *United Eur Gastroent* 2017; **5**: A1-A160 [DOI: 10.1177/2050640617725668]
35 **Madhok BM**, Carr WR, McCormack C, Boyle M, Jennings N, Schroeder N, Balupuri S, Small PK. Preoperative endoscopy may reduce the need for revisional surgery for gastro-oesophageal reflux disease following laparoscopic sleeve gastrectomy. *Clin Obes* 2016; **6**: 268-272 [PMID: 27400631 DOI:

10.1111/cob.12153]
36 **Cottam D**, Qureshi FG, Mattar SG, Sharma S, Holover S, Bonanomi G, Ramanathan R, Schauer P. Laparoscopic sleeve gastrectomy as an initial weight-loss procedure for high-risk patients with morbid obesity. *Surg Endosc* 2006; **20**: 859-863 [PMID: 16738970 DOI: 10.1007/s00464-005-0134-5]
37 **Moon Han S**, Kim WW, Oh JH. Results of laparoscopic sleeve gastrectomy (LSG) at 1 year in morbidly obese Korean patients. *Obes Surg* 2005; **15**: 1469-1475 [PMID: 16354529 DOI: 10.1381/096089205774859227]
38 **Melissas J**, Koukouraki S, Askoxylakis J, Stathaki M, Daskalakis M, Perisinakis K, Karkavitsas N. Sleeve gastrectomy: A restrictive procedure? *Obes Surg* 2007; **17**: 57-62 [PMID: 17355769 DOI: 10.1007/s11695-007-9006-5]
39 **Melissas J**, Daskalakis M, Koukouraki S, Askoxylakis I, Metaxari M, Dimitriadis E, Stathaki M, Papadakis JA. Sleeve gastrectomy-a "food limiting" operation. *Obes Surg* 2008; **18**: 1251-1256 [PMID: 18663545 DOI: 10.1007/s11695-008-9634-4]
40 **Gibson SC**, Le Page PA, Taylor CJ. Laparoscopic sleeve gastrectomy: Review of 500 cases in single surgeon Australian practice. *ANZ J Surg* 2015; **85**: 673-677 [PMID: 24354405 DOI: 10.1111/ans.12483]
41 **DuPree CE**, Blair K, Steele SR, Martin MJ. Laparoscopic sleeve gastrectomy in patients with preexisting gastroesophageal reflux disease: A national analysis. *JAMA Surg* 2014; **149**: 328-334 [PMID: 24500799 DOI: 10.1001/jamasurg.2013.4323]
42 **Sheppard CE**, Sadowski DC, de Gara CJ, Karmali S, Birch DW. Rates of reflux before and after laparoscopic sleeve gastrectomy for severe obesity. *Obes Surg* 2015; **25**: 763-768 [PMID: 25411120 DOI: 10.1007/s11695-014-1480-y]
43 **Carter PR**, LeBlanc KA, Hausmann MG, Kleinpeter KP, deBarros SN, Jones SM. Association between gastroesophageal reflux disease and laparoscopic sleeve gastrectomy. *Surg Obes Relat Dis* 2011; **7**: 569-572 [PMID: 21429818 DOI: 10.1016/j.soard.2011.01.040]
44 **Tai CM**, Huang CK, Lee YC, Chang CY, Lee CT, Lin JT. Increase in gastroesophageal reflux disease symptoms and erosive esophagitis 1 year after laparoscopic sleeve gastrectomy among obese adults. *Surg Endosc* 2013; **27**: 1260-1266 [PMID: 23232995 DOI: 10.1007/s00464-012-2593-9]
45 **Howard DD**, Caban AM, Cendan JC, Ben-David K. Gastroesophageal reflux after sleeve gastrectomy in morbidly obese patients. *Surg Obes Relat Dis* 2011; **7**: 709-713 [PMID: 21955743 DOI: 10.1016/j.soard.2011.08.003]
46 **Rebecchi F**, Allaix ME, Giaccone C, Ugliono E, Scozzari G, Morino M. Gastroesophageal reflux disease and laparoscopic sleeve gastrectomy: A physiopathologic evaluation. *Ann Surg* 2014; **260**: 909-914; discussion 914-915 [PMID: 25379861 DOI: 10.1097/SLA.0000000000000967]
47 **Rebecchi F**, Allaix ME, Patti MG, Schlottmann F, Morino M. Gastroesophageal reflux disease and morbid obesity: To sleeve or not to sleeve? *World J Gastroenterol* 2017; **23**: 2269-2275 [PMID: 28428706 DOI: 10.3748/wjg.v23.i13.2269]
48 **Del Genio G**, Tolone S, Limongelli P, Brusciano L, D'Alessandro A, Docimo G, Rossetti G, Silecchia G, Iannelli A, del Genio A, del Genio F, Docimo L. Sleeve gastrectomy and development of "*de novo*" gastroesophageal reflux. *Obes Surg* 2014; **24**: 71-77 [PMID: 24249251 DOI: 10.1007/s11695-013-1046-4]
49 **Gorodner V**, Buxhoeveden R, Clemente G, Solé L, Caro L, Grigaites A. Does laparoscopic sleeve gastrectomy have any influence on gastroesophageal reflux disease? Preliminary results. *Surg Endosc* 2015; **29**: 1760-1768 [PMID: 25303918 DOI: 10.1007/s00464-014-3902-2]
50 **Georgia D**, Stamatina T, Maria N, Konstantinos A, Konstantinos F, Emmanouil L, Georgios Z, Dimitrios T. 24-h Multichannel Intraluminal Impedance PH-metry 1 Year After Laparocopic Sleeve Gastrectomy: An Objective Assessment of Gastroesophageal Reflux Disease. *Obes Surg* 2017; **27**: 749-753 [PMID: 27592124 DOI: 10.1007/s11695-016-2359-x]
51 **Langer FB**, Bohdjalian A, Shakeri-Leidenmühler S, Schoppmann SF, Zacherl J, Prager G. Conversion from sleeve gastrectomy to Roux-en-Y gastric bypass--indications and outcome. *Obes Surg* 2010; **20**: 835-840 [PMID: 20393810 DOI: 10.1007/s11695-010-0125-z]
52 **Juodeikis Ž**, Brimas G. Long-term results after sleeve gastrectomy: A systematic review. *Surg Obes Relat Dis* 2017; **13**: 693-699 [PMID: 27876332 DOI: 10.1016/j.soard.2016.10.006]
53 **Sebastianelli L**, Benois M, Vanbiervliet G, Bailly L, Robert M, Turrin N, Gizard E, Foletto M, Bisello M, Albanese A, Santonicola A, Iovino P, Piche T, Angrisani L, Turchi L, Schiavo L, Iannelli A. Systematic Endoscopy 5 Years After Sleeve Gastrectomy Results in a High Rate of Barrett's Esophagus: Results of a Multicenter Study. *Obes Surg* 2019; **29**: 1462-1469 [PMID: 30666544 DOI: 10.1007/s11695-019-03704-y]
54 **Mion F**, Tolone S, Garros A, Savarino E, Pelascini E, Robert M, Poncet G, Valette PJ, Marjoux S, Docimo L, Roman S. High-resolution Impedance Manometry after Sleeve Gastrectomy: Increased Intragastric Pressure and Reflux are Frequent Events. *Obes Surg* 2016; **26**: 2449-2456 [PMID: 26956879 DOI: 10.1007/s11695-016-2127-y]
55 **Altieri MS**, Shroyer KR, Pryor A, Pagnotti GM, Ete Chan M, Talamini M, Telem DA. The association between sleeve gastrectomy and histopathologic changes consistent with esophagitis in a rodent model. *Surg Obes Relat Dis* 2015; **11**: 1289-1294 [PMID: 26048523 DOI: 10.1016/j.soard.2015.01.012]
56 **Klaus A**, Weiss H. Is preoperative manometry in restrictive bariatric procedures necessary? *Obes Surg* 2008; **18**: 1039-1042 [PMID: 18386106 DOI: 10.1007/s11695-007-9399-1]
57 **Lazoura O**, Zacharoulis D, Triantafyllidis G, Fanariotis M, Sioka E, Papamargaritis D, Tzovaras G. Symptoms of gastroesophageal reflux following laparoscopic sleeve gastrectomy are related to the final shape of the sleeve as depicted by radiology. *Obes Surg* 2011; **21**: 295-299 [PMID: 21165778 DOI: 10.1007/s11695-010-0339-0]
58 **Hayat JO**, Wan A. The effects of sleeve gastectomy on gastro-esophageal reflux and gastro-esophageal motility. *Expert Rev Gastroenterol Hepatol* 2014; **8**: 445-452 [PMID: 24580041 DOI: 10.1586/17474124.2014.888951]
59 **Himpens J**, Dapri G, Cadière GB. A prospective randomized study between laparoscopic gastric banding and laparoscopic isolated sleeve gastrectomy: Results after 1 and 3 years. *Obes Surg* 2006; **16**: 1450-1456 [PMID: 17132410 DOI: 10.1381/096089206778869933]
60 **Baumann T**, Kuesters S, Grueneberger J, Marjanovic G, Zimmermann L, Schaefer AO, Hopt UT, Langer M, Karcz WK. Time-resolved MRI after ingestion of liquids reveals motility changes after laparoscopic sleeve gastrectomy--preliminary results. *Obes Surg* 2011; **21**: 95-101 [PMID: 21088924 DOI: 10.1007/s11695-010-0317-6]
61 **Keidar A**, Appelbaum L, Schweiger C, Elazary R, Baltasar A. Dilated upper sleeve can be associated with severe postoperative gastroesophageal dysmotility and reflux. *Obes Surg* 2010; **20**: 140-147 [PMID:

19949885 DOI: 10.1007/s11695-009-0032-3]
62 **Dapri G**, Cadière GB, Himpens J. Laparoscopic seromyotomy for long stenosis after sleeve gastrectomy with or without duodenal switch. *Obes Surg* 2009; **19**: 495-499 [PMID: 19169764 DOI: 10.1007/s11695-009-9803-0]

World Journal of Gastroenterology

Submit a Manuscript: https://www.f6publishing.com

World J Gastroenterol 2019 September 7; 25(33): 4814-4834

DOI: 10.3748/wjg.v25.i33.4814

ISSN 1007-9327 (print) ISSN 2219-2840 (online)

REVIEW

Intestinal permeability in the pathogenesis of liver damage: From non-alcoholic fatty liver disease to liver transplantation

Alberto Nicoletti, Francesca Romana Ponziani, Marco Biolato, Venanzio Valenza, Giuseppe Marrone, Gabriele Sganga, Antonio Gasbarrini, Luca Miele, Antonio Grieco

ORCID number: Alberto Nicoletti (0000-0003-0658-4310); Francesca Romana Ponziani (0000-0002-5924-6238); Marco Biolato (0000-0002-5172-8208); Venanzio Valenza (0000-0002-0023-6625); Giuseppe Marrone (0000-0002-9475-3948); Gabriele Sganga (0000-0001-5079-0395); Antonio Gasbarrini (0000-0003-4863-6924); Luca Miele (0000-0003-3464-0068); Antonio Grieco (0000-0002-0544-8993).

Author contributions: Grieco A was the guarantor and designed the review. Nicoletti A, Ponziani FR, Biolato M and Marrone G revised literature and wrote the initial manuscript. Nicoletti A conceived and draw the figures. Valenza V, Gasbarrini A, Sganga G and Miele L critically revised the article for important intellectual content.

Conflict-of-interest statement: Nothing to declare.

Alberto Nicoletti, Francesca Romana Ponziani, Marco Biolato, Venanzio Valenza, Giuseppe Marrone, Gabriele Sganga, Antonio Gasbarrini, Luca Miele, Antonio Grieco, Fondazione Policlinico Universitario A Gemelli IRCCS, Rome 00168, Italy

Alberto Nicoletti, Francesca Romana Ponziani, Marco Biolato, Venanzio Valenza, Giuseppe Marrone, Gabriele Sganga, Antonio Gasbarrini, Luca Miele, Antonio Grieco, Università Cattolica del Sacro Cuore, Rome 00168, Italy

Corresponding author: Antonio Grieco, MD, Associate Professor, Chief of Liver Transplant Medicine Unit, Fondazione Policlinico Universitario A. Gemelli IRCCS, Università Cattolica del Sacro Cuore, Roma, Institute of Internal Medicine, Largo Agostino Gemelli No. 8, Rome 00168, Italy. antonio.grieco@unicatt.it
Telephone: +39-6-30155451
Fax: +39-6-35502775

Abstract

The intimate connection and the strict mutual cooperation between the gut and the liver realizes a functional entity called gut-liver axis. The integrity of intestinal barrier is crucial for the maintenance of liver homeostasis. In this mutual relationship, the liver acts as a second firewall towards potentially harmful substances translocated from the gut, and is, in turn, is implicated in the regulation of the barrier. Increasing evidence has highlighted the relevance of increased intestinal permeability and consequent bacterial translocation in the development of liver damage. In particular, in patients with non-alcoholic fatty liver disease recent hypotheses are considering intestinal permeability impairment, diet and gut dysbiosis as the primary pathogenic trigger. In advanced liver disease, intestinal permeability is enhanced by portal hypertension. The clinical consequence is an increased bacterial translocation that further worsens liver damage. Furthermore, this pathogenic mechanism is implicated in most of liver cirrhosis complications, such as spontaneous bacterial peritonitis, hepatorenal syndrome, portal vein thrombosis, hepatic encephalopathy, and hepatocellular carcinoma. After liver transplantation, the decrease in portal pressure should determine beneficial effects on the gut-liver axis, although are incompletely understood data on the modifications of the intestinal permeability and gut microbiota composition are still lacking. How the modulation of the intestinal permeability could prevent the initiation and progression of liver disease is still an uncovered area, which deserves further attention.

Manuscript source: Invited manuscript

Received: May 21, 2019
Peer-review started: May 21, 2019
First decision: June 9, 2019
Revised: July 4, 2019
Accepted: July 19, 2019
Article in press: July 19, 2019
Published online: September 7, 2019

P-Reviewer: Hilmi I, Hori T, Kohla MAS, Pop TL
S-Editor: Ma RY
L-Editor: A
E-Editor: Ma YJ

Key words: Bacterial translocation; Gut microbiota; Gut-liver axis; Liver disease; Cirrhosis; Mediterranean diet; Personalized medicine

Core tip: The integrity of the gut-liver axis is crucial for the maintenance of the homestasis of the organism. The disruption of the intestinal barrier and consequent increased intestinal permeability has been recently associated with the development of liver damage. This review summarizes present evidence on the relevance of the derangement of the gut-liver axis in the pathogenesis of liver damage and non-alcoholic fatty liver disease, the development of the complications of liver cirrhosis and its modifications after liver transplantation.

Citation: Nicoletti A, Ponziani FR, Biolato M, Valenza V, Marrone G, Sganga G, Gasbarrini A, Miele L, Grieco A. Intestinal permeability in the pathogenesis of liver damage: From non-alcoholic fatty liver disease to liver transplantation. *World J Gastroenterol* 2019; 25(33): 4814-4834
URL: https://www.wjgnet.com/1007-9327/full/v25/i33/4814.htm
DOI: https://dx.doi.org/10.3748/wjg.v25.i33.4814

INTRODUCTION

The gut is one of the largest mucosal surfaces of the human body. Besides being involved in the absorption of nutrients and water introduced with ingested food, it acts as a barrier that guarantees protection against pathogenic microorganisms and potentially harmful substances, such as toxins and pollutants[1]. In addition, the interaction that occurs between the gut microbiota and immunological cells at this level is crucial for the development and maintenance of the immune system[2,3].

The gut and the liver are anatomically connected by portal circulation, and their functional unit realizes the gut-liver axis[4]. Thus, any type of substance that goes beyond the gut barrier can reach the liver where is processed into metabolic pathways or interacts with the immune system cells or resident cells.

Liver disease affects gut homeostasis, altering intestinal permeability (IP) and the gut microbiota composition, proportionally to the degree of liver function impairment. Indeed, once portal hypertension (PHT) is established, the intestinal barrier functions are altered, causing the passage of substances that are normally kept in the intestinal lumen[5]. In particular, the translocation of bacterial fragments or products into the bloodstream activates the immune system, stimulating inflammation. This process not only could further worsen liver function, but it is implicated in a series of chain reactions involving the whole organism, realizing a systemic inflammatory condition typical of advanced liver cirrhosis[5].

PHYSIOLOGICAL GUT BARRIER

Normally, the gut constitutes a complex physical, chemical, functional and immunological barrier. In order to perform its tasks, different components are necessary[1,6]. Proceeding from the lumen inwards, they can be classified into the following levels: The microbiota, the extracellular elements, the epithelial cells, the immune system, the vascular structure (Figure 1).

The microbial barrier

The human gut microbiota harbors one hundred trillions of microorganisms, about ten times the number of eukaryotic cells. It has about ten times the genes of the human genome and has a mass of about 1-2 kg[7].

Several factors, such as birth mode, age, diet and lifestyle, influence the human gut microbiota. In physiological conditions, its compositional and functional armony is quite stable over time. However, the onset of disease and/or the use of certain drugs (*e.g.*, antibiotics) can break this balance, resulting in dysbiosis with significant consequences on human homeostasis. Indeed, the gut microbiota integrates the metabolism of the organism providing crucial pathways to process nutrients, vitamins

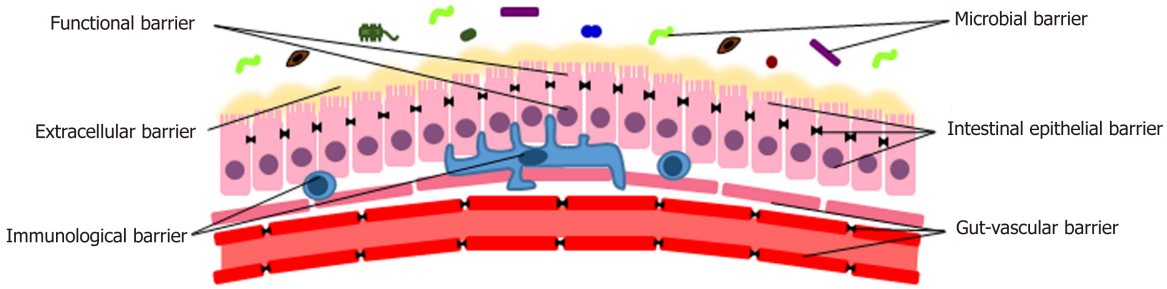

Figure 1 Physiological gut barrier.

and endogenous substances[8]. Microorganisms host in the lumen interact with the intestinal mucosa, shaping the mucus[9], exerting a trophic and protective function towards enterocytes. Moreover, it plays a pivotal role in the development, maturation and maintenance of the immune system[10-15] and induces local production of antimicrobial peptides and immunoglobulins[8,12].

Extracellular barrier

Intestinal mucus is a gel formed by glycosylated proteins secreted by intestinal goblet cells called mucins[16]. It covers the whole gut and its thickness depends on the location, being almost absent in the stomach and maximum in the colon[17]. Mucus prevents harmful substances and bacteria from directly contacting cell surface, causing inflammation[18-20]. Thus, a proper structure of mucins is crucial for the maintenance of the gut barrier, and alterations could facilitate the absorption of harmful substances, leading to inflammation[20]. Indeed, quantitative or qualitative alterations of the mucus layer has been documented in several diseases, such as cystic fibrosis[21] and inflammatory bowel disease (IBD)[22]. In addition, it has been demonstrated in mice models that a high MUC2 mucin production increases the susceptibility of goblet cells to apoptosis and endoplasmic reticulum stress[23]. An increased mucus thickness has been related to alcohol intake and cirrhosis[24]. Conversely, an incorrect assembly of MUC2 inside the epithelial cells leads to the development of an inflammatory disease resembling ulcerative colitis in mice[23,25]. This process may be responsible of the depletion of goblet cells documented in IBD[16].

The inner side of the intestinal mucus is made of a fluid, which is not reached by the mixing forces of the luminal flow and peristalsis, called unstirred layer. The inner face of the mucin layer is devoid of bacteria[18] and directly contacts the intestinal epithelial cells, modulating the absorption of water and nutrients due to its static nature. A thicker unstirred layer has been observed in patients with coeliac disease and has been related to malabsorption[26].

Functional barrier

To make the picture more complex, it has to be considered that this system is dynamic and subject to regulation by gastrointestinal motility and secretions. The outer part of the mucus layer is continuously moved forward by peristalsis. The luminal flow prevents the proliferations of microorganism and a prompt clearance of detrimental elements. This is crucial in the protection against pathogens[1,27]. Gastric acid decreases microbial colonization of the small intestine. Only acid resistant microorganism, such as *Helicobacter pylori* and Lactobacilli are able to survive at low pH[28]. Bile acids, the main constituents of bile, have direct antimicrobial properties interfering with membrane and protein production and integrity[29-32]. Thus, alterations of the bile and gastric fluid and impairment of the peristalsis cause both qualitative and quantitative modifications of the gut microbiota composition up to the derangement of intestinal homeostasis and the development of pathology[28,33].

Intestinal epithelial barrier

Underneath the intestinal mucus, there is a continuous monocellular layer of enterocytes. Goblet cells, responsible for the production of the mucus, and Paneth cells, which produce antimicrobial peptides, provide additional functions and support to the homeostasis of the gut barrier. Enterocytes plasma membrane represents the main mechanical element of the mucosal barrier. Because of its lipidic structure, it is impermeable to most solutes that need a specific transporter to cross the barrier (transcellular pathway)[1]. In order to limit the gut permeability, intercellular spaces are sealed by the presence of a specific apical junctional complex, which is composed by a tight junction (TJ) and an adherens junction. Overall, over 40 proteins form a TJ,

being claudins, peripheral membrane proteins, such as zonula occludens (ZO) 1 and 2, and occludin the main components[34,35]. Both tight and adherens junctions are connected to the cytoskeleton[36]. TJ are important elements for both active and passive transport through the gut barrier[37]. They regulate the passive flow of the solutes and water through the paracellular pathway, operating both as a size- and charge-selective filter[38]. The passive movement of substances across TJ occurs through two different routes: The leak pathway, that allows the transport of larger substances (*e.g.*, proteins, bacterial components), and a second pathway mediated by claudin proteins, that is charge selective and limits the flow to molecules smaller than 4 Å[1,38-40].

As for active transport, an intact intestinal epithelial barrier, formed by TJ and the plasma membrane of intestinal cell, realizes a gradient between the lumen and the inner interstice. This condition prevents an uncontrolled translocation of substances and allows an active transcellular transport through the enterocytes[1]. Moreover, the complex system of TJ is finely regulated by the influence of cytokines, particularly tumor necrosis factor-alfa (TNFα)[41] and interferon gamma (IFNγ)[42], and by signaling kinases and cytoskeleton, like myosin light chain kinases (MLCK)[43,44]. Both qualitative and quantitative alterations of TJ have been described in the context of liver disease[45,46]. Finally, intestinal cells own another defensive element. In fact, apical brush border microvilli are negatively charged, owing to the presence of polar carbohydrates and charged transmembrane proteins, and cause an electrostatic repulsive force towards bacterial cell wall, that is negatively charged as well[47].

Immunological barrier

In response to the exposure to bacteria and to their components, Paneth cells produce antimicrobial peptides, such as defensins, cathelicidines, resistin-like molecules, bactericidial-permeability-inducing proteins and lectins, and immunoglobulins, particularly secretory IgA[5]. These elements are secreted into the gut lumen and are host in the inner face of the mucin layer hosts[48]. Whenever microbial and pathogen-associated molecular patterns cross the intestinal barrier, they are identified through the interaction between pattern-recognition receptors, such as Toll-like receptors (TLRs) and nucleotide binding oligomerization domain-like receptors on the intestinal epithelial cells. Then, recruited dendritic cells are responsible for the transport of the captured antigens to the mesenteric lymph nodes (MLNs) for antigen presentation. This mechanism allows the priming and maturation of B and T lymphocytes, that become part of the adaptive immune response in the gut associated lymphoid tissue[49-51]. Hence, immune response is compartmentalized in mucosal lymphatics in healthy individuals.

Gut-vascular barrier

Since 2015, the knowledge about barrier mechanisms for the modulation of IP stopped to the basocellular membrane of the enterocytes. Recent studies have successively revealed that the intestinal defense mechanisms actually go further, and also include a gut-vascular barrier[52]. Observing functional similarities between blood-brain barrier and intestinal barrier, Spadoni *et al*[52,53] hypothesized that a parallel structure in the gut could be responsible for the prevention of the translocation of bacteria and/or microbial components passed through the extracellular and the intestinal epithelial barrier.

The fundamental structure of this entity is the gut-vascular unit. It is composed by the intestinal endothelium, which is anatomically and functionally associated with pericytes and enteric glial cells that surround it. The barrier is completed by TJ and adherens junctions, which are permeable to most of the small nutrients. Endothelial plasma membrane provides isolation and is equipped with active and passive transporters[53,54]. Glial cells play an important role in the homeostasis of the gut and in the regulation of IP[52,53]. In fact, in murine models, it has been demonstrated that either genetical or autoimmune targeting of glial cells determines the development of fulminant enteritis with increased translocation of microbes and evidence of bacteremia[55,56]. When the endothelium is intact, it allows the free diffusion of 4 kD dextran, whereas 70 kD dextran is blocked. Infection with *Salmonella enterica* serovar Typhimurium disrupts the gut-vascular barrier, allowing the translocation of larger substances, and this happens independently of the increase in the blood flow provoked by inflammation[52,53]. Furthermore, 70 kD dextran was only found in the liver and not in the spleen, demonstrating that dissemination occurs through the portal circulation rather than the lymphatic vessels. The increase in plasmalemma vesicle-associated protein-1 (PV1), a marker of endothelial permeability, during Salmonella infection confirms this evidence. Finally, the authors demonstrated that bacteria with the ability to cross the intestinal epithelial barrier do not disseminate to liver and spleen, blocked by a second barrier[52]. These experiments definitively prove the existence of a gut-vascular barrier.

ALTERED GUT BARRIER, INTESTINAL PERMEABILITY AND BACTERIAL TRANSLOCATION IN THE PATHOGENESIS OF LIVER DAMAGE

In liver diseases, increased IP is the consequence of multiple disorders that affect the homeostasis of the barrier. Several studies in animal models and in human pathology correlated liver damage and dysfunction to alterations of the gut microbiota composition[57], mucus quality and quantity[24], gastrointestinal motility[33], intestinal epithelial barrier and TJ[45], and the immune system[58].

Nevertheless, bacterial translocation (BT) is a physiological process that consists in the passage of small amounts of microorganisms and their constituents from the intestinal lumen to the MLNs[5]. At this site, microbial killing occurs without systemic inflammatory response[59,60]. This process is crucial for the modulation of the immune system and the development of immune tolerance[2,3]. Despite the fact that the liver is usually devoid of bacteria[61], in healthy individuals it is physiologically exposed to trace amounts of bacterial mRNAs and lipopolysaccharide (LPS)[4,62,63], mainly acting as a firewall detoxifying bacterial components[61,64]. In healthy mice, it has been demonstrated that the liver can act as a second firewall for microorganisms penetrated after mucosal damage and escaped from MLNs surveillance activity[4,61,64]. This function is supposed to be mainly exerted by the hepatic sinusoids, where Kupffer cells - representing over the 80% of all tissue macrophages - are able to phagocytize and kill microbes derived from the bloodstream[4,61,65-67]. Several experiments have demonstrated the importance of liver resident macrophages in the clearance of microorganisms and microbial- and pathogen- associated molecular patterns (MAMPs and PAMPs). In fact, ^{3}H- and ^{14}C-labelled endotoxin purified from *E. coli* is actively processed by Kupffer cells[68]. Similarly, lipopolysaccharide binding protein (LBP), an acute-phase protein synthesized in the liver and secreted after interleukin-1 (IL-1), interleukin-6 (IL-6), and glucocorticoids stimulation, after binding with LPS mediates the activation of liver mononuclear cells in a way that is dependent on the presence of functional Toll-like receptor 4 (TLR4)[69,70]. CD14, either expressed on myeloid cells (mCD14) or the isoform secreted into the bloodstream by monocytes and hepatocytes (sCD14), acts as a co-receptor of TLR4 binding the LPS-LBP complex and allowing its uptake by liver resident myeloid cells[71-73]. Moreover, an elegant imaging-based study by Lee *et al*[65] documented the ability of Kupffer cells to perform filtration of blood, phagocytosis and killing of green fluorescent protein expressing *B. burgdorferii* and antigen presentation to natural killer (NK) cells. Finally, in Kupffer cells depleted mice, the clearance of *E. coli* K-12 during bacteremia is delayed[61].

Yet, the "liver buffer" is exhaustible too. The disruption of the intestinal barrier at any level leads to an increase inIP (Figure 2). Thus, harmful substances, such as MAMPs and PAMPs (LPS, microbial DNA, peptidoglycans and lipopeptides), metabolic products, and whole bacteria massively reach local MLNs, that are unable to provide an adequate clearance[74-77]. Hence, a variable amount of detrimental products is delivered to the liver through the mesenteric and portal circulation[4]. The maintenance of a damaging insult triggers a systemic inflammatory response, developing from the liver[78-81]. Kupffer cells play a pivotal role in orchestrating this mechanism[67,80,82-84]. Indeed, the interaction between pathogen-associated molecular patterns and TLRs activate intracellular molecular pathways, either MyD88-dependent or MyD88-independent, resulting in the activation of NF-κB and the expression of inflammatory cytokines (TNF-α, IL-1β, IL-6, IL-12, IL-18), chemokines (CXCL1, CXCL2, CCL2, CCL5, CCL3, CCL4), vasoactive factors [nitric oxide (NO)] and reactive oxygen species (ROS)[85]. This local inflammatory storm leads to the recruitment of systemic leukocytes, such as neutrophils, $CD4^{+}$ T cells and monocytes, that perpetuate liver inflammation[80,82]. Net result of this process is the induction of hepatocyte apoptosis and necrosis[86]. Both inflammatory cytokines and cell death cause the activation and proliferation of hepatic stellate cells (HSC) and the development of fibrosis under the stimulation of transforming growth factor-β (TGFβ)[84,87].

As a consequence of inflammatory cytokines, HSCs and several other liver cells upregulate the expression of matrix metalloproteinases (MMPs). The overexpression and hyperactivation of MMPs result in the destruction of the hepatic tissue[88,89].

Tissue inhibitors of matrix metalloproteinases (TIMPs) are the main modulators of the activity of MMPs. While a decrease in the levels of TIMPs have been associated with liver damage in acute liver injury, an increase in their expression in chronic liver diseases favor the accumulation of collagen and liver fibrogenesis, by inhibiting degradation of collagen[88-91]. Furthermore, as proof of the relevance of these enzymes in the pathogenesis of liver damage, TIMP-1 has been identified as a predictive marker for the presence of non-alcoholic steatohepatitis (NASH)[92]

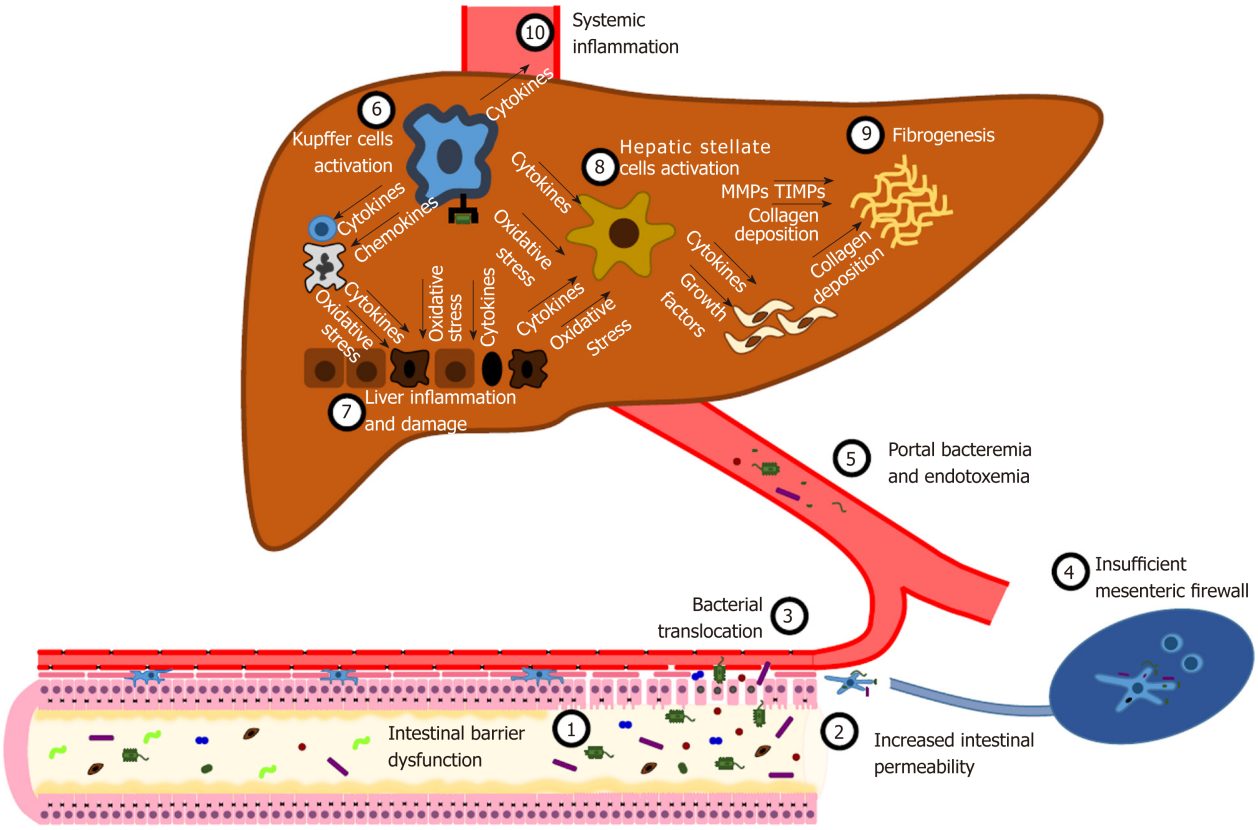

Figure 2 Intestinal permeability in the pathogenesis of liver damage. Several disorders, such as gut dysbiosis and primary and secondary intestinal diseases, can cause increased intestinal permeability. Consequently, viable bacteria and microbial- associated molecular patterns cross the intestinal epithelial barrier, a process known as bacterial translocation. An efficient immunological barrier limits this process, promoting a local immune response in activated mesenteric lymph nodes. When this primary firewall fails, microbes and microbial compounds reach the liver, where they activate Kupffer cells by binding Toll-like receptors. Kupffer cells orchestrate several processes, such as the release of inflammatory cytokines and reactive oxygen species, the recruitment of innate immune cells, the activation of hepatic stellate cells. The uncontrolled perpetuation of this pathogenic mechanism results in liver inflammation and damage, fibrogenesis and systemic inflammation. See text for further details.

Oxidative stress plays a critical role in the development of liver damage[93]. The production of reactive oxygen species is a physiological consequence of aerobic life. Hence, organisms have developed antioxidant mechanisms in order to face the harmful effects of these agents. The detrimental effect of these species depends on the balance with antioxidant elements[94].

When this equilibrium is deranged, ROS can negatively affect both sides of the gut-liver axis. On the one hand, oxidative stress is responsible for intestinal barrier damage. Indeed, diet[95], alcohol[96], infectious[97] and primary inflammatory diseases[98], and drugs[99] are able to cause an imbalance in the redox state in the gut, resulting in increased IP. Furthermore, in advanced liver diseases PHT causes hypoperfusion of the intestinal mucosa. Subsequent hypoxia enhances the activity of xanthine oxidase, resulting in increased ROS release and oxidative damage[100]. On the other hand, the liver is an important scavenger of free radicals, since it plays a crucial role in the restoration of endogenous antioxidants and metabolism of exogenous ones[101,102]. A significant increase in the level of oxidative stress has been observed in all chronic liver diseases, irrespective of the etiology of the liver disorder. Moreover, all the liver cells are sensitive to oxidative stress-related molecules[93,103,104]. The activation of TLR causes the generation of ROS by Kupffer cells[105]. ROS signaling causes the activation and proliferation of HSC[106]. Conversely, as a consequence to the exposure to ROS, Kupffer cells produce cytokines and chemokines, which further stimulate HSCs[104].

Nevertheless, there are some protective mechanisms. IL-10 mediates remarkable protective effects towards the intestinal mucosa and liver. At the intestinal level, the release of IL-10 by macrophages modulates innate immune activation, preventing an excessive response and consequent tissue damage[107]. Hence, adequate IL-10 levels improve the integrity of the gut barrier, resulting in a decrease in endotoxin absorption[108]. In the liver, IL-10 reduces liver inflammations and fibrosis, inhibiting several Kupffer cells functions[109,110].

Similarly, NK cells regulate fibrogenetic mechanisms in the liver. Indeed, NK cells

perform immunosurveillance activity by killing early activated and senescent HSCs, thus limiting fibrogenesis[111,112]. Interestingly, TIMP-1-expressing HSCs are resistant to NK cells activity[113].

Coeliac disease is the hallmark of the pathogenic mechanism linking increased IP and liver inflammation[45]. Liver damage is a common disorder associated with coeliac disease[114-119]. In a recent meta-analysis, the prevalence of cryptogenic hypertransaminasaemia in newly diagnosed coeliac disease is 27%[120]. In coeliac patients, increased permeability has been proved as well[121]. Although the pathogenesis is poorly understood, the theory that liver involvement could be secondary to increased IP and BT is widely accepted[114,115,118]. Bardella *et al*[115] reported a normalization of transaminases levels in about 90% of patients with increased levels at the time of coeliac disease diagnosis after six months of gluten free diet (GFD). In the remaining 10% other possible causes of liver damage were proven by liver biopsy. Another study demonstrated a significant correlation between serum transaminases levels and IP, assessed with lactulose/mannitol test. The authors found similar response to GFD (64/72 patients, 88.9%) and reported that IP index significantly decreased in conjunction with the normalization of serum transaminases levels within one year of diet. Conversely, in patients who were not compliant with GFD, liver injury persisted and permeability tests remained altered[122]. Furthermore, histological alterations in the liver of patients with newly diagnosed coeliac disease and transaminases elevation suggest that increased IP could be responsible for liver damage in this setting. As reported by Jacobsen *et al*[119], among 37 liver biopsies performed in coeliac patients, 25 showed non-specific patterns, 7 were diagnostic for other diseases, 5 were classified as normal. Liver histological features of the 25 non-specific specimens documented an increased number of Kupffer cells (52.0%), expanded portal tracts (48.0%) and parenchymal or portal mononuclear infiltration (36% and 20% respectively). Interestingly, some of these alterations are comparable to those observed in other experiments reproducing liver damage in context of increased IP[123]. Thus, these results are consistent with the hypothesis that IP *per se* could trigger the development of liver damage.

Also in the setting of primary liver disease, increasing evidence is linking IP to liver damage. Occludin deficient ($Ocln^{-/-}$) mice do not show intestinal TJ alteration[124], but ethanol feeding induces a decrease in E-cadherin and β-catenin distribution, which are other proteins involved in the maintenance of TJ integrity, causing gut barrier dysfunction[125]. Although both ethanol fed $Ocln^{-/-}$ and wild type mice had increased plasma transaminase levels, liver damage was worse in occludin deficient mice, and histopathological examination of the liver confirmed the presence of inflammatory lesions only in $Ocln^{-/-}$ mice[125]. As for human studies, Cariello *et al*[126] demonstrated that plasma levels of inflammatory cytokines (TNF-α and IL-6) are higher in patients with both liver disease and increased IP compared to those with normal IP. A positive correlation between altered IP and liver inflammation and fibrosis was observed in a population of children with non-alcoholic fatty liver disease (NAFLD)[127]. Finally, a recent meta-analysis showed that patients with NAFLD, particularly those with increased liver injury markers, more frequently exhibit altered IP[128]. Altogether, these data suggest a pathogenic mechanism that determines liver damage through the alteration of the gut barrier.

GUT-LIVER AXIS: ROLE IN THE PATHOGENESIS OF NAFLD

The pathogenesis of liver damage in patients with NAFLD is still incompletely understood. However, a growing body of experimental and clinical data suggests a primary role of the gut-liver axis dysfunction. Traditionally, a "double-hit" pathogenetic model has been hypothesized for NAFLD development. Lipid accumulation into the liver (steatosis) represents the first step. Then, a second insult is needed to cause liver injury and inflammation[129,130]. The discovery of a linkage between small intestinal bacterial overgrowth (SIBO) and NAFLD[131-133] and the observation that endotoxin triggers liver inflammation in mice with steatosis[134] brought to the formulation of this hypothesis[130]. Several experiments in animal and human models confirmed the influence of increased IP both in the development of liver steatosis and in the pathogenesis of liver inflammation and fibrosis.

Brun *et al*[62] reported gut barrier dysfunction, tested as higher epithelial permeability to horseradish peroxidase in obese mice, both genetically deficient in leptin (C57BL/6Job/ob) and functionally deficient for the long-form leptin receptor (C57BL/6Jdb/db). Immunochemistry and Western blot confirmed important alterations of TJ proteins (ZO-1 and Occludin) distribution in obese mice. Hence, endotoxin in portal circulation and levels of circulating proinflammatory cytokines

(IL-1, IL-6, INF-γ, and TNF-α) were significantly higher both in ob/ob and in db/db mice compared to controls. Interestingly, HSC isolated from obese mice showed enhanced sensitivity to LPS and produced higher levels of cytokines.

Junctional adhesion molecule A (JAM-A) is a constituent of the TJ encoded by the murine gene *F11r*. It modulates the epithelial barrier function, regulating IP and inflammation[135-138]. F11r$^{-/-}$ mice, fed a diet high in saturated fat, fructose and cholesterol (HFCD) for 8 weeks, developed a severe steatohepatitis, assessed by the presence of histological features of liver inflammation (hepatocyte ballooning and inflammatory cells infiltration) and fibrogenesis and increase in serum transaminases compared to controls[123].

In a recent study, male C57BL/6 mice were fed with dextran sulfate sodium (DSS), a chemical compound able to determine gut inflammation, and a high-fat diet (HFD) for 12 wk. Fat vacuoles and leukocyte infiltration in the liver were higher in DSS and HFD-fed mice compared to HFD-fed mice. Concordantly, levels of hepatic mRNA coding for inflammatory cytokines (IL-1, IL-6, TNF-α, MCP-1) were increased as well. Moreover, DSS + HFD showed higher expression of collagen I and profibrogenic factors mRNA (TGF-β, Actin α2, tissue inhibitor of metalloproteinase-1 and plasminogen activator inhibitor-1). Although there were no significant differences in the levels of serum endotoxin, an upregulation of TLR4 and TLR 9 was observed in DSS HFD mice. Finally, the downregulation of ZO-1 and Claudin-1 and the increased expression of PV1 confirmed both the intestinal and gut-vascular barrier dysfunction after DSS treatment[139].

As for human models, the first strong evidence of increased IP in NAFLD patients emerged from a study testing the intestinal absorption and urine excretion of orally administered ^{51}Cr-EDTA[45]. Indeed, ^{51}Cr-EDTA is normally not metabolized and poorly absorbed (1%-3%) from the gastrointestinal tract and it crosses the intestinal barrier through the paracellular pathway in the presence of TJ disruption[27,140,141]. ^{51}Cr-EDTA excretion levels were significantly higher than values of healthy volunteers in a fashion that resulted proportional to the degree of liver steatosis. Furthermore, duodenal histology showed reduced ZO-1 expression in patients with NAFLD. In this population of patients, the prevalence of SIBO was about three times compared to controls, an observation that confirmed findings of previous studies[142]. However, increased IP was not associated with the severity of liver inflammation, fibrosis and the presence of NASH[45]. Similarly, in children with NALFD liver damage has been linked to alterations of the gut barrier. The ratio between urinary excretion of lactulose and mannitol (L/M ratio) after oral administration was used to measure the degree of IP[27,127,143]. L/M ratio was significantly higher in NAFLD children and further increased in NASH patients. In order to ascertain the presence of BT, serum LPS was quantified and resulted significantly higher in children with confirmed liver damage. Interestingly, the extent of hepatic inflammation and fibrosis was proportional to the degree of IP[127]. The association between SIBO and NAFLD and the finding of increased endotoxemia across the studies underlines the role of the gut microbiota in the initiation and development of metabolic liver disease[45,127,142,144]. Once increased IP is established, dysbiosis affects liver homeostasis through different mechanisms. Gut microorganisms directly cause liver damage either by means of MAMPs and PAMPs (*e.g.*, LPS) or by products of their metabolism (*e.g.*, ethanol, short-chain fatty acids (SCFAs) and trimethylamine)[145].

Proteobacteria, particularly *Enterobacteriaceae*, can ferment carbohydrates to ethanol[146]. In the presence of adequate conditions, the amount produced can be remarkable[147]; indeed, a significant correlation between ethanol-producing bacteria abundance, blood ethanol concentration and liver inflammation has been demonstrated[146]. Besides causing direct toxic effects to the liver, this overproduction determine the activation of hepatic ethanol metabolic pathways and increases liver oxidative stress[148]. These evidences have confirmed the relevance of endogenous ethanol production in the pathogenesis of NASH.

Acetic, propionic and butyric acid are the main SCFAs produced by the gut microbiota in physiological conditions as a result of carbohydrates fermentation[149]. Following the intestinal absorption, SCFAs reach the liver through the portal circulation, where they serve as energy source and exert a relevant role in lipogenesis and gluconeogenesis[145,150,151]. Interacting with Gprotein coupled receptors GPR41 and GPR43 of intestinal enteroendocrine L cells, SCFAs stimulate the release of the peptide YY (PYY), a hormone able to slow gastric emptying and intestinal transit and favor energy absorption[152]. Another important consequence is the release of glucagon-like peptide-1, which enhances glucose-dependent insulin release[153]. Altogether, these effects may favor the development of NAFLD and NASH[145].

Furthermore, the intestinal microbiota inhibits the production and secretion of fasting-induced adipocyte factor (FIAF) by the intestinal L cells and the enterocytes. FIAF is an inhibitor of lipoprotein lipase (LPL), which determines, when suppressed,

the activation of LPL and the increase in triglyceride accumulation in the liver and the adipocytes[154]. Hence, increased hepatic lipid storage activates the carbohydrate-responsive element-binding protein and the sterol regulatory element-binding protein 1, perpetuating fat accumulation[155].

Finally, choline is implicated in the synthesis of very-low density lipoprotein (VLDL). Hence, choline deficiency cause a decrease in the production and release of VLDL and triglyceride accumulation in the liver[156]. Bacteria of the taxa *Erysipelotrichia* are able to metabolize choline to methylamines, toxic compounds that have been correlated to liver damage[157,158]. In NAFLD patients, augmented intestinal metabolism of choline, choline deficiency and abundance of *Erysipelotrichia* taxa have been observed[157].

Recent studies reported qualitative alterations of the gut microbiota composition in patients with NAFLD. Particularly, *Bacteroides* genus is correlated with NASH and a parallel decrease in *Prevotella* abundance was found[159,160]. In fact, diet enriched in fat, proteins of animal origin and simple sugars, like Western one, promotes *Bacteroides* abundance, whilst an increase in *Prevotella* abundance is favored by a diet rich in fibers and vegetal carbohydrates[159,161]. *Ruminococcus* genus has been positively associated with significant liver fibrosis (≥ F2) in humans[159], and a correlation between the abundance of this genus and the development of metabolic impairment has been observed in animal models[162]. Alcohol production, due to the ability of *Ruminococcus* to ferment complex carbohydrates, may be responsible for further liver damage[163]. An increase in *Proteobacteria*/*Enterobacteriaceae*/*Escherichia* abundance has been described in NASH and correlates with serum levels of alcohol[146].

Furthermore, NAFLD-related liver cirrhosis patients showed a low gut microbiota diversity compared to healthy controls. At the genus level, an abundance in *Lactobacillus*, *Bacteroides*, *Ruminococcus*, *Klebsiella*, *Prevotella*, *Enterococcus*, *Haemophilus*, *Pseudomonas*, *Parabacteroides*, *Phascolarctobacterium*, *Veillonella*, *Streptococcus*, *Atopobium*, *Dialister*, *Christensenella*, and decrease in *Methanobrevibacter* and *Akkermansia* was observed[164].

It is well known that di*et al*so is a key regulator of IP[165]. In animal models of NAFLD, adaptation of a high-fat diet or high-fructose intake has been associated with increased gut permeability[166,167]. Elevated concentrations of saturated fat or fructose favors pro-inflammatory microbiota; on one hand, suppressing production of SCFAs that are essential for intestinal barrier function, on the other hand recruiting macrophages and leading to the release of TNF-α and other cytokines causing mucosal inflammation[168,169]. The consequence is a decreased expression of TJ proteins and a higher permeability of the gut barrier[170]. Diet-induced increases in blood LPS levels are known as metabolic endotoxaemia and play an important role in the activation of TLR-mediated low-grade liver inflammation, which are associated with NAFLD and NASH[171]. Current evidence from animal studies suggests that a high-fat diet or a high-fructose diet can induce metabolic endotoxaemia by altering the intestinal TJ proteins, mainly ZO-1 and occluding[62,172-174]. In NAFLD adolescents, postprandial endotoxin levels were increased compared to healthy subjects in response to fructose, but not glucose, beverages (consumed with meals) in a 24-h feeding challenge[175].

There are currently no data concerning diet modulation of IP in patients with NAFLD, and it is plausible that a healthy diet can reduce IP in patients with NAFLD by restoring the integrity of tight junctions. The Mediterranean diet contains a high intake of mono- and polyunsaturated fatty acids, fibres, polyphenols, antioxidants and phytochemicals; many of these components promote short-chain fatty acid-producing gut bacteria and have significant prebiotic effects[176]. As such, Mediterranean diet was an attractive tool for reducing impaired IP in patients with NAFLD. In a cross-over pilot study[177], twenty patients with NAFLD underwent 16 weeks of a Mediterranean diet and 16 weeks of a low-fat diet; although the majority of patients presented at baseline, as expected, high IP evaluated according to 51Cr-EDTA, none of the two diets were sufficient to modulate it. Diet-modulation of IP in humans is much more difficult to obtain than in animal models and further research is needed.

GUT-LIVER AXIS: ROLE IN THE PATHOGENESIS OF CIRRHOSIS

Increased IP and BT are hallmarks of liver cirrhosis[5,27]. As previously described, the contribution of BT to liver damage could be crucial for the progression to liver cirrhosis. On the other hand, the once liver cirrhosis is establishment it further enhances IP. The magnitude of BT is proportional to the stage of the disease[5] and

correlates with prognosis[178].

PHT can reasonably be considered the primary determinant of the onset of altered IP in the setting of advanced liver disease. Indeed, increased splanchnic vasodilation induces a decrease in the blood flow and venous congestion at the intestinal mucosa level, leading to ischemia and edema, up to the disruption of the TJ and epithelial barrier dysfunction[179,180]. Consequently, BT is enhanced and in most cases it becomes clinically relevant, due to the large extent of the mucosa involved in the pathogenic mechanism[181-184]. To confirm of the importance of PHT in the pathogenesis of increased IP, the reduction of hepatic venous pressure gradient by non-selective beta-blocker therapy decreases IP[180].

Endotoxemia further worsens the hemodynamics of cirrhotic patients. In fact, the systemic inflammatory response activated by bacteria and their products/fragments leads to the release of cytokines and the consequent synthesis of (NO) by inducible nitric oxide synthase (iNOS)[185-187]. The result is a decrease in systemic vascular resistance and the secondary development of hyperdynamic circulation[74,75,188] that further worsen IP and BT[189]. In fact, there is evidence that intestinal decontamination improves the hyperdynamic state in liver cirrhosis[190,191].

Furthermore, increased IP and consequent BT are fundamental pathogenic steps in the development of complications of chronic liver disease[74]. In cirrhotic patients, impaired hemodynamics in advanced phases may negatively affect renal function, causing the hepatorenal syndrome (HRS). LPS per se leads to renal vasoconstriction, but it can worsen renal function *via* the increase of plasma levels of endothelin[192-194]. Furthermore, TLR4 may play a role in the pathogenesis of HRS *via* the consequent activation of NF-κB and TNF-α pathways, since it is overexpressed in the kidney during endotoxemia[195]. The importance of this pathogenic mechanism in the development of HRS is highlighted by the fact that in both animal and human studies, intestinal decontamination, achieved either by norfloxacin, paromomycin or rifaximin, showed beneficial effects on renal function[195-197]. Similarly, among the ancillary effects of albumin infusion, the scavenging of LPS is involved in the amelioration of renal hemodynamics[198].

In the first clinical reports of spontaneous bacterial peritonitis (SBP) in the 1960s, a pathogenetic mechanism involving BT from the gastrointestinal tract has already been hypothesized[199-202]. However, clear scientific evidence was only produced in the 1990s. These experiments showed in murine models of liver cirrhosis a high correspondence between the isolation of bacteria from cultures of MLNs and ascites. Positive cultures were obtained from both mice with or without SBP, demonstrating that BT is a frequent event in advanced liver disease[203-205]. Another evidence that elucidates the causal association between intestinal dysbiosis, impaired IP, BT and SBP is the decrease in the incidence of SBP (-72%) in patients with ascites treated with rifaximin[206]. Similar results in SBP primary and secondary prophylaxis have been obtained with norfloxacin[207,208].

In liver cirrhosis, the liver capacity to detoxify ammonia, neurotoxic substances and false neurotransmitters, produced by the gut microbiota from the catabolism of dietary proteins, is insufficient[209,210]. On the other hand, the formation of portosystemic shunts further decrease the part of blood depurated[211]. Thus, entering the bloodstream, these substances are delivered to the brain, where they have detrimental effects, causing edema and altering neurotransmission, causing hepatic encephalopathy (HE)[209,210].

A perturbation in the gut microbiota composition has been linked to the development of HE. In particular, *Alcaligeneceae*, *Porphyromonadaceae*, *Enterobacteriaceae* abundance has been correlated with cognitive impairment and neuroinflammation in cirrhotic patients[212]. Moreover, the systemic inflammatory state resulting from the perpetuation of BT independently affects brain functions and worsens cognitive performance[213-217], and finally, inflammation secondarily extends to the brain, where a self-maintaining process is then established[214,218-220]. Hence, the modulation of the gut microbiota and its metabolism represents the basis for the treatment and prevention of overt HE[221-223].

The pathogenesis of portal vein thrombosis (PVT) is incompletely understood. However, besides reduced portal vein flow velocity and prothrombotic state, BT into portal vein could favor the activation of the coagulative cascade[224,225]. Indeed, it is known that endotoxin is able to increase thrombin generation *via* the increased production of tissue factor (TF)[226]. Similarly, LPS stimulates the release of factor VIII and von Willebrand factor release, in a way that could be mediated by TLR4 activation[227]. Since the liver acts as a firewall towards BT[61], there is a gradient between the concentration of LPS in the portal vein and in the systemic circulation[228]. Hence, this could be a significant pathogenic mechanism for the development of PVT in cirrhotic patients[224,225]. Interestingly, endotoxin-induced prothrombotic state in the portal system can cause microembolism to hepatic sinusoids, contributing to liver

damage and inflammation[229].

Increasing evidence supports the involvement of the gut-liver axis in hepatocarcinogenesis. As aforementioned, intestinal hyperpermeability and consequent BT activate TLRs through the binding with LPS[85]. The subsequent activation of NF-κB signaling initiates the inflammatory cascade that favors carcinogenesis[230,231]. Indeed, in animal models, it has been demonstrated that the infusion of LPS stimulates the development as well as the growth of liver tumors[232,233]. Conversely, the lack of IKK-b, a kinase that frees NF-κB from inhibitory proteins, decreases hepatocarcinogenesis[234]. An inflammatory environment is crucial for the development of hepatocellular carcinoma (HCC). Cytokines modify the micro-enviroment by recruiting innate immune cells and altering the extracellular matrix[231,235]. Moreover, the production of ROS cause direct DNA damage[236] and inflammation stimulate cell turnover and proliferation, favoring the accumulation of DNA mutations[231,235].

Other MAMPs and PAMPs and microbial metabolites have also been proposed as potential carcinogens[237,238]. Hence, recent studies have analyzed the gut microbiota of patients with HCC in order to find a microbial fingerprint of the disease. Ponziani *et al*[164] described the gut microbiota of NAFLD cirrhotic patients with HCC. At the genus level, a significant increased abundance of the *Phascolarctobacterium*, *Enterococcus*, *Streptococcus*, *Gemella*, *Bilophila* genera was observed. In another recent study, the abundance of the *Haemophilus*, *Eggerthella*, *Bifidobacterium*, *Butyricimonas*, *Christensella*, *Odoribacter* genera, an unknown genus from Tenericutes phylum and an unknown genus from Firmicutes phylum was significantly increased by 2-3 fold in the HCC group. Interestingly, the authors found a correlation between changes in the gut microbiota and liver inflammation[239].

Finally, as regards the gut microbiome in liver cirrhosis, a decreased bacterial diversity has been observed compared to healthy controls. At the phylum level, the abundance of *Bacteroidetes* is reduced, whilst *Proteobacteria* and *Fusobacteria* are increased. The increase in the abundance of potentially pathogenic bacteria, such as *Streptococcus*, *Veilonella*, and *Enterobacteriaceae*, may explain the frequent involvement of these bacteria in the pathogenesis of infectious complications in these patients[240,241]. A relocation in the distribution of microorganisms along the gastrointestinal tract has been correlated with the onset of the complications of liver cirrhosis, as well[240]. In particular, a higher abundance of *Streptococcus salivarius* has been correlated with the minimal HE[242]. In parallel, a decrease in the abundance of potentially beneficial *Lachnospiraceae* and *Clostridium* cluster XIVa has been reported[240,241].

GUT-LIVER AXIS AFTER LIVER TRANSPLANTATION

PHT, which is responsible for increased IP in the setting of liver cirrhosis, is reverted by liver transplantation (LT)[243,244]. Accordingly, IP should decrease after LT. In a study analyzing IP 2 to 3 years after LT in patients on immunosuppressant drugs (tacrolimus and cyclosporine), Parrilli *et al*[245] reported an increase in lactulose /rhamnose ratio (Lacl/L-Rh ratio) that was only due to a decrease in L-Rh excretion. The authors concluded that IP was restored, in spite of the effects of antirejection drugs on intestinal barrier function. Moreover, serum endotoxin levels were similar between LT patients and controls. Another study soon after LT in patients receiving tacrolimus therapy showed that IP, assessed with L/R ratio, was elevated compared to healthy controls. Furthermore, about 50% of the patients had increased serum levels of endotoxin[246]. Therefore, IP could still be impaired soon after LT and improve later. However, further studies are needed to analyze the modification of IP in patients with cirrhosis after LT.

Few studies analyzed the alterations of the gut microbiota after LT. In particular, a decrease in *Eubacteria*, *Bifidobacterium spp*, *Fecalibacterium prausnitzii* and *Lactobacillus spp* abundance and a decrease in Enterobacteriaceae and *Enterococcus spp* has been observed[247]. Interestingly, in a recent study microbial diversity did not show significant modification during the first week after LT. Instead, during postoperative days 8 to 14 the influence of surgical operation, antibiotics and antirejection therapy reduced microbial diversity[248]. Afterwards diversity was progressively restored[247,248]. No association was been found between intestinal dysbiosis and acute cellular rejection, post-transplant bloodstream infections and/or the recurrence of liver disease[248,249].

CONCLUSION

Increased IP, BT and alterations of the gut microbiota composition are important pathogenetic elements responsible for the development of liver damage, the initiation of fibrosis changes up to the development of liver cirrhosis and its complications. At present, there are very few evidences of the efficacy of the role of the gut microbiota modulation in the modification of the natural course of liver disease. Further studies are needed to investigate the efficacy of these strategies.

REFERENCES

1 **Turner JR**. Intestinal mucosal barrier function in health and disease. *Nat Rev Immunol* 2009; **9**: 799-809 [PMID: 19855405 DOI: 10.1038/nri2653]
2 **Macpherson AJ**, Harris NL. Interactions between commensal intestinal bacteria and the immune system. *Nat Rev Immunol* 2004; **4**: 478-485 [PMID: 15173836 DOI: 10.1038/nri1373]
3 **Maynard CL**, Elson CO, Hatton RD, Weaver CT. Reciprocal interactions of the intestinal microbiota and immune system. *Nature* 2012; **489**: 231-241 [PMID: 22972296 DOI: 10.1038/nature11551]
4 **Brandl K**, Kumar V, Eckmann L. Gut-liver axis at the frontier of host-microbial interactions. *Am J Physiol Gastrointest Liver Physiol* 2017; **312**: G413-G419 [PMID: 28232456 DOI: 10.1152/ajpgi.00361.2016]
5 **Wiest R**, Lawson M, Geuking M. Pathological bacterial translocation in liver cirrhosis. *J Hepatol* 2014; **60**: 197-209 [PMID: 23993913 DOI: 10.1016/j.jhep.2013.07.044]
6 **Okumura R**, Takeda K. Maintenance of intestinal homeostasis by mucosal barriers. *Inflamm Regen* 2018; **38**: 5 [PMID: 29619131 DOI: 10.1186/s41232-018-0063-z]
7 **Lynch SV**, Pedersen O. The Human Intestinal Microbiome in Health and Disease. *N Engl J Med* 2016; **375**: 2369-2379 [PMID: 27974040 DOI: 10.1056/NEJMra1600266]
8 **Jandhyala SM**, Talukdar R, Subramanyam C, Vuyyuru H, Sasikala M, Nageshwar Reddy D. Role of the normal gut microbiota. *World J Gastroenterol* 2015; **21**: 8787-8803 [PMID: 26269668 DOI: 10.3748/wjg.v21.i29.8787]
9 **Jakobsson HE**, Rodríguez-Piñeiro AM, Schütte A, Ermund A, Boysen P, Bemark M, Sommer F, Bäckhed F, Hansson GC, Johansson ME. The composition of the gut microbiota shapes the colon mucus barrier. *EMBO Rep* 2015; **16**: 164-177 [PMID: 25525071 DOI: 10.15252/embr.201439263]
10 **Hooper LV**, Littman DR, Macpherson AJ. Interactions between the microbiota and the immune system. *Science* 2012; **336**: 1268-1273 [PMID: 22674334 DOI: 10.1126/science.1223490]
11 **Thaiss CA**, Zmora N, Levy M, Elinav E. The microbiome and innate immunity. *Nature* 2016; **535**: 65-74 [PMID: 27383981 DOI: 10.1038/nature18847]
12 **Britanova L**, Diefenbach A. Interplay of innate lymphoid cells and the microbiota. *Immunol Rev* 2017; **279**: 36-51 [PMID: 28856740 DOI: 10.1111/imr.12580]
13 **Belkaid Y**, Hand TW. Role of the microbiota in immunity and inflammation. *Cell* 2014; **157**: 121-141 [PMID: 24679531 DOI: 10.1016/j.cell.2014.03.011]
14 **Rescigno M**. Mucosal immunology and bacterial handling in the intestine. *Best Pract Res Clin Gastroenterol* 2013; **27**: 17-24 [PMID: 23768549 DOI: 10.1016/j.bpg.2013.03.004]
15 **Rescigno M**. Intestinal microbiota and its effects on the immune system. *Cell Microbiol* 2014; **16**: 1004-1013 [PMID: 24720613 DOI: 10.1111/cmi.12301]
16 **Kim YS**, Ho SB. Intestinal goblet cells and mucins in health and disease: recent insights and progress. *Curr Gastroenterol Rep* 2010; **12**: 319-330 [PMID: 20703838 DOI: 10.1007/s11894-010-0131-2]
17 **Pelaseyed T**, Bergström JH, Gustafsson JK, Ermund A, Birchenough GM, Schütte A, van der Post S, Svensson F, Rodríguez-Piñeiro AM, Nyström EE, Wising C, Johansson ME, Hansson GC. The mucus and mucins of the goblet cells and enterocytes provide the first defense line of the gastrointestinal tract and interact with the immune system. *Immunol Rev* 2014; **260**: 8-20 [PMID: 24942678 DOI: 10.1111/imr.12182]
18 **Johansson ME**, Phillipson M, Petersson J, Velcich A, Holm L, Hansson GC. The inner of the two Muc2 mucin-dependent mucus layers in colon is devoid of bacteria. *Proc Natl Acad Sci U S A* 2008; **105**: 15064-15069 [PMID: 18806221 DOI: 10.1073/pnas.0803124105]
19 **Hollingsworth MA**, Swanson BJ. Mucins in cancer: protection and control of the cell surface. *Nat Rev Cancer* 2004; **4**: 45-60 [PMID: 14681689 DOI: 10.1038/nrc1251]
20 **Vereecke L**, Beyaert R, van Loo G. Enterocyte death and intestinal barrier maintenance in homeostasis and disease. *Trends Mol Med* 2011; **17**: 584-593 [PMID: 21741311 DOI: 10.1016/j.molmed.2011.05.011]
21 **Gustafsson JK**, Ermund A, Ambort D, Johansson ME, Nilsson HE, Thorell K, Hebert H, Sjövall H, Hansson GC. Bicarbonate and functional CFTR channel are required for proper mucin secretion and link cystic fibrosis with its mucus phenotype. *J Exp Med* 2012; **209**: 1263-1272 [PMID: 22711878 DOI: 10.1084/jem.20120562]
22 **Schultsz C**, Van Den Berg FM, Ten Kate FW, Tytgat GN, Dankert J. The intestinal mucus layer from patients with inflammatory bowel disease harbors high numbers of bacteria compared with controls. *Gastroenterology* 1999; **117**: 1089-1097 [PMID: 10535871]
23 **Tawiah A**, Cornick S, Moreau F, Gorman H, Kumar M, Tiwari S, Chadee K. High MUC2 Mucin Expression and Misfolding Induce Cellular Stress, Reactive Oxygen Production, and Apoptosis in Goblet Cells. *Am J Pathol* 2018; **188**: 1354-1373 [PMID: 29545196 DOI: 10.1016/j.ajpath.2018.02.007]
24 **Hartmann P**, Chen P, Wang HJ, Wang L, McCole DF, Brandl K, Stärkel P, Belzer C, Hellerbrand C, Tsukamoto H, Ho SB, Schnabl B. Deficiency of intestinal mucin-2 ameliorates experimental alcoholic liver disease in mice. *Hepatology* 2013; **58**: 108-119 [PMID: 23408358 DOI: 10.1002/hep.26321]
25 **Heazlewood CK**, Cook MC, Eri R, Price GR, Tauro SB, Taupin D, Thornton DJ, Png CW, Crockford TL, Cornall RJ, Adams R, Kato M, Nelms KA, Hong NA, Florin TH, Goodnow CC, McGuckin MA. Aberrant mucin assembly in mice causes endoplasmic reticulum stress and spontaneous inflammation resembling ulcerative colitis. *PLoS Med* 2008; **5**: e54 [PMID: 18318598 DOI: 10.1371/journal.pmed.0050054]
26 **Strocchi A**, Corazza G, Furne J, Fine C, Di Sario A, Gasbarrini G, Levitt MD. Measurements of the jejunal unstirred layer in normal subjects and patients with celiac disease. *Am J Physiol* 1996; **270**: G487-

G491 [PMID: 8638715 DOI: 10.1152/ajpgi.1996.270.3.G487]
27 **Ponziani FR**, Zocco MA, Cerrito L, Gasbarrini A, Pompili M. Bacterial translocation in patients with liver cirrhosis: physiology, clinical consequences, and practical implications. *Expert Rev Gastroenterol Hepatol* 2018; **12**: 641-656 [PMID: 29806487 DOI: 10.1080/17474124.2018.1481747]
28 **Ponziani FR**, Gerardi V, Gasbarrini A. Diagnosis and treatment of small intestinal bacterial overgrowth. *Expert Rev Gastroenterol Hepatol* 2016; **10**: 215-227 [PMID: 26636484 DOI: 10.1586/17474124.2016.1110017]
29 **Russell DW**. The enzymes, regulation, and genetics of bile acid synthesis. *Annu Rev Biochem* 2003; **72**: 137-174 [PMID: 12543708 DOI: 10.1146/annurev.biochem.72.121801.161712]
30 **Duparc T**, Plovier H, Marrachelli VG, Van Hul M, Essaghir A, Ståhlman M, Matamoros S, Geurts L, Pardo-Tendero MM, Druart C, Delzenne NM, Demoulin JB, van der Merwe SW, van Pelt J, Bäckhed F, Monleon D, Everard A, Cani PD. Hepatocyte MyD88 affects bile acids, gut microbiota and metabolome contributing to regulate glucose and lipid metabolism. *Gut* 2017; **66**: 620-632 [PMID: 27196572 DOI: 10.1136/gutjnl-2015-310904]
31 **Lorenzo-Zúñiga V**, Bartolí R, Planas R, Hofmann AF, Viñado B, Hagey LR, Hernández JM, Mañé J, Alvarez MA, Ausina V, Gassull MA. Oral bile acids reduce bacterial overgrowth, bacterial translocation, and endotoxemia in cirrhotic rats. *Hepatology* 2003; **37**: 551-557 [PMID: 12601352 DOI: 10.1053/jhep.2003.50116]
32 **Bertók L**. Bile acids in physico-chemical host defence. *Pathophysiology* 2004; **11**: 139-145 [PMID: 15561510 DOI: 10.1016/j.pathophys.2004.09.002]
33 **Theocharidou E**, Dhar A, Patch D. Gastrointestinal Motility Disorders and Their Clinical Implications in Cirrhosis. *Gastroenterol Res Pract* 2017; **2017**: 8270310 [PMID: 28584525 DOI: 10.1155/2017/8270310]
34 **Yamazaki Y**, Okawa K, Yano T, Tsukita S, Tsukita S. Optimized proteomic analysis on gels of cell-cell adhering junctional membrane proteins. *Biochemistry* 2008; **47**: 5378-5386 [PMID: 18416558 DOI: 10.1021/bi8002567]
35 **Schneeberger EE**, Lynch RD. The tight junction: a multifunctional complex. *Am J Physiol Cell Physiol* 2004; **286**: C1213-C1228 [PMID: 15151915 DOI: 10.1152/ajpcell.00558.2003]
36 **Van Itallie CM**, Anderson JM. Architecture of tight junctions and principles of molecular composition. *Semin Cell Dev Biol* 2014; **36**: 157-165 [PMID: 25171873 DOI: 10.1016/j.semcdb.2014.08.011]
37 **Anderson JM**, Van Itallie CM. Physiology and function of the tight junction. *Cold Spring Harb Perspect Biol* 2009; **1**: a002584 [PMID: 20066090 DOI: 10.1101/cshperspect.a002584]
38 **Van Itallie CM**, Holmes J, Bridges A, Gookin JL, Coccaro MR, Proctor W, Colegio OR, Anderson JM. The density of small tight junction pores varies among cell types and is increased by expression of claudin-2. *J Cell Sci* 2008; **121**: 298-305 [PMID: 18198187 DOI: 10.1242/jcs.021485]
39 **Colegio OR**, Van Itallie C, Rahner C, Anderson JM. Claudin extracellular domains determine paracellular charge selectivity and resistance but not tight junction fibril architecture. *Am J Physiol Cell Physiol* 2003; **284**: C1346-C1354 [PMID: 12700140 DOI: 10.1152/ajpcell.00547.2002]
40 **Amasheh S**, Meiri N, Gitter AH, Schöneberg T, Mankertz J, Schulzke JD, Fromm M. Claudin-2 expression induces cation-selective channels in tight junctions of epithelial cells. *J Cell Sci* 2002; **115**: 4969-4976 [PMID: 12432083]
41 **Taylor CT**, Dzus AL, Colgan SP. Autocrine regulation of epithelial permeability by hypoxia: role for polarized release of tumor necrosis factor alpha. *Gastroenterology* 1998; **114**: 657-668 [PMID: 9516386]
42 **Madara JL**, Stafford J. Interferon-gamma directly affects barrier function of cultured intestinal epithelial monolayers. *J Clin Invest* 1989; **83**: 724-727 [PMID: 2492310 DOI: 10.1172/JCI113938]
43 **Turner JR**, Rill BK, Carlson SL, Carnes D, Kerner R, Mrsny RJ, Madara JL. Physiological regulation of epithelial tight junctions is associated with myosin light-chain phosphorylation. *Am J Physiol* 1997; **273**: C1378-C1385 [PMID: 9357784 DOI: 10.1152/ajpcell.1997.273.4.C1378]
44 **Hartmann P**, Haimerl M, Mazagova M, Brenner DA, Schnabl B. Toll-like receptor 2-mediated intestinal injury and enteric tumor necrosis factor receptor I contribute to liver fibrosis in mice. *Gastroenterology* 2012; **143**: 1330-1340.e1 [PMID: 22841787 DOI: 10.1053/j.gastro.2012.07.099]
45 **Miele L**, Valenza V, La Torre G, Montalto M, Cammarota G, Ricci R, Mascianà R, Forgione A, Gabrieli ML, Perotti G, Vecchio FM, Rapaccini G, Gasbarrini G, Day CP, Grieco A. Increased intestinal permeability and tight junction alterations in nonalcoholic fatty liver disease. *Hepatology* 2009; **49**: 1877-1887 [PMID: 19291785 DOI: 10.1002/hep.22848]
46 **Assimakopoulos SF**, Tsamandas AC, Tsiaoussis GI, Karatza E, Triantos C, Vagianos CE, Spiliopoulou I, Kaltezioti V, Charonis A, Nikolopoulou VN, Scopa CD, Thomopoulos KC. Altered intestinal tight junctions' expression in patients with liver cirrhosis: a pathogenetic mechanism of intestinal hyperpermeability. *Eur J Clin Invest* 2012; **42**: 439-446 [PMID: 22023490 DOI: 10.1111/j.1365-2362.2011.02609.x]
47 **Bennett KM**, Walker SL, Lo DD. Epithelial microvilli establish an electrostatic barrier to microbial adhesion. *Infect Immun* 2014; **82**: 2860-2871 [PMID: 24778113 DOI: 10.1128/IAI.01681-14]
48 **Meyer-Hoffert U**, Hornef MW, Henriques-Normark B, Axelsson LG, Midtvedt T, Pütsep K, Andersson M. Secreted enteric antimicrobial activity localises to the mucus surface layer. *Gut* 2008; **57**: 764-771 [PMID: 18250125 DOI: 10.1136/gut.2007.141481]
49 **Gautreaux MD**, Deitch EA, Berg RD. T lymphocytes in host defense against bacterial translocation from the gastrointestinal tract. *Infect Immun* 1994; **62**: 2874-2884 [PMID: 7911786]
50 **Gautreaux MD**, Gelder FB, Deitch EA, Berg RD. Adoptive transfer of T lymphocytes to T-cell-depleted mice inhibits Escherichia coli translocation from the gastrointestinal tract. *Infect Immun* 1995; **63**: 3827-3834 [PMID: 7558287]
51 **Hapfelmeier S**, Lawson MA, Slack E, Kirundi JK, Stoel M, Heikenwalder M, Cahenzli J, Velykoredko Y, Balmer ML, Endt K, Geuking MB, Curtiss R, McCoy KD, Macpherson AJ. Reversible microbial colonization of germ-free mice reveals the dynamics of IgA immune responses. *Science* 2010; **328**: 1705-1709 [PMID: 20576892 DOI: 10.1126/science.1188454]
52 **Spadoni I**, Zagato E, Bertocchi A, Paolinelli R, Hot E, Di Sabatino A, Caprioli F, Bottiglieri L, Oldani A, Viale G, Penna G, Dejana E, Rescigno M. A gut-vascular barrier controls the systemic dissemination of bacteria. *Science* 2015; **350**: 830-834 [PMID: 26564856 DOI: 10.1126/science.aad0135]
53 **Spadoni I**, Fornasa G, Rescigno M. Organ-specific protection mediated by cooperation between vascular and epithelial barriers. *Nat Rev Immunol* 2017; **17**: 761-773 [PMID: 28869253 DOI: 10.1038/nri.2017.100]
54 **Spadoni I**, Pietrelli A, Pesole G, Rescigno M. Gene expression profile of endothelial cells during perturbation of the gut vascular barrier. *Gut Microbes* 2016; **7**: 540-548 [PMID: 27723418 DOI:

10.1080/19490976.2016.1239681]
55 **Bush TG**, Savidge TC, Freeman TC, Cox HJ, Campbell EA, Mucke L, Johnson MH, Sofroniew MV. Fulminant jejuno-ileitis following ablation of enteric glia in adult transgenic mice. *Cell* 1998; **93**: 189-201 [PMID: 9568712]
56 **Cornet A**, Savidge TC, Cabarrocas J, Deng WL, Colombel JF, Lassmann H, Desreumaux P, Liblau RS. Enterocolitis induced by autoimmune targeting of enteric glial cells: a possible mechanism in Crohn's disease? *Proc Natl Acad Sci USA* 2001; **98**: 13306-13311 [PMID: 11687633 DOI: 10.1073/pnas.231474098]
57 **Betrapally NS**, Gillevet PM, Bajaj JS. Gut microbiome and liver disease. *Transl Res* 2017; **179**: 49-59 [PMID: 27477080 DOI: 10.1016/j.trsl.2016.07.005]
58 **Albillos A**, Lario M, Álvarez-Mon M. Cirrhosis-associated immune dysfunction: distinctive features and clinical relevance. *J Hepatol* 2014; **61**: 1385-1396 [PMID: 25135860 DOI: 10.1016/j.jhep.2014.08.010]
59 **Macpherson AJ**, Uhr T. Induction of protective IgA by intestinal dendritic cells carrying commensal bacteria. *Science* 2004; **303**: 1662-1665 [PMID: 15016999 DOI: 10.1126/science.1091334]
60 **Macpherson AJ**, Gatto D, Sainsbury E, Harriman GR, Hengartner H, Zinkernagel RM. A primitive T cell-independent mechanism of intestinal mucosal IgA responses to commensal bacteria. *Science* 2000; **288**: 2222-2226 [PMID: 10864873]
61 **Balmer ML**, Slack E, de Gottardi A, Lawson MA, Hapfelmeier S, Miele L, Grieco A, Van Vlierberghe H, Fahrner R, Patuto N, Bernsmeier C, Ronchi F, Wyss M, Stroka D, Dickgreber N, Heim MH, McCoy KD, Macpherson AJ. The liver may act as a firewall mediating mutualism between the host and its gut commensal microbiota. *Sci Transl Med* 2014; **6**: 237ra66 [PMID: 24848256 DOI: 10.1126/scitranslmed.3008618]
62 **Brun P**, Castagliuolo I, Di Leo V, Buda A, Pinzani M, Palù G, Martines D. Increased intestinal permeability in obese mice: new evidence in the pathogenesis of nonalcoholic steatohepatitis. *Am J Physiol Gastrointest Liver Physiol* 2007; **292**: G518-G525 [PMID: 17023554 DOI: 10.1152/ajpgi.00024.2006]
63 **Etienne-Mesmin L**, Vijay-Kumar M, Gewirtz AT, Chassaing B. Hepatocyte Toll-Like Receptor 5 Promotes Bacterial Clearance and Protects Mice Against High-Fat Diet-Induced Liver Disease. *Cell Mol Gastroenterol Hepatol* 2016; **2**: 584-604 [PMID: 28090564 DOI: 10.1016/j.jcmgh.2016.04.007]
64 **Wood NJ**. Liver: the liver as a firewall--clearance of commensal bacteria that have escaped from the gut. *Nat Rev Gastroenterol Hepatol* 2014; **11**: 391 [PMID: 24935420 DOI: 10.1038/nrgastro.2014.90]
65 **Lee WY**, Moriarty TJ, Wong CH, Zhou H, Strieter RM, van Rooijen N, Chaconas G, Kubes P. An intravascular immune response to Borrelia burgdorferi involves Kupffer cells and iNKT cells. *Nat Immunol* 2010; **11**: 295-302 [PMID: 20228796 DOI: 10.1038/ni.1855]
66 **Knook DL**, Barkway C, Sleyster EC. Lysosomal enzyme content of Kupffer and endothelial liver cells isolated from germfree and clean conventional rats. *Infect Immun* 1981; **33**: 620-622 [PMID: 7275320]
67 **Schwabe RF**, Seki E, Brenner DA. Toll-like receptor signaling in the liver. *Gastroenterology* 2006; **130**: 1886-1900 [PMID: 16697751 DOI: 10.1053/j.gastro.2006.01.038]
68 **Fox ES**, Thomas P, Broitman SA. Clearance of gut-derived endotoxins by the liver. Release and modification of 3H, 14C-lipopolysaccharide by isolated rat Kupffer cells. *Gastroenterology* 1989; **96**: 456-461 [PMID: 2642878]
69 **Su GL**, Klein RD, Aminlari A, Zhang HY, Steinstraesser L, Alarcon WH, Remick DG, Wang SC. Kupffer cell activation by lipopolysaccharide in rats: role for lipopolysaccharide binding protein and toll-like receptor 4. *Hepatology* 2000; **31**: 932-936 [PMID: 10733550 DOI: 10.1053/he.2000.5634]
70 **Schumann RR**, Kirschning CJ, Unbehaun A, Aberle HP, Knope HP, Lamping N, Ulevitch RJ, Herrmann F. The lipopolysaccharide-binding protein is a secretory class 1 acute-phase protein whose gene is transcriptionally activated by APRF/STAT/3 and other cytokine-inducible nuclear proteins. *Mol Cell Biol* 1996; **16**: 3490-3503 [PMID: 8668165]
71 **Frey EA**, Miller DS, Jahr TG, Sundan A, Bazil V, Espevik T, Finlay BB, Wright SD. Soluble CD14 participates in the response of cells to lipopolysaccharide. *J Exp Med* 1992; **176**: 1665-1671 [PMID: 1281215]
72 **Pugin J**, Schürer-Maly CC, Leturcq D, Moriarty A, Ulevitch RJ, Tobias PS. Lipopolysaccharide activation of human endothelial and epithelial cells is mediated by lipopolysaccharide-binding protein and soluble CD14. *Proc Natl Acad Sci USA* 1993; **90**: 2744-2748 [PMID: 7681988]
73 **Landmann R**, Knopf HP, Link S, Sansano S, Schumann R, Zimmerli W. Human monocyte CD14 is upregulated by lipopolysaccharide. *Infect Immun* 1996; **64**: 1762-1769 [PMID: 8613389]
74 **Lin RS**, Lee FY, Lee SD, Tsai YT, Lin HC, Lu RH, Hsu WC, Huang CC, Wang SS, Lo KJ. Endotoxemia in patients with chronic liver diseases: relationship to severity of liver diseases, presence of esophageal varices, and hyperdynamic circulation. *J Hepatol* 1995; **22**: 165-172 [PMID: 7790704]
75 **Bellot P**, García-Pagán JC, Francés R, Abraldes JG, Navasa M, Pérez-Mateo M, Such J, Bosch J. Bacterial DNA translocation is associated with systemic circulatory abnormalities and intrahepatic endothelial dysfunction in patients with cirrhosis. *Hepatology* 2010; **52**: 2044-2052 [PMID: 20979050 DOI: 10.1002/hep.23918]
76 **Cirera I**, Bauer TM, Navasa M, Vila J, Grande L, Taurá P, Fuster J, García-Valdecasas JC, Lacy A, Suárez MJ, Rimola A, Rodés J. Bacterial translocation of enteric organisms in patients with cirrhosis. *J Hepatol* 2001; **34**: 32-37 [PMID: 11211904]
77 **Garcia-Tsao G**, Lee FY, Barden GE, Cartun R, West AB. Bacterial translocation to mesenteric lymph nodes is increased in cirrhotic rats with ascites. *Gastroenterology* 1995; **108**: 1835-1841 [PMID: 7768390]
78 **Kudo H**, Takahara T, Yata Y, Kawai K, Zhang W, Sugiyama T. Lipopolysaccharide triggered TNF-alpha-induced hepatocyte apoptosis in a murine non-alcoholic steatohepatitis model. *J Hepatol* 2009; **51**: 168-175 [PMID: 19446916 DOI: 10.1016/j.jhep.2009.02.032]
79 **Brenner C**, Galluzzi L, Kepp O, Kroemer G. Decoding cell death signals in liver inflammation. *J Hepatol* 2013; **59**: 583-594 [PMID: 23567086 DOI: 10.1016/j.jhep.2013.03.033]
80 **Heymann F**, Tacke F. Immunology in the liver--from homeostasis to disease. *Nat Rev Gastroenterol Hepatol* 2016; **13**: 88-110 [PMID: 26758786 DOI: 10.1038/nrgastro.2015.200]
81 **Ramadori G**, Moriconi F, Malik I, Dudas J. Physiology and pathophysiology of liver inflammation, damage and repair. *J Physiol Pharmacol* 2008; **59** Suppl 1: 107-117 [PMID: 18802219]
82 **Wenfeng Z**, Yakun W, Di M, Jianping G, Chuanxin W, Chun H. Kupffer cells: increasingly significant role in nonalcoholic fatty liver disease. *Ann Hepatol* 2014; **13**: 489-495 [PMID: 25152980]
83 **Duffield JS**, Forbes SJ, Constandinou CM, Clay S, Partolina M, Vuthoori S, Wu S, Lang R, Iredale JP. Selective depletion of macrophages reveals distinct, opposing roles during liver injury and repair. *J Clin Invest* 2005; **115**: 56-65 [PMID: 15630444 DOI: 10.1172/JCI22675]

84 **Seki E**, De Minicis S, Osterreicher CH, Kluwe J, Osawa Y, Brenner DA, Schwabe RF. TLR4 enhances TGF-beta signaling and hepatic fibrosis. *Nat Med* 2007; **13**: 1324-1332 [PMID: 17952090 DOI: 10.1038/nm1663]

85 **Seki E**, Schnabl B. Role of innate immunity and the microbiota in liver fibrosis: crosstalk between the liver and gut. *J Physiol* 2012; **590**: 447-458 [PMID: 22124143 DOI: 10.1113/jphysiol.2011.219691]

86 **Wree A**, Broderick L, Canbay A, Hoffman HM, Feldstein AE. From NAFLD to NASH to cirrhosis-new insights into disease mechanisms. *Nat Rev Gastroenterol Hepatol* 2013; **10**: 627-636 [PMID: 23958599 DOI: 10.1038/nrgastro.2013.149]

87 **Tsuchida T**, Friedman SL. Mechanisms of hepatic stellate cell activation. *Nat Rev Gastroenterol Hepatol* 2017; **14**: 397-411 [PMID: 28487545 DOI: 10.1038/nrgastro.2017.38]

88 **Benyon RC**, Arthur MJ. Extracellular matrix degradation and the role of hepatic stellate cells. *Semin Liver Dis* 2001; **21**: 373-384 [PMID: 11586466 DOI: 10.1055/s-2001-17552]

89 **Roderfeld M**. Matrix metalloproteinase functions in hepatic injury and fibrosis. *Matrix Biol* 2018; **68-69**: 452-462 [PMID: 29221811 DOI: 10.1016/j.matbio.2017.11.011]

90 **Knittel T**, Mehde M, Kobold D, Saile B, Dinter C, Ramadori G. Expression patterns of matrix metalloproteinases and their inhibitors in parenchymal and non-parenchymal cells of rat liver: regulation by TNF-alpha and TGF-beta1. *J Hepatol* 1999; **30**: 48-60 [PMID: 9927150]

91 **Schuppan D**, Ruehl M, Somasundaram R, Hahn EG. Matrix as a modulator of hepatic fibrogenesis. *Semin Liver Dis* 2001; **21**: 351-372 [PMID: 11586465 DOI: 10.1055/s-2001-17556]

92 **Miele L**, Forgione A, La Torre G, Vero V, Cefalo C, Racco S, Vellone VG, Vecchio FM, Gasbarrini G, Rapaccini GL, Neuman MG, Grieco A. Serum levels of hyaluronic acid and tissue metalloproteinase inhibitor-1 combined with age predict the presence of nonalcoholic steatohepatitis in a pilot cohort of subjects with nonalcoholic fatty liver disease. *Transl Res* 2009; **154**: 194-201 [PMID: 19766963 DOI: 10.1016/j.trsl.2009.06.007]

93 **Cichoż-Lach H**, Michalak A. Oxidative stress as a crucial factor in liver diseases. *World J Gastroenterol* 2014; **20**: 8082-8091 [PMID: 25009380 DOI: 10.3748/wjg.v20.i25.8082]

94 **Valko M**, Leibfritz D, Moncol J, Cronin MT, Mazur M, Telser J. Free radicals and antioxidants in normal physiological functions and human disease. *Int J Biochem Cell Biol* 2007; **39**: 44-84 [PMID: 16978905 DOI: 10.1016/j.biocel.2006.07.001]

95 **Gil-Cardoso K**, Ginés I, Pinent M, Ardévol A, Terra X, Blay M. A cafeteria diet triggers intestinal inflammation and oxidative stress in obese rats. *Br J Nutr* 2017; **117**: 218-229 [PMID: 28132653 DOI: 10.1017/S0007114516004608]

96 **Keshavarzian A**, Farhadi A, Forsyth CB, Rangan J, Jakate S, Shaikh M, Banan A, Fields JZ. Evidence that chronic alcohol exposure promotes intestinal oxidative stress, intestinal hyperpermeability and endotoxemia prior to development of alcoholic steatohepatitis in rats. *J Hepatol* 2009; **50**: 538-547 [PMID: 19155080 DOI: 10.1016/j.jhep.2008.10.028]

97 **van Ampting MT**, Schonewille AJ, Vink C, Brummer RJ, van der Meer R, Bovee-Oudenhoven IM. Intestinal barrier function in response to abundant or depleted mucosal glutathione in Salmonella-infected rats. *BMC Physiol* 2009; **9**: 6 [PMID: 19374741 DOI: 10.1186/1472-6793-9-6]

98 **Novak EA**, Mollen KP. Mitochondrial dysfunction in inflammatory bowel disease. *Front Cell Dev Biol* 2015; **3**: 62 [PMID: 26484345 DOI: 10.3389/fcell.2015.00062]

99 **Utzeri E**, Usai P. Role of non-steroidal anti-inflammatory drugs on intestinal permeability and nonalcoholic fatty liver disease. *World J Gastroenterol* 2017; **23**: 3954-3963 [PMID: 28652650 DOI: 10.3748/wjg.v23.i22.3954]

100 **Ramachandran A**, Prabhu R, Thomas S, Reddy JB, Pulimood A, Balasubramanian KA. Intestinal mucosal alterations in experimental cirrhosis in the rat: role of oxygen free radicals. *Hepatology* 2002; **35**: 622-629 [PMID: 11870376 DOI: 10.1053/jhep.2002.31656]

101 **Casas-Grajales S**, Muriel P. Antioxidants in liver health. *World J Gastrointest Pharmacol Ther* 2015; **6**: 59-72 [PMID: 26261734 DOI: 10.4292/wjgpt.v6.i3.59]

102 **Maellaro E**, Casini AF, Del Bello B, Comporti M. Lipid peroxidation and antioxidant systems in the liver injury produced by glutathione depleting agents. *Biochem Pharmacol* 1990; **39**: 1513-1521 [PMID: 2337408]

103 **Luangmonkong T**, Suriguga S, Mutsaers HAM, Groothuis GMM, Olinga P, Boersema M. Targeting Oxidative Stress for the Treatment of Liver Fibrosis. *Rev Physiol Biochem Pharmacol* 2018; **175**: 71-102 [PMID: 29728869 DOI: 10.1007/112_2018_10]

104 **Li S**, Tan HY, Wang N, Zhang ZJ, Lao L, Wong CW, Feng Y. The Role of Oxidative Stress and Antioxidants in Liver Diseases. *Int J Mol Sci* 2015; **16**: 26087-26124 [PMID: 26540040 DOI: 10.3390/ijms161125942]

105 **Liang S**, Kisseleva T, Brenner DA. The Role of NADPH Oxidases (NOXs) in Liver Fibrosis and the Activation of Myofibroblasts. *Front Physiol* 2016; **7**: 17 [PMID: 26869935 DOI: 10.3389/fphys.2016.00017]

106 **Nieto N**. Oxidative-stress and IL-6 mediate the fibrogenic effects of [corrected] Kupffer cells on stellate cells. *Hepatology* 2006; **44**: 1487-1501 [PMID: 17133487 DOI: 10.1002/hep.21427]

107 **Krause P**, Morris V, Greenbaum JA, Park Y, Bjoerheden U, Mikulski Z, Muffley T, Shui JW, Kim G, Cheroutre H, Liu YC, Peters B, Kronenberg M, Murai M. IL-10-producing intestinal macrophages prevent excessive antibacterial innate immunity by limiting IL-23 synthesis. *Nat Commun* 2015; **6**: 7055 [PMID: 25959063 DOI: 10.1038/ncomms8055]

108 **Gómez-Hurtado I**, Moratalla A, Moya-Pérez Á, Peiró G, Zapater P, González-Navajas JM, Giménez P, Such J, Sanz Y, Francés R. Role of interleukin 10 in norfloxacin prevention of luminal free endotoxin translocation in mice with cirrhosis. *J Hepatol* 2014; **61**: 799-808 [PMID: 24882049 DOI: 10.1016/j.jhep.2014.05.031]

109 **Thompson K**, Maltby J, Fallowfield J, McAulay M, Millward-Sadler H, Sheron N. Interleukin-10 expression and function in experimental murine liver inflammation and fibrosis. *Hepatology* 1998; **28**: 1597-1606 [PMID: 9828224 DOI: 10.1002/hep.510280620]

110 **de Souza-Cruz S**, Victória MB, Tarragô AM, da Costa AG, Pimentel JP, Pires EF, Araújo Lde P, Coelho-dos-Reis JG, Gomes Mde S, Amaral LR, Teixeira-Carvalho A, Martins-Filho OA, Victória Fda S, Malheiro A. Liver and blood cytokine microenvironment in HCV patients is associated to liver fibrosis score: a proinflammatory cytokine ensemble orchestrated by TNF and tuned by IL-10. *BMC Microbiol* 2016; **16**: 3 [PMID: 26742960 DOI: 10.1186/s12866-015-0610-6]

111 **Melhem A**, Muhanna N, Bishara A, Alvarez CE, Ilan Y, Bishara T, Horani A, Nassar M, Friedman SL, Safadi R. Anti-fibrotic activity of NK cells in experimental liver injury through killing of activated HSC. *J*

Hepatol 2006; **45**: 60-71 [PMID: 16515819 DOI: 10.1016/j.jhep.2005.12.025]
112 **Krizhanovsky V**, Yon M, Dickins RA, Hearn S, Simon J, Miething C, Yee H, Zender L, Lowe SW. Senescence of activated stellate cells limits liver fibrosis. *Cell* 2008; **134**: 657-667 [PMID: 18724938 DOI: 10.1016/j.cell.2008.06.049]
113 **Yoshiji H**, Kuriyama S, Yoshii J, Ikenaka Y, Noguchi R, Nakatani T, Tsujinoue H, Yanase K, Namisaki T, Imazu H, Fukui H. Tissue inhibitor of metalloproteinases-1 attenuates spontaneous liver fibrosis resolution in the transgenic mouse. *Hepatology* 2002; **36**: 850-860 [PMID: 12297832 DOI: 10.1053/jhep.2002.35625]
114 **Volta U**. Pathogenesis and clinical significance of liver injury in celiac disease. *Clin Rev Allergy Immunol* 2009; **36**: 62-70 [PMID: 18496773 DOI: 10.1007/s12016-008-8086-x]
115 **Bardella MT**, Fraquelli M, Quatrini M, Molteni N, Bianchi P, Conte D. Prevalence of hypertransaminasemia in adult celiac patients and effect of gluten-free diet. *Hepatology* 1995; **22**: 833-836 [PMID: 7657290]
116 **Grieco A**, Miele L, Pignatoro G, Pompili M, Rapaccini GL, Gasbarrini G. Is coeliac disease a confounding factor in the diagnosis of NASH? *Gut* 2001; **49**: 596 [PMID: 11589191]
117 **Duggan JM**, Duggan AE. Systematic review: the liver in coeliac disease. *Aliment Pharmacol Ther* 2005; **21**: 515-518 [PMID: 15740533 DOI: 10.1111/j.1365-2036.2005.02361.x]
118 **Casella G**, Antonelli E, Di Bella C, Villanacci V, Fanini L, Baldini V, Bassotti G. Prevalence and causes of abnormal liver function in patients with coeliac disease. *Liver Int* 2013; **33**: 1128-1131 [PMID: 23601438 DOI: 10.1111/liv.12178]
119 **Jacobsen MB**, Fausa O, Elgjo K, Schrumpf E. Hepatic lesions in adult coeliac disease. *Scand J Gastroenterol* 1990; **25**: 656-662 [PMID: 2396080]
120 **Sainsbury A**, Sanders DS, Ford AC. Meta-analysis: Coeliac disease and hypertransaminasaemia. *Aliment Pharmacol Ther* 2011; **34**: 33-40 [PMID: 21545472 DOI: 10.1111/j.1365-2036.2011.04685.x]
121 **van Elburg RM**, Uil JJ, Mulder CJ, Heymans HS. Intestinal permeability in patients with coeliac disease and relatives of patients with coeliac disease. *Gut* 1993; **34**: 354-357 [PMID: 8472983]
122 **Novacek G**, Miehsler W, Wrba F, Ferenci P, Penner E, Vogelsang H. Prevalence and clinical importance of hypertransaminasaemia in coeliac disease. *Eur J Gastroenterol Hepatol* 1999; **11**: 283-288 [PMID: 10333201]
123 **Rahman K**, Desai C, Iyer SS, Thorn NE, Kumar P, Liu Y, Smith T, Neish AS, Li H, Tan S, Wu P, Liu X, Yu Y, Farris AB, Nusrat A, Parkos CA, Anania FA. Loss of Junctional Adhesion Molecule A Promotes Severe Steatohepatitis in Mice on a Diet High in Saturated Fat, Fructose, and Cholesterol. *Gastroenterology* 2016; **151**: 733-746.e12 [PMID: 27342212 DOI: 10.1053/j.gastro.2016.06.022]
124 **Saitou M**, Furuse M, Sasaki H, Schulzke JD, Fromm M, Takano H, Noda T, Tsukita S. Complex phenotype of mice lacking occludin, a component of tight junction strands. *Mol Biol Cell* 2000; **11**: 4131-4142 [PMID: 11102513 DOI: 10.1091/mbc.11.12.4131]
125 **Mir H**, Meena AS, Chaudhry KK, Shukla PK, Gangwar R, Manda B, Padala MK, Shen L, Turner JR, Dietrich P, Dragatsis I, Rao R. Occludin deficiency promotes ethanol-induced disruption of colonic epithelial junctions, gut barrier dysfunction and liver damage in mice. *Biochim Biophys Acta* 2016; **1860**: 765-774 [PMID: 26721332 DOI: 10.1016/j.bbagen.2015.12.013]
126 **Cariello R**, Federico A, Sapone A, Tuccillo C, Scialdone VR, Tiso A, Miranda A, Portincasa P, Carbonara V, Palasciano G, Martorelli L, Esposito P, Cartenì M, Del Vecchio Blanco C, Loguercio C. Intestinal permeability in patients with chronic liver diseases: Its relationship with the aetiology and the entity of liver damage. *Dig Liver Dis* 2010; **42**: 200-204 [PMID: 19502117 DOI: 10.1016/j.dld.2009.05.001]
127 **Giorgio V**, Miele L, Principessa L, Ferretti F, Villa MP, Negro V, Grieco A, Alisi A, Nobili V. Intestinal permeability is increased in children with non-alcoholic fatty liver disease, and correlates with liver disease severity. *Dig Liver Dis* 2014; **46**: 556-560 [PMID: 24631029 DOI: 10.1016/j.dld.2014.02.010]
128 **Luther J**, Garber JJ, Khalili H, Dave M, Bale SS, Jindal R, Motola DL, Luther S, Bohr S, Jeoung SW, Deshpande V, Singh G, Turner JR, Yarmush ML, Chung RT, Patel SJ. Hepatic Injury in Nonalcoholic Steatohepatitis Contributes to Altered Intestinal Permeability. *Cell Mol Gastroenterol Hepatol* 2015; **1**: 222-232 [PMID: 26405687 DOI: 10.1016/j.jcmgh.2015.01.001]
129 **Day CP**, James OF. Steatohepatitis: a tale of two "hits"? *Gastroenterology* 1998; **114**: 842-845 [PMID: 9547102]
130 **Farrell GC**, Larter CZ. Nonalcoholic fatty liver disease: from steatosis to cirrhosis. *Hepatology* 2006; **43**: S99-S112 [PMID: 16447287 DOI: 10.1002/hep.20973]
131 **Nazim M**, Stamp G, Hodgson HJ. Non-alcoholic steatohepatitis associated with small intestinal diverticulosis and bacterial overgrowth. *Hepatogastroenterology* 1989; **36**: 349-351 [PMID: 2516007]
132 **Lichtman SN**, Sartor RB, Keku J, Schwab JH. Hepatic inflammation in rats with experimental small intestinal bacterial overgrowth. *Gastroenterology* 1990; **98**: 414-423 [PMID: 2295397]
133 **Lichtman SN**, Keku J, Schwab JH, Sartor RB. Hepatic injury associated with small bowel bacterial overgrowth in rats is prevented by metronidazole and tetracycline. *Gastroenterology* 1991; **100**: 513-519 [PMID: 1985047]
134 **Diehl AM**, Li ZP, Lin HZ, Yang SQ. Cytokines and the pathogenesis of non-alcoholic steatohepatitis. *Gut* 2005; **54**: 303-306 [PMID: 15647199 DOI: 10.1136/gut.2003.024935]
135 **Laukoetter MG**, Nava P, Lee WY, Severson EA, Capaldo CT, Babbin BA, Williams IR, Koval M, Peatman E, Campbell JA, Dermody TS, Nusrat A, Parkos CA. JAM-A regulates permeability and inflammation in the intestine in vivo. *J Exp Med* 2007; **204**: 3067-3076 [PMID: 18039951 DOI: 10.1084/jem.20071416]
136 **Monteiro AC**, Sumagin R, Rankin CR, Leoni G, Mina MJ, Reiter DM, Stehle T, Dermody TS, Schaefer SA, Hall RA, Nusrat A, Parkos CA. JAM-A associates with ZO-2, afadin, and PDZ-GEF1 to activate Rap2c and regulate epithelial barrier function. *Mol Biol Cell* 2013; **24**: 2849-2860 [PMID: 23885123 DOI: 10.1091/mbc.E13-06-0298]
137 **Ménard S**, Cerf-Bensussan N, Heyman M. Multiple facets of intestinal permeability and epithelial handling of dietary antigens. *Mucosal Immunol* 2010; **3**: 247-259 [PMID: 20404811 DOI: 10.1038/mi.2010.5]
138 **Vetrano S**, Rescigno M, Cera MR, Correale C, Rumio C, Doni A, Fantini M, Sturm A, Borroni E, Repici A, Locati M, Malesci A, Dejana E, Danese S. Unique role of junctional adhesion molecule-a in maintaining mucosal homeostasis in inflammatory bowel disease. *Gastroenterology* 2008; **135**: 173-184 [PMID: 18514073 DOI: 10.1053/j.gastro.2008.04.002]
139 **Cheng C**, Tan J, Qian W, Zhang L, Hou X. Gut inflammation exacerbates hepatic injury in the high-fat diet induced NAFLD mouse: Attention to the gut-vascular barrier dysfunction. *Life Sci* 2018; **209**: 157-166

[PMID: 30096384 DOI: 10.1016/j.lfs.2018.08.017]
140 **DeMeo MT**, Mutlu EA, Keshavarzian A, Tobin MC. Intestinal permeation and gastrointestinal disease. *J Clin Gastroenterol* 2002; **34**: 385-396 [PMID: 11907349]
141 **Arslan G**, Atasever T, Cindoruk M, Yildirim IS. (51)CrEDTA colonic permeability and therapy response in patients with ulcerative colitis. *Nucl Med Commun* 2001; **22**: 997-1001 [PMID: 11505209]
142 **Wigg AJ**, Roberts-Thomson IC, Dymock RB, McCarthy PJ, Grose RH, Cummins AG. The role of small intestinal bacterial overgrowth, intestinal permeability, endotoxaemia, and tumour necrosis factor alpha in the pathogenesis of non-alcoholic steatohepatitis. *Gut* 2001; **48**: 206-211 [PMID: 11156641]
143 **Dastych M**, Dastych M, Novotná H, Cíhalová J. Lactulose/mannitol test and specificity, sensitivity, and area under curve of intestinal permeability parameters in patients with liver cirrhosis and Crohn's disease. *Dig Dis Sci* 2008; **53**: 2789-2792 [PMID: 18320320 DOI: 10.1007/s10620-007-0184-8]
144 **Cani PD**, Amar J, Iglesias MA, Poggi M, Knauf C, Bastelica D, Neyrinck AM, Fava F, Tuohy KM, Chabo C, Waget A, Delmée E, Cousin B, Sulpice T, Chamontin B, Ferrières J, Tanti JF, Gibson GR, Casteilla L, Delzenne NM, Alessi MC, Burcelin R. Metabolic endotoxemia initiates obesity and insulin resistance. *Diabetes* 2007; **56**: 1761-1772 [PMID: 17456850 DOI: 10.2337/db06-1491]
145 **Leung C**, Rivera L, Furness JB, Angus PW. The role of the gut microbiota in NAFLD. *Nat Rev Gastroenterol Hepatol* 2016; **13**: 412-425 [PMID: 27273168 DOI: 10.1038/nrgastro.2016.85]
146 **Zhu L**, Baker SS, Gill C, Liu W, Alkhouri R, Baker RD, Gill SR. Characterization of gut microbiomes in nonalcoholic steatohepatitis (NASH) patients: a connection between endogenous alcohol and NASH. *Hepatology* 2013; **57**: 601-609 [PMID: 23055155 DOI: 10.1002/hep.26093]
147 **Dawes EA**, Foster SM. The formation of ethanol in Escherichia coli. *Biochim Biophys Acta* 1956; **22**: 253-265 [PMID: 13382840]
148 **Baker SS**, Baker RD, Liu W, Nowak NJ, Zhu L. Role of alcohol metabolism in non-alcoholic steatohepatitis. *PLoS One* 2010; **5**: e9570 [PMID: 20221393 DOI: 10.1371/journal.pone.0009570]
149 **Duncan SH**, Louis P, Thomson JM, Flint HJ. The role of pH in determining the species composition of the human colonic microbiota. *Environ Microbiol* 2009; **11**: 2112-2122 [PMID: 19397676 DOI: 10.1111/j.1462-2920.2009.01931.x]
150 **Brüssow H**, Parkinson SJ. You are what you eat. *Nat Biotechnol* 2014; **32**: 243-245 [PMID: 24727777 DOI: 10.1038/nbt.2845]
151 **Subramanian S**, Goodspeed L, Wang S, Kim J, Zeng L, Ioannou GN, Haigh WG, Yeh MM, Kowdley KV, O'Brien KD, Pennathur S, Chait A. Dietary cholesterol exacerbates hepatic steatosis and inflammation in obese LDL receptor-deficient mice. *J Lipid Res* 2011; **52**: 1626-1635 [PMID: 21690266 DOI: 10.1194/jlr.M016246]
152 **Musso G**, Gambino R, Cassader M. Obesity, diabetes, and gut microbiota: the hygiene hypothesis expanded? *Diabetes Care* 2010; **33**: 2277-2284 [PMID: 20876708 DOI: 10.2337/dc10-0556]
153 **Svegliati-Baroni G**, Saccomanno S, Rychlicki C, Agostinelli L, De Minicis S, Candelaresi C, Faraci G, Pacetti D, Vivarelli M, Nicolini D, Garelli P, Casini A, Manco M, Mingrone G, Risaliti A, Frega GN, Benedetti A, Gastaldelli A. Glucagon-like peptide-1 receptor activation stimulates hepatic lipid oxidation and restores hepatic signalling alteration induced by a high-fat diet in nonalcoholic steatohepatitis. *Liver Int* 2011; **31**: 1285-1297 [PMID: 21745271 DOI: 10.1111/j.1478-3231.2011.02462.x]
154 **Bäckhed F**, Ding H, Wang T, Hooper LV, Koh GY, Nagy A, Semenkovich CF, Gordon JI. The gut microbiota as an environmental factor that regulates fat storage. *Proc Natl Acad Sci USA* 2004; **101**: 15718-15723 [PMID: 15505215 DOI: 10.1073/pnas.0407076101]
155 **Alex S**, Lange K, Amolo T, Grinstead JS, Haakonsson AK, Szalowska E, Koppen A, Mudde K, Haenen D, Al-Lahham S, Roelofsen H, Houtman R, van der Burg B, Mandrup S, Bonvin AM, Kalkhoven E, Müller M, Hooiveld GJ, Kersten S. Short-chain fatty acids stimulate angiopoietin-like 4 synthesis in human colon adenocarcinoma cells by activating peroxisome proliferator-activated receptor γ. *Mol Cell Biol* 2013; **33**: 1303-1316 [PMID: 23339868 DOI: 10.1128/MCB.00858-12]
156 **Wang Z**, Klipfell E, Bennett BJ, Koeth R, Levison BS, Dugar B, Feldstein AE, Britt EB, Fu X, Chung YM, Wu Y, Schauer P, Smith JD, Allayee H, Tang WH, DiDonato JA, Lusis AJ, Hazen SL. Gut flora metabolism of phosphatidylcholine promotes cardiovascular disease. *Nature* 2011; **472**: 57-63 [PMID: 21475195 DOI: 10.1038/nature09922]
157 **Spencer MD**, Hamp TJ, Reid RW, Fischer LM, Zeisel SH, Fodor AA. Association between composition of the human gastrointestinal microbiome and development of fatty liver with choline deficiency. *Gastroenterology* 2011; **140**: 976-986 [PMID: 21129376 DOI: 10.1053/j.gastro.2010.11.049]
158 **Dumas ME**, Barton RH, Toye A, Cloarec O, Blancher C, Rothwell A, Fearnside J, Tatoud R, Blanc V, Lindon JC, Mitchell SC, Holmes E, McCarthy MI, Scott J, Gauguier D, Nicholson JK. Metabolic profiling reveals a contribution of gut microbiota to fatty liver phenotype in insulin-resistant mice. *Proc Natl Acad Sci USA* 2006; **103**: 12511-12516 [PMID: 16895997 DOI: 10.1073/pnas.0601056103]
159 **Boursier J**, Mueller O, Barret M, Machado M, Fizanne L, Araujo-Perez F, Guy CD, Seed PC, Rawls JF, David LA, Hunault G, Oberti F, Calès P, Diehl AM. The severity of nonalcoholic fatty liver disease is associated with gut dysbiosis and shift in the metabolic function of the gut microbiota. *Hepatology* 2016; **63**: 764-775 [PMID: 26600078 DOI: 10.1002/hep.28356]
160 **de Wit NJ**, Afman LA, Mensink M, Müller M. Phenotyping the effect of diet on non-alcoholic fatty liver disease. *J Hepatol* 2012; **57**: 1370-1373 [PMID: 22796155 DOI: 10.1016/j.jhep.2012.07.003]
161 **Wu GD**, Chen J, Hoffmann C, Bittinger K, Chen YY, Keilbaugh SA, Bewtra M, Knights D, Walters WA, Knight R, Sinha R, Gilroy E, Gupta K, Baldassano R, Nessel L, Li H, Bushman FD, Lewis JD. Linking long-term dietary patterns with gut microbial enterotypes. *Science* 2011; **334**: 105-108 [PMID: 21885731 DOI: 10.1126/science.1208344]
162 **O'Sullivan A**, He X, McNiven EM, Haggarty NW, Lönnerdal B, Slupsky CM. Early diet impacts infant rhesus gut microbiome, immunity, and metabolism. *J Proteome Res* 2013; **12**: 2833-2845 [PMID: 23651394 DOI: 10.1021/pr4001702]
163 **Christopherson MR**, Dawson JA, Stevenson DM, Cunningham AC, Bramhacharya S, Weimer PJ, Kendziorski C, Suen G. Unique aspects of fiber degradation by the ruminal ethanologen Ruminococcus albus 7 revealed by physiological and transcriptomic analysis. *BMC Genomics* 2014; **15**: 1066 [PMID: 25477200 DOI: 10.1186/1471-2164-15-1066]
164 **Ponziani FR**, Bhoori S, Castelli C, Putignani L, Rivoltini L, Del Chierico F, Sanguinetti M, Morelli D, Paroni Sterbini F, Petito V, Reddel S, Calvani R, Camisaschi C, Picca A, Tuccitto A, Gasbarrini A, Pompili M, Mazzaferro V. Hepatocellular Carcinoma Is Associated With Gut Microbiota Profile and Inflammation in Nonalcoholic Fatty Liver Disease. *Hepatology* 2019; **69**: 107-120 [PMID: 29665135 DOI: 10.1002/hep.30036]

165 **Bischoff SC**, Barbara G, Buurman W, Ockhuizen T, Schulzke JD, Serino M, Tilg H, Watson A, Wells JM. Intestinal permeability--a new target for disease prevention and therapy. *BMC Gastroenterol* 2014; **14**: 189 [PMID: 25407511 DOI: 10.1186/s12876-014-0189-7]

166 **Serino M**, Luche E, Gres S, Baylac A, Bergé M, Cenac C, Waget A, Klopp P, Iacovoni J, Klopp C, Mariette J, Bouchez O, Lluch J, Ouarné F, Monsan P, Valet P, Roques C, Amar J, Bouloumié A, Théodorou V, Burcelin R. Metabolic adaptation to a high-fat diet is associated with a change in the gut microbiota. *Gut* 2012; **61**: 543-553 [PMID: 22110050 DOI: 10.1136/gutjnl-2011-301012]

167 **Spruss A**, Kanuri G, Wagnerberger S, Haub S, Bischoff SC, Bergheim I. Toll-like receptor 4 is involved in the development of fructose-induced hepatic steatosis in mice. *Hepatology* 2009; **50**: 1094-1104 [PMID: 19637282 DOI: 10.1002/hep.23122]

168 **Lambertz J**, Weiskirchen S, Landert S, Weiskirchen R. Fructose: A Dietary Sugar in Crosstalk with Microbiota Contributing to the Development and Progression of Non-Alcoholic Liver Disease. *Front Immunol* 2017; **8**: 1159 [PMID: 28970836 DOI: 10.3389/fimmu.2017.01159]

169 **Ray K**. NAFLD. Leaky guts: intestinal permeability and NASH. *Nat Rev Gastroenterol Hepatol* 2015; **12**: 123 [PMID: 25645967 DOI: 10.1038/nrgastro.2015.15]

170 **Miele L**, Marrone G, Lauritano C, Cefalo C, Gasbarrini A, Day C, Grieco A. Gut-liver axis and microbiota in NAFLD: insight pathophysiology for novel therapeutic target. *Curr Pharm Des* 2013; **19**: 5314-5324 [PMID: 23432669]

171 **Kirpich IA**, Marsano LS, McClain CJ. Gut-liver axis, nutrition, and non-alcoholic fatty liver disease. *Clin Biochem* 2015; **48**: 923-930 [PMID: 26151226 DOI: 10.1016/j.clinbiochem.2015.06.023]

172 **Cani PD**, Bibiloni R, Knauf C, Waget A, Neyrinck AM, Delzenne NM, Burcelin R. Changes in gut microbiota control metabolic endotoxemia-induced inflammation in high-fat diet-induced obesity and diabetes in mice. *Diabetes* 2008; **57**: 1470-1481 [PMID: 18305141 DOI: 10.2337/db07-1403]

173 **Ding S**, Chi MM, Scull BP, Rigby R, Schwerbrock NM, Magness S, Jobin C, Lund PK. High-fat diet: bacteria interactions promote intestinal inflammation which precedes and correlates with obesity and insulin resistance in mouse. *PLoS One* 2010; **5**: e12191 [PMID: 20808947 DOI: 10.1371/journal.pone.0012191]

174 **Kavanagh K**, Wylie AT, Tucker KL, Hamp TJ, Gharaibeh RZ, Fodor AA, Cullen JM. Dietary fructose induces endotoxemia and hepatic injury in calorically controlled primates. *Am J Clin Nutr* 2013; **98**: 349-357 [PMID: 23783298 DOI: 10.3945/ajcn.112.057331]

175 **Jin R**, Willment A, Patel SS, Sun X, Song M, Mannery YO, Kosters A, McClain CJ, Vos MB. Fructose induced endotoxemia in pediatric nonalcoholic Fatty liver disease. *Int J Hepatol* 2014; **2014**: 560620 [PMID: 25328713 DOI: 10.1155/2014/560620]

176 **Bifulco M**. Mediterranean diet: the missing link between gut microbiota and inflammatory diseases. *Eur J Clin Nutr* 2015; **69**: 1078 [PMID: 26014263 DOI: 10.1038/ejcn.2015.81]

177 **Biolato M**, Manca F, Marrone G, Cefalo C, Racco S, Miggiano GA, Valenza V, Gasbarrini A, Miele L, Grieco A. Intestinal permeability after Mediterranean diet and low-fat diet in non-alcoholic fatty liver disease. *World J Gastroenterol* 2019; **25**: 509-520 [PMID: 30700946 DOI: 10.3748/wjg.v25.i4.509]

178 **Zapater P**, Francés R, González-Navajas JM, de la Hoz MA, Moreu R, Pascual S, Monfort D, Montoliu S, Vila C, Escudero A, Torras X, Cirera I, Llanos L, Guarner-Argente C, Palazón JM, Carnicer F, Bellot P, Guarner C, Planas R, Solá R, Serra MA, Muñoz C, Pérez-Mateo M, Such J. Serum and ascitic fluid bacterial DNA: a new independent prognostic factor in noninfected patients with cirrhosis. *Hepatology* 2008; **48**: 1924-1931 [PMID: 19003911 DOI: 10.1002/hep.22564]

179 **Iwao T**, Toyonaga A, Ikegami M, Oho K, Sumino M, Harada H, Sakaki M, Shigemori H, Aoki T, Tanikawa K. Reduced gastric mucosal blood flow in patients with portal-hypertensive gastropathy. *Hepatology* 1993; **18**: 36-40 [PMID: 8325619]

180 **Reiberger T**, Ferlitsch A, Payer BA, Mandorfer M, Heinisch BB, Hayden H, Lammert F, Trauner M, Peck-Radosavljevic M, Vogelsang H; Vienna Hepatic Hemodynamic Lab. Non-selective betablocker therapy decreases intestinal permeability and serum levels of LBP and IL-6 in patients with cirrhosis. *J Hepatol* 2013; **58**: 911-921 [PMID: 23262249 DOI: 10.1016/j.jhep.2012.12.011]

181 **Garcia-Tsao G**, Albillos A, Barden GE, West AB. Bacterial translocation in acute and chronic portal hypertension. *Hepatology* 1993; **17**: 1081-1085 [PMID: 8514258]

182 **De Palma GD**, Rega M, Masone S, Persico F, Siciliano S, Patrone F, Matantuono L, Persico G. Mucosal abnormalities of the small bowel in patients with cirrhosis and portal hypertension: a capsule endoscopy study. *Gastrointest Endosc* 2005; **62**: 529-534 [PMID: 16185966]

183 **Higaki N**, Matsui H, Imaoka H, Ikeda Y, Murakami H, Hiasa Y, Matsuura B, Onji M. Characteristic endoscopic features of portal hypertensive enteropathy. *J Gastroenterol* 2008; **43**: 327-331 [PMID: 18592149 DOI: 10.1007/s00535-008-2166-9]

184 **Baffy G**. Potential mechanisms linking gut microbiota and portal hypertension. *Liver Int* 2019; **39**: 598-609 [PMID: 30312513 DOI: 10.1111/liv.13986]

185 **Francés R**, Muñoz C, Zapater P, Uceda F, Gascón I, Pascual S, Pérez-Mateo M, Such J. Bacterial DNA activates cell mediated immune response and nitric oxide overproduction in peritoneal macrophages from patients with cirrhosis and ascites. *Gut* 2004; **53**: 860-864 [PMID: 15138214]

186 **Albillos A**, de la Hera A, González M, Moya JL, Calleja JL, Monserrat J, Ruiz-del-Arbol L, Alvarez-Mon M. Increased lipopolysaccharide binding protein in cirrhotic patients with marked immune and hemodynamic derangement. *Hepatology* 2003; **37**: 208-217 [PMID: 12500206 DOI: 10.1053/jhep.2003.50038]

187 **Mishima S**, Xu D, Lu Q, Deitch EA. Bacterial translocation is inhibited in inducible nitric oxide synthase knockout mice after endotoxin challenge but not in a model of bacterial overgrowth. *Arch Surg* 1997; **132**: 1190-1195 [PMID: 9366711]

188 **McAvoy NC**, Semple S, Richards JM, Robson AJ, Patel D, Jardine AG, Leyland K, Cooper AS, Newby DE, Hayes PC. Differential visceral blood flow in the hyperdynamic circulation of patients with liver cirrhosis. *Aliment Pharmacol Ther* 2016; **43**: 947-954 [PMID: 26947424 DOI: 10.1111/apt.13571]

189 **Du Plessis J**, Vanheel H, Janssen CE, Roos L, Slavik T, Stivaktas PI, Nieuwoudt M, van Wyk SG, Vieira W, Pretorius E, Beukes M, Farré R, Tack J, Laleman W, Fevery J, Nevens F, Roskams T, Van der Merwe SW. Activated intestinal macrophages in patients with cirrhosis release NO and IL-6 that may disrupt intestinal barrier function. *J Hepatol* 2013; **58**: 1125-1132 [PMID: 23402745 DOI: 10.1016/j.jhep.2013.01.038]

190 **Zhu Q**, Zou L, Jagavelu K, Simonetto DA, Huebert RC, Jiang ZD, DuPont HL, Shah VH. Intestinal decontamination inhibits TLR4 dependent fibronectin-mediated cross-talk between stellate cells and endothelial cells in liver fibrosis in mice. *J Hepatol* 2012; **56**: 893-899 [PMID: 22173161 DOI:

10.1016/j.jhep.2011.11.013]
191 **Guarner C**, Runyon BA, Heck M, Young S, Sheikh MY. Effect of long-term trimethoprim-sulfamethoxazole prophylaxis on ascites formation, bacterial translocation, spontaneous bacterial peritonitis, and survival in cirrhotic rats. *Dig Dis Sci* 1999; **44**: 1957-1962 [PMID: 10548343]
192 **O'Hair DP**, Adams MB, Tunberg TC, Osborn JL. Relationships among endotoxemia, arterial pressure, and renal function in dogs. *Circ Shock* 1989; **27**: 199-210 [PMID: 2650915]
193 **Huang LT**, Hung JF, Chen CC, Hsieh CS, Yu HR, Hsu CN, Tain YL. Endotoxemia exacerbates kidney injury and increases asymmetric dimethylarginine in young bile duct-ligated rats. *Shock* 2012; **37**: 441-448 [PMID: 22193869 DOI: 10.1097/SHK.0b013e318244b787]
194 **Uchihara M**, Izumi N, Sato C, Marumo F. Clinical significance of elevated plasma endothelin concentration in patients with cirrhosis. *Hepatology* 1992; **16**: 95-99 [PMID: 1535610]
195 **Shah N**, Dhar D, El Zahraa Mohammed F, Habtesion A, Davies NA, Jover-Cobos M, Macnaughtan J, Sharma V, Olde Damink SW, Mookerjee RP, Jalan R. Prevention of acute kidney injury in a rodent model of cirrhosis following selective gut decontamination is associated with reduced renal TLR4 expression. *J Hepatol* 2012; **56**: 1047-1053 [PMID: 22266601 DOI: 10.1016/j.jhep.2011.11.024]
196 **Tarao K**, Moroi T, Hirabayashi Y, Ikeuchi T, Endo O, Takamura Y. Effect of paromomycin sulfate on endotoxemia in patients with cirrhosis. *J Clin Gastroenterol* 1982; **4**: 263-267 [PMID: 7096960]
197 **Kalambokis GN**, Mouzaki A, Rodi M, Pappas K, Fotopoulos A, Xourgia X, Tsianos EV. Rifaximin improves systemic hemodynamics and renal function in patients with alcohol-related cirrhosis and ascites. *Clin Gastroenterol Hepatol* 2012; **10**: 815-818 [PMID: 22391344 DOI: 10.1016/j.cgh.2012.02.025]
198 **Garcia-Martinez R**, Noiret L, Sen S, Mookerjee R, Jalan R. Albumin infusion improves renal blood flow autoregulation in patients with acute decompensation of cirrhosis and acute kidney injury. *Liver Int* 2015; **35**: 335-343 [PMID: 24620819 DOI: 10.1111/liv.12528]
199 **Matz R**, Jurmann J. Spontaneous peritonitis in cirrhosis of the liver. *Lancet* 1966; **1**: 1242-1243 [PMID: 4161392]
200 **Kerr DN**, Pearson DT, Read AE. Infection of ascitic fluid in patients with hepatic cirrhosis. *Gut* 1963; **4**: 394-398 [PMID: 14084751]
201 **Conn HO**. Spontaneous peritonitis and bacteremia in laennec's cirrhosis caused by enteric organisms. A relatively common but rarely recognized syndrome. *Ann Intern Med* 1964; **60**: 568-580 [PMID: 14138877]
202 **Whipple RL**, Harris JF. B. coli septicemia in Laennec's cirrhosis of the liver. *Ann Intern Med* 1950; **33**: 462-466 [PMID: 15433136]
203 **Runyon BA**, Squier S, Borzio M. Translocation of gut bacteria in rats with cirrhosis to mesenteric lymph nodes partially explains the pathogenesis of spontaneous bacterial peritonitis. *J Hepatol* 1994; **21**: 792-796 [PMID: 7890896]
204 **Llovet JM**, Bartolí R, Planas R, Cabré E, Jimenez M, Urban A, Ojanguren I, Arnal J, Gassull MA. Bacterial translocation in cirrhotic rats. Its role in the development of spontaneous bacterial peritonitis. *Gut* 1994; **35**: 1648-1652 [PMID: 7828991]
205 **Llovet JM**, Bartolí R, March F, Planas R, Viñado B, Cabré E, Arnal J, Coll P, Ausina V, Gassull MA. Translocated intestinal bacteria cause spontaneous bacterial peritonitis in cirrhotic rats: molecular epidemiologic evidence. *J Hepatol* 1998; **28**: 307-313 [PMID: 9580278]
206 **Hanouneh MA**, Hanouneh IA, Hashash JG, Law R, Esfeh JM, Lopez R, Hazratjee N, Smith T, Zein NN. The role of rifaximin in the primary prophylaxis of spontaneous bacterial peritonitis in patients with liver cirrhosis. *J Clin Gastroenterol* 2012; **46**: 709-715 [PMID: 22878533 DOI: 10.1097/MCG.0b013e3182506dbb]
207 **Soriano G**, Guarner C, Tomás A, Villanueva C, Torras X, González D, Sainz S, Anguera A, Cussó X, Balanzó J. Norfloxacin prevents bacterial infection in cirrhotics with gastrointestinal hemorrhage. *Gastroenterology* 1992; **103**: 1267-1272 [PMID: 1397884]
208 **Ginés P**, Rimola A, Planas R, Vargas V, Marco F, Almela M, Forné M, Miranda ML, Llach J, Salmerón JM. Norfloxacin prevents spontaneous bacterial peritonitis recurrence in cirrhosis: results of a double-blind, placebo-controlled trial. *Hepatology* 1990; **12**: 716-724 [PMID: 2210673]
209 **Wijdicks EF**. Hepatic Encephalopathy. *N Engl J Med* 2016; **375**: 1660-1670 [PMID: 27783916 DOI: 10.1056/NEJMra1600561]
210 **Butterworth RF**, Giguère JF, Michaud J, Lavoie J, Layrargues GP. Ammonia: key factor in the pathogenesis of hepatic encephalopathy. *Neurochem Pathol* 1987; **6**: 1-12 [PMID: 3306479]
211 **Olde Damink SW**, Deutz NE, Dejong CH, Soeters PB, Jalan R. Interorgan ammonia metabolism in liver failure. *Neurochem Int* 2002; **41**: 177-188 [PMID: 12020618]
212 **Bajaj JS**, Ridlon JM, Hylemon PB, Thacker LR, Heuman DM, Smith S, Sikaroodi M, Gillevet PM. Linkage of gut microbiome with cognition in hepatic encephalopathy. *Am J Physiol Gastrointest Liver Physiol* 2012; **302**: G168-G175 [PMID: 21940902 DOI: 10.1152/ajpgi.00190.2011]
213 **Shawcross DL**, Sharifi Y, Canavan JB, Yeoman AD, Abeles RD, Taylor NJ, Auzinger G, Bernal W, Wendon JA. Infection and systemic inflammation, not ammonia, are associated with Grade 3/4 hepatic encephalopathy, but not mortality in cirrhosis. *J Hepatol* 2011; **54**: 640-649 [PMID: 21163546 DOI: 10.1016/j.jhep.2010.07.045]
214 **Murta V**, Farías MI, Pitossi FJ, Ferrari CC. Chronic systemic IL-1β exacerbates central neuroinflammation independently of the blood-brain barrier integrity. *J Neuroimmunol* 2015; **278**: 30-43 [PMID: 25595250 DOI: 10.1016/j.jneuroim.2014.11.023]
215 **Jain L**, Sharma BC, Sharma P, Srivastava S, Agrawal A, Sarin SK. Serum endotoxin and inflammatory mediators in patients with cirrhosis and hepatic encephalopathy. *Dig Liver Dis* 2012; **44**: 1027-1031 [PMID: 22883217 DOI: 10.1016/j.dld.2012.07.002]
216 **Luo M**, Li L, Yang EN, Dai CY, Liang SR, Cao WK. Correlation between interleukin-6 and ammonia in patients with overt hepatic encephalopathy due to cirrhosis. *Clin Res Hepatol Gastroenterol* 2013; **37**: 384-390 [PMID: 23084463 DOI: 10.1016/j.clinre.2012.08.007]
217 **Shawcross DL**, Davies NA, Williams R, Jalan R. Systemic inflammatory response exacerbates the neuropsychological effects of induced hyperammonemia in cirrhosis. *J Hepatol* 2004; **40**: 247-254 [PMID: 14739095]
218 **Kang DJ**, Betrapally NS, Ghosh SA, Sartor RB, Hylemon PB, Gillevet PM, Sanyal AJ, Heuman DM, Carl D, Zhou H, Liu R, Wang X, Yang J, Jiao C, Herzog J, Lippman HR, Sikaroodi M, Brown RR, Bajaj JS. Gut microbiota drive the development of neuroinflammatory response in cirrhosis in mice. *Hepatology* 2016; **64**: 1232-1248 [PMID: 27339732 DOI: 10.1002/hep.28696]
219 **Jayakumar AR**, Rama Rao KV, Norenberg MD. Neuroinflammation in hepatic encephalopathy: mechanistic aspects. *J Clin Exp Hepatol* 2015; **5**: S21-S28 [PMID: 26041953 DOI:

10.1016/j.jceh.2014.07.006]
220 **Rodrigo R**, Cauli O, Gomez-Pinedo U, Agusti A, Hernandez-Rabaza V, Garcia-Verdugo JM, Felipo V. Hyperammonemia induces neuroinflammation that contributes to cognitive impairment in rats with hepatic encephalopathy. *Gastroenterology* 2010; **139**: 675-684 [PMID: 20303348 DOI: 10.1053/j.gastro.2010.03.040]
221 **American Association for the Study of Liver Diseases**. European Association for the Study of the Liver. Hepatic encephalopathy in chronic liver disease: 2014 practice guideline by the European Association for the Study of the Liver and the American Association for the Study of Liver Diseases. *J Hepatol* 2014; **61**: 642-659 [PMID: 25015420 DOI: 10.1016/j.jhep.2014.05.042]
222 **Ponziani FR**, Gerardi V, Pecere S, D'Aversa F, Lopetuso L, Zocco MA, Pompili M, Gasbarrini A. Effect of rifaximin on gut microbiota composition in advanced liver disease and its complications. *World J Gastroenterol* 2015; **21**: 12322-12333 [PMID: 26604640 DOI: 10.3748/wjg.v21.i43.12322]
223 **Garcovich M**, Zocco MA, Roccarina D, Ponziani FR, Gasbarrini A. Prevention and treatment of hepatic encephalopathy: focusing on gut microbiota. *World J Gastroenterol* 2012; **18**: 6693-6700 [PMID: 23239905 DOI: 10.3748/wjg.v18.i46.6693]
224 **Violi F**, Ferro D, Basili S, Lionetti R, Rossi E, Merli M, Riggio O, Bezzi M, Capoccaccia L. Ongoing prothrombotic state in the portal circulation of cirrhotic patients. *Thromb Haemost* 1997; **77**: 44-47 [PMID: 9031447]
225 **Violi F**, Lip GY, Cangemi R. Endotoxemia as a trigger of thrombosis in cirrhosis. *Haematologica* 2016; **101**: e162-e163 [PMID: 27033239 DOI: 10.3324/haematol.2015.139972]
226 **Moore KL**, Andreoli SP, Esmon NL, Esmon CT, Bang NU. Endotoxin enhances tissue factor and suppresses thrombomodulin expression of human vascular endothelium in vitro. *J Clin Invest* 1987; **79**: 124-130 [PMID: 3025256 DOI: 10.1172/JCI112772]
227 **Carnevale R**, Raparelli V, Nocella C, Bartimoccia S, Novo M, Severino A, De Falco E, Cammisotto V, Pasquale C, Crescioli C, Scavalli AS, Riggio O, Basili S, Violi F. Gut-derived endotoxin stimulates factor VIII secretion from endothelial cells. Implications for hypercoagulability in cirrhosis. *J Hepatol* 2017; **67**: 950-956 [PMID: 28716745 DOI: 10.1016/j.jhep.2017.07.002]
228 **Lumsden AB**, Henderson JM, Kutner MH. Endotoxin levels measured by a chromogenic assay in portal, hepatic and peripheral venous blood in patients with cirrhosis. *Hepatology* 1988; **8**: 232-236 [PMID: 3281884]
229 **Shibayama Y**. Sinusoidal circulatory disturbance by microthrombosis as a cause of endotoxin-induced hepatic injury. *J Pathol* 1987; **151**: 315-321 [PMID: 3585589 DOI: 10.1002/path.1711510412]
230 **Pikarsky E**, Porat RM, Stein I, Abramovitch R, Amit S, Kasem S, Gutkovich-Pyest E, Urieli-Shoval S, Galun E, Ben-Neriah Y. NF-kappaB functions as a tumour promoter in inflammation-associated cancer. *Nature* 2004; **431**: 461-466 [PMID: 15329734 DOI: 10.1038/nature02924]
231 **Bishayee A**. The role of inflammation and liver cancer. *Adv Exp Med Biol* 2014; **816**: 401-435 [PMID: 24818732 DOI: 10.1007/978-3-0348-0837-8_16]
232 **Dapito DH**, Mencin A, Gwak GY, Pradere JP, Jang MK, Mederacke I, Caviglia JM, Khiabanian H, Adeyemi A, Bataller R, Lefkowitch JH, Bower M, Friedman R, Sartor RB, Rabadan R, Schwabe RF. Promotion of hepatocellular carcinoma by the intestinal microbiota and TLR4. *Cancer Cell* 2012; **21**: 504-516 [PMID: 22516259 DOI: 10.1016/j.ccr.2012.02.007]
233 **Liu WT**, Jing YY, Gao L, Li R, Yang X, Pan XR, Yang Y, Meng Y, Hou XJ, Zhao QD, Han ZP, Wei LX. Lipopolysaccharide induces the differentiation of hepatic progenitor cells into myofibroblasts constitutes the hepatocarcinogenesis-associated microenvironment. *Cell Death Differ* 2019 [PMID: 31065105 DOI: 10.1038/s41418-019-0340-7]
234 **Maeda S**, Kamata H, Luo JL, Leffert H, Karin M. IKKbeta couples hepatocyte death to cytokine-driven compensatory proliferation that promotes chemical hepatocarcinogenesis. *Cell* 2005; **121**: 977-990 [PMID: 15989949 DOI: 10.1016/j.cell.2005.04.014]
235 **Nakagawa H**, Maeda S. Inflammation- and stress-related signaling pathways in hepatocarcinogenesis. *World J Gastroenterol* 2012; **18**: 4071-4081 [PMID: 22919237 DOI: 10.3748/wjg.v18.i31.4071]
236 **Ma-On C**, Sanpavat A, Whongsiri P, Suwannasin S, Hirankarn N, Tangkijvanich P, Boonla C. Oxidative stress indicated by elevated expression of Nrf2 and 8-OHdG promotes hepatocellular carcinoma progression. *Med Oncol* 2017; **34**: 57 [PMID: 28281193 DOI: 10.1007/s12032-017-0914-5]
237 **Yoshimoto S**, Loo TM, Atarashi K, Kanda H, Sato S, Oyadomari S, Iwakura Y, Oshima K, Morita H, Hattori M, Honda K, Ishikawa Y, Hara E, Ohtani N. Obesity-induced gut microbial metabolite promotes liver cancer through senescence secretome. *Nature* 2013; **499**: 97-101 [PMID: 23803760 DOI: 10.1038/nature12347]
238 **Loo TM**, Kamachi F, Watanabe Y, Yoshimoto S, Kanda H, Arai Y, Nakajima-Takagi Y, Iwama A, Koga T, Sugimoto Y, Ozawa T, Nakamura M, Kumagai M, Watashi K, Taketo MM, Aoki T, Narumiya S, Oshima M, Arita M, Hara E, Ohtani N. Gut Microbiota Promotes Obesity-Associated Liver Cancer through PGE_2-Mediated Suppression of Antitumor Immunity. *Cancer Discov* 2017; **7**: 522-538 [PMID: 28202625 DOI: 10.1158/2159-8290.CD-16-0932]
239 **Piñero F**, Vazquez M, Baré P, Rohr C, Mendizabal M, Sciara M, Alonso C, Fay F, Silva M. A different gut microbiome linked to inflammation found in cirrhotic patients with and without hepatocellular carcinoma. *Ann Hepatol* 2019; **18**: 480-487 [PMID: 31023615 DOI: 10.1016/j.aohep.2018.10.003]
240 **Qin N**, Yang F, Li A, Prifti E, Chen Y, Shao L, Guo J, Le Chatelier E, Yao J, Wu L, Zhou J, Ni S, Liu L, Pons N, Batto JM, Kennedy SP, Leonard P, Yuan C, Ding W, Chen Y, Hu X, Zheng B, Qian G, Xu W, Ehrlich SD, Zheng S, Li L. Alterations of the human gut microbiome in liver cirrhosis. *Nature* 2014; **513**: 59-64 [PMID: 25079328 DOI: 10.1038/nature13568]
241 **Chen Y**, Yang F, Lu H, Wang B, Chen Y, Lei D, Wang Y, Zhu B, Li L. Characterization of fecal microbial communities in patients with liver cirrhosis. *Hepatology* 2011; **54**: 562-572 [PMID: 21574172 DOI: 10.1002/hep.24423]
242 **Zhang Z**, Zhai H, Geng J, Yu R, Ren H, Fan H, Shi P. Large-scale survey of gut microbiota associated with MHE *via* 16S rRNA-based pyrosequencing. *Am J Gastroenterol* 2013; **108**: 1601-1611 [PMID: 23877352 DOI: 10.1038/ajg.2013.221]
243 **Korda D**, Deák Kiss G, Gerlei Z, Kóbori L, Görög D, Fehérvári I, Piros L, Máthé Z, Doros A. Management of Portal Hypertension After Liver Transplantation. *Transplant Proc* 2017; **49**: 1530-1534 [PMID: 28838434 DOI: 10.1016/j.transproceed.2017.06.015]
244 **Unger LW**, Berlakovich GA, Trauner M, Reiberger T. Management of portal hypertension before and after liver transplantation. *Liver Transpl* 2018; **24**: 112-121 [PMID: 28752925 DOI: 10.1002/lt.24830]
245 **Parrilli G**, Abazia C, Sarnelli G, Corsaro MM, Coccoli P, Viglione L, Cuomo R, Budillon G. Effect of

chronic administration of tacrolimus and cyclosporine on human gastrointestinal permeability. *Liver Transpl* 2003; **9**: 484-488 [PMID: 12740791 DOI: 10.1053/jlts.2003.50088]

246 **Gabe SM**, Bjarnason I, Tolou-Ghamari Z, Tredger JM, Johnson PG, Barclay GR, Williams R, Silk DB. The effect of tacrolimus (FK506) on intestinal barrier function and cellular energy production in humans. *Gastroenterology* 1998; **115**: 67-74 [PMID: 9649460]

247 **Wu ZW**, Ling ZX, Lu HF, Zuo J, Sheng JF, Zheng SS, Li LJ. Changes of gut bacteria and immune parameters in liver transplant recipients. *Hepatobiliary Pancreat Dis Int* 2012; **11**: 40-50 [PMID: 22251469]

248 **Kato K**, Nagao M, Miyamoto K, Oka K, Takahashi M, Yamamoto M, Matsumura Y, Kaido T, Uemoto S, Ichiyama S. Longitudinal Analysis of the Intestinal Microbiota in Liver Transplantation. *Transplant Direct* 2017; **3**: e144 [PMID: 28405600 DOI: 10.1097/TXD.0000000000000661]

249 **Doycheva I**, Leise MD, Watt KD. The Intestinal Microbiome and the Liver Transplant Recipient: What We Know and What We Need to Know. *Transplantation* 2016; **100**: 61-68 [PMID: 26647107 DOI: 10.1097/TP.0000000000001008]

World Journal of Gastroenterology

Submit a Manuscript: https://www.f6publishing.com

World J Gastroenterol 2019 September 7; 25(33): 4835-4849

DOI: 10.3748/wjg.v25.i33.4835

ISSN 1007-9327 (print) ISSN 2219-2840 (online)

REVIEW

Crosstalk network among multiple inflammatory mediators in liver fibrosis

Han-Jing Zhangdi, Si-Biao Su, Fei Wang, Zi-Yu Liang, Yu-Dong Yan, Shan-Yu Qin, Hai-Xing Jiang

ORCID number: Han-Jing Zhangdi (0000-0001-6288-5885); Si-Biao Su (0000-0002-5502-075X); Fei Wang (0000-0003-2031-3883); Zi-Yu Liang (0000-0002-4349-6662); Yu-Dong Yan (0000-0002-7536-3645); Shan-Yu Qin (0000-0002-8566-1427); Hai-Xing Jiang (0000-0002-7941-856X).

Author contributions: Zhangdi HJ wrote the manuscript; Zhangdi HJ and Jiang HX designed the study; all other authors equally contributed to this paper with regard to manuscript drafting, critical revision, and editing.

Conflict-of-interest statement: No potential conflicts of interest.

Manuscript source: Unsolicited manuscript

Received: July 12, 2019
Peer-review started: July 12, 2019
First decision: July 22, 2019
Revised: July 24, 2019
Accepted: August 7, 2019
Article in press: August 7, 2019

Han-Jing Zhangdi, Si-Biao Su, Fei Wang, Zi-Yu Liang, Yu-Dong Yan, Shan-Yu Qin, Hai-Xing Jiang, Department of Gastroenterology, the First Affiliated Hospital of Guangxi Medical University, Nanning 530021, Guangxi Zhuang Autonomous Region, China

Corresponding author: Hai-Xing Jiang, PhD, Director, Department of Gastroenterology, the First Affiliated Hospital of Guangxi Medical University, No. 6, Shuangyong Road, Nanning 530021, Guangxi Zhuang Autonomous Region, China. ce28meseq@sina.com
Telephone: +86-13978867818
Fax: +86-771-78867818

Abstract

Liver fibrosis is the common pathological basis of all chronic liver diseases, and is the necessary stage for the progression of chronic liver disease to cirrhosis. As one of pathogenic factors, inflammation plays a predominant role in liver fibrosis *via* communication and interaction between inflammatory cells, cytokines, and the related signaling pathways. Damaged hepatocytes induce an increase in pro-inflammatory factors, thereby inducing the development of inflammation. In addition, it has been reported that inflammatory response related signaling pathway is the main signal transduction pathway for the development of liver fibrosis. The crosstalk regulatory network leads to hepatic stellate cell activation and proinflammatory cytokine production, which in turn initiate the fibrotic response. Compared with the past, the research on the pathogenesis of liver fibrosis has been greatly developed. However, the liver fibrosis mechanism is complex and many pathways involved need to be further studied. This review mainly focuses on the crosstalk regulatory network among inflammatory cells, cytokines, and the related signaling pathways in the pathogenesis of chronic inflammatory liver diseases. Moreover, we also summarize the recent studies on the mechanisms underlying liver fibrosis and clinical efforts on the targeted therapies against the fibrotic response.

Key words: Crosstalk network; Inflammatory cell; Cytokine signal pathway; Liver fibrosis

Core tip: Liver fibrosis is a chronic liver lesion with inflammation. Reciprocally, increased inflammatory response exacerbates the severity of liver disease. Clinical data reveal that an aberrant increase of inflammatory cytokines is highly correlated with poor outcome of patients with liver fibrosis. However, the mechanism underlying liver fibrosis is not completely understood. It is urgently needed to enrich the knowledge of

Published online: September 7, 2019

P-Reviewer: El-Bendary M, Tanabe S
S-Editor: Gong ZM
L-Editor: Wang TQ
E-Editor: Ma YJ

liver fibrosis. This review focuses on the role of inflammation in liver fibrosis and discusses the crosstalk network involving immune cells, cytokines, and the related signaling pathways.

Citation: Zhangdi HJ, Su SB, Wang F, Liang ZY, Yan YD, Qin SY, Jiang HX. Crosstalk network among multiple inflammatory mediators in liver fibrosis. *World J Gastroenterol* 2019; 25(33): 4835-4849
URL: https://www.wjgnet.com/1007-9327/full/v25/i33/4835.htm
DOI: https://dx.doi.org/10.3748/wjg.v25.i33.4835

INTRODUCTION

Chronic inflammatory lesions results in extracellular matrix accumulation and hepatic fibrosis, eventually leading to cirrhosis[1]. Liver cirrhosis is a life-threatening factor for human health in the world. Sustained stimulations by a series of pathogenic mediators impair the regeneration capacity of the liver and thus result in the development of liver fibrosis. Among many pathogenic factors, inflammation is a key inducer for liver fibrosis progression. Cross activation of hepatic stellate cells (HSCs), Kupffer cells, and other immune cells is a hallmark for the pathogenesis of liver fibrosis. Furthermore, critical cell signal pathway-related apoptosis, autophagy, collagen and inflammatory cytokine production are involved in the development of liver fibrosis by crosstalk with immune cells. Chronic pathogenic factors activated abundant hepacytes to generate inflammatory cytokines and chemokine mediators, which subsequently form a crosstalk network in liver fibrosis. Until now, liver fibrosis is still a serious unsolved problem in chronic liver disease. This review focuses on this crosstalk network in liver fibrosis and discusses the detailed mechanism by which the process of liver fibrosis is modulated.

CELLS INVOLVED IN LIVER FIBROSIS

HSCs

As the precursor of myofibroblasts, HSCs differentiate into an activated myofibroblastic phenotype with the assistance of Kupffer cells and cytokine-cytokine receptor signaling pathways. HSCs comprise 15% of total resident cells in the normal human liver. Through secretion of interleukins and chemokines, HSCs communicate with Kupffer cells and other liver cells in quiescent conditions[2]. However, deregulation of HSC activation can initiate inflammation and enhance the susceptibility to liver fibrosis. Activated HSCs produce endothelin-1 to promote fibrogenesis[3]. A homologous protein of YB1 (a negative mediator for liver fibrosis) mediated anti-fibrotic activity by suppressing the expression of collagen type I in HSCs[4]. Moreover, Wnt signaling can also enhance HSC activation and promote liver fibrosis[5]. Some data showed that loss of interleukin (IL)-1Ra in mice decreased the number of HSCs and Kupffer cells in the liver compared to the other groups, which suggested that IL-1 signaling is also involved in this process[6]. Additionally, mature HSCs have been reported to stimulate allogeneic regulatory T cell proliferation in a cell-cell contact-dependent manner[7]. Mast cells might crosstalk with HSCs to inhibit liver fibrosis *via* the HLA-G-mediated decrease of collagen I, and IL-10 also mediates crosstalk between mast cells and HSCs[8]. Endothelial progenitor cells dramatically inhibit the proliferation, adhesion, and migration of HSCs, promote the apoptosis of HSCs, and down-regulate the mRNA and protein expression of collagen I and collagen III in HSCs[9]. Epigenetic crosstalk between histone acetylation and miRNAs inhibited HSC activation[10]. Researchers have explored drugs targeting HSCs. A number of protein markers were found to be overexpressed in activated HSCs, and their ligands have been utilized to specifically deliver various anti-fibrotic agents[11]. Natural killer (NK) cells are important in regulating hepatic fibrosis, and their cytotoxic killing of HSCs has been reported. Activated NK cells lead HSCs to death in a TRAIL-involved mechanism *via* the p38/PI3K/AKT pathway, which suggested that the p38/PI3K/AKT pathway in NK cells may be a novel drug target to inhibit liver fibrosis[12]. It has been confirmed that activation of HSCs could be inhibited by reducing the production of transforming growth factor-β1 (TGF-β1) in HSCs *via* inhibition of the NF-κB pathway through downregulation of the TGF-β1/Smad3

pathway[13].

Kupffer cells

Kupffer cells as resident macrophages are one of important liver inflammatory cell types, and account for 30% of sinusoidal cells[14]. Activated Kupffer cells secrete abundant cytokines and signaling molecules, which enhance liver immunopathology. Activated Kupffer cells participate in the initial injury/fibrogenic response to TGF-β1 and methotrexate, which results in upregulated production of cytokines, including IL-10, IL-4, IL-6, and IL-13[15]. CXCL6 stimulates the phosphorylation of epidermal growth factor receptor (EGFR) and the expression of TGF-β in cultured Kupffer cells, thereby resulting in activation of HSCs[16]. In response to liver injury induced by endotoxin, IL-35 can promote Kupffer cells to secrete IL-10 and reduce acute liver injury[17]. A crosstalk network including Ly6C+ monocytes, CCL2-CCR2, and Kupffer cells determines HBV clearance/tolerance, and manipulation of these two cell types may be a potential strategy for immunotherapy of HBV-related liver diseases[18]. Activation of Kupffer cells by pathogens and the CCL2/CCR2 axis can be the key factor to recruit innate effector cells to the injured liver[19]. In alcoholic liver disease mice, a crosstalk network including Kupffer cells, T cells, CCL2/CCR2, and CCL5/CCR5 sensitizes hepatocytes[20]. NLRP3 inflammasome from Kupffer cells is involved in the occurrence of schistosomiasis-induced liver fibrosis (SSLF) *via* NF-κB signaling and IL-1β in serum increased strongly[21]. An effective method of isolating Kupffer cells was explored to eliminate endothelial cell contamination, which could be meaningful for illuminating Kupffer cell function and mechanism in diseases[22]. RAMP 1 in Kupffer cells mediates a crosstalk network involving infiltration of immune cells and pro-inflammatory cytokines secreted by Kupffer cells and splenic T cells, and such crosstalk network can regulate the immune response[23]. ATG5-dependent autophagy involved in crosstalk between Kupffer cells and cytokines (IL-6 and IL-10) mediated acute liver injury response[24]. The cross communication of Sphk1 with HSCs and Kupffer cells regulated the CCL2-CCR2 axis in liver fibrosis[25]. Fas ligand stimulated Fas-expressing Kupffer cells or macrophages to secrete active IL-18 in a caspase-1-independent manner and finally resulted in acute liver injury in mice[26]. Kupffer cells with high expression of CD1d only presented lipid antigen to NKT cells for activation of the pro-inflammatory cytokine pathway[27]. Huangqi decoction activated Kupffer cells to promote liver fibrosis[28]. The crosstalk between Th2 microenvironment and Kupffer cells promoted liver fibrodsis[29]. The interaction between NK cells and Kupffer cells mediated by the CD205-TLR9-IL-12 axis promoted liver injury[30]. MM9 from Kupffer cell can remodel the matrix and repair the architecture during liver fibrosis regression[31]. Taken together, multiple functions of Kupffer cells modified by different molecules, signal pathways, inflammatory cytokines, and immune cells are essential in the development of liver fibrosis.

Other inflammation-related cells

NKT cells are activated in an NKG2D-dependent manner, and the crosstalk of IL-30 with NKG2D activates NKT cells to remove collagen-produced HSCs[32]. Regulatory CD4 T cells modulate the crosstalk network between NK cells and HSCs[33]. Neutrophils are the source of many inflammation cytokines and important inflammatory cells for acute liver injury and chronic fibrosis. Neutrophil-to-lymphocyte ratio is determined to be related with inflammatory activity and fibrosis in non-alcohol fatty liver disease[34]. A latest report shows that Th22 cells are closely associated with chronic liver fibrosis; moreover, the close crosstalk in the cell number of $CD4^+$ T cells and Th22 cells suggests that Th22 plays an important role in chronic liver fibrosis[35]. One report demonstrates that NK cells migrate into the fibrosis scar and play a role in immune surveillance by clearing senescent activated HSC cells[36]. However, the chemokine CXCL-10 reverses NK cell-mediated HSC inactivation function and promotes liver fibrosis[37]. Therefore, liver fibrosis progresses in the inflammatory mediator crosstalk network microenvironment.

Inflammatory cytokines

Proinflammatory cytokines: IL-17A in combination with TGF-βRI can phosphorylate SMAD2/3 in HSCs to activate liver fibrosis[38]. A cross communication involving BM-MSCs and IL-6/STAT3 can down-regulate IL-17 and affect liver fibrosis[39]. In a new mouse model with a pre-injured liver (Abcb4/Mdr2$^{-/-}$), IL-6-driven inflammatory response may determine the outcome of acute liver injury[40]. IL-6 is a primary regulator of both acute and chronic inflammation, which exhibits two contrasting functions. It acts as a pro-inflammatory cytokine in models of chronic inflammatory diseases[41], and contrarily shows anti-inflammatory effects in acute inflammation. Therefore, as a classic pro-inflammatory cytokine biomarker, IL-6 is used to clinically diagnose chronic liver fibrosis[42]. A crosstalk axis involving IL-6 and polymorphism of

its gene (C174G) accelerates progression of chronic liver fibrosis[43]. As a potent chemoattractant for neutrophils, IL-8 and its receptor CXCR1 are involved in inflammation activation and liver fibrosis[44]. As potent predictors of liver injury, IL-8, MCP-1, and OPN are associated with advanced liver fibrosis in nonalcoholic fatty liver disease[45]. CXCL-6 can phosphorylate EGFR and activate the TGF-β pathway in Kupffer cells in liver fibrosis[16]. A latest report shows that IL-9-derived interaction between Raf/MEK/ERK and CXCL-10 can promote liver fibrosis[46]. As a profibrogenic factor, IL-34 may become a diagnostic biomarker for liver fibrosis[47]. In a mouse model, the crosstalk between IL-13 and STAT6 signaling pathways activates schistosomiasis-induced liver fibrosis[48]. In non-alcoholic fatty liver disease, fibroblast-derived marker IL-34 is developed as a feasible diagnostic marker[49]. IL-34, together with macrophage colony-stimulating factor, activates HSCs to promote collagen synthesis[50]. Plasma IL-18 in children with nonalcoholic fatty liver disease has been proposed as a novel biomarker for liver fibrosis[51]. CCL2-dependent monocytes may promote angiogenesis induced by inflammation in the progression of liver fibrosis[52]. The communication of TGF-β with JAK1-STAT3 may promote HSC proliferation as well as collagen I and α-SMA up-regulation in CCL4-derived live fibrosis[53]. In fibrotic liver, activated HSC-derived CTGF may respond to TGF-β stimulation in order to form a crosstalk regulatory network, and this crosstalk contributes to extracellular matrix production in a STAT3-dependent mode[54]. Alternatively, the interaction of TGF-β with long non-coding RNA-21 may promote hepatocyte apoptosis in liver fibrosis[55]. Neutralizing of IL-1α and IL-1 can inhibit the progression of liver fibrosis, which suggests that IL-1α and IL-1β promote inflammatory liver fibrosis[56]. Higher IL-9-derived Th9 cell expression was investigated in patients with HBV associated liver cirrhosis, and the result suggested that IL-9 may relate closely to the liver fibrosis. IL-9 is reported to promote hepatic dysfunction in CCL4-mediated liver fibrosis[57].

Anti-fibrosis cytokines: As an autophagy inhibitor, IL-10 crosstalks with STAT3 to exert an anti-fibrogenic function in liver injury[58]. IL-10 producing regulatory B cells can enhance regulatory T cell function in chronic liver fibrosis mediated by HBV[59]. Through restriction fragment length polymorphism (RFLP) analysis, IL-10 gene promoter (rs1800896) polymorphism was correlated with an increased risk of chronic liver fibrosis, especially that mediated by HBV[60]. IL-22 belongs to the IL-10 family and is produced by Th17 cells, Th22 cells, and NKT cells. IL-22 crosstalks with the microRNA (miRNA) and inflammatory cytokine pathways to attenuate HSC activation and inhibit liver fibrosis[61,62]. Crosstalk of IL-22 with p53-p21 in a STAT3 dependent way may induce the senescence of activated HSCs in liver fibrosis[63]. Crosstalk of IL-22 with Nrf2-keap1-ARE inhibits acetaldehyde-induced HSC activation and proliferation[64]. As a liver protector, IL-22 may activate liver cell STAT3 to inhibit liver injury[65]. Moreover, IL-22 inhibits ConA-induced acute liver inflammation[66]. Crosstalk of IL-22 with STAT3 exerts an anti-apoptotic and mitogenic activity[67]. IL-22 is up-regulated strongly in patients with HCV infection, and administration of IL-22 promotes α-SMA expression and collagen production from HSCs[68]. However, crosstalk between IL-22 and HSC-derived IL-22-R1 may induce up-regulation of HSC-derived chemokines (CXCL10 and CCL20) to recruit Th17 cells to migrate into the inflammatory liver in response to chronic liver inflammation and fibrosis mediated by HBV. Therefore, the ultimate effect of IL-22 in liver fibrosis needs to be determined by the balance between induction of HSC apoptosis and promotion of liver inflammation[69]. Crosstalk between IL-22 and the TGF-β1/Notch signaling pathway may induce HSC inactivation and inhibit liver fibrosis[70]. Therefore, liver fibrosis progresses gradually *via* a crosstalk regulatory network involving multiple cytokines and their related downstream signaling pathways. IL-23 produced by Th2 cells down-regulates proinflammatory cytokines and inhibits liver fibrosis[71]. High expression of IL-23R on the Th17 cell surface in acute-on-chronic liver injury patients suggests that it strongly correlates with liver disease severity[72]. High expression of IL-23 in monocyte-derived dendritic cells presents in a TRAF6/NF-κB dependent manner and is closely associated with HBV-mediated acute-on-chronic liver injury[73]. Besides, IL-23 on the basis of IL-17A-producing γδT cells has a protective effect against ConA-mediated liver injury[74].

SIGNALING PATHWAY CROSSTALK IN LIVER FIBROSIS

TGF-β signaling pathway

A crosstalk involving TGF-β and TGF-β R exerts a regulatory effect on cell plasticity in liver fibrosis (Figure 1). In CCL4 induced acute liver injury mice, CCL2/CCR2 recruits monocytes to infiltrate to the injury liver, then monocytes differentiate

preferentially into inducible nitric oxide synthase-producing macrophages exerting pro-inflammatory and pro-fibrogenic actions, *e.g.*, promoting HSC activation *via* the TGF-β pathway[75]. Collagen triple helix repeat containing 1 (CTHRC1) promotes HSC proliferation, migration, and contractility for supporting liver fibrosis *via* crosstalk with the TGF-β signal pathway[76]. IL-13 activates the TGF-β signaling pathway to promote HSC proliferation and cell viability[77]. M2 Kupffer cells produce TGF-β and IL-10, which mediate immune tolerance in mouse liver injury by down-regulating the production of TNF-α and IL-12. In addition, M2 polarization of Kupffer cells contributes to the apoptosis of M1 Kupffer cells in fatty liver disease[78]. Therefore, TGF-β is critical for the activation of HSCs to transdifferentiate into fibrogenic myofibroblasts. Crosstalk between TGF-β and SMAD3 contributes to CCL4-induced liver fibrosis[79]. Activated HSCs may impair NK cell-mediated anti-fibrosis function through crosstalk with TGF-β in HBV-induced chronic liver fibrosis[80]. Some small compounds may crosstalk with the TGF-β pathway and exert an effect on liver fibrosis. Crosstalk of paeoniflorin with the TGF-β pathway may exert a protective role in radiation-induced liver fibrosis[81]. Sauchinone also reduces activation of HSCs and liver fibrosis through crosstalk with the TGF-β1 pathway[82]. Isorhamnetin may control liver fibrosis progression through inhibitive crosstalk with TGF-β1 and relieving oxidative stress[83]. Synthetic oligodeoxynucleotide may prevent fibrogenesis and deposition of collagen by targeting the TGF-β1/Smad pathway[84]. Platelets are a rich source of TGF-β1 and platelet TGF-β1 deficiency decreases liver fibrosis in a mouse model of live injury[85]. TGF-β mediates the transformation of mesothelial cells to myofibroblast[86].

MiRNA signaling pathways

MiRNAs as an important regulatory element are involved in liver fibrosis. Crosstalk between miR-101 and the PI3K/Akt/mTOR signaling pathway presents an anti-fibrotic effect in a CCL4 induced mouse model[87]. MiRNA-29b can target the PI3K/AKT pathway to prevent liver fibrosis by attenuating HSC activation and inducing apoptosis[88]. MiRNA-29b and its crosstalk with the TGF-β1/Smad3 may suppress HSC activation[89]. MiRNA-34a-5p inhibits liver fibrosis by regulating the TGF-β1/Smad3 pathway in HSCs[90]. A cross-communication between miR-130a-3p and its down-regulatory TGFBR1 and TGFBR2 induces HSC apoptosis[91]. MiR-19b can down-regulate CCL2 in HSCs and further inhibit liver fibrosis[25]. A crosstalk involving miRNA-21 and the NLRP3 inflammasome/IL-1β axis mediates angiotensin II-induced liver fibrosis[92]. As a Wnt/β-catenin activator, miR-17-5p contributes to progression of liver fibrosis *via* activating HSCs[93]. Much evidence suggests that miR-17-5p promotes HSC proliferation and activation, on the contrary, down-regulation of miR-17-5p expression contributes to the suppression of activated HSCs[94]. MiRNA-142-3p inhibits TGF-β-induced fibrosis by targeting the TGF-RI pathway and was found to decrease the plasma of chronic liver fibrosis patients[95]. A considerable amount of evidence has shown that miRNA-200 participates in fibrosis[96]. As a PI3K/Akt pathway activator, interaction of miR-200c with its related FOG2 results in HSC activation and liver fibrosis[97]. MiRNA-181b-3p and its target importin α5 may regulate sensitivity of TLR4 in Kupffer cells[98]. MiRNA-193a/b-3p relives liver fibrosis by inhibiting the activation and proliferation of HSCs[99]. MiRNA-26b-5p inhibits mouse liver fibrosis by targeting platelet-derived growth factor receptor-β[100]. MiRNA-219 plays a protective role in liver fibrosis by targeting TGF-βRII[101]. MiRNA-145 promotes HSC activation by targeting Krüppel-like factor 4[102]. The effects of alcohol on DNA methylation in hepatocytes in liver fibrosis and miRNA regulation have been elucidated[103]. Therefore, the core miRNAs and the related downstream targets form a complicate regulatory miRNA-mRNA communication network in liver fibrosis, and this provides a basis for the development of more effective therapy for liver fibrosis.

TLR pathway in liver fibrosis

TLR has the ability to recognize pathogens and contains ten members: TLR1-10. Among the TLR family, TLR3, 7, 8, 9, and 10 are located in the endolysosome[104,105], and TLR1, 2, 4, 5, and 6 are located on the membrane. A crosstalk between TLR and their ligands activates the liver fibrosis pathway (Figure 2). TLR2 and its ligand stimulate Kupffer cells to secret IL-10 in HBV-dependent liver fibrosis[106,107]. In HBV-induced chronic liver fibrosis, TLR2 acts in a homodimer form or in a heterodimer form with TLR1 or TLR6 and activates NF-kB in a MyD-88 dependent manner[108]. TLR3 silencing induces HSC and Kupffer cell activation, suggesting that TLR3 is related closely to liver injury. This supports the basis for TLR3-targeted therapy of liver disease[109]. Crosstalk between TLR3 and CCL5 plays a key role in HCV-mediated liver fibrosis[110]. Exosome-mediated TLR3 promotes liver fibrosis by enhancing IL-17A production from γδT cells[111]. In a non-alcoholic steatohepatitis rat

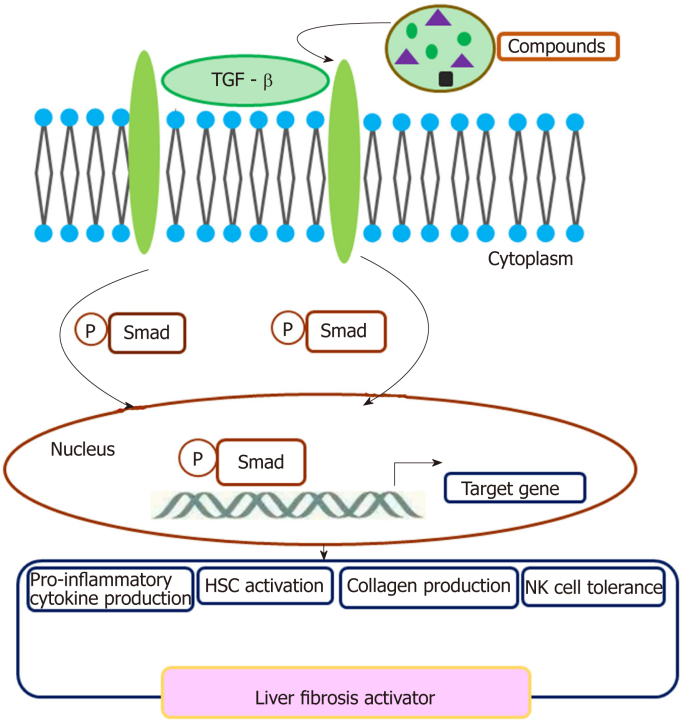

Figure 1 Transforming growth factor-β mediated crosstalk network in liver fibrosis. TGF-β is primarily signaled by intracellular Smads. TGF-β: Transforming growth factor-β; HSC: Hepatic stellate cell; NK: Natural killer.

model, TLR4-p38 MAPK signaling may induce Kupffer cell activation, suggesting that TLR4 is closely associated with steatofibrosis[112]. Ethyl pyruvate may protect the liver from CCL4-mediated fibrosis by inhibition of TLR4[113]. TLR5 promotes liver bacterial clearance and protects from liver injury and fibrosis[114]. Bioactive compound luteolin may protect the liver from fibrosis through up-regulation of TLR5, and knockdown of TLR5 induces metabolic syndrome[115]. These data suggest that TLR5 is a possible key transcription factor for preventing lipotoxicity. TLR2, together with the TLR9-dependent myD88-dependent pathway, may activate HSCs to secret CXCL1, and the CXCL1/CXCR2 axis recruits neutrophils to the liver, which contributes to the development of alcohol-mediated liver injury[116]. TLR7 may activate dendritic cells to secret type I interferon (IFN) to activate Kupffer cells to produce profibrogenic IL-1ra. The TLR7/type I IFN/IL-1ra axis opens a selective target therapy for liver fibrosis[117]. Besides TLR3, other TLR family members are dependent on the MyD88 pathway. Curcumin promotes apoptosis of activated HSCs by inhibiting the MyD-88 pathway[118].

Other signaling pathways

There are other signaling pathways, such as STAT-3, Wnt/β-catenin, and NF-κB signaling pathways, involved in liver fibrosis (Figure 3). A crosstalk involving IL-17 and the STAT3 signaling pathway activates HSCs to produce collagen I[119]. A crosstalk network involving IL-6 and IL-10 with STAT3 may protect the liver against alcohol-mediated inflammation and injury[120]. STAT3/IL-10/IL-6 signaling regulates hepatocyte proliferation and is a key factor associated with acute injury and chronic liver fibrosis[121]. Moreover, crosstalk of IL-22 with STAT3 induces senescence of HSCs in liver fibrosis[53]. STAT3 is required to for TGF-β-induced proliferation and fibrosis in LX-2 cells, and this supports that there is a close crosstalk between the TGF-β and STAT3 pathways[122]. STAT3-EGFR signaling promotes liver protective function in cholestatic liver injury and fibrosis[123]. STAT3 and MAPK are necessary for IL-6-mediated liver fibrosis[63]. STX-0119 reduces liver fibrosis by inhibition of STAT3 and inactivation of HSCs in mice[124]. Crosstalk of FGF21 with the NF-κB and JNK signaling pathways protects the liver from inflammation and fibrosis[125]. Crosstalk between NF-κB and type I IFN signaling promotes liver inflammation and fibrosis, while crosstalk of ADAR1 with this pathway restrains this function[126]. The Wnt/β-catenin pathway exerts a function in HSC activation induced collagen I formation and liver fibrosis, and crosstalk of hBM-MSC with this pathway may inhibit liver fibrosis[127]. HGF activation promotes HSC apoptosis through the Rho pathway[128].

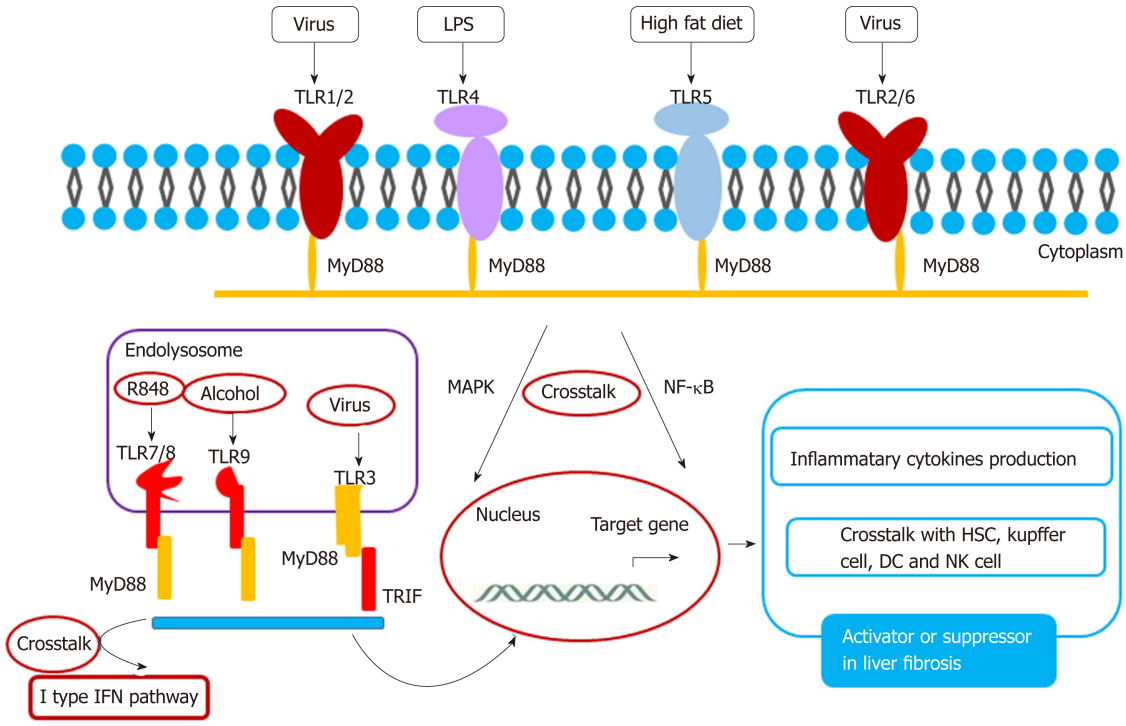

Figure 2 Toll-like receptor mediated crosstalk network in liver fibrosis. Toll-like receptor is a member of DAMPs that recognize pathogen-associated molecules and thereby transmit inflammatory signals that cause inflammatory responses. TLR: Toll-like receptor; MAPK: Mitogen-activated protein kinase; NF-κB: Nuclear factor-κB; HSC: Hepatic stellate cell; DC: Dendritic cells; NK: Natural killer.

TARGETED THERAPIES FOR LIVER FIBROSIS

There are currently some drugs available for the therapy of liver fibrosis, however, their efficacy is limited (Table 1). It is the time to explore promising drugs to improve the treatment of liver fibrosis by developing promising therapeutic strategies, such as inhibition of HSC activation and anti-inflammation. Following molecular targeted therapy increasingly development, protein marker on HSC, signal pathway molecule may be potential marker to be selected for improving liver fibrosis. Many anti-fibrotic compounds are being on road. Tumor necrosis factor-related apoptosis-inducing ligand (TRAIL) has been evaluated to improve liver fibrosis. TRAIL can reverse liver fibrosis by promoting apoptosis of primary HSCs and inhibiting Kupffer cells in a CCL4-mediated liver fibrosis model. Therefore, TRAIL-based therapy is a useful direction for exploring new anti-fibrotic drugs[129]. Wnt/β-based ICG-001 has been assessed to selectively induce target cell apoptosis, with encouraging results obtained in terms of reversing fibrosis and improving survival rate of model animals[130]. 24-nor-ursodeoxycholic acid (norUDCA) has been found to have anti-fibrotic effects and improve inflammation-mediated liver fibrosis[131]. Cenicriviroc, an inhibitor of CCR2/CCR5, is on a phase III clinical trial, which presents an anti-liver fibrosis effect[132]. Accumulating experiments of tyrosine kinase inhibitors make it possible to exploit their beneficial effects on fibrotic disease, although it should not also neglect the side effects of TK inhibitors for liver fibrosis, such as rash and gastrointestinal symptoms[133]. Taken together, these new drug therapies will provide a new avenue for the treatment of liver fibrosis.

CONCLUSION

A better understanding of the crosstalk among inflammation-related cells, cytokines, and signaling pathways in liver fibrosis could help clarify the pathogenesis of liver fibrosis. The aim of this review is to describe the present knowledge about inflammation-related crosstalk networks, which effectively perform regulatory functions in HSC activation and liver fibrosis. Moreover, we discuss different interactions among crosstalk-related members in liver fibrosis. The crosstalk-related complex regulatory network modulates several important aspects of cell function, including proliferation, activation, and differentiation (Table 1, Figure 4). Targeting each node of the crosstalk network can be a promising direction for liver fibrosis

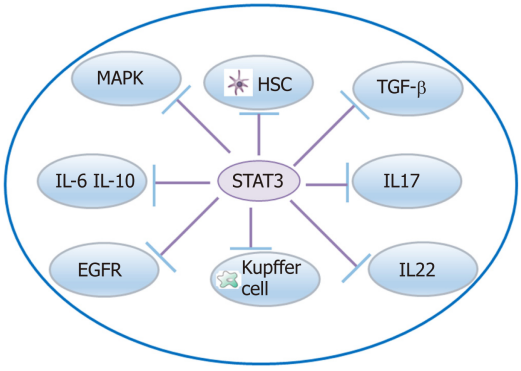

Figure 3 STAT3-mediated inflammatory mediator crosstalk network in liver fibrosis. EGFR: Epidermal growth factor receptor; HSC: Hepatic stellate cell; TGF-β: Transforming growth factor-β; MAPK: Mitogen-activated protein kinase; IL: Interleukin.

treatment. Interaction of IL-34 with the PI3K/Akt signal pathway promotes the M2 polarization of Kupffer cells to inhibit acute rejection in rat liver transplantation[134]. IL-17 stimulates Kupffer cells to secret TGF-β and activates HSCs to form myofibroblasts by stimulating collagen synthesis *via* the STAT3 signal pathway. In the future, we will focus on the function of IL-22 in the crosstalk between Kupffer cells and the CCL2-CCR2 pathway in order to enrich our knowledge on inflammatory cytokines in liver fibrosis. This will provide a basis for the therapy of liver fibrosis[118]. In addition, it should be noted that impaired macroautophagy/autophagy is involved in the pathogenesis of hepatic fibrosis.

Table 1 Signal pathway-inflammatory mediator crosstalk network in liver fibrosis

Crosstalk family member	Mechanism	Function in liver fibrosis	Biological basis as therapeutic target
TGF-β	Proliferation Migration Collagen production Crosstalk with small compounds Induces NK cell tolerance	Fibrosis activator	Deficiency of TGF-β inhibits liver fibrosis
Wnt/β-catenin	Promotes activation of HSC Collagen I production	Fibrosis activator	
TLR-2 TLR1/2 TLR2/6	Activates NF-kB pathway Pro-inflammatory cytokines Activates Kupffer cell and IL-10 production	Inducer or suppressor in liver fibrosis	
TLR-3	Crosstalk with IL-17A and γδT cell Crosstalk with CCL5	Inducer or suppressor in liver fibrosis	Loss of TLR3 aggravates liver inflammation
TLR-4	Pro-inflammatory cytokine production	Fibrosis activator	Inhibition of TLR4 promotes liver protection
TLR-5	Crosstalk other pathway Regulates metabolism Anti-inflammatory cytokine production	Fibrosis inhibitor	Activation of TLR5 reduces liver fibrosis
TLR7	Pro-inflammatory cytokine production Activates DCs Crosstalk with IFN signaling pathway	Fibrosis inhibitor	
TLR-9	CXCL1 production Neutrophil infiltration	Fibrosis activator	
STAT3	Crosstalk with IL-17, IL-10, and IL-6 Crosstalk with other signal pathways	Fibrosis activator or suppressor	Inhibition of STAT3 may inactivate HSCs and prevent liver fibrosis
miR-29b	Crosstalk with PI3K/AKT pathway Crosstalk with TGF-β1/SMAD3 pathway Induces HSC apoptosis	Fibrosis inhibitor	
miR-34a-5p	Crosstalk with TGF-β1/SMAD3	Fibrosis inhibitor	
miR-130a-3p	Crosstalk with TGFBR1 and TGFBR2 Induces HSC apoptosis	Fibrosis inhibitor	
miR-19b	Crosstalk with HSC CCL2	Fibrosis inhibitor	
miR-21	Crosstalk with NLRP3 inflammasome/IL-1β axis	Fibrosis regulator	
miR-17-5p	Crosstalk with Wnt/β-catenin Activation of HSCs	Fibrosis promoter	
miR-142-3p	Crosstalk with TGF-β	Fibrosis inhibitor	
miR-200c	Crosstalk with PI3K/Akt	Fibrosis promoter	
miR-181b-3p	Crosstalk with TLR4 Kupffer cells	Fibrosis regulator	
miR-193a/b-3p	Inhibits activation of HSCs	Fibrosis regulator	
miR-26b-5p	Crosstalk with platelet-derived growth factor receptor-β	Fibrosis inhibition	
miR-219	Crosstalk with TGF-βRII	Fibrosis inhibition	
miR-145	Crosstalk with Krüppel-like factor 4 Promotes activation of HSCs	Fibrosis inhibition	

TGF-β: Transforming growth factor-β; TLR: Toll-like receptor; NF-κB: Nuclear factor-κB; HSC: Hepatic stellate cell; DCs: Dendritic cells; NK: Natural killer; IL: Interleukin.

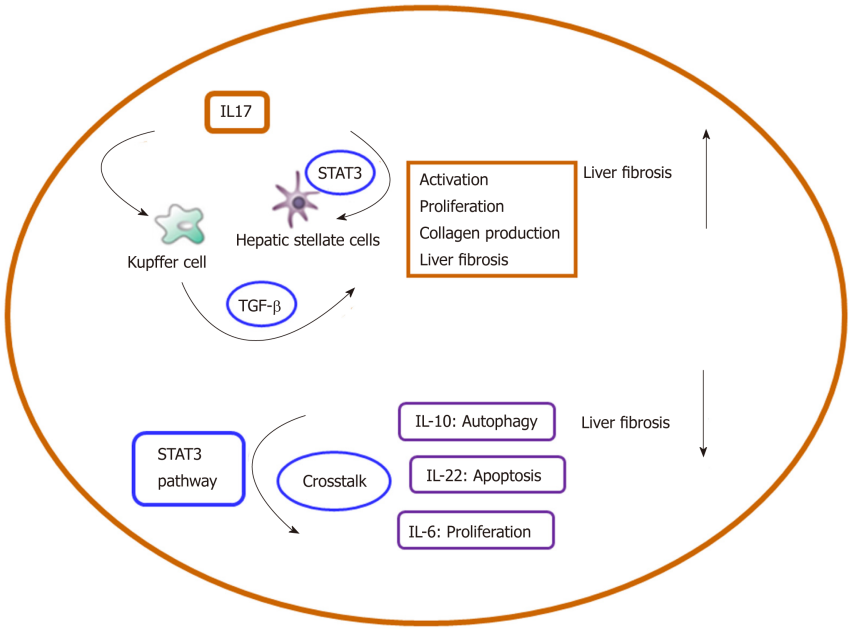

Figure 4 Inflammatory mediator network between cytokines and signaling pathway in liver fibrosis. TGF-β: Transforming growth factor-β; IL: Interleukin.

REFERENCES

1 **Chen L**, Brenner DA, Kisseleva T. Combatting Fibrosis: Exosome-Based Therapies in the Regression of Liver Fibrosis. *Hepatol Commun* 2018; **3**: 180-192 [PMID: 30766956 DOI: 10.1002/hep4.1290]
2 **Friedman SL**. Hepatic stellate cells: protean, multifunctional, and enigmatic cells of the liver. *Physiol Rev* 2008; **88**: 125-172 [PMID: 18195085 DOI: 10.1152/physrev.00013.2007]
3 **Li T**, Shi Z, Rockey DC. Preproendothelin-1 expression is negatively regulated by IFNγ during hepatic stellate cell activation. *Am J Physiol Gastrointest Liver Physiol* 2012; **302**: G948-G957 [PMID: 22301113 DOI: 10.1152/ajpgi.00359.2011]
4 **Chen L**, Ji Z, Duan L, Zhu D, Chen J, Sun X, Yu Y, Duan Y. rSJYB1 inhibits collagen type I protein expression in hepatic stellate cells via down-regulating activity of collagen α1 (I) promoter. *J Cell Mol Med* 2019; **23**: 3676-3682 [PMID: 30895719 DOI: 10.1111/jcmm.14271]
5 **Miao CG**, Yang YY, He X, Huang C, Huang Y, Zhang L, Lv XW, Jin Y, Li J. Wnt signaling in liver fibrosis: progress, challenges and potential directions. *Biochimie* 2013; **95**: 2326-2335 [PMID: 24036368 DOI: 10.1016/j.biochi.2013.09.003]
6 **Meier RPH**, Meyer J, Montanari E, Lacotte S, Balaphas A, Muller YD, Clément S, Negro F, Toso C, Morel P, Buhler LH. Interleukin-1 Receptor Antagonist Modulates Liver Inflammation and Fibrosis in Mice in a Model-Dependent Manner. *Int J Mol Sci* 2019; **20**: pii: E1295 [PMID: 30875826 DOI: 10.3390/ijms20061295]
7 **Huang H**, Deng Z. Adoptive transfer of regulatory T cells stimulated by Allogeneic Hepatic Stellate Cells mitigates liver injury in mice with concanavalin A-induced autoimmune hepatitis. *Biochem Biophys Res Commun* 2019; **512**: 14-21 [PMID: 30853178 DOI: 10.1016/j.bbrc.2019.02.147]
8 **Amiot L**, Vu N, Drenou B, Scrofani M, Chalin A, Devisme C, Samson M. The anti-fibrotic role of mast cells in the liver is mediated by HLA-G and interaction with hepatic stellate cells. *Cytokine* 2019; **117**: 50-58 [PMID: 30825834 DOI: 10.1016/j.cyto.2019.02.002]
9 **Chen XX**, Zhang XY, Ding YZ, Li X, Guan XM, Li H, Cheng M, Cui XD. [Effects of endothelial progenitor cells on proliferation and biological function of hepatic stellate cells under shear stress]. *Zhongguo Ying Yong Sheng Li Xue Za Zhi* 2018; **34**: 404-407 [PMID: 30788918 DOI: 10.12047/j.cjap.5624.2018.092]
10 **Lu P**, Yan M, He L, Li J, Ji Y, Ji J. Crosstalk between Epigenetic Modulations in Valproic Acid Deactivated Hepatic Stellate Cells: An Integrated Protein and miRNA Profiling Study. *Int J Biol Sci* 2019; **15**: 93-104 [PMID: 30662350 DOI: 10.7150/ijbs.28642]
11 **D'Ippolito D**, Pisano M. Dupilumab (Dupixent): An Interleukin-4 Receptor Antagonist for Atopic Dermatitis. *P T* 2018; **43**: 532-535 [PMID: 30186024]
12 **Li T**, Yang Y, Song H, Li H, Cui A, Liu Y, Su L, Crispe IN, Tu Z. Activated NK cells kill hepatic stellate cells via p38/PI3K signaling in a TRAIL-involved degranulation manner. *J Leukoc Biol* 2019; **105**: 695-704 [PMID: 30748035 DOI: 10.1002/JLB.2A0118-031RR]
13 **Feng J**, Chen K, Xia Y, Wu L, Li J, Li S, Wang W, Lu X, Liu T, Guo C. Salidroside ameliorates autophagy and activation of hepatic stellate cells in mice via NF-κB and TGF-β1/Smad3 pathways. *Drug Des Devel Ther* 2018; **12**: 1837-1853 [PMID: 29970958 DOI: 10.2147/DDDT.S162950]
14 **Bouwens L**, Baekeland M, De Zanger R, Wisse E. Quantitation, tissue distribution and proliferation kinetics of Kupffer cells in normal rat liver. *Hepatology* 1986; **6**: 718-722 [PMID: 3733004]
15 **Norona LM**, Nguyen DG, Gerber DA, Presnell SC, Mosedale M, Watkins PB. Bioprinted liver provides early insight into the role of Kupffer cells in TGF-β1 and methotrexate-induced fibrogenesis. *PLoS One* 2019; **14**: e0208958 [PMID: 30601836 DOI: 10.1371/journal.pone.0208958]
16 **Cai X**, Li Z, Zhang Q, Qu Y, Xu M, Wan X, Lu L. CXCL6-EGFR-induced Kupffer cells secrete TGF-β1 promoting hepatic stellate cell activation via the SMAD2/BRD4/C-MYC/EZH2 pathway in liver fibrosis. *J Cell Mol Med* 2018; **22**: 5050-5061 [PMID: 30106235 DOI: 10.1111/jcmm.13787]

17 **Zheng XF**, Hu XY, Ma B, Fang H, Zhang F, Mao YF, Yang FY, Xiao SC, Xia ZF. Interleukin-35 Attenuates D-Galactosamine/Lipopolysaccharide-Induced Liver Injury via Enhancing Interleukin-10 Production in Kupffer Cells. *Front Pharmacol* 2018; **9**: 959 [PMID: 30197594 DOI: 10.3389/fphar.2018.00959]

18 **Wu LL**, Peng WH, Wu HL, Miaw SC, Yeh SH, Yang HC, Liao PH, Lin JS, Chen YR, Hong YT, Wang HY, Chen PJ, Chen DS. Lymphocyte Antigen 6 Complex, Locus C⁺ Monocytes and Kupffer Cells Orchestrate Liver Immune Responses Against Hepatitis B Virus in Mice. *Hepatology* 2019; **69**: 2364-2380 [PMID: 30661248 DOI: 10.1002/hep.30510]

19 **Triantafyllou E**, Woollard KJ, McPhail MJW, Antoniades CG, Possamai LA. The Role of Monocytes and Macrophages in Acute and Acute-on-Chronic Liver Failure. *Front Immunol* 2018; **9**: 2948 [PMID: 30619308 DOI: 10.3389/fimmu.2018.02948]

20 **Ambade A**, Lowe P, Kodys K, Catalano D, Gyongyosi B, Cho Y, Iracheta-Vellve A, Adejumo A, Saha B, Calenda C, Mehta J, Lefebvre E, Vig P, Szabo G. Pharmacological Inhibition of CCR2/5 Signaling Prevents and Reverses Alcohol-Induced Liver Damage, Steatosis, and Inflammation in Mice. *Hepatology* 2019; **69**: 1105-1121 [PMID: 30179264 DOI: 10.1002/hep.30249]

21 **Daghestani MH**, Daghestani MH, Daghistani MH, Bjørklund G, Chirumbolo S, Warsy A. The influence of the rs1137101 genotypes of leptin receptor gene on the demographic and metabolic profile of normal Saudi females and those suffering from polycystic ovarian syndrome. *BMC Womens Health* 2019; **19**: 10 [PMID: 30635060 DOI: 10.1186/s12905-018-0706-x]

22 **Lynch RW**, Hawley CA, Pellicoro A, Bain CC, Iredale JP, Jenkins SJ. An efficient method to isolate Kupffer cells eliminating endothelial cell contamination and selective bias. *J Leukoc Biol* 2018; **104**: 579-586 [PMID: 29607532 DOI: 10.1002/JLB.1TA0517-169R]

23 **Inoue T**, Ito Y, Nishizawa N, Eshima K, Kojo K, Otaka F, Betto T, Yamane S, Tsujikawa K, Koizumi W, Majima M. RAMP1 in Kupffer cells is a critical regulator in immune-mediated hepatitis. *PLoS One* 2018; **13**: e0200432 [PMID: 30462657 DOI: 10.1371/journal.pone.0200432]

24 **Zhou S**, Gu J, Liu R, Wei S, Wang Q, Shen H, Dai Y, Zhou H, Zhang F, Lu L. Spermine Alleviates Acute Liver Injury by Inhibiting Liver-Resident Macrophage Pro-Inflammatory Response Through ATG5-Dependent Autophagy. *Front Immunol* 2018; **9**: 948 [PMID: 29770139 DOI: 10.3389/fimmu.2018.00948]

25 **Lan T**, Li C, Yang G, Sun Y, Zhuang L, Ou Y, Li H, Wang G, Kisseleva T, Brenner D, Guo J. Sphingosine kinase 1 promotes liver fibrosis by preventing miR-19b-3p-mediated inhibition of CCR2. *Hepatology* 2018; **68**: 1070-1086 [PMID: 29572892 DOI: 10.1002/hep.29885]

26 **Nakanishi K**. Unique Action of Interleukin-18 on T Cells and Other Immune Cells. *Front Immunol* 2018; **9**: 763 [PMID: 29731751 DOI: 10.3389/fimmu.2018.00763]

27 **Tang T**, Sui Y, Lian M, Li Z, Hua J. Pro-inflammatory activated Kupffer cells by lipids induce hepatic NKT cells deficiency through activation-induced cell death. *PLoS One* 2013; **8**: e81949 [PMID: 24312613 DOI: 10.1371/journal.pone.0081949]

28 **Liu C**, Wang G, Chen G, Mu Y, Zhang L, Hu X, Sun M, Liu C, Liu P. Huangqi decoction inhibits apoptosis and fibrosis, but promotes Kupffer cell activation in dimethylnitrosamine-induced rat liver fibrosis. *BMC Complement Altern Med* 2012; **12**: 51 [PMID: 22531084 DOI: 10.1186/1472-6882-12-51]

29 **López-Navarrete G**, Ramos-Martínez E, Suárez-Álvarez K, Aguirre-García J, Ledezma-Soto Y, León-Cabrera S, Gudiño-Zayas M, Guzmán C, Gutiérrez-Reyes G, Hernández-Ruíz J, Camacho-Arroyo I, Robles-Díaz G, Kershenobich D, Terrazas LI, Escobedo G. Th2-associated alternative Kupffer cell activation promotes liver fibrosis without inducing local inflammation. *Int J Biol Sci* 2011; **7**: 1273-1286 [PMID: 22110380 DOI: 10.7150/ijbs.7.1273]

30 **Hou X**, Hao X, Zheng M, Xu C, Wang J, Zhou R, Tian Z. CD205-TLR9-IL-12 axis contributes to CpG-induced oversensitive liver injury in HBsAg transgenic mice by promoting the interaction of NKT cells with Kupffer cells. *Cell Mol Immunol* 2017; **14**: 675-684 [PMID: 27041637 DOI: 10.1038/cmi.2015.111]

31 **Feng M**, Ding J, Wang M, Zhang J, Zhu X, Guan W. Kupffer-derived matrix metalloproteinase-9 contributes to liver fibrosis resolution. *Int J Biol Sci* 2018; **14**: 1033-1040 [PMID: 29989076 DOI: 10.7150/ijbs.25589]

32 **Mitra A**, Satelli A, Yan J, Xueqing X, Gagea M, Hunter CA, Mishra L, Li S. IL-30 (IL27p28) attenuates liver fibrosis through inducing NKG2D-rae1 interaction between NKT and activated hepatic stellate cells in mice. *Hepatology* 2014; **60**: 2027-2039 [PMID: 25351459 DOI: 10.1002/hep.27392]

33 **Langhans B**, Alwan AW, Krämer B, Glässner A, Lutz P, Strassburg CP, Nattermann J, Spengler U. Regulatory CD4+ T cells modulate the interaction between NK cells and hepatic stellate cells by acting on either cell type. *J Hepatol* 2015; **62**: 398-404 [PMID: 25195554 DOI: 10.1016/j.jhep.2014.08.038]

34 **Khoury T**, Mari A, Nseir W, Kadah A, Sbeit W, Mahamid M. Neutrophil-to-lymphocyte ratio is independently associated with inflammatory activity and fibrosis grade in nonalcoholic fatty liver disease. *Eur J Gastroenterol Hepatol* 2019 [PMID: 30888972 DOI: 10.1097/MEG.0000000000001393]

35 **Qin S**, Chen M, Guo X, Luo W, Wang J, Jiang H. The clinical significance of intrahepatic Th22 cells in liver cirrhosis. *Adv Clin Exp Med* 2019; **28**: 765-770 [PMID: 30740944 DOI: 10.17219/acem/94062]

36 **Krizhanovsky V**, Yon M, Dickins RA, Hearn S, Simon J, Miething C, Yee H, Zender L, Lowe SW. Senescence of activated stellate cells limits liver fibrosis. *Cell* 2008; **134**: 657-667 [PMID: 18724938 DOI: 10.1016/j.cell.2008.06.049]

37 **Hintermann E**, Bayer M, Pfeilschifter JM, Luster AD, Christen U. CXCL10 promotes liver fibrosis by prevention of NK cell mediated hepatic stellate cell inactivation. *J Autoimmun* 2010; **35**: 424-435 [PMID: 20932719 DOI: 10.1016/j.jaut.2010.09.003]

38 **Fabre T**, Kared H, Friedman SL, Shoukry NH. IL-17A enhances the expression of profibrotic genes through upregulation of the TGF-β receptor on hepatic stellate cells in a JNK-dependent manner. *J Immunol* 2014; **193**: 3925-3933 [PMID: 25210118 DOI: 10.4049/jimmunol.1400861]

39 **Farouk S**, Sabet S, Abu Zahra FA, El-Ghor AA. Bone marrow derived-mesenchymal stem cells downregulate IL17A dependent IL6/STAT3 signaling pathway in CCl4-induced rat liver fibrosis. *PLoS One* 2018; **13**: e0206130 [PMID: 30346985 DOI: 10.1371/journal.pone.0206130]

40 **Tang LX**, He RH, Yang G, Tan JJ, Zhou L, Meng XM, Huang XR, Lan HY. Asiatic acid inhibits liver fibrosis by blocking TGF-beta/Smad signaling in vivo and in vitro. *PLoS One* 2012; **7**: e31350 [PMID: 22363627 DOI: 10.1371/journal.pone.0031350]

41 **Pradere JP**, Kluwe J, De Minicis S, Jiao JJ, Gwak GY, Dapito DH, Jang MK, Guenther ND, Mederacke I, Friedman R, Dragomir AC, Aloman C, Schwabe RF. Hepatic macrophages but not dendritic cells contribute to liver fibrosis by promoting the survival of activated hepatic stellate cells in mice. *Hepatology* 2013; **58**: 1461-1473 [PMID: 23553591 DOI: 10.1002/hep.26429]

42 **Yakut M**, Özkan H, F Karakaya M, Erdal H. Diagnostic and Prognostic Role of Serum Interleukin-6 in

Malignant Transformation of Liver Cirrhosis. *Euroasian J Hepatogastroenterol* 2018; **8**: 23-30 [PMID: 29963457 DOI: 10.5005/jp-journals-10018-1253]

43 **Bulatova IA**, Schekotova AP, Paducheva SV, Dolgikh OV, Krivtsov AV, Tretyakova YI. [The significance of interleukin-6 and polymorphism of its gene (C174G) under viral, alcoholic and mixed cirrhosis of liver]. *Klin Lab Diagn* 2017; **62**: 100-103 [PMID: 30615393]

44 **Zimmermann HW**, Seidler S, Gassler N, Nattermann J, Luedde T, Trautwein C, Tacke F. Interleukin-8 is activated in patients with chronic liver diseases and associated with hepatic macrophage accumulation in human liver fibrosis. *PLoS One* 2011; **6**: e21381 [PMID: 21731723 DOI: 10.1371/journal.pone.0021381]

45 **Glass O**, Henao R, Patel K, Guy CD, Gruss HJ, Syn WK, Moylan CA, Streilein R, Hall R, Mae Diehl A, Abdelmalek MF. Serum Interleukin-8, Osteopontin, and Monocyte Chemoattractant Protein 1 Are Associated With Hepatic Fibrosis in Patients With Nonalcoholic Fatty Liver Disease. *Hepatol Commun* 2018; **2**: 1344-1355 [PMID: 30411081 DOI: 10.1002/hep4.1237]

46 **Guo X**, Cen Y, Wang J, Jiang H. CXCL10-induced IL-9 promotes liver fibrosis via Raf/MEK/ERK signaling pathway. *Biomed Pharmacother* 2018; **105**: 282-289 [PMID: 29860220 DOI: 10.1016/j.biopha.2018.05.128]

47 **Wang YQ**, Cao WJ, Gao YF, Ye J, Zou GZ. Serum interleukin-34 level can be an indicator of liver fibrosis in patients with chronic hepatitis B virus infection. *World J Gastroenterol* 2018; **24**: 1312-1320 [PMID: 29599606 DOI: 10.3748/wjg.v24.i12.1312]

48 **Du P**, Ma Q, Zhu ZD, Li G, Wang Y, Li QQ, Chen YF, Shang ZZ, Zhang J, Zhao L. Mechanism of Corilagin interference with IL-13/STAT6 signaling pathways in hepatic alternative activation macrophages in schistosomiasis-induced liver fibrosis in mouse model. *Eur J Pharmacol* 2016; **793**: 119-126 [PMID: 27845069 DOI: 10.1016/j.ejphar.2016.11.018]

49 **Shoji H**, Yoshio S, Mano Y, Kumagai E, Sugiyama M, Korenaga M, Arai T, Itokawa N, Atsukawa M, Aikata H, Hyogo H, Chayama K, Ohashi T, Ito K, Yoneda M, Nozaki Y, Kawaguchi T, Torimura T, Abe M, Hiasa Y, Fukai M, Kamiyama T, Taketomi A, Mizokami M, Kanto T. Interleukin-34 as a fibroblast-derived marker of liver fibrosis in patients with non-alcoholic fatty liver disease. *Sci Rep* 2016; **6**: 28814 [PMID: 27363523 DOI: 10.1038/srep28814]

50 **Preisser L**, Miot C, Le Guillou-Guillemette H, Beaumont E, Foucher ED, Garo E, Blanchard S, Frémaux I, Croué A, Fouchard I, Lunel-Fabiani F, Boursier J, Roingeard P, Calès P, Delneste Y, Jeannin P. IL-34 and macrophage colony-stimulating factor are overexpressed in hepatitis C virus fibrosis and induce profibrotic macrophages that promote collagen synthesis by hepatic stellate cells. *Hepatology* 2014; **60**: 1879-1890 [PMID: 25066464 DOI: 10.1002/hep.27328]

51 **Mandelia C**, Collyer E, Mansoor S, Lopez R, Lappe S, Nobili V, Alkhouri N. Plasma Cytokeratin-18 Level As a Novel Biomarker for Liver Fibrosis in Children With Nonalcoholic Fatty Liver Disease. *J Pediatr Gastroenterol Nutr* 2016; **63**: 181-187 [PMID: 26835904 DOI: 10.1097/MPG.0000000000001136]

52 **Ehling J**, Bartneck M, Wei X, Gremse F, Fech V, Möckel D, Baeck C, Hittatiya K, Eulberg D, Luedde T, Kiessling F, Trautwein C, Lammers T, Tacke F. CCL2-dependent infiltrating macrophages promote angiogenesis in progressive liver fibrosis. *Gut* 2014; **63**: 1960-1971 [PMID: 24561613 DOI: 10.1136/gutjnl-2013-306294]

53 **Tang LY**, Heller M, Meng Z, Yu LR, Tang Y, Zhou M, Zhang YE. Transforming Growth Factor-β (TGF-β) Directly Activates the JAK1-STAT3 Axis to Induce Hepatic Fibrosis in Coordination with the SMAD Pathway. *J Biol Chem* 2017; **292**: 4302-4312 [PMID: 28154170 DOI: 10.1074/jbc.M116.773085]

54 **Liu Y**, Liu H, Meyer C, Li J, Nadalin S, Königsrainer A, Weng H, Dooley S, ten Dijke P. Transforming growth factor-β (TGF-β)-mediated connective tissue growth factor (CTGF) expression in hepatic stellate cells requires Stat3 signaling activation. *J Biol Chem* 2013; **288**: 30708-30719 [PMID: 24005672 DOI: 10.1074/jbc.M113.478685]

55 **Tu X**, Zhang Y, Zheng X, Deng J, Li H, Kang Z, Cao Z, Huang Z, Ding Z, Dong L, Chen J, Zang Y, Zhang J. TGF-β-induced hepatocyte lincRNA-p21 contributes to liver fibrosis in mice. *Sci Rep* 2017; **7**: 2957 [PMID: 28592847 DOI: 10.1038/s41598-017-03175-0]

56 **Kamari Y**, Shaish A, Vax E, Shemesh S, Kandel-Kfir M, Arbel Y, Olteanu S, Barshack I, Dotan S, Voronov E, Dinarello CA, Apte RN, Harats D. Lack of interleukin-1α or interleukin-1β inhibits transformation of steatosis to steatohepatitis and liver fibrosis in hypercholesterolemic mice. *J Hepatol* 2011; **55**: 1086-1094 [PMID: 21354232 DOI: 10.1016/j.jhep.2011.01.048]

57 **de Lira Silva NS**, Borges BC, da Silva AA, de Castilhos P, Teixeira TL, Teixeira SC, Dos Santos MA, Servato JPS, Justino AB, Caixeta DC, Tomiosso TC, Espindola FS, da Silva CV. The Deleterious Impact of Interleukin 9 to Hepatorenal Physiology. *Inflammation* 2019; **42**: 1360-1369 [PMID: 30887397 DOI: 10.1007/s10753-019-00997-0]

58 **Hu BL**, Shi C, Lei RE, Lu DH, Luo W, Qin SY, Zhou Y, Jiang HX. Interleukin-22 ameliorates liver fibrosis through miR-200a/beta-catenin. *Sci Rep* 2016; **6**: 36436 [PMID: 27819314 DOI: 10.1038/srep36436]

59 **Liu Y**, Cheng LS, Wu SD, Wang SQ, Li L, She WM, Li J, Wang JY, Jiang W. IL-10-producing regulatory B-cells suppressed effector T-cells but enhanced regulatory T-cells in chronic HBV infection. *Clin Sci (Lond)* 2016; **130**: 907-919 [PMID: 26980345 DOI: 10.1042/CS20160069]

60 **Yao L**, Xing S, Fu X, Song H, Wang Z, Tang J, Zhao Y. Association between interleukin-10 gene promoter polymorphisms and susceptibility to liver cirrhosis. *Int J Clin Exp Pathol* 2015; **8**: 11680-11684 [PMID: 26617910]

61 **Zhang XW**, Mi S, Li Z, Zhou JC, Xie J, Hua F, Li K, Cui B, Lv XX, Yu JJ, Hu ZW. Antagonism of Interleukin-17A ameliorates experimental hepatic fibrosis by restoring the IL-10/STAT3-suppressed autophagy in hepatocytes. *Oncotarget* 2017; **8**: 9922-9934 [PMID: 28039485 DOI: 10.18632/oncotarget.14266]

62 **Lu DH**, Guo XY, Qin SY, Luo W, Huang XL, Chen M, Wang JX, Ma SJ, Yang XW, Jiang HX. Interleukin-22 ameliorates liver fibrogenesis by attenuating hepatic stellate cell activation and downregulating the levels of inflammatory cytokines. *World J Gastroenterol* 2015; **21**: 1531-1545 [PMID: 25663772 DOI: 10.3748/wjg.v21.i5.1531]

63 **Kong X**, Feng D, Wang H, Hong F, Bertola A, Wang FS, Gao B. Interleukin-22 induces hepatic stellate cell senescence and restricts liver fibrosis in mice. *Hepatology* 2012; **56**: 1150-1159 [PMID: 22473749 DOI: 10.1002/hep.25744]

64 **Ni YH**, Huo LJ, Li TT. Antioxidant axis Nrf2-keap1-ARE in inhibition of alcoholic liver fibrosis by IL-22. *World J Gastroenterol* 2017; **23**: 2002-2011 [PMID: 28373766 DOI: 10.3748/wjg.v23.i11.2002]

65 **Pan H**, Hong F, Radaeva S, Gao B. Hydrodynamic gene delivery of interleukin-22 protects the mouse

liver from concanavalin A-, carbon tetrachloride-, and Fas ligand-induced injury via activation of STAT3. *Cell Mol Immunol* 2004; **1**: 43-49 [PMID: 16212920]

66 **Zenewicz LA**, Yancopoulos GD, Valenzuela DM, Murphy AJ, Karow M, Flavell RA. Interleukin-22 but not interleukin-17 provides protection to hepatocytes during acute liver inflammation. *Immunity* 2007; **27**: 647-659 [PMID: 17919941 DOI: 10.1016/j.immuni.2007.07.023]

67 **Radaeva S**, Sun R, Pan HN, Hong F, Gao B. Interleukin 22 (IL-22) plays a protective role in T cell-mediated murine hepatitis: IL-22 is a survival factor for hepatocytes via STAT3 activation. *Hepatology* 2004; **39**: 1332-1342 [PMID: 15122762 DOI: 10.1002/hep.20184]

68 **Wu LY**, Liu S, Liu Y, Guo C, Li H, Li W, Jin X, Zhang K, Zhao P, Wei L, Zhao J. Up-regulation of interleukin-22 mediates liver fibrosis via activating hepatic stellate cells in patients with hepatitis C. *Clin Immunol* 2015; **158**: 77-87 [PMID: 25771172 DOI: 10.1016/j.clim.2015.03.003]

69 **Zhao J**, Zhang Z, Luan Y, Zou Z, Sun Y, Li Y, Jin L, Zhou C, Fu J, Gao B, Fu Y, Wang FS. Pathological functions of interleukin-22 in chronic liver inflammation and fibrosis with hepatitis B virus infection by promoting T helper 17 cell recruitment. *Hepatology* 2014; **59**: 1331-1342 [PMID: 24677193 DOI: 10.1002/hep.26916]

70 **Chen E**, Cen Y, Lu D, Luo W, Jiang H. IL-22 inactivates hepatic stellate cells via downregulation of the TGF-β1/Notch signaling pathway. *Mol Med Rep* 2018; **17**: 5449-5453 [PMID: 29393435 DOI: 10.3892/mmr.2018.8516]

71 **Hassoba H**, Leheta O, Sayed A, Fahmy H, Fathy A, Abbas F, Attia F, Serwah A. IL-10 and IL-12p40 in Egyptian patients with HCV-related chronic liver disease. *Egypt J Immunol* 2003; **10**: 1-8 [PMID: 15719617]

72 **Khanam A**, Trehanpati N, Sarin SK. Increased interleukin-23 receptor (IL-23R) expression is associated with disease severity in acute-on-chronic liver failure. *Liver Int* 2019; **39**: 1062-1070 [PMID: 30506912 DOI: 10.1111/liv.14015]

73 **Bao S**, Zheng J, Li N, Huang C, Chen M, Cheng Q, Li Q, Lu Q, Zhu M, Ling Q, Yu K, Chen S, Shi G. Role of interleukin-23 in monocyte-derived dendritic cells of HBV-related acute-on-chronic liver failure and its correlation with the severity of liver damage. *Clin Res Hepatol Gastroenterol* 2017; **41**: 147-155 [PMID: 28041935 DOI: 10.1016/j.clinre.2016.10.005]

74 **Meng Z**, Wang J, Yuan Y, Cao G, Fan S, Gao C, Wang L, Li Z, Wu X, Wu Z, Zhao L, Yin Z. γδ T cells are indispensable for interleukin-23-mediated protection against Concanavalin A-induced hepatitis in hepatitis B virus transgenic mice. *Immunology* 2017; **151**: 43-55 [PMID: 28092402 DOI: 10.1111/imm.12712]

75 **Karlmark KR**, Weiskirchen R, Zimmermann HW, Gassler N, Ginhoux F, Weber C, Merad M, Luedde T, Trautwein C, Tacke F. Hepatic recruitment of the inflammatory Gr1+ monocyte subset upon liver injury promotes hepatic fibrosis. *Hepatology* 2009; **50**: 261-274 [PMID: 19554540 DOI: 10.1002/hep.22950]

76 **Li J**, Wang Y, Ma M, Jiang S, Zhang X, Zhang Y, Yang X, Xu C, Tian G, Li Q, Wang Y, Zhu L, Nie H, Feng M, Xia Q, Gu J, Xu Q, Zhang Z. Autocrine CTHRC1 activates hepatic stellate cells and promotes liver fibrosis by activating TGF-β signaling. *EBioMedicine* 2019; **40**: 43-55 [PMID: 30639416 DOI: 10.1016/j.ebiom.2019.01.009]

77 **Sui G**, Cheng G, Yuan J, Hou X, Kong X, Niu H. Interleukin (IL)-13, Prostaglandin E2 (PGE2), and Prostacyclin 2 (PGI2) Activate Hepatic Stellate Cells via Protein kinase C (PKC) Pathway in Hepatic Fibrosis. *Med Sci Monit* 2018; **24**: 2134-2141 [PMID: 29633755 DOI: 10.12659/msm.906442]

78 **Pan G**, Zhao Z, Tang C, Ding L, Li Z, Zheng D, Zong L, Wu Z. Soluble fibrinogen-like protein 2 ameliorates acute rejection of liver transplantation in rat via inducing Kupffer cells M2 polarization. *Cancer Med* 2018 [PMID: 29749104 DOI: 10.1002/cam4.1528]

79 **Niu L**, Cui X, Qi Y, Xie D, Wu Q, Chen X, Ge J, Liu Z. Involvement of TGF-β1/Smad3 Signaling in Carbon Tetrachloride-Induced Acute Liver Injury in Mice. *PLoS One* 2016; **11**: e0156090 [PMID: 27224286 DOI: 10.1371/journal.pone.0156090]

80 **Shi J**, Zhao J, Zhang X, Cheng Y, Hu J, Li Y, Zhao X, Shang Q, Sun Y, Tu B, Shi L, Gao B, Wang FS, Zhang Z. Activated hepatic stellate cells impair NK cell anti-fibrosis capacity through a TGF-β-dependent emperipolesis in HBV cirrhotic patients. *Sci Rep* 2017; **7**: 44544 [PMID: 28291251 DOI: 10.1038/srep44544]

81 **Hu Z**, Qin F, Gao S, Zhen Y, Huang D, Dong L. Paeoniflorin exerts protective effect on radiation-induced hepatic fibrosis in rats via TGF-β1/Smads signaling pathway. *Am J Transl Res* 2018; **10**: 1012-1021 [PMID: 29636890]

82 **Lee JH**, Jang EJ, Seo HL, Ku SK, Lee JR, Shin SS, Park SD, Kim SC, Kim YW. Sauchinone attenuates liver fibrosis and hepatic stellate cell activation through TGF-β/Smad signaling pathway. *Chem Biol Interact* 2014; **224**: 58-67 [PMID: 25451574 DOI: 10.1016/j.cbi.2014.10.005]

83 **Yang JH**, Kim SC, Kim KM, Jang CH, Cho SS, Kim SJ, Ku SK, Cho IJ, Ki SH. Isorhamnetin attenuates liver fibrosis by inhibiting TGF-β/Smad signaling and relieving oxidative stress. *Eur J Pharmacol* 2016; **783**: 92-102 [PMID: 27151496 DOI: 10.1016/j.ejphar.2016.04.042]

84 **Kim JY**, An HJ, Kim WH, Gwon MG, Gu H, Park YY, Park KK. Anti-fibrotic Effects of Synthetic Oligodeoxynucleotide for TGF-β1 and Smad in an Animal Model of Liver Cirrhosis. *Mol Ther Nucleic Acids* 2017; **8**: 250-263 [PMID: 28918026 DOI: 10.1016/j.omtn.2017.06.022]

85 **Ghafoory S**, Varshney R, Robison T, Kouzbari K, Woolington S, Murphy B, Xia L, Ahamed J. Platelet TGF-β1 deficiency decreases liver fibrosis in a mouse model of liver injury. *Blood Adv* 2018; **2**: 470-480 [PMID: 29490978 DOI: 10.1182/bloodadvances.2017010868]

86 **Li Y**, Lua I, French SW, Asahina K. Role of TGF-β signaling in differentiation of mesothelial cells to vitamin A-poor hepatic stellate cells in liver fibrosis. *Am J Physiol Gastrointest Liver Physiol* 2016; **310**: G262-G272 [PMID: 26702136 DOI: 10.1152/ajpgi.00257.2015]

87 **Lei Y**, Wang QL, Shen L, Tao YY, Liu CH. MicroRNA-101 suppresses liver fibrosis by downregulating PI3K/Akt/mTOR signaling pathway. *Clin Res Hepatol Gastroenterol* 2019; **pii**: S2210-7401(19)30041-5 [PMID: 30857885 DOI: 10.1016/j.clinre.2019.02.003]

88 **Wang J**, Chu ES, Chen HY, Man K, Go MY, Huang XR, Lan HY, Sung JJ, Yu J. microRNA-29b prevents liver fibrosis by attenuating hepatic stellate cell activation and inducing apoptosis through targeting PI3K/AKT pathway. *Oncotarget* 2015; **6**: 7325-7338 [PMID: 25356754 DOI: 10.18632/oncotarget.2621]

89 **Liang C**, Bu S, Fan X. Suppressive effect of microRNA-29b on hepatic stellate cell activation and its crosstalk with TGF-β1/Smad3. *Cell Biochem Funct* 2016; **34**: 326-333 [PMID: 27273381 DOI: 10.1002/cbf.3193]

90 **Feili X**, Wu S, Ye W, Tu J, Lou L. MicroRNA-34a-5p inhibits liver fibrosis by regulating TGF-β1/Smad3

pathway in hepatic stellate cells. *Cell Biol Int* 2018; **42**: 1370-1376 [PMID: 29957876 DOI: 10.1002/cbin.11022]

91 **Wang Y**, Du J, Niu X, Fu N, Wang R, Zhang Y, Zhao S, Sun D, Nan Y. MiR-130a-3p attenuates activation and induces apoptosis of hepatic stellate cells in nonalcoholic fibrosing steatohepatitis by directly targeting TGFBR1 and TGFBR2. *Cell Death Dis* 2017; **8**: e2792 [PMID: 28518142 DOI: 10.1038/cddis.2017.10]

92 **Ning ZW**, Luo XY, Wang GZ, Li Y, Pan MX, Yang RQ, Ling XG, Huang S, Ma XX, Jin SY, Wang D, Li X. MicroRNA-21 Mediates Angiotensin II-Induced Liver Fibrosis by Activating NLRP3 Inflammasome/IL-1β Axis via Targeting Smad7 and Spry1. *Antioxid Redox Signal* 2017; **27**: 1-20 [PMID: 27502441 DOI: 10.1089/ars.2016.6669]

93 **Yu F**, Lu Z, Huang K, Wang X, Xu Z, Chen B, Dong P, Zheng J. MicroRNA-17-5p-activated Wnt/β-catenin pathway contributes to the progression of liver fibrosis. *Oncotarget* 2016; **7**: 81-93 [PMID: 26637809 DOI: 10.18632/oncotarget.6447]

94 **Yu F**, Guo Y, Chen B, Dong P, Zheng J. MicroRNA-17-5p activates hepatic stellate cells through targeting of Smad7. *Lab Invest* 2015; **95**: 781-789 [PMID: 25915722 DOI: 10.1038/labinvest.2015.58]

95 **Yang X**, Dan X, Men R, Ma L, Wen M, Peng Y, Yang L. MiR-142-3p blocks TGF-β-induced activation of hepatic stellate cells through targeting TGFβRI. *Life Sci* 2017; **187**: 22-30 [PMID: 28823564 DOI: 10.1016/j.lfs.2017.08.017]

96 **Besheer T**, Elalfy H, Abd El-Maksoud M, Abd El-Razek A, Taman S, Zalata K, Elkashef W, Zaghloul H, Elshahawy H, Raafat D, Elemshaty W, Elsayed E, El-Gilany AH, El-Bendary M. Diffusion-weighted magnetic resonance imaging and micro-RNA in the diagnosis of hepatic fibrosis in chronic hepatitis C virus. *World J Gastroenterol* 2019; **25**: 1366-1377 [PMID: 30918429 DOI: 10.3748/wjg.v25.i11.1366]

97 **Ma T**, Cai X, Wang Z, Huang L, Wang C, Jiang S, Hua Y, Liu Q. miR-200c Accelerates Hepatic Stellate Cell-Induced Liver Fibrosis via Targeting the FOG2/PI3K Pathway. *Biomed Res Int* 2017; **2017**: 2670658 [PMID: 28691020 DOI: 10.1155/2017/2670658]

98 **Saikia P**, Bellos D, McMullen MR, Pollard KA, de la Motte C, Nagy LE. MicroRNA 181b-3p and its target importin α5 regulate toll-like receptor 4 signaling in Kupffer cells and liver injury in mice in response to ethanol. *Hepatology* 2017; **66**: 602-615 [PMID: 28257601 DOI: 10.1002/hep.29144]

99 **Ju B**, Nie Y, Yang X, Wang X, Li F, Wang M, Wang C, Zhang H. miR-193a/b-3p relieves hepatic fibrosis and restrains proliferation and activation of hepatic stellate cells. *J Cell Mol Med* 2019; **23**: 3824-3832 [PMID: 30945448 DOI: 10.1111/jcmm.14210]

100 **Ma L**, Ma J, Ou HL. MicroRNA219 overexpression serves a protective role during liver fibrosis by targeting tumor growth factor β receptor 2. *Mol Med Rep* 2019; **19**: 1543-1550 [PMID: 30592264 DOI: 10.3892/mmr.2018.9787]

101 **Yang L**, Dong C, Yang J, Yang L, Chang N, Qi C, Li L. MicroRNA-26b-5p Inhibits Mouse Liver Fibrogenesis and Angiogenesis by Targeting PDGF Receptor-Beta. *Mol Ther Nucleic Acids* 2019; **16**: 206-217 [PMID: 30901579 DOI: 10.1016/j.omtn.2019.02.014]

102 **Men R**, Wen M, Zhao M, Dan X, Yang Z, Wu W, Wang MH, Liu X, Yang L. MircoRNA-145 promotes activation of hepatic stellate cells via targeting krüppel-like factor 4. *Sci Rep* 2017; **7**: 40468 [PMID: 28091538 DOI: 10.1038/srep40468]

103 **Mandrekar P**. Epigenetic regulation in alcoholic liver disease. *World J Gastroenterol* 2011; **17**: 2456-2464 [PMID: 21633650 DOI: 10.3748/wjg.v17.i20.2456]

104 **Fakhir FZ**, Lkhider M, Badre W, Alaoui R, Meurs EF, Pineau P, Ezzikouri S, Benjelloun S. Genetic variations in toll-like receptors 7 and 8 modulate natural hepatitis C outcomes and liver disease progression. *Liver Int* 2018; **38**: 432-442 [PMID: 28752959 DOI: 10.1111/liv.13533]

105 **El-Bendary M**, Neamatallah M, Elalfy H, Besheer T, Elkholi A, El-Diasty M, Elsareef M, Zahran M, El-Aarag B, Gomaa A, Elhammady D, El-Setouhy M, Hegazy A, Esmat G. The association of single nucleotide polymorphisms of Toll-like receptor 3, Toll-like receptor 7 and Toll-like receptor 8 genes with the susceptibility to HCV infection. *Br J Biomed Sci* 2018; **75**: 175-181 [PMID: 29947302 DOI: 10.1080/09674845.2018.1492186]

106 **Liu J**, Yu Q, Wu W, Huang X, Broering R, Werner M, Roggendorf M, Yang D, Lu M. TLR2 Stimulation Strengthens Intrahepatic Myeloid-Derived Cell-Mediated T Cell Tolerance through Inducing Kupffer Cell Expansion and IL-10 Production. *J Immunol* 2018; **200**: 2341-2351 [PMID: 29459406 DOI: 10.4049/jimmunol.1700540]

107 **Li M**, Sun R, Xu L, Yin W, Chen Y, Zheng X, Lian Z, Wei H, Tian Z. Kupffer Cells Support Hepatitis B Virus-Mediated CD8+ T Cell Exhaustion via Hepatitis B Core Antigen-TLR2 Interactions in Mice. *J Immunol* 2015; **195**: 3100-3109 [PMID: 26304988 DOI: 10.4049/jimmunol.1500839]

108 **Bagheri V**, Askari A, Arababadi MK, Kennedy D. Can Toll-Like Receptor (TLR) 2 be considered as a new target for immunotherapy against hepatitis B infection? *Hum Immunol* 2014; **75**: 549-554 [PMID: 24530748 DOI: 10.1016/j.humimm.2014.02.018]

109 **Lee YS**, Kim DY, Kim TJ, Kim SY, Jeong JM, Jeong WI, Jung JK, Choi JK, Yi HS, Byun JS. Loss of toll-like receptor 3 aggravates hepatic inflammation but ameliorates steatosis in mice. *Biochem Biophys Res Commun* 2018; **497**: 957-962 [PMID: 29410095 DOI: 10.1016/j.bbrc.2018.01.191]

110 **Gong XW**, Xu YJ, Yang QH, Liang YJ, Zhang YP, Wang GL, Li YY. Effect of Soothing Gan (Liver) and Invigorating Pi (Spleen) Recipes on TLR4-p38 MAPK Pathway in Kupffer Cells of Non-alcoholic Steatohepatitis Rats. *Chin J Integr Med* 2019; **25**: 216-224 [PMID: 29335857 DOI: 10.1007/s11655-018-2829-6]

111 **Seo W**, Eun HS, Kim SY, Yi HS, Lee YS, Park SH, Jang MJ, Jo E, Kim SC, Han YM, Park KG, Jeong WI. Exosome-mediated activation of toll-like receptor 3 in stellate cells stimulates interleukin-17 production by γδ T cells in liver fibrosis. *Hepatology* 2016; **64**: 616-631 [PMID: 27178735 DOI: 10.1002/hep.28644]

112 **Zhang M**, Hu X, Li S, Lu C, Li J, Zong Y, Qi W, Yang H. Hepatoprotective effects of ethyl pyruvate against CCl4-induced hepatic fibrosis via inhibition of TLR4/NF-κB signaling and up-regulation of MMPs/TIMPs ratio. *Clin Res Hepatol Gastroenterol* 2018; **42**: 72-81 [PMID: 28601590 DOI: 10.1016/j.clinre.2017.04.008]

113 **Etienne-Mesmin L**, Vijay-Kumar M, Gewirtz AT, Chassaing B. Hepatocyte Toll-Like Receptor 5 Promotes Bacterial Clearance and Protects Mice Against High-Fat Diet-Induced Liver Disease. *Cell Mol Gastroenterol Hepatol* 2016; **2**: 584-604 [PMID: 28090564 DOI: 10.1016/j.jcmgh.2016.04.007]

114 **Kwon EY**, Choi MS. Luteolin Targets the Toll-Like Receptor Signaling Pathway in Prevention of Hepatic and Adipocyte Fibrosis and Insulin Resistance in Diet-Induced Obese Mice. *Nutrients* 2018; **10** [PMID: 30282902 DOI: 10.3390/nu10101415]

115 **Roh YS**, Zhang B, Loomba R, Seki E. TLR2 and TLR9 contribute to alcohol-mediated liver injury through induction of CXCL1 and neutrophil infiltration. *Am J Physiol Gastrointest Liver Physiol* 2015; **309**: G30-G41 [PMID: 25930080 DOI: 10.1152/ajpgi.00031.2015]

116 **Roh YS**, Park S, Kim JW, Lim CW, Seki E, Kim B. Toll-like receptor 7-mediated type I interferon signaling prevents cholestasis- and hepatotoxin-induced liver fibrosis. *Hepatology* 2014; **60**: 237-249 [PMID: 24375615 DOI: 10.1002/hep.26981]

117 **He YJ**, Kuchta K, Deng YM, Cameron S, Lin Y, Liu XY, Ye GR, Lv X, Kobayashi Y, Shu JC. Curcumin Promotes Apoptosis of Activated Hepatic Stellate Cells by Inhibiting Protein Expression of the MyD88 Pathway. *Planta Med* 2017; **83**: 1392-1396 [PMID: 28628927 DOI: 10.1055/s-0043-113044]

118 **Meng F**, Wang K, Aoyama T, Grivennikov SI, Paik Y, Scholten D, Cong M, Iwaisako K, Liu X, Zhang M, Österreicher CH, Stickel F, Ley K, Brenner DA, Kisseleva T. Interleukin-17 signaling in inflammatory, Kupffer cells, and hepatic stellate cells exacerbates liver fibrosis in mice. *Gastroenterology* 2012; **143**: 765-776.e3 [PMID: 22687286 DOI: 10.1053/j.gastro.2012.05.049]

119 **Miller AM**, Wang H, Bertola A, Park O, Horiguchi N, Ki SH, Yin S, Lafdil F, Gao B. Inflammation-associated interleukin-6/signal transducer and activator of transcription 3 activation ameliorates alcoholic and nonalcoholic fatty liver diseases in interleukin-10-deficient mice. *Hepatology* 2011; **54**: 846-856 [PMID: 21725996 DOI: 10.1002/hep.24517]

120 **Campana L**, Starkey Lewis PJ, Pellicoro A, Aucott RL, Man J, O'Duibhir E, Mok SE, Ferreira-Gonzalez S, Livingstone E, Greenhalgh SN, Hull KL, Kendall TJ, Vernimmen D, Henderson NC, Boulter L, Gregory CD, Feng Y, Anderton SM, Forbes SJ, Iredale JP. The STAT3-IL-10-IL-6 Pathway Is a Novel Regulator of Macrophage Efferocytosis and Phenotypic Conversion in Sterile Liver Injury. *J Immunol* 2018; **200**: 1169-1187 [PMID: 29263216 DOI: 10.4049/jimmunol.1701247]

121 **Katsounas A**, Trippler M, Wang B, Polis M, Lempicki RA, Kottilil S, Gerken G, Schlaak JF. CCL5 mRNA is a marker for early fibrosis in chronic hepatitis C and is regulated by interferon-α therapy and toll-like receptor 3 signalling. *J Viral Hepat* 2012; **19**: 128-137 [PMID: 22239502 DOI: 10.1111/j.1365-2893.2011.01503.x]

122 **Svinka J**, Pflügler S, Mair M, Marschall HU, Hengstler JG, Stiedl P, Poli V, Casanova E, Timelthaler G, Sibilia M, Eferl R. Epidermal growth factor signaling protects from cholestatic liver injury and fibrosis. *J Mol Med (Berl)* 2017; **95**: 109-117 [PMID: 27568040 DOI: 10.1007/s00109-016-1462-8]

123 **Kagan P**, Sultan M, Tachlytski I, Safran M, Ben-Ari Z. Both MAPK and STAT3 signal transduction pathways are necessary for IL-6-dependent hepatic stellate cells activation. *PLoS One* 2017; **12**: e0176173 [PMID: 28472150 DOI: 10.1371/journal.pone.0176173]

124 **Choi S**, Jung HJ, Kim MW, Kang JH, Shin D, Jang YS, Yoon YS, Oh SH. A novel STAT3 inhibitor, STX-0119, attenuates liver fibrosis by inactivating hepatic stellate cells in mice. *Biochem Biophys Res Commun* 2019; **513**: 49-55 [PMID: 30935693 DOI: 10.1016/j.bbrc.2019.03.156]

125 **Lee KJ**, Jang YO, Cha SK, Kim MY, Park KS, Eom YW, Baik SK. Expression of Fibroblast Growth Factor 21 and β-Klotho Regulates Hepatic Fibrosis through the Nuclear Factor-κB and c-Jun N-Terminal Kinase Pathways. *Gut Liver* 2018; **12**: 449-456 [PMID: 29699061 DOI: 10.5009/gnl17443]

126 **Ben-Shoshan SO**, Kagan P, Sultan M, Barabash Z, Dor C, Jacob-Hirsch J, Harmelin A, Pappo O, Marcu-Malina V, Ben-Ari Z, Amariglio N, Rechavi G, Goldstein I, Safran M. ADAR1 deletion induces NFκB and interferon signaling dependent liver inflammation and fibrosis. *RNA Biol* 2017; **14**: 587-602 [PMID: 27362366 DOI: 10.1080/15476286.2016.1203501]

127 **Rong X**, Liu J, Yao X, Jiang T, Wang Y, Xie F. Human bone marrow mesenchymal stem cells-derived exosomes alleviate liver fibrosis through the Wnt/β-catenin pathway. *Stem Cell Res Ther* 2019; **10**: 98 [PMID: 30885249 DOI: 10.1186/s13287-019-1204-2]

128 **Shen YH**, Jiang HX, Qin SY, Wei LP, Meng YC, Luo W. [Activation of hepatocyte growth factor promotes apoptosis of hepatic stellate cells via the Rho pathway]. *Zhonghua Gan Zang Bing Za Zhi* 2014; **22**: 136-141 [PMID: 24735597 DOI: 10.3760/cma.j.issn.1007-3418.2014.02.013]

129 **Oh Y**, Park O, Swierczewska M, Hamilton JP, Park JS, Kim TH, Lim SM, Eom H, Jo DG, Lee CE, Kechrid R, Mastorakos P, Zhang C, Hahn SK, Jeon OC, Byun Y, Kim K, Hanes J, Lee KC, Pomper MG, Gao B, Lee S. Systemic PEGylated TRAIL treatment ameliorates liver cirrhosis in rats by eliminating activated hepatic stellate cells. *Hepatology* 2016; **64**: 209-223 [PMID: 26710118 DOI: 10.1002/hep.28432]

130 **Henderson WR**, Chi EY, Ye X, Nguyen C, Tien YT, Zhou B, Borok Z, Knight DA, Kahn M. Inhibition of Wnt/beta-catenin/CREB binding protein (CBP) signaling reverses pulmonary fibrosis. *Proc Natl Acad Sci U S A* 2010; **107**: 14309-14314 [PMID: 20660310 DOI: 10.1073/pnas.1001520107]

131 **Sombetzki M**, Fuchs CD, Fickert P, Österreicher CH, Mueller M, Claudel T, Loebermann M, Engelmann R, Langner C, Sahin E, Schwinge D, Guenther ND, Schramm C, Mueller-Hilke B, Reisinger EC, Trauner M. 24-nor-ursodeoxycholic acid ameliorates inflammatory response and liver fibrosis in a murine model of hepatic schistosomiasis. *J Hepatol* 2015; **62**: 871-878 [PMID: 25463533 DOI: 10.1016/j.jhep.2014.11.020]

132 **Lefebvre E**, Gottwald M, Lasseter K, Chang W, Willett M, Smith PF, Somasunderam A, Utay NS. Pharmacokinetics, Safety, and CCR2/CCR5 Antagonist Activity of Cenicriviroc in Participants With Mild or Moderate Hepatic Impairment. *Clin Transl Sci* 2016; **9**: 139-148 [PMID: 27169903 DOI: 10.1111/cts.12397]

133 **Qu K**, Huang Z, Lin T, Liu S, Chang H, Yan Z, Zhang H, Liu C. New Insight into the Anti-liver Fibrosis Effect of Multitargeted Tyrosine Kinase Inhibitors: From Molecular Target to Clinical Trials. *Front Pharmacol* 2016; **6**: 300 [PMID: 26834633 DOI: 10.3389/fphar.2015.00300]

134 **Zhao Z**, Pan G, Tang C, Li Z, Zheng D, Wei X, Wu Z. IL-34 Inhibits Acute Rejection of Rat Liver Transplantation by Inducing Kupffer Cell M2 Polarization. *Transplantation* 2018; **102**: e265-e274 [PMID: 29570162 DOI: 10.1097/TP.0000000000002194]

World Journal of Gastroenterology

Submit a Manuscript: https://www.f6publishing.com

World J Gastroenterol 2019 September 7; 25(33): 4850-4869

DOI: 10.3748/wjg.v25.i33.4850

ISSN 1007-9327 (print) ISSN 2219-2840 (online)

MINIREVIEWS

Neoadjuvant radiotherapy for rectal cancer management

Gerard Feeney, Rishabh Sehgal, Margaret Sheehan, Aisling Hogan, Mark Regan, Myles Joyce, Michael Kerin

ORCID number: Gerard Feeney (0000-0002-1527-793X); Rishabh Sehgal (0000-0002-1905-3378); Margaret Sheehan (0000-0001-5475-392X); Aisling Hogan (0000-0002-8166-732X); Mark Regan (0000-0003-1348-7877); Myles Joyce (0000-0002-9102-8636); Michael Kerin (0000-0003-4164-5561).

Author contributions: All authors contributed equally to this paper. All authors had equal input in conception, literature review, drafting, editing and final approval of the paper.

Supported by NBCRI, Symptomatic Breast Unit, University Hospital Galway.

Conflict-of-interest statement: There is no conflict of interest associated with any of the senior authors or other coauthors contributed their efforts in this manuscript.

Manuscript source: Invited manuscript

Received: May 9, 2019

Gerard Feeney, Rishabh Sehgal, Aisling Hogan, Mark Regan, Myles Joyce, Michael Kerin, Department of General/Colorectal Surgery, Galway University Hospital, Galway H91 YR71, Ireland

Margaret Sheehan, Department of Histopathology, Galway University Hospital, Galway H91 YR71, Ireland

Corresponding author: Gerard Feeney, MBChB, Doctor, Department of General/Colorectal Surgery, Lambe Institute, Galway University Hospital, Newcastle Road, Galway H91 YR71, Ireland. g.feeney3@outlook.com
Telephone: +353-91-524222

Abstract

Thirty per cent of all colorectal tumours develop in the rectum. The location of the rectum within the bony pelvis and its proximity to vital structures presents significant therapeutic challenges when considering neoadjuvant options and surgical interventions. Most patients with early rectal cancer can be adequately managed by surgery alone. However, a significant proportion of patients with rectal cancer present with locally advanced disease and will potentially benefit from down staging prior to surgery. Neoadjuvant therapy involves a variety of options including radiotherapy, chemotherapy used alone or in combination. Neoadjuvant radiotherapy in rectal cancer has been shown to be effective in reducing tumour burden in advance of curative surgery. The gold standard surgical rectal cancer management aims to achieve surgical removal of the tumour and all draining lymph nodes, within an intact mesorectal package, in order to minimise local recurrence. It is critically important that all rectal cancer cases are discussed at a multidisciplinary meeting represented by all relevant specialties. Pre-operative staging including CT thorax, abdomen, pelvis to assess for distal disease and magnetic resonance imaging to assess local involvement is essential. Staging radiology and MDT discussion are integral in identifying patients who require neoadjuvant radiotherapy. While Neoadjuvant radiotherapy is potentially beneficial it may also result in morbidity and thus should be reserved for those patients who are at a high risk of local failure, which includes patients with nodal involvement, extramural venous invasion and threatened circumferential margin. The aim of this review is to discuss the role of neoadjuvant radiotherapy in the management of rectal cancer.

Key words: Rectal cancer; Neoadjuvant therapy; Low anterior resection syndrome; Stoma; Transanal endoscopic microsurgery; Trans-anal total mesorectal excision; Robotic surgery; Watch and wait

Peer-review started: May 10, 2019
First decision: July 21, 2019
Revised: July 28, 2019
Accepted: August 7, 2019
Article in press: August 7, 2019
Published online: September 7, 2019

P-Reviewer: Brisinda G, Gerard JP, Horne J, Perse M
S-Editor: Ma RY
L-Editor: A
E-Editor: Ma YJ

Core tip: Neoadjuvant radiotherapy aims to downstage tumours for a more effective oncological resection. Studies have shown that both long and short course pre-operative radiotherapy confers benefits to local recurrence. Some patients completely respond to radiotherapy and have been enrolled in surveillance programmes without undergoing surgery. It is essential to be aware of the disadvantages associated with radiotherapy. Radiation therapy increases the risk of anorectal and genitourinary dysfunction which have a deleterious impact on quality of life. Thus it is imperative to accurately identify patients who are likely to benefit from neoadjuvant radiotherapy in order to minimise morbidity and improve patient outcomes.

Citation: Feeney G, Sehgal R, Sheehan M, Hogan A, Regan M, Joyce M, Kerin M. Neoadjuvant radiotherapy for rectal cancer management. *World J Gastroenterol* 2019; 25(33): 4850-4869
URL: https://www.wjgnet.com/1007-9327/full/v25/i33/4850.htm
DOI: https://dx.doi.org/10.3748/wjg.v25.i33.4850

INTRODUCTION

Colorectal cancer (CRC) is the third most common cancer diagnosed in both sexes in the Western World. In 2019 there were approximately 44180 new cases of rectal cancer diagnosed in the United States[1]. Several risk factors have been implicated in rectal tumorigenesis including genetics, age, obesity, smoking, and diet. Cancers of the rectum and rectosigmoid junction account for 30% of all CRC diagnosed. Rectal cancer is defined as tumours arising within 15 cm of the anal verge. While histologically similar to cancers occurring at other sites in the colon, rectal cancers, given the anatomical confinements of the bony pelvis, blood supply, lymphatic drainage and nervous innervation rectal cancer are considered a distinct entity, specifically in regards to the invasive growth pattern, surgical approach, and treatment outcomes[2,3]. The use of neoadjuvant chemoradiotherapy is recommended for all newly diagnosed rectal adenocarcinoma with a clinical (c) stage T3 or T4 based on transrectal endoscopic ultrasound (EUS) or pelvic magnetic resonance imaging (MRI). Neoadjuvant therapy may comprise of either radiotherapy alone or in combination with chemotherapy. Commonly prescribed chemotherapy agents include 5-Fluorouracil (5-FU) and Oxaliplatin. These agents act to limit tumour cell division in several ways. Oxaliplatin acts *via* the formation of DNA-platinum adducts which deprives tumour cells of the necessary building blocks for cell replication. Similarly, 5-FU prevents the formation of nucleosides essential for tumour cell division. Following the completion of neoadjuvant chemoradiotherapy, the patient proceeds to curative surgery. The overarching aim of rectal cancer management is surgical removal of the tumour and all draining lymph node basins, in an intact mesenteric package, in order to achieve an R0 resection, with negative resection margins, with the aim of reducing local recurrence rates. Radiotherapy plays an integral role, as it aids in downsizing or downstaging large tumours (cT3/T4) in the neoadjuvant setting. It is important however to note that not every patient responds favourably to radiotherapy and that treatment-related toxicity can occur, which negatively impact patients' overall and health-related quality of life (QoL)[4]. Furthermore, neoadjuvant radiotherapy can cause excessive tissue oedema, leading to a loss of surgical planes, thereby posing an increased surgical challenge, especially in the narrow male pelvis[5].

The aim of this review is to discuss the role of radiotherapy for the management of rectal cancer in the neoadjuvant setting.

EVOLUTION OF SURGERY IN MANAGEMENT OF RECTAL CANCER

Surgery with curative intent provides the best chance of survival from rectal adenocarcinoma. Due to the challenges posed by the confinement of the bony pelvis, surgical approaches to rectal cancer have undergone several landmark technical milestones, which have lead to improved local recurrence rates and reduced overall

morbidity and mortality. Historically rectal tumours were excised *via* a perineal approach, which was associated with poor mortality, morbidity, and local recurrence rates[6]. The first successful rectal resection was performed in 1826 by Lisfranc, where the rectum was everted and a minimal resection of the distal rectum was performed. There was no consideration for resection of the mesorectum and draining lymph nodes. As anaesthesia was still in the nascent stages, success was based primarily on patients' survival and fitness for discharge. These procedures were principally performed with palliative intent. A review conducted by Vogel of 1500 cases performed in the 19th century found an average operative mortality rate of 20% and a local recurrence rate of 80%[6]. In 1908, the English surgeon William Ernest Miles described the first radical procedure using an abdominal and perineal approach, i.e. abdominoperineal resection (APR). This involved resection of the distal rectum and anal canal. The proximal rectum was exteriorized as an end colostomy. Miles published his case series between 1908 to 1923 and reported local recurrence in 5 patients of the 12 reported (41.6%)[7]. Miles influenced generations of future surgeons who adopted his technique. Subsequent improvements to the technique included performing a high-tie of the inferior mesenteric artery (IMA)[8]. This served to maximise lymph node yield and reduce local recurrence.

In 1938, Henri Hartmann published a case series of 38 patients with sigmoid tumours. Hartmann performed a sub-total colectomy and fashioned an end-colostomy, with oversewing of the rectal stump preserving anal anatomy. First described in 1921, the case series quoted a mortality rate of 8.8% which was a significant reduction, when compared to the 38% mortality rate associated with APR[9]. Hartmann did not advocate for the restoration of bowel continuity in his case series, as he felt the risk to the patient would be too high. This was challenged by the American surgeon Claude Dixon in 1948 when he published a series of 426 patients between 1930 and 1947 in which he performed an anterior resection. In this procedure, upper rectal tumours were resected with bowel continuity restored during the same procedure. A temporary diverting stoma may also be fashioned mitigating the clinical severity of any potential anastomotic leak. Dixon reported a mortality rate of 5.6% and a 5-year survival rate of 67.7% in 272 patients[10]. Dixon concluded that anterior resection was a safe and efficacious procedure for the treatment of upper rectal tumours.

In order to reduce local recurrence rates even further, Professor Richard J Heald developed the technique that is now known as total mesorectal excision (TME)[11]. This is a standardized and reproducible anatomical approach to pelvic dissection, which interrogates surgical planes in order to completely excise the lymphovascular fatty tissue surrounding the rectum and mesorectum under direct vision. Heald postulated that local recurrence was a result of leaving residual mesorectal tissue within the pelvis. In a case series performed at Basingstoke between 1978 and 1997, 519 patients underwent TME for rectal cancer. Neoadjuvant radiotherapy was administered to 49 of the patients in the series. The predominant surgical procedure performed was an anterior resection, although APR and Hartmann resections were also included. The findings of the case series demonstrated a 5-year cancer-specific survival rate of 68% for all patients. The local recurrence rate for curative resections, defined as disease-free proximal, distal and circumferential margins, was 3%. Local recurrence had been, on average, 20% before the publication of this study. Disease-free survival at 5 years was calculated at 80% for those patients treated with curative intent[12]. TME highlights the importance of utilizing natural anatomical planes and performing meticulous dissection during the surgical approach. TME is associated with the lowest rates of local recurrence and has become the surgical gold standard for the management of rectal cancer. Moreover, Quirke *et al*[13] examined 1156 surgical specimens from patients managed with TME. The authors graded the quality of the resections as Good (52%), Poor (13%) or Intermediate (38%), based on the integrity of the mesorectal envelope post-resection. The authors very elegantly demonstrated a significant direct correlation between a positive circumferential resection margin and rates of local recurrence thereby validating Heald's embryological theory underpinning TME.

Restoration of intestinal continuity posed new challenges to rectal cancer management, principally the risk of anastomotic leakage. This feared complication occurs due to failure in the integrity of the anastomosis leading to an abnormal communication between the peritoneal cavity and the intraluminal contents of the bowel. Studies investigating anastomotic leaks have quoted incidence rates of 15%-20%[14,15]. To mitigate the severity of this event, a diverting stoma can be formed at the time of surgery. The creation of a diverting stoma does not reduce the incidence of anastomotic failure, however, it has been shown to minimize the risk of reoperation[14]. The fashioning of a stoma is not without risk. A meta-analysis comprising of 6 studies and 1063 patients demonstrated a complication rate of 18.2% for loop ileostomy and

30.6% for loop colostomy (P = 0.001)[16]. The authors found that rates of clinical dehydration (3.1% *vs* 0%, P = 0.13) and post-operative ileus (5.2% *vs* 1.7%, P = 0.02) were greater in those patients with a loop ileostomy. Emmanuel *et al*[14], published a study in 2018 investigating outcomes for rectal cancer patients with diverting stomas. The authors found that those with such stomas experienced a higher rate of post-operative complications (57.1% *vs* 34.9%, P = 0.003) and an increased average length of hospital stay (13 d *vs* 6.9 d, P = 0.005).

For the majority of these patients, diverting stomas are intended as a temporary measure. A prospective observational study of 275 patients with diverting stomas was published in 2017. Following an average follow-up of 4.9 years, the rate of permanent stoma formation was 16.7%[15]. A retrospective study in Sweden of 3564 patients with loop ileostomies outlined a 9-mo reversal rate of 68.4%. Risk factors for prolonged interval to reversal and for conversion to permanent stoma included, post-operative complications (HR = 0.67, 0.62-0.73), adjuvant chemotherapy (0.63, 0.57-0.69) and advanced cancer stage (Stage III 0.74, 0.66-0.83 and Stage IV 0.38, 0.32-0.46)[17] (Figure 1).

RADIOTHERAPY

Staging

Neoadjuvant therapy comprises a combination of radiotherapy and chemotherapy. The European Society of Medical Oncology (ESMO) recommend neoadjuvant therapy in cases of advanced disease (> T3), lymph node involvement on imaging and where the adequacy of TME surgery is in question (circumferential resection margin)[18]. The goal of neoadjuvant therapy is to downsize or downstage the tumour in anticipation of surgical resection. In instances where there is involvement of the anal sphincters, successful neoadjuvant therapy can potentially downsize a tumour, to allow for the creation of a safe resection margin thereby preserving the anal sphincters and maintaining anal continence. In certain cases, tumours may completely respond to neoadjuvant therapy. Complete Response is defined as the replacement of tumour with fibrous tissue post-radiotherapy. Analysis of the National Cancer Database in 2017 detailed a pathologic complete response (pCR) rate of 13% in an overall patient cohort of 27532[19]. The decision to treat a patient with neoadjuvant therapy is dependent on the clinical tumour stage at presentation. This entails taking a full medical history and clinical examination, including digital rectal examination (DRE), and radiological examinations. Local staging is performed through MRI of the pelvis and EUS of the rectal lesion. MRI provides detailed images of the pelvis allowing for accurate staging of the tumour and facilitating pre-operative planning. Furthermore, MRI aids in assessing the circumferential resection margin (CRM) status. In a prospective observational study of 408 patients, 87% (95%CI: 83%-90%) had clear margins on MRI. Surgical resection specimens of this cohort demonstrated clear margins in 94% (95%CI: 93%-96%). Specificity was found to be 92% (95%CI: 90%-95%)[20]. EUS is effective at measuring the depth of tumour invasion in early rectal cancers[21]. Accuracy in assessing T stage for EUS has been quoted in the range of 85%-90%[22]. Computed tomography (CT) of the Thorax, Abdomen, and Pelvis is useful for both local and distant staging. CT has an accuracy rate of 85.1%, a positive predictive value of 96.1% and a negative predictive value of 3.9% in detecting hepatic metastases[23].

Short course vs long course neoadjuvant radiotherapy

The clear advantages of neoadjuvant radiotherapy were first recognised in 1997 by the Swedish Rectal Cancer Study Group[24]. Between 1987 and 1990 1168 patients diagnosed with rectal cancer were randomly assigned to an intervention arm, *i.e.*, patients received neoadjuvant therapy prior to surgery and a control arm defined as those patients who underwent surgery alone. The neoadjuvant regime involved 25 Gy of radiotherapy in 5 fractions over the duration of one week. These patients were operated one week after completing neoadjuvant therapy. This study found that there was a significant reduction in local recurrence rates between intervention and control (11% *vs* 27%, P < 0.001). The overall rate of local recurrence reduction in patients who received radiotherapy was 58% (95%CI: 46%-69%). Even though neoadjuvant therapy had no bearing on postoperative mortality the 5-year survival was significantly higher in the radiotherapy group (58% *vs* 48%). This landmark study was the first to demonstrate improved overall survival in those patients receiving radiotherapy prior to undergoing curative surgery.

In 2001, The Dutch Rectal Cancer Study Group performed a randomized control trial comparing the effects of pre-operative radiotherapy and TME surgery in 1861

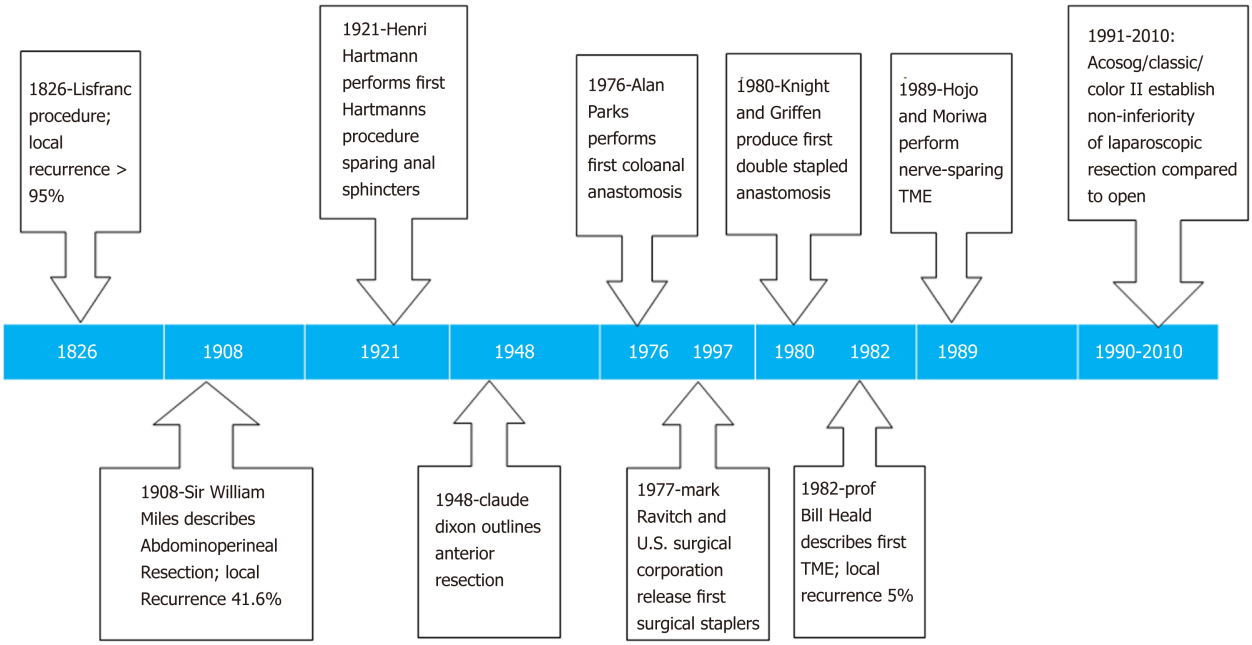

Figure 1 Timeline of surgical innovations in the treatment of rectal cancer[81-87]**.** TME: Total mesorectal excision.

patients[25]. The protocol for neoadjuvant therapy involved 5 Gy of radiotherapy per day for five days which was followed by TME surgery. Patients were regularly followed up every three months for one year and annually thereafter for at least two years. The overall rate of local recurrence was found to be 5.3%. The cohort treated with radiotherapy and surgery exhibited local recurrence in 2.4% of cases *vs* 8.2% in the surgery only group ($P < 0.001$). Unlike the Swedish trial, however, there was no difference in overall survival between the two study arms.

Sebag-Montefiore *et al*[26] performed a multicentre, randomised, control trial comparing preoperative radiotherapy *vs* selective postoperative chemoradiotherapy in patients with rectal cancer. This study encompassed 80 centres spanning four countries. A total of 1350 patients with locally advanced adenocarcinoma of the rectum were randomly assigned to a short-course preoperative radiotherapy (25 Gy in five fractions; $n = 674$) arm *vs* surgery with selective postoperative chemoradiotherapy (45 Gy in 25 fractions with concurrent 5-FU) arm, restricted to patients with a positive circumferential resection margin ($n = 676$). The primary outcome was local recurrence and the median follow-up was 4 years. Ninety-nine patients had developed a local recurrence (27 in the preoperative radiotherapy group *vs* 72 in the selective postoperative chemoradiotherapy cohort). The authors noted a reduction of 61% in the relative risk of local recurrence for patients receiving preoperative radiotherapy (95%CI: 0.27-0.58, $P < 0.0001$), and an absolute difference at 3-years of 6.2% (95%CI: 5.3-7.1). Moreover, there was a relative improvement in disease-free survival of 24% in patients who received preoperative radiotherapy (HR = 0.76, 95%CI: 0.62-0.94, $P = 0.013$), and an absolute difference at 3-years of 6.0% (95%CI: 5.3-6.8) (77.5% *vs* 71.5%). Overall survival did not differ between the groups (HR 0.91, 95%CI: 0.73-1.13, $P = 0.40$). The authors were able to demonstrate an overall relative risk reduction of 61% in local recurrence for patients receiving neoadjuvant therapy. The rate of anastomotic leak in anterior resection patients was similar at one month (9% pre-op radiotherapy *vs* 7% post-op chemotherapy). Patients undergoing pre-operative radiotherapy were more likely to have poor perineal wound healing post-APR (35% *vs* 22%). Rates of CRM involvement were also similar between groups (10% *vs* 12%). Taken with results from other randomised trials, the MRC CR-07 findings provided convincing and consistent evidence that short-course preoperative radiotherapy is an effective treatment option for patients with locally advanced rectal cancer.

In 2004 Sauer *et al*[27] demonstrated favourable outcomes in relation to long-course combination therapy of chemotherapy and radiotherapy in the neoadjuvant setting (nCRT) for the management of rectal cancer. A total of 823 patients with T3/T4 rectal adenocarcinoma were randomised to either a neoadjuvant long course chemoradiotherapy arm or an adjuvant chemoradiotherapy arm. Neoadjuvant therapy involved 28 fractions totalling 50.4 Gy. This was supplemented with Fluorouracil (5-FU) infusions at weeks one and five. Surgery was performed 6-wk followed by four cycles of 5-FU at one month post-operatively. Adjuvant patients

underwent the same adjuvant regimen except for the addition of 540-cGy boost of radiation. The results confirmed an improvement in 5-year local recurrence rates for the pre-operative treatment (13% *vs* 6%) arm. Moreover, 5-year survival rates between the two arms were not dissimilar (76% *vs* 74%, $P = 0.8$). Overall morbidity rates were 36% in the pre-operative arm and 34% in the post-operative arm ($P = 0.68$). Incidence of anastomotic leak (11% *vs* 12%, $P = 0.77$), post-operative ileus (2% *vs* 1%, P = 0.26), post-operative bleeding (3% vs 2%, $P = 0.5$) and sacral wound healing (10% *vs* 8%, $P = 0.1$) demonstrated no significant difference. This study utilised not only long-course neoadjuvant therapy but also combined chemoradiotherapy in the neoadjuvant phase. The benefits of combined chemoradiotherapy had been previously described by Fryckholm *et al*[28] in 2001. In this study, 70 patients were divided into a combined therapy group and a radiotherapy monotherapy group. Both groups underwent surgery within 3-4 wk after completing neoadjuvant therapy. Combined therapy consisted of 40Gy of radiotherapy over 7 wk with weekly infusions of chemotherapy. The authors concluded that treatment with combined therapy resulted in improved local control. Post radical resection surgery, local recurrence rates were 4% and 35% for the combined group compared to the radiotherapy alone group respectively ($P = 0.02$). Even with this regimen, no significant difference was appreciated in 5-year survival between the two cohorts. The combined cohort had a five-year survival rate of 29% with the radiotherapy group at 18% ($P = 0.3$).

A recent meta-analysis comparing short-course with long-course preoperative neoadjuvant therapy for rectal cancer included eight robust studies[29]. The qualifying studies included a total of 1475 patients (short treatment: $n = 665$; long treatment: $n = 810$). No significant difference was detected in each outcome between the short- and long-course preoperative treatments. Interestingly, subgroup analysis indicated that the outcome of distant metastasis was significantly higher in long-course radiotherapy, compared with short-course radiotherapy (OR = 2.65, 95%CI: 1.05-6.68).

Total neoadjuvant therapy

Intensified treatment has been proposed, in certain cases, for patients who present with advanced local disease or those who are partial responders to neoadjuvant radiation. Studies have investigated whether the addition of further cycles of chemotherapy in the neoadjuvant phase, known as total neoadjuvant therapy (TNT), had any impact on response rates or long-term outcomes such as local recurrence and survival.

The GCR-3 trial was a Phase II randomised controlled trial incorporating 108 patients that were randomised to either receive neoadjuvant chemoradiotherapy and 4 cycles of adjuvant capecitabine/oxaliplatin (CAPOX) chemotherapy or receive 4 cycles of CAPOX in conjunction with radiation in the neoadjuvant phase. Both groups demonstrated similar pCR rates (13% *vs* 14%), 5- year overall survival (62% *vs* 64%) and 5-year disease free survival (77% *vs* 74%). Median follow-up was 69.5 months. The authors noted a significant reduction in the incidence of treatment toxicity (19% *vs* 54%, $P = 0.004$) and increased rate of therapy completion (91% *vs* 51%, $P < 0.0001$) in the TNT cohort[30].

INTERVAL TO SURGERY

To date, there is no consensus regarding the interval between the end of neoadjuvant chemoradiotherapy and time to surgery. In 1999, the Lyon R90-01 trial aimed to identify any benefits between short intervals to surgery (< 2 wk) and long intervals to surgery (6-8 wk) in 201 patients[31]. The trial demonstrated that a long interval was associated with a greater treatment response rate (53.1% *vs* 71.7%, $P = 0.007$). Furthermore, the long interval cohort had increased rates of downstaging relative to the short interval cohort (26% *vs* 10.3%, $P = 0.0054$). Patients were routinely followed up twice a year for 5 years. The median follow-up was 33.5 mo (range, 1-79 mo) The overall local recurrence rate was 9%. Both study arms had similar rates of local recurrence. There was no significant difference in overall survival between both study arms. The 3-year survival was 78% and 73% for the short interval and long interval group respectively. In 2016, patient outcomes in this cohort were reanalyzed post follow-up of 15 years[32]. The long interval group demonstrated superior pathological response rates (26% *vs* 10.3%, $P = 0.015$). Pathological response was related with improved survival outcomes for patients (P-0.0048). No differences were noted between both study arms in relation to local recurrence or survival. Of note, the majority of local recurrences presented within 5 years of treatment (96%). In 2017, the Stockholm III trial results were published in the Lancet[33]. This multicentre, randomised, non-blinded, non-inferiority trial aimed to determine the optimal

interval to surgery between neoadjuvant therapy and upfront surgery in 840 patients. Furthermore, the study also sought to determine whether the short course or long course neoadjuvant therapy had a stronger impact on local recurrence. The first study arm received 5 fractions of 5Gy radiation followed by surgery within one week, *i.e.*, the short course group. The second study arm received a similar dose of radiation with surgery performed between 4-8 wk, the delayed short course group. The final study group underwent 25 fractions of 2 Gy radiation with surgery carried out after 4-8 wk *i.e.*, the delayed long course radiotherapy arm. The study demonstrated no significant difference in local recurrence between the three study arms. Interestingly there was an increased rate of post-operative complications in the short course cohort when compared to the delayed short course group (53% *vs* 41%, $P = 0.001$) in a pooled analysis. The overall complication rate was 50% for the Short Course Group, 38% for the Short Course Delayed Group and 39% for the Long Course Group. Patients who received short-course therapy had a reoperation rate of 11% *vs* 7% for the other intervention arms. Surgical complications occurred in 31% of short course patients with a rate of 26% and 23% for the short course delayed and long course groups, respectively. Surgical complications were defined as surgical site infections (SSI), post-operative bleeding, anastomotic leak, wound dehiscence, *etc*.

A comprehensive meta-analysis and systematic review was conducted by Donlin Du *et al*[34] in 2018. This review sought to determine if an extended interval to surgery (≥ 8 wk) influenced patient outcomes, in particular, pathological complete response (pCR) rates (defined as the replacement of tumour cells with fibrous tissue on a resected pathological specimen after neoadjuvant therapy). Thirteen studies involving 19652 patients were included. The meta-analysis demonstrated that pCR was significantly increased in patients with locally advanced rectal cancer and a waiting interval of ≥ 8 wk between preoperative nCRT and surgery compared to a waiting interval of < 8 wk, or a waiting interval of > 8 wk compared to ≤ 8 wk (risk ratio ¼ 1.25; 95%CI: 1.16-1.35; $P < 0.0001$). There were no significant differences in overall survival, disease-free survival, operative time, or incidence of local recurrence, postoperative complications, or sphincter-preserving surgery. This study revealed that performing surgery after a waiting interval of 8 wk after the end of preoperative nCRT is safe and efficacious for patients with locally advanced rectal cancer, significantly improving pCR without increasing operative time or incidence of postoperative complications when compared to a waiting interval of 8 wk.

Moreover in 2018 Kim *et al*[35] analysed outcomes for rectal cancer patients who received differing intervals to surgery after completion of neoadjuvant therapy. The primary outcomes measured were pCR and tumour downstaging. Overall 249 patients with differing intervals to surgery were included. The majority (45.4%) underwent surgery within 7 to 9 wk. The shortest time to surgery was within 5 wk whereas some patients' surgery was performed over 11 wk after neoadjuvant therapy was completed. The authors noted a higher rate of pCR in the 9 to 11-wk interval with a pCR of 8.6% ($P = 0.886$). Downstaging occurred most frequently in the 7 to 9-wk cohort with a downstaging rate of 52.9% ($P = 0.087$).

A meta-analysis incorporating 3584 patients examined the correlations between interval to surgery and the rate of pCR[36]. The control for this study was patients treated with surgery 6 to 8 wk after neoadjuvant therapy. There was a higher rate of pCR in patients operated on after 8 wk ($P < 0.0001$). The rates of pCR were found to increase from 13.7% to 19.5%. Other patient outcomes such as survival, local recurrence, and post-operative complication rates were similar between both groups.

A further multicentre study investigated outcomes for rectal cancer patients treated with surgery over 12 wk after completing neoadjuvant therapy[37]. Seventy-six patients were enrolled in the long interval group, with 48 patients undergoing surgery within 12 wk. There was no statistically significant difference between both groups regarding post-operative complications ($P = 0.547$), readmission rates post-operatively ($P = 0.183$) and 30-d mortality (0.148). Histopathological analysis of the resected surgical specimens demonstrated a pCR rate of 8.3% for those undergoing surgery within 12 wk and 15.8% in those with an extended interval to surgery ($P = 0.28$). Similarly, there were no significant differences found regarding morbidity and mortality in either group.

Overall, debate still continues as to the benefit of long *vs* short interval to surgery post neoadjuvant therapy. Patients who undergo prompt resection post neoadjuvant therapy (< 6 wk) have a shorter duration of treatment yet are at a higher risk of post-operative complication and downstaging of the tumour. Alternatively, patients with prolonged interval to surgery (> 8 wk) have a reduced rate of post-operative complications with a higher incidence of treatment response and downstaging. If rectal preservation is the aim of treatment, then long-course radiotherapy is essential (Table 1).

Table 1 Impact of radiotherapy on local recurrence and survival

Study	*n*	Interventions	Local recurrence	Overall survival	5-yr disease free survival
Swedish Rectal Cancer Trial, NEJM, 1997[24]	1168	25 Gy in 5 fractions in one week surgery	27% 11% ($P \leq 0.001$)	58% 48% ($P = 0.004$)	74% 65% (after nine years) ($P = 0.002$)
Dutch Rectal Cancer Trial, NEJM, 2001[25]	1861	25 Gy in one week TME surgery	2.4% 8.2% ($P \leq 0.001$)	82% 81.8% ($P = 0.2$)	N/A
MRC CR-07, Lancet, 2009[26]	1350	25 Gy in one week TME surgery and adjuvant therapy	27 (674) = 4% 72 (676) = 10.7%	70.3% 67.9% ($P = 0.4$)	73.6% 66.7% ($P = 0.013$)
Sauer *et al*[27], NEJM, 2004	850	50.4 Gy over 5 wk with 5-FU TME surgery	6% 13%	76% 74%	68% 65%
Fryckholm *et al*[28], 2001	70	40 Gy and 5-FU 40 Gy	4% 35% ($P = 0.02$)	66% 38% ($P = 0.03$)	29% 18% ($P = 0.3$)
Stockholm III trial, 2017[33]	840	Short course Short course w/ delay Long course w/ delay	2.24% 2.8% 5.5%	73% 76% 78%	65% 64% 65%
Bujko *et al*[88], 2016	515	5 × 5 Gy and FOLFOX 50.4 Gy in 28 fractions w/ 5-FU	22% 21% ($P = 0.82$)	73% 64.5% ($P = 0.055$)	53% 52% ($P = 0.74$)
Trans-Tasman Oncology Group, 2012[89]	326	5 × 5 Gy in 1 wk 50.4 Gy in 5 wk	7.5% 4.4% ($P = 0.24$)	74% 70% ($P = 0.62$)	N/A
Wawok *et al*[90], 2018	51	5 × 5 Gy 50.4 Gy w/5-FU	35% 5% ($P = 0.036$)	47% 86% ($P = 0.009$)	N/A
German CAO/ARO/AIO-04 study, 2012[91]	1236	50.4 Gy w/ 5-FU (Control) 50.4 Gy w/5-FU and Oxaliplatin	4.6% 2.9%	88% 88.7%	71.2% 75.9%

TME: Total mesorectal excision; FU: Fluorouracil; FOLFOX: Folinic Acid, Fluorouracil, Oxaliplatin; 5-FU: 5-Fluorouracil.

COMPLICATIONS OF RADIOTHERAPY

The introduction of neoadjuvant radiotherapy to the management of rectal cancer has resulted in improved outcomes for patients. This has now been demonstrated by multiple studies, with all reporting reduced rates of local recurrence. It has been suggested that patients who receive a complete pathological response to radiotherapy could potentially avoid surgery and the morbidities associated with surgery or at the very least the adjuvant chemotherapy limb of the current neoadjuvant protocols. The survival outcome data from these studies are ambiguous, however. The potential benefit of radiotherapy in treating a rectal tumour must also be balanced against the risk of patients developing serious side effects secondary to radiation exposure. Numerous side effects, complications, and toxicities from radiotherapy have been reported, ranging from immediate complications such as wound dehiscence, surgical site infection and anastomotic leak to long-term functional disorders such as low anterior resection syndrome (LARS) and genitourinary dysfunction.

Radiotherapy toxicity

Radiation toxicity has been recognised since the discovery of radiation in the early 20th century. Symptoms of toxicity are manifold and of variable severity. In order to accurately quantify and measure such adverse events, a grading system was devised by the Radiation Therapy Oncology Group (RTOG) and the European Organisation for the Research and Treatment of Cancer (EORTC). This grading system is specific to each system or organ exposed to radiation (Table 2).

In 2004 Sauer *et al*[27] recorded all incidences of Grades 3 and 4 toxicity in their patient cohort. In the acute phase, 27% of neoadjuvant patients experienced Grade 3-4 toxicity with 12% of neoadjuvant patients reporting diarrhoea. Long-term data on the same cohort demonstrated an incidence rate of 14% for Grade 3-4 toxicity. This included 4% of neoadjuvant patients developing a stricture at their anastomosis site. Of note, the incidence of toxicity was greater in the adjuvant cohort (40% in acute *vs* 24% in long-term).

The Stockholm III trial reported on the frequency of post-operative complications and found that the rate of complications was similar overall between patients who received long-course therapy and those who received a short course[33]. The authors did note, that in a pooled analysis, there was an increased risk of post-operative complications in the cohort of patients who received short-course radiotherapy

Table 2 RTOG/EORTC radiation toxicity grading system for lower gastrointestinal tract

	Grade 1	Grade 2	Grade 3	Grade 4
Early radiation toxicity (< 6 mo post radiotherapy)	Increased frequency of bowel movements not requiring medical therapy	Increased frequency of bowel movements requiring medication or causing abdominal pain	Diarrhoea requiring IV treatment, mucous or bloody discharge PR, abdominal distention	Acute/subacute bowel obstruction, fistula formation, GI bleed requiring transfusion, abdominal pain requiring tube decompression
Late radiation toxicity (> 6 mo post radiotherapy)	Bowel movements of 5 per day, mild abdominal cramping, mild PR bleeding	Bowel movements > 5 per day, increased mucous PR, intermittent PR bleeding	Obstruction or bleeding requiring operative management	Necrosis, perforation, fistula formation

PR: Per rectum; IV: Intravenous; GI: Gastrointestinal.

without a delay to surgery (53% *vs* 44%, $P = 0.001$).

Differences in immediate post-operative outcomes between short course and long course neoadjuvant patients were analysed by the Trans-Tasman Oncology Group in 2017[38]. The findings of this study indicated increased rates of Grade 3 events in patients who underwent short-course radiotherapy. These adverse events included proctitis (0% *vs* 3.7%, $P = 0.016$) and diarrhoea (1.3% *vs* 14.2%, $P < 0.001$). Conversely, patients who were administered radiotherapy over a longer course were at higher risk of developing an anastomotic leak (7.1% *vs* 3.5%) and perineal wound breakdown (50% *vs* 38.3%), however, neither of these were found to be statistically significant.

Anorectal dysfunction and LARS

As noted in the Sauer and Trans-Tasman studies above[27,38], one of the most frequent and often most distressing side effects of radiotherapy for patients was diarrhoea. Patients who receive neoadjuvant treatment and undergo anterior resection for distal rectal tumours are at risk of developing LARS. LARS can present with a myriad of symptoms including faecal incontinence, faecal urgency and abdominal bloating. The prevalence of LARS was found to be 42%[39]. The pathophysiology of this syndrome is attributed to impaired function of the anal sphincters, colonic dysmotility, and dysfunction of the neorectal reservoir. The causes of this condition are thought to be secondary to physical and neural factors. It is postulated that a reduction in the volume of rectum post-resection contributes to reduced colonic transit times and therefore increased the frequency of bowel motions. A systematic review in 2008 investigated bowel function outcomes after alternative rectal reconstructive techniques. Only two studies included in this review investigated long-term bowel function outcomes in patients post rectal surgery. The authors concluded that patients who received a Colonic J Pouch (CJP) demonstrated better outcomes in bowel function than their counterparts who received a Straight Coloanal Anastomosis (SCA) ($P < 0.05$[40], $P < 0.001$)[41]. The authors noted, however, that these benefits were only apparent for the first 18 mo post-operatively[42].

Neural factors also play a significant role in the development of LARS. Neural dysfunction can occur post-treatment either as a result of denervation post-surgery or as a consequence of radiotherapy. In a cross-sectional study on rectal cancer patients published in 2013, 41% of the total patient cohort of 938 experienced LARS[43]. The authors observed that those who received neoadjuvant therapy (long and short course) and TME surgery demonstrated an increased risk of developing LARS.

In a 14-year follow up study of patients enrolled in the Dutch Rectal Cancer Trial, the authors observed a 46% incidence of LARS in the 242 patients who responded to questionnaires[44]. Neoadjuvant radiotherapy and age < 75 years were found to be significant risk factors. Furthermore, LARS was also associated with a reduction in Health-Related Quality of Life (HRQOL). In a recent study by Kupsch *et al*[45,46], reported a significant reduction in HRQOL scores for patients reporting major LARS using the standardised EORCT-30 and CR38 questionnaire. Patients with major LARS scored 56 ± 19 compared to minor/no LARS who scored 67 ± 20 ($P < 0.001$).

Genitourinary dysfunction

Urinary and sexual dysfunction post-treatment for rectal cancer can be very distressing for patients and greatly impacts on their HRQOL. Dysfunction is secondary to autonomic nerve damage during surgery. The principal autonomic nerves damaged are the superior and inferior hypogastric plexus, the nervi erigenti and pudendal nerves. Nerve damage is attributed to several factors, including pre-operative radiotherapy resulting in inflammation of the local tissues. This makes

delineating surgical planes difficult at the time of surgery. A retrospective study of 288 rectal cancer patients treated laparoscopically was conducted in 2017 in order to determine risk factors for prolonged pelvic pain post-treatment. Multivariate analysis demonstrated that extended operating time ($P < 0.001$) and resection margins in proximity to the anal verge ($P < 0.001$) were independent risk factors for prolonged pelvic pain[47]. Patients with distal tumours are also more likely to suffer some degree of genitourinary dysfunction post-operatively as the autonomic nerves are in close proximity to the rectum.

In a study by Hendren *et al*[48], questionnaires were sent to living rectal cancer patients who had been treated at Mount Sinai Hospital, Toronto, Canada between 1980 and 2003. The study found that 29% of women and 45% of men experienced some degree of sexual dysfunction after treatment. The authors described how radiation therapy had a strong association ($P = 0.0001$). The type of surgical procedure was also related to worse outcomes ($P = 0.005$) with most patients treated with APR reporting sexual dysfunction. Moreover, an observational retrospective study performed by Costa *et al*[49] in 2018 found the presence of a stoma post-operatively to be associated with sexual dysfunction. Attaallah *et al*[50] compared rates of sexual dysfunction in patients treated with laparoscopic TME and those treated with open TME in 187 patients and reported reduced rates of dysfunction in the laparoscopic arm compared to open. The authors noted that post-operative radiotherapy and chemotherapy was associated with male sexual dysfunction only on univariate analysis ($P = 0.003$, $P = 0.03$) however failed to maintain significance on multivariate analysis ($P = 0.112$, $P = 0.818$).

Urinary dysfunction encompasses a constellation of symptoms including urinary incontinence, difficulty in initiating micturition, and urinary retention. Similar to sexual dysfunction, urinary dysfunction most commonly occurs after neoadjuvant radiotherapy and surgery for distal tumours. A retrospective observational study in Sweden found that 36% of men and 57% of women reported urinary incontinence 3 years after undergoing APR[51].

Pelvic fractures

Insufficiency fractures in the pelvis are an underreported adverse event secondary to neoadjuvant therapy for rectal cancer. Stress fractures are commonly due to loss of mineralisation in the bone itself. This process is accentuated by radiotherapy which serves to exacerbate osteopenia *via* small vessel ischaemia in the bone[52].

A prospective case-control study involving 403 rectal cancer patients was published in 2018[53]. These patients underwent MRI pelvis imaging 3 years post resection of their rectal tumour to assess for local recurrence and the presence of pelvic insufficiency fractures. Fractures were identified in 49 patients with 39 of these patients having received neoadjuvant treatment ($P < 0.001$). Multivariate analysis demonstrated pre-operative CRT (OR: 14.2, 6.1-33.1), female gender (OR: 3.52, 1.7-7.5) and age over 65 (OR: 3.2, 1.5-6.9) to be significantly associated with the development of a pelvic fracture. Moreover, a retrospective review of 492 rectal cancer patients who received adjuvant radiotherapy was conducted with a median follow-up of 3.5 years[54]. The incidence of sacral fracture in this cohort was 7.1% and identified osteoporosis as a risk factor for the development of a sacral fracture (HR: 3.23, 1.23-8.5).

WATCH AND WAIT IN CLINICAL COMPLETE RESPONDERS

In those patients who receive neoadjuvant radiotherapy, there is a small cohort that has been shown to develop a complete pathological response. This occurs when the tumour cells are completely replaced with fibrous tissue. The relative extent of tumour response is objectively measured using the Mandard Tumour Regression Grade (TRG). Patients may also develop a Complete Clinical Response (cCR). cCR is defined in accordance with the Response Evaluation Criteria of Solid Tumours (RECIST)[55]. This defines cCR as the absence of tumour on clinical examination and endoscopy at least 4 wk after completion of neoadjuvant therapy. In 1998, Habr Gama *et al*[56] proposed that those patients who demonstrate a (cCR) to neoadjuvant radiotherapy could be managed by observation alone. When investigating the outcomes of combined neoadjuvant chemoradiotherapy on 118 patients, it was found that 30.5% exhibited a (cCR) after a follow-up of approximately 36 mo. Furthermore, 26.2% of patients did not require surgical management and 38.1% underwent sphincter-sparing management after diagnosis of low rectal cancer. In 2004, Habr-Gama published a controlled trial where complete clinical responders were followed up by surveillance and incomplete responders proceeded to surgery. The surveillance

protocol consisted of monthly clinical examinations (including digital rectal examination), CEA levels and proctoscopy. Chest X-Rays in addition to CT imaging of the abdomen and pelvis were performed every 6 mo for the first year. Clinical follow-up frequency was increased to between two and six monthly visits after year one of surveillance. The long-term results of this study demonstrated local recurrence in 2 (cCR) patients (n = 99). Both patients underwent successful treatment with comparable survival outcomes to the incomplete responder group. It was noted that recurrence tended to occur after approximately 4-5 years indicating the need for prolonged surveillance. Distant recurrence was found to be higher in the surgery cohort (12.5% *vs* 6%). Finally, disease-specific mortality was found to be 8% in the surveillance group and 17% in the surgery cohort[57].

Long-term outcomes of watch and wait patients from multiple countries contributing to the International Watch and Wait Database (IWWD) were assessed in 2018[58]. Each patient included in the study had received neoadjuvant radiotherapy and were enrolled in frequent surveillance programmes. A total of 880 patients were included from 47 centres across 15 countries, 87% of which exhibited clinical complete response (cCR). Two-year cumulative rates of local regrowth were noted in 25.2%. Five-year overall survival was 85% with 5-year disease-free survival of 94%. The OnCore Project, published in 2016, was a propensity score-matched cohort analysis study[59]. Each patient underwent long course chemoradiotherapy. Patients who demonstrated (cCR) were offered surgery or surveillance. Overall, 129 patients were observed. Thirty-one patients were prospectively recruited with the remaining data obtained from a retrospective database of surveillance patients. The authors found that 34% of surveillance patients developed local regrowth with 88% requiring salvage surgery. There was no significant difference in 3-year overall survival in the matched analysis of the resection group and surveillance group (96% *vs* 87%, P = 0.024).

Innovative methods of delivering radiotherapy have demonstrated encouraging results in cCR rates of rectal cancer patients. An example of such a method is endocavitary irradiation. This involves the application of X-Ray radiation directly to the primary tumour, *via* a proctoscope, in addition to standard external beam radiotherapy (EBRT). In 1994, Gerard *et al*[60], published the results of a study investigating the outcomes of 414 patients with T2/T3 rectal cancers treated with this method. This technique resulted in a 91% local control rate in patients who did not undergo surgery with 90% local control in patients who went on to have curative surgery. The authors noted that 60% of patients with low/middle rectal tumours progressed to sphincter-sparing surgery. These results were replicated in a retrospective 1996 study where 25 patients long-term outcomes were assessed[61]. Within this cohort, 20 patients were managed with curative intent with the remaining 5 patients palliative cases. Local control was accomplished in 18 of the 20 curative patients and in 4 of the 5 palliative patients. In the curative study arm, 5-year local control was quoted at 89% with a 5-year survival rate of 76%.

The benefits of endocavitary radiation were confirmed in a Phase III randomised controlled trial in 2004[62]. Patients (n = 88) with low rectal tumours were randomised into receiving EBRT (39 Gy over 17 d) or EBRT with Contact X-Ray Radiotherapy boost (CXRT) of 85Gy in three fractions. Complete clinical response was greatly increased in patients who received endocavitary treatment compared to EBRT alone (24% *vs* 2%). There was also an increase in the rate of sphincter preserving surgeries performed on patients post endocavitary treatment (76% *vs* 44%, P = 0.004). These patients were followed up after a median follow-up of 132 mo[63] .

Local recurrence was lower in the CXRT group compared to EBRT (10% *vs* 15%, P = 0.69). Overall survival was similar between both study arms (53% *vs* 54%). Clinical response data demonstrated that a greater proportion of CXRT patients remained in a state of cCR after 10 years compared to EBRT (11 patients vs 1 patient). These studies highlighted the association between endocavitary radiation and cCR in patients with rectal cancer (Table 3).

Minimally invasive surgery

While radical resection provides the best chance for definitive management for rectal cancer it may also carry a high risk of poor functional outcome and quality of life for the patient. This is particularly pertinent for those rectal cancer patients diagnosed with early-stage disease (cT1-T2). New surgical techniques and surgical tools have been developed which aim to adequately resect and treat early rectal cancers whilst minimising the risk of poor functional outcomes post-operatively. Traditional transanal excision (TAE) is utilized for tumours that measure less than 3 cm or equal to 2 cm in diameter and located within 6-8 cm from the anal verge. It entails accessing the rectal lesion *via* the anal canal utilizing specialized laparoscopic equipment. Difficulties with resecting early rectal tumours *via* TAE have been noted in the

Table 3 Studies on watch and wait outcomes, *n* (%)

Study	*n*	NA regime	Recurrence	Salvage therapy	Survival post salvage therapy	Survival
Habr-Gama *et al*[57], 2004	71	Long-course radiotherapy w/ 5-FU	Local:2 Distant: 3	2 (100)	100%	OS: 100% DFS: 92%
Habr-Gama *et al*[92], 2014	90	Long course radiotherapy w/ 5-FU	Local: 28 (31%)	26 (92.8)	OS: 94%	OS: 91% DFS: 68%
OnCore Project, 2016[59]	129	45 Gy w/ 5-FU	Local: 44 (34%)	36 (88)	N/A	OS: 96% at 3 yr DFS: 88% at 3 yr
IWWD Consortium, 2015[58]	880	Chemoradiotherapy: 91%	Local: 25.2%	141 (69)	OS: 75.4% DFS: 84%	OS: 85% DFS: 94%
Appelt *et al*[93], 2015	40	Chemoradiotherapy	Local: 25.9% at 2 yr	9	OS: 100% at 2 yr DFS: 100% at 2 yr	OS: 100% at 2 years DFS: 70% at 2 years
Smith *et al*[94], 2012	32	Long-course chemoradiotherapy	Local: 6 (18.75)	6 (100)	OS: 100% at 17 mo	OS: 96% DFS: 88% all at 17 mo
Smith *et al*[95], 2019	113		Local: 22 (19.5)	22 (100)	DFS: 91%	OS: 73% DFS: 75%
Martens *et al*[96], 2016	100	Long-Course: 95% Short Course: 5%	Local: 15% Distant: 5%	13	OS: 92.3%	OS: 96.6% DFS: 80.6% all after 3 yr
Lai *et al*[97], 2016	18	Chemoradiotherapy	Local: 2	2	100%	OS: 100%
Rijkmans *et al*[98], 2017	38	External beam radiotherapy and brachytherapy (iridium)				DFS: 42% OS: 63%
Vuong *et al*[99], 2007	100	External beam radiotherapy with brachytherapy (iridium)	Local recurrence at 5 yr: 5%			DFS: 65% OS: 70%
Gerard *et al*[100], 2019	74	Contact X-ray brachytherapy	10% at 3 yr	2		DFS: 88%
Sun Myint *et al*[101], 2018	83	Contact X-ray brachytherapy	13.2% after 2.5 yr (*n* = 7)	6		DFS: 83.1%
Ortholan *et al*[63], 2012	45	External beam radiotherapy with contact X-ray boost				DFS: 53% OS: 55%

DFS: Disease-free survival; OS: Overall survival.

literature[64,65]. TAE is only suitable for resection of distal tumours as access to proximal rectal lesions is limited. Precision of TAE is reduced, thereby, increasing rates of tumour fragmentation during resection. Tumour fragmentation during surgery increases the risk of incomplete resection and consequently local recurrence.

In 1983 Professor Gerhard Buess described transanal endoscopic microsurgery (TEMS) for resecting low rectal lesions[66]. The specialised equipment required for this procedure allows access to tumours up to 24 cm from the anal verge, greater precision in tumour resection and a magnified 3D view of the rectum. An endoscope is inserted in the anal canal to the level of the rectal lesion. This lesion is subsequently resected *via* electrocautery. In a single centre retrospective review, 92 TEMS patients were followed up for approximately 5 years[67]. The study detailed a post-operative complication rate of 10.9%, the most common being urinary retention and bleeding (both 4.3%). The overall recurrence rate stood at 6.7% with disease-free survival of 98.6% and overall survival of 89.4%[67].

Promising patient outcomes have been reported in those treated with neoadjuvant chemoradiotherapy preceding TEMS. The CARTS study (Chemoradiation Therapy for Rectal Cancer in the Distal Rectum followed by organ-sparing Transanal Endoscopic Microsurgery) followed neoadjuvant patients treated with TEMS for an average of 4.5 years[68]. Of the 55 patients enrolled in the study, 35 (74%) underwent TEMS with 16 patients receiving TME surgery. Local recurrence at 5 years was 7.7% with an overall survival of 82.8% and disease-free survival of 81.6%. The authors found that TEMS patients were more likely to gain improved QoL post-operatively. However, 78% of TEMS patients did report a degree of LARS in the aftermath of their procedure (50% major LARS, 28% minor LARS).

The outcomes of TEMS in incomplete responders to neoadjuvant therapy has also

been studied. In a prospective single centre study, 53 patients who were restaged as T1-T2 after completing neoadjuvant therapy were offered TEMS. This cohort of patients was found to have a 3-year local recurrence rate of 23% (n = 12). Nine of these patients exhibited local recurrence and 8 were subsequently managed with salvage therapy[69] (Table 4).

The primary disadvantages of the TEMS procedure include the high cost of specialised equipment, in addition to the risk of anorectal dysfunction as outlined above. To mitigate this, a novel hybrid between single-port laparoscopy and TEM for transanal excision was introduced. Transanal minimally invasive surgery (TAMIS) involves access to the rectum *via* a single multichannel port with the use of ordinary laparoscopic instruments. In the original case series describing TAMIS, in 6 patients, with an average tumour location at 9.3 cm from the anal verge, were recruited[70]. When compared to TEM, the operative time for TAMIS was shorter compared to TEMS (86 min *vs* 120-140 min). Three of the patients were discharged on the same day. The longer length of hospital stay for some patients was primarily due to technical difficulties encountered during the procedure such as an anterior lying tumour and inadvertent violation of the peritoneum. There was no incidence of morbidity or mortality observed in the TAMIS patients after an average follow-up period of 6.2 wk.

A multi-institutional matched analysis study of both techniques was published in 2017 with the quality of excision examined[71]. Patients requiring excision of benign and malignant rectal lesions were included. Overall, 428 patients were enrolled and the quality of excision was assessed based on tumour fragmentation and positive resection margins. Both TEMS and TAMIS demonstrated similar rates of poor excision (8% *vs* 11%, P = 0.223). Post-operative complication rates were also similar between both groups (11% *vs* 9%, P = 0.477). Local recurrence in both cohorts was 7% (P = 0.864). The authors noted that TAMIS did allow for shorter operating times and a reduced length of hospital stay compared to TEMS. This study highlighted the non-inferiority of TAMIS excision compared to TEMS[71].

Several studies were subsequently published examining the adequacy of TAMIS excision. The primary determinant of excision quality was the presence of a positive excision margin on histological examination of resected specimens. Studies also examined the average distance of lesions from the anal verge, to analyse the extent of access TAMIS could achieve within the rectum. A systematic review of 390 TAMIS procedures conducted over three years was published in 2014[72]. The average distance of the tumour from the anal verge was 7.6 cm (3-15 cm). Of studies that recorded margin status, 4.36% of resected specimens demonstrated a positive margin on pathological analysis. Recurrence rates were recorded for 259 patients. The average rate of recurrence over a 7 mo period was 2.7%. Furthermore, a prospective observational study of 50 TAMIS patients was published in 2013[73]. Patients underwent TAMIS for both benign (n = 25) and malignant (n = 25) rectal lesions. Patients were recruited between 2009 and 2011 and received an average follow-up of 20 mo. The average distance of tumour to the anal verge was 8.1 cm (3-14 cm). The rate of positive margins on histology was 6%. There was a 4% recurrence rate documented after 20 mo of follow-up.

A larger study published in 2016 involved 75 patients[74]. The majority of lesions excised *via* TAMIS were benign with 17 patients treated for malignant lesions *via* TAMIS [59 benign (77.3%), 17 malignant (22.7%)]. The average distance from the anal verge was 10 cm (6-16 cm). Of note, two patients required temporary ileostomies after the peritoneal cavity was inadvertently entered. Average follow-up was over 39.5 mo. Of the 17 patients treated for rectal cancer, 5 (29%) had positive margins on pathology. Within this group, 2 patients went on to have a radical resection, 1 patient was deemed too high risk for radical surgery whilst another declined further surgery altogether. The fifth patient underwent a period of surveillance and was referred to medical oncology. Only one patient treated for rectal cancer and with negative margins on histology developed local recurrence and underwent an APR. This study was unique relative to those described above as it detailed the frequency and severity of post-operative complications from TAMIS. The common theme of the studies outlined above is that rectal lesions, both benign and early malignant tumours, can be safely and adequately resected *via* TAMIS. The average local recurrence rate for TAMIS resections is similar to those resected *via* traditional TME. It is essential however that appropriate patient selection is conducted in advance of any TAMIS procedure in order to further minimise the incidence of local recurrence.

The description of techniques such as TAMIS, TEMS, and TAE is in keeping with the global focus on minimally invasive surgery. The trials described above serve to demonstrate that minimally invasive surgery is a safe and effective means of surgically managing early, localised rectal cancer. Further advances in this field are being achieved through the use of robotics and novel techniques such as transanal

Table 4 Outcomes in transanal endoscopic microsurgery

Study	*n*	Post-op complications	Local recurrence	Survival
Lee *et al*[71], 2017	247	11%	7%	DFS: 80%
CARTS study, Stijns *et al*[68], 2019	47	N/A	7.7%	DFS: 81.6% OS: 82.8%
O'Neill *et al*[67], 2017	92	10.9%	6.7%	DFS: 98.6% OS: 89.4% (after 3 yr)
Jeong *et al*[102], 2009	45	0	15.5%	DFS: 88.5% OS: 96.2%
Stipa *et al*[103], 2012	86 (T1 patients)	N/A	11.6% (for T1 tumours)	OS: 92% (for T1 patients)
Baatrup *et al*[104],2009	143	N/A	18%	DFS: 87% OS: 66%
Van Den Eynde, 2019[105]	53	40%	N/A	N/A

DFS: Disease-free survival; OS: Overall survival.

total mesorectal excision (taTME). Robotic transanal surgery (RTS) involves multiple robotic arms being utilised to resect a rectal lesion *via* a transanal approach. The robotic arms are introduced transanally through a multichannel port. Robotic Transanal Surgery was first described in 2011[75]. Initial studies were performed in a dry lab setting, to assess feasibility. Later studies were performed on cadaveric models. The first documented description of RTS on a human patient was performed in 2012[76]. There were no immediate post-operative complications and the patient was discharged home on day one. The patient was followed up for 6 wk. In 2019 Tomassi *et al* performed a retrospective study of 58 patients who underwent RTS[77]. Within this cohort, 28 patients were operated for early localised rectal cancer, 11 for rectal carcinoid, 1 patient for rectal GI stromal tumour and the remainder for excision of rectal polyps. Specimen fragmentation was recorded in 1.7% of cases and 94.8% demonstrated negative margins on histopathology. After a mean follow-up of 11.5 mo (range, 0.3-33.3 mo), 3 patients (5.5%) demonstrated local recurrence with all 3 patients proceeding to salvage surgery.

taTME involves resecting rectal tumours *via* a transanal and transabdominal approach. The transabdominal approach involves an operating team mobilising the sigmoid colon and resecting the rectum proximal to the tumour allowing for adequate margins. A multichannel port is inserted into the anal canal by a second operating team with dissection proceeding distal to the rectal tumour. The transanal dissection proceeds proximally with simultaneous abdominal dissection distally[78]. A long-term follow-up of 373 patients treated with taTME was performed in 2017[79]. The majority of patients were treated for distal rectal tumours (91%) and received long-course neoadjuvant therapy preceding resection (97.7%). Good quality TME was performed in 96% of cases with a negative circumferential resection margin documented in 94% of patients. Morbidity and mortality rates following the procedure were 13.4% and 0.3% respectively. Local recurrence rates in this cohort were 7.4% with a 5-year survival rate of 90%. Furthermore, a systematic review and meta-analysis was conducted comparing outcomes between rectal cancer patients treated with open, laparoscopic, robotic and transanal excision of their tumours[80]. Overall, 29 studies were included incorporating 6237 patients. Post-operative morbidity was decreased in patients treated *via* laparoscopic and robotic surgery when compared to open. Similar findings were demonstrated in regards to the length of hospital stay. Quality of TME resection was found to be higher in open (OR = 1.52, 1.19-1.93) and transanal resections compared to laparoscopy. No significant differences were described regarding the incidence of anastomotic leaks, local recurrence rates and 5-year survival among patients (Table 5).

CONCLUSION

Management of rectal cancer has evolved significantly over the course of the past century. Local recurrence rates and overall survival have increased progressively as a consequence of refinements in surgical techniques and instrumentation, culminating with the description of the TME. Studies outlining novel minimally invasive approaches to accessing rectal lesions are producing intriguing results. These newer approaches require strict criteria for patient selection and are most effective for treating early, localised rectal cancers. The advent of neoadjuvant therapy, and neoadjuvant radiotherapy, in particular, has resulted in further improvements in local recurrence. There have been numerous studies examining the benefit in enrolling patients with a complete response to radiotherapy into surveillance programmes.

Table 5 Transanal minimally invasive surgery studies

Study	Pt numbers (*n*)	Average distance from Anal Verge (cm)	Positive margins	Local recurrence	Average length of follow-up
Atallah *et al*[70], 2010	6	9.3	0	N/A	N/A
Albert *et al*[73], 2013	50	8.1	6%	2 (4%)	N/A
Keller *et al*[74], 2016	75 17 (malignant) 58 (benign)	10	5		
Garcia-Florez *et al*[106], 2017	32	5.6	1	10.3%	26 mo
Van den Eynde *et al*[105], 2019	68	6	12%	N/A	30 d
Melin *et al*[107], 2016	29	6.79	3	1	Retrospective study

Medical professionals must be mindful of the side effect profile of radiotherapy such as long-term genitourinary and anorectal dysfunction. Therefore, it is essential that the nomination of patients for neoadjuvant radiotherapy should occur only after careful consideration and discussion by a multidisciplinary team of rectal cancer specialists.

REFERENCES

1 **Bray F**, Ferlay J, Soerjomataram I, Siegel RL, Torre LA, Jemal A. Global cancer statistics 2018: GLOBOCAN estimates of incidence and mortality worldwide for 36 cancers in 185 countries. *CA Cancer J Clin* 2018; **68**: 394-424 [PMID: 30207593 DOI: 10.3322/caac.21492]

2 **Tamas K**, Walenkamp AM, de Vries EG, van Vugt MA, Beets-Tan RG, van Etten B, de Groot DJ, Hospers GA. Rectal and colon cancer: Not just a different anatomic site. *Cancer Treat Rev* 2015; **41**: 671-679 [PMID: 26145760 DOI: 10.1016/j.ctrv.2015.06.007]

3 **Paschke S**, Jafarov S, Staib L, Kreuser ED, Maulbecker-Armstrong C, Roitman M, Holm T, Harris CC, Link KH, Kornmann M. Are Colon and Rectal Cancer Two Different Tumor Entities? A Proposal to Abandon the Term Colorectal Cancer. *Int J Mol Sci* 2018; **19** [PMID: 30200215 DOI: 10.3390/ijms19092577]

4 **Couwenberg AM**, Burbach JPM, van Grevenstein WMU, Smits AB, Consten ECJ, Schiphorst AHW, Wijffels NAT, Heikens JT, Intven MPW, Verkooijen HM. Effect of Neoadjuvant Therapy and Rectal Surgery on Health-related Quality of Life in Patients With Rectal Cancer During the First 2 Years After Diagnosis. *Clin Colorectal Cancer* 2018; **17**: e499-e512 [PMID: 29678514 DOI: 10.1016/j.clcc.2018.03.009]

5 **Ashburn JH**, Kalady MF. Radiation-Induced Problems in Colorectal Surgery. *Clin Colon Rectal Surg* 2016; **29**: 85-91 [PMID: 27247532 DOI: 10.1055/s-0036-1580632]

6 **Lirici MM**, Hüscher CG. Techniques and technology evolution of rectal cancer surgery: a history of more than a hundred years. *Minim Invasive Ther Allied Technol* 2016; **25**: 226-233 [PMID: 27415777 DOI: 10.1080/13645706.2016.1198381]

7 **Miles WE**. A method of performing abdomino-perineal excision for carcinoma of the rectum and of the terminal portion of the pelvic colon (1908). *CA Cancer J Clin* 1971; **21**: 361-364 [PMID: 5001853]

8 **Moynihan B**. The surgical treatment of cancer of the sigmoid flexure and rectum. *Surg Gynecol Obstet* 1908; **6**: 463

9 **Ronel DN**, Hardy MA. Henri Albert Hartmann: labor and discipline. *Curr Surg* 2002; **59**: 59-64 [PMID: 16093106]

10 **Dixon CF**. Anterior Resection for Malignant Lesions of the Upper Part of the Rectum and Lower Part of the Sigmoid. *Ann Surg* 1948; **128**: 425-442 [PMID: 17859211]

11 **Heald RJ**, Husband EM, Ryall RD. The mesorectum in rectal cancer surgery--the clue to pelvic recurrence? *Br J Surg* 1982; **69**: 613-616 [PMID: 6751457 DOI: 10.1002/bjs.1800691019]

12 **Heald RJ**, Moran BJ, Ryall RD, Sexton R, MacFarlane JK. Rectal cancer: the Basingstoke experience of total mesorectal excision, 1978-1997. *Arch Surg* 1998; **133**: 894-899 [PMID: 9711965 DOI: 10.1001/archsurg.133.8.894]

13 **Quirke P**, Steele R, Monson J, Grieve R, Khanna S, Couture J, O'Callaghan C, Myint AS, Bessell E, Thompson LC, Parmar M, Stephens RJ, Sebag-Montefiore D; MRC CR07/NCIC-CTG CO16 Trial Investigators; NCRI Colorectal Cancer Study Group. Effect of the plane of surgery achieved on local recurrence in patients with operable rectal cancer: a prospective study using data from the MRC CR07 and NCIC-CTG CO16 randomised clinical trial. *Lancet* 2009; **373**: 821-828 [PMID: 19269520 DOI: 10.1016/S0140-6736(09)60485-2]

14 **Emmanuel A**, Chohda E, Lapa C, Miles A, Haji A, Ellul J. Defunctioning Stomas Result in Significantly More Short-Term Complications Following Low Anterior Resection for Rectal Cancer. *World J Surg* 2018; **42**: 3755-3764 [PMID: 29777268 DOI: 10.1007/s00268-018-4672-0]

15 **Miura T**, Sakamoto Y, Morohashi H, Yoshida T, Sato K, Hakamada K. Risk factor for permanent stoma and incontinence quality of life after sphincter-preserving surgery for low rectal cancer without a diverting stoma. *Ann Gastroenterol Surg* 2017; **2**: 79-86 [PMID: 29863122 DOI: 10.1002/ags3.12033]

16 **Chudner A**, Gachabayov M, Dyatlov A, Lee H, Essani R, Bergamaschi R. The influence of diverting loop ileostomy vs. colostomy on postoperative morbidity in restorative anterior resection for rectal cancer: a systematic review and meta-analysis. *Langenbecks Arch Surg* 2019; **404**: 129-139 [PMID: 30747281 DOI: 10.1007/s00423-019-01758-1]

17 **Gustafsson CP**, Gunnarsson U, Dahlstrand U, Lindforss U. Loop-ileostomy reversal-patient-related characteristics influencing time to closure. *Int J Colorectal Dis* 2018; **33**: 593-600 [PMID: 29508050 DOI: 10.1007/s00384-018-2994-x]

18 **Glynne-Jones R**, Wyrwicz L, Tiret E, Brown G, Rödel C, Cervantes A, Arnold D; ESMO Guidelines Committee. Rectal cancer: ESMO Clinical Practice Guidelines for diagnosis, treatment and follow-up. *Ann Oncol* 2017; **28**: iv22-iv40 [PMID: 28881920 DOI: 10.1093/annonc/mdx224]

19 **Lorimer PD**, Motz BM, Kirks RC, Boselli DM, Walsh KK, Prabhu RS, Hill JS, Salo JC. Pathologic Complete Response Rates After Neoadjuvant Treatment in Rectal Cancer: An Analysis of the National Cancer Database. *Ann Surg Oncol* 2017; **24**: 2095-2103 [PMID: 28534080 DOI: 10.1245/s10434-017-5873-8]

20 **MERCURY Study Group**. Diagnostic accuracy of preoperative magnetic resonance imaging in predicting curative resection of rectal cancer: prospective observational study. *BMJ* 2006; **333**: 779 [PMID: 16984925 DOI: 10.1136/bmj.38937.646400.55]

21 **Brown G**. Staging rectal cancer: endoscopic ultrasound and pelvic MRI. *Cancer Imaging* 2008; **8** Spec No A: S43-S45 [PMID: 18852080 DOI: 10.1102/1470-7330.2008.9008]

22 **Siddiqui AA**, Fayiga Y, Huerta S. The role of endoscopic ultrasound in the evaluation of rectal cancer. *Int Semin Surg Oncol* 2006; **3**: 36 [PMID: 17049086 DOI: 10.1186/1477-7800-3-36]

23 **Valls C**, Andía E, Sánchez A, Gumà A, Figueras J, Torras J, Serrano T. Hepatic metastases from colorectal cancer: preoperative detection and assessment of resectability with helical CT. *Radiology* 2001; **218**: 55-60 [PMID: 11152779 DOI: 10.1148/radiology.218.1.r01dc1155]

24 **Swedish Rectal Cancer Trial**. Cedermark B, Dahlberg M, Glimelius B, Påhlman L, Rutqvist LE, Wilking N. Improved survival with preoperative radiotherapy in resectable rectal cancer. *N Engl J Med* 1997; **336**: 980-987 [PMID: 9091798 DOI: 10.1056/NEJM199704033361402]

25 **Kapiteijn E**, Marijnen CA, Nagtegaal ID, Putter H, Steup WH, Wiggers T, Rutten HJ, Pahlman L, Glimelius B, van Krieken JH, Leer JW, van de Velde CJ; Dutch Colorectal Cancer Group. Preoperative radiotherapy combined with total mesorectal excision for resectable rectal cancer. *N Engl J Med* 2001; **345**: 638-646 [PMID: 11547717 DOI: 10.1056/NEJMoa010580]

26 **Sebag-Montefiore D**, Stephens RJ, Steele R, Monson J, Grieve R, Khanna S, Quirke P, Couture J, de Metz C, Myint AS, Bessell E, Griffiths G, Thompson LC, Parmar M. Preoperative radiotherapy versus selective postoperative chemoradiotherapy in patients with rectal cancer (MRC CR07 and NCIC-CTG C016): a multicentre, randomised trial. *Lancet* 2009; **373**: 811-820 [PMID: 19269519 DOI: 10.1016/S0140-6736(09)60484-0]

27 **Sauer R**, Becker H, Hohenberger W, Rödel C, Wittekind C, Fietkau R, Martus P, Tschmelitsch J, Hager E, Hess CF, Karstens JH, Liersch T, Schmidberger H, Raab R; German Rectal Cancer Study Group. Preoperative versus postoperative chemoradiotherapy for rectal cancer. *N Engl J Med* 2004; **351**: 1731-1740 [PMID: 15496622 DOI: 10.1056/NEJMoa040694]

28 **Frykholm GJ**, Påhlman L, Glimelius B. Combined chemo- and radiotherapy vs. radiotherapy alone in the treatment of primary, nonresectable adenocarcinoma of the rectum. *Int J Radiat Oncol Biol Phys* 2001; **50**: 427-434 [PMID: 11380230 DOI: 10.1016/s0360-3016(01)01479-1]

29 **Chen K**, Xie G, Zhang Q, Shen Y, Zhou T. Comparison of short-course with long-course preoperative neoadjuvant therapy for rectal cancer: A meta-analysis. *J Cancer Res Ther* 2018; **14**: S224-S231 [PMID: 29578178 DOI: 10.4103/0973-1482.202231]

30 **Fernandez-Martos C**, Garcia-Albeniz X, Pericay C, Maurel J, Aparicio J, Montagut C, Safont MJ, Salud A, Vera R, Massuti B, Escudero P, Alonso V, Bosch C, Martin M, Minsky BD. Chemoradiation, surgery and adjuvant chemotherapy versus induction chemotherapy followed by chemoradiation and surgery: long-term results of the Spanish GCR-3 phase II randomized trial†. *Ann Oncol* 2015; **26**: 1722-1728 [PMID: 25957330 DOI: 10.1093/annonc/mdv223]

31 **Francois Y**, Nemoz CJ, Baulieux J, Vignal J, Grandjean JP, Partensky C, Souquet JC, Adeleine P, Gerard JP. Influence of the interval between preoperative radiation therapy and surgery on downstaging and on the rate of sphincter-sparing surgery for rectal cancer: the Lyon R90-01 randomized trial. *J Clin Oncol* 1999; **17**: 2396 [PMID: 10561302 DOI: 10.1200/JCO.1999.17.8.2396]

32 **Cotte E**, Passot G, Decullier E, Maurice C, Glehen O, François Y, Lorchel F, Chapet O, Gerard JP. Pathologic Response, When Increased by Longer Interval, Is a Marker but Not the Cause of Good Prognosis in Rectal Cancer: 17-year Follow-up of the Lyon R90-01 Randomized Trial. *Int J Radiat Oncol Biol Phys* 2016; **94**: 544-553 [PMID: 26723110 DOI: 10.1016/j.ijrobp.2015.10.061]

33 **Erlandsson J**, Holm T, Pettersson D, Berglund Å, Cedermark B, Radu C, Johansson H, Machado M, Hjern F, Hallböök O, Syk I, Glimelius B, Martling A. Optimal fractionation of preoperative radiotherapy and timing to surgery for rectal cancer (Stockholm III): a multicentre, randomised, non-blinded, phase 3, non-inferiority trial. *Lancet Oncol* 2017; **18**: 336-346 [PMID: 28190762 DOI: 10.1016/S1470-2045(17)30086-4]

34 **Du D**, Su Z, Wang D, Liu W, Wei Z. Optimal Interval to Surgery After Neoadjuvant Chemoradiotherapy in Rectal Cancer: A Systematic Review and Meta-analysis. *Clin Colorectal Cancer* 2018; **17**: 13-24 [PMID: 29153429 DOI: 10.1016/j.clcc.2017.10.012]

35 **Kim MJ**, Cho JS, Kim EM, Ko WA, Oh JH. Optimal Time Interval for Surgery After Neoadjuvant Chemoradiotherapy in Patients With Locally Advanced Rectal Cancer: Analysis of Health Insurance Review and Assessment Service Data. *Ann Coloproctol* 2018; **34**: 241-247 [PMID: 30419721 DOI: 10.3393/ac.2018.01.01]

36 **Petrelli F**, Sgroi G, Sarti E, Barni S. Increasing the Interval Between Neoadjuvant Chemoradiotherapy and Surgery in Rectal Cancer: A Meta-analysis of Published Studies. *Ann Surg* 2016; **263**: 458-464 [PMID: 24263329 DOI: 10.1097/SLA.0000000000000368]

37 **Figueiredo N**, Panteleimonitis S, Popeskou S, Cunha JF, Qureshi T, Beets GL, Heald RJ, Parvaiz A. Delaying surgery after neoadjuvant chemoradiotherapy in rectal cancer has no influence in surgical approach or short-term clinical outcomes. *Eur J Surg Oncol* 2018; **44**: 484-489 [PMID: 29398323 DOI: 10.1016/j.ejso.2018.01.088]

38 **Ansari N**, Solomon MJ, Fisher RJ, Mackay J, Burmeister B, Ackland S, Heriot A, Joseph D, McLachlan SA, McClure B, Ngan SY. Acute Adverse Events and Postoperative Complications in a Randomized Trial of Preoperative Short-course Radiotherapy Versus Long-course Chemoradiotherapy for T3 Adenocarcinoma of the Rectum: Trans-Tasman Radiation Oncology Group Trial (TROG 01.04). *Ann Surg* 2017; **265**: 882-888 [PMID: 27631775 DOI: 10.1097/SLA.0000000000001987]

39 **Croese AD**, Lonie JM, Trollope AF, Vangaveti VN, Ho YH. A meta-analysis of the prevalence of Low Anterior Resection Syndrome and systematic review of risk factors. *Int J Surg* 2018; **56**: 234-241 [PMID:

29936195 DOI: 10.1016/j.ijsu.2018.06.031]
40 **Ho YH**, Seow-Choen F, Tan M. Colonic J-pouch function at six months versus straight coloanal anastomosis at two years: randomized controlled trial. *World J Surg* 2001; **25**: 876-881 [PMID: 11572027]
41 **Lazorthes F**, Chiotasso P, Gamagami RA, Istvan G, Chevreau P. Late clinical outcome in a randomized prospective comparison of colonic J pouch and straight coloanal anastomosis. *Br J Surg* 1997; **84**: 1449-1451 [PMID: 9361611]
42 **Brown CJ**, Fenech DS, McLeod RS. Reconstructive techniques after rectal resection for rectal cancer. *Cochrane Database Syst Rev* 2008; CD006040 [PMID: 18425933 DOI: 10.1002/14651858.CD006040.pub2]
43 **Bregendahl S**, Emmertsen KJ, Lous J, Laurberg S. Bowel dysfunction after low anterior resection with and without neoadjuvant therapy for rectal cancer: a population-based cross-sectional study. *Colorectal Dis* 2013; **15**: 1130-1139 [PMID: 23581977 DOI: 10.1111/codi.12244]
44 **Chen TY**, Wiltink LM, Nout RA, Meershoek-Klein Kranenbarg E, Laurberg S, Marijnen CA, van de Velde CJ. Bowel function 14 years after preoperative short-course radiotherapy and total mesorectal excision for rectal cancer: report of a multicenter randomized trial. *Clin Colorectal Cancer* 2015; **14**: 106-114 [PMID: 25677122 DOI: 10.1016/j.clcc.2014.12.007]
45 **Kupsch J**, Jackisch T, Matzel KE, Zimmer J, Schreiber A, Sims A, Witzigmann H, Stelzner S. Outcome of bowel function following anterior resection for rectal cancer-an analysis using the low anterior resection syndrome (LARS) score. *Int J Colorectal Dis* 2018; **33**: 787-798 [PMID: 29541896 DOI: 10.1007/s00384-018-3006-x]
46 **Kupsch J**, Kuhn M, Matzel KE, Zimmer J, Radulova-Mauersberger O, Sims A, Witzigmann H, Stelzner S. To what extent is the low anterior resection syndrome (LARS) associated with quality of life as measured using the EORTC C30 and CR38 quality of life questionnaires? *Int J Colorectal Dis* 2019; **34**: 747-762 [PMID: 30721417 DOI: 10.1007/s00384-019-03249-7]
47 **Lee JY**, Kim HC, Huh JW, Sim WS, Lim HY, Lee EK, Park HG, Bang YJ. Incidence and risk factors for rectal pain after laparoscopic rectal cancer surgery. *J Int Med Res* 2017; **45**: 781-791 [PMID: 28415928 DOI: 10.1177/0300060517693421]
48 **Hendren SK**, O'Connor BI, Liu M, Asano T, Cohen Z, Swallow CJ, Macrae HM, Gryfe R, McLeod RS. Prevalence of male and female sexual dysfunction is high following surgery for rectal cancer. *Ann Surg* 2005; **242**: 212-223 [PMID: 16041212 DOI: 10.1097/01.sla.0000171299.43954.ce]
49 **Costa P**, Cardoso JM, Louro H, Dias J, Costa L, Rodrigues R, Espiridião P, Maciel J, Ferraz L. Impact on sexual function of surgical treatment in rectal cancer. *Int Braz J Urol* 2018; **44**: 141-149 [PMID: 29219281 DOI: 10.1590/S1677-5538.IBJU.2017.0318]
50 **Attaallah W**, Ertekin SC, Yegen C. Prospective study of sexual dysfunction after proctectomy for rectal cancer. *Asian J Surg* 2018; **41**: 454-461 [PMID: 28800864 DOI: 10.1016/j.asjsur.2017.04.005]
51 **Ledebo A**, Bock D, Prytz M, Haglind E, Angenete E. Urogenital function 3 years after abdominoperineal excision for rectal cancer. *Colorectal Dis* 2018; **20**: O123-O134 [PMID: 29679517 DOI: 10.1111/codi.14229]
52 **Hopewell JW**. Radiation-therapy effects on bone density. *Med Pediatr Oncol* 2003; **41**: 208-211 [PMID: 12868120 DOI: 10.1002/mpo.10338]
53 **Jørgensen JB**, Bondeven P, Iversen LH, Laurberg S, Pedersen BG. Pelvic insufficiency fractures frequently occur following preoperative chemo-radiotherapy for rectal cancer - a nationwide MRI study. *Colorectal Dis* 2018; **20**: 873-880 [PMID: 29673038 DOI: 10.1111/codi.14224]
54 **Kim HJ**, Boland PJ, Meredith DS, Lis E, Zhang Z, Shi W, Yamada YJ, Goodman KA. Fractures of the sacrum after chemoradiation for rectal carcinoma: incidence, risk factors, and radiographic evaluation. *Int J Radiat Oncol Biol Phys* 2012; **84**: 694-699 [PMID: 22867889 DOI: 10.1016/j.ijrobp.2012.01.021]
55 **Eisenhauer EA**, Therasse P, Bogaerts J, Schwartz LH, Sargent D, Ford R, Dancey J, Arbuck S, Gwyther S, Mooney M, Rubinstein L, Shankar L, Dodd L, Kaplan R, Lacombe D, Verweij J. New response evaluation criteria in solid tumours: revised RECIST guideline (version 1.1). *Eur J Cancer* 2009; **45**: 228-247 [PMID: 19097774 DOI: 10.1016/j.ejca.2008.10.026]
56 **Habr-Gama A**, de Souza PM, Ribeiro U, Nadalin W, Gansl R, Sousa AH, Campos FG, Gama-Rodrigues J. Low rectal cancer: impact of radiation and chemotherapy on surgical treatment. *Dis Colon Rectum* 1998; **41**: 1087-1096 [PMID: 9749491 DOI: 10.1007/bf02239429]
57 **Habr-Gama A**, Perez RO, Nadalin W, Sabbaga J, Ribeiro U, Silva e Sousa AH, Campos FG, Kiss DR, Gama-Rodrigues J. Operative versus nonoperative treatment for stage 0 distal rectal cancer following chemoradiation therapy: long-term results. *Ann Surg* 2004; **240**: 711-7; discussion 717-8 [PMID: 15383798 DOI: 10.1097/01.sla.0000141194.27992.32]
58 **van der Valk MJM**, Hilling DE, Bastiaannet E, Meershoek-Klein Kranenbarg E, Beets GL, Figueiredo NL, Habr-Gama A, Perez RO, Renehan AG, van de Velde CJH; IWWD Consortium. Long-term outcomes of clinical complete responders after neoadjuvant treatment for rectal cancer in the International Watch & Wait Database (IWWD): an international multicentre registry study. *Lancet* 2018; **391**: 2537-2545 [PMID: 29976470 DOI: 10.1016/S0140-6736(18)31078-X]
59 **Renehan AG**, Malcomson L, Emsley R, Gollins S, Maw A, Myint AS, Rooney PS, Susnerwala S, Blower A, Saunders MP, Wilson MS, Scott N, O'Dwyer ST. Watch-and-wait approach versus surgical resection after chemoradiotherapy for patients with rectal cancer (the OnCoRe project): a propensity-score matched cohort analysis. *Lancet Oncol* 2016; **17**: 174-183 [PMID: 26705854 DOI: 10.1016/S1470-2045(15)00467-2]
60 **Gerard JP**, Coquard R, Fric D, Ayzac L, Romestaing P, Ardiet JM, Rocher FP, Baron MH, Trillet-Lenoir V. Curative endocavitary irradiation of small rectal cancers and preoperative radiotherapy in T2 T3 (T4) rectal cancer. A brief overview of the Lyon experience. *Eur J Surg Oncol* 1994; **20**: 644-647 [PMID: 7995415]
61 **Schild SE**, Martenson JA, Gunderson LL. Endocavitary radiotherapy of rectal cancer. *Int J Radiat Oncol Biol Phys* 1996; **34**: 677-682 [PMID: 8621292 DOI: 10.1016/0360-3016(95)02098-5]
62 **Gerard JP**, Chapet O, Nemoz C, Hartweig J, Romestaing P, Coquard R, Barbet N, Maingon P, Mahe M, Baulieux J, Partensky C, Papillon M, Glehen O, Crozet B, Grandjean JP, Adeleine P. Improved sphincter preservation in low rectal cancer with high-dose preoperative radiotherapy: the lyon R96-02 randomized trial. *J Clin Oncol* 2004; **22**: 2404-2409 [PMID: 15197202 DOI: 10.1200/JCO.2004.08.170]
63 **Ortholan C**, Romestaing P, Chapet O, Gerard JP. Correlation in rectal cancer between clinical tumor response after neoadjuvant radiotherapy and sphincter or organ preservation: 10-year results of the Lyon R 96-02 randomized trial. *Int J Radiat Oncol Biol Phys* 2012; **83**: e165-e171 [PMID: 22579379 DOI: 10.1016/j.ijrobp.2011.12.002]

64 **Pigot F**, Bouchard D, Mortaji M, Castinel A, Juguet F, Chaume JC, Faivre J. Local excision of large rectal villous adenomas: long-term results. *Dis Colon Rectum* 2003; **46**: 1345-1350 [PMID: 14530673 DOI: 10.1007/s10350-004-6748-1]

65 **Rai V**, Mishra N. Transanal Approach to Rectal Polyps and Cancer. *Clin Colon Rectal Surg* 2016; **29**: 65-70 [PMID: 26929754 DOI: 10.1055/s-0035-1570395]

66 **Buess G**, Theiss R, Günther M, Hutterer F, Pichlmaier H. [Transanal endoscopic microsurgery]. *Leber Magen Darm* 1985; **15**: 271-279 [PMID: 4079630]

67 **O'Neill CH**, Platz J, Moore JS, Callas PW, Cataldo PA. Transanal Endoscopic Microsurgery for Early Rectal Cancer: A Single-Center Experience. *Dis Colon Rectum* 2017; **60**: 152-160 [PMID: 28059911 DOI: 10.1097/DCR.0000000000000764]

68 **Stijns RCH**, de Graaf EJR, Punt CJA, Nagtegaal ID, Nuyttens JJME, van Meerten E, Tanis PJ, de Hingh IHJT, van der Schelling GP, Acherman Y, Leijtens JWA, Bremers AJA, Beets GL, Hoff C, Verhoef C, Marijnen CAM, de Wilt JHW; CARTS Study Group. Long-term Oncological and Functional Outcomes of Chemoradiotherapy Followed by Organ-Sparing Transanal Endoscopic Microsurgery for Distal Rectal Cancer: The CARTS Study. *JAMA Surg* 2019; **154**: 47-54 [PMID: 30304338 DOI: 10.1001/jamasurg.2018.3752]

69 **Perez RO**, Habr-Gama A, São Julião GP, Proscurshim I, Fernandez LM, de Azevedo RU, Vailati BB, Fernandes FA, Gama-Rodrigues J. Transanal Endoscopic Microsurgery (TEM) Following Neoadjuvant Chemoradiation for Rectal Cancer: Outcomes of Salvage Resection for Local Recurrence. *Ann Surg Oncol* 2016; **23**: 1143-1148 [PMID: 26577119 DOI: 10.1245/s10434-015-4977-2]

70 **Atallah S**, Albert M, Larach S. Transanal minimally invasive surgery: a giant leap forward. *Surg Endosc* 2010; **24**: 2200-2205 [PMID: 20174935 DOI: 10.1007/s00464-010-0927-z]

71 **Lee L**, Edwards K, Hunter IA, Hartley JE, Atallah SB, Albert MR, Hill J, Monson JR. Quality of Local Excision for Rectal Neoplasms Using Transanal Endoscopic Microsurgery Versus Transanal Minimally Invasive Surgery: A Multi-institutional Matched Analysis. *Dis Colon Rectum* 2017; **60**: 928-935 [PMID: 28796731 DOI: 10.1097/DCR.0000000000000884]

72 **Martin-Perez B**, Andrade-Ribeiro GD, Hunter L, Atallah S. A systematic review of transanal minimally invasive surgery (TAMIS) from 2010 to 2013. *Tech Coloproctol* 2014; **18**: 775-788 [PMID: 24848524 DOI: 10.1007/s10151-014-1148-6]

73 **Albert MR**, Atallah SB, deBeche-Adams TC, Izfar S, Larach SW. Transanal minimally invasive surgery (TAMIS) for local excision of benign neoplasms and early-stage rectal cancer: efficacy and outcomes in the first 50 patients. *Dis Colon Rectum* 2013; **56**: 301-307 [PMID: 23392143 DOI: 10.1097/DCR.0b013e31827ca313]

74 **Keller DS**, Tahilramani RN, Flores-Gonzalez JR, Mahmood A, Haas EM. Transanal Minimally Invasive Surgery: Review of Indications and Outcomes from 75 Consecutive Patients. *J Am Coll Surg* 2016; **222**: 814-822 [PMID: 27016903 DOI: 10.1016/j.jamcollsurg.2016.02.003]

75 **Atallah SB**, Albert MR, deBeche-Adams TH, Larach SW. Robotic TransAnal Minimally Invasive Surgery in a cadaveric model. *Tech Coloproctol* 2011; **15**: 461-464 [PMID: 21953243 DOI: 10.1007/s10151-011-0762-9]

76 **Hompes R**, Rauh SM, Hagen ME, Mortensen NJ. Preclinical cadaveric study of transanal endoscopic da Vinci® surgery. *Br J Surg* 2012; **99**: 1144-1148 [PMID: 22619046 DOI: 10.1002/bjs.8794]

77 **Tomassi MJ**, Taller J, Yuhan R, Ruan JH, Klaristenfeld DD. Robotic Transanal Minimally Invasive Surgery for the Excision of Rectal Neoplasia: Clinical Experience With 58 Consecutive Patients. *Dis Colon Rectum* 2019; **62**: 279-285 [PMID: 30451744 DOI: 10.1097/DCR.0000000000001223]

78 **Trépanier JS**, Fernandez-Hevia M, Lacy AM. Transanal total mesorectal excision: surgical technique description and outcomes. *Minim Invasive Ther Allied Technol* 2016; **25**: 234-240 [PMID: 27336195 DOI: 10.1080/13645706.2016.1199434]

79 **Marks JH**, Myers EA, Zeger EL, Denittis AS, Gummadi M, Marks GJ. Long-term outcomes by a transanal approach to total mesorectal excision for rectal cancer. *Surg Endosc* 2017; **31**: 5248-5257 [PMID: 28643051 DOI: 10.1007/s00464-017-5597-7]

80 **Simillis C**, Lal N, Thoukididou SN, Kontovounisios C, Smith JJ, Hompes R, Adamina M, Tekkis PP. Open Versus Laparoscopic Versus Robotic Versus Transanal Mesorectal Excision for Rectal Cancer: A Systematic Review and Network Meta-analysis. *Ann Surg* 2019; **270**: 59-68 [PMID: 30720507 DOI: 10.1097/SLA.0000000000003227]

81 **Ravitch MM**, Steichen FM. A stapling instrument for end-to-end inverting anastomoses in the gastrointestinal tract. *Ann Surg* 1979; **189**: 791-797 [PMID: 453950 DOI: 10.1097/00000658-197906000-00017]

82 **Parks AG**, Percy JP. Resection and sutured colo-anal anastomosis for rectal carcinoma. *Br J Surg* 1982; **69**: 301-304 [PMID: 7082951 DOI: 10.1002/bjs.1800690602]

83 **van der Pas MH**, Haglind E, Cuesta MA, Fürst A, Lacy AM, Hop WC, Bonjer HJ; COlorectal cancer Laparoscopic or Open Resection II (COLOR II) Study Group. Laparoscopic versus open surgery for rectal cancer (COLOR II): short-term outcomes of a randomised, phase 3 trial. *Lancet Oncol* 2013; **14**: 210-218 [PMID: 23395398 DOI: 10.1016/S1470-2045(13)70016-0]

84 **Guillou PJ**, Quirke P, Thorpe H, Walker J, Jayne DG, Smith AM, Heath RM, Brown JM; MRC CLASICC trial group. Short-term endpoints of conventional versus laparoscopic-assisted surgery in patients with colorectal cancer (MRC CLASICC trial): multicentre, randomised controlled trial. *Lancet* 2005; **365**: 1718-1726 [PMID: 15894098 DOI: 10.1016/S0140-6736(05)66545-2]

85 **Fleshman J**, Branda M, Sargent DJ, Boller AM, George V, Abbas M, Peters WR, Maun D, Chang G, Herline A, Fichera A, Mutch M, Wexner S, Whiteford M, Marks J, Birnbaum E, Margolin D, Larson D, Marcello P, Posner M, Read T, Monson J, Wren SM, Pisters PW, Nelson H. Effect of Laparoscopic-Assisted Resection vs Open Resection of Stage II or III Rectal Cancer on Pathologic Outcomes: The ACOSOG Z6051 Randomized Clinical Trial. *JAMA* 2015; **314**: 1346-1355 [PMID: 26441179 DOI: 10.1001/jama.2015.10529]

86 **Hojo K**, Sawada T, Moriya Y. An analysis of survival and voiding, sexual function after wide iliopelvic lymphadenectomy in patients with carcinoma of the rectum, compared with conventional lymphadenectomy. *Dis Colon Rectum* 1989; **32**: 128-133 [PMID: 2914526 DOI: 10.1007/bf02553825]

87 **Knight CD**, Griffen FD. An improved technique for low anterior resection of the rectum using the EEA stapler. *Surgery* 1980; **88**: 710-714 [PMID: 7434211]

88 **Bujko K**, Wyrwicz L, Rutkowski A, Malinowska M, Pietrzak L, Kryński J, Michalski W, Olędzki J, Kuśnierz J, Zając L, Bednarczyk M, Szczepkowski M, Tarnowski W, Kosakowska E, Zwoliński J, Winiarek M, Wiśniowska K, Partycki M, Bęczkowska K, Polkowski W, Styliński R, Wierzbicki R, Bury

P, Jankiewicz M, Paprota K, Lewicka M, Ciseł B, Skórzewska M, Mielko J, Bębenek M, Maciejczyk A, Kapturkiewicz B, Dybko A, Hajac Ł, Wojnar A, Leśniak T, Zygulska J, Jantner D, Chudyba E, Zegarski W, Las-Jankowska M, Jankowski M, Kołodziejski L, Radkowski A, Żelazowska-Omiotek U, Czeremszyńska B, Kępka L, Kolb-Sielecki J, Toczko Z, Fedorowicz Z, Dziki A, Danek A, Nawrocki G, Sopyło R, Markiewicz W, Kędzierawski P, Wydmański; Polish Colorectal Study Group. Long-course oxaliplatin-based preoperative chemoradiation versus 5 × 5 Gy and consolidation chemotherapy for cT4 or fixed cT3 rectal cancer: results of a randomized phase III study. *Ann Oncol* 2016; **27**: 834-842 [PMID: 26884592 DOI: 10.1093/annonc/mdw062]

89 **Ngan SY**, Burmeister B, Fisher RJ, Solomon M, Goldstein D, Joseph D, Ackland SP, Schache D, McClure B, McLachlan SA, McKendrick J, Leong T, Hartopeanu C, Zalcberg J, Mackay J. Randomized trial of short-course radiotherapy versus long-course chemoradiation comparing rates of local recurrence in patients with T3 rectal cancer: Trans-Tasman Radiation Oncology Group trial 01.04. *J Clin Oncol* 2012; **30**: 3827-3833 [PMID: 23008301 DOI: 10.1200/JCO.2012.42.9597]

90 **Wawok P**, Polkowski W, Richter P, Szczepkowski M, Olędzki J, Wierzbicki R, Gach T, Rutkowski A, Dziki A, Kołodziejski L, Sopyło R, Pietrzak L, Kryński J, Wiśniowska K, Spałek M, Pawlewicz K, Polkowski M, Kowalska T, Paprota K, Jankiewicz M, Radkowski A, Chalubińska-Fendler J, Michalski W, Bujko K; Polish Colorectal Cancer Study Group. Preoperative radiotherapy and local excision of rectal cancer: Long-term results of a randomised study. *Radiother Oncol* 2018; **127**: 396-403 [PMID: 29680321 DOI: 10.1016/j.radonc.2018.04.004]

91 **Rödel C**, Liersch T, Becker H, Fietkau R, Hohenberger W, Hothorn T, Graeven U, Arnold D, Lang-Welzenbach M, Raab HR, Sülberg H, Wittekind C, Potapov S, Staib L, Hess C, Weigang-Köhler K, Grabenbauer GG, Hoffmanns H, Lindemann F, Schlenska-Lange A, Folprecht G, Sauer R; German Rectal Cancer Study Group. Preoperative chemoradiotherapy and postoperative chemotherapy with fluorouracil and oxaliplatin versus fluorouracil alone in locally advanced rectal cancer: initial results of the German CAO/ARO/AIO-04 randomised phase 3 trial. *Lancet Oncol* 2012; **13**: 679-687 [PMID: 22627104 DOI: 10.1016/S1470-2045(12)70187-0]

92 **Habr-Gama A**, Gama-Rodrigues J, São Julião GP, Proscurshim I, Sabbagh C, Lynn PB, Perez RO. Local recurrence after complete clinical response and watch and wait in rectal cancer after neoadjuvant chemoradiation: impact of salvage therapy on local disease control. *Int J Radiat Oncol Biol Phys* 2014; **88**: 822-828 [PMID: 24495589 DOI: 10.1016/j.ijrobp.2013.12.012]

93 **Appelt AL**, Pløen J, Harling H, Jensen FS, Jensen LH, Jørgensen JC, Lindebjerg J, Rafaelsen SR, Jakobsen A. High-dose chemoradiotherapy and watchful waiting for distal rectal cancer: a prospective observational study. *Lancet Oncol* 2015; **16**: 919-927 [PMID: 26156652 DOI: 10.1016/S1470-2045(15)00120-5]

94 **Smith JD**, Ruby JA, Goodman KA, Saltz LB, Guillem JG, Weiser MR, Temple LK, Nash GM, Paty PB. Nonoperative management of rectal cancer with complete clinical response after neoadjuvant therapy. *Ann Surg* 2012; **256**: 965-972 [PMID: 23154394 DOI: 10.1097/SLA.0b013e3182759f1c]

95 **Smith JJ**, Strombom P, Chow OS, Roxburgh CS, Lynn P, Eaton A, Widmar M, Ganesh K, Yaeger R, Cercek A, Weiser MR, Nash GM, Guillem JG, Temple LKF, Chalasani SB, Fuqua JL, Petkovska I, Wu AJ, Reyngold M, Vakiani E, Shia J, Segal NH, Smith JD, Crane C, Gollub MJ, Gonen M, Saltz LB, Garcia-Aguilar J, Paty PB. Assessment of a Watch-and-Wait Strategy for Rectal Cancer in Patients With a Complete Response After Neoadjuvant Therapy. *JAMA Oncol* 2019; e185896 [PMID: 30629084 DOI: 10.1001/jamaoncol.2018.5896]

96 **Martens MH**, Maas M, Heijnen LA, Lambregts DM, Leijtens JW, Stassen LP, Breukink SO, Hoff C, Belgers EJ, Melenhorst J, Jansen R, Buijsen J, Hoofwijk TG, Beets-Tan RG, Beets GL. Long-term Outcome of an Organ Preservation Program After Neoadjuvant Treatment for Rectal Cancer. *J Natl Cancer Inst* 2016; **108** [PMID: 27509881 DOI: 10.1093/jnci/djw171]

97 **Lai CL**, Lai MJ, Wu CC, Jao SW, Hsiao CW. Rectal cancer with complete clinical response after neoadjuvant chemoradiotherapy, surgery, or "watch and wait". *Int J Colorectal Dis* 2016; **31**: 413-419 [PMID: 26607907 DOI: 10.1007/s00384-015-2460-y]

98 **Rijkmans EC**, Cats A, Nout RA, van den Bongard DHJG, Ketelaars M, Buijsen J, Rozema T, Franssen JH, Velema LA, van Triest B, Marijnen CAM. Endorectal Brachytherapy Boost After External Beam Radiation Therapy in Elderly or Medically Inoperable Patients With Rectal Cancer: Primary Outcomes of the Phase 1 HERBERT Study. *Int J Radiat Oncol Biol Phys* 2017; **98**: 908-917 [PMID: 28366579 DOI: 10.1016/j.ijrobp.2017.01.033]

99 **Vuong T**, Devic S, Podgorsak E. High dose rate endorectal brachytherapy as a neoadjuvant treatment for patients with resectable rectal cancer. *Clin Oncol (R Coll Radiol)* 2007; **19**: 701-705 [PMID: 17714925 DOI: 10.1016/j.clon.2007.07.006]

100 **Gérard JP**, Barbet N, Gal J, Dejean C, Evesque L, Doyen J, Coquard R, Gugenheim J, Benizri E, Schiappa R, Baudin G, Benezery K, François E. Planned organ preservation for early T2-3 rectal adenocarcinoma: A French, multicentre study. *Eur J Cancer* 2019; **108**: 1-16 [PMID: 30580125 DOI: 10.1016/j.ejca.2018.11.022]

101 **Sun Myint A**, Smith FM, Gollins S, Wong H, Rao C, Whitmarsh K, Sripadam R, Rooney P, Hershman M, Pritchard DM. Dose Escalation Using Contact X-ray Brachytherapy After External Beam Radiotherapy as Nonsurgical Treatment Option for Rectal Cancer: Outcomes From a Single-Center Experience. *Int J Radiat Oncol Biol Phys* 2018; **100**: 565-573 [PMID: 29229327 DOI: 10.1016/j.ijrobp.2017.10.022]

102 **Jeong WK**, Park JW, Choi HS, Chang HJ, Jeong SY. Transanal endoscopic microsurgery for rectal tumors: experience at Korea's National Cancer Center. *Surg Endosc* 2009; **23**: 2575-2579 [PMID: 19347399 DOI: 10.1007/s00464-009-0466-7]

103 **Stipa F**, Giaccaglia V, Burza A. Management and outcome of local recurrence following transanal endoscopic microsurgery for rectal cancer. *Dis Colon Rectum* 2012; **55**: 262-269 [PMID: 22469792 DOI: 10.1097/DCR.0b013e318241ef22]

104 **Baatrup G**, Breum B, Qvist N, Wille-Jørgensen P, Elbrønd H, Møller P, Hesselfeldt P. Transanal endoscopic microsurgery in 143 consecutive patients with rectal adenocarcinoma: results from a Danish multicenter study. *Colorectal Dis* 2009; **11**: 270-275 [PMID: 18573118 DOI: 10.1111/j.1463-1318.2008.01600.x]

105 **Van den Eynde F**, Jaekers J, Fieuws S, D'Hoore AM, Wolthuis AM. TAMIS is a valuable alternative to TEM for resection of intraluminal rectal tumors. *Tech Coloproctol* 2019; **23**: 161-166 [PMID: 30859349 DOI: 10.1007/s10151-019-01954-7]

106 **García-Flórez LJ**, Otero-Díez JL, Encinas-Muñiz AI, Sánchez-Domínguez L. Indications and Outcomes From 32 Consecutive Patients for the Treatment of Rectal Lesions by Transanal Minimally Invasive

Surgery. *Surg Innov* 2017; **24**: 336-342 [PMID: 28355962 DOI: 10.1177/1553350617700803]
107 **Melin AA**, Kalaskar S, Taylor L, Thompson JS, Ternent C, Langenfeld SJ. Transanal endoscopic microsurgery and transanal minimally invasive surgery: is one technique superior? *Am J Surg* 2016; **212**: 1063-1067 [PMID: 27810138 DOI: 10.1016/j.amjsurg.2016.08.017]

World Journal of Gastroenterology

Submit a Manuscript: https://www.f6publishing.com

World J Gastroenterol 2019 September 7; 25(33): 4870-4884

DOI: 10.3748/wjg.v25.i33.4870

ISSN 1007-9327 (print) ISSN 2219-2840 (online)

MINIREVIEWS

Helicobacter pylori virulence genes

Anja Šterbenc, Erika Jarc, Mario Poljak, Matjaž Homan

ORCID number: Anja Šterbenc (0000-0001-8522-3753); Erika Jarc (0000-0001-8516-9179); Mario Poljak (0000-0002-3216-7564); Matjaž Homan (0000-0001-5764-5430).

Author contributions: All authors contributed equally to this paper, with conception and design of the study, literature review and analysis, drafting and critical revision and editing, and final approval of the final version.

Conflict-of-interest statement: No potential conflicts of interest. No financial support.

Manuscript source: Invited manuscript

Received: May 18, 2019
Peer-review started: May 20, 2019
First decision: July 21, 2019
Revised: July 29, 2019
Accepted: August 7, 2019
Article in press: August 7, 2019
Published online: September 7, 2019

P-Reviewer: Amiri M, Chmiela M, Giordano A

Anja Šterbenc, Erika Jarc, Mario Poljak, Institute of Microbiology and Immunology, Faculty of Medicine, University of Ljubljana, Ljubljana 1000, Slovenia

Matjaž Homan, Department of Gastroenterology, Hepatology and Nutrition, University Children's Hospital, Faculty of Medicine, University of Ljubljana, Ljubljana 1000, Slovenia

Corresponding author: Matjaž Homan, MD, PhD, Assistant Professor, Department of Gastroenterology, Hepatology and Nutrition, University Children's Hospital, Faculty of Medicine, University of Ljubljana, Bohoričeva 20, Ljubljana 1000, Slovenia.
matjaz.homan@guest.arnes.si
Telephone: +386-1-5229276
Fax: +386-1-5229350

Abstract

Helicobacter pylori (*H. pylori*) is one of the most important human pathogens, infecting approximately half of the global population. Despite its high prevalence, only a subset of *H. pylori* infected individuals develop serious gastroduodenal pathology. The pathogenesis of *H. pylori* infection and disease outcome is thus thought to be mediated by an intricate interplay between host, environmental and bacterial virulence factors. *H. pylori* has adapted to the harsh milieu of the human stomach through possession of various virulence genes that enable survival of the bacteria in the acidic environment, movement towards the gastric epithelium, and attachment to gastric epithelial cells. These virulence factors enable successful colonization of the gastric mucosa and sustain persistent *H. pylori* infection, causing chronic inflammation and tissue damage, which may eventually lead to the development of peptic ulcers and gastric cancer. Numerous studies have focused on the prevalence and role of putative *H. pylori* virulence genes in disease pathogenesis. While several virulence factors with various functions have been identified, disease associations appear to be less evident, especially among different study populations. This review presents key findings on the most important *H. pylori* virulence genes, including several bacterial adhesins and toxins, in children and adults, and focuses on their prevalence, clinical significance and potential relationships.

Key words: *Helicobacter pylori*; Virulence genes; Disease association; Children; Adults; Outer membrane proteins; Bacterial toxins

Core tip: The assessment of pathogenicity of a plethora of *Helicobacter pylori* (*H. pylori*) virulence genes appears to be relatively difficult. In specific, *H. pylori* isolates show a

S-Editor: Yan JP
L-Editor: A
E-Editor: Ma YJ

high degree of geographic variability, with certain *H. pylori* genotypes being associated with a more severe clinical outcome in some regions, while presenting as virtually harmless variants in other studied populations. To date, *cagA* and certain allelic variants of *vacA* have been most consistently associated with severe gastroduodenal disease in both children and adults, whereas the role of outer membrane proteins, such as *babA2*, *sabA*, *homB* and *oipA*, is somewhat more ambiguous.

Citation: Šterbenc A, Jarc E, Poljak M, Homan M. *Helicobacter pylori* virulence genes. *World J Gastroenterol* 2019; 25(33): 4870-4884
URL: https://www.wjgnet.com/1007-9327/full/v25/i33/4870.htm
DOI: https://dx.doi.org/10.3748/wjg.v25.i33.4870

INTRODUCTION

As one of the most common bacterial infections, *Helicobacter pylori* (*H. pylori*) infects approximately half of the world's population, although substantial regional variation exists[1]. The infection is usually acquired in childhood and persists lifelong in the absence of appropriate antibiotic treatment. In order to survive the harsh milieu of the human stomach, *H. pylori* had to adapt by possessing various virulence genes. However, the significance of these virulence genes extends beyond the pure survival needs of the bacteria, making *H. pylori* one of the most well-adapted human pathogens, capable of sustaining extremely efficient persistent infection. *H. pylori* has in fact developed mechanisms to withstand gastric acidity through the possession of urease and multiple sheathed flagella, which enable the bacteria to move toward gastric epithelial cells. *H. pylori* then needs to establish permanent colonization of the gastric mucosa, which is accomplished by the action of outer membrane proteins (OMPs) and adhesins, which enable adherence to the gastric epithelial cells. Finally, *H. pylori* possesses an arsenal of virulence genes that encode for effector proteins, which directly impair the gastric epithelium[2,3]. Although infection with *H. pylori* almost inevitably leads to chronic active gastritis, only approximately 10%-15% of infected individuals develop severe gastroduodenal diseases, such as peptic ulcer disease (PUD), gastric carcinoma (GC) and mucosa associated lymphoid tissue (MALT) lymphoma[4,5]. Nevertheless, the high global prevalence of *H. pylori* is considered an important public health issue, especially since *H. pylori* is classified as a class I carcinogen. More than one million (1033701) new cases of GC were estimated to occur worldwide in 2018, accounting for 6.1% of all new cancer cases, ranking GC as the fifth most common malignancy among males and females on a global scale[6].

H. pylori infection in children and adults differs in several aspects. In children, it is thought that environmental factors, such as smoking, are implicated in disease development to a far lesser degree than in adults. Whereas several factors influence the prevalence rates of *H. pylori* infection in children (*e.g.*, gender, age, low socioeconomic status and family education, poor hygiene, household crowding and certain geographical regions), it has been shown that the infection is acquired in early childhood in both industrialized and non-industrialized countries[7]. The most frequent form of gastritis in children is nodular gastritis, while atrophic gastritis and intestinal metaplasia, which occur more often in adults, are relatively rarely found in children[7]. Because the degree of *H. pylori* colonization and repertoire of virulence genes are comparable in both children and adults, it is thought that the lower levels of gastric inflammation and lower rates of severe clinical outcome in children indicate downregulation of immune responses[8].

Over the past few decades, inclusion of proteomic and transcriptomic methods, as well as the availability of an increasing number of *H. pylori* partial and complete genomes, have significantly improved knowledge of the intricate gene regulatory networks of *H. pylori*. While the exact molecular mechanisms by which *H. pylori* infection induces a severe clinical outcome have not yet been clearly elucidated, they are thought to involve various elements, including host genetic and environmental factors, as well as certain bacterial virulence genes. In this review, we present the most important *H. pylori* virulence genes and discuss their prevalence and clinical significance in children and adults.

GENES ENCODING OUTER MEMBRANE PROTEINS

OMPs are a large group of proteins that confer durable colonization of *H. pylori* through specific interactions with the host receptors. It has been estimated that approximately 4% of the *H. pylori* genome encodes OMPs, suggesting that these proteins are of vital importance to the bacterial lifecycle[3,9]. Several OMPs have been described in detail to date, with most studies focusing on *babA2*, *oipA*, *homB*, and *sabA* genes.

babA2

To date, three allelic types of *bab* have been identified: *babA1*, *babA2* and *babB*. The *babA2* gene encodes a blood group antigen binding adhesin (BabA), a major adhesin on the outer bacterial membrane that enables binding of *H. pylori* to the mucosal Lewis^b blood group antigens, thus facilitating colonization and determining bacterial density. Strains carrying the *babA2* gene can be classified based on protein production as BabA high producers (BabA-H), which possess Lewis^b binding activity, and BabA low producers (BabA-L), which are not able to bind to Lewis^b antigens, while strains carrying the *babA1* gene lack BabA. Unfortunately, PCR was used in most studies evaluating the prevalence and clinical significance of *babA2*, although it has been shown that this method does not accurately reflect the functional status of BabA as determined by Lewis^b binding activity or immunoblotting[10,11]. Moreover, expression of BabA is generally regulated by phase variation and intragenomic recombination events between the *babA* gene and its highly homologous gene *babB*[11,12].

Adults: The prevalence of the *babA2* gene varies significantly among different geographic regions, from moderate (44.0% and 44.6% in strains from Portugal and Germany, respectively) to high (70.4% and 79.7% in strains from Iran and United States, respectively) and even universal presence in strains from Japan, South Korea, Taiwan and Brazil[13]. *H. pylori* strains from East Asia uniformly express the BabA protein[10,14], whereas only 9.8% of Western strains were shown to lack the BabA[10].

A meta-analysis of 38 case-control studies evaluating the relationship between the presence of the *babA2* and clinical outcome showed that detection of the *babA2* gene significantly increases the risk of PUD [odds ratio (OR) = 2.069, 95% confidence interval (CI): 1.532-2.794], especially in the duodenal ulcer subgroup (OR = 1.588, 95%CI: 1.141-2.209), with significant associations being more apparent in studies on Western isolates. Namely, the presence of the *babA2* gene substantially increased PUD risk in Western populations (OR = 2.739, 95%CI: 1.860-4.032), whereas the association with PUD was only marginal in Asian populations (OR = 1.370, 95%CI: 0.941-1.994), due to the very high overall prevalence of the *babA2* gene. Conversely, no significant risk correlation was observed for GC among Western (OR = 1.303, 95%CI: 0.881-1.927) or Asian populations (OR = 1.132, 95%CI: 0.763-1.680)[13]. The lack of association found in this meta-analysis could be due to significant heterogeneity among the performed studies, contradicting several reports that suggest *babA2* is indeed an important virulence factor in GC development, especially when co-expressed with other virulence factors. For example, it has been shown that the "triple-positive" genotype, simultaneously containing *babA2*, *vacA* s1 and *cagA*, serves as a better discriminative factor for PUD and GC than the *vacA* s1 and *cagA* only genotype[15]. Moreover, a study focusing on expression of the BabA protein has shown that patients from Western countries with BabA-H and BabA-L had a 18.2- (95%CI: 1.7-198) and 33.9-fold (95%CI: 2.8-411) increased risk of GC compared to those who were *babA2* negative[10]. Interestingly, a recent genome-wide association study on 173 European *H. pylori* isolates showed that, compared to strains obtained from gastritis patients, the GC phenotype was associated with certain single nucleotide polymorphisms and a specific array of genes, including the *babA2* gene[16]. Although the majority of studies on isolates from East Asia have failed to find an association between the *babA2* gene and disease status, a study from Taiwan highlighted the importance of the recombinant *babA/B* genotype, which was found to be associated with both precancerous lesions and GC[12].

Children: Data on the significance of the *babA2* gene in children is less abundant. To date, nine studies have evaluated the prevalence and clinical relevance of the *babA2* gene in children[17-20]. The prevalence ranged from 17.2% in Portuguese[21,22] to 84.4% in Brazilian strains[23]. Moreover, associations between the *babA2* gene and clinical outcome are inconsistent[17,24,25], with only two studies[17,22] correlating the presence of the *babA2* gene with a higher degree of gastric mucosal damage.

Associations with other virulence genes: The influence of the *babA2* gene on clinical outcome is generally associated with *cagA*, *vacA* s1, *vacA* m1[17] and *oipA* "on" status[26,27].

Comment: Unfortunately, despite a multitude of clinical and epidemiological studies that have attempted to identify possible links between the presence of the *babA2* gene and disease outcome, definite conclusions are difficult to reach, due to several factors that influence interpretation of the results. In addition to the distinct genotypic profile of Western and Asian isolates, considerable performance differences in *babA2* gene detection methods[17], as well as poor correlation between the presence of the *babA2* gene and actual expression and activity of the BabA2 protein[10], thus prevent simple comparisons between studies.

Outer inflammatory protein A

Outer inflammatory protein A (OipA) is encoded by the *oipA* gene and its expression is thought to be dependent on a slipped strand mispairing system. The proposed mechanisms by which a functional OipA (*e.g.*, *oipA* "on" status) promotes severe gastric pathology include the capacity of the bacteria to attach to the gastric epithelium, followed by subsequent apoptosis of host cells, toxicity and the induction of inflammation through increased interleukin- 8 (IL-8) production[28-35].

Adults: The overall prevalence of *oipA* "on" status in adult patients was shown to be remarkably consistent among certain geographical regions: Approximately 100%, 80% and 60% of East Asian, Latin American and Western strains, respectively, contained *oipA* "on" (Table 1). Unfortunately, the clinical significance of the *oipA* status remains controversial, although numerous studies have investigated its relevance. It has been proposed by some authors that OipA increases the risk for PUD and GC development by disrupting the balance between apoptosis and cell proliferation during *H. pylori* infection, causing PUD when apoptosis is promoted and metaplasia and GC when gastric cell proliferation is increased[36-39]. A meta-analysis of PUD and GC risk, based on *oipA* "on/off" status, showed increased overall risk of PUD (OR = 3.97, 95%CI: 2.89-5.45) and GC (OR = 2.43, 95%CI: 1.45-4.07) in individuals with *oipA* "on" status, while the presence of the *oipA* gene alone did not reflect its specific functional status, since it was not found to be associated with PUD or GC[40]. However, results from some studies contradict the findings from this meta-analysis, since no correlation between *oipA* and disease status or increased gastroduodenal damage was identified[27,31,32,35]. Moreover, it seems that *oipA* status by itself is not a useful marker for predicting the clinical outcome of *H. pylori* infection, especially in populations with a high prevalence of infection with virulent strains[32].

Children: In children, the frequency of the *oipA* "on" status tends to be somewhat lower than in adults (49.6%, 67.6% and 68.8% in children from Portugal, United States and Brazil, respectively)[22,30,41], with higher frequencies among pediatric strains from high risk populations in which the incidence of *H. pylori* infection and related disease is significant. Moreover, the OR for PUD risk was shown to be higher in children (OR= 7.03, 95%CI: 3.71-13.34) compared to that in adults, suggesting increased risk for PUD in children with *oipA* "on" status[40,42]. However, the observed differences between children and adults regarding the significance of *oipA* status were based on a relatively small number of strains tested and thus need to be confirmed in future studies.

Associations with other virulence genes: The *oipA* "on" status was found to be closely associated with *cagA* positivity[26,27,33,38], although it has also been linked to the presence of other *H. pylori* virulence genes, such as *vacA* s1[27,33,38], *vacA* m1[26,27,33], *vacA* m2[33] and *babA2*[26,27].

homB

The *hom* family contains four OMPs, of which *homA* and *homB* are the most studied. Strains can carry a single *homA* or *homB* gene, with one locus remaining empty, two copies of each gene (*homA*/*homA* or *homB*/*homB*), a single copy of each gene (*homA*/*homB*), or they can lack *homA* and *homB* genes, leaving both loci empty. HomB enables adherence to host gastric epithelial cells and has been shown to increase cellular IL-8 production *in vitro*[42]. The level of adherence and IL-8 secretion is proportional to the number of *homB* copies with strains that carry two copies of the *homB* gene, inducing more pronounced actions, leading to a higher degree of gastric mucosal damage[42].

Adults: Studies have found a relatively comparable prevalence of the *homB* gene in Western countries, with slightly more than half of the evaluated strains being *homB* positive (Table 2). However, it seems that the *homB* gene is more common in East Asia and West Africa than in the Middle East, where only approximately one third of strains contain *homB* (Table 2). In addition, the distribution, location and copy number of the *homB* gene seem to be dependent on geographical region, influencing potential

Table 1 Prevalence of *oipA* "on" status among isolates from various geographical regions

Country	Number of patients	Study population	*oipA* "on" prevalence	Association with other virulence genes
North-Eastern Brazil[30]	95	Adults with gastritis, GC and their first degree relatives, asymptomatic children	81.1%	*cagA* and *vacA* s1 m1
Iran[31]	53	Adults and children with chronic gastritis, PUD, intestinal metaplasia and GC	79.0%	*cagA*, *vacA* s1 m1
Venezuela[32]	113	Adults with chronic gastritis	83.0%	NA
Bulgaria[33]	70	Symptomatic adults	81.0%	*cagA*, *vacA* s1, m1 and m2
Malaysia and Singapore[34]	159	Adults with functional dyspepsia, GC and PUD	89.4%	*vacA* m1/m2
Italy[35]	90	Adults with chronic gastritis and PUD	77.4%	*babA2*, *hopQ*
Colombia and United States[36]	200	Patients with gastritis, PUD and GC	79.3%	*cagA*, *babA*
Germany[26]	58	Patients with chronic gastritis	59.0%	*cagA*, *vacA* s1, *babA*
Netherlands[37]	96	Adults with chronic gastritis, PUD, GC and lymphoma	72.0%	cag PAI+
Italy[27]	60	Adults with chronic gastritis, PUD and duodenitis	60.0%	*cagA*, *vacA* s1 and m1, *babA*
East Asia and India[38]	54	Adults with gastritis and PUD	100%	*cagA*, *vacA* s1
Western countries[38]	55	Adults with gastritis and PUD	63.6%	*cagA*, *vacA* s1

NA: Not available; PUD: Peptic ulcer disease; GC: Gastric cancer.

differences in disease outcome[42,43]. Whereas Western strains carry a single *hom* gene at locus A, East Asian strains only carry a single *hom* gene at locus B[42,44]. Interestingly, strains from Iran were shown to carry only one of the *hom* genes, *homA* and *homB* were not detected simultaneously in any of the 138 evaluated strains[45].

Whereas the two genes exhibit 90% sequence identity, they are correlated with different spectra of the disease[46-51]; *homA* has been associated with non-ulcer dyspepsia (NUD), whereas *homB* is presumed to be implicated in the development of PUD and GC, although this association is geographically dependent (Table 2). Moreover, strains carrying two copies of the *homB* gene were found to be most strongly correlated with PUD (OR = 4.91, 95%CI: 1.77-14.02)[42].

Children: Only three studies[22,42,50] have specifically focused on the prevalence and clinical significance of the *homB* gene in children. Whereas two studies from Portugal found a strong association between *homB* and PUD[22,42], *homB* was not considered to be an important individual virulence factor in Slovenian children and was only associated with a higher degree of mucosal damage when co-present with other virulence genes (*i.e.*, *cagA*, *vacA* and *babA2*)[50].

sabA

In addition to Lewis^b blood group antigens, sialyl-Lewis^x and sialyl-Lewis^a antigens are considered to be functional receptors, enabling *H. pylori* adherence. They are recognized by the corresponding sialic acid binding adhesin SabA, encoded by the *sabA* gene. In contrast to SabA, its homologue SabB does not seem to be able to bind to sialyl-Lewis^x and sialyl-Lewis^a receptors. Similar to *oipA*, the expression of SabA is regulated by phase variation, meaning only certain strains are capable of producing functional proteins[52,53]. The level of expression of SabA can rapidly adjust to the changing environment of the human stomach by switching "on" or "off". The sialyl-Lewis^x and sialyl-Lewis^a antigens are otherwise rarely present in normal gastric mucosa, and only after persistent *H. pylori* infection induces chronic inflammation of the gastric mucosa does replacement of naturally produced Lewis antigens occur[53]. Moreover, the *sabA* "on" status inversely correlates with the degree of gastric acid secretion, suggesting that differences in pH and/or antigen expression on atrophic mucosa can influence SabA expression[53].

Adults: In adults, *sabA* "on" was found in 63.2%, 49.0% and 35.5% of strains from

Table 2 Overview of studies on *homB* prevalence and clinical significance in adults and children

Country	Study population	Number of patients	*homB* prevalence	Clinical relevance of *homB*	Association with other virulence genes
Western countries[43]	Adults	234	53.8	Significant, PUD	*vacA* s1, *cagA*+
East Asian countries[43]	Adults	138	86.8	NS	NS
Western countries[46]	Adults	300	56.0	NA	NA
East Asian countries[46]	Adults	138	86.6	NA	NA
Burkina Faso[46]	Adults	11	90.9	NA	NA
Colombia, United States[47]	Adults	286	61.2	Significant, GC	*cagA*+
Iran[45]	Adults	138	43.5	Significant, GC	*cagA*+
Iraq[48]	NA	70	29.9	NS	NS
Turkey[48]	NA	64	33.9	NS	NS
South Korea[44]	Children and adults	260	69.2	NS	*vacA*
Portugal[49]	Children	45	58.4	Significant, PUD	NA
	Adults	90	57.7	NS	NA
Portugal[42]	Children	84	57.3	Significant, PUD	*cagA*+, *vacA* s1, *babA2*+, *hopQI*, *oipA* "on"
	Adults	106	56.8	Significant only in ≤ 40 yr of age, PUD	
Portugal[22]	Children	117	53.5	Significant, PUD	*jhp0562*
Slovenia[50]	Children	285	40.7	NS	NS

NS: Non-significant; NA: Not available; PUD: Peptic ulcer disease; NUD: Non-ulcer dyspepsia; GC: Gastric cancer.

Portugal[42], the Netherlands[37] and Italy[35], respectively. The rates are higher in Iran, with *sabA* "on" being detected in 85.3% of strains[31]. Similarly, functional *sabA* was found to be highly prevalent in Japan, it was present in 81.5% of patients with chronic gastritis, PUD and GC[54]. Interestingly, an analysis of strains from Taiwan showed that the *sabA* gene was present in 80.0% (116/145) of strains, whereas only 31.0% (45/145) actually expressed SabA[14].

In a study on 200 patients from Colombia and the United States, *sabA* "on" status was shown to be associated with the presence of pre-neoplastic lesions (*e.g.*, gastric atrophy and severe intestinal metaplasia) and GC. Moreover, *sabA* "on" was the only predictor of GC versus duodenal ulcer (OR = 2.8, 95%CI: 1.2-6.7) among several investigated OMPs in this study[36]. However, there were no statistically significant differences among Taiwanese patients with *sabA* "on" and *sabA* "off" in terms of the prevalence of gastric atrophy or intestinal metaplasia[14]. Although all *H. pylori* isolates from Iranian patients with GC were found to be *sabA* "on" (5/5, 100%), the link did not appear to be statistically significant[31]. Similarly, there was no correlation between *sabA* "on" and clinical outcome among Italian and Japanese patients[35,54], although *sabA* "on" was associated with atrophy and severe neutrophil infiltration in patients from Japan[54].

Children: In children, the prevalence of the *sabA* "on" genotype was found to be 44.0% among strains from Portugal and the *sabA* "on" status significantly correlated with NUD (P = 0.028, OR = 0.298)[42]. Similarly, a low rate of SabA producing strains (38.0%) was detected in a collection of gastric biopsies from children and young adults[55]. Interestingly, it has recently been proposed that high expression of *sabA* may be responsible for iron deficiency anemia in children and young adults[56].

Associations with other virulence genes: Studies evaluating associations between *sabA* and other virulence genes are somewhat contradictory. Whereas *sabA* was closely related to *cagA* and *babA2* positivity in European strains[52], subsequent studies could not confirm these findings[36,37].

Comment: Again, identification of the *sabA* "on" status by using PCR and sequencing may not reliably reflect the actual production of SabA, thus affecting the result interpretation of studies on *sabA* clinical relevance, which have primarily used sequencing-based methods[3,14].

VIRULENCE GENES THAT PRODUCE TOXINS AND CAUSE HOST TISSUE DAMAGE

cagA, cagPAI and EPIYA motifs

It has been previously shown that highly virulent *H. pylori* strains harbor the cytotoxin-associated genes pathogenicity island (*cag*PAI), which is a 40 kb region containing 31 genes that encode for components of a type IV secretion system, involved in CagA translocation and the host's inflammatory response[4]. *cagA* is arguably the most extensively studied *H. pylori* virulence gene to date. It is located at the end of the *cag*PAI and encodes a 120-145 kDa immunodominant protein, CagA[57]. Based on CagA production, *H. pylori* isolates can be divided into two groups: *cagA* negative and *cagA* positive. During infection, CagA is localized on the plasma membrane, where it is phosphorylated at specific Glu-Pro-Ile-Tyr-Ala (EPIYA)-motifs by host Src and Abl kinases. Four distinct segments harboring EPIYA-motifs have been described so far, designated as segments A, B, C, and D[11,57,58]. The biological activity of CagA depends on the number and types of the EPIYA-motifs at the C-terminal region. Following translocation, CagA interacts with multiple host cell molecules and is responsible for dysregulation of homeostatic signal transduction of gastric epithelial cells, induction of pro-inflammatory responses that lead to chronic inflammation of gastric mucosa, and induction of carcinogenesis through the modulation of apoptosis, disruption of cell polarity and promotion of genetic instability. Hence, due to its cancer-inducing traits, CagA was designated as the first bacterial oncoprotein[57,59].

Adults: An analysis of a global collection of *H. pylori* strains from 53 different geographical/ethnic sources showed the presence of *cag*PAI in more than 95% of strains from Western and South Africa and East and Central Asia, whereas the presence of *cag*PAI in other regions ranged from 81% (Northeastern Africa) to only 28% (Latin America). The prevalence of *cag*PAI in Europe was shown to be intermediate, with approximately 58% of strains harboring *cag*PAI[60]. The prevalence of *cagA* positive strains is approximately 60% and > 90% in Western and Asian countries, respectively[2]. In the Middle East, *cagA* is detected in nearly half of the strains[61].

Since the majority of East Asian strains harbor *cagA* irrespective of the disease status, it cannot be considered a useful marker of the disease. Nevertheless, based on mosaicism within the EPIYA-motifs, *cagA* positive strains can be further divided into Western (EPIYA-ABC, EPIYA-ABCC and EPIYA-ABCCC) and East Asian strains (EPIYA-ABD)[5,62]. Although very rarely, a subset of East Asian strains can possess a Western type EPIYA motif, whereas the reverse is not true for Western strains[32,58]. In Latin America, EPIYA-ABC is the most common motif, detected in approximately 51.6%-73.6% of strains, although strains with multiple EPIYA-C segments were found to be rare (2.7%) in a Venezuelan population[32].

When assessing the risk of infection with *cagA* positive strains for the development of GC, one must be aware of the considerable global variation, not only in the prevalence of *cagA* positive strains but also in the incidence of GC[60,63]. In Western countries, the presence of *cagA* is associated with a higher risk of GC and PUD development, whereas in East Asia, where almost all *H. pylori* strains contain *cagA*, this association is evident but less prominent[5]. Specifically, patients infected with *H. pylori* who had CagA antibodies were shown to have a 5.8-fold (95%CI: 2.6-13.0) increase in the likelihood of developing GC compared to uninfected individuals, whereas those who were CagA seronegative only had a slightly but not statistically significantly (OR 2.2, 95%CI: 0.9-5.4) increased risk of GC[64]. Moreover, a meta-analysis of CagA serostatus performed on 10 non-cardia gastric cancer case–control studies from Western populations showed marked differences in CagA seropositivity in *H. pylori* infected cases (62.8%, n = 1707) and controls (37.5%, n = 2124), with CagA seropositive status associated with a higher risk of GC development (OR = 2.87, 95%CI: 1.95-4.22) compared to the risk of being infected with *H. pylori* only (OR = 2.31, 95%CI: 1.58-3.39)[65]. Similarly, a meta-analysis of 10 gastric cancer case–control studies from East Asia also identified an association between CagA seropositivity and increased risk of GC[66], although OR (OR = 1.81, 95%CI: 1.30-2.11) was lower compared to that of Western populations[65,66]. In addition, a large meta-analysis on more than 17000 individuals identified a 1.69-fold risk (95%CI: 1.12-2.55) of PUD among *cagA* positive Western and Asian populations, with an even higher risk of GC (OR = 2.09, 95%CI: 1.48-2.94)[67]. CagA is also one of the few virulence factors associated with the development of gastric high-grade B cell lymphoma[11].

Different diagnostic approaches should be applied in different geographical regions—due to the almost universal presence of the *cagA* gene in East Asian strains,

the sensitivity of *cagA* gene detection is suboptimal, rendering *cagA* subtyping in order to identify those with high risk infections[11]. The number of EPIYA segments in the second repeat region is thought to be associated with GC. Namely, initial trials showed that the incidence of GC was considerably higher if patients were infected with strains harboring multiple EPIYA-C segments (EPIYA-ABCCC) than if patients were infected with strains harboring only one EPIYA-C segment (EPIYA-C). Unfortunately, because East Asian strains only harbor a single EPIYA-D segment, differentiation between chronic gastritis and GC using only the number of repeat regions has proved to be somewhat problematic[5,62]. To clarify this issue, a recent meta-analysis evaluated the differences in PUD and GC risk among strains carrying one EPIYA-D motif or multiple EPIYA-C motifs. In Asian strains, the presence of one EPIYA-D motif was significantly associated with increased GC risk (OR = 1.91, 95%CI: 1.19-3.07) compared with the presence of one EPIYA-C motif, whereas it was not significantly associated with PUD (OR = 0.90, 95%CI: 0.46-1.76). Moreover, multiple EPIYA-C motifs were associated with increased PUD risk (OR = 2.33, 95%CI: 1.29-4.20) in Asian countries and with increased GC risk (OR = 3.28, 95%CI: 2.32-4.64) in Western countries[68].

Children: In children, *cagA* is the best characterized among all virulence genes. Similar to adults, the prevalence of *cagA* in children varies among different countries/regions. The *cagA* gene can be found in more than half of *H. pylori* isolates obtained from symptomatic children from Western countries, namely 60.8% in Poland[18], 59.6% in Slovenia[69] and 70.0% in United States[41]. A surprisingly low prevalence of *cagA* was found in Portuguese children (22.4%)[21]. In Iran, the reported prevalence of *cagA* in symptomatic children ranges between 60.0 and 72.7%[70,71] and is similar to that in Turkish children (55.6%-61.0%)[25,72]. A high prevalence of *cagA* (73.0%) was also observed in symptomatic Venezuelan children with recurrent abdominal pain[73]. In Mexican children, *cagA* and *cag*PAI were detected in 63.3% and 71.4% of strains, respectively[74]. Similar to adults, strains from Korean and Japanese children almost exclusively carry the *cagA* gene (94.0% and 100%, respectively)[75,76]. Interestingly, it has previously been shown that the prevalence of *cagA* can be surprisingly high (66.1% and 75.0% in Colombia and Brazil, respectively) in asymptomatic children from high-risk populations, with rates that are comparable or even higher than those in symptomatic children from other regions[30,77]. It is thus possible that the high prevalence of virulent *H. pylori* variants in Colombian and Brazilian children contributes to the increased GC incidence in adults from the same region[77]. The high proportion (40.0%) of strains with multiple EPIYA-C motifs further confirms previous observations that this population may already be exposed to the most virulent variants of *H. pylori* at a young age[30]. The fact that infection with *H. pylori* is a risk factor for GC highlights the importance of early detection of *H. pylori* virulence factors in children, especially those residing in areas with a high prevalence of GC[77].

In China, the rates of *cagA* positivity in the pediatric population closely resemble those in adults, with the prevalence of *cagA* among children with symptomatic gastroduodenal disease being 94.4%, with no clinical relevance[78]. Similarly, because the *cagA* positive genotype is present in virtually all Korean and Japanese pediatric strains, no associations with severity of gastritis or PUD were found[75,76]. In contrast, *cagA* was significantly associated with PUD (OR = 14.06, 95%CI: 4.78-41.29)[42], higher *H. pylori* density score, and the degree of chronic and acute inflammation[69] in European children.

Associations with other virulence genes: Interestingly, almost all *vacA* s1 strains also carry *cagA*, whereas almost all *cagA* negative strains harbor the less virulent genotype *vacA* s2/m2[69,79]. In addition, *cagA* is also more commonly detected in *babA2* positive strains[77].

Vacuolating cytotoxin A

The vacuolating cytotoxin A (VacA) derives its name from its capacity to induce the formation of vacuoles in eukaryotic cells. Several other cellular functions of VacA with a potential influence on host cell death have been described thus far, including disruption of endocytic trafficking, release of organic anions and HCO_3, promotion of immune tolerance and chronic infection through inhibition of various immune cells, activation of mitogen-activated protein kinases, and modulation of autophagy[80,81]. All *H. pylori* strains carry the *vacA* gene, although with different vacuolating ability, which is conferred by variations in five *vacA* regions: s-region (s1 and s2), i-region (i1, i2, i3), m-region (m1 and m2), d-region (d1 and d2), and the recently identified c-region (c1 and c2). The *vacA* s2 variant is considered less pathogenic than the s1, since VacA s2 toxins are produced and secreted at lower rates and are also unable to form

membrane channels through which VacA s1 induces vacuolation of cells[3,79,81]. VacA i1 is also associated with increased activity compared to VacA i2. Unlike VacA m2, VacA m1 induces a decrease in intracellular levels of glutathione and an increase in oxidative stress, leading to autophagy and apoptosis of host cells[81,82].

Adults: The distribution of *vacA* alleles is geographically dependent, with s1c being the most prevalent allele in East Asia, while the *vacA* s1a allele is detected more often in Northern Europe and *vacA* s1b in Portugal and Spain. In Northern America, *vacA* s1a and *vacA* s1b are relatively evenly distributed, whereas virtually all strains from Latin America carry *vacA* s1b. The *vacA* s1 allele prevalence ranges from 36.0% in North Africa to 95.0% in East Asia. *vacA* m1 and m2 are equally distributed, except in Portugal, Spain and Latin America, where *vacA* m1 is more prevalent (86.2%). The *vacA* m2b allele is found solely in East Asian strains carrying *vacA* s1c[83]. Interestingly, mixed *vacA* s1a/s1b/m2 was found to be the most common genotype in Saudi Arabia[61].

Several studies have intensely focused on potential associations between *vacA* alleles and risk of PUD and GC. Results were relatively consistent, since most studies identified *vacA* s1, *vacA* i1 and *vacA* m1 alleles as being associated with a higher risk of precancerous lesions and GC[67,84]. Interestingly, *vacA* i1 and d1 were shown to be significantly associated with non-cardia GC (OR = 37.52, 95%CI: 3.04-462.17 and OR = 7.17, 95%CI: 1.43-35.94, respectively), but not with cardia GC. The presence of these alleles may also predict the risk according to the GC type, as *vacA* i1 was linked to intestinal-type adenocarcinoma (OR = 14.04, 95%CI: 2.15-91.77) and *vacA* d1 to diffuse-type adenocarcinoma (OR = 7.71, 95%CI: 1.13-52.28)[85]. Furthermore, strains harboring *vacA* s1 and *vacA* m1 genotypes were also more commonly detected in patients with severe inflammation and gastric epithelial damage and PUD than in those who were *vacA* s2/m2 positive. In Western countries and the Middle East, the presence of *vacA* s1/m1 is associated with an increased risk of PUD, whereas in East Asia, the *vacA* s1/i1/m1 genotype is not a useful differentiating factor since most strains harbor this genotype[11,34,61]. Moreover, a meta-analysis showed that *vacA* i1 confers higher risk of GC (OR = 5.12, 95%CI: 2.66-9.85), especially among the Central Asian population (OR = 10.89, 95%CI: 4.11-20.88). Conversely, *vacA* i1 was not associated with increased risk of PUD (OR = 1.38, 95%CI: 0.87-2.17)[86]. As shown by Van Doorn *et al*[83], the *vacA* s1/*cagA*+ genotype is associated with PUD in all regions of the world.

Children: Genotype *vacA* s1/m2 is the most common genotype in children from Iran (45.5%) and Turkey (57.1%)[25,70]. In Venezuela, 85.0% of strains obtained from symptomatic children harbored *vacA* s1/m1[73]. In Slovenia, pediatric *H. pylori* strains more commonly contain *vacA* s1 and m2 than *vacA* s2 and m1, with most strains harboring the *vacA* s1/m1 genotype[17,50,69]. In asymptomatic Brazilian children, *vacA* s1 (82.5%) and *vacA* i1 (75.0%) were the most common alleles, whereas m1 and m2 were found to be equally distributed (48.2% each)[30]. Using stool samples, the prevalence of the *vacA* s1 gene in asymptomatic Colombian children was shown to be very high (91.7%) and similar to that in the adult population (93.2%)[77]. Results from Brazil, a high-risk region for GC, also suggest that asymptomatic children from this area are more often colonized with strains harboring the toxigenic *vacA* s1 allele[87].

In Iranian children, nodular gastritis was commonly found and was significantly associated with the presence of *vacA* m1[70]. Similar to *cagA*, *vacA* s1 has been strongly associated with PUD risk (OR = 14.13, 95%CI: 4.75-42.04) among Portuguese children[42], whereas there were no significant correlations between *vacA* status and PUD in Iranian children[71]. Moreover, studies on Korean, Japanese and North American children found no associations between the *vacA* genotype and clinical outcome or severity of inflammation[75,76,88,89].

Associations with other virulence genes: Compared to *vacA* s2, strains that harbor *vacA* s1 more commonly contain *cag*PAI, *babA2*, *homB* and *oipA* "on"[81]. *vacA* i1 is strongly associated with *vacA* s1 and *vacA* m1 and *cagA*[30,84].

VIRULENCE GENES WITH OTHER FUNCTIONS

Duodenal ulcer promoting gene

The duodenal ulcer promoting (*dupA*) gene encompasses *jhp0917* and *jhp0918*, located in the plasticity region of the *H. pylori* genome. Due to its high homology with the *virB4* factor, *dupA* presumably forms a type IV secretion system together with *vir* genes, although its exact functions are not yet fully understood. The detection of the *dupA* gene correlates with increased IL-8 production from gastric epithelial cells, both

in vivo and *in vitro*. Increased IL-8 secretion from the gastric antrum thus leads to the development of predominantly antral gastritis, a well-known characteristic of duodenal ulcer disease[90].

Adults: Worldwide, approximately 48.0% of strains carry *dupA*[91], with the highest rates in Brazil (89.5%) and South Africa (84.8%)[92,93] and lowest in East Asian countries[91]. A study on 500 isolates from patients with gastritis, PUD and GC originating in Japan, Korea and Colombia showed an overall prevalence of *dupA* of 26.3%[94]. Surprisingly, the prevalence of the *dupA* gene was higher in Colombia (36.5%) than in Korea (16.8%), regardless of the clinical outcome[94]. In relation to the prevalence in strains from patients with functional dyspepsia, *dupA* was detected in 65.0%, 37.8%, 35.7%, 28.9% and 7.1% of strains from Swedish, Australian, Malay, Chinese and Indian patients, respectively[95].

Interestingly, in contrast to other virulence factors, such as *cag*PAI, *vacA*, *oipA* and *babA*2, which are reportedly associated with an increased risk of both PUD and GC, *dupA* was the first *H. pylori* virulence factor to be correlated with a differential susceptibility to PUD and GC, with protection against pre-neoplastic lesions and GC (OR for GC = 0.42, 95%CI: 0.2-0.9, compared with gastritis)[94]. However, some subsequent studies failed to reproduce these results. A meta-analysis on the relationship between the *dupA* gene and clinical outcomes was therefore performed and it showed that infection with *H. pylori* strains carrying *dupA* had a 1.41-fold (95%CI: 1.12-1.76) increased overall risk of duodenal ulcer. A subgroup analysis identified higher ORs in Asian countries (OR 1.57, 95%CI: 1.19-2.06) than in Western countries (OR 1.09, 95%CI: 0.73-1.62), suggesting that *dupA* can be considered a disease-specific virulence factor, especially in Asian countries. No associations between the presence of *dupA* and GC or gastric ulcer were found[66]. In addition, the same authors reported that the presence of *dupA* may also be an independent risk factor (OR = 3.71, 95%CI: 1.07-12.38) for *H. pylori* eradication failure[90]. Interestingly, a recent study showed protective effects of the *dupA* gene against severe outcome in infected females (OR = 0.05, 95%CI: 0.01-0.42). Moreover, whereas the sole presence of *vacA* i1 carried the highest risk for a severe clinical outcome, the simultaneous presence of the *dupA* gene resulted in a delay of severe disease outcome by almost 20 years[96].

Children: The prevalence of *dupA* was found to be 37.5% in Mexican children with recurrent abdominal pain[74]. In contrast, all *H. pylori* strains from Brazilian children were found to be *dupA* positive, with a significantly higher prevalence than in adults from the same region[92]. However, despite using the same primers for detecting the *dupA* gene as Gomes *et al*[92], another study analyzing Brazilian children showed a much lower (37.0%) prevalence of this gene[97]. These discrepancies may be due to the presence of significant geographic differences even within the same country/region, variations in studied populations or rearrangements within the plasticity zone, which is prone to frequent change[92,97].

Associations with other virulence genes: The *dupA* gene has previously been associated with *cagA*[74,92,97] and *cag*PAI[74].

COMBINATIONS OF VIRULENCE GENES

Since some genes are almost exclusively associated with one another (*e.g.*, *vacA* s1/i1/m1 and *cagA*), it is impossible to consider each of these virulence genes separately as independent markers for disease outcome. For example, the presence of *oipA* "on" is tightly linked to the presence of *cag*PAI and some studies even suggest that *cag*PAI and OipA act synergistically by regulating the signaling pathways that induce inflammation and actin dynamics[29]. Here, we briefly summarize some of the most intriguing combinations of *H. pylori* virulence genes.

As expected, the risk of a severe clinical outcome increases if multiple virulence genes are simultaneously detected. It has been shown that strains harboring the *vacA* s1/m1/*cagA*+ genotype carry a 4.8-fold (95%CI: 1.71-13.5) increased risk of progression of pre-cancerous lesions in comparison to the strains carrying *vacA* s2/m2/*cagA*-, with higher ORs than if each of these virulence genes was evaluated individually[98]. In addition, strains carrying *cagA*, *vacA* s1 and *babA*2 were associated with duodenal ulcer and adenocarcinoma[15], whereas *cagA*, *vacA* s1/m1 and *babA*2 were found to work synergistically in causing intestinal metaplasia[27]. Furthermore, a study from Portugal identified an increased risk of PUD in strains that simultaneously harbored *homB*, *cagA* and *vacA*[43]. Using binary logistic regression, *cagA*+/*homB*+ and *cagA*+/*vacA*s1 genotypes were found to have the highest discriminatory capacity to

distinguish PUD from NUD in children, among the evaluated combinations of virulence factors[42]. Another study on pediatric strains showed that quadruple-positive strains (*vacA* s1/m1/*cagA*+/*babA*2+) had the highest discriminating value for detecting the severity of gastritis compared to other groups evaluated[17]. Interestingly, whereas *homB* was not associated with a severe finding on gastric histology when considered as an individual marker of the disease, a correlation between the *vacA* s2/m2/*cagA*−/*babA*2−/*homB*+ genotype and the presence of atrophic changes in Slovenian children was found[50]. Moreover, a study evaluating the prevalence and relevance of various *H. pylori* virulence factors in the pathogenesis of low-grade gastric MALT lymphoma was unable to identify correlations between any of the putative virulence genes and MALT lymphoma when evaluated individually. However, when using multiple correspondence analysis, patients infected with strains carrying *iceA1*, *sabA* "on" and *hopZ* "off" had 10-fold higher odds (OR = 10.3, 95%CI: 1.2-86.0) of developing MALT lymphoma than age-matched patients with gastritis[99].

CONCLUSION

H. pylori isolates show a high degree of geographic variability. It is thus possible that certain *H. pylori* genotypes are associated with a more severe clinical outcome in some regions, while presenting as virtually harmless variants in other studied populations. The observed discrepancies in several studies on *H. pylori* virulence genes may be due to various factors: different definitions or diagnoses of gastroduodenal disease, limitations of PCR and sequencing methods for detecting virulence genes (*e.g.*, inadequate PCR primer design, disregarding frameshift mutations that could have a considerable influence on protein expression and/or function, and poor correlation of the genotypic methods with the actual expression profile of the protein), and inability to detect mixed infections with more than one strain at a time. Moreover, differences between East Asian and Western strains confirm the hypothesis that the degree of gastroduodenal pathology depends on complex relationships between host genetics, environmental factors and the presence, as well as combinations, of various *H. pylori* virulence genes. Although the importance of the majority of *H. pylori* virulence genes has not yet been uniformly clarified, knowledge on their role in pathogenesis, as well as disease outcome, has substantially improved in the last two decades. Careful monitoring and continuous refining of their roles will not only contribute to novel strategies for *H. pylori* vaccine development but also impact potential alternative therapies and facilitate the discovery of novel virulence genes. Although sequencing methods have dramatically improved over the years, enabling better and in-depth information on *H. pylori* genome structure, future studies should not only focus on these methods but also account for differences in protein expression profiles. Nevertheless, enriched knowledge on the pathogenicity of *H. pylori* virulence genes may be of clinical significance, since the detection of more virulent variants of strains, such as those with an increased number of CagA EPIYA-motifs, could be used to improve clinical prediction of the disease risk and identify those who need more intensive surveillance and eradication of the infection to prevent serious health-related consequences. In addition, focusing on a single virulence factor is probably too restrictive, since clear linkages between various virulence factors with different biological roles and significances exist, which may act synergistically to induce serious gastroduodenal pathology. Moreover, in the light of recent studies demonstrating that early exposure to *H. pylori* provides some protection against subsequent atopy and allergic conditions in childhood[100], identification of reliable discriminative virulence factors of bacterial strains could be extremely helpful in the event that triaging of *H. pylori* infection is applied in the future.

REFERENCES

1 **Peleteiro B**, Bastos A, Ferro A, Lunet N. Prevalence of Helicobacter pylori infection worldwide: A systematic review of studies with national coverage. *Dig Dis Sci* 2014; **59**: 1698-1709 [PMID: 24563236 DOI: 10.1007/s10620-014-3063-0]

2 **Kao CY**, Sheu BS, Wu JJ. Helicobacter pylori infection: An overview of bacterial virulence factors and pathogenesis. *Biomed J* 2016; **39**: 14-23 [PMID: 27105595 DOI: 10.1016/j.bj.2015.06.002]

3 **Whitmire JM**, Merrell DS. Helicobacter pylori Genetic Polymorphisms in Gastric Disease Development. *Adv Exp Med Biol* 2019 [PMID: 31016629 DOI: 10.1007/5584_2019_365]

4 **Kalali B**, Mejías-Luque R, Javaheri A, Gerhard M. H. pylori virulence factors: Influence on immune system and pathology. *Mediators Inflamm* 2014; **2014**: 426309 [PMID: 24587595 DOI: 10.1155/2014/426309]

5 **Yamaoka Y**. Mechanisms of disease: Helicobacter pylori virulence factors. *Nat Rev Gastroenterol*

Hepatol 2010; **7**: 629-641 [PMID: 20938460 DOI: 10.1038/nrgastro.2010.154]
6 New Global Cancer Data: GLOBOCAN 2018; 2018 [cited 2019 Apr 14]. Available from: https://www.uicc.org/new-global-cancer-data-globocan-2018
7 **Kori M**, Daugule I, Urbonas V. Helicobacter pylori and some aspects of gut microbiota in children. *Helicobacter* 2018; **23** Suppl 1: e12524 [PMID: 30203591 DOI: 10.1111/hel.12524]
8 **Razavi A**, Bagheri N, Azadegan-Dehkordi F, Shirzad M, Rahimian G, Rafieian-Kopaei M, Shirzad H. Comparative Immune Response in Children and Adults with H. pylori Infection. *J Immunol Res* 2015; **2015**: 315957 [PMID: 26495322 DOI: 10.1155/2015/315957]
9 **Alm RA**, Bina J, Andrews BM, Doig P, Hancock RE, Trust TJ. Comparative genomics of Helicobacter pylori: Analysis of the outer membrane protein families. *Infect Immun* 2000; **68**: 4155-4168 [PMID: 10858232 DOI: 10.1128/IAI.68.7.4155-4168.2000]
10 **Fujimoto S**, Olaniyi Ojo O, Arnqvist A, Wu JY, Odenbreit S, Haas R, Graham DY, Yamaoka Y. Helicobacter pylori BabA expression, gastric mucosal injury, and clinical outcome. *Clin Gastroenterol Hepatol* 2007; **5**: 49-58 [PMID: 17157077 DOI: 10.1016/j.cgh.2006.09.015]
11 **Chang WL**, Yeh YC, Sheu BS. The impacts of H. pylori virulence factors on the development of gastroduodenal diseases. *J Biomed Sci* 2018; **25**: 68 [PMID: 30205817 DOI: 10.1186/s12929-018-0466-9]
12 **Sheu SM**, Sheu BS, Chiang WC, Kao CY, Wu HM, Yang HB, Wu JJ. H. pylori clinical isolates have diverse babAB genotype distributions over different topographic sites of stomach with correlation to clinical disease outcomes. *BMC Microbiol* 2012; **12**: 89 [PMID: 22646246 DOI: 10.1186/1471-2180-12-89]
13 **Chen MY**, He CY, Meng X, Yuan Y. Association of Helicobacter pylori babA2 with peptic ulcer disease and gastric cancer. *World J Gastroenterol* 2013; **19**: 4242-4251 [PMID: 23864790 DOI: 10.3748/wjg.v19.i26.4242]
14 **Sheu BS**, Odenbreit S, Hung KH, Liu CP, Sheu SM, Yang HB, Wu JJ. Interaction between host gastric Sialyl-Lewis X and H. pylori SabA enhances H. pylori density in patients lacking gastric Lewis B antigen. *Am J Gastroenterol* 2006; **101**: 36-44 [PMID: 16405531 DOI: 10.1111/j.1572-0241.2006.00358.x]
15 **Gerhard M**, Lehn N, Neumayer N, Borén T, Rad R, Schepp W, Miehlke S, Classen M, Prinz C. Clinical relevance of the Helicobacter pylori gene for blood-group antigen-binding adhesin. *Proc Natl Acad Sci U S A* 1999; **96**: 12778-12783 [PMID: 10535999 DOI: 10.1073/pnas.96.22.12778]
16 **Berthenet E**, Yahara K, Thorell K, Pascoe B, Meric G, Mikhail JM, Engstrand L, Enroth H, Burette A, Megraud F, Varon C, Atherton JC, Smith S, Wilkinson TS, Hitchings MD, Falush D, Sheppard SK. A GWAS on Helicobacter pylori strains points to genetic variants associated with gastric cancer risk. *BMC Biol* 2018; **16**: 84 [PMID: 30071832 DOI: 10.1186/s12915-018-0550-3]
17 **Homan M**, Šterbenc A, Kocjan BJ, Luzar B, Zidar N, Orel R, Poljak M. Prevalence of the Helicobacter pylori babA2 gene and correlation with the degree of gastritis in infected Slovenian children. *Antonie Van Leeuwenhoek* 2014; **106**: 637-645 [PMID: 25055876 DOI: 10.1007/s10482-014-0234-0]
18 **Biernat MM**, Gościniak G, Iwańczak B. Prevalence of Helicobacter pylori cagA, vacA, iceA, babA2 genotypes in Polish children and adolescents with gastroduodenal disease. *Postepy Hig Med Dosw (Online)* 2014; **68**: 1015-1021 [PMID: 25228509 DOI: 10.5604/17322693.1118211]
19 **Podzorski RP**, Podzorski DS, Wuerth A, Tolia V. Analysis of the vacA, cagA, cagE, iceA, and babA2 genes in Helicobacter pylori from sixty-one pediatric patients from the Midwestern United States. *Diagn Microbiol Infect Dis* 2003; **46**: 83-88 [PMID: 12812722 DOI: 10.1016/S0732-8893(03)00034-8]
20 **Talarico S**, Gold BD, Fero J, Thompson DT, Guarner J, Czinn S, Salama NR. Pediatric Helicobacter pylori isolates display distinct gene coding capacities and virulence gene marker profiles. *J Clin Microbiol* 2009; **47**: 1680-1688 [PMID: 19386830 DOI: 10.1128/JCM.00273-09]
21 **Oleastro M**, Gerhard M, Lopes AI, Ramalho P, Cabral J, Sousa Guerreiro A, Monteiro L. Helicobacter pylori virulence genotypes in Portuguese children and adults with gastroduodenal pathology. *Eur J Clin Microbiol Infect Dis* 2003; **22**: 85-91 [PMID: 12627281 DOI: 10.1007/s10096-002-0865-3]
22 **Oleastro M**, Santos A, Cordeiro R, Nunes B, Mégraud F, Ménard A. Clinical relevance and diversity of two homologous genes encoding glycosyltransferases in Helicobacter pylori. *J Clin Microbiol* 2010; **48**: 2885-2891 [PMID: 20554820 DOI: 10.1128/JCM.00401-10]
23 **Garcia GT**, Aranda KR, Gonçalves ME, Cardoso SR, Iriya K, Silva NP, Scaletsky IC. High prevalence of clarithromycin resistance and cagA, vacA, iceA2, and babA2 genotypes of Helicobacter pylori in Brazilian children. *J Clin Microbiol* 2010; **48**: 4266-4268 [PMID: 20826649 DOI: 10.1128/JCM.01034-10]
24 **Boyanova L**, Yordanov D, Gergova G, Markovska R, Mitov I. Association of iceA and babA genotypes in Helicobacter pylori strains with patient and strain characteristics. *Antonie Van Leeuwenhoek* 2010; **98**: 343-350 [PMID: 20454856 DOI: 10.1007/s10482-010-9448-y]
25 **Ozbey G**, Dogan Y, Demiroren K. Prevalence of Helicobacter pylori virulence genotypes among children in Eastern Turkey. *World J Gastroenterol* 2013; **19**: 6585-6589 [PMID: 24151385 DOI: 10.3748/wjg.v19.i39.6585]
26 **Dossumbekova A**, Prinz C, Mages J, Lang R, Kusters JG, Van Vliet AH, Reindl W, Backert S, Saur D, Schmid RM, Rad R. Helicobacter pylori HopH (OipA) and bacterial pathogenicity: Genetic and functional genomic analysis of hopH gene polymorphisms. *J Infect Dis* 2006; **194**: 1346-1355 [PMID: 17054063 DOI: 10.1086/508426]
27 **Zambon CF**, Navaglia F, Basso D, Rugge M, Plebani M. Helicobacter pylori babA2, cagA, and s1 vacA genes work synergistically in causing intestinal metaplasia. *J Clin Pathol* 2003; **56**: 287-291 [PMID: 12663641 DOI: 10.1136/jcp.56.4.287]
28 **Teymournejad O**, Mobarez AM, Hassan ZM, Talebi Bezmin Abadi A. Binding of the Helicobacter pylori OipA causes apoptosis of host cells via modulation of Bax/Bcl-2 levels. *Sci Rep* 2017; **7**: 8036 [PMID: 28808292 DOI: 10.1038/s41598-017-08176-7]
29 **Yamaoka Y**, Kikuchi S, el-Zimaity HM, Gutierrez O, Osato MS, Graham DY. Importance of Helicobacter pylori oipA in clinical presentation, gastric inflammation, and mucosal interleukin 8 production. *Gastroenterology* 2002; **123**: 414-424 [PMID: 12145793 DOI: 10.1053/gast.2002.34781]
30 **Braga LL**, Oliveira MA, Gonçalves MH, Chaves FK, Benigno TG, Gomes AD, Silva CI, Anacleto C, Batista Sde A, Queiroz DM. CagA phosphorylation EPIYA-C motifs and the vacA i genotype in Helicobacter pylori strains of asymptomatic children from a high-risk gastric cancer area in northeastern Brazil. *Mem Inst Oswaldo Cruz* 2014; **109**: 1045-1049 [PMID: 25494468 DOI: 10.1590/0074-0276140279]
31 **Farzi N**, Yadegar A, Aghdaei HA, Yamaoka Y, Zali MR. Genetic diversity and functional analysis of oipA gene in association with other virulence factors among Helicobacter pylori isolates from Iranian patients with different gastric diseases. *Infect Genet Evol* 2018; **60**: 26-34 [PMID: 29452293 DOI:

10.1016/j.meegid.2018.02.017]
32 **Torres K**, Valderrama E, Sayegh M, Ramírez JL, Chiurillo MA. Study of the oipA genetic diversity and EPIYA motif patterns in cagA-positive Helicobacter pylori strains from Venezuelan patients with chronic gastritis. *Microb Pathog* 2014; **76**: 26-32 [PMID: 25223715 DOI: 10.1016/j.micpath.2014.09.006]
33 **Markovska R**, Boyanova L, Yordanov D, Gergova G, Mitov I. Helicobacter pylori oipA genetic diversity and its associations with both disease and cagA, vacA s, m, and i alleles among Bulgarian patients. *Diagn Microbiol Infect Dis* 2011; **71**: 335-340 [PMID: 21937185 DOI: 10.1016/j.diagmicrobio.2011.08.008]
34 **Schmidt HM**, Andres S, Nilsson C, Kovach Z, Kaakoush NO, Engstrand L, Goh KL, Fock KM, Forman D, Mitchell H. The cag PAI is intact and functional but HP0521 varies significantly in Helicobacter pylori isolates from Malaysia and Singapore. *Eur J Clin Microbiol Infect Dis* 2010; **29**: 439-451 [PMID: 20157752 DOI: 10.1007/s10096-010-0881-7]
35 **Chiarini A**, Calà C, Bonura C, Gullo A, Giuliana G, Peralta S, D'Arpa F, Giammanco A. Prevalence of virulence-associated genotypes of Helicobacter pylori and correlation with severity of gastric pathology in patients from western Sicily, Italy. *Eur J Clin Microbiol Infect Dis* 2009; **28**: 437-446 [PMID: 18958508 DOI: 10.1007/s10096-008-0644-x]
36 **Yamaoka Y**, Ojo O, Fujimoto S, Odenbreit S, Haas R, Gutierrez O, El-Zimaity HM, Reddy R, Arnqvist A, Graham DY. Helicobacter pylori outer membrane proteins and gastroduodenal disease. *Gut* 2006; **55**: 775-781 [PMID: 16322107 DOI: 10.1136/gut.2005.083014]
37 **de Jonge R**, Pot RG, Loffeld RJ, van Vliet AH, Kuipers EJ, Kusters JG. The functional status of the Helicobacter pylori sabB adhesin gene as a putative marker for disease outcome. *Helicobacter* 2004; **9**: 158-164 [PMID: 15068418 DOI: 10.1111/j.1083-4389.2004.00213.x]
38 **Ando T**, Peek RM, Pride D, Levine SM, Takata T, Lee YC, Kusugami K, van der Ende A, Kuipers EJ, Kusters JG, Blaser MJ. Polymorphisms of Helicobacter pylori HP0638 reflect geographic origin and correlate with cagA status. *J Clin Microbiol* 2002; **40**: 239-246 [PMID: 11773122 DOI: 10.1128/JCM.40.1.239-246.2002]
39 **Leung WK**, Yu J, To KF, Go MY, Ma PK, Chan FK, Sung JJ. Apoptosis and proliferation in Helicobacter pylori-associated gastric intestinal metaplasia. *Aliment Pharmacol Ther* 2001; **15**: 1467-1472 [PMID: 11552920 DOI: 10.1046/j.1365-2036.2001.01057.x]
40 **Liu J**, He C, Chen M, Wang Z, Xing C, Yuan Y. Association of presence/absence and on/off patterns of Helicobacter pylori oipA gene with peptic ulcer disease and gastric cancer risks: A meta-analysis. *BMC Infect Dis* 2013; **13**: 555 [PMID: 24256489 DOI: 10.1186/1471-2334-13-555]
41 **Yamaoka Y**, Reddy R, Graham DY. Helicobacter pylori virulence factor genotypes in children in the United States: Clues about genotype and outcome relationships. *J Clin Microbiol* 2010; **48**: 2550-2551 [PMID: 20421443 DOI: 10.1128/JCM.00114-10]
42 **Oleastro M**, Cordeiro R, Ferrand J, Nunes B, Lehours P, Carvalho-Oliveira I, Mendes AI, Penque D, Monteiro L, Mégraud F, Ménard A. Evaluation of the clinical significance of homB, a novel candidate marker of Helicobacter pylori strains associated with peptic ulcer disease. *J Infect Dis* 2008; **198**: 1379-1387 [PMID: 18811585 DOI: 10.1086/592166]
43 **Oleastro M**, Cordeiro R, Yamaoka Y, Queiroz D, Mégraud F, Monteiro L, Ménard A. Disease association with two Helicobacter pylori duplicate outer membrane protein genes, homB and homA. *Gut Pathog* 2009; **1**: 12 [PMID: 19545429 DOI: 10.1186/1757-4749-1-12]
44 **Kang J**, Jones KR, Jang S, Olsen CH, Yoo YJ, Merrell DS, Cha JH. The geographic origin of Helicobacter pylori influences the association of the homB gene with gastric cancer. *J Clin Microbiol* 2012; **50**: 1082-1085 [PMID: 22205793 DOI: 10.1128/JCM.06293-11]
45 **Talebi Bezmin Abadi A**, Rafiei A, Ajami A, Hosseini V, Taghvaei T, Jones KR, Merrell DS. Helicobacter pylori homB, but not cagA, is associated with gastric cancer in Iran. *J Clin Microbiol* 2011; **49**: 3191-3197 [PMID: 21734027 DOI: 10.1128/JCM.00947-11]
46 **Oleastro M**, Cordeiro R, Ménard A, Yamaoka Y, Queiroz D, Mégraud F, Monteiro L. Allelic diversity and phylogeny of homB, a novel co-virulence marker of Helicobacter pylori. *BMC Microbiol* 2009; **9**: 248 [PMID: 19954539 DOI: 10.1186/1471-2180-9-248]
47 **Jung SW**, Sugimoto M, Graham DY, Yamaoka Y. homB status of Helicobacter pylori as a novel marker to distinguish gastric cancer from duodenal ulcer. *J Clin Microbiol* 2009; **47**: 3241-3245 [PMID: 19710266 DOI: 10.1128/JCM.00293-09]
48 **Hussein NR**. A study of Helicobacter pylori outer-membrane proteins (hom) A and B in Iraq and Turkey. *J Infect Public Health* 2011; **4**: 135-139 [PMID: 21843859 DOI: 10.1016/j.jiph.2011.03.004]
49 **Oleastro M**, Monteiro L, Lehours P, Mégraud F, Ménard A. Identification of markers for Helicobacter pylori strains isolated from children with peptic ulcer disease by suppressive subtractive hybridization. *Infect Immun* 2006; **74**: 4064-4074 [PMID: 16790780 DOI: 10.1128/IAI.00123-06]
50 **Šterbenc A**, Poljak M, Zidar N, Luzar B, Homan M. Prevalence of the Helicobacter pylori homA and homB genes and their correlation with histological parameters in children. *Microb Pathog* 2018; **125**: 26-32 [PMID: 30195645 DOI: 10.1016/j.micpath.2018.09.005]
51 **Oleastro M**, Cordeiro R, Ménard A, Gomes JP. Allelic diversity among Helicobacter pylori outer membrane protein genes homB and homA generated by recombination. *J Bacteriol* 2010; **192**: 3961-3968 [PMID: 20525831 DOI: 10.1128/JB.00395-10]
52 **Mahdavi J**, Sondén B, Hurtig M, Olfat FO, Forsberg L, Roche N, Angstrom J, Larsson T, Teneberg S, Karlsson KA, Altraja S, Wadström T, Kersulyte D, Berg DE, Dubois A, Petersson C, Magnusson KE, Norberg T, Lindh F, Lundskog BB, Arnqvist A, Hammarström L, Borén T. Helicobacter pylori SabA adhesin in persistent infection and chronic inflammation. *Science* 2002; **297**: 573-578 [PMID: 12142529 DOI: 10.1126/science.1069076]
53 **Yamaoka Y**. Increasing evidence of the role of Helicobacter pylori SabA in the pathogenesis of gastroduodenal disease. *J Infect Dev Ctries* 2008; **2**: 174-181 [PMID: 19738347 DOI: 10.3855/jidc.259]
54 **Yanai A**, Maeda S, Hikiba Y, Shibata W, Ohmae T, Hirata Y, Ogura K, Yoshida H, Omata M. Clinical relevance of Helicobacter pylori sabA genotype in Japanese clinical isolates. *J Gastroenterol Hepatol* 2007; **22**: 2228-2232 [PMID: 18031386 DOI: 10.1111/j.1440-1746.2007.04831.x]
55 **Odenbreit S**, Swoboda K, Barwig I, Ruhl S, Borén T, Koletzko S, Haas R. Outer membrane protein expression profile in Helicobacter pylori clinical isolates. *Infect Immun* 2009; **77**: 3782-3790 [PMID: 19546190 DOI: 10.1128/IAI.00364-09]
56 **Kato S**, Osaki T, Kamiya S, Zhang XS, Blaser MJ. Helicobacter pylori sabA gene is associated with iron deficiency anemia in childhood and adolescence. *PLoS One* 2017; **12**: e0184046 [PMID: 28854239 DOI: 10.1371/journal.pone.0184046]
57 **Backert S**, Blaser MJ. The Role of CagA in the Gastric Biology of Helicobacter pylori. *Cancer Res* 2016;

76: 4028-4031 [PMID: 27655809 DOI: 10.1158/0008-5472.CAN-16-1680]
58 **Xia Y**, Yamaoka Y, Zhu Q, Matha I, Gao X. A comprehensive sequence and disease correlation analyses for the C-terminal region of CagA protein of Helicobacter pylori. *PLoS One* 2009; **4**: e7736 [PMID: 19893742 DOI: 10.1371/journal.pone.0007736]
59 **Jones KR**, Whitmire JM, Merrell DS. A Tale of Two Toxins: Helicobacter Pylori CagA and VacA Modulate Host Pathways that Impact Disease. *Front Microbiol* 2010; **1**: 115 [PMID: 21687723 DOI: 10.3389/fmicb.2010.00115]
60 **Olbermann P**, Josenhans C, Moodley Y, Uhr M, Stamer C, Vauterin M, Suerbaum S, Achtman M, Linz B. A global overview of the genetic and functional diversity in the Helicobacter pylori cag pathogenicity island. *PLoS Genet* 2010; **6**: e1001069 [PMID: 20808891 DOI: 10.1371/journal.pgen.1001069]
61 **Akeel M**, Shehata A, Elhafey A, Elmakki E, Aboshouk T, Ageely H, Mahfouz M. Helicobacter pylori vacA, cagA and iceA genotypes in dyspeptic patients from southwestern region, Saudi Arabia: Distribution and association with clinical outcomes and histopathological changes. *BMC Gastroenterol* 2019; **19**: 16 [PMID: 30683054 DOI: 10.1186/s12876-019-0934-z]
62 **Yamaoka Y**. Pathogenesis of Helicobacter pylori-Related Gastroduodenal Diseases from Molecular Epidemiological Studies. *Gastroenterol Res Pract* 2012; **2012**: 371503 [PMID: 22829807 DOI: 10.1155/2012/371503]
63 **Park JY**, Forman D, Waskito LA, Yamaoka Y, Crabtree JE. Epidemiology of Helicobacter pylori and CagA-Positive Infections and Global Variations in Gastric Cancer. *Toxins (Basel)* 2018; **10**: pii: E163 [PMID: 29671784 DOI: 10.3390/toxins10040163]
64 **Parsonnet J**, Friedman GD, Orentreich N, Vogelman H. Risk for gastric cancer in people with CagA positive or CagA negative Helicobacter pylori infection. *Gut* 1997; **40**: 297-301 [PMID: 9135515 DOI: 10.1136/gut.40.3.297]
65 **Huang JQ**, Zheng GF, Sumanac K, Irvine EJ, Hunt RH. Meta-analysis of the relationship between cagA seropositivity and gastric cancer. *Gastroenterology* 2003; **125**: 1636-1644 [PMID: 14724815 DOI: 10.1053/j.gastro.2003.08.033]
66 **Shiota S**, Matsunari O, Watada M, Hanada K, Yamaoka Y. Systematic review and meta-analysis: The relationship between the Helicobacter pylori dupA gene and clinical outcomes. *Gut Pathog* 2010; **2**: 13 [PMID: 21040520 DOI: 10.1186/1757-4749-2-13]
67 **Matos JI**, de Sousa HA, Marcos-Pinto R, Dinis-Ribeiro M. Helicobacter pylori CagA and VacA genotypes and gastric phenotype: A meta-analysis. *Eur J Gastroenterol Hepatol* 2013; **25**: 1431-1441 [PMID: 23929249 DOI: 10.1097/MEG.0b013e328364b53e]
68 **Li Q**, Liu J, Gong Y, Yuan Y. Association of CagA EPIYA-D or EPIYA-C phosphorylation sites with peptic ulcer and gastric cancer risks: A meta-analysis. *Medicine (Baltimore)* 2017; **96**: e6620 [PMID: 28445260 DOI: 10.1097/MD.0000000000006620]
69 **Homan M**, Luzar B, Kocjan BJ, Orel R, Mocilnik T, Shrestha M, Kveder M, Poljak M. Prevalence and clinical relevance of cagA, vacA, and iceA genotypes of Helicobacter pylori isolated from Slovenian children. *J Pediatr Gastroenterol Nutr* 2009; **49**: 289-296 [PMID: 19525870 DOI: 10.1097/MPG.0b013e31818f09f2]
70 **Rafeey M**, Ghotaslou R, Milani M, Farokhi N, Ghojazadeh M. Association between Helicobacter pylori, cagA, and vacA Status and Clinical Presentation in Iranian Children. *Iran J Pediatr* 2013; **23**: 551-556 [PMID: 24800016 DOI: 10.1089/bfm.2013.9982]
71 **Falsafi T**, Khani A, Mahjoub F, Asgarani E, Sotoudeh N. Analysis of vacA/cagA genotypes/status in Helicobacter pylori isolates from Iranian children and their association with clinical outcome. *Turk J Med Sci* 2015; **45**: 170-177 [PMID: 25790548 DOI: 10.3906/sag-1311-2]
72 **Saltik IN**, Demir H, Engin D, Ertunç OD, Akyön Y, Koçak N. The cagA status of Helicobacter pylori isolates from dyspeptic children in Turkey. *FEMS Immunol Med Microbiol* 2003; **36**: 147-149 [PMID: 12738384 DOI: 10.1016/S0928-8244(03)00024-5]
73 **Ortiz-Princz D**, Daoud G, Salgado-Sabel A, Cavazza ME. Helicobacter pylori infection in children: Should it be carefully assessed? *Eur Rev Med Pharmacol Sci* 2016; **20**: 1798-1813 [PMID: 27212173]
74 **Romo-González C**, Consuelo-Sánchez A, Camorlinga-Ponce M, Velázquez-Guadarrama N, García-Zúñiga M, Burgueño-Ferreira J, Coria-Jiménez R. Plasticity Region Genes jhp0940, jhp0945, jhp0947, and jhp0949 of Helicobacter pylori in Isolates from Mexican Children. *Helicobacter* 2015; **20**: 231-237 [PMID: 25735460 DOI: 10.1111/hel.12194]
75 **Ko JS**, Kim KM, Oh YL, Seo JK. cagA, vacA, and iceA genotypes of Helicobacter pylori in Korean children. *Pediatr Int* 2008; **50**: 628-631 [PMID: 19261108 DOI: 10.1111/j.1442-200X.2008.02641.x]
76 **Azuma T**, Kato S, Zhou W, Yamazaki S, Yamakawa A, Ohtani M, Fujiwara S, Minoura T, Iinuma K, Kato T. Diversity of vacA and cagA genes of Helicobacter pylori in Japanese children. *Aliment Pharmacol Ther* 2004; **20** Suppl 1: 7-12 [PMID: 15298599 DOI: 10.1111/j.1365-2036.2004.01980.x]
77 **Sicinschi LA**, Correa P, Bravo LE, Peek RM, Wilson KT, Loh JT, Yepez MC, Gold BD, Thompson DT, Cover TL, Schneider BG. Non-invasive genotyping of Helicobacter pylori cagA, vacA, and hopQ from asymptomatic children. *Helicobacter* 2012; **17**: 96-106 [PMID: 22404439 DOI: 10.1111/j.1523-5378.2011.00919.x]
78 **Zhang SH**, Xie Y, Li BM, Liu DS, Wan SH, Luo LJ, Xiao ZJ, Li H, Yi LJ, Zhou J, Zhu X. [Prevalence of Helicobacter pylori cagA, vacA, and iceA genotypes in children with gastroduodenal diseases]. *Zhongguo Dang Dai Er Ke Za Zhi* 2016; **18**: 618-624 [PMID: 27412545]
79 **Atherton JC**, Cao P, Peek RM, Tummuru MK, Blaser MJ, Cover TL. Mosaicism in vacuolating cytotoxin alleles of Helicobacter pylori. Association of specific vacA types with cytotoxin production and peptic ulceration. *J Biol Chem* 1995; **270**: 17771-17777 [PMID: 7629077 DOI: 10.1074/jbc.270.30.17771]
80 **Foegeding NJ**, Caston RR, McClain MS, Ohi MD, Cover TL. An Overview of Helicobacter pylori VacA Toxin Biology. *Toxins (Basel)* 2016; **8**: pii: E173 [PMID: 27271669 DOI: 10.3390/toxins8060173]
81 **McClain MS**, Beckett AC, Cover TL. Helicobacter pylori Vacuolating Toxin and Gastric Cancer. *Toxins (Basel)* 2017; **9**: pii: E316 [PMID: 29023421 DOI: 10.3390/toxins9100316]
82 **Calore F**, Genisset C, Casellato A, Rossato M, Codolo G, Esposti MD, Scorrano L, de Bernard M. Endosome-mitochondria juxtaposition during apoptosis induced by H. pylori VacA. *Cell Death Differ* 2010; **17**: 1707-1716 [PMID: 20431599 DOI: 10.1038/cdd.2010.42]
83 **Van Doorn LJ**, Figueiredo C, Mégraud F, Pena S, Midolo P, Queiroz DM, Carneiro F, Vanderborght B, Pegado MD, Sanna R, De Boer W, Schneeberger PM, Correa P, Ng EK, Atherton J, Blaser MJ, Quint WG. Geographic distribution of vacA allelic types of Helicobacter pylori. *Gastroenterology* 1999; **116**: 823-830 [PMID: 10092304 DOI: 10.1016/S0016-5085(99)70065-X]
84 **Ferreira RM**, Machado JC, Letley D, Atherton JC, Pardo ML, Gonzalez CA, Carneiro F, Figueiredo C. A

novel method for genotyping the Helicobacter pylori vacA intermediate region directly in gastric biopsy specimens. *J Clin Microbiol* 2012; **50**: 3983-3989 [PMID: 23035185 DOI: 10.1128/JCM.02087-12]

85 **Abdi E**, Latifi-Navid S, Zahri S, Yazdanbod A, Safaralizadeh R. Helicobacter pylori genotypes determine risk of non-cardia gastric cancer and intestinal- or diffuse-type GC in Ardabil: A very high-risk area in Northwestern Iran. *Microb Pathog* 2017; **107**: 287-292 [PMID: 28390977 DOI: 10.1016/j.micpath.2017.04.007]

86 **Liu X**, He B, Cho WC, Pan Y, Chen J, Ying H, Wang F, Lin K, Peng H, Wang S. A systematic review on the association between the Helicobacter pylori vacA i genotype and gastric disease. *FEBS Open Bio* 2016; **6**: 409-417 [PMID: 27419046 DOI: 10.1002/2211-5463.12046]

87 **Goncalves MH**, Silva CI, Braga-Neto MB, Fialho AB, Fialho AM, Queiroz DM, Braga LL. Helicobacter pylori virulence genes detected by string PCR in children from an urban community in northeastern Brazil. *J Clin Microbiol* 2013; **51**: 988-989 [PMID: 23254125 DOI: 10.1128/JCM.02583-12]

88 **Yamaoka Y**, Kodama T, Kita M, Imanishi J, Kashima K, Graham DY. Relationship of vacA genotypes of Helicobacter pylori to cagA status, cytotoxin production, and clinical outcome. *Helicobacter* 1998; **3**: 241-253 [PMID: 9844065 DOI: 10.1046/j.1523-5378.1998.08056.x]

89 **Gold BD**, van Doorn LJ, Guarner J, Owens M, Pierce-Smith D, Song Q, Hutwagner L, Sherman PM, de Mola OL, Czinn SJ. Genotypic, clinical, and demographic characteristics of children infected with Helicobacter pylori. *J Clin Microbiol* 2001; **39**: 1348-1352 [PMID: 11283055 DOI: 10.1128/JCM.39.4.1348-1352.2001]

90 **Shiota S**, Nguyen LT, Murakami K, Kuroda A, Mizukami K, Okimoto T, Kodama M, Fujioka T, Yamaoka Y. Association of helicobacter pylori dupA with the failure of primary eradication. *J Clin Gastroenterol* 2012; **46**: 297-301 [PMID: 22298090 DOI: 10.1097/MCG.0b013e318243201c]

91 **Hussein NR**. The association of dupA and Helicobacter pylori-related gastroduodenal diseases. *Eur J Clin Microbiol Infect Dis* 2010; **29**: 817-821 [PMID: 20419465 DOI: 10.1007/s10096-010-0933-z]

92 **Gomes LI**, Rocha GA, Rocha AM, Soares TF, Oliveira CA, Bittencourt PF, Queiroz DM. Lack of association between Helicobacter pylori infection with dupA-positive strains and gastroduodenal diseases in Brazilian patients. *Int J Med Microbiol* 2008; **298**: 223-230 [PMID: 17897881 DOI: 10.1016/j.ijmm.2007.05.006]

93 **Argent RH**, Burette A, Miendje Deyi VY, Atherton JC. The presence of dupA in Helicobacter pylori is not significantly associated with duodenal ulceration in Belgium, South Africa, China, or North America. *Clin Infect Dis* 2007; **45**: 1204-1206 [PMID: 17918084 DOI: 10.1086/522177]

94 **Lu H**, Hsu PI, Graham DY, Yamaoka Y. Duodenal ulcer promoting gene of Helicobacter pylori. *Gastroenterology* 2005; **128**: 833-848 [PMID: 15825067 DOI: 10.1053/j.gastro.2005.01.009]

95 **Schmidt HM**, Andres S, Kaakoush NO, Engstrand L, Eriksson L, Goh KL, Fock KM, Hilmi I, Dhamodaran S, Forman D, Mitchell H. The prevalence of the duodenal ulcer promoting gene (dupA) in Helicobacter pylori isolates varies by ethnic group and is not universally associated with disease development: a case-control study. *Gut Pathog* 2009; **1**: 5 [PMID: 19338650 DOI: 10.1186/1757-4749-1-5]

96 **Paredes-Osses E**, Sáez K, Sanhueza E, Hebel S, González C, Briceño C, García Cancino A. Association between cagA, vacAi, and dupA genes of Helicobacter pylori and gastroduodenal pathologies in Chilean patients. *Folia Microbiol (Praha)* 2017; **62**: 437-444 [PMID: 28283946 DOI: 10.1007/s12223-017-0514-y]

97 **Pereira WN**, Ferraz MA, Zabaglia LM, de Labio RW, Orcini WA, Bianchi Ximenez JP, Neto AC, Payão SL, Rasmussen LT. Association among H. pylori virulence markers dupA, cagA and vacA in Brazilian patients. *J Venom Anim Toxins Incl Trop Dis* 2014; **20**: 1 [PMID: 24456629 DOI: 10.1186/1678-9199-20-1]

98 **González CA**, Figueiredo C, Lic CB, Ferreira RM, Pardo ML, Ruiz Liso JM, Alonso P, Sala N, Capella G, Sanz-Anquela JM. Helicobacter pylori cagA and vacA genotypes as predictors of progression of gastric preneoplastic lesions: A long-term follow-up in a high-risk area in Spain. *Am J Gastroenterol* 2011; **106**: 867-874 [PMID: 21285949 DOI: 10.1038/ajg.2011.1]

99 **Lehours P**, Ménard A, Dupouy S, Bergey B, Richy F, Zerbib F, Ruskoné-Fourmestraux A, Delchier JC, Mégraud F. Evaluation of the association of nine Helicobacter pylori virulence factors with strains involved in low-grade gastric mucosa-associated lymphoid tissue lymphoma. *Infect Immun* 2004; **72**: 880-888 [PMID: 14742532 DOI: 10.1128/IAI.72.2.880-888.2004]

100 **Taye B**, Enquselassie F, Tsegaye A, Medhin G, Davey G, Venn A. Is Helicobacter Pylori infection inversely associated with atopy? A systematic review and meta-analysis. *Clin Exp Allergy* 2015; **45**: 882-890 [PMID: 25207960 DOI: 10.1111/cea.12404]

World Journal of Gastroenterology

Submit a Manuscript: https://www.f6publishing.com

World J Gastroenterol 2019 September 7; 25(33): 4885-4891

DOI: 10.3748/wjg.v25.i33.4885

ISSN 1007-9327 (print) ISSN 2219-2840 (online)

MINIREVIEWS

Occupational exposure to vinyl chloride and liver diseases

Ugo Fedeli, Paolo Girardi, Giuseppe Mastrangelo

ORCID number: Ugo Fedeli (0000-0002-9939-3398); Paolo Girardi (0000-0001-8330-9414); Giuseppe Mastrangelo (0000-0003-4204-045X).

Author contributions: Fedeli U, Girardi P, Mastrangelo G reviewed the literature and wrote the manuscript.

Conflict-of-interest statement: All the Authors have no conflict of interest related to the manuscript.

Manuscript source: Unsolicited manuscript

Received: March 26, 2019
Peer-review started: March 26, 2019
First decision: May 30, 2019
Revised: June 10, 2019
Accepted: June 25, 2019
Article in press: June 26, 2019
Published online: September 7, 2019

P-Reviewer: Guo K, Sun WB
S-Editor: Yan JP
L-Editor: A
E-Editor: Ma YJ

Ugo Fedeli, Paolo Girardi, Epidemiological Department, Azienda Zero, Padova 35131, Italy

Giuseppe Mastrangelo, Department of Cardiac, Thoracic and Vascular Sciences, University of Padova, Padova 35128, Italy

Corresponding author: Ugo Fedeli, MD, Senior Scientist, Epidemiological Department, Azienda Zero, Veneto Region, Passaggio Gaudenzio 1, Padova 35131, Italy.
ugo.fedeli@azero.veneto.it
Telephone: +39-49-8778542
Fax: +39-49-8778235

Abstract

Portal hypertension, liver fibrosis, and angiosarcoma of the liver (ASL) have been reported among workers exposed to vinyl chloride monomer (VCM) since the 1970s. In 2007, the International Agency for Research on Cancer established the association of VCM with hepatocellular carcinoma (HCC), though only on the basis of the few cases available. Thereafter, recent reports from the United States cohort and a European sub-cohort of vinyl chloride workers provided compelling evidence of a strong association between cumulative VCM exposure and HCC risk. Further areas of research include the risk of liver cancer at lower levels of exposure and different patterns of risk of ASL and HCC with the time since exposure. The evidence of interaction between VCM exposure and other known liver carcinogens such as alcohol and chronic viral infection provides clues for the health surveillance of exposed workers. Notably, also the risk of VCM-associated chronic liver disease is modulated by alcohol consumption, viral infection, and genetic polymorphism. A counter-intuitive finding from cohort studies of exposed workers is the lower mortality from liver cirrhosis with respect to the general population; this can be attributed to the healthy worker effect and to the selection of liver cancer as the cause of death in the presence of concomitant chronic liver disease. Studies designed to overcome these intricacies confirmed an association between cumulative VCM exposure and the risk of liver cirrhosis.

Key words: Vinyl chloride; Occupational exposure; Epidemiology; Liver cancer; Angiosarcoma; Hepatocellular carcinoma; Liver cirrhosis

Core tip: Occupational exposure to vinyl chloride monomer (VCM) causes chronic liver disease, liver angiosarcoma, and hepatocellular carcinoma. VCM exposure has a synergistic effect with other known risk factors of liver diseases such as alcohol consumption and chronic viral infection. Further research is warranted to assess the risk

of liver cancer at low levels of exposure and to investigate the patterns of risk with time since exposure.

Citation: Fedeli U, Girardi P, Mastrangelo G. Occupational exposure to vinyl chloride and liver diseases. *World J Gastroenterol* 2019; 25(33): 4885-4891
URL: https://www.wjgnet.com/1007-9327/full/v25/i33/4885.htm
DOI: https://dx.doi.org/10.3748/wjg.v25.i33.4885

INTRODUCTION

Vinyl chloride monomer (VCM) is a synthetic gas mostly used in the manufacture of polyvinyl chloride (PVC), a widely used plastic material. Occupational exposure to VCM primarily occurs in the VCM/PVC production and processing industry[1]. The role of occupational exposure to VCM in the development of angiosarcoma of the liver (ASL) is well known since the mid-1970s. In 2007, the International Agency for Research on Cancer (IARC) established that exposure to VCM causes both ASL and hepatocellular carcinoma (HCC)[2]. The evidence on HCC was mainly derived from studies carried out in the early 2000s, demonstrating a relationship between HCC incidence and cumulative VCM exposure, as well as an association of VCM exposure with liver cirrhosis[3-5].

However, some controversy remained because findings on HCC were based only on a limited number of confirmed cases. Such controversy was fueled by reviews issued by VCM industry consultants, claiming that the results about HCC might have been biased due to misclassification between HCC and ASL, and underlining the fact that overall among VCM workers mortality from liver cirrhosis was lower with respect to the general population[6-8]. Notably, one of these reviews deduced that a firm conclusion about the role of VCM in the development of liver diseases other than ASL is unlikely to be reached in the future, because of the contrasting personal views given by experts[8]. The statements regarding irresolvable controversies might be used in the legal setting, yet the scientific evidence usually proceeds by slowly accumulating new original studies that shed light on gray areas of the available knowledge.

In fact, after the IARC assessment, new epidemiological studies updating previous results from cohorts of workers employed in VCM/PVC production in the United States[9], Europe[10,11], and Taiwan[12] have been published. Aim of this review is to summarize such new findings within the frame of the previous evidence.

HEPATOCELLULAR CARCINOMA

An increase in mortality from liver cancer among vinyl chloride workers has been reported by several studies carried out in the past decades, especially two large multicentric cohort studies from the United States[9,13-15] and Europe[3,16]. However, the association between VCM exposure and HCC is difficult to investigate because most studies did not collect histological or clinical information distinguishing HCC from ASL or other primary/secondary neoplasms[1]. The IARC assessment carried out in 2007 relied mostly on the results from the European cohort of workers employed in the vinyl chloride industry[3], from an Italian sub-cohort[4], and a case-control study nested in the latter sub-cohort[5]. Overall, a clear association of HCC risk with cumulative exposure was found, although based only on a few confirmed cases (ranging from 10 to 13).

Two studies have recently confirmed the IARC assessment. For the first time in 2017, data were published from the US cohort of vinyl chloride workers specifically addressing HCC risk, with the diagnosis based on information reported in death certificates. The risk of HCC steeply increased with increasing duration of employment and VCM cumulative exposure. The authors warned that in the absence of histopathological confirmation, such figures might have been influenced by misclassification of ASL and HCC in the earlier decades[9]. However, such misclassification did not probably affect the main results since findings were confirmed after exposures were lagged by 10-40 years. More recently, an update of an Italian cohort of vinyl chloride workers found a strong association with VCM cumulative exposure in a large series of HCC confirmed by histology and/or clinical records[11]. In

summary, all the original studies available provide compelling evidence of the causal role of occupational VCM exposure in the development of HCC (Table 1).

It must be remarked that vinyl chloride is mutagenic, being associated to chromosomal aberrations, micronucleus formation, sister chromatid exchange, Ki-ras and p53 gene mutations[2]; furthermore, the development of liver cirrhosis per se increases the risk of HCC through multiple mechanism, including chromosomal instability[17]. Within this framework, specific aspects of the association between VCM and HCC, namely, the absence of risk below a threshold of exposure, a decrease in the rates of liver cancer in historical cohorts through the more recent decades of follow-up, and interactions with other known risk factors for HCC, need further clarification.

Analyses on the risk of HCC at low levels of cumulative VCM exposure are hampered by the limited number of available cases. In the United States cohort, based on 32 cases of HCC as identified from death certificates, mortality rates did not increase except for the highest quintile of cumulative exposure (≥ 2271 ppm-years). However, after exposures were lagged by 30 years, HCC mortality significantly increased already in the 865-2271 ppm-years class (or in the 1021-3301 ppm-years class using high cut-points based on quintiles for all liver cancers, see also Table 1). The authors suggested a possible threshold at about 1000 ppm-years cumulative exposure[9]. In the European cohort of vinyl chloride workers, an increase in liver cancer risk (all types) with increasing exposure was confirmed in analyses restricted to subjects with cumulative exposure < 1500 ppm-years[3]. In an Italian cohort, an approach based on a non-parametric regression was adopted to model in continuous form the relationship between exposure and mortality considering 31 confirmed HCC cases; HCC mortality rates were found to increase with cumulative VCM exposure already in the range below 2000 ppm-years[11]. In view of the above data, the risk of HCC seems not to be confined only to a few subjects in the highest exposure categories, but probably involves most workers from the United States and Europe, who had relevant exposures to VCM before the major improvements in working conditions achieved in the mid-1970s.

The second issue is represented by the possible decline in liver cancer risk among previously exposed workers decades after the large decrease in the VCM exposure levels that were achieved in the chemical industry. According to the last update of the cohort of vinyl chloride workers in Taiwan[12], liver cancer mortality reached a peak during 1991–1996, and thereafter showed a decline. Although information on histological type was missing for most patients who died of liver cancer, the limited number of cases with available medical records were all confirmed HCC, with no case of ASL identified[18]. In the United States cohort, the peak of standardized mortality ratios (SMR) for liver cancer (all types) was observed during the 1970s; however, in subsequent decades a more than two-fold excess risk for liver cancer was still observed[15]. Among the confirmed cases, the median latency for HCC (48 years) was found to be considerably longer than that for ASL (36 years)[9]. In an Italian cohort of vinyl chloride workers, SMRs for liver cancer remained increased through the most recent period of follow-up[11]; analyses by latency showed that the highest SMR was reached after more than 40 years from the first exposure[10,11]. Once again among the confirmed cases, latency was observed to be longer for HCC as compared to ASL, being mean latency 39 and 32 years, respectively[11]. The overall picture from the historical cohorts is consistent with a first major peak of liver cancer deaths, mostly represented by ASL; in the more recent decades, mortality for liver cancer remained significantly increased, mainly sustained by the occurrence of HCC.

A common criticism of cohort studies is the lack of adjustment for known risk factors such as alcohol consumption and hepatitis B virus (HBV) or hepatitis C virus (HCV) infection. Two nested case-control studies, already included in the IARC review, investigated such an issue. A multiplicative effect between employment in jobs with high VCM exposure and HBsAg carrier status was reported for liver cancer (mostly HCC) in the Taiwanese cohort[19]. Furthermore, a study from Italy reported that cumulative VCM exposure was an independent risk factor for HCC, interacting synergistically with alcohol consumption and additively with viral infection[5]. Such studies provide useful clues for the health surveillance and disease prevention in previously exposed workers, as the interaction between multiple exposures further increases the risk for HCC. Therefore, cessation of alcohol consumption and treatment of chronic viral infection should be prioritized among vinyl chloride workers, especially in the view of the recent availability of directly acting antivirals for HCV treatment.

Table 1 Studies investigating the association between occupational exposure and hepatocellular carcinoma in vinyl chloride workers

Ref. location	Study description	Disease assessment	Exposure assessment	Exposure categories	Number of cases	Relative risk (95%CI)	Notes
Ward *et al*[3] (2001), European cohort	Cohort study, 12700 workers	HCC, best evidence	Job exposure matrix: Cumulative exposure (ppm-years)	0-734	3	1.0	Trend test
				735-2379	2	3.02 (0.50-1.81)	$P = 0.004$
				2380-5188	1	2.47 (0.26-23.9)	
				5189-7531	1	5.33 (0.54-52.8)	
				≥ 7532	2	20.3 (2.98-138)	
Mundt *et al*[9] (2017), United States cohort	Cohort study, 9951 workers	HCC, death certificates	Job exposure matrix: Cumulative exposure (ppm-years)	high cut-points:			30-yr lagged exp
				< 1021	8	1.0	1.0
				1021-3300	4	1.2 (0.4-3.8)	3.8 (1.4-10.4)
				3301-5685	7	7.2 (2.6-20.0)	8.9 (2.8-28.5)
				5686-10551	6	7.3 (2.5-21.1)	14.6 (4.7-45.1)
				≥ 10551	7	18.8 (6.8-51.9)	34.6 (10.3-115.8)
Fedeli *et al*[11] (2019), Italian plant	Cohort study, 1685 workers	HCC, histology or clinical records	Job exposure matrix: cumulative exposure (ppm-years)	0-734	12	1.00	
				735-2379	4	1.72 (0.55-5.32)	
				2380-5188	9	5.24 (2.20-12.5)	
				≥ 5189	6	5.52 (2.03-14.9)	
Wong *et al*[19] (2003), Taiwanese cohort	Nested case-control study: 18 cases, 68 referents	Liver cancer: 10 confirmed HCC, no angiosarcoma	Job title based on job history	Tank cleaning	18 liver cancers	3.6 (1.4-9.2)	Additional analyses on joint effects
				High exposure jobs		2.9 (1.1-7.3)	
Mastrangelo *et al*[5] (2004), Italian plant	Nested case-control study: 13 cases, 139 referents	HCC, histology or clinical records	Job exposure matrix: Cumulative exposure (ppm-years)	Each 1000 ppm-years increase	13	1.71 (1.29-2.44) alcohol/virus adjusted	Additional analyses on joint effects

HCC: Hepatocellular carcinoma; CI: Confidence interval.

CHRONIC LIVER DISEASE

Portal hypertension and fibrosis at liver biopsy have been reported among VCM production workers since the 1970s[20]. Thereafter, multiple studies adopting different approaches have investigated the association between occupational exposure to VCM and chronic liver disease: Prevalence surveys among active workers, cohort mortality studies, nested case-control studies. Ultrasonography was advocated as the preferred method for health surveillance of workers exposed to VCM since the mid-1970s: Enlarged portal vein, splenomegaly, and changes in hepatic structure were the most commonly observed abnormalities; by contrast, liver function tests were reported to be unsuitable for the detection of VCM-associated liver diseases[21]. Subsequent studies reported contrasting results for liver function tests, and a possible role for cholestasis indices was suggested for the surveillance of exposed workers[22]. In spite of the early recognition of the role of liver ultrasonography, only a few studies describing the findings associated with VCM exposure have been published. An increased prevalence of periportal liver fibrosis among workers with past high VCM exposure was reported among 757 Italian workers, whereas no association with steatosis and changes in liver function tests was observed[23,24]. Among 347 male workers in Taiwan, those with a history of high VCM-exposure jobs were at a higher risk of liver fibrosis (a category combining cirrhotic and pre-cirrhotic sonographic changes of the liver). Other risk factors for liver fibrosis included overweight/obesity and HBV/HCV infection; workers with both viral infection and high exposure were at the highest risk of liver fibrosis[25]. A possible role of genetic polymorphism of Cytochrome P450 2E1 (CYP2E1) in the development of VCM-induced liver fibrosis was suggested[26]. Among Taiwanese workers, a synergistic effect between high VCM exposure and hepatitis viral infection was also found responsible for increased transaminase levels[27]. The association between occupational VCM exposure and chronic liver disease was confirmed by higher rates of hospital admissions for cirrhosis with respect to non-exposed reference workers[28]. Lastly, an increasing prevalence of abnormalities (all types) was detected at liver ultrasonography across workers with no, low, and high VCM exposures in China; once again, a joint effect with CYP2E1 polymorphism was reported[29].

The studies investigating ultrasonography findings among VCM workers still employed in Western countries and Taiwan were carried out about twenty years after the end of high exposure periods, with a possible underestimation of risks due to workers quitting job as a consequence of liver diseases[25]. More recently, Cave and colleagues reviewed slides from liver biopsies and analyzed frozen sera obtained during 1974-1977 from 25 United States workers with extremely high exposure submitted to intensive medical surveillance (four had concomitant ASL, with a fifth case developing ASL in subsequent years)[30]. Steatohepatitis was observed in 20 (80%) biopsies, among which, liver fibrosis was present in 11. Notably, among these cases, called "Toxicant Associated Steatohepatitis" (TASH), serum transaminases were not altered with respect to healthy chemical workers. TASH, the consequence of current high VCM exposures, may not always be reversible after exposure has been withdrawn and may further evolve into progressive liver injury and fibrosis[30].

The role of VCM exposure in the development of chronic liver disease has been confirmed by a case-control study carried out within an Italian cohort of VCM workers[5]. The case group comprising 40 patients with cirrhosis diagnosed at histology or on a clinical basis was compared to 139 reference workers without any liver disease. Cumulative VCM exposure was an independent risk factor for cirrhosis, interacting with both alcohol consumption and viral infection.

By contrast, cohort studies on vinyl chloride workers usually report a risk of mortality from liver cirrhosis/chronic liver disease lower than the expected based on rates registered in the general population; this finding can be attributed to the healthy worker effect[7]. Within-cohort analyses avoiding bias derived from comparison with an external reference have been performed in the European and the United States cohorts. In both cohorts, increased mortality rates were observed in highly exposed groups with respect to the reference group having the lowest exposure (Table 2), although a linear trend across the categories of cumulative exposure could not be demonstrated[3,9]. It must be remarked that mortality from cirrhosis can be underestimated especially among highly exposed workers. In the presence of ASL or HCC, liver cancer will be selected as the underlying cause of death, whereas the co-existing chronic liver disease will be mentioned only as a concomitant cause (or even omitted)[11,31]. To overcome this limit, deaths from liver cirrhosis were analyzed together with the deaths of patients with histologically or clinically evident cirrhosis, yet having liver cancer as the underlying cause: A strong association with cumulative VCM exposure was demonstrated[11].

CONCLUSION

Occupational exposure to VCM causes a substantial burden of liver diseases; in the last update of an Italian cohort, as much as 29% of overall deaths among workers in the highest exposure category were from liver cancer (all types) or liver cirrhosis[11]. Available original studies reviewed by IARC and published after the IARC assessment confirm the association between occupational VCM exposure and chronic liver disease as well as HCC. Further research is warranted to assess the disease risk in the lower range of cumulative exposure and to investigate the pattern of risk with the time elapsed since exposure. The evidence of additive or multiplicative interactions with other known risk factors should prompt health surveillance and promotion programs among exposed workers, aimed at reduction of alcohol consumption and body weight, and identification and treatment of chronic viral infection.

Table 2 Studies investigating the association between occupational exposure and liver fibrosis/liver cirrhosis in vinyl chloride workers

Ref. location	Study description	Disease assessment	Exposure assessment	Exposure categories	Number of cases	Relative risk (95%CI)	Notes
Maroni *et al*[23] (2003), Italy, four VC plants	Survey of 757 active workers	Liver ultrasonography: Periportal fibrosis	Job exposure matrix: Max Exposure (ppm)	0	Overall prevalence 16.0%	1.0	Adjusted for age, alcohol, body mass index, viral hepatitis
				1-10		1.55 (P = 0.276)	
				50		1.54 (P = 0.405)	
				200		4.12 (P = 0.005)	
				500		2.47 (P = 0.064)	
Hsiao *et al*[25] (2003), Taiwan, five VC plants	Survey of 347 active workers	Liver ultrasonography: Liver fibrosis including pre-cirrhosis and cirrhosis	Job exposure matrix: Cumulative exposure (ppm-years)	Low	3	1.0	Adjusted for age, alcohol, body mass index
				Moderate	5	4.6 (1.0–25.5)	
				High (> 2400)	12	5.9 (1.7–28.2)	
Mastrangelo *et al*[5] (2004), Italian plant	Nested case-control study: 40 Cases and 139 controls	Cirrhosis at histology and/or clinical records	Job exposure matrix: Cumulative exposure (ppm-years)	Each 1000 ppm-years increase	40	1.37 (1.13-1.69) alcohol/virus adjusted	Additional analyses on joint effects
Ward *et al*[3] (2001), European cohort	Cohort study, 12700 workers	Cause of death from death certificates	Job exposure matrix: Cumulative exposure (ppm-years)	< 524	8	1.0	
				524-998	8	9.38 (3.52-25.0)	
				999-3428	9	4.01 (1.55-10.4)	
				3430-5148	8	9.77 (3.66-26.1)	
				5149+	9	8.28 (3.15-21.8)	
Mundt *et al*[9] (2017), United States cohort	Cohort study, 9951 workers	Cause of death from death certificates	Job exposure matrix: Cumulative exposure (ppm-years)	< 63	11	1.0	
				63-286	19	1.8 (0.9-3.8)	
				287-864	22	2.0 (1.0-4.1)	
				865-2270	24	2.1 (1.0-4.3)	
				2271+	21	1.7 (0.9-3.7)	
Fedeli *et al*[11] (2019), Italian plant	Cohort study, 1685 workers	Deaths from cirrhosis + deaths from liver cancer with histological/clinical evidence of cirrhosis	Job exposure matrix: Cumulative exposure (ppm-years)	< 734	35	1.0	
				734-2378	8	1.18 (0.55-2.55)	
				2379-5187	12	2.43 (1.26-4.70)	
				≥ 5188	8	2.60 (1.19-5.67)	

VC: Vinyl chloride; CI: Confidence interval.

REFERENCES

1 **IARC Working Group on the Evaluation of Carcinogenic Risks to Humans**. Chemical agents and related occupations. *IARC Monogr Eval Carcinog Risks Hum* 2012; **100**: 9-562 [PMID: 23189753]
2 **IARC Working Group on the Evaluation of Carcinogenic Risks to Humans**. IARC monographs on the evaluation of carcinogenic risks to humans. Volume 97. 1,3-butadiene, ethylene oxide and vinyl halides (vinyl fluoride, vinyl chloride and vinyl bromide). *IARC Monogr Eval Carcinog Risks Hum* 2008; **97**: 3-471 [PMID: 20232717]
3 **Ward E**, Boffetta P, Andersen A, Colin D, Comba P, Deddens JA, De Santis M, Engholm G, Hagmar L, Langard S, Lundberg I, McElvenny D, Pirastu R, Sali D, Simonato L. Update of the follow-up of mortality and cancer incidence among European workers employed in the vinyl chloride industry. *Epidemiology* 2001; **12**: 710-718 [PMID: 11679801 DOI: 10.1097/00001648-200111000-00021]
4 **Pirastu R**, Baccini M, Biggeri A, Comba P. [Epidemiologic study of workers exposed to vinyl chloride in Porto Marghera: Mortality update]. *Epidemiol Prev* 2003; **27**: 161-172 [PMID: 12958735]
5 **Mastrangelo G**, Fedeli U, Fadda E, Valentini F, Agnesi R, Magarotto G, Marchì T, Buda A, Pinzani M, Martines D. Increased risk of hepatocellular carcinoma and liver cirrhosis in vinyl chloride workers: Synergistic effect of occupational exposure with alcohol intake. *Environ Health Perspect* 2004; **112**: 1188-1192 [PMID: 15289165 DOI: 10.1289/ehp.6972]
6 **Fedeli U**, Mastroangelo G. Vinyl chloride industry in the courtroom and corporate influences on the scientific literature. *Am J Ind Med* 2011; **54**: 470-473 [PMID: 21456080 DOI: 10.1002/ajim.20941]
7 **Frullanti E**, La Vecchia C, Boffetta P, Zocchetti C. Vinyl chloride exposure and cirrhosis: A systematic review and meta-analysis. *Dig Liver Dis* 2012; **44**: 775-779 [PMID: 22440240 DOI: 10.1016/j.dld.2012.02.007]
8 **Lotti M**. Do occupational exposures to vinyl chloride cause hepatocellular carcinoma and cirrhosis? *Liver Int* 2017; **37**: 630-633 [PMID: 28063180 DOI: 10.1111/liv.13326]
9 **Mundt KA**, Dell LD, Crawford L, Gallagher AE. Quantitative estimated exposure to vinyl chloride and risk of angiosarcoma of the liver and hepatocellular cancer in the US industry-wide vinyl chloride cohort:

Mortality update through 2013. *Occup Environ Med* 2017; **74**: 709-716 [PMID: 28490663 DOI: 10.1136/oemed-2016-104051]
10 **Scarnato C**, Rambaldi R, Mancini G, Olanda S, Spagnolo MR, Previati E, Parmeggiani V, Minisci S, Comba P, Pirastu R. [Mortality study update of workers exposed to vinyl chloride in plants located in Ferrara and Ravenna (Emilia-Romagna Region, Northern Italy)]. *Epidemiol Prev* 2017; **41**: 271-278 [PMID: 29119762 DOI: 10.19191/EP17.5-6.P271.088]
11 **Fedeli U**, Girardi P, Gardiman G, Zara D, Scoizzato L, Ballarin MN, Baccini M, Pirastu R, Comba P, Mastrangelo G. Mortality from liver angiosarcoma, hepatocellular carcinoma, and cirrhosis among vinyl chloride workers. *Am J Ind Med* 2019; **62**: 14-20 [PMID: 30474170 DOI: 10.1002/ajim.22922]
12 **Hsieh HI**, Chen PC, Wong RH, Du CL, Chang YY, Wang JD, Cheng TJ. Mortality from liver cancer and leukaemia among polyvinyl chloride workers in Taiwan: An updated study. *Occup Environ Med* 2011; **68**: 120-125 [PMID: 20798004 DOI: 10.1136/oem.2010.056978]
13 **Cooper WC**. Epidemiologic study of vinyl chloride workers: Mortality through December 31, 1972. *Environ Health Perspect* 1981; **41**: 101-106 [PMID: 7199425 DOI: 10.1289/ehp.8141101]
14 **Wong O**, Whorton MD, Foliart DE, Ragland D. An industry-wide epidemiologic study of vinyl chloride workers, 1942-1982. *Am J Ind Med* 1991; **20**: 317-334 [PMID: 1928109 DOI: 10.1002/ajim.4700200305]
15 **Mundt KA**, Dell LD, Austin RP, Luippold RS, Noess R, Bigelow C. Historical cohort study of 10 109 men in the North American vinyl chloride industry, 1942-72: Update of cancer mortality to 31 December 1995. *Occup Environ Med* 2000; **57**: 774-781 [PMID: 11024202 DOI: 10.1136/oem.57.11.774]
16 **Simonato L**, L'Abbé KA, Andersen A, Belli S, Comba P, Engholm G, Ferro G, Hagmar L, Langård S, Lundberg I. A collaborative study of cancer incidence and mortality among vinyl chloride workers. *Scand J Work Environ Health* 1991; **17**: 159-169 [PMID: 2068554 DOI: 10.5271/sjweh.1715]
17 **El-Serag HB**, Rudolph KL. Hepatocellular carcinoma: Epidemiology and molecular carcinogenesis. *Gastroenterology* 2007; **132**: 2557-2576 [PMID: 17570226 DOI: 10.1053/j.gastro.2007.04.061]
18 **Wong RH**, Chen PC, Du CL, Wang JD, Cheng TJ. An increased standardised mortality ratio for liver cancer among polyvinyl chloride workers in Taiwan. *Occup Environ Med* 2002; **59**: 405-409 [PMID: 12040117 DOI: 10.1136/oem.59.6.405]
19 **Wong RH**, Chen PC, Wang JD, Du CL, Cheng TJ. Interaction of vinyl chloride monomer exposure and hepatitis B viral infection on liver cancer. *J Occup Environ Med* 2003; **45**: 379-383 [PMID: 12708141 DOI: 10.1097/01.jom.0000063622.37065.fd]
20 **Smith PM**, Crossley IR, Williams DM. Portal hypertension in vinyl-chloride production workers. *Lancet* 1976; **2**: 602-604 [PMID: 61343 DOI: 10.1016/S0140-6736(76)90668-1]
21 **Williams DM**, Smith PM, Taylor KJ, Crossley IR, Duck BW. Monitoring liver disorders in vinyl chloride monomer workers using greyscale ultrasonography. *Br J Ind Med* 1976; **33**: 152-157 [PMID: 962999 DOI: 10.1136/oem.33.3.152]
22 **Attarchi MS**, Aminian O, Dolati M, Mazaheri M. Evaluation of liver enzyme levels in workers exposed to vinyl chloride vapors in a petrochemical complex: A cross-sectional study. *J Occup Med Toxicol* 2007; **2**: 6 [PMID: 17686177 DOI: 10.1186/1745-6673-2-6]
23 **Maroni M**, Mocci F, Visentin S, Preti G, Fanetti AC. Periportal fibrosis and other liver ultrasonography findings in vinyl chloride workers. *Occup Environ Med* 2003; **60**: 60-65 [PMID: 12499459 DOI: 10.1136/oem.60.1.60]
24 **Maroni M**, Fanetti AC. Liver function assessment in workers exposed to vinyl chloride. *Int Arch Occup Environ Health* 2006; **79**: 57-65 [PMID: 16091976 DOI: 10.1007/s00420-005-0018-y]
25 **Hsiao TJ**, Wang JD, Yang PM, Yang PC, Cheng TJ. Liver fibrosis in asymptomatic polyvinyl chloride workers. *J Occup Environ Med* 2004; **46**: 962-966 [PMID: 15354062 DOI: 10.1097/01.jom.0000137722.66767.38]
26 **Hsieh HI**, Chen PC, Wong RH, Wang JD, Yang PM, Cheng TJ. Effect of the CYP2E1 genotype on vinyl chloride monomer-induced liver fibrosis among polyvinyl chloride workers. *Toxicology* 2007; **239**: 34-44 [PMID: 17659824 DOI: 10.1016/j.tox.2007.06.089]
27 **Hsieh HI**, Wang JD, Chen PC, Cheng TJ. Synergistic effect of hepatitis virus infection and occupational exposures to vinyl chloride monomer and ethylene dichloride on serum aminotransferase activity. *Occup Environ Med* 2003; **60**: 774-778 [PMID: 14504367 DOI: 10.1136/oem.60.10.774]
28 **Du CL**, Wang JD. Increased morbidity odds ratio of primary liver cancer and cirrhosis of the liver among vinyl chloride monomer workers. *Occup Environ Med* 1998; **55**: 528-532 [PMID: 9849539 DOI: 10.1136/oem.55.8.528]
29 **Zhu SM**, Ren XF, Wan JX, Xia ZL. Evaluation in vinyl chloride monomer-exposed workers and the relationship between liver lesions and gene polymorphisms of metabolic enzymes. *World J Gastroenterol* 2005; **11**: 5821-5827 [PMID: 16270392 DOI: 10.3748/wjg.v11.i37.5821]
30 **Cave M**, Falkner KC, Ray M, Joshi-Barve S, Brock G, Khan R, Bon Homme M, McClain CJ. Toxicant-associated steatohepatitis in vinyl chloride workers. *Hepatology* 2010; **51**: 474-481 [PMID: 19902480 DOI: 10.1002/hep.23321]
31 **Fedeli U**, Schievano E, Lisiero M, Avossa F, Mastrangelo G, Saugo M. Descriptive epidemiology of chronic liver disease in northeastern Italy: An analysis of multiple causes of death. *Popul Health Metr* 2013; **11**: 20 [PMID: 24112320 DOI: 10.1186/1478-7954-11-20]

World Journal of Gastroenterology

Submit a Manuscript: https://www.f6publishing.com

World J Gastroenterol 2019 September 7; 25(33): 4892-4903

DOI: 10.3748/wjg.v25.i33.4892

ISSN 1007-9327 (print) ISSN 2219-2840 (online)

ORIGINAL ARTICLE

Basic Study

Ex vivo effect of vascular wall stromal cells secretome on enteric ganglia

Giovanni Dothel, Chiara Bernardini, Augusta Zannoni, Maria Rosaria Spirito, Roberta Salaroli, Maria Laura Bacci, Monica Forni, Fabrizio De Ponti

ORCID number: Giovanni Dothel (0000-0002-8588-9018); Chiara Bernardini (0000-0003-3384-0244); Augusta Zannoni (0000-0002-2972-4921); Maria Rosaria Spirito (0000-0003-1963-5340); Roberta Salaroli (0000-0002-8819-2857); Maria Laura Bacci (0000-0001-6702-5868); Monica Forni (0000-0003-1310-6202); Fabrizio De Ponti (0000-0002-0367-9595).

Author contributions: Dothel G, Zannoni A, Bernardini C and Forni M conceived and designed the study; Dothel G, Salaroli R and Spirito MR performed the experiments; Dothel G, Bernardini C and Forni M wrote the paper; Dothel G performed the data analysis; Bacci ML carried out the procedures on pigs; De Ponti F and Forni M coordinated the research; all authors reviewed and participated to the paper drafting.

Supported by Fondazione del Monte di Bologna e Ravenna (ID ROL: FdM/3208).

Institutional review board statement: This study was approved by the institutional review board of National Institute of Health.

Institutional animal care and use committee statement: All procedures involving animals were reviewed and approved by the Institutional Animal Care and Use Committee of the University of Bologna (approved experimental protocol for the use of guinea pigs: protocol number - 18/79/14;

Giovanni Dothel, Maria Rosaria Spirito, Fabrizio De Ponti, Department of Medical and Surgical Sciences, University of Bologna, Bologna 40126, Italy

Chiara Bernardini, Augusta Zannoni, Roberta Salaroli, Maria Laura Bacci, Monica Forni, Department of Veterinary Medical Sciences, University of Bologna, Bologna 40064, Italy

Corresponding author: Monica Forni, PhD, Associate Professor, Department of Veterinary Medical Sciences, University of Bologna, Via Tolara di Sopra 50, Ozzano dell'Emilia, Bologna 40064, Italy. monica.forni@unibo.it
Telephone: +39-51-2097913
Fax: +39-51-2097899

Abstract

BACKGROUND

Mesenchymal stromal cell (MSC)-based therapy is currently under study to treat inflammatory bowel diseases. MSC bioactive products could represent a valid alternative to overcome issues associated with systemic whole-cell therapies. However, MSC anti-inflammatory mechanisms differ between rodents and humans, impairing the reliability of preclinical models.

AIM

To evaluate the effect of conditioned medium (CM) derived from porcine vascular wall MSCs (pVW-MSCs) on survival and differentiation of porcine and guinea pig enteric ganglia exposed to lipopolysaccharide (LPS).

METHODS

Primary cultures of enteric ganglia were obtained by mechanic and enzymatic digestion of ileum resections from guinea pigs (*Cavia porcellus*) (GPEG) and pigs (*Suus scrofa*) (PEG). pVW-MSCs were derived by enzymatic digestion from vascular wall resections of porcine aorta and tested by immunoflowcytometry for MSC immune profile. Enteric ganglia were treated with increasing concentrations of LPS, CM derived by pVW-MSCs or a combination of CM and LPS 1 μg/mL. Cell count and morphometric analysis of HuD positive neurons and glial fibrillary acidic protein positive glial cells were performed by immunofluorecent staining of cultured ganglia.

RESULTS

PEG showed a higher number of neurons compared to GPEG. Overall, CM exerted a protective role on LPS-treated enteric ganglia. CM in combination with

approved experimental protocol for the use of pigs: protocol number - 43-IX/9 all.37; 15/04/2013).

Conflict-of-interest statement: None of the authors have any potential conflicts of interest associated with this research.

ARRIVE guidelines statement: The present study was conceived, designed and performed following the ARRIVE guidelines. All the authors have read the ARRIVE guidelines and reviewed the manuscript accordingly.

Manuscript source: Unsolicited manuscript

Received: April 11, 2019
Peer-review started: April 11, 2019
First decision: May 17, 2019
Revised: May 31, 2019
Accepted: June 8, 2019
Article in press: June 8, 2019
Published online: September 7, 2019

P-Reviewer: Bagyánszki M, Krishnan T, Tang ST, Xu WX
S-Editor: Yan JP
L-Editor: A
E-Editor: Li X

LPS increased the number of glial cells per ganglion in both cultures evoking glial cells differentiation in porcine cultures.

CONCLUSION
These findings suggest an immunomodulating activity of pVW-MSCs mediators on the enteric nervous system in inflammatory conditions.

Key words: Enteric nervous system; Mesenchymal stromal cells; Inflammatory bowel disease; Ganglia; Translational models

Core tip: Secretome of porcine vascular wall mesenchymal stromal cells (pVW-MSCs) induced an increase of glial cell number in swine and guinea pig-derived enteric ganglia. Co-treatment of enteric ganglia with lipopolysaccharide and conditioned medium promoted glial cell differentiation only in pigs. These data indicate an immune activation promoted by pVW-MSCs which could be more specific in higher mammals, suggesting a careful consideration of the animal models used in research studies on cell-based therapies.

Citation: Dothel G, Bernardini C, Zannoni A, Spirito MR, Salaroli R, Bacci ML, Forni M, Ponti FD. *Ex vivo* effect of vascular wall stromal cells secretome on enteric ganglia. *World J Gastroenterol* 2019; 25(33): 4892-4903
URL: https://www.wjgnet.com/1007-9327/full/v25/i33/4892.htm
DOI: https://dx.doi.org/10.3748/wjg.v25.i33.4892

INTRODUCTION

Inflammatory bowel diseases (IBDs), encompassing the two major forms Crohn's disease (CD) and ulcerative colitis (UC), are characterized by an overactive immune response to unknown environmental triggers associated with specific genetic traits[1]. Genome-wide association studies advanced previous knowledge of genetic variants associated with innate and adaptive immunity (*e.g.*, *NOD2*, *IL23R*) revealing novel pathophysiological mechanisms linked to autophagy and loss of epithelial barrier function[2,3]. In IBD, chronic intestinal inflammation induces several morpho-functional changes of the enteric nervous system (ENS), including swallowing of enteric nerve bundles and higher expression of several neurotransmitters[4].

Mesenchymal stromal cells (MSCs) are currently under study as a therapeutic option in regenerative medicine and as a novel treatment for autoimmune and chronic inflammatory disorders including IBDs[5]. Although the mechanism underlying the immunoregulatory effect of MSCs is still to be clarified, their role in balancing immune homeostasis has been acknowledged[6]. Notably, pro- or anti-inflammatory activity[7] along with other MSC biomolecules is settled by toll-like receptors 3 and 4, the latter being one of the main sensors of bacterial lipopolysaccharide (LPS)[8,9].

MSCs respond to an inflammatory environment releasing CC chemokine ligand 2 and IL-10, which inhibits CD4 Th17 cells proliferation and IL-17 production[10] and polarizes naïve T-cells to the regulatory Foxp3-positive phenotype (T-reg)[6]. These pleiotropic, anti-inflammatory properties justify a proof of concept study for a possible application of MSCs in IBDs, where Th-17 and Th-4/5 lymphocytes drive the aberrant immune reaction of CD and UC, respectively. A phase III clinical trial of CD with a systemic infusion of MSCs is currently ongoing[11], while local treatment of the severe fistulizing form of CD was recently approved by EMA[12].

One of the main drawbacks of cell-based therapy regards uncertainty about biodistribution and homing of cells to the target site of action. In particular, MSCs tend to remain trapped in the microcirculation of pulmonary alveoli, allegedly for an increased diameter acquired during *in vitro* expansion[13]. For these reasons, MSC-derived exosomes as well as MSC secretome are gaining attention in current research[14-17]. Furthermore, a recent study showed that a vascular wall mesenchymal stem cells isolated by porcine aortic tissue (pVW-MSCs) showed mesenchymal features[18] and the ability to differentiate in all the cellular components of a mature vessel[19]. A deeper characterization demonstrated their metabolic properties[20] and

their intrinsic attitude to promote angiogenesis also by paracrine action[21].

Interestingly, the key factor responsible for MSC anti-inflammatory action varies among species and is related to a specific phylogenetic tree[22]. On this basis, this study aims at investigating a possible gap between rodent and swine neuro-immune response to MSC-derived bioactive products assuming pVW-MSC secretome as a closer model from a translational point of view. To this purpose, we first compared the effect of LPS on cell survival and differentiation in primary enteric ganglia derived from guinea pig and pig myenteric plexus (MP) (GPEG and PEG, respectively); thereafter, we evaluated the effect of pVW-MSC secretome in these two *ex-vivo* models of ENS.

MATERIALS AND METHODS

Animals

Animals were used after approval of the protocol by the local ethics committee and following the guidelines of 3Rs implied in the EU directive 2010/63/EU for the use of animal for experimental purposes and in accordance with the national legislation (Decree 116/1992). In accordance with the 3Rs principle of Reduction[23] the animals used in the present study served as controls in other experimental protocols carried out in our facility.

Swine (Protocol number n.43-IX/9 all.37; 20/11/2012): Young commercial hybrids of *Sus scrofa* (4 males–aged 4-5 wk, 7 ± 0.5 Kg live weight), born at the ASA Unit (DIMEVET, University of Bologna), were enrolled in the study. Piglets were bred under the lactating sow till 28 d, then weaned and kept in a multiple box for young piglets, temperature was kept at 28 ± 1 °C with adequate ventilation and humidity in relation to the young age. Surgical procedures were carried out during the morning in the surgical theatre of the DIMEVET facilities. Animal received an i.m. bolus of tiletamine-zolazepam (5 mg/kg) 10 min before induction; general anesthesia was achieved using sevoflurane with an induction mask[24]. Animals were then sacrificed with a single bolus (0.3 mL/kg) of Tanax (embutramide/mebezonium iodide/tetracaine hydrochloride; Msd Animal Health Srl) and the abdomen was opened to remove the small intestine.

Guinea pigs (Protocol number 18/79/14): Male Dunkin-Hartley guinea pigs (*Cavia porcellus*, 8 males–aged 3-5 wk, weight 200-280 g, Harlan Italy, Udine, IT) were kept in home cages with a controlled environment (12 h dark/light cycle, 20-24 °C temperature, 40%-70% humidity) with unlimited access to water and chow. The day of the experiment, animals were sacrificed through isoflurane inhalation followed by exsanguination through jugular excision. All the procedures were carried out in the operating room of Medical and Surgical Department.

Isolation and culture of ganglia by pig and guinea pig myenteric plexus

Isolation of MP from 8 guinea pigs (3-5 wk) and 4 pigs (4-5 wk) was performed as previously described[25,26]. Briefly, the small intestine was washed with sterile, oxygenated Krebs solution containing (mM) NaCl 120.9, KCl 5, $MgCl_2$ 1.2, $CaCl_2$ 2.5, glucose 11.5, $NaHCO_3$ 14.4, NaH_2PO_4 1.2 additioned with fungizone and penicillin-streptomycin 10 ml/L (Sigma Aldrich-Merck, Darmstadt, Germany). MP was peeled by 2-cm traits of small intestine cut in 1 mm × 1 mm fragments and digested in T25 plastic flasks with an enzymatic solution containing 1.25 mg/mL collagenase IV from *Clostridium histolyticum*, 1 mg/mL dispase II from *Bacillus polymyxa* and 1 mg/mL bovine serum albumin (Sigma Aldrich-Merck) in gentle agitation 30 min (guinea pig tissues) or 45 min (pig tissues) at 37 °C. Reaction was stopped by placing flasks in ice for 3 min. Digested tissues were washed with cold Krebs solution and collected in DMEM. Fragmented neuronal fibers were selected over muscle bundles with a stereomicroscope (Nikon C-PSCN - Nikon, Tokyo, Japan) and seeded on polyornithine-covered coverslips in 24-well plates with M199 medium enriched with 5% fetal bovine serum, 10 mL/L penicillin-streptomycin and 5% glucose (complete M199-cM199). Plates were kept 24 h in a humidified chamber at 37 °C with 5% CO_2.

Immune profiling and collection of media conditioned by porcine vascular wall mesenchymal stromal cells

pVW-MSCs were isolated, characterized and maintained as previously described[27]. In order to confirm the mesenchymal immunophenotype after cryopreservation, flow cytometry analysis was performed before media collection. Briefly, 2 × 10^5 cells were resuspended in 100 μL of phosphate buffered saline (PBS) and incubated for 1 h at 4 °C in the dark with appropriate fluorochrome-conjugated antibodies at the titers

reported in Table 1. Unstained controls to evaluate inherent background or autofluorescence were obtained omitting primary antibodies. After incubation, cells were washed twice and resuspended in 200 µl of PBS then analyzed with MacsQuant Analyzer10 (Miltenyi Biotec, Bergisch Gladbach, Germany). For CD34 staining, after the first incubation with the primary antibody, cells were washed and incubated with PE-conjugated secondary antibody (Table 1) for 40 min at 4 °C in the dark. Data were analyzed using the Flowlogic™ software (Miltenyi Biotec).

After thawing cellular suspensions were plated in a 24-multi well plate at a concentration of 3 × 10^4 cells/well in PGM medium (Promocell, Heidelberg, Germany), the day after, cells were washed with PBS and cultured for additional 24 h in PGM, then media were collected, centrifuged at 800 × g for 10 min, filtered through a 0.20-µm syringe filter, immediately frozen in liquid nitrogen and stored at -80 °C until use.

Treatments

Enteric ganglia derived from each animal were seeded in 24 wells plates, a pool of 35 ganglia per well from 3 wells (triplicates) were considered for the analysis. After 2 d, ganglia were incubated for 24 h with cM199 (CRTL) or one of the followings: cM199 + 0-0.1-1-10 µg/mL LPS (LPS from Escherichia coli O111:B4, Sigma Aldrich-Merck); conditioned medium (CM) derived by culture flasks containing adherent pVW-MSCs (10% in M199) or CM combined with LPS 1 µg/mL. Treatments were coded arbitrary so that a second operator could carry on the operation blindly.

Immunocytochemistry analysis of enteric ganglia

At the end of 24-h treatment, cells were washed twice in cold PBS and fixed in 4% paraformaldehyde for 1 h. After three washes with cold PBS, unspecific epitopes were blocked by incubating fixed ganglia with a blocking solution of 0.5% Triton and donkey serum 5% for 1 h. Ganglia were double-stained by overnight incubation at 4°C with a mix containing antibodies directed to the pan-neuronal marker HuD and to the glial fibrillary acidic protein (GFAP). The following day, cells were washed three times with PBS and incubated 2 h at room temperature with appropriate fluorescent anti-antibodies (Table 1). Negative controls included a pre-adsorption step for 2 h with the specific blocking peptides in the preliminary tests and the omission of the primary antibody in every run experiment. At the end of the procedure, coverslips were mounted on slides with an anti-fade solution (10% Mowiol 4-88, Sigma Aldrich-Merck) containing 0.1 µg/mL DAPI. Photomicrographs of single ganglion were obtained with a Zeiss Imager M1 microscope with dedicated software (AxioVision, Carl Zeiss, Jena, Germany).

Imaging analysis of cultured ganglia

Cell count and morphometric analysis of photomicrographs were carried out blindly with Image J software on the basis of a previously applied method[28]. Briefly, two axis intersecting at a 90° angle were traced from the furthest ends of the cluster of cell bodies. A first circle representing the core area was traced considering the intersection of the two axis as the center and the longest axis as the diameter. Likewise, an outer circle, having the same center as the former and the diameter extending to the furthest fillopodium, was considered as the total area. The percentage of ganglion expansion (Gang. Exp. %) on total area was calculated as follows: Gang.Exp.% = [(total area-core area)]%100/(total area).

Statistical analysis

Results are reported as Tukey box-plots (middle lines-median values; lower and upper sides of the rectangles - 1st and 3rd percentile, whiskers - confidence intervals; black dots - outliers). Statistical analysis was performed through GraphPad Prism software (GraphPad, La Jolla, CA, United States) on data retrieved from 35 ganglia/well analyzed in triplicates for each experimental group. Normal distribution was confirmed by Shapiro-Wilk test and Student *t* test was used to determine statistical significance of the differences observed. Data significance was considered when $P < 0.05$ or as reported in text.

RESULTS

Comparison of ganglia derived by pig and guinea pig myenteric plexa

After 2 d of culture *in vitro*, GPEG showed a more consistent morphology and cell composition in comparison with PEG. GPEG showed a globular or bean-like shapes with a core of cell bodies and glial cells radially protruding outward (Figure 1A). Conversely, PEG were characterized by larger globular, bi- or tri-lobed shapes (Figure

Table 1 Antibody reporting

Name	Target	Clonality	Conjugation	Research resource identifiers	Species	Supplier	Catalog number	Application	Concentrati-on used
Anti-HuD	Hu N-terminus of human HuD	Poly	-	AB_2101223	Gt	Santa Cruz Biotechnologies	sc-5977	IC	5 μg/mL
Anti-GFAP	Hu Glial Fibrillary Acidic Protein	Mono	-	AB_10689630	Ms	BD Biosciences	561483	IC	1 μg/mL
Alexa 488	Gt IgM heavy and light chains	Poly	Alexa Fluor® 488	AB_2535792	Dk	Thermo Fisher Scientific	A-21206	IC	0.5 μg/mL
Alexa 555	Ms IgM heavy and light chains	Poly	Alexa Fluor® 555	AB_2535853	Dk	Thermo Fisher Scientific	A-21432	IC	0.5 μg/mL
Anti-CD 105	Hu CD105 (L-isoform) cell surface antigen	Mono	FITC	AB_868768	Ms	Abcam	Ab53318	FC	2 μL/10^5 cells/100 μL
Anti-CD90	Hu CD90/Thy-1 cell surface antigen	Mono	APC	AB_10677422	Ms	Abcam	Ab139364	FC	1 μL/10^5 cells/100 μL
PE anti-human CD56	Hu CD56 cell surface antigen	Mono	PE	AB_314448	Ms	Biolegend	304606	FC	2 μL/10^5 cells/100 μL
Human CD44 antibody	Hu CD44 isoforms, 80-95 Kd cell surface antigen	Mono	PerCP	AB_10645506	Rt	Biolegend	103036	FC	0.5 μL/10^5 cells/100 μL
CD34 antibody [EP373Y]	Hu CD34 cell surface antigen	Mono	-	AB_1640331	Rb	Abcam	Ab81289	FC	0.8 μL/10^5 cells/100 μL
Rabbit-PE	Rb IgG heavy and light chains	Poly	PE	AB_10680576	Gt	Abcam	Ab97070	FC	0.5 μL/10^5 cells/100 μL

FITC: Fluorescein isothiocyanate; APC: Allophycocyanin; PE: Phycoerythrin; PerCP: Peridinin-chlorophyll-protein; Ms: Mouse; Rt: Rat; Gt: Goat; Dk: Donkey; Hu: Human; GFAP: Glial fibrillary acidic protein IC: Immunocitochemistry; FC: Flowcitometry.

1E) with a number of total cells per ganglion about 4-fold higher when compared to GPEG (213.7 ± 50.4/PEG *vs* 53.3 ± 5.2 cells/GPEG, $P < 0.001$, Figure 1B) and a higher number of HuD-immunoreactive (HuD-IR) neurons per ganglion (+13.7%, Figure 1C). Frequency analysis in Figure 1F and Figure 1G describes differences between GPEG and PEG in terms of number of ganglia presenting 5 to 205 neurons. Moreover, PEG showed a different proportion of HuD-IR neurons and GFAP-immunoreactive (GFAP-IR) glial cells (+12.7%, $P < 0.05$), whereas GPEG presented a more homogenous distribution of both cell types. Notably, a higher number of neurons/ganglion (+12.7%, $P < 0.05$) and a lower number of glial cells/ganglion (-15.7%, $P < 0.05$) were detected in PEG compared to GPEG (Figure 1D).

Effect of LPS on the number of cells in pig and guinea pig enteric ganglia

GPEG exposed to increasing concentrations of LPS displayed a trend towards a decreased number of neurons/ganglion, which was statistically significant only at the concentration of 10 μg/ml (-22.3%, $P < 0.05$, Figure 2A). This effect was paralleled by an increased number of glial cells/ganglion (+22.2%, $P < 0.05$, Figure 2A). Conversely, no effect of LPS was detected on cell number in PEG cultures at any of the concentrations tested. Notably, the observed lower number of GFAP-IR glial cells compared with HuD-IR neurons was similar in all the experimental groups ($P < 0.05$, Figure 2B).

Characterization of pVW-MSCs phenotype

Flowcytometric analysis confirmed an unvaried immunophenotype of pVW-MSCs at the third passage after cryopreservation, displaying MSC profile. In line with the

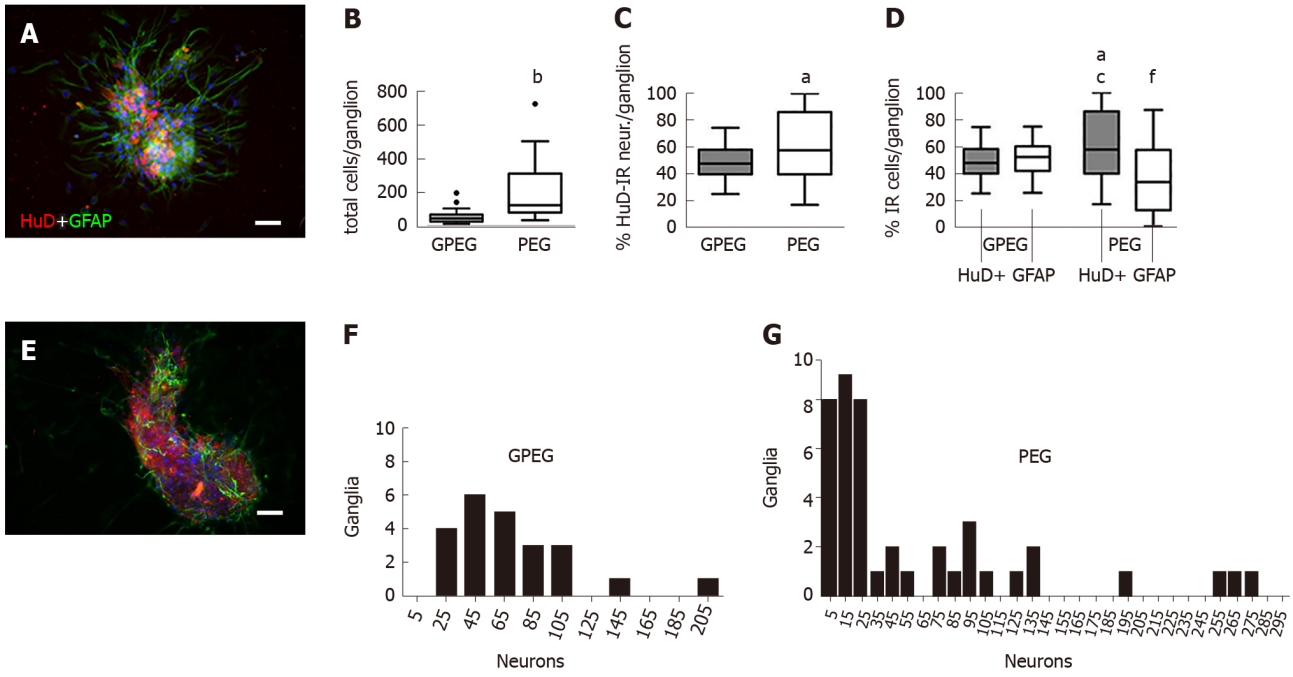

Figure 1 Descriptive analysis of the morphology and cellular composition of guinea pig and pig enteric ganglia after 2 d *in vitro*. A and E: Representative photomicrographs of guinea pig enteric ganglia (GPEG) and pig enteric ganglia (PEG) stained with HuD (red) and glial fibrillary acidic protein (GFAP) (green) antibodies directed to neurons and glial cells respectively (scale bar: 100 μm); B: Total number of cells per ganglion in GPEG, left gray box plot, and PEG, right white bars, cultures (53.3 ± 5.2 *vs* 213.7 ± 50.4 neurons per ganglion, $^{b}P < 0.001$ *vs* GPEG); C: PEG showed a higher number of HuD-immunoreactive (HuD-IR) neurons compared to GPEG (+13.7%, $^{a}P < 0.05$); D: PEG and GPEG comparison of HuD-IR neurons and GFAP-immunoreactive (GFAP-IR) glial cells: PEG presented a higher number of HuD-IR neurons compared to GFAP-IR glial cells (+28.4%, $^{a}P < 0.05$). In comparison to GPEG, PEG showed a higher number of neurons (+12.7%, $^{c}P < 0.05$) and a lower number of GFAP-IR glial cells (-15.7%, $^{f}P < 0.01$); B-D: Values reported as Tukey box-plots were obtained by three independent experiments. F and G: Frequency analysis indicating the number of GPEG (F) and PEG (G) presenting 5 to 205 neurons. GPEG: Guinea pig enteric ganglia; PEG: Pig enteric ganglia; GFAP: Glial fibrillary acidic protein; GFAP-IR: Glial fibrillary acidic protein-immunoreactive; HuD-IR: HuD-immunoreactive.

criteria for MSC characterization[18] more than 96% of the cell population analyzed was positive for the markers of mesenchymal stemness, CD105, CD90, CD56, CD44, and less than 2.5% was positive for the hematopoietic markers CD45 and CD34 (Figure 3).

Effect of pVW-MSCs mediators on GPEG and PEG exposed to LPS

Thereafter, we tested the effect of medium conditioned by pVW-MSCs (CM) on GPEG and PEG cultured with LPS 1 μg/mL (LPS1). The concentration of 1 μg/mL was chosen in order to resemble a plausible pathophysiological condition of a high bacterial overload. Both guinea pig and pig cultures did not show any significant change in the number of HuD+ neurons after treatments (Figure 4A and B, white columns), whereas glial cell number varied significantly (Figure 4A and B, gray columns). In particular, GPEG cultures showed a higher number of glial cells as a result of co-treatment with CM+LPS1, compared to control and LPS1 groups (+13.9%, $P < 0.001$; +16.5%, $P < 0.01$, respectively). As for PEG cultures an increased number of GFAP+ glial cells was observed in CM group compared to control (+13.6%, $P < 0.05$) and LPS1 groups (+20.2%, $P < 0.05$). In addition, number of glial cells was higher in GPEG treated with CM+LPS1 compared to LPS1 (+14.2%, $P < 0.05$). The main interspecies difference was the variation of number of glial cells exposed to CM, which increased in PEG but not in GPEG cultures compared to the relative control (Figure 4A and B, third gray columns).

Morphometric analysis of ganglia upon treatment with pVW-MSC-conditioned medium

As most of the observed differences regarded glial rather than neuronal cells, we proceeded with a morphometric analysis of glial processes protruding outward the ganglion center area measuring the extent of the ganglion expanded area (Gang. Exp.%, Figure 5A). PEG morphology underwent more substantial changes in comparison to GPEG cultures which did not show any significant change following treatments showing a trend towards decreased Neur.Exp. (not statistically significant) after LPS1 treatment compared to control and CM groups. Furthermore, CM+LPS1 induced a marked increase of Gang.Exp. which was approximately 2 fold higher compared to both LPS1 and control groups (+43.2% *vs* CTRL, $P < 0.01$, Figure 5B).

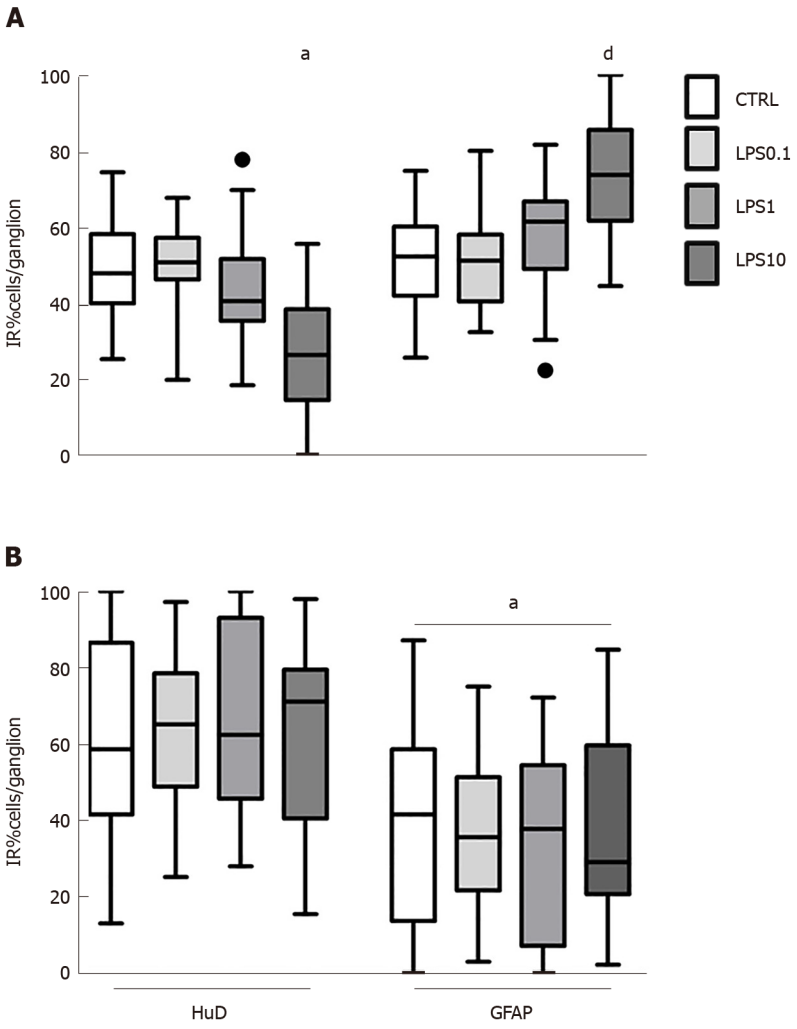

Figure 2 Effect of increasing concentration of lipopolysaccharide on enteric ganglia' HUD+ neurons and GFAP+ glial cells. A: In guinea pig-derived enteric ganglia - lipopolysaccharide (LPS) at 10 μg/mL decreased number of HuD-immunoreactive (HuD-IR) neurons (left columns) and increased proliferation of glial fibrillary acidic protein-immunoreactive (GFAP-IR) glial cells (right columns - HuD-IR neurons LPS10 *vs* CTRL, 22.3%, $^{a}P < 0.05$; GFAP-IR glial cells LPS10 *vs* CTRL, +22.2%, $^{d}P < 0.01$); B: Conversely, in pig enteric ganglia the number of glial cells at every LPS concentration tested did not change and was significatively lower compared to ganglionic neurons. $^{a}P < 0.05$. LPS: lipopolysaccharide; GFAP-IR: Glial fibrillary acidic protein-immunoreactive; HuD-IR: HuD-immunoreactive.

DISCUSSION

The present study shows higher reactivity to MSC mediators of glial cells in pig compared to guinea pig myenteric ganglia. In particular, we tested the effect of CM derived by pVW-MSCs cultures on myenteric ganglia isolated from ileal tissue of GPEG and PEG. These primary cultures exposed to LPS combined with pVW-MSCs medium showed a more pronounced proliferation and differentiation in PEG compared to GPEG. This finding suggests a different and higher response of neuroimmune cells in higher mammals, which could impact on translational aspects of current research on cell-based therapies.

In the present study, we reported interspecies differences in the cellular composition of GPEG and PEG, with a higher neuronal/glial cells ratio in the latter, which is in line with previous findings[29]. Furthermore, we described a slight decrease in the number of neurons with a correspondent increase of glial cells as a result of increasing micromolar concentrations of LPS in GPEG, but not in PEG. Finally, we detected a marked modification of glial cell number and morphological modifications of PEG in response to CM derived by pVW-MSCs cultures.

The higher number of neurons detected in PEG is in line with previous findings describing an anatomical correlation in the size of myenteric ganglia and number of cells per ganglion in large mammals[30]. Moreover, PEG size and number of cells were more variable compared to GPEG, partially reflecting ganglia composition observed

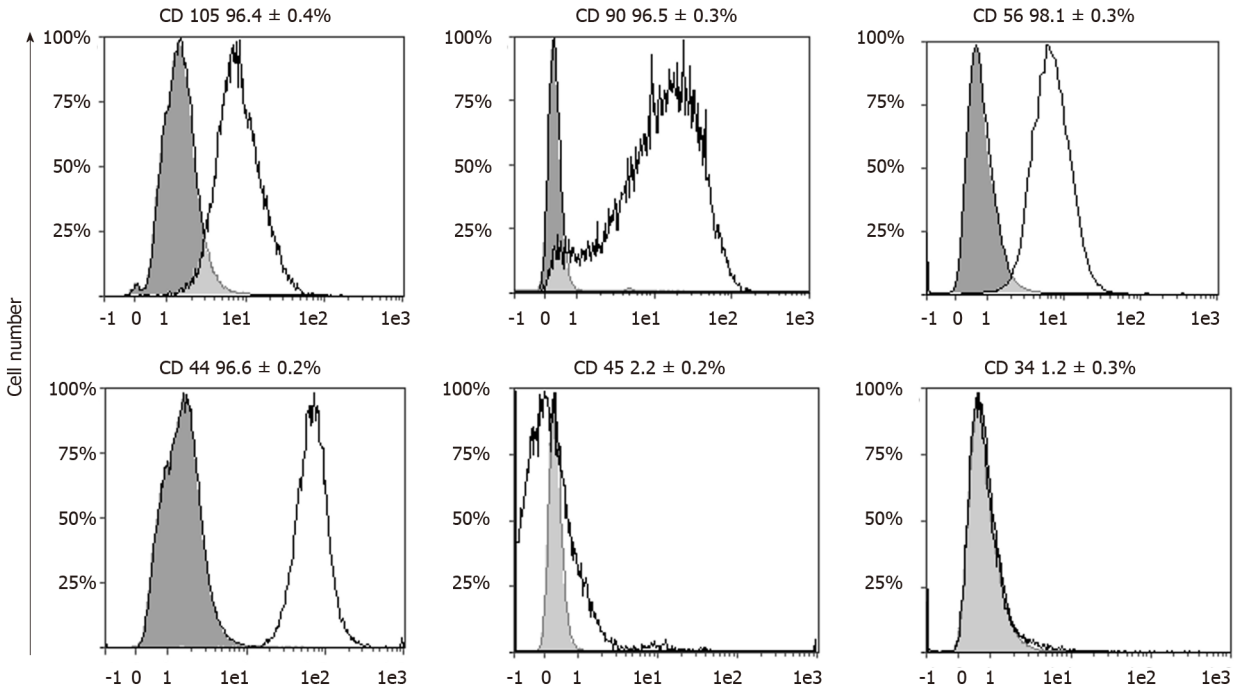

Figure 3 Flowcytometric analysis of cell-surface markers in porcine vascular wall mesenchymal stromal cells. Each graph shows the percentage of cells expressing the specific marker reported [white area under the curve (AUC)] and the relative negative control (gray AUC, cells not incubated with any antibodies). This analysis confirmed the mesenchymal stromal cell-like immune profile of porcine vascular wall mesenchymal stromal cells: CD105, CD90, CD56, CD44 were highly expressed (> 96%) while the hematopoietic markers CD45 and CD43 were nearly absent (< 2.5%). AUC: Area under the curve.

in larger mammals, including humans[31]. Our findings show a low glial cells/neurons ratio, particularly in PEG, which is in line with previous published data[29]. This disproportion is easily filled within 48 h of culture, due to the rapid proliferation of glial cells. In order to avoid a possible confounder, we chose a shorter time (24 h) to limit the proliferation of glial cells, so as to detect small variations in number and morphology of ganglia resulting after treatment.

Notably, our data of cell count analysis correspond to micromolar LPS concentrations as a result of previous tests performed with nanomolar concentrations. This analysis did not provide any measurable difference between groups (10-100 nM, data not shown). Moreover, the scarce decrease of cell number in GPEG and the absence of any effect in PEG cultures even with LPS at the highest concentrations (10 μM) reflects a remarkable resilience of myenteric neurons, already reported in previous works[32]. The slight decrease of neuronal cells at 10 μM of LPS in GPEG could be ascribed to a lower sensitivity of guinea pigs to LPS compared to pigs, which was tested in previous studies on LPS-induced endotoxic shock[33,34]. However, Schuster and colleagues described a counterintuitive effect of LPS promoting neuronal viability and stemness in myenteric ganglia derived by MP of newborn mice[32]. Differently from this work, our data did not show a higher neuron number as a result of LPS treatment. Rather, most of the variations observed, as probably due to age-related features of the animals used (young animals rather than newborns), regarded glial cell number, which markedly varied upon treatment with pVW-MSCs supernatants, while it did not evoke any measurable change on the neuronal component in either pig or guinea pig cultures. Indeed, CM derived by pVW-MSCs alone or combined with 1 μg/mL LPS induced a higher number of glial cells in PEG, while in GPEG-treated samples an akin effect was found only after the co-treatment, suggesting a synergic activity of pVW-MSC-secreted molecules and LPS in promoting glial cells mitosis in both models. This observation is in accordance with the properties showed by brain vascular pericytes which favor glial cells' phenotype, being also spatially in close relation with this cell type in brain vessels[35,36]. Indeed, pVW-MSCs, along with a MSC-like immune profile, exhibited an intrinsic pro-angiogenic features in previous studies[19,27]. In addition, both LPS and MSCs promote the activation of glial cells in brain-derived ganglia. In particular, a recent study *in vitro* described the induction of glia proliferation induced by Wharton-jelly-derived MSCs[37], while *in vivo* injection of LPS induced an overexpression of the glial marker GFAP in brain tissue[38]. Interestingly, we observed a substantial variation of this cell population in swine but not in guinea pig primary cultures. Allegedly, this might be

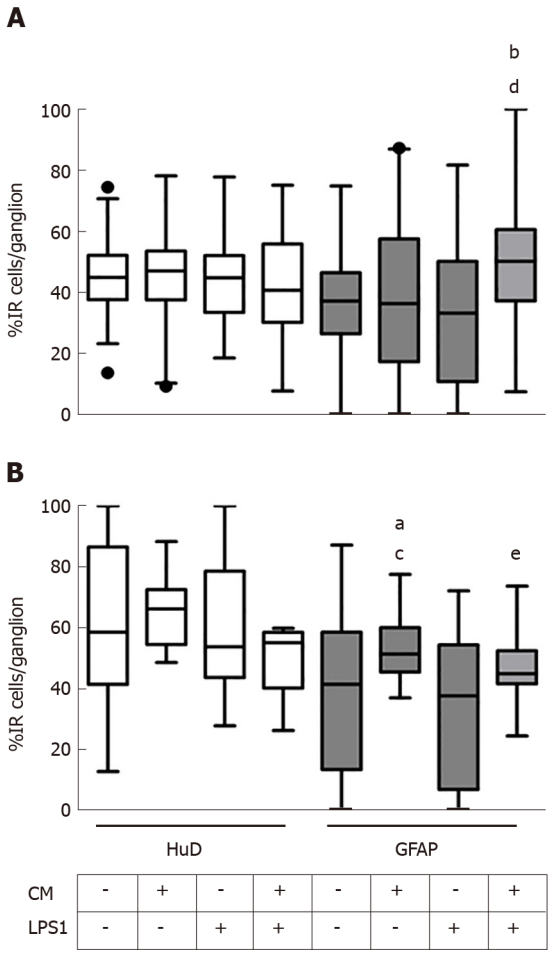

Figure 4 Effect of porcine vascular wall mesenchymal stromal cells supernatants on the number of neurons (left white bars) and glial cells (gray right bars) exposed to lipopolysaccharide 1 μg/mL. A: The number of neurons in guinea pig enteric ganglia did not change significantly upon any of the treatment tested, whereas co-treatment with conditioned medium (CM) and lipopolysaccharide 1 μg/mL (LPS1) (CM+LPS1) increased the number of glial cells compared to control (CTRL) and LPS1-treated ganglia (+13.9%, $^{b}P < 0.001$; +16.5%, $^{d}P < 0.01$, respectively); B: The number of neurons in pig enteric ganglia did not change as a result of any of the treatment tested. Conversely glial cell number was higher in the CM group compared to control (+13.6%, $^{a}P < 0.05$) and LPS1 (+20.2%, $^{c}P < 0.05$). CM+LPS1 co-treatment increased the number of glial cells compared to LPS1-treated ganglia (+14.2, $^{e}P < 0.05$). LPS1: Lipopolysaccharide 1 μg/mL; CM: Conditioned medium. GFAP: Glial fibrillary acidic protein.

due to the species correspondence of porcine enteric glia with pVW-MSCs, which would reflect the phylogenetic differences previously reported in signaling modalities for MSC immunomodulation[39]. Indeed, in humans, non-human primates and pigs, immunomodulation is a mechanism dependent by indoleamine 2,3-dioxygenase secretion whereas in rodents the same mechanism is associated with inducible nitric oxide synthase expression and nitric oxide production[21,39]. Whether the observed increase in number and shape of glial cells should be associated with a compensative/therapeutic rather than a noxious *stimulus* should be addressed by further investigations on cytokine expression patterns. In this sense, an exhaustive characterization of molecular mechanisms activated by MSC-derived bioactive molecules was beyond the scope of our analysis.

Taken together, these lines of evidence suggest an effect of pVW-MSCs mediators on glial cells promoting neuronal remodeling and confirm the paramount role of this cell type in modulating immune-mediated changes of the ENS. A further characterization of the type of glial cells involved in these changes is warranted. Moreover, the observed interspecies differences should be taken into consideration in future investigations of immune-mediated response to MSCs secretome in rodents models.

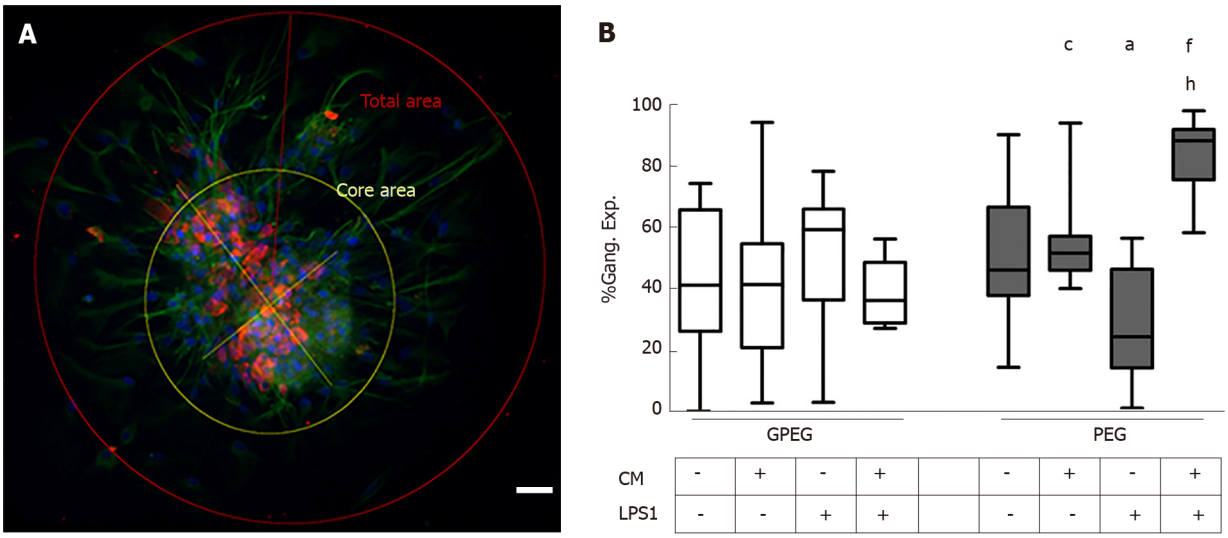

Figure 5 Effect of porcine vascular wall mesenchymal stromal cells supernatants on ganglion expansion. A: Representative photo of the morphometric analysis performed to compare glial cells processes elongating from ganglion's cores under different experimental conditions (scale bar: 100 μm); B: Relative area occupied by glial processes of guinea pig (left, gray bars) and pig enteric ganglia (right white bars). Guinea pig enteric ganglia did not show any significant difference between the different treatment groups. Conversely, pig enteric ganglia were more subjected to morphological changes: There was a decrease of the expanded area in the group treated with lipopolysaccharide 1 μg/mL (LPS1) compared to control (-42.88%, $^{a}P < 0.05$). Moreover, conditioned medium (CM) derived by porcine vascular wall mesenchymal stromal cells evoked a higher protrusion of glial processes than LPS1 alone (+36.8%, $^{c}P < 0.05$) which was remarkably higher in combination with LPS1 (CM+LPS1, +43.2% *vs* CTRL, $^{f}P < 0.01$; +60.9% *vs* LPS1, $^{h}P < 0.01$). LPS1: Lipopolysaccharide 1 μg/mL; CM: Conditioned medium; GPEG: Guinea pig enteric ganglia; PEG: Pig enteric ganglia.

ARTICLE HIGHLIGHTS

Research background

There is growing interest on mesenchymal stromal cells (MSC) as a novel therapeutic strategy to treat auto-immune and inflammatory diseases. However, identifying optimal MSC sources and limited reliability of current experimental models still represent a challenge in this field. Pigs represent more closely human physiology and an accessible resource for *ex vivo* procedures. Recently, our group isolated a population of pericytes from porcine aortic wall with an MSC profile, currently cited as porcine vascular wall-MSC (pVW-MSC).

Research motivation

Inflammatory bowel diseases (IBDs), comprising the two major forms ulcerative colitis and Crohn's disease, are characterized by an aberrant immune response leading to severe damage of the intestinal wall and functioning. Current trials are evaluating the application of cell-based therapies for the treatment of IBDs. The present study describes the effect of pVW-MSC-conditioned medium (CM) on enteric ganglia in two *ex vivo* models of IBDs in order to investigate a potential development of MSC-based treatment of IBDs.

Research objective

To evaluate the effect of pVW-MSC secretome on survival and differentiation of enteric ganglionic cells isolated by guinea pigs (GPEG) and pigs (PEG) and exposed to lipopolysaccharide (LPS).

Research methods

The expression of standard MSC markers in pVW-MSC were assessed by flow cytometry. Increasing concentration of LPS were tested in both GPEG and PEG cultures. CM derived by pVW-MSC cultures were added alone or in combination with 1μg of LPS in GPEG and PEG cultures. Ganglionic cells were double-stained with antibodies directed to the pan-neuronal marker, HuD and the glial fibrillary acidic protein, GFAP. Cell count and morphometric analysis were performed to determine changes of neuronal and glial population.

Research results

Guinea-pig neurons and glial cells decreased and increased respectively in response to high concentrations of LPS. These changes were not observed in pig primary cultures. pVW-MSC secretome increased the number and differentiation of glial cells compared to neurons with a more pronounced effect in PEG and in combination with LPS.

Research conclusions

These data showed a higher resilience of pig enteric ganglia to the main bacterial product LPS compared to guinea pig and a higher responsiveness of glial cells to pVW-MSC secreted mediators.

Research perspectives

Neuro-immune changes induced by pVW-MSC represent an essential aspect in the development of cell-based therapies. Further studies are warranted to investigate inter-species differences of pVW-MSC secretome.

ACKNOWLEDGEMENTS

Professor Patrizia Hrelia (Department of Pharmacology and Biotechnology, University of Bologna) kindly provided access to the imaging facility (Zeiss Imager M1 microscope and AxioVision software). Doctor Alberto Elmi kindly gave his support for the statistical analysis. Doctor Giulio Bassi gave his excellent support for flowcytometry analysis.

REFERENCES

1 **Baumgart DC**, Carding SR. Inflammatory bowel disease: Cause and immunobiology. *Lancet* 2007; **369**: 1627-1640 [PMID: 17499605 DOI: 10.1016/S0140-6736(07)60750-8]
2 **Salim SY**, Söderholm JD. Importance of disrupted intestinal barrier in inflammatory bowel diseases. *Inflamm Bowel Dis* 2011; **17**: 362-381 [PMID: 20725949 DOI: 10.1002/ibd.21403]
3 **Cleynen I**, Vermeire S. The genetic architecture of inflammatory bowel disease: Past, present and future. *Curr Opin Gastroenterol* 2015; **31**: 456-463 [PMID: 26444824 DOI: 10.1097/MOG.0000000000000215]
4 **Vasina V**, Barbara G, Talamonti L, Stanghellini V, Corinaldesi R, Tonini M, De Ponti F, De Giorgio R. Enteric neuroplasticity evoked by inflammation. *Auton Neurosci* 2006; **126-127**: 264-272 [PMID: 16624634 DOI: 10.1016/j.autneu.2006.02.025]
5 **Sherman LS**, Shaker M, Mariotti V, Rameshwar P. Mesenchymal stromal/stem cells in drug therapy: New perspective. *Cytotherapy* 2017; **19**: 19-27 [PMID: 27765601 DOI: 10.1016/j.jcyt.2016.09.007]
6 **Ma S**, Xie N, Li W, Yuan B, Shi Y, Wang Y. Immunobiology of mesenchymal stem cells. *Cell Death Differ* 2014; **21**: 216-225 [PMID: 24185619 DOI: 10.1038/cdd.2013.158]
7 **Waterman RS**, Tomchuck SL, Henkle SL, Betancourt AM. A new mesenchymal stem cell (MSC) paradigm: Polarization into a pro-inflammatory MSC1 or an Immunosuppressive MSC2 phenotype. *PLoS One* 2010; **5**: e10088 [PMID: 20436665 DOI: 10.1371/journal.pone.0010088]
8 **Rashedi I**, Gómez-Aristizábal A, Wang XH, Viswanathan S, Keating A. TLR3 or TLR4 Activation Enhances Mesenchymal Stromal Cell-Mediated Treg Induction via Notch Signaling. *Stem Cells* 2017; **35**: 265-275 [PMID: 27571579 DOI: 10.1002/stem.2485]
9 **Najar M**, Krayem M, Meuleman N, Bron D, Lagneaux L. Mesenchymal Stromal Cells and Toll-Like Receptor Priming: A Critical Review. *Immune Netw* 2017; **17**: 89-102 [PMID: 28458620 DOI: 10.4110/in.2017.17.2.89]
10 **Rafei M**, Campeau PM, Aguilar-Mahecha A, Buchanan M, Williams P, Birman E, Yuan S, Young YK, Boivin MN, Forner K, Basik M, Galipeau J. Mesenchymal stromal cells ameliorate experimental autoimmune encephalomyelitis by inhibiting CD4 Th17 T cells in a CC chemokine ligand 2-dependent manner. *J Immunol* 2009; **182**: 5994-6002 [PMID: 19414750 DOI: 10.4049/jimmunol.0803962]
11 **UCSF Clinical Trials**. Evaluation of PROCHYMAL® for Treatment-refractory Moderate-to-severe Crohn's Disease [accessed 2019 Feb 28]. Available from: https://clinicaltrials.ucsf.edu/trial/NCT01233960
12 **European Medicines Agency**. Summary of Opinion (initial authorisation) -Alofisel [Internet], 2017 [cited 2018 Jan 17]. Available from: http://www.ema.europa.eu/docs/en_GB/document_library/Summary_of_opinion_-_Initial_authorisation/human/004258/WC500240363.pdf
13 **Karp JM**, Leng Teo GS. Mesenchymal stem cell homing: The devil is in the details. *Cell Stem Cell* 2009; **4**: 206-216 [PMID: 19265660 DOI: 10.1016/j.stem.2009.02.001]
14 **Watanabe S**, Arimura Y, Nagaishi K, Isshiki H, Onodera K, Nasuno M, Yamashita K, Idogawa M, Naishiro Y, Murata M, Adachi Y, Fujimiya M, Imai K, Shinomura Y. Conditioned mesenchymal stem cells produce pleiotropic gut trophic factors. *J Gastroenterol* 2014; **49**: 270-282 [PMID: 24217964 DOI: 10.1007/s00535-013-0901-3]
15 **Harting MT**, Srivastava AK, Zhaorigetu S, Bair H, Prabhakara KS, Toledano Furman NE, Vykoukal JV, Ruppert KA, Cox CS, Olson SD. Inflammation-Stimulated Mesenchymal Stromal Cell-Derived Extracellular Vesicles Attenuate Inflammation. *Stem Cells* 2018; **36**: 79-90 [PMID: 29076623 DOI: 10.1002/stem.2730]
16 **Eirin A**, Zhu XY, Puranik AS, Tang H, McGurren KA, van Wijnen AJ, Lerman A, Lerman LO. Mesenchymal stem cell-derived extracellular vesicles attenuate kidney inflammation. *Kidney Int* 2017; **92**: 114-124 [PMID: 28242034 DOI: 10.1016/j.kint.2016.12.023]
17 **Börger V**, Bremer M, Ferrer-Tur R, Gockeln L, Stambouli O, Becic A, Giebel B. Mesenchymal Stem/Stromal Cell-Derived Extracellular Vesicles and Their Potential as Novel Immunomodulatory Therapeutic Agents. *Int J Mol Sci* 2017; 18 [PMID: 28684664 DOI: 10.3390/ijms18071450]
18 **Dominici M**, Le Blanc K, Mueller I, Slaper-Cortenbach I, Marini F, Krause D, Deans R, Keating A, Prockop Dj, Horwitz E. Minimal criteria for defining multipotent mesenchymal stromal cells. The International Society for Cellular Therapy position statement. *Cytotherapy* 2006; **8**: 315-317 [PMID: 16923606 DOI: 10.1080/14653240600855905]
19 **Zaniboni A**, Bernardini C, Alessandri M, Mangano C, Zannoni A, Bianchi F, Sarli G, Calzà L, Bacci ML, Forni M. Cells derived from porcine aorta tunica media show mesenchymal stromal-like cell properties in in vitro culture. *Am J Physiol Cell Physiol* 2014; **306**: C322-C333 [PMID: 24304832 DOI: 10.1152/ajpcell.00112.2013]
20 **Nesci S**, Bernardini C, Salaroli R, Zannoni A, Trombetti F, Ventrella V, Pagliarani A, Forni M. Characterization of metabolic profiles and lipopolysaccharide effects on porcine vascular wall mesenchymal stem cells. *J Cell Physiol* 2019 [PMID: 30825197 DOI: 10.1002/jcp.28429]

21 **Bernardini C**, Bertocchi M, Zannoni A, Salaroli R, Tubon I, Dothel G, Fernandez M, Bacci ML, Calzà L, Forni M. Constitutive and LPS-stimulated secretome of porcine Vascular Wall-Mesenchymal Stem Cells exerts effects on in vitro endothelial angiogenesis. *Bmc Vet Res* 2019; **15**: 123 [PMID: 31029157 DOI: 10.1186/s12917-019-1873-1]

22 **Su J**, Chen X, Huang Y, Li W, Li J, Cao K, Cao G, Zhang L, Li F, Roberts AI, Kang H, Yu P, Ren G, Ji W, Wang Y, Shi Y. Phylogenetic distinction of iNOS and IDO function in mesenchymal stem cell-mediated immunosuppression in mammalian species. *Cell Death Differ* 2014; **21**: 388-396 [PMID: 24162664 DOI: 10.1038/cdd.2013.149]

23 **Russell WMS**, Burch RL. The Principles of Humane Experimental Technique, 1959. Available from: http://altweb.jhsph.edu/pubs/books/humane_exp/het-toc

24 **Romagnoli N**, Ventrella D, Giunti M, Dondi F, Sorrentino NC, Fraldi A, Surace EM, Bacci ML. Access to cerebrospinal fluid in piglets via the cisterna magna: Optimization and description of the technique. *Lab Anim* 2014; **48**: 345-348 [PMID: 24968696 DOI: 10.1177/0023677214540881]

25 **Kugler EM**, Mazzuoli G, Demir IE, Ceyhan GO, Zeller F, Schemann M. Activity of protease-activated receptors in primary cultured human myenteric neurons. *Front Neurosci* 2012; **6**: 133 [PMID: 22988431 DOI: 10.3389/fnins.2012.00133]

26 **Schäfer KH**, Saffrey MJ, Burnstock G, Mestres-Ventura P. A new method for the isolation of myenteric plexus from the newborn rat gastrointestinal tract. *Brain Res Brain Res Protoc* 1997; **1**: 109-113 [PMID: 9385071 DOI: 10.1016/S1385-299X(96)00017-7]

27 **Zaniboni A**, Bernardini C, Bertocchi M, Zannoni A, Bianchi F, Avallone G, Mangano C, Sarli G, Calzà L, Bacci ML, Forni M. In vitro differentiation of porcine aortic vascular precursor cells to endothelial and vascular smooth muscle cells. *Am J Physiol Cell Physiol* 2015; **309**: C320-C331 [PMID: 26135800 DOI: 10.1152/ajpcell.00049.2015]

28 **Kim HJ**, Shaker MR, Cho B, Cho HM, Kim H, Kim JY, Sun W. Dynamin-related protein 1 controls the migration and neuronal differentiation of subventricular zone-derived neural progenitor cells. *Sci Rep* 2015; **5**: 15962 [PMID: 26514444 DOI: 10.1038/srep15962]

29 **di Giancamillo A**, Vitari F, Bosi G, Savoini G, Domeneghini C. The chemical code of porcine enteric neurons and the number of enteric glial cells are altered by dietary probiotics. *Neurogastroenterol Motil* 2010; **22**: e271-e278 [PMID: 20524986 DOI: 10.1111/j.1365-2982.2010.01529.x]

30 **Gabella G**, Trigg P. Size of neurons and glial cells in the enteric ganglia of mice, guinea-pigs, rabbits and sheep. *J Neurocytol* 1984; **13**: 49-71 [PMID: 6707713 DOI: 10.1007/BF01148318]

31 **Ippolito C**, Segnani C, De Giorgio R, Blandizzi C, Mattii L, Castagna M, Moscato S, Dolfi A, Bernardini N. Quantitative evaluation of myenteric ganglion cells in normal human left colon: Implications for histopathological analysis. *Cell Tissue Res* 2009; **336**: 191-201 [PMID: 19322590 DOI: 10.1007/s00441-009-0770-5]

32 **Schuster A**, Klotz M, Schwab T, Di Liddo R, Bertalot T, Schrenk S, Martin M, Nguyen TD, Nguyen TN, Gries M, Faßbender K, Conconi MT, Parnigotto PP, Schäfer KH. Maintenance of the enteric stem cell niche by bacterial lipopolysaccharides? Evidence and perspectives. *J Cell Mol Med* 2014; **18**: 1429-1443 [PMID: 24780093 DOI: 10.1111/jcmm.12292]

33 **Chiang CE**, Luk HN, Wang TM. Swelling-activated chloride current is activated in guinea pig cardiomyocytes from endotoxic shock. *Cardiovasc Res* 2004; **62**: 96-104 [PMID: 15023556 DOI: 10.1016/j.cardiores.2004.01.007]

34 **Forni M**, Mazzola S, Ribeiro LA, Pirrone F, Zannoni A, Bernardini C, Bacci ML, Albertini M. Expression of endothelin-1 system in a pig model of endotoxic shock. *Regul Pept* 2005; **131**: 89-96 [PMID: 16043243 DOI: 10.1016/j.regpep.2005.07.001]

35 **Sakuma R**, Kawahara M, Nakano-Doi A, Takahashi A, Tanaka Y, Narita A, Kuwahara-Otani S, Hayakawa T, Yagi H, Matsuyama T, Nakagomi T. Brain pericytes serve as microglia-generating multipotent vascular stem cells following ischemic stroke. *J Neuroinflammation* 2016; **13**: 57 [PMID: 26952098 DOI: 10.1186/s12974-016-0523-9]

36 **Barón M**, Gallego A. The relation of the microglia with the pericytes in the cat cerebral cortex. *Z Zellforsch Mikrosk Anat* 1972; **128**: 42-57 [PMID: 4336601 DOI: 10.1007/BF00306887]

37 **Oppliger B**, Joerger-Messerli MS, Simillion C, Mueller M, Surbek DV, Schoeberlein A. Mesenchymal stromal cells from umbilical cord Wharton's jelly trigger oligodendroglial differentiation in neural progenitor cells through cell-to-cell contact. *Cytotherapy* 2017; **19**: 829-838 [PMID: 28457739 DOI: 10.1016/j.jcyt.2017.03.075]

38 **Drommelschmidt K**, Serdar M, Bendix I, Herz J, Bertling F, Prager S, Keller M, Ludwig AK, Duhan V, Radtke S, de Miroschedji K, Horn PA, van de Looij Y, Giebel B, Felderhoff-Müser U. Mesenchymal stem cell-derived extracellular vesicles ameliorate inflammation-induced preterm brain injury. *Brain Behav Immun* 2017; **60**: 220-232 [PMID: 27847282 DOI: 10.1016/j.bbi.2016.11.011]

39 **Ren G**, Su J, Zhang L, Zhao X, Ling W, L'huillie A, Zhang J, Lu Y, Roberts AI, Ji W, Zhang H, Rabson AB, Shi Y. Species variation in the mechanisms of mesenchymal stem cell-mediated immunosuppression. *Stem Cells* 2009; **27**: 1954-1962 [PMID: 19544427 DOI: 10.1002/stem.118]

World Journal of Gastroenterology

Submit a Manuscript: https://www.f6publishing.com

World J Gastroenterol 2019 September 7; 25(33): 4904-4920

DOI: 10.3748/wjg.v25.i33.4904

ISSN 1007-9327 (print) ISSN 2219-2840 (online)

ORIGINAL ARTICLE

Basic Study

Towards a standard diet-induced and biopsy-confirmed mouse model of non-alcoholic steatohepatitis: Impact of dietary fat source

Michelle L Boland, Denise Oró, Kirstine S Tølbøl, Sebastian T Thrane, Jens Christian Nielsen, Taylor S Cohen, David E Tabor, Fiona Fernandes, Andrey Tovchigrechko, Sanne S Veidal, Paul Warrener, Bret R Sellman, Jacob Jelsing, Michael Feigh, Niels Vrang, James L Trevaskis, Henrik H Hansen

ORCID number: Michelle L Boland (0000-0002-9920-2088); Denise Oró (0000-0001-5255-3692); Kirstine S Tølbøl (0000-0001-6817-7441); Sebastian T Thrane (0000-0002-4802-8665); Jens Christian Nielsen (0000-0002-6522-9987); Taylor S Cohen (0000-0001-9368-0903); David E Tabor (0000-0002-8016-9281); Fiona Fernandes (0000-0003-3117-5543); Andrey Tovchigrechko (0000-0002-0959-4429); Sanne S Veidal (0000-0003-1240-2034); Paul Warrener (0000-0001-8597-7029); Bret R Sellman (0000-0002-1172-8799); Jacob Jelsing (0000-0002-4583-1022); Michael Feigh (0000-0001-5274-8799); Niels Vrang (0000-0002-7203-9532); James L Trevaskis (0000-0002-5356 -6118); Henrik H Hansen (0000-0002-3732-0281).

Author contributions: Boland ML, Cohen TS, Warrener P, Sellman BR, Feigh M, Vrang N, Trevaskis JL, and Hansen HH designed and coordinated the study; Boland ML, Oró D, Tølbøl KS, Thrane ST, Nielsen JC, Tabor DE, and Fernandes F performed the experiments, acquired and analyzed data; Boland ML, Cohen TS, Tabor DE, Fernandes F, Oró D, Tølbøl KS, Thrane ST, Nielsen JC, Tovchigrechko A, Veidal SS, Feigh M, Jelsing J, Vrang N, Trevaskis JL, and Hansen HH interpreted the data; Boland ML, Jelsing J, Trevaskis JL, and Hansen HH wrote the manuscript; all authors approved the final version of the

Michelle L Boland, Taylor S Cohen, David E Tabor, Fiona Fernandes, Andrey Tovchigrechko, Paul Warrener, Bret R Sellman, James L Trevaskis, Cardiovascular, Renal and Metabolic Diseases, MedImmune, Gaithersburg, MD 20878, United States

Michelle L Boland, Denise Oró, Kirstine S Tølbøl, Sebastian T Thrane, Jens Christian Nielsen, Sanne S Veidal, Jacob Jelsing, Michael Feigh, Niels Vrang, Henrik H Hansen, Pharmacology, Gubra, Hørsholm DK-2970, Denmark

Corresponding author: Henrik H Hansen, PhD, Senior Scientist, Pharmacology, Gubra, Hørsholm Kongevej 11B, Hørsholm DK-2970, Denmark. hbh@gubra.dk
Telephone: +45-31-522-651

Abstract

BACKGROUND

The trans-fat containing AMLN (amylin liver non-alcoholic steatohepatitis, NASH) diet has been extensively validated in C57BL/6J mice with or without the Lep^{ob}/Lep^{ob} (*ob/ob*) mutation in the leptin gene for reliably inducing metabolic and liver histopathological changes recapitulating hallmarks of NASH. Due to a recent ban on trans-fats as food additive, there is a marked need for developing a new diet capable of promoting a compatible level of disease in *ob/ob* and C57BL/6J mice.

AIM

To develop a biopsy-confirmed mouse model of NASH based on an obesogenic diet with trans-fat substituted by saturated fat.

METHODS

Male *ob/ob* mice were fed AMLN diet or a modified AMLN diet with trans-fat (Primex shortening) substituted by equivalent amounts of palm oil [Gubra amylin NASH, (GAN) diet] for 8, 12 and 16 wk. C57BL/6J mice were fed the same diets for 28 wk. AMLN and GAN diets had similar caloric content (40% fat kcal), fructose (22%) and cholesterol (2%) level.

RESULTS

The GAN diet was more obesogenic compared to the AMLN diet and impaired glucose tolerance. Biopsy-confirmed steatosis, lobular inflammation, hepatocyte ballooning, fibrotic liver lesions and hepatic transcriptome changes were similar in *ob/ob* mice fed the GAN or AMLN diet. C57BL/6J mice developed a mild to

article.

Supported by the Innovation Fund Denmark, Tølbøl KS, No. 5016-00168B.

Institutional review board statement: The study was reviewed and approved by the Institutional Review Board at MedImmune and Gubra.

Institutional animal care and use committee statement: All animal experiments conformed to the internationally accepted principles for the care and use of laboratory animals (licence No. 2013-15-2934-00784, The Animal Experiments Inspectorate, Denmark; protocol no. MI-17-0005, The Institutional Animal Care and Use Committee at MedImmune, Gaitherburg, MD, United States).

Conflict-of-interest statement: Michelle L. Boland and James L. Trevaskis were previously employed by MedImmune, LLC. Taylor S. Cohen, David Tabor, Fiona Fernandes, Andrey Tovchigrechko, Paul Warrener, and Bret R. Sellman are employed by MedImmune LLC. All other authors have nothing to disclose.

Data sharing statement: No additional data are available.

ARRIVE guidelines statement: The authors have read the ARRIVE guidelines, and the manuscript was prepared and revised according to the ARRIVE guidelines.

Manuscript source: Unsolicited manuscript

Received: April 26, 2019
Peer-review started: April 26, 2019
First decision: May 24, 2019
Revised: June 28, 2019
Accepted: July 19, 2019
Article in press: July 19, 2019
Published online: September 7, 2019

moderate fibrotic NASH phenotype when fed the same diets.

CONCLUSION
Substitution of Primex with palm oil promotes a similar phenotype of biopsy-confirmed NASH in *ob/ob* and C57BL/6J mice, making GAN diet-induced obese mouse models suitable for characterizing novel NASH treatments.

Key words: Non-alcoholic steatohepatitis; High-fat diet; Mouse model; Histopathology; Fibrosis; Liver biopsy; Liver transcriptome

Core tip: The trans-fat containing amylin liver non-alcoholic steatohepatitis (NASH) (AMLN) diet has been extensively validated in mice for reliably inducing metabolic and liver histopathological changes recapitulating hallmarks of NASH. A recent ban on trans-fats as food additive prompted the development of a new diet with similar disease-inducing properties as the AMLN diet. Here, we introduce a trans-fat-free diet high in pal m oil (Gubra amylin NASH, GAN diet) that promotes a highly similar phenotype of biopsy-confirmed fibrotic NASH in both *ob/ob* and C57BL/6J mice, highlighting the suitability of GAN diet-induced obese mouse models of biopsy-confirmed NASH for the characterization of novel drug therapies for NASH.

Citation: Boland ML, Oró D, Tølbøl KS, Thrane ST, Nielsen JC, Cohen TS, Tabor DE, Fernandes F, Tovchigrechko A, Veidal SS, Warrener P, Sellman BR, Jelsing J, Feigh M, Vrang N, Trevaskis JL, Hansen HH. Towards a standard diet-induced and biopsy-confirmed mouse model of non-alcoholic steatohepatitis: Impact of dietary fat source. *World J Gastroenterol* 2019; 25(33): 4904-4920
URL: https://www.wjgnet.com/1007-9327/full/v25/i33/4904.htm
DOI: https://dx.doi.org/10.3748/wjg.v25.i33.4904

INTRODUCTION

Liver-related complications have in recent years become widely recognized as among the most prevalent co-morbidities in obesity and diabetes. Non-alcoholic steatohepatitis (NASH) is the most severe form of non-alcoholic fatty liver disease (NAFLD), an umbrella term for a range of medical conditions with hepatic steatosis unrelated to significant alcohol consumption, use of steatogenic medication or hereditary disorders[1]. Notably, presence of obesity, dyslipidemia and type 2 diabetes constitutes the strongest risk factors for NASH[2,3], which has led to the concept that NASH represents the hepatic manifestation of the metabolic syndrome[4,5]. Liver biopsy represents the gold standard method for diagnosing and grading of NASH[6]. In NASH, lobular inflammation and liver cell damage (hepatocyte ballooning) are mandatory histopathological features in addition to steatosis[7]. Notably, the vast majority of patients with NAFLD across the disease spectrum is asymptomatic with an unpredictable onset of NASH and with rates of fibrosis progression not linear with time. As a result, disease severity varies considerably among affected NASH patients and may progress to cirrhosis undiagnosed[8,9]. Among the various histology-based scoring systems applied, the NAFLD activity scoring (NAS) system is the most prevalent diagnostic tool for defining NASH and assess disease activity[10]. While not initially designed for the specific purpose of assessing therapeutic drug efficacy, the NAS system is now the most widely used scoring system in clinical trials for NASH.

The conspicuous clustering of obesity, diabetes and metabolic comorbidities in NASH patients underscores that overnutrition and dietary factors play an important role in the transition from mild NAFLD to manifest NASH. The pathogenesis of NASH is complex and multifactorial, implicating multiple parallel and converging signaling pathways. Current "multiple-hit" hypotheses consider several insults acting sequentially or together on a background of genetical predisposition to promote NAFLD and transition to NASH. Early pathogenic events are associated with hepatic triglyceride accumulation as result of excessive caloric intake, stimulation of hepatic *de novo* lipogenesis secondary to insulin resistance, and impaired free fatty acid clearance. Increasing triglyceride levels in hepatocytes can lead to overproduction of

P-Reviewer: Suda T, Yuan YS
S-Editor: Yan JP
L-Editor: A
E-Editor: Ma YJ

reactive lipid metabolites (lipotoxicity) that eventually override hepatic adaptive and regenerative mechanisms[11-13], triggering detrimental immune cell responses with downstream activation of resident fibrogenic myofibroblasts that produce and secrete collagens[13-15]. In the event of continuing insufficient regenerative responses, progressive extracellular matrix deposition may result in excessive fibrotic liver damage and hepatocellular cancer.

The emergence of these theories has played an important role in the development of animal models of NASH with more reproducible and robust liver histopathology. Diet-induced obese (DIO) mice fed Western diets are attractive as they recapitulate the natural history of NASH[16]. In addition, the human NAS system largely correlates with similar histopathologic lesions in these models[17], which makes obese mouse models of NASH increasingly employed in preclinical NASH research. Conventional obesogenic high-fat diets promote dyslipidemia, fatty liver, and mild-stage NASH without appreciable fibrosis in rodents[16]. Hence, additional dietary stimuli ("hits") are therefore applied to enhance the pro-fibrogenic properties of the high-fat diets employed in preclinical NASH research. Among the various dietary approaches, specific modifications in Western-type obesogenic diets have consistently been reported to promote fibrotic NASH in mice. Accordingly, C57BL/6J mice fed a high-fat/fructose diet supplemented with trans-fat and cholesterol (amylin liver NASH diet, *i.e.*, AMLN diet[18]) develop manifest NASH, characterized by steatosis, lobular inflammation and hepatocyte ballooning. Notably, a significant proportion of C57BL/6J mice fed the AMLN diet (AMLN DIO-NASH mice) develop mild to moderate fibrosis following ≥ 26 wk of feeding[18-23]. The hepatopathology is similar, but accentuated, in leptin-deficient C57BL6J-Lep^{ob}/Lep^{ob} (*ob/ob*) mice fed the AMLN diet, demonstrating a fibrotic NASH phenotype after ≥ 12 wk of feeding[22,24-26]. The two AMLN DOI models of NASH have been extensively characterized in pharmacology studies with employment of biopsy-confirmed histopathology for grading and staging of baseline liver pathology[23,24,27]. As in the clinic, DIO mouse models of NASH have unpredictable onset of disease with varying rates of progression. Consequently, any given cohort of DIO mice may represent all stages of NAFLD following long-term high-fat feeding[18,22,28,29]. This makes it imperative to control for inherently variable dynamics in NAFLD progression that could otherwise lead to misinterpretation of data obtained in longitudinal studies. Liver biopsy procedures have therefore recently been introduced to prevent bias and enable stringent within-subject analyses in both mice[18,22,23,27] and rats[30].

Addition of dietary trans-fats (also called trans-unsaturated fatty acids or trans fatty acids) has been reported to enhance the steatogenic and pro-fibrotic properties of obesogenic diets in mice, including the AMLN diet[24] and variants thereof[21,31-33]. The underlying molecular mechanisms are not fully understood, but trans-fats may likely sensitize to the hepatotoxic effects of high-fat/carbohydrate diets by increasing insulin resistance, hepatic lipogenesis and oxidative stress[24,32,34-36]. A recent FDA ban on trans-fats as food additive[37], however, has prompted the development of a non-trans-fat Western diet capable of promoting metabolic and liver histopathological changes comparable to that afforded by the AMLN diet. The present study therefore aimed to develop and characterize a compatible biopsy-confirmed obese mouse model of NASH based on an isocaloric palmitic acid-enriched diet with a nutrient composition similar to the AMLN diet.

MATERIALS AND METHODS

Animals

Male *ob/ob* and C57BL/6J (C57) mice were from Jackson Laboratory (Bar Harbor, ME, United States) or Janvier Labs (Le Genest Saint Isle, France), arrived at 5-8 wk of age and housed in a controlled environment (12 h light/dark cycle, 21 ± 2 °C, humidity 50 ± 10%). Mice were stratified and randomized to individual diet groups according to baseline body weight and had *ad libitum* access to tap water and chow (2018 Teklad Rodent Diet, Envigo, Madison, WI, United States; Altromin 1324, Brogaarden, Hoersholm, Denmark), AMLN diet (40 kcal-% fat (of these 22% trans-fat and 26% saturated fatty acids by weight), 22% fructose, 10% sucrose, 2% cholesterol; D09100301, Research Diets, New Brunswick, NJ, United States)[22,24] or Gubra amylin NASH diet [GAN diet; 40 kcal-% fat (of these 0% trans-fat and 46% saturated fatty acids by weight), 22% fructose, 10% sucrose, 2% cholesterol; D09100310, Research Diets]. Mice were fed chow, AMLN or GAN diet for 8, 12 or 16 wk (*ob/ob*) and 28 wk (C57BL/6J), respectively. The study was approved by The Institutional Animal Care and Use Committee at MedImmune (Gaitherburg, MD, United States) and The Danish Animal Experiments Inspectorate (license 2013-15-2934-00784) in accordance with

internationally accepted principles for the use of laboratory animals.

Body weight, body composition and liver fat mass

Body weight was monitored weekly. Whole-body fat mass was analyzed at week 8, 12 and 16 of the feeding period by non-invasive EchoMRI scanning using EchoMRI-900 (EchoMRI, Houston, TX, United States). During the scanning procedure, mice were placed in a restrainer for 90-120 s.

Intraperitoneal glucose tolerance test

An intraperitoneal glucose tolerance test (ipGTT) was performed in week 7 of the feeding period. Animals were fasted for 4 h prior to administration of the glucose bolus (1.5 g/kg). Cages were changed at the time of fasting. At t = 0, C57 and *ob/ob* mice received a bolus of glucose by intraperitoneal injection (5 mL/kg). Blood samples were collected from the tail vein and blood glucose was measured at time points t = 0, 15, 30, 45, 60, 90 and 120 min after the glucose bolus. Mice were re-fed after the last blood sampling.

Biochemical analyses

Biochemical analyses were performed as reported previously[22,26]. Terminal plasma samples from fed animals were assayed for alanine aminotransferase (ALT), aspartate aminotransferase (AST), total triglycerides (TG) and total cholesterol. Total liver lipid mass was determined using a Bruker LF-90 minispec system (Bruker Biospin Corporation, Billerica, MA, United States) and expressed relative (%) to total liver weight.

Liver biopsy

A separate cohort of *ob/ob* mice were fed AMLN or GAN diet for 9 wk before a liver biopsy procedure was applied as described in detail previously[22]. On the surgery day, mice were anesthetized with isoflurane (2%-3%, in 100% oxygen), a small abdominal incision in the midline was made, and the left lateral lobe of the liver was exposed. A cone-shaped wedge of liver tissue (50-100 mg) was excised from the distal part of the lobe. The cut surface of the liver was closed by electrosurgical bipolar coagulation using an electrosurgical unit (ERBE VIO 100C, ERBE, Marietta, GA, United States). The liver was returned to the abdominal cavity, the abdominal wall was sutured and skin stapled. Carprofen (5 mg/kg, i.p.) was administered at the time of surgery and at post-operative day one and two. After the procedure, animals were single-housed and kept on the respective diet for a total period of 16 wk.

Liver histology and digital image analysis

Biopsy and terminal liver samples (both from the left lateral lobe) were fixed overnight in 4% paraformaldehyde. Liver tissue was paraffin-embedded and sectioned (3 μm thickness). Sections were stained with hematoxylin-eosin (HE, Dako, Glostrup, Denmark), Picro-Sirius red (Sigma-Aldrich, Broendby, Denmark), anti-galectin-3 (cat. 125402, Biolegend, San Diego, CA, United States), or anti-type I collagen (Col1a1; cat. 1310-01, Southern Biotech, Birmingham, AL, United States) using standard procedures[22,23]. The NAS and fibrosis staging system was applied to liver pre-biopsies and terminal samples for scoring of steatosis, lobular inflammation, hepatocyte ballooning, and fibrosis outlined by Kleiner *et al*[10]. Quantitative histomorphometry was analyzed using digital imaging software (VIS Software, Visiopharm, Hørsholm, Denmark)[22,23]. Proportional (fractional) areas of liver fat (HE-staining), galectin-3 and Col1a1 were expressed relative to total sectional area. All histological assessments were performed by histologists blinded to the experimental groups.

RNA sequencing

Liver transcriptome analysis was performed by RNA sequencing on RNA extracts from terminal liver samples (15 mg fresh tissue), as described in detail elsewhere[22,23]. The RNA quantity was measured using Qubit® (Thermo Scientific, Eugene, OR, United States). The RNA quality was determined using a bioanalyzer with RNA 6000 Nano kit (Agilent, Waldbronn, Germany). RNA sequence libraries were prepared with NeoPrep (Illumina, San Diego, CA, United States) using Illumina TruSeq stranded mRNA Library kit for NeoPrep (Illumina, San Diego, CA, United States) and sequenced on the NextSeq 500 (Illumina, San Diego, CA, United States) with NSQ 500 hi-Output KT v2 (75 CYS, Illumina, San Diego, CA, United States). Reads were aligned to the GRCm38 v84 Ensembl Mus musculus genome using STAR v.2.5.2a with default parameters[38]. Differential gene expression analysis was performed with DEseq237. Genes with a Benjamini and Hochberg adjusted $P \leq 0.05$ (5% false discovery rate, FDR) were regarded as statistically significantly regulated. The

Reactome pathway database[39] was used as gene annotation in a gene set analysis using the R package PIANO v.1.18.1[40], with the Stouffer method and Benjamini-Hochberg adjusted *P* values (FDR < 0.01).

Statistical analyses

Except for RNA sequencing, data were analyzed using GraphPad Prism v7.03 software (GraphPad, La Jolla, CA, United States). All results are shown as mean ± standard error of mean. A two-way ANOVA with Tukey's multiple comparisons test was performed for body weight and quantitative histological analyses. A one-way ANOVA with Dunnett's post-hoc test was used for all other parameters. A *P* value < 0.05 was considered statistically significant.

RESULTS

Metabolic changes in ob/ob mice fed GAN or AMLN diet for up to 16 wk

The temporal progression of metabolic deficits was determined in *ob/ob* mice fed the GAN (GAN *ob/ob*-NASH) or AMLN (AMLN *ob/ob*-NASH) diet for up to 16 wk. Body weight curves were significantly different in GAN and AMLN *ob/ob*-NASH mice (overall $P < 0.001$, two-way ANOVA). Compared to the AMLN diet, the GAN diet induced greater body weight gain in *ob/ob* mice from diet week 7 and onwards (Figure 1A). Relative body weight gain over the 16-week feeding period was 141.6 ± 2.9% (GAN *ob/ob*-NASH) and 125.2 ± 3.6% (AMLN *ob/ob*-NASH). GAN-*ob/ob* mice displayed more pronounced increases in whole-body fat mass at all time points measured (Figure 1B). The GAN and AMLN diets promoted similar degree of hepatomegaly in *ob/ob* mice (Figure 1C). An ipGTT was performed in diet week 7 and demonstrated impaired glucose tolerance in GAN, but not AMLN, *ob/ob*-NASH mice compared to chow-fed C57 controls (Figure 1D and E). During the ipGTT, plasma insulin levels were equally elevated in GAN and AMLN *ob/ob*-NASH mice (Figure 1F). Plasma ALT and AST levels were significantly increased in GAN and AMLN *ob/ob*-NASH mice after 8 wk on the diet and did not change further during the 16-wk feeding period. The GAN and AMLN diets promoted a similar degree of hypercholesterolemia (diet week 8-16, $P < 0.05$) in *ob/ob* mice with slightly reduced TG levels (diet week 16, $P < 0.05$), as compared to chow-fed C57 mice (Table 1).

Terminal liver lipid levels in GAN and AMLN *ob/ob*-NASH mice were approximately 10-fold higher than that of age-matched C57 mice and were maximally elevated after 8 weeks of feeding (Table 1).

Gut microbiome changes in ob/ob mice fed GAN or AMLN diet for up to 16 wk

In addition to metabolic changes, the gut microbiome composition in GAN and AMLN *ob/ob* mice was characterized by bacterial 16S rDNA gene sequencing performed on serial fecal samples. The GAN and AMLN diets promoted similar taxonomic shifts compared to baseline (chow feeding). The structural modulation of the gut microbiota was largely manifest two weeks after the change to GAN or AMLN diet, being slightly more accentuated following 16 wk of feeding (Supplemental Figure 1). Compared to baseline, the changes in microbiome composition in GAN and AMLN *ob/ob* mice was mainly driven by increases in the relative abundance of *Akkermansia, Bacteroides* and *Parasutterella* with reciprocal decreases in *Clostridiales* and *Porphyromonadaceae*. Consistently lowered relative abundance of *Lactobacillus* was also observed in GAN *ob/ob*-NASH mice.

Biopsy-confirmed progression of liver histopathology in ob/ob mice fed GAN or AMLN diet for 16 wk

Liver histopathological changes in GAN *ob/ob* mice were assessed in *ob/ob* mice fed GAN or AMLN diet for 16 wk (n = 8-10 per group). A liver biopsy was sampled after 9 wk on the respective diet for within-subject analysis of disease progression. Representative histological stainings are shown in Figure 2A. Comparable changes in composite NAS and fibrosis scores from feeding week 9 to 16 were observed in GAN *ob/ob* and AMLN *ob/ob* mice (Figure 2B). At feeding week 9, GAN *ob/ob* and AMLN *ob/ob* mice showed mild-to-moderate fibrosis (F1-F2) with an equal distribution of mice progressing in fibrosis severity. A major proportion of GAN or AMLN diet fed *ob/ob* mice demonstrated moderate fibrosis after 16 weeks of feeding (Figure 2C). Individual pre-biopsy and terminal histopathological scores on steatosis, lobular inflammation and hepatocyte ballooning are indicated in Supplemental Figure 2. Steatosis severity was severe (score 3) and sustained after 9 weeks of feeding in both GAN and AMLN *ob/ob*-NASH mice. Both diets induced moderate-grade (score 2) lobular inflammation in almost all *ob/ob* mice without significant changes from

Table 1 Plasma and liver biomarkers in *ob/ob* mice fed amylin liver non-alcoholic steatohepatitis (AMLN) or Gubra amylin non-alcoholic steatohepatitis (GAN) diet for 8-16 wk

Group	Weeks on diet	*n*	ALT (U/L)	AST (U/L)	Plasma TG (mmol/L)	Plasma TC(mmol/L)	Liver lipid mass (% of liver weight)
Chow C57	8	6	115 ± 60	192 ± 77	1.7 ± 0.2	3.8 ± 0.2	3.5 ± 0.4
	12	6	67 ± 10	93 ± 16	1.7 ± 0.1	3.5 ± 0.1	4.9 ± 0.7
	16	6	61 ± 18	82 ± 18	2.2 ± 0.2	3.8 ± 0.3	3.6 ± 0.4
GAN *ob/ob*	8	4	913 ± 113[a]	663 ± 37[a]	1.2 ± 0.2	11.8 ± 0.9[a]	31.6 ± 1.3[a]
	12	5	959 ± 93[a]	660 ± 52[a]	1.4 ± 0.1	12.4 ± 1.3[a]	33.3 ± 0.7[a]
	16	5	868 ± 102[a]	674 ± 25[ad]	1.5 ± 0.2[a]	14.3 ± 0.8[ad]	28.4 ± 1.4[ad]
AMLN *ob/ob*	16	6	654 ± 39[a]	399 ± 23[a]	1.0 ± 0.1[a]	11.0 ± 0.4[a]	35.4 ± 0.8[ad]

[a]$P < 0.05$ *vs* corresponding feeding period in chow-fed C57BL/6J (Chow C57) mice,
[d]$P < 0.05$ *vs* corresponding feeding period in amylin liver non-alcoholic steatohepatitis (AMLN) *ob/ob* mice. TC: Total cholesterol; ALT: Alanine aminotransferase; AST: Aspartate aminotransferase; TG: Total triglycerides; AMLN: Amylin liver non-alcoholic steatohepatitis diet; GAN: Gubra amylin non-alcoholic steatohepatitis diet; NASH: Non-alcoholic steatohepatitis.

feeding week 9 to 16. The rate of hepatocyte ballooning was low in *ob/ob* mice fed the GAN or AMLN diet for 9 weeks, however, increased during the remainder of the feeding period. Hepatocyte ballooning did not progress beyond grade 1 in *ob/ob* mice. Terminal quantitative histopathological changes were also similar in *ob/ob* mice fed the GAN or AMLN diet, as indicated by morphometric analyses of steatosis, inflammation and Col1a1 (Figure 3).

Liver transcriptome changes in ob/ob mice fed AMLN or GAN diet for 16 wk

To characterize the effect of 16-week feeding on global liver gene expression, the transcriptome of GAN and AMLN *ob/ob*-NASH mice vs. chow-fed C57 mice were analyzed by RNA sequencing. To assess the overall similarity of the individual transcriptome samples, a principal component analysis (PCA) was performed. The primary PCA, accounting for the major variability in the data set, yielded conspicuous clustering of transcriptome samples from GAN and AMLN *ob/ob*-NASH mice, being clearly separated from chow-fed C57 controls (Figure 4A), indicating that the two NASH-promoting diets overall promoted substantial, however highly similar, alterations in liver global gene signatures of *ob/ob* mice. In accordance, a total pool of 9725 and 9760 differentially expressed genes (DEGs) were identified in GAN and AMLN *ob/ob*-NASH mice, respectively, with virtually all regulated genes being shared in the two *ob/ob*-NASH groups (Figure 4B). For initial evaluation of the DEGs identified, we probed for candidate gene transcripts associated with NASH and fibrosis (see Supplemental Table 1). GAN and AMLN *ob/ob*-NASH mice showed significant and overlapping regulations of candidate genes (Figure 4C), particularly associated to modulated fatty acid synthesis (*Fasn, Scd1*), reduced fatty acid β-oxidation (*Cpt-1*), lowered triglyceride synthesis (*Gpat4*), reduced cholesterol synthesis (*Hmgcr, Hmgcs1*) and transport (*ApoCIII, Ldlr, Lrp1, Scarb1*); impaired insulin (*Akt, Irs1, Irs2*) and FXR (*Cyp7a1, Cyp8b1, Ostb*) signaling; enhanced monocyte differentiation/recruitment (*Ccr1, Ccr2, Cd14, Cd68, Cd86, Il1a, Il1a, Mac-2, Mcp-1*), pro-inflammatory signaling (*Nfkb, P38, Tgfbr, Tnfa*); inflammasome (*Ipaf, Nlrp1b, Nlrp3, Tlr4)* and pro-apoptotic activity (*Casp-8, Rip-1, Rip-3*), and enhanced extracellular matrix (ECM) reorganization (a-*Sma, Col1a1, Col1a2, Col3a1, Col5a1/2/3, Col6a1/2/3, Mmp2, Mmp13, Timp1/2/3*). When performing a group-wise comparison of global gene expression profiles in GAN vs. AMLN *ob/ob* mice, liver transcriptome signatures were distinguished by only nine DEGs (*Ces3b, Cfhr1, Cyp1a1, Cyp2f2, Gm4788, Keg1, Serpina3k, Ugt1a9, Ugt2a3*). To obtain further resolution of the liver transcriptome changes in GAN and AMLN *ob/ob*-NASH mice vs. chow-fed C57 controls, a gene set enrichment analysis was subsequently conducted. The Reactome gene annotation analysis identified several disease-relevant biological pathways significantly enriched in both GAN and AMLN *ob/ob*-NASH mice. Notably, all significantly enriched pathways were completely overlapping between GAN and AMLN *ob/ob*-NASH mice (Figure 4D).

Liver histopathology in C57 mice fed GAN or AMLN diet for 28 wk

To investigate liver histological changes in wild-type mice, C57 mice were fed chow (n = 15), GAN (n = 30) or AMLN (n = 30) diet for 28 wk. Histopathological scores and proportionate area of Col1a1 are shown in Figure 5. GAN and AMLN diets were both highly obesogenic in C57 mice. GAN DIO-NASH mice showed significantly higher

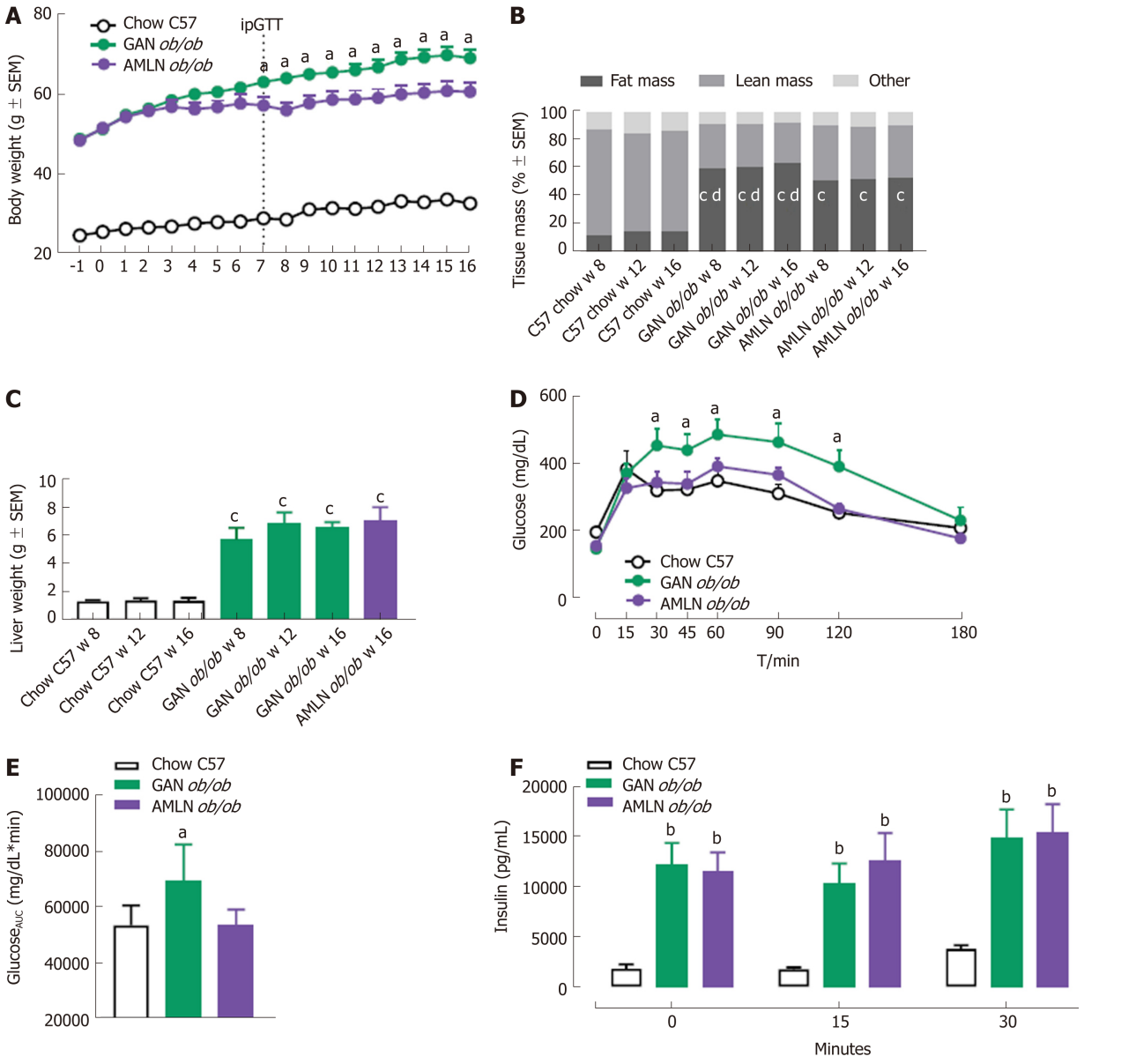

Figure 1 Metabolic parameters in *ob/ob* mice fed amylin liver non-alcoholic steatohepatitis (AMLN) or Gubra amylin non-alcoholic steatohepatitis (GAN) diet for 8-16 wk. A: Body weight; B: Body composition; C: Terminal liver weight (week 16); D: An intraperitoneal glucose tolerance test (ipGTT) was performed in week 7 of the feeding period, glucose excursion curves; E: Glucose area under the curve (AUC, 0-180 min); F: Plasma insulin (0, 15, 30 min). [a]$P < 0.05$, [b]$P < 0.01$, [c]$P < 0.001$ *vs* chow-fed C57BL/6J (Chow C57) controls; [d]$P < 0.001$ *vs* amylin liver non-alcoholic steatohepatitis (AMLN) diet (n = 5-6 mice per group). AMLN: Amylin liver non-alcoholic steatohepatitis diet; GAN: Gubra amylin non-alcoholic steatohepatitis diet; iPGTT: Intraperitoneal glucose tolerance test.

endpoint body weight (46.0 ± 0.8 g) compared to AMLN DIO-NASH (40.6 ± 0.6 g, $P < 0.001$) and chow-fed C57 mice (30.7 ± 0.4 g, $P < 0.001$ *vs* GAN DIO-NASH and AMLN-DIO NASH mice). While age-matched chow-fed C57 mice displayed normal liver histology, GAN DIO-NASH mice developed severe steatosis (score 3, 30/30 mice) and moderate-to-severe lobular inflammation (score 0, 1/30 mice; score 1, 3/30 mice; score 2, 19/30 mice; score 3, 7/30 mice) upon 28 wk of feeding (Figure 5A and B). Hepatocyte ballooning was largely absent in GAN DIO-NASH mice (score 0, 26/30 mice; score 1, 4/30 mice, Figure 5C). Generally, a NAS of 5-6 was observed in GAN DIO-NASH mice (score 3, 1/30 mice; score 4, 3/30 mice; score 5, 17/30 mice; score 6, 7/30 mice; score 7, 2/30 mice, Figure 5D). Fibrosis was typically mild to moderate in GAN DIO-NASH mice (F0, 1/30 mice; F1, 10/30 mice; F2, 18/30 mice; F3, 1/30 mice), see Figure 5E. AMLN DIO-NASH mice showed a liver histological phenotype very similar to GAN DIO-NASH mice, as indicated by severe steatosis (score 3, 30/30 mice), moderate to severe lobular inflammation (score 0, 1/30 mice; score 1, 3/30 mice; score 2, 19/30 mice; score 3, 7/30 mice), inconsistent hepatocyte ballooning (score 0, 17/30 mice; score 1, 13/30 mice), and mild-to-moderate fibrosis (F0, 3/30 mice; F1, 4/30 mice; F2, 23/30 mice; F3, 0/30 mice). In addition, Col1a1 proportionate areas were increased to a similar degree in GAN and AMLN DIO-NASH mice, as

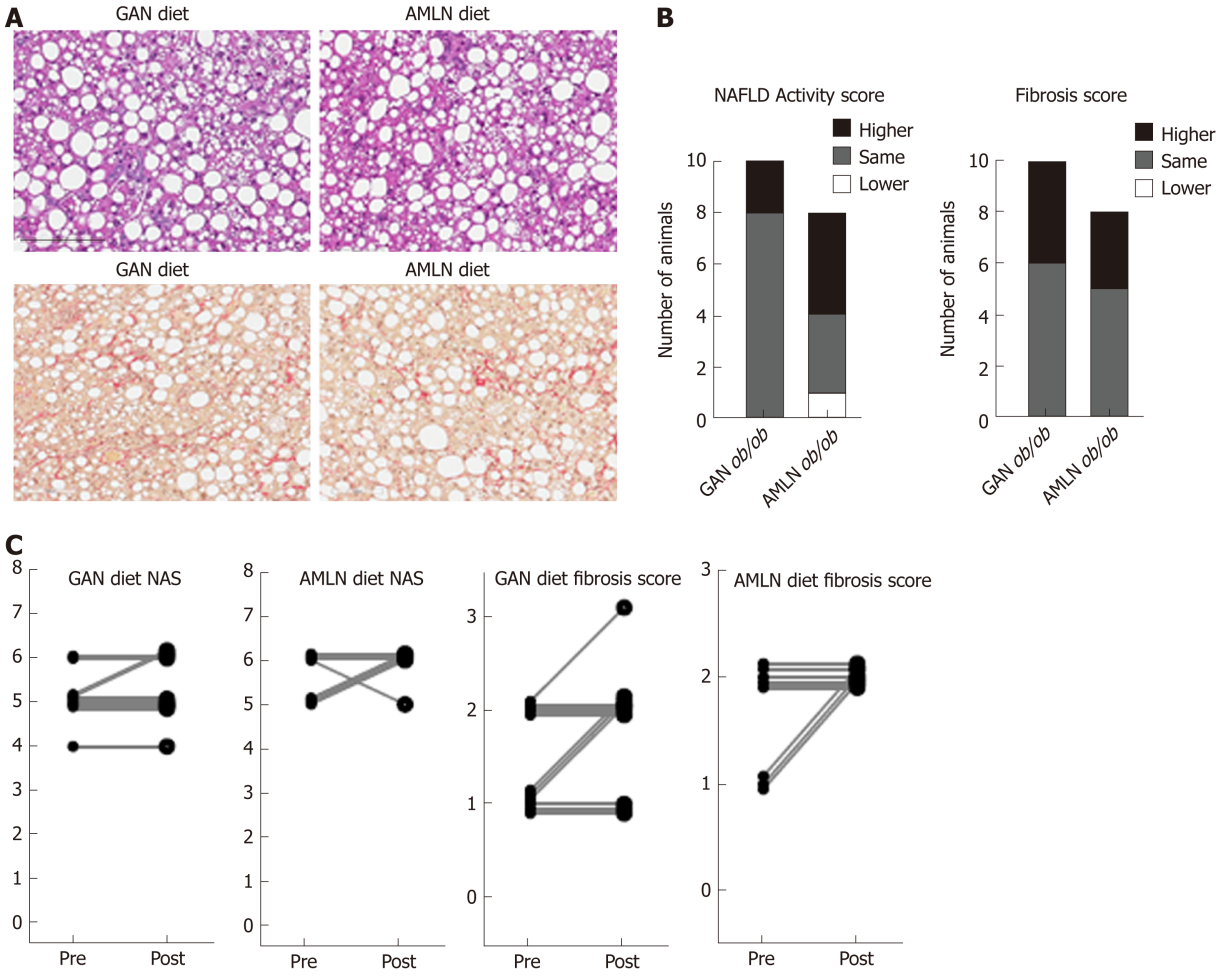

Figure 2 Liver biopsy-confirmed non-alcoholic fatty liver disease activity score and fibrosis scores in *ob/ob* mice fed amylin liver non-alcoholic steatohepatitis (AMLN) or Gubra amylin non-alcoholic steatohepatitis (GAN) diet for 16 wk. A: Representative images of terminal liver morphology (upper panel: hematoxylin-eosin staining, lower panel: Picro-Sirus red staining, 20× magnification, scale bar 100 μm); B: Number of animals with higher, same or lower post-biopsy histopathology score compared to corresponding pre-biopsy score (n = 8-10 mice per group). Left panel: Non-alcoholic fatty liver disease activity score (NAS); right panel: Fibrosis score; C: Individual pre-biopsy and terminal NAS and fibrosis scores. AMLN: Amylin liver non-alcoholic steatohepatitis diet; GAN: Gubra amylin non-alcoholic steatohepatitis diet; NAFLD: Non-alcoholic fatty liver disease; NAS: Non-alcoholic fatty liver disease activity score.

compared to chow-fed C57 mice, see Figure 5F.

DISCUSSION

The AMLN DIO-NASH and *ob/ob*-NASH mouse models have been extensively validated and characterized in an increasing number of pharmacology studies. Here, we compared the metabolic and liver histological phenotype in *ob/ob* mice fed the AMLN diet or a modified AMLN diet (GAN diet) with Primex shortening, a trans-fat containing food additive, substituted with equivalent amounts of palm oil. The GAN and AMLN diets promoted similar biopsy-confirmed liver lesions with hallmarks of fibrotic NASH in both *ob/ob* and C57 mice. Hence, the maintained NASH phenotype in both *ob/ob* and C57 mice indicates the utility of GAN DIO mouse models of biopsy-confirmed NASH for the preclinical characterization of novel drug therapies for NASH.

The composition of the AMLN diet, containing high levels of saturated fat, fructose, trans-fat and cholesterol, reflects dietary factors considered important in the pathogenesis of NAFLD/NASH. Accordingly, excess energy intake from dietary fat and simple sugars (Western diets) has been strongly linked to NAFLD/NASH[41,42]. In particular, increased consumption of saturated fats and fructose has been associated with the deleterious effects of intrahepatic lipid accumulation, enhanced lipogenesis, insulin resistance, hepatocyte oxidative stress and inflammation in NAFLD/NASH[43-47]. Although less well-characterized in NASH, *trans*-unsaturated fat consumption and dietary cholesterol may sensitize to the hepatotoxic effects of

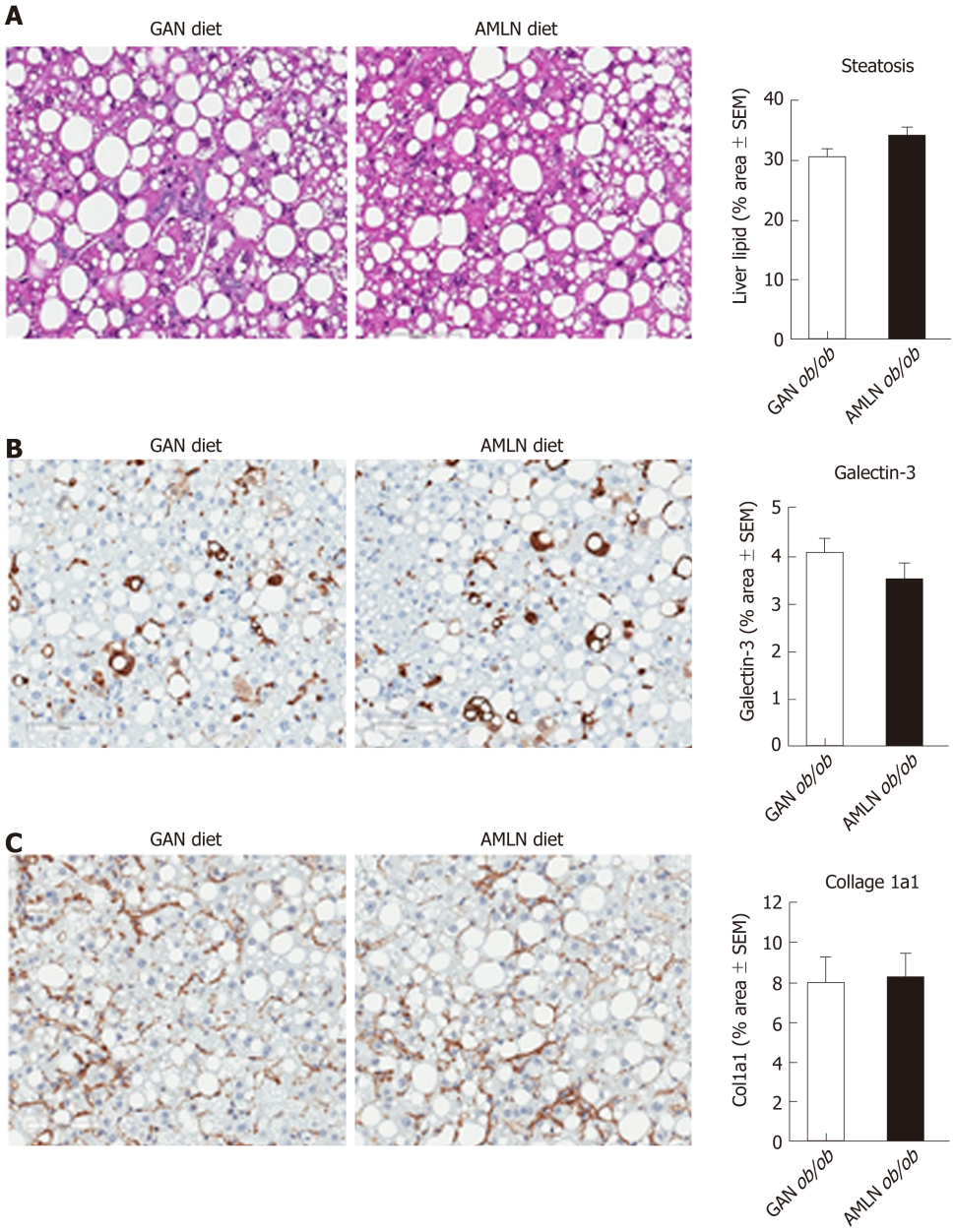

Figure 3 Quantitative histopathological changes in *ob/ob* mice fed amylin liver non-alcoholic steatohepatitis (AMLN) or Gubra amylin non-alcoholic steatohepatitis (GAN) diet for 16 wk. Fractional (%) area of steatosis (hematoxylin-eosin staining), inflammation [galectin-3 immunostaining and fibrosis (collagen-1a1) immunostaining] determined by imaging-based morphometry (n = 8-10 mice per group). A: Steatosis; Galectin-3; C: Collagen-1a1. Scale bar 100 μm. AMLN: Amylin liver non-alcoholic steatohepatitis diet; GAN: Gubra amylin non-alcoholic steatohepatitis diet; Col1a1: Collagen-1a1.

excessive fat and fructose intake[31,32,48,49]. Because the FDA has recently imposed a ban on the use of trans-fat additives in foods, this prompted us to develop a compatible mouse model of NASH based on an obesogenic diet high in saturated fat and with a nutrient composition and caloric density similar to the AMLN diet.

The GAN and AMLN diets were both highly obesogenic in *ob/ob* mice. Notably, weight gain and adiposity were even more pronounced in mice fed the GAN diet. Other high-fat/trans-fat diets have been reported inducing slightly less weight gain in wild-type mice compared to trans-fat-free hypercaloric diets[36]. Although not specifically addressed in the present study, it may be speculated that substitution of trans-fat with palm oil led to improved diet palatability and/or fat absorption rates. This is also indirectly supported by the observation that hyperphagic *ob/ob* mice fed the AMLN diet attain slightly less weight gain compared to chow feeding[22,23]. Consistent with previous reports[22,24,27], the AMLN diet did not influence glucose homeostasis in *ob/ob* mice which contrasts findings of mild glucose intolerance in obese wild-type mice fed other high-fat/trans-fat diet types[31,36,50]. The AMLN diet has been reported to elevate endogenous glucose production in C57 mice[51], suggesting development of peripheral insulin resistance. As also C57 mice fed the AMLN diet

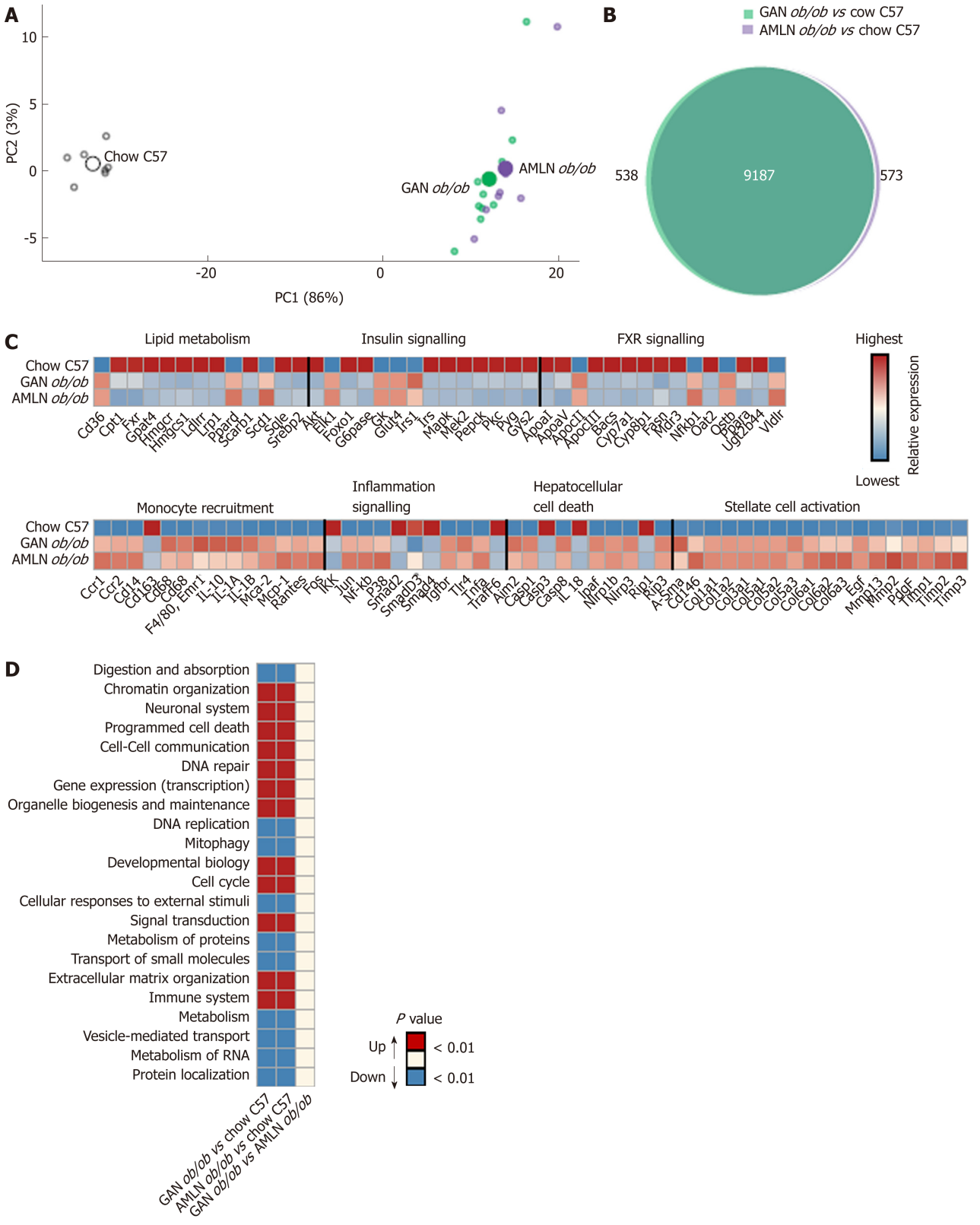

Figure 4 Liver transcriptome changes in *ob/ob* mice fed amylin liver non-alcoholic steatohepatitis (AMLN) or Gubra amylin non-alcoholic steatohepatitis (GAN) diet for 16 wk. Overview of hepatic gene expression profiles in *ob/ob* mice fed amylin liver non-alcoholic steatohepatitis (AMLN) or Gubra amylin non-alcoholic steatohepatitis (GAN) diet compared to age-matched chow-fed *ob/ob* mice (n = 8-10 mice per group). A: Principal component analysis of samples based on top 500 most variable gene expression levels; B: Group-wise comparison of total number of differentially expressed genes (false discovery rate < 0.05) between *ob/ob* mice fed AMLN or GAN diet for 16 wk *vs* chow-fed C57BL/6J (Chow C57) mice; C: Relative gene expression levels (z-scores) of differentially regulated candidate genes associated with NASH and fibrosis. In-house gene panel on candidate genes is indicated in Supplemental Table 1; D: Group-wise comparison of global liver transcriptome changes according to enrichment of individual gene sets in the Reactome pathway database. Regulated pathways are ranked according to level of statistical significance (P value). AMLN: Amylin liver non-alcoholic steatohepatitis diet; GAN: Gubra amylin non-alcoholic steatohepatitis diet; NASH: Non-alcoholic steatohepatitis.

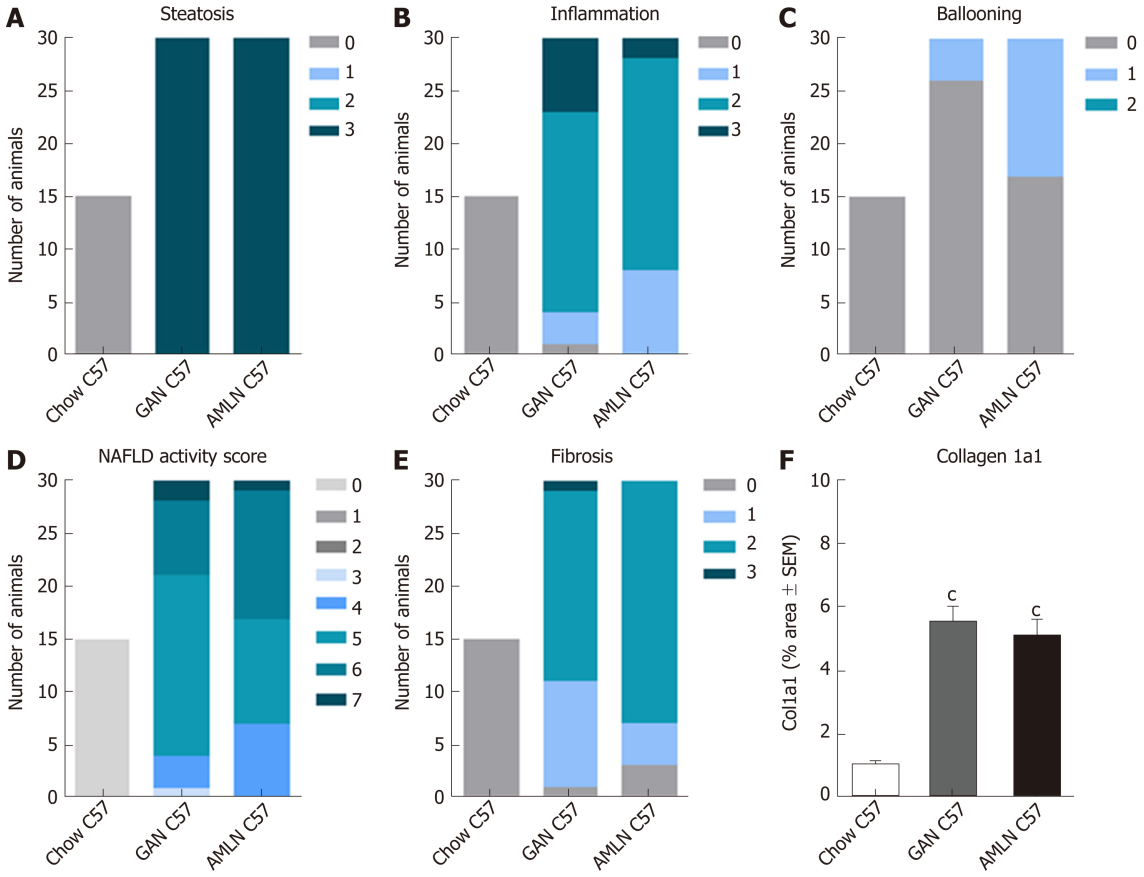

Figure 5 Liver histopathological scores and collagen 1a1 deposition in C57BL/6J mice fed chow, amylin liver non-alcoholic steatohepatitis (AMLN) or Gubra amylin non-alcoholic steatohepatitis (GAN) diet for 28 wk. A: Steatosis; B: Lobular inflammation; C: Hepatocyte ballooning; D: Non-alcoholic fatty liver disease activity score (NAS); E: Fibrosis score; F: Collagen-1a1 fractional area (mean ± SEM). $^{c}P < 0.001$ *vs* chow-fed C57BL/6J (Chow C57) mice. AMLN: Amylin liver non-alcoholic steatohepatitis diet; GAN: Gubra amylin non-alcoholic steatohepatitis diet; NASH: Non-alcoholic steatohepatitis.

maintain normal oral glucose tolerance[22,24], it may be speculated that glucoregulatory effects of trans-fats depend on the composition of trans-fat species in obesogenic diets. In contrast, GAN *ob/ob*-NASH mice displayed significantly impaired glucose tolerance compared to chow-fed C57 mice, indicating a more robust insulin-resistant phenotype in GAN *ob/ob*-NASH mice. Because insulin resistance is closely associated with NAFLD and is recognized as an important pathophysiological factor in the progression to NASH[52-54], this lends further support to the translatability of the GAN *ob/ob*-NASH mouse model. It should be noted that GAN and AMLN *ob/ob*-NASH mice both showed suppressed expression of hepatic genes related to lipid and glucose handling. This points to the possibility that extrahepatic mechanisms contribute to impaired glucose handling in GAN *ob/ob*-NASH mice. GAN and AMLN *ob/ob*-NASH mice demonstrated similarly profound hyperinsulinemia, which argues for sustained pancreatic β-cell compensation in both models. Importantly, however, glucose intolerance in leptin-deficient *ob/ob* mice has been attributed to failure to suppress hepatic glucose production in conjunction with impaired muscle glucose uptake, likely precipitated by defective triglyceride handling in these tissues[55-57]. *ob/ob* mice also demonstrate impaired glucose uptake in adipose tissues[58,59], suggesting a contributory role of adipose tissue insulin resistance. Although the present study did not specifically determine insulin sensitivity by hyperinsulinemic-euglycemic clamp techniques, the marked adipogenic properties of the GAN diet may therefore promote insulin resistance at both the hepatic and extrahepatic level to facilitate manifest glucose intolerance in GAN *ob/ob*-NASH mice.

Consistent with the obese phenotype in GAN and AMLN *ob/ob*-NASH mice, the two models demonstrated pronounced hepatomegaly and intrahepatic lipid accumulation. Development of hypercholesterolemia, but not hypertriglyceridemia, was also a shared feature in GAN and AMLN *ob/ob*-NASH mice, possibly attributed to suppressed hepatic triglyceride secretion, as high dietary cholesterol intake can downregulate hepatic cholesterol ester and lipoprotein synthesis[60,61]. This is supported by our finding of reduced expression of several hepatic genes involved in cholesterol synthesis and transport. Enhanced hepatic fat uptake combined with

impaired capacity to secrete fatty acids may thus be important mechanisms leading to marked steatosis in GAN and AMLN *ob/ob* mice. Hepatic injury was suggested by increased levels of plasma transaminases in GAN and AMLN *ob/ob* mice, subsequently confirmed by liver histology. We have previously reported that *ob/ob* mice develop reliably manifest NASH when maintained on AMLN diet for a relatively short feeding period (≥ 12 wk). The AMLN *ob/ob*-NASH model is characterized by biopsy-confirmed severe hepatic steatosis, moderate to severe lobular inflammation, mild hepatocyte ballooning and fibrotic lesions increasing in severity with prolonged feeding periods[22,24-26], recapitulating clinical histopathological criteria for the diagnosis of fibrosing NASH[7,62]. Also, the AMLN *ob/ob*-NASH model has been extensively characterized in pharmacology studies[23-25,27]. Notably, *ob/ob* mice fed the GAN and AMLN diet, respectively, developed a highly similar fibrotic NASH phenotype with comparable within-subject disease progression rates during the feeding period. Accordingly, GAN and AMLN-*ob/ob*-NASH mice demonstrated similar liver histopathology, as determined by both standard clinical histopathological scoring and imaging-based quantitative histological assessment of steatosis, inflammation and fibrosis.

The GAN and AMLN diets induced virtually identical hepatic transcriptome signatures with marked alterations in candidate genes associated with NAFLD/NASH. An unsupervised analysis for full-scale mapping and functional annotation of liver transcriptome signatures confirmed completely overlapping GAN and AMLN diet-induced hepatic signaling pathway perturbations with signatures of inefficient intrahepatic lipid and carbohydrate handling, stimulated immune cell activity, increased apoptotic activity, ECM remodeling and cell cycle modulation. In addition to suppressed transcription of genes associated with cholesterol metabolism (discussed above), a subset of genes involved in fatty acid catabolism (β-oxidation) and storage (triglyceride synthesis) were also downregulated. This could indirectly suggest free fatty acid overload and defective lipid compartmentation, which has been associated with hepatocyte cytotoxicity (lipotoxicity), inflammation and apoptosis in NASH[11-13]. Also, increased immune activity and hepatocyte damage was supported by upregulation of genes involved in monocyte differentiation /recruitment, pro-inflammatory cytokine production, inflammasome activation and pro-apoptotic signaling. The significant upregulation of a-Sma, multiple collagen isoforms (Col1a1, Col1a2, Col3a1, Col5a1/2/3, Col6a1/2/3) and molecules involved in ECM reorganization (Mmp2, Mmp13, Timp1/2/3), suggests that hepatic collagen accumulation in GAN and AMLN *ob/ob*-NASH mice is a combined effect of stimulated fibrogenesis and altered balance between the activity of collagen-degrading matrix metalloproteinases and tissue inhibitors of meta-lloproteinases.

The observation that the GAN and AMLN diets both promoted consistent fibrotic NASH in *ob/ob* mice indicates that palm oil supplementation fully compensated for the lack of trans-fat in the GAN diet. The extent of hepatic saturated fatty acid accumulation parallels disease severity in NAFLD/NASH patients[63], and inefficient disposal of saturated free fatty acids is considered hepatotoxic[64,65]. Specifically, the particularly high levels of palmitic acid in the GAN diet (37% of total fat by weight) compared to the AMLN diet (17% of total fat by weight) invites the possibility that this nutritional component played an integral role in the development and progression of liver pathology in GAN *ob/ob*-NASH mice. In support of this view, high palmitic acid (palmitate at physiological pH) levels in hepatocytes and non-parenchymal liver cells can trigger substantial lipotoxic damage through various mechanism associated with NASH pathology, including oxidative stress[66], endoplasmic reticulum stress[67], pro-apoptotic signaling[68] as well as Kupffer cell[69] and hepatic stellate cell activation[70]. In addition to direct cytotoxicity, hepatic palmitic acid overload can also promote hepatotoxic effects via increased formation palmitate-derived complex lipids, including ceramides[71]. Interestingly, long-term AMLN diet feeding has been reported to elevate hepatic levels of palmitate-containing ceramides in C57 mice, most likely due to incomplete mitochondrial fatty acid oxidation nutritional as result of nutritional overload[20].

Compared to AMLN *ob/ob*-NASH mice, longer AMLN diet feeding periods (≥ 26 wk) are required for inducing consistent fibrotic NASH in C57 mice[18,19,22,23], which is likely explained by hyperphagia-driven excessive AMLN diet intake in leptin-deficient *ob/ob*-NASH mice. A comparative study was therefore also performed in C57 mice fed the GAN or AMLN diet for 28 wk (DIO-NASH mice). Similar to *ob/ob* mice, C57 mice showed significantly greater weight gain when fed the GAN diet compared to AMLN diet. Histological assessments of biopsied liver specimens revealed highly compatible liver lesions in GAN and AMLN DIO-NASH mice. Both models presented with manifest NASH (NAS ≥ 4), characterized by severe steatosis and moderate-to-severe lobular inflammation. In GAN DIO-NASH mice, fibrosis stage was mild to moderate with significantly increased proportionate area of Col1a1 compared to

chow-fed C57 mice showing normal liver histology. Consistent with previously reported studies in AMLN DIO-NASH mice[23,72], hepatocyte ballooning was only detected in a subset of GAN and AMLN DIO-NASH mice. In addition to the GAN diet, we tested other isocaloric variants of the AMLN diet for the ability to induce a metabolic and NASH phenotype comparable to the AMLN diet. Compared to the GAN diet, *ob/ob* and C57 mice did not consistently develop fibrotic NASH when fed these diets, including diets supplemented with trans-fat from partially hydrogenated corn oil (Supplemental Table 2). As the trans-fatty acids (largely *trans*-oleic acid) in the AMLN diet are derived from partially hydrogenated soybean and palm oils, the differences in liver histopathology may therefore relate to the source of dietary fat used to prepare the partially hydrogenated vegetable oil.

We also characterized the gut microbiome composition in *ob/ob* mice fed the GAN and AMLN diet. GAN and AMLN *ob/ob*-NASH mice exhibited a similar gut microbiome signature, which further emphasizes the comparable phenotype in GAN and AMLN *ob/ob*-NASH mice. Both high-fat diets promoted sustained bacterial taxonomic shifts which were evident only two weeks after switching from chow feeding. Other high-fat diet feeding regimens have been reported to induce rapid gut microbiome structural changes in mice[73-75], suggesting that dietary fat played a major role in modulating gut bacterial communities in GAN and AMLN *ob/ob*-NASH mice. At the genus level, the microbiome signature in GAN and AMLN *ob/ob*-NASH mice was dominated by increased abundance of *Bacteroides* and *Akkermansia* paralleled by reductions in unclassified *Porphyromonadaceae*. Although various fecal microbiome profiles have been associated with NASH[76], recent studies have indicated increased *Bacteroides*[77-79] and reduced *Porphyromonadaceae*[80] abundance in NASH patients compared to healthy control subjects. *Bacteroides* have a large number and diversity of genes encoding enzymes converting complex polysaccharides to short-chain fatty acids that serve as energy substrates and signaling molecules[81,82]. Increased energy harvest from bacterial degradation of dietary polysaccharides has been suggested to contribute to adiposity in *ob/ob* mice[83]. In addition, *Bacteroides* and *Akkermansia* include prominent mucosa-degrading species[84], which have been linked to modulation of gut barrier integrity and immune responses in obesity-associated diseases, including NASH[85,86]. It should be considered that high-fat diet feeding has been reported to promote similar gut microbiome signatures in obesity-prone and obesity-resistant mice, which signifies efficient gut ecosystem adaptations to dietary changes independent of the metabolic phenotype[87]. Given the early and stable changes in dominant gut bacterial genera following the shift from chow to GAN/AMLN diet feeding, it cannot be ruled out that microbial adaptive responses secondary to altered nutrient intake played a role in shaping the gut microbiome in GAN and AMLN *ob/ob* mice.

In conclusion, modification of the AMLN diet by substitution of Primex shortening with palm oil (GAN diet) resulted in a maintained NASH phenotype in both *ob/ob* and C57 mice. The GAN diet was more obesogenic than the AMLN diet in both *ob/ob* and C57 mice and impaired glucose intolerance in *ob/ob* mice. Hence, the clear metabolic and histopathological hallmarks of NASH in *ob/ob* and C57 mice fed the GAN diet highlights the suitability of these mouse model for characterizing novel drug therapies for NASH.

ARTICLE HIGHLIGHTS

Research background

Non-alcoholic steatohepatitis (NASH) is an obesity-associated liver disease with marked unmet medical need. Various diet-induced obese animal models of NASH have been employed in preclinical research, target discovery and drug development. The trans-fat containing amylin liver NASH (AMLN) diet, high in fat, fructose and cholesterol, has been widely used in *ob/ob* and C57BL/6J mice for reliably inducing metabolic and liver histopathological changes recapitulating hallmarks of NASH.

Research motivation

A recent ban on trans-fats as food additive has prompted the development of a trans-fat free high-fat diet capable of promoting a compatible level of disease in *ob/ob* and C57BL/6J mice.

Research objectives

The present study aimed to develop and characterize a liver biopsy-confirmed obese mouse model of NASH based on an isocaloric palmitic acid-enriched diet with a nutrient composition similar to the AMLN diet.

Research methods

Male *ob/ob* mice were fed AMLN diet or a modified AMLN diet with trans-fat (Primex

shortening) substituted by equivalent amounts of palm oil [Gubra Amylin NASH, (GAN) diet] for 8, 12 and 16 wk. In addition, C57BL/6J mice were fed AMLN or GAN diet for 28 wk. AMLN and GAN diets were isocaloric (40% fat kcal; 10% sucrose, 22% fructose, 2% cholesterol). Disease phenotyping included metabolic, liver biochemical/histopathological/transcriptomics as well as gut microbiome analyses.

Research results

In *ob/ob* mice, the GAN diet was more obesogenic and adipogenic compared to the AMLN diet. Whereas the GAN diet promoted impaired oral glucose tolerance in *ob/ob* mice, the AMLN diet had no effect on glucose regulation. The GAN and AMLN diets induced similar severity of liver biopsy-confirmed steatosis, lobular inflammation, hepatocyte ballooning and fibrotic lesions. In addition, hepatic transcriptome and gut microbiome changes were similar in *ob/ob* mice fed the GAN and AMLN diet. Also, C57BL/6J mice fed the GAN and AMLN developed a similar histological phenotype of mild to moderate fibrotic NASH.

Research conclusions

Substitution of trans-fat (Primex in the AMLN diet) with saturated fat (palm oil in the GAN diet) promotes a consistent phenotype of biopsy-confirmed fibrotic NASH in both *ob/ob* and C57BL/6J mice.

Research perspectives

GAN diet-based *ob/ob* and C57BL/6J mouse models of biopsy-confirmed NASH are applicable for preclinical characterization of novel NASH treatments.

ACKNOWLEDGEMENTS

The authors would like to acknowledge Benji Gill, Stephanie Oldham (MedImmune, Gaithersburg, MD), Mikkel Christensen-Dalsgaard and Lillian Petersen (Gubra) for skillful technical assistance.

REFERENCES

1 **Bedossa P**. Current histological classification of NAFLD: Strength and limitations. *Hepatol Int* 2013; **7** Suppl 2: 765-770 [PMID: 26202292 DOI: 10.1007/s12072-013-9446-z]
2 **Angulo P**, Keach JC, Batts KP, Lindor KD. Independent predictors of liver fibrosis in patients with nonalcoholic steatohepatitis. *Hepatology* 1999; **30**: 1356-1362 [PMID: 10573511 DOI: 10.1002/hep.510300604]
3 **Ratziu V**, Giral P, Charlotte F, Bruckert E, Thibault V, Theodorou I, Khalil L, Turpin G, Opolon P, Poynard T. Liver fibrosis in overweight patients. *Gastroenterology* 2000; **118**: 1117-1123 [PMID: 10833486 DOI: 10.1016/S0016-5085(00)70364-7]
4 **Younossi ZM**, Koenig AB, Abdelatif D, Fazel Y, Henry L, Wymer M. Global epidemiology of nonalcoholic fatty liver disease-Meta-analytic assessment of prevalence, incidence, and outcomes. *Hepatology* 2016; **64**: 73-84 [PMID: 26707365 DOI: 10.1002/hep.28431]
5 **Tilg H**, Moschen AR, Roden M. NAFLD and diabetes mellitus. *Nat Rev Gastroenterol Hepatol* 2017; **14**: 32-42 [PMID: 27729660 DOI: 10.1038/nrgastro.2016.147]
6 **Bedossa P**. Diagnosis of non-alcoholic fatty liver disease/non-alcoholic steatohepatitis: Why liver biopsy is essential. *Liver Int* 2018; **38** Suppl 1: 64-66 [PMID: 29427497 DOI: 10.1111/liv.13653]
7 **Bedossa P**. Pathology of non-alcoholic fatty liver disease. *Liver Int* 2017; **37** Suppl 1: 85-89 [PMID: 28052629 DOI: 10.1111/liv.13301]
8 **McPherson S**, Hardy T, Henderson E, Burt AD, Day CP, Anstee QM. Evidence of NAFLD progression from steatosis to fibrosing-steatohepatitis using paired biopsies: Implications for prognosis and clinical management. *J Hepatol* 2015; **62**: 1148-1155 [PMID: 25477264 DOI: 10.1016/j.jhep.2014.11.034]
9 **Singh S**, Allen AM, Wang Z, Prokop LJ, Murad MH, Loomba R. Fibrosis progression in nonalcoholic fatty liver vs nonalcoholic steatohepatitis: A systematic review and meta-analysis of paired-biopsy studies. *Clin Gastroenterol Hepatol* 2015; **13**: 643-54.e1-9; quiz e39-40 [PMID: 24768810 DOI: 10.1016/j.cgh.2014.04.014]
10 **Kleiner DE**, Brunt EM, Van Natta M, Behling C, Contos MJ, Cummings OW, Ferrell LD, Liu YC, Torbenson MS, Unalp-Arida A, Yeh M, McCullough AJ, Sanyal AJ; Nonalcoholic Steatohepatitis Clinical Research Network. Design and validation of a histological scoring system for nonalcoholic fatty liver disease. *Hepatology* 2005; **41**: 1313-1321 [PMID: 15915461 DOI: 10.1002/hep.20701]
11 **Rosso N**, Chavez-Tapia NC, Tiribelli C, Bellentani S. Translational approaches: From fatty liver to non-alcoholic steatohepatitis. *World J Gastroenterol* 2014; **20**: 9038-9049 [PMID: 25083077 DOI: 10.3748/wjg.v20.i27.9038]
12 **Berlanga A**, Guiu-Jurado E, Porras JA, Auguet T. Molecular pathways in non-alcoholic fatty liver disease. *Clin Exp Gastroenterol* 2014; **7**: 221-239 [PMID: 25045276 DOI: 10.2147/CEG.S62831]
13 **Friedman SL**, Neuschwander-Tetri BA, Rinella M, Sanyal AJ. Mechanisms of NAFLD development and therapeutic strategies. *Nat Med* 2018; **24**: 908-922 [PMID: 29967350 DOI: 10.1038/s41591-018-0104-9]
14 **Tsuchida T**, Friedman SL. Mechanisms of hepatic stellate cell activation. *Nat Rev Gastroenterol Hepatol* 2017; **14**: 397-411 [PMID: 28487545 DOI: 10.1038/nrgastro.2017.38]
15 **Szabo G**, Petrasek J. Inflammasome activation and function in liver disease. *Nat Rev Gastroenterol Hepatol* 2015; **12**: 387-400 [PMID: 26055245 DOI: 10.1038/nrgastro.2015.94]
16 **Hansen HH**, Feigh M, Veidal SS, Rigbolt KT, Vrang N, Fosgerau K. Mouse models of nonalcoholic steatohepatitis in preclinical drug development. *Drug Discov Today* 2017; **22**: 1707-1718 [PMID: 28687459 DOI: 10.1016/j.drudis.2017.06.007]

17 **Liang W**, Menke AL, Driessen A, Koek GH, Lindeman JH, Stoop R, Havekes LM, Kleemann R, van den Hoek AM. Establishment of a general NAFLD scoring system for rodent models and comparison to human liver pathology. *PLoS One* 2014; **9**: e115922 [PMID: 25535951 DOI: 10.1371/journal.pone.0115922]

18 **Clapper JR**, Hendricks MD, Gu G, Wittmer C, Dolman CS, Herich J, Athanacio J, Villescaz C, Ghosh SS, Heilig JS, Lowe C, Roth JD. Diet-induced mouse model of fatty liver disease and nonalcoholic steatohepatitis reflecting clinical disease progression and methods of assessment. *Am J Physiol Gastrointest Liver Physiol* 2013; **305**: G483-G495 [PMID: 23886860 DOI: 10.1152/ajpgi.00079.2013]

19 **Ding ZM**, Xiao Y, Wu X, Zou H, Yang S, Shen Y, Xu J, Workman HC, Usborne AL, Hua H. Progression and Regression of Hepatic Lesions in a Mouse Model of NASH Induced by Dietary Intervention and Its Implications in Pharmacotherapy. *Front Pharmacol* 2018; **9**: 410 [PMID: 29765319 DOI: 10.3389/fphar.2018.00410]

20 **Patterson RE**, Kalavalapalli S, Williams CM, Nautiyal M, Mathew JT, Martinez J, Reinhard MK, McDougall DJ, Rocca JR, Yost RA, Cusi K, Garrett TJ, Sunny NE. Lipotoxicity in steatohepatitis occurs despite an increase in tricarboxylic acid cycle activity. *Am J Physiol Endocrinol Metab* 2016; **310**: E484-E494 [PMID: 26814015 DOI: 10.1152/ajpendo.00492.2015]

21 **Kawashita E**, Ishihara K, Nomoto M, Taniguchi M, Akiba S. A comparative analysis of hepatic pathological phenotypes in C57BL/6J and C57BL/6N mouse strains in non-alcoholic steatohepatitis models. *Sci Rep* 2019; **9**: 204 [PMID: 30659241 DOI: 10.1038/s41598-018-36862-7]

22 **Kristiansen MN**, Veidal SS, Rigbolt KT, Tølbøl KS, Roth JD, Jelsing J, Vrang N, Feigh M. Obese diet-induced mouse models of nonalcoholic steatohepatitis-tracking disease by liver biopsy. *World J Hepatol* 2016; **8**: 673-684 [PMID: 27326314 DOI: 10.4254/wjh.v8.i16.673]

23 **Tølbøl KS**, Kristiansen MN, Hansen HH, Veidal SS, Rigbolt KT, Gillum MP, Jelsing J, Vrang N, Feigh M. Metabolic and hepatic effects of liraglutide, obeticholic acid and elafibranor in diet-induced obese mouse models of biopsy-confirmed nonalcoholic steatohepatitis. *World J Gastroenterol* 2018; **24**: 179-194 [PMID: 29375204 DOI: 10.3748/wjg.v24.i2.179]

24 **Trevaskis JL**, Griffin PS, Wittmer C, Neuschwander-Tetri BA, Brunt EM, Dolman CS, Erickson MR, Napora J, Parkes DG, Roth JD. Glucagon-like peptide-1 receptor agonism improves metabolic, biochemical, and histopathological indices of nonalcoholic steatohepatitis in mice. *Am J Physiol Gastrointest Liver Physiol* 2012; **302**: G762-G772 [PMID: 22268099 DOI: 10.1152/ajpgi.00476.2011]

25 **Jouihan H**, Will S, Guionaud S, Boland ML, Oldham S, Ravn P, Celeste A, Trevaskis JL. Superior reductions in hepatic steatosis and fibrosis with co-administration of a glucagon-like peptide-1 receptor agonist and obeticholic acid in mice. *Mol Metab* 2017; **6**: 1360-1370 [PMID: 29107284 DOI: 10.1016/j.molmet.2017.09.001]

26 **Boland ML**, Oldham S, Boland BB, Will S, Lapointe JM, Guionaud S, Rhodes CJ, Trevaskis JL. Nonalcoholic steatohepatitis severity is defined by a failure in compensatory antioxidant capacity in the setting of mitochondrial dysfunction. *World J Gastroenterol* 2018; **24**: 1748-1765 [PMID: 29713129 DOI: 10.3748/wjg.v24.i16.1748]

27 **Roth JD**, Feigh M, Veidal SS, Fensholdt LK, Rigbolt KT, Hansen HH, Chen LC, Petitjean M, Friley W, Vrang N, Jelsing J, Young M. INT-767 improves histopathological features in a diet-induced ob/ob mouse model of biopsy-confirmed non-alcoholic steatohepatitis. *World J Gastroenterol* 2018; **24**: 195-210 [PMID: 29375205 DOI: 10.3748/wjg.v24.i2.195]

28 **Farrell GC**, Mridha AR, Yeh MM, Arsov T, Van Rooyen DM, Brooling J, Nguyen T, Heydet D, Delghingaro-Augusto V, Nolan CJ, Shackel NA, McLennan SV, Teoh NC, Larter CZ. Strain dependence of diet-induced NASH and liver fibrosis in obese mice is linked to diabetes and inflammatory phenotype. *Liver Int* 2014; **34**: 1084-1093 [PMID: 24107103 DOI: 10.1111/liv.12335]

29 **Haczeyni F**, Poekes L, Wang H, Mridha AR, Barn V, Geoffrey Haigh W, Ioannou GN, Yeh MM, Leclercq IA, Teoh NC, Farrell GC. Obeticholic acid improves adipose morphometry and inflammation and reduces steatosis in dietary but not metabolic obesity in mice. *Obesity (Silver Spring)* 2017; **25**: 155-165 [PMID: 27804232 DOI: 10.1002/oby.21701]

30 **Tølbøl KS**, Stierstorfer B, Rippmann JF, Veidal SS, Rigbolt KTG, Schönberger T, Gillum MP, Hansen HH, Vrang N, Jelsing J, Feigh M, Broermann A. Disease Progression and Pharmacological Intervention in a Nutrient-Deficient Rat Model of Nonalcoholic Steatohepatitis. *Dig Dis Sci* 2019; **64**: 1238-1256 [PMID: 30511198 DOI: 10.1007/s10620-018-5395-7]

31 **Tetri LH**, Basaranoglu M, Brunt EM, Yerian LM, Neuschwander-Tetri BA. Severe NAFLD with hepatic necroinflammatory changes in mice fed trans fats and a high-fructose corn syrup equivalent. *Am J Physiol Gastrointest Liver Physiol* 2008; **295**: G987-G995 [PMID: 18772365 DOI: 10.1152/ajpgi.90272.2008]

32 **Machado RM**, Stefano JT, Oliveira CP, Mello ES, Ferreira FD, Nunes VS, de Lima VM, Quintão EC, Catanozi S, Nakandakare ER, Lottenberg AM. Intake of trans fatty acids causes nonalcoholic steatohepatitis and reduces adipose tissue fat content. *J Nutr* 2010; **140**: 1127-1132 [PMID: 20357081 DOI: 10.3945/jn.109.117937]

33 **Obara N**, Fukushima K, Ueno Y, Wakui Y, Kimura O, Tamai K, Kakazu E, Inoue J, Kondo Y, Ogawa N, Sato K, Tsuduki T, Ishida K, Shimosegawa T. Possible involvement and the mechanisms of excess trans-fatty acid consumption in severe NAFLD in mice. *J Hepatol* 2010; **53**: 326-334 [PMID: 20462650 DOI: 10.1016/j.jhep.2010.02.029]

34 **Morinaga M**, Kon K, Saito H, Arai K, Kusama H, Uchiyama A, Yamashina S, Ikejima K, Watanabe S. Sodium 4-phenylbutyrate prevents murine dietary steatohepatitis caused by trans-fatty acid plus fructose. *J Clin Biochem Nutr* 2015; **57**: 183-191 [PMID: 26566303 DOI: 10.3164/jcbn.15-75]

35 **Ibrahim A**, Natrajan S, Ghafoorunissa R. Dietary trans-fatty acids alter adipocyte plasma membrane fatty acid composition and insulin sensitivity in rats. *Metabolism* 2005; **54**: 240-246 [PMID: 15789505 DOI: 10.1016/j.metabol.2004.08.019]

36 **Koppe SW**, Elias M, Moseley RH, Green RM. Trans fat feeding results in higher serum alanine aminotransferase and increased insulin resistance compared with a standard murine high-fat diet. *Am J Physiol Gastrointest Liver Physiol* 2009; **297**: G378-G384 [PMID: 19541924 DOI: 10.1152/ajpgi.90543.2008]

37 **US Food Drug Administration**. Final Determination Regarding Partially Hydrogenated Oils (Removing Trans Fat). 2018; Available from: https://www.federalregister.gov/documents/2018/05/21/2018-10714/final-determination-regarding-partially-hydrogenated-oils

38 **Dobin A**, Davis CA, Schlesinger F, Drenkow J, Zaleski C, Jha S, Batut P, Chaisson M, Gingeras TR. STAR: Ultrafast universal RNA-seq aligner. *Bioinformatics* 2013; **29**: 15-21 [PMID: 23104886 DOI: 10.1093/bioinformatics/bts635]

39 **Fabregat A**, Jupe S, Matthews L, Sidiropoulos K, Gillespie M, Garapati P, Haw R, Jassal B, Korninger F, May B, Milacic M, Roca CD, Rothfels K, Sevilla C, Shamovsky V, Shorser S, Varusai T, Viteri G, Weiser J, Wu G, Stein L, Hermjakob H, D'Eustachio P. The Reactome Pathway Knowledgebase. *Nucleic Acids Res* 2018; **46**: D649-D655 [PMID: 29145629 DOI: 10.1093/nar/gkx1132]

40 **Väremo L**, Nielsen J, Nookaew I. Enriching the gene set analysis of genome-wide data by incorporating directionality of gene expression and combining statistical hypotheses and methods. *Nucleic Acids Res* 2013; **41**: 4378-4391 [PMID: 23444143 DOI: 10.1093/nar/gkt111]

41 **Oddy WH**, Herbison CE, Jacoby P, Ambrosini GL, O'Sullivan TA, Ayonrinde OT, Olynyk JK, Black LJ, Beilin LJ, Mori TA, Hands BP, Adams LA. The Western dietary pattern is prospectively associated with nonalcoholic fatty liver disease in adolescence. *Am J Gastroenterol* 2013; **108**: 778-785 [PMID: 23545714 DOI: 10.1038/ajg.2013.95]

42 **Asrih M**, Jornayvaz FR. Diets and nonalcoholic fatty liver disease: The good and the bad. *Clin Nutr* 2014; **33**: 186-190 [PMID: 24262589 DOI: 10.1016/j.clnu.2013.11.003]

43 **Lim JS**, Mietus-Snyder M, Valente A, Schwarz JM, Lustig RH. The role of fructose in the pathogenesis of NAFLD and the metabolic syndrome. *Nat Rev Gastroenterol Hepatol* 2010; **7**: 251-264 [PMID: 20368739 DOI: 10.1038/nrgastro.2010.41]

44 **Alkhouri N**, Dixon LJ, Feldstein AE. Lipotoxicity in nonalcoholic fatty liver disease: Not all lipids are created equal. *Expert Rev Gastroenterol Hepatol* 2009; **3**: 445-451 [PMID: 19673631 DOI: 10.1586/egh.09.32]

45 **Abdelmalek MF**, Suzuki A, Guy C, Unalp-Arida A, Colvin R, Johnson RJ, Diehl AM; Nonalcoholic Steatohepatitis Clinical Research Network. Increased fructose consumption is associated with fibrosis severity in patients with nonalcoholic fatty liver disease. *Hepatology* 2010; **51**: 1961-1971 [PMID: 20301112 DOI: 10.1002/hep.23535]

46 **Moore JB**, Gunn PJ, Fielding BA. The role of dietary sugars and de novo lipogenesis in non-alcoholic fatty liver disease. *Nutrients* 2014; **6**: 5679-5703 [PMID: 25514388 DOI: 10.3390/nu6125679]

47 **Della Pepa G**, Vetrani C, Lombardi G, Bozzetto L, Annuzzi G, Rivellese AA. Isocaloric Dietary Changes and Non-Alcoholic Fatty Liver Disease in High Cardiometabolic Risk Individuals. *Nutrients* 2017; **9** pii: E1065 [PMID: 28954437 DOI: 10.3390/nu9101065]

48 **Walenbergh SM**, Shiri-Sverdlov R. Cholesterol is a significant risk factor for non-alcoholic steatohepatitis. *Expert Rev Gastroenterol Hepatol* 2015; **9**: 1343-1346 [PMID: 26395315 DOI: 10.1586/17474124.2015.1092382]

49 **Jeyapal S**, Putcha UK, Mullapudi VS, Ghosh S, Sakamuri A, Kona SR, Vadakattu SS, Madakasira C, Ibrahim A. Chronic consumption of fructose in combination with trans fatty acids but not with saturated fatty acids induces nonalcoholic steatohepatitis with fibrosis in rats. *Eur J Nutr* 2018; **57**: 2171-2187 [PMID: 28676973 DOI: 10.1007/s00394-017-1492-1]

50 **Zhao X**, Shen C, Zhu H, Wang C, Liu X, Sun X, Han S, Wang P, Dong Z, Ma X, Hu K, Sun A, Ge J. Trans-Fatty Acids Aggravate Obesity, Insulin Resistance and Hepatic Steatosis in C57BL/6 Mice, Possibly by Suppressing the IRS1 Dependent Pathway. *Molecules* 2016; **21**: pii: E705 [PMID: 27248994 DOI: 10.3390/molecules21060705]

51 **Kalavalapalli S**, Bril F, Guingab J, Vergara A, Garrett TJ, Sunny NE, Cusi K. Impact of exenatide on mitochondrial lipid metabolism in mice with nonalcoholic steatohepatitis. *J Endocrinol* 2019; **241**: 293-305 [PMID: 31082799 DOI: 10.1530/JOE-19-0007]

52 **Marchesini G**, Brizi M, Morselli-Labate AM, Bianchi G, Bugianesi E, McCullough AJ, Forlani G, Melchionda N. Association of nonalcoholic fatty liver disease with insulin resistance. *Am J Med* 1999; **107**: 450-455 [PMID: 10569299 DOI: 10.1016/S0002-9343(99)00271-5]

53 **Loomba R**, Abraham M, Unalp A, Wilson L, Lavine J, Doo E, Bass NM; Nonalcoholic Steatohepatitis Clinical Research Network. Association between diabetes, family history of diabetes, and risk of nonalcoholic steatohepatitis and fibrosis. *Hepatology* 2012; **56**: 943-951 [PMID: 22505194 DOI: 10.1002/hep.25772]

54 **Williams CD**, Stengel J, Asike MI, Torres DM, Shaw J, Contreras M, Landt CL, Harrison SA. Prevalence of nonalcoholic fatty liver disease and nonalcoholic steatohepatitis among a largely middle-aged population utilizing ultrasound and liver biopsy: A prospective study. *Gastroenterology* 2011; **140**: 124-131 [PMID: 20858492 DOI: 10.1053/j.gastro.2010.09.038]

55 **Haluzik M**, Colombo C, Gavrilova O, Chua S, Wolf N, Chen M, Stannard B, Dietz KR, Le Roith D, Reitman ML. Genetic background (C57BL/6J versus FVB/N) strongly influences the severity of diabetes and insulin resistance in ob/ob mice. *Endocrinology* 2004; **145**: 3258-3264 [PMID: 15059949 DOI: 10.1210/en.2004-0219]

56 **Grefhorst A**, van Dijk TH, Hammer A, van der Sluijs FH, Havinga R, Havekes LM, Romijn JA, Groot PH, Reijngoud DJ, Kuipers F. Differential effects of pharmacological liver X receptor activation on hepatic and peripheral insulin sensitivity in lean and ob/ob mice. *Am J Physiol Endocrinol Metab* 2005; **289**: E829-E838 [PMID: 15941783 DOI: 10.1152/ajpendo.00165.2005]

57 **Muurling M**, Mensink RP, Pijl H, Romijn JA, Havekes LM, Voshol PJ. Rosiglitazone improves muscle insulin sensitivity, irrespective of increased triglyceride content, in ob/ob mice. *Metabolism* 2003; **52**: 1078-1083 [PMID: 12898477 DOI: 10.1016/s0026-0495(03)00109-4]

58 **Tan SX**, Fisher-Wellman KH, Fazakerley DJ, Ng Y, Pant H, Li J, Meoli CC, Coster AC, Stöckli J, James DE. Selective insulin resistance in adipocytes. *J Biol Chem* 2015; **290**: 11337-11348 [PMID: 25720492 DOI: 10.1074/jbc.M114.623686]

59 **Jager J**, Corcelle V, Grémeaux T, Laurent K, Waget A, Pagès G, Binétruy B, Le Marchand-Brustel Y, Burcelin R, Bost F, Tanti JF. Deficiency in the extracellular signal-regulated kinase 1 (ERK1) protects leptin-deficient mice from insulin resistance without affecting obesity. *Diabetologia* 2011; **54**: 180-189 [PMID: 20953578 DOI: 10.1007/s00125-010-1944-0]

60 **Henkel J**, Coleman CD, Schraplau A, Jöhrens K, Weber D, Castro JP, Hugo M, Schulz TJ, Krämer S, Schürmann A, Püschel GP. Induction of steatohepatitis (NASH) with insulin resistance in wildtype B6 mice by a western-type diet containing soybean oil and cholesterol. *Mol Med* 2017; **23**: 70-82 [PMID: 28332698 DOI: 10.2119/molmed.2016.00203]

61 **Ma K**, Malhotra P, Soni V, Hedroug O, Annaba F, Dudeja A, Shen L, Turner JR, Khramtsova EA, Saksena S, Dudeja PK, Gill RK, Alrefai WA. Overactivation of intestinal SREBP2 in mice increases serum cholesterol. *PLoS One* 2014; **9**: e84221 [PMID: 24465397 DOI: 10.1371/journal.pone.0084221]

62 **Brown GT**, Kleiner DE. Histopathology of nonalcoholic fatty liver disease and nonalcoholic steatohepatitis. *Metabolism* 2016; **65**: 1080-1086 [PMID: 26775559 DOI: 10.1016/j.metabol.2015.11.008]

63 **Chiappini F**, Coilly A, Kadar H, Gual P, Tran A, Desterke C, Samuel D, Duclos-Vallée JC, Touboul D,

Bertrand-Michel J, Brunelle A, Guettier C, Le Naour F. Metabolism dysregulation induces a specific lipid signature of nonalcoholic steatohepatitis in patients. *Sci Rep* 2017; **7**: 46658 [PMID: 28436449 DOI: 10.1038/srep46658]

64 **Mota M**, Banini BA, Cazanave SC, Sanyal AJ. Molecular mechanisms of lipotoxicity and glucotoxicity in nonalcoholic fatty liver disease. *Metabolism* 2016; **65**: 1049-1061 [PMID: 26997538 DOI: 10.1016/j.metabol.2016.02.014]

65 **Liangpunsakul S**, Chalasani N. Lipid mediators of liver injury in nonalcoholic fatty liver disease. *Am J Physiol Gastrointest Liver Physiol* 2019; **316**: G75-G81 [PMID: 30383414 DOI: 10.1152/ajpgi.00170.2018]

66 **Zhang K**, Kim H, Fu Z, Qiu Y, Yang Z, Wang J, Zhang D, Tong X, Yin L, Li J, Wu J, Qi NR, Houten SM, Zhang R. Deficiency of the Mitochondrial NAD Kinase Causes Stress-Induced Hepatic Steatosis in Mice. *Gastroenterology* 2018; **154**: 224-237 [PMID: 28923496 DOI: 10.1053/j.gastro.2017.09.010]

67 **Wei Y**, Wang D, Topczewski F, Pagliassotti MJ. Saturated fatty acids induce endoplasmic reticulum stress and apoptosis independently of ceramide in liver cells. *Am J Physiol Endocrinol Metab* 2006; **291**: E275-E281 [PMID: 16492686 DOI: 10.1152/ajpendo.00644.2005]

68 **Cazanave SC**, Mott JL, Bronk SF, Werneburg NW, Fingas CD, Meng XW, Finnberg N, El-Deiry WS, Kaufmann SH, Gores GJ. Death receptor 5 signaling promotes hepatocyte lipoapoptosis. *J Biol Chem* 2011; **286**: 39336-39348 [PMID: 21941003 DOI: 10.1074/jbc.M111.280420]

69 **Luo W**, Xu Q, Wang Q, Wu H, Hua J. Effect of modulation of PPAR-γ activity on Kupffer cells M1/M2 polarization in the development of non-alcoholic fatty liver disease. *Sci Rep* 2017; **7**: 44612 [PMID: 28300213 DOI: 10.1038/srep44612]

70 **Hetherington AM**, Sawyez CG, Zilberman E, Stoianov AM, Robson DL, Borradaile NM. Differential Lipotoxic Effects of Palmitate and Oleate in Activated Human Hepatic Stellate Cells and Epithelial Hepatoma Cells. *Cell Physiol Biochem* 2016; **39**: 1648-1662 [PMID: 27626926 DOI: 10.1159/000447866]

71 **Hirsova P**, Ibrahim SH, Gores GJ, Malhi H. Lipotoxic lethal and sublethal stress signaling in hepatocytes: Relevance to NASH pathogenesis. *J Lipid Res* 2016; **57**: 1758-1770 [PMID: 27049024 DOI: 10.1194/jlr.R066357]

72 **Honda Y**, Imajo K, Kato T, Kessoku T, Ogawa Y, Tomeno W, Kato S, Mawatari H, Fujita K, Yoneda M, Saito S, Nakajima A. The Selective SGLT2 Inhibitor Ipragliflozin Has a Therapeutic Effect on Nonalcoholic Steatohepatitis in Mice. *PLoS One* 2016; **11**: e0146337 [PMID: 26731267 DOI: 10.1371/journal.pone.0146337]

73 **Turnbaugh PJ**, Ridaura VK, Faith JJ, Rey FE, Knight R, Gordon JI. The effect of diet on the human gut microbiome: A metagenomic analysis in humanized gnotobiotic mice. *Sci Transl Med* 2009; **1**: 6ra14 [PMID: 20368178 DOI: 10.1126/scitranslmed.3000322]

74 **Zheng X**, Huang F, Zhao A, Lei S, Zhang Y, Xie G, Chen T, Qu C, Rajani C, Dong B, Li D, Jia W. Bile acid is a significant host factor shaping the gut microbiome of diet-induced obese mice. *BMC Biol* 2017; **15**: 120 [PMID: 29241453 DOI: 10.1186/s12915-017-0462-7]

75 **Frank DN**, Bales ES, Monks J, Jackman MJ, MacLean PS, Ir D, Robertson CE, Orlicky DJ, McManaman JL. Perilipin-2 Modulates Lipid Absorption and Microbiome Responses in the Mouse Intestine. *PLoS One* 2015; **10**: e0131944 [PMID: 26147095 DOI: 10.1371/journal.pone.0131944]

76 **de Faria Ghetti F**, Oliveira DG, de Oliveira JM, de Castro Ferreira LEVV, Cesar DE, Moreira APB. Influence of gut microbiota on the development and progression of nonalcoholic steatohepatitis. *Eur J Nutr* 2018; **57**: 861-876 [PMID: 28875318 DOI: 10.1007/s00394-017-1524-x]

77 **Wong VW**, Tse CH, Lam TT, Wong GL, Chim AM, Chu WC, Yeung DK, Law PT, Kwan HS, Yu J, Sung JJ, Chan HL. Molecular characterization of the fecal microbiota in patients with nonalcoholic steatohepatitis--a longitudinal study. *PLoS One* 2013; **8**: e62885 [PMID: 23638162 DOI: 10.1371/journal.pone.0062885]

78 **Zhu L**, Baker SS, Gill C, Liu W, Alkhouri R, Baker RD, Gill SR. Characterization of gut microbiomes in nonalcoholic steatohepatitis (NASH) patients: A connection between endogenous alcohol and NASH. *Hepatology* 2013; **57**: 601-609 [PMID: 23055155 DOI: 10.1002/hep.26093]

79 **Boursier J**, Mueller O, Barret M, Machado M, Fizanne L, Araujo-Perez F, Guy CD, Seed PC, Rawls JF, David LA, Hunault G, Oberti F, Calès P, Diehl AM. The severity of nonalcoholic fatty liver disease is associated with gut dysbiosis and shift in the metabolic function of the gut microbiota. *Hepatology* 2016; **63**: 764-775 [PMID: 26600078 DOI: 10.1002/hep.28356]

80 **Da Silva HE**, Teterina A, Comelli EM, Taibi A, Arendt BM, Fischer SE, Lou W, Allard JP. Nonalcoholic fatty liver disease is associated with dysbiosis independent of body mass index and insulin resistance. *Sci Rep* 2018; **8**: 1466 [PMID: 29362454 DOI: 10.1038/s41598-018-19753-9]

81 **El Kaoutari A**, Armougom F, Gordon JI, Raoult D, Henrissat B. The abundance and variety of carbohydrate-active enzymes in the human gut microbiota. *Nat Rev Microbiol* 2013; **11**: 497-504 [PMID: 23748339 DOI: 10.1038/nrmicro3050]

82 **Koh A**, De Vadder F, Kovatcheva-Datchary P, Bäckhed F. From Dietary Fiber to Host Physiology: Short-Chain Fatty Acids as Key Bacterial Metabolites. *Cell* 2016; **165**: 1332-1345 [PMID: 27259147 DOI: 10.1016/j.cell.2016.05.041]

83 **Turnbaugh PJ**, Ley RE, Mahowald MA, Magrini V, Mardis ER, Gordon JI. An obesity-associated gut microbiome with increased capacity for energy harvest. *Nature* 2006; **444**: 1027-1031 [PMID: 17183312 DOI: 10.1038/nature05414]

84 **Donaldson GP**, Lee SM, Mazmanian SK. Gut biogeography of the bacterial microbiota. *Nat Rev Microbiol* 2016; **14**: 20-32 [PMID: 26499895 DOI: 10.1038/nrmicro3552]

85 **Miura K**, Ohnishi H. Role of gut microbiota and Toll-like receptors in nonalcoholic fatty liver disease. *World J Gastroenterol* 2014; **20**: 7381-7391 [PMID: 24966608 DOI: 10.3748/wjg.v20.i23.7381]

86 **Derrien M**, Belzer C, de Vos WM. Akkermansia muciniphila and its role in regulating host functions. *Microb Pathog* 2017; **106**: 171-181 [PMID: 26875998 DOI: 10.1016/j.micpath.2016.02.005]

87 **Hildebrandt MA**, Hoffmann C, Sherrill-Mix SA, Keilbaugh SA, Hamady M, Chen YY, Knight R, Ahima RS, Bushman F, Wu GD. High-fat diet determines the composition of the murine gut microbiome independently of obesity. *Gastroenterology* 2009; **137**: 1716-24.e1-2 [PMID: 19706296 DOI: 10.1053/j.gastro.2009.08.042]

World Journal of Gastroenterology

Submit a Manuscript: https://www.f6publishing.com

World J Gastroenterol 2019 September 7; 25(33): 4921-4932

DOI: 10.3748/wjg.v25.i33.4921

ISSN 1007-9327 (print) ISSN 2219-2840 (online)

ORIGINAL ARTICLE

Basic Study

Identification of hepatitis B virus and liver cancer bridge molecules based on functional module network

Xiao-Bing Huang, Yong-Gang He, Lu Zheng, Huan Feng, Yu-Ming Li, Hong-Yan Li, Feng-Xia Yang, Jing Li

ORCID number: Xiao-Bing Huang (0000-0001-7143-1114); Yong-Gang He (0000-0001-5714-6826); Lu Zheng (0000-0001-5714-6827); Huan Feng (0000-0001-5714-6828); Yu-Ming Li (0000-0001-5714-6830); Hong-Yan Li (0000-0001-5714-6829); Feng-Xia Yang (0000-0001-5714-6831); Jing Li (0000-0001-7143-1113).

Author contributions: Huang XB wrote the majority of the paper, performed experiments, and analyzed the data; He YG, Zheng L, Feng H, Li YM, Li HY, and Yang FX performed experiments and analyzed the data; Li J designed and coordinated the research.

Supported by the Basic and Advanced Research Projects of Chongqing, No. cstc2015jcyjA10123.

Institutional review board statement: This study was reviewed and approved by the Second Hospital Affiliated to Third Military Medical University of Xinqiao Hospital Ethics Committee.

Conflict-of-interest statement: The authors declare no conflict of interest.

Data sharing statement: No additional data are available.

Xiao-Bing Huang, Yong-Gang He, Lu Zheng, Yu-Ming Li, Hong-Yan Li, Feng-Xia Yang, Jing Li, Department of Hepatobiliary Surgery, Second Hospital Affiliated to Third Military Medical University of Xinqiao Hospital, Chongqing 400037, China

Huan Feng, Division of Nursing, Second Hospital Affiliated to Third Military Medical University, Xinqiao Hospital, Chongqing 400037, China

Corresponding author: Jing Li, MD, MSc, Attending Doctor, Doctor, Department of Hepatobiliary Surgery, Second Hospital Affiliated to Third Military Medical University of Xinqiao Hospital, Xinqiao street 183, Shapingba District, Chongqing 400037, China.
xqyylijing@tom.com
Telephone: +86-23-68755000
Fax: +86-23-68755114

Abstract

BACKGROUND

The potential role of chronic inflammation in the development of cancer has been widely recognized. However, there has been little research fully and thoroughly exploring the molecular link between hepatitis B virus (HBV) and hepatocellular carcinoma (HCC).

AIM

To elucidate the molecular links between HBV and HCC through analyzing the molecular processes of HBV-HCC using a multidimensional approach.

METHODS

First, maladjusted genes shared between HBV and HCC were identified by disease-related differentially expressed genes. Second, the protein-protein interaction network based on dysfunctional genes identified a series of dysfunctional modules and significant crosstalk between modules based on the hypergeometric test. In addition, key regulators were detected by pivot analysis. Finally, targeted drugs that have regulatory effects on diseases were predicted by modular methods and drug target information.

RESULTS

The study found that 67 genes continued to increase in the HBV-HCC process. Moreover, 366 overlapping genes in the module network participated in multiple functional blocks. It could be presumed that these genes and their interactions play an important role in the relationship between inflammation and cancer. Correspondingly, significant crosstalk constructed a module level bridge for

Manuscript source: Unsolicited manuscript

Received: April 25, 2019
Peer-review started: April 25, 2019
First decision: May 30, 2019
Revised: June 29, 2019
Accepted: July 19, 2019
Article in press: July 19, 2019
Published online: September 7, 2019

P-Reviewer: Dourakis SP, Rostami-Nejad M, Yakoot M
S-Editor: Yan JP
L-Editor: Filipodia
E-Editor: Ma YJ

HBV-HCC molecular processes. On the other hand, a series of non-coding RNAs and transcription factors that have potential pivot regulatory effects on HBV and HCC were identified. Among them, some of the regulators also had persistent disorders in the process of HBV-HCC including microRNA-192, microRNA-215, and microRNA-874, and early growth response 2, FOS, and Kruppel-like factor 4. Therefore, the study concluded that these pivots are the key bridge molecules outside the module. Last but not least, a variety of drugs that may have some potential pharmacological or toxic side effects on HBV-induced HCC were predicted, but their mechanisms still need to be further explored.

CONCLUSION
The results suggest that the persistent inflammatory environment of HBV can be utilized as an important risk factor to induce the occurrence of HCC, which is supported by molecular evidence.

Key words: Hepatitis B virus; Hepatocellular carcinoma; Molecular linkage; Transcription factors; non-coding RNA

Core tip: The potential role of chronic inflammation in the development of cancer has been widely recognized. However, the molecular link between hepatitis B virus (HBV) and hepatocellular carcinoma (HCC) has not been fully and thoroughly explored. Therefore, this study analyzed the molecular processes of HBV-HCC using a multidimensional approach to elucidate the molecular links between the two groups. The results suggest that the persistent inflammatory environment of HBV can be used as an important risk factor to induce the occurrence of HCC, which is supported by molecular evidence.

Citation: Huang XB, He YG, Zheng L, Feng H, Li YM, Li HY, Yang FX, Li J. Identification of hepatitis B virus and liver cancer bridge molecules based on functional module network. *World J Gastroenterol* 2019; 25(33): 4921-4932
URL: https://www.wjgnet.com/1007-9327/full/v25/i33/4921.htm
DOI: https://dx.doi.org/10.3748/wjg.v25.i33.4921

INTRODUCTION

Epidemiological research has shown that chronic low levels of inflammation can significantly increase the risk of cancer[1]. A series of genes including inflammatory molecules and transcription factors (TFs), adhesion molecules, AP-1, chemokines, C-reactive protein and enzymes are involved in inflammation, which have crucial impacts on inflammatory-mediated tumors[2]. In the process of chronic inflammation caused by virus infection, abnormal long-term expression of related proteins may induce physiological disorders such as oxidative stress and inflammation in tissues and organs. Thereby, a potential carcinogenic microenvironment has been formed within it, and different functions are exerted in different stages of cancer development[3]. On the other hand, the occurrence and development of tumors also affect inflammatory response processes. Many types of cancer can change the secretion levels of chemokines and inflammatory cytokines in the microenvironment, which is conducive to promoting immune escape in cancer[4,5]. Specifically, chronic hepatitis B virus (HBV) infection seriously threatens human health, which is one of the most common infectious diseases in the world, and has become a public health problem worldwide[6]. Long-term infection of HBV has the possibility of inducing liver failure, cirrhosis, and liver cancer[7]. The key mechanism is that viral DNA is integrated into the genome of host cells to alter the genetic mechanism and gene expression of host cells[8]. Studies have shown that the large surface of HBV surface antigen can induce DNA damage and polo-like kinase 1-mediated cell cycle G2/M cell division failure, which leads to unstable reproductive cycle of chromatin to drive the development of hepatocellular carcinoma (HCC)[9]. In addition, protein 4 (VSIG4) with immunoglobulin domain contains VSIG4 has poor prognosis in patients with HBV-positive HCC, but has no predictive significance in patients with HBV-negative

HCC[10]. This indicates that HBV infection not only affects the occurrence of HCC, but also affects its development, and has a negative effect on the prognosis of patients. Therefore, a systematic and in-depth understanding of the potential molecular links between HBV and HCC is essential for the exploration of the mechanism of HBV-induced HCC process and the development of targeted therapies. On the other hand, HCC is one of the most common cancers and has a higher mortality. Although the treatment of HCC has improved in the past few decades, the survival rate of patients is still very low[11]. Accumulating evidence has indicated that liver cancer is a complex disease with multiple factors and steps. In terms of risk factors, chronic persistent infection of hepatitis C virus or HBV, chronic untreated hepatitis inflammation with different etiologies, oxidative stress, and fatty liver disease may lead to the occurrence of HCC[12]. From the molecular mechanism, the increased expression of A-Raf and fatty acid 2-hydrolase (FA2H) in HCC cells leads to lipid metabolism disorder and promotes the development of cancer[13]. However, in drug sensitivity tests, overexpression of FA2H also increases the drug sensitivity of human colorectal and cervical cancer cells, while silencing FA2H makes the cells resistant to the drug[14]. Furthermore, studies have suggested that arginase 1 (ARG1) can participate in the proliferation of HBV-specific CD8 (+) T cells and regulate the occurrence of HBV[15]. At the same time, ARG1 may also promote the epithelial to mesenchymal transition process by upregulating Vimentin, N-cadherin, and beta-catenin, thus mediating the development and invasion of HCC[16]. Therefore, it is speculated that it is the key molecule in the HBV-HCC process, which needs further exploration. On the other hand, NOP7 interacts with beta-catenin to activate the inflammatory signaling pathway of beta-catenin/TCF, and its upregulation promotes the proliferation and migration of HCC cancer cells[17]. To some extent, these results indicate that HBV may mediate the occurrence and development of HCC, and guide a comprehensive and in-depth discussion on the bridge mechanism between them.

The study explored the co-imbalance bridging molecules between HBV and HCC and their potential drugs based on the dysfunction module. The results not only help to clarify the potential molecular links between HBV and HCC, but also provide biologists with abundant candidate resources for further research.

MATERIALS AND METHODS

Data resource

The National Center for Biotechnology Information Gene contains numerous published results on HBV. To systematically analyze the molecular links between HBV and HCC, 128 expression profiles of HBV-related RNA (GSE83148) and 16 microRNAs (miRNAs) (GSE33857) were collected from the Gene Expression Omnibus (http://www.ncbi.nlm.nih.gov/geo/). All of these were assessed using Affymetrix Human Genome U133 Plus 2.0 Array, including normal and disease samples. Subsequently, 424 RNA-seq data (original count) and 850 miRNA expression profile data of HCC-related genes were collected from The Cancer Genome Atlas (TCGA) database.

Identification of differentially expressed genes

In this study, differences in the expression of RNA and miRNAs in both disease and normal samples were calculated using the R-language limma package. For chip data, we first used the background correct function for background correction and standardization. Then the control probes and low-expression probes were filtered out to obtain high-quality standardized data based on the quantile normalization method of normalizing Between Array function. For RNA-seq gene expression data, the voom function was utilized to standardize reads counts. Finally, these standardized chips and RNA-seq data were analyzed by using lmFit and eBayes functions with default parameters, and the differentially expressed genes (DEGs) of HBV and HCC were screened by R language limma package, with a screening threshold P value < 0.01. The DEGs of hepatitis B and HCC were screened for logFC > 1 and logFC < 1, respectively.

Generating inflammatory and cancer-related functional modules

The database STRING (a search tool for retrieving interacting genes/proteins) is specially designed for protein-protein interaction (PPI). It provides the most comprehensive view of the current most complete PPI, so it can be used as a metadata base for extensive PPI analysis. All human protein interaction data in this study were derived from STRING data, involving 405916 interaction pairs of 10514 proteins. Then the inflammation and cancer DEGs were mapped onto the PPI network, and the

maximum connected component was obtained. Based on the maximum connected component generated above, we used the perfect MCODE method with default parameters to identify the functional modules related to inflammation and cancer. Cytoscape 3.6.1 network visualization software and ClusterONE algorithm were used to select modules with node degree > 50, and 16 modules were obtained

Crosstalk analysis to build a module level bridge

The roles of HBV- and HCC-related genes in the pathogenesis of HBV and HCC are intricate, and there are innumerable links between them. Correspondingly, the functions of the modules are also rich and colorful, and the interactions between modules are intricate as well. In order to clarify the interactions between modules and build a bridge between HBV and HCC at the module level, we used human PPI information as a background set to conduct comprehensive crosstalk analysis of all modules to further understand the interaction mechanism of co-expression modules between HBV and HCC diseases. First, based on the hypothesis that the crosstalk between functional modules is significant when the number of interactions is significantly greater than the random distribution, we constructed 1000 random PPI networks with a network size and degree of each node unchanged. Subsequently, for each pair of modules between HBV and HCC, we compared the actual number of interactions with the random distribution extracted from 1000 random PPI networks. According to the computational rules, the number of interaction pairs between modules is larger than the interaction pairs under random background. These interactions are called crosstalk. The method of calculating significant crosstalk was as follows: First, under the background of random network, the number of interaction pairs between modules in N random networks was larger than that in real networks, and the number of interaction pairs between modules was counted as n. Then the formula for calculating p value was $P = n/N$ (in this study, N = 1000). When $P \leq 0.05$, it can be considered that these crosstalk modules are more significant than random ones. Finally, Cytoscape was utilized to elucidate the significant crosstalk to intuitively observe the complex regulatory relationship between co-expression modules.

Functional and pathway enrichment analysis

Functions and signaling pathways are often important mediators of genes and diseases, and the study of them is often an effective means to explore the molecular pathways and potential mechanisms of diseases. Therefore, enrichment analysis of Gene Ontology (GO) function (P value cutoff = 0.01, q value cutoff = 0.01) and KEGG pathway (P value cutoff = 0.01, q value cutoff = 0.01) was carried out for all modules related to HBV and HCC using R language Cluster profiler package, respectively. Subsequently, we extracted the functions and pathways involved in both HBV and HCC, and considered them to be the molecular bridges between the two diseases at the levels of function and pathway.

Pivot analysis predicts module transcriptional regulators and potential drugs

Pivot node is a node that not only interacts with two modules but also has at least two pairs of interactions with each module. The hypergeometric test significance analysis of the interaction between the node and each module is $P \leq 0.05$. Python program was written to find the pivot node of the interaction module for further analysis. Gene transcription and post-transcriptional regulation are often driven by non-coding RNA (ncRNA) and TFs. Hence, we scientifically predicted and detected their role in HBV- and HCC-related dysfunction modules. Pivot is defined as a regulator that has significant regulatory effects on modules in the pathogenesis of HBV and HCC including ncRNA, TFs, and potential drugs. More than two control links between each regulator and each module were required, and the significance of enriched targets in each module based on the hypergeometric test calculation was $P < 0.01$. In addition, we examined the overlap of DEGs between HBV and HCC in these significant pivot regulators.

RESULTS

Identification of liver functional inflammation and cancer-related modules

Biologists have conducted many experiments and studies on the relationship between HBV and HCC, and determined that HBV infection is a key factor that induces HCC. However, the complex interaction mechanism between them remains unclear. Therefore, molecular links and functional effects of HBV and HCC were explored during the course of disease. We integrated related genes of the samples and screened the DEGs of HBV and HCC. Through significant screening of DEG, 394 HBV

significant DEGs and 4185 HCC significant DEGs were obtained. After screening of HBV- and HCC-related DEGs, 135 common genes were obtained (Figure 1).

In order to determine the functional clusters of hepatitis B and HCC DEGs, we searched 4444 differential gene interactions based on the PPI network. In our results, 16 dysfunction modules were obtained including 1585 nodes and 145616 edges. As shown in the table, inflammation and cancer DEGs were closely clustered together in the modules. We also observed that butyrylcholinesterase had the largest connectivity (16) in the modular network among the common genes of HBV and HCC, while lipoprotein metabolism and fatty acid-binding protein 5 were linked to 15 other genes respectively, which means that the 3 genes played a central role in their modules. At the same time, their modules were significantly involved in hepatitis B and HCC, which could be a bridge molecule between HBV and HCC. Therefore, we inferred that HBV and HCC may promote their own proliferation through some common function module-related genes, and are closely related to the microenvironment of liver diseases.

Key bridge molecules between HBV and HCC

The expression level of the same gene in two related diseases is different, which may represent the progressive bridge between diseases. Therefore, to identify key bridge molecules between HBV and HCC, we screened 135 common DEGs of diseases to identify key molecules that could characterize the process of HBV to HCC. Sixty-seven persistent dysregulated genes were obtained. Interestingly, these genes were upregulated, and most of the genes in HCC were significantly higher than those in HBV. Thus, these significantly elevated genes could characterize the progression of disease from HBV to HCC and are key genes for bridging the two diseases. On the other hand, overlapping screening of pathogenic module genes clustered by DEGs clarified that the same genes existed among multiple modules. A total of 366 overlapping genes were screened, which indicated that these genes could be associated with the disease process of HBV-related HCC at the same time. Subsequently, the connectivity of module genes was calculated and analyzed. The results suggested that the highest connectivity of PIK3CD was 670, and there were 15 genes larger than 600. The higher the connectivity, the more significant the role of the gene in the whole regulatory network, and the more important influence it has in the process of two diseases.

Significant crosstalk and shared signal pathway between common modules of HBV and HCC

A total of 54% of all HCC cases are associated with HBV, making it the most common cause of cancer worldwide[18]. In addition to directly overlapping nodes as the most direct bridge between HBV and HCC, we also analyzed other possible links between inflammation and cancer. In other words, PPI was used to find the crosstalk interaction among modules, and 40 significant crosstalk connections were obtained by screening the significant crosstalk. Because Module 7 had the highest connectivity among them, focusing on the genes of Module 7 allowed us to further understand the bridge mechanism. Inflammatory mediators play an important role in the microenvironment of tumors, which can affect all stages of tumorigenesis and development, especially the initial stage of formation. Based on GO functional analysis, we found that DEGs of the central dysfunction module tended to significantly enrich multiple disease functions (Figure 2). These pathways included positive regulation of lipid kinase activity, protein kinase B signal transduction, phosphorylation of phosphatidylinositol, acute inflammatory response, and myocyte proliferation. The modules not only shared some DEGs, but also participated in the same or similar functions and paths through crosstalk interaction. In conclusion, exploration of bridge mechanism at the module level suggested that the connections of HBV and HCC could communicate and transit through module bridging to a certain extent, demonstrating the process of disease under the global effect. Therefore, exploring the potential processes of crosstalk and molecular linkage through crosstalk may further our understanding of the detailed pathogenesis of HBV-related HCC.

TF and ncRNA driving liver inflammation and cancer progression

Although the regulation of HBV-related HCC by single or several TFs and ncRNA has been extensively studied, little attention has been paid to their comprehensive regulation of dysfunctional modules. Therefore, in order to explore these transcriptional regulators, we applied the predictive analysis of regulators to the dysfunction module based on the relationship between transcription and post-transcriptional regulation. We obtained 496 ncRNAs and 158 TFs involving 739 ncRNA-Module interaction pairs and 213 TF-Module interaction pairs. Statistical analysis of the predicted results showed that there were five regulatory modules,

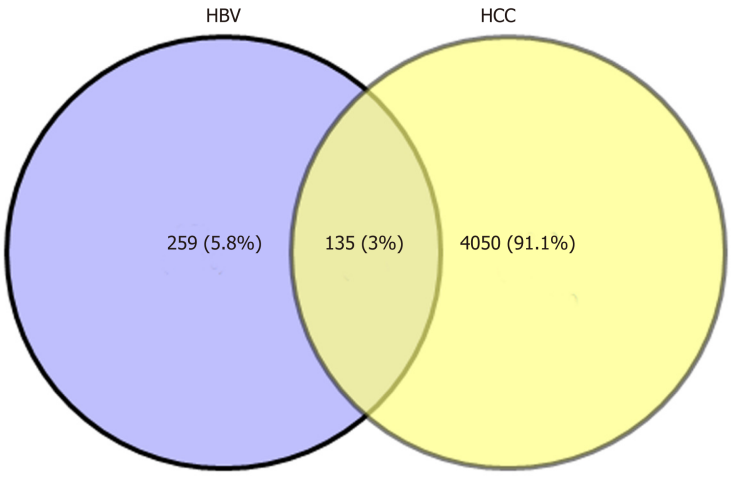

Figure 1 Common differentially expressed genes between HBV and HCC. Veen map shows the same and different genes between HBV-differentially expressed genes and HCC-differentially expressed genes. A total of 135 identical genes were obtained. HBV: Hepatitis B virus; HCC: Hepatocellular carcinoma.

which were targeted by long-chain ncRNA MALAT1, and three modules were targeted by mi410-3p. Other ncRNAs also regulated multiple dysfunction modules to varying degrees, and had potential regulatory effects on HBV and HCC. According to statistics, TF PPARA could regulate five modules, and NFKB1 and RELA also had significant regulatory effect on the four modules. These TFs may mediate the occurrence and development of HBV-related HCC and play a crucial role in the process of disease.

Three of the same miRNAs in HBV and HCC were identical to the predicted ncRNA including miR-192, miR-215, and miR-874. At the same time, it was predicted that three genes in the TFs of the regulatory module were identical to those of the persistent disorder including EGR2, FOS, and KLF4 involved in modules 1 and 9. According to the analysis of GO function, these two modules mainly play a role in regulating the JAK-STAT and MAPK signaling pathways. Therefore, we presume that these six TFs and ncRNAs are key regulatory factors and key components of connecting HBV and HCC bridges. Generally speaking, it is convenient for us to understand the potential mechanism of disease by exploring the regulatory role of pivot regulators in dysfunction modules. The pivot regulators can also be used as candidates for further experimental studies by other biologists.

Prediction of potential drugs and targets for effective inhibition of HBV-HCC process based on bridge mechanism

Potential drug prediction was made based on the bridge mechanism and drug target information between HBV and HCC explored previously. The results reported that 1,633 drug-module drug target pairs of 953 drugs may represent the potential therapeutic mechanism of the disease. In the statistical results, Sarilumab had significant pharmacological effects on six modules, while Capsaicin, Imipramine, and Mirtazapine had potential therapeutic or side effects on five modules. Other drugs also had different degree of targeting dysfunction modules, which had a certain regulatory effect on HBV and HCC. After screening the same DEGs of the two diseases, 21 drug target genes were found, and each gene corresponded to multiple drugs (Figure 3). In conclusion, these targeted drug predictions of bridge molecules and functional dysfunction modules provide references and inspirations for biologists in the treatment of diseases and the analysis of pharmacodynamics, and it can be used as candidate drugs as well. Potential target drug prediction based on dysfunction module has become an important research method for personalized treatment and drug use.

DISCUSSION

HCC is the most difficult end-stage liver disease to cure. A total of 60%-80% of HCC patients worldwide are potential liver diseases caused by HCV or HBV[19]. Although scientists have done extensive research on the close relationship between hepatitis and HCC, there has been a lack of exploration of molecular bridges based on

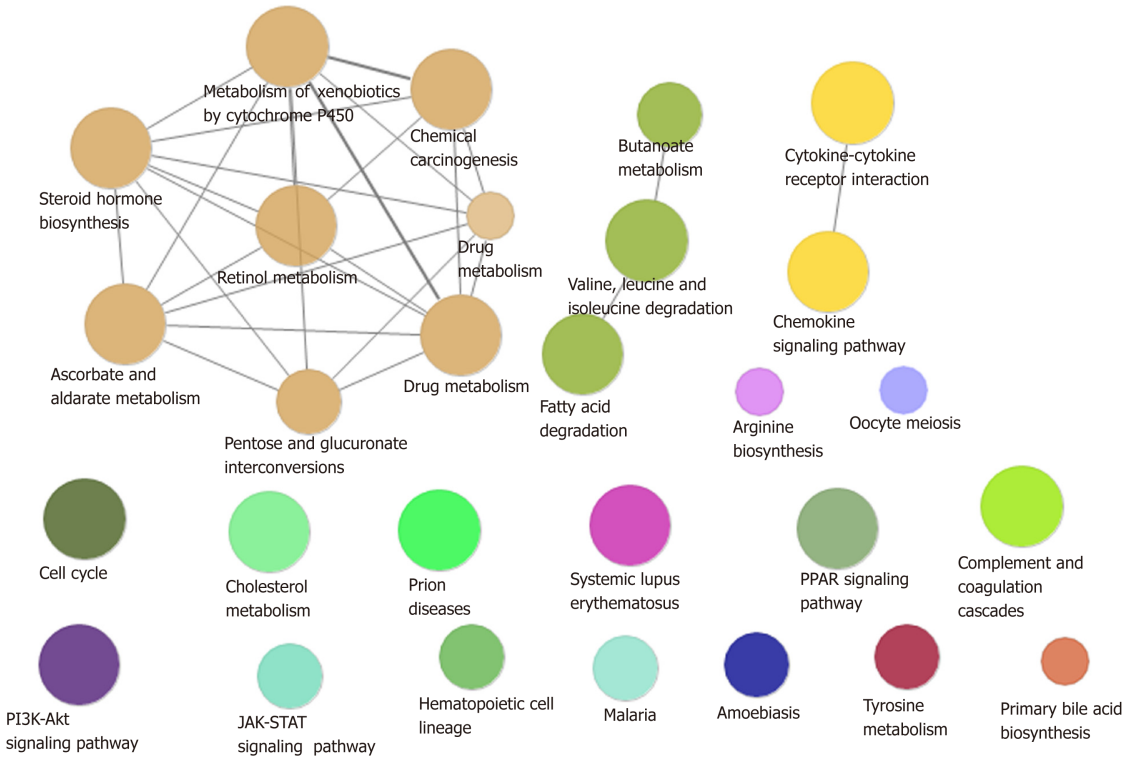

Figure 2 Module path enrichment. The larger the node, the more genes involved in the pathway. The connections between nodes reflect the correlation between signaling pathways.

functional modules of HBV and HCC. Therefore, resources from several databases were integrated including gene transcription and miRNA level changes in normal and disease patients, PPI network, transcriptional and post-transcriptional regulation, and other related data to study the potential molecular bridge of HBV-mediated HCC. The combination of PPI and crosstalk analysis showed that the functional module-based method can provide abundant resources for potential candidate genes, interactions, ncRNA, and TFs of molecular bridges between the two diseases.

In our analysis, there were 135 identical genes in the DEGs of HBV and HCC and 67 genes were assumed to be persistent dysfunctional genes among them with the increased expression of TOP5, GRHL2, VIPR1, CHST4, SLC25A47, and FXYD1 from hepatitis to HCC. We postulate that these genes play an important role in the occurrence and development of HCC induced by HBV, which has been confirmed in some previous studies. GRHL2 levels in alcoholic liver patients and model mice increased significantly among them, which seems to increase the level of hepatic inflammation by targeting the inhibition of the transcription of microRNA122, while HIF1 alpha can promote the metastasis of cancer cells and angiogenesis[20,21]. Inhibitory effect on miRNA 122 can also affect the differentiation potential of hepatic stem/progenitor cells and aggravate the occurrence of liver diseases[22]. GRHL2 can also promote cell proliferation in a variety of HCC cell lines and is significantly associated with early recurrence of HCC[23]. In addition, the binding of VIP to receptors can participate in neutrophil recruitment, adhesion molecule expression, and fibrinogen synthesis in different target organs to regulate inflammation[24]. VIPR1 is expressed in the majority of most common human tumors including breast cancer, prostate cancer, pancreatic cancer, lung cancer, colon cancer, gastric cancer, liver and bladder cancers, lymphoma, and meningioma[25]. In addition, Jinawath *et al*[26] identified a significant increase in CHST4 expression in intrahepatic cholangiocarcinoma disease samples by gene expression profile. As an organ with metabolic function, the liver plays a major role in metabolism-related proteins in tissues and cells, and the imbalance of metabolism-related proteins may cause liver dysfunction, even the occurrence of diseases. SLC transporters, as the "metabolic gates" of cells, mediate the transport of many essential nutrients and metabolites. Human genome studies have identified SLC transporters as susceptible or pathogenic genes in various diseases such as cancer, cardiovascular disease, metabolic disorders, autoimmune diseases, and neurological dysfunction[27]. Finally, FXYD proteins can act as Na, K-ATPase functional regulators by reducing the affinity of the system to potassium and sodium. The expression level of FXYD proteins in normal liver tissues

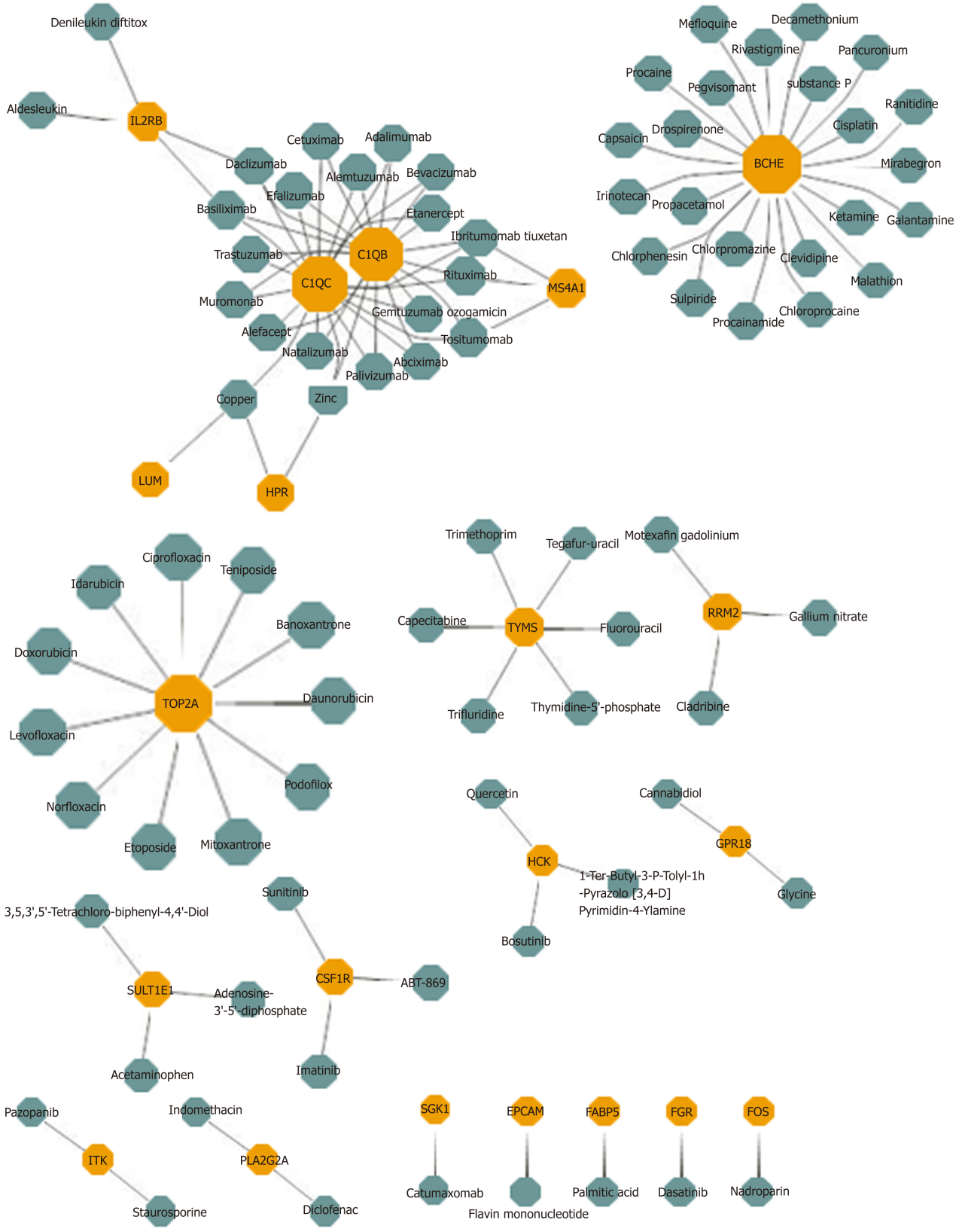

Figure 3 Potential drugs with significant effects on common gene. Yellow nodes represent common genes, and green nodes represent potential drugs.

is low, but it has a significant increase in the detection data in this study, demonstrating that FXYD is also a key gene causing liver diseases[28].

Through in-depth analysis of HBV-related HCC dysfunction module, it was found that overlapping genes existed among multiple modules, including a variety of

chemokines that have the ability to chemoattract white blood cells to the site of infection, thereby regulating the inflammatory response. CCL21 also participated in five modules. CCL21 chemokines bind to CR7 receptors and T cells of mature DCs regulated DC migration to the white pulp of the spleen, where physical contacts with lymphocytes triggers immune cell responses and regulates tumor-mediated immunosuppression[29,30]. Another chemokine CCL20 participated in four modules simultaneously, and its expression level in HBV-infected cells was markedly increased. CCL20/CCR6 chemokine/receptor axis is able to recruit CCR6-positive white blood cells into the tumor microenvironment and promote the initiation and progression of HCC[31,32]. While some chemokine receptors also existed in several modules. The knockdown of CCR1 results in the reduction of HCC metastasis promoter osteopontin *in vitro* and *in vivo* induced liver cancer migration, invasion, and lung metastasis[33]. In addition, PIK3CD had the highest 670 connectivity among all modules, which is a key regulatory gene with one-stop and whole-body effects. The high expression of PIK3CD can promote the proliferation and migration of HCC cells, and also participates in acute liver injury model in mice. Long-term inflammation of liver injury is an important factor leading to liver fibrosis and even cirrhosis and HCC[34,35]. Later, interesting module pairs were observed and module 4 and module 6 showed significant crosstalk, including the most common DEGs of which most were related to chemokines and receptors. Functional analysis showed that they may regulate pivot regulators by regulating inflammation, cell cycle regulation, and cell adhesion, thus completing the potential relationship between HBV and HCC.

Transcriptional and post-transcriptional regulation are regarded as key factors in the occurrence and development of diseases. Evaluating the transcriptional regulation of dysfunction module has become an important means to explore the bridge molecules of HBV-mediated HCC pathogenesis in a comprehensive manner. To elucidate the transcriptional regulatory factors associated with the molecular links between the two diseases, pivot regulators were analyzed based on transcriptional and post-transcriptional regulatory relationships. The results showed that MALAT1, ANCR, and BANCR were the main long-chain ncRNAs, miRNAs dominated by miRNA-410-3p, TFs dominated by PPARA, NFKB1, and RELA had significant regulatory effects on dysfunction modules. For common DEGs of HBV and HCC persistent disorder genes and miRNAs, the same genes were found with these pivot regulators including EGR2, FOS, and KLF4, as well as miR-192, miR-215, and miR-874. These genes exist in two disease-related modules and play a regulatory role in these modules, so they can be presumed to be key bridge molecules between diseases. These genes regulated activation of T cell, production of cytokine, change of cell cycle, activation of inflammatory and cancer-related signaling pathways by targeting multiple genes in the module. EGR plays a crucial role in the expression of FasL mediated by HBx, thus affecting the occurrence of HBV-related HCC[36]. Inhibition of EGR2 in HCC cell lines reduces the expression of SOCS-1 and the phosphorylation of JAK2 and STAT3, thus affecting cell proliferation[37]. FOS signal transduction is associated with TLR9-mediated IFN production in plasma-like dendritic cells, and the gene expression level of it is also significantly changed in HCC[38,39]. KLF4 affects inflammation by regulating M1/M2 macrophage polarization, and can also be used as a candidate marker for HCC development[40,41]. The regulation of small RNA is the focus of biological mechanism research. Among them, miRNA-192 not only affects the replication of HBV, but also affects the proliferation of HCC cell lines through the regulation of apoptotic proteins and ER stress[42]. MiRNA-215 is significantly correlated with hepatitis grade, fibrosis stage, and tumor tissue differentiation[43]. MiRNA-874 can inhibit the angiogenesis of endothelial cells derived from tumors. Overexpression of miRNA-874-3p in HCC cell lines can significantly inhibit cell growth and colony formation, and promote cell apoptosis[44,45]. Based on the functions of these transcriptional and post-transcriptional regulators, it is believed that they may represent key linkages in the development of HBV to HCC. TFs mediated modules 1 and 9, which is an important mechanism of dysfunction. All pivot regulators mediated dysfunction modules and played an overall regulatory role including the recombinant genes, indicating the potential pathogenesis of HBV-related HCC.

Drug prediction results based on multi-regulator-driven dysfunction module and drug target information showed that Sarilumab had significant regulatory effects on six dysfunction modules. Sarilumab is a human monoclonal antibody against IL-6 receptor-alpha, which has the ability to reduce neutrophils, showing that the drug has a certain effect on inflammation[46]. 26 DEGs results were obtained with DEGs targeting HBV and HCC. Among them, butyrylcholinesterase targeted predictive drug Mefloquine acts on the beta-catenin pathway and plays a role in the treatment of HCC[47]. Sulpiride induces fatty liver in rats by phosphorylating IRS-1 in Ser 307-

mediated adipose tissue insulin resistance, so the drug may have potential toxic side effects on the liver[48]. Many drugs need to be further explored for their treatment or side effects. However, this study provides a new method for choosing common drugs for HBV and HCC. This is not just helpful for drug research and development personnel to conduct drug screening, but also provides theoretical guidance for clinical medical personnel to conduct personalized treatment. Generally speaking, the functional module-based approach can not only comprehensively and thoroughly explore the mechanism of the occurrence and development of disease, but also predict its potential therapeutic methods and mechanisms.

ARTICLE HIGHLIGHTS

Research background

The potential role of chronic inflammation in the development of cancer has been widely recognized. However, there has been little research fully and thoroughly exploring the molecular link between hepatitis B virus (HBV) and hepatocellular carcinoma (HCC).

Research motivation

To conduct a comprehensive and in-depth discussion on the bridge mechanism between HBV and HCC.

Research objectives

The purpose of this study was to explore the co-imbalance bridging molecules between HBV and HCC and their potential drugs based on the dysfunction module.

Research methods

First, maladjusted genes shared between HBV and HCC were identified by disease-related DEGs. Second, the PPI network based on dysfunctional genes identified a series of dysfunctional modules and significant crosstalk between modules based on the hypergeometric test. In addition, key regulators were detected by pivot analysis. Finally, targeted drugs that have regulatory effects on diseases were predicted by modular methods and drug target information.

Research results

The study found that 67 genes continued to increase in the HBV-HCC process. Moreover, 366 overlapping genes in the module network participated in multiple functional blocks. It could be presumed that these genes and their interactions play an important role in the relationship between inflammation and cancer. Correspondingly, significant crosstalk constructed a module level bridge for HBV-HCC molecular processes. On the other hand, a series of ncRNAs and TFs that have potential pivot regulatory effects on HBV and HCC were identified. Among them, some of the regulators also had persistent disorders in the process of HBV-HCC including miRNA-192, miRNA-215, and miRNA-874, and EGR2, FOS, and KLF4. Therefore, the study concluded that these pivots are the key bridge molecules outside the module. Last but not least, a variety of drugs that may have some potential pharmacological or toxic side effects on HBV-induced HCC were predicted, but their mechanisms need to be further explored.

Research conclusions

The results suggest that the persistent inflammatory environment of HBV can be utilized as an important risk factor to induce the occurrence of HCC, which is supported by molecular evidence.

Research perspectives

In the future, research may comprehensively and thoroughly explore the mechanism of HCC occurrence and development and predict the potential therapeutic methods and mechanisms.

REFERENCES

1 **Colotta F**, Allavena P, Sica A, Garlanda C, Mantovani A. Cancer-related inflammation, the seventh hallmark of cancer: Links to genetic instability. *Carcinogenesis* 2009; **30**: 1073-1081 [PMID: 19468060 DOI: 10.1093/carcin/bgp127]

2 **Gupta SC**, Kunnumakkara AB, Aggarwal S, Aggarwal BB. Inflammation, a Double-Edge Sword for Cancer and Other Age-Related Diseases. *Front Immunol* 2018; **9**: 2160 [PMID: 30319623 DOI: 10.3389/fimmu.2018.02160]

3 **Virzì A**, Roca Suarez AA, Baumert TF, Lupberger J. Oncogenic Signaling Induced by HCV Infection. *Viruses* 2018; **10**: pii: E538 [PMID: 30279347 DOI: 10.3390/v10100538]

4 **Susek KH**, Karvouni M, Alici E, Lundqvist A. The Role of CXC Chemokine Receptors 1-4 on Immune Cells in the Tumor Microenvironment. *Front Immunol* 2018; **9**: 2159 [PMID: 30319622 DOI: 10.3389/fimmu.2018.02159]

5 **Zang M**, Li Y, He H, Ding H, Chen K, Du J, Chen T, Wu Z, Liu H, Wang D, Cai J, Qu C. IL-23 production of liver inflammatory macrophages to damaged hepatocytes promotes hepatocellular carcinoma development after chronic hepatitis B virus infection. *Biochim Biophys Acta Mol Basis Dis* 2018; **1864**: 3759-3770 [PMID: 30292634 DOI: 10.1016/j.bbadis.2018.10.004]

6 **Mysore KR**, Leung DH. Hepatitis B and C. *Clin Liver Dis* 2018; **22**: 703-722 [PMID: 30266158 DOI: 10.1016/j.cld.2018.06.002]
7 **Maddrey WC**. Hepatitis B: An important public health issue. *J Med Virol* 2000; **61**: 362-366 [PMID: 10861647]
8 **Yang L**, Ye S, Zhao X, Ji L, Zhang Y, Zhou P, Sun J, Guan Y, Han Y, Ni C, Hu X, Liu W, Wang H, Zhou B, Huang J. Molecular Characterization of HBV DNA Integration in Patients with Hepatitis and Hepatocellular Carcinoma. *J Cancer* 2018; **9**: 3225-3235 [PMID: 30271481 DOI: 10.7150/jca.26052]
9 **Musa J**, Li J, Grünewald TG. Hepatitis B virus large surface protein is priming for hepatocellular carcinoma development via induction of cytokinesis failure. *J Pathol* 2019; **247**: 6-8 [PMID: 30246253 DOI: 10.1002/path.5169]
10 **Zhu S**, Tan W, Li W, Zhou R, Wu X, Chen X, Li W, Shang C, Chen Y. Low expression of VSIG4 is associated with poor prognosis in hepatocellular carcinoma patients with hepatitis B infection. *Cancer Manag Res* 2018; **10**: 3697-3705 [PMID: 30288101 DOI: 10.2147/CMAR.S165822]
11 **Xu X**, Tao Y, Shan L, Chen R, Jiang H, Qian Z, Cai F, Ma L, Yu Y. The Role of MicroRNAs in Hepatocellular Carcinoma. *J Cancer* 2018; **9**: 3557-3569 [PMID: 30310513 DOI: 10.7150/jca.26350]
12 **Abdel-Hamid NM**, Abass SA, Mohamed AA, Muneam Hamid D. Herbal management of hepatocellular carcinoma through cutting the pathways of the common risk factors. *Biomed Pharmacother* 2018; **107**: 1246-1258 [PMID: 30257339 DOI: 10.1016/j.biopha.2018.08.104]
13 **Ranjpour M**, Wajid S, Jain SK. Elevated expression of A-Raf and FA2H in hepatocellular carcinoma is associated with lipid metabolism dysregulation and cancer progression. *Anticancer Agents Med Chem* 2018 [PMID: 30324893 DOI: 10.2174/1871520618666181015142810]
14 **Herrero AB**, Astudillo AM, Balboa MA, Cuevas C, Balsinde J, Moreno S. Levels of SCS7/FA2H-mediated fatty acid 2-hydroxylation determine the sensitivity of cells to antitumor PM02734. *Cancer Res* 2008; **68**: 9779-9787 [PMID: 19047157 DOI: 10.1158/0008-5472.CAN-08-1981]
15 **Kong X**, Sun R, Chen Y, Wei H, Tian Z. γδT cells drive myeloid-derived suppressor cell-mediated CD8+ T cell exhaustion in hepatitis B virus-induced immunotolerance. *J Immunol* 2014; **193**: 1645-1653 [PMID: 25015833 DOI: 10.4049/jimmunol.1303432]
16 **You J**, Chen W, Chen J, Zheng Q, Dong J, Zhu Y. The Oncogenic Role of ARG1 in Progression and Metastasis of Hepatocellular Carcinoma. *Biomed Res Int* 2018; **2018**: 2109865 [PMID: 30320132 DOI: 10.1155/2018/2109865]
17 **Wu N**, Zhao J, Yuan Y, Lu C, Zhu W, Jiang Q. NOP7 interacts with β-catenin and activates β-catenin/TCF signaling in hepatocellular carcinoma cells. *Onco Targets Ther* 2018; **11**: 6369-6376 [PMID: 30319277 DOI: 10.2147/OTT.S164601]
18 **Pazgan-Simon M**, Simon KA, Jarowicz E, Rotter K, Szymanek-Pasternak A, Zuwała-Jagiełło J. Hepatitis B virus treatment in hepatocellular carcinoma patients prolongs survival and reduces the risk of cancer recurrence. *Clin Exp Hepatol* 2018; **4**: 210-216 [PMID: 30324148 DOI: 10.5114/ceh.2018.78127]
19 **Park JW**, Chen M, Colombo M, Roberts LR, Schwartz M, Chen PJ, Kudo M, Johnson P, Wagner S, Orsini LS, Sherman M. Global patterns of hepatocellular carcinoma management from diagnosis to death: The BRIDGE Study. *Liver Int* 2015; **35**: 2155-2166 [PMID: 25752327 DOI: 10.1111/liv.12818]
20 **Satishchandran A**, Ambade A, Rao S, Hsueh YC, Iracheta-Vellve A, Tornai D, Lowe P, Gyongyosi B, Li J, Catalano D, Zhong L, Kodys K, Xie J, Bala S, Gao G, Szabo G. MicroRNA 122, Regulated by GRLH2, Protects Livers of Mice and Patients From Ethanol-Induced Liver Disease. *Gastroenterology* 2018; **154**: 238-252.e7 [PMID: 28987423 DOI: 10.1053/j.gastro.2017.09.022]
21 **Kim A**, Ma JY. Rhaponticin decreases the metastatic and angiogenic abilities of cancer cells via suppression of the HIF1α pathway. *Int J Oncol* 2018; **53**: 1160-1170 [PMID: 30015877 DOI: 10.3892/ijo.2018.4479]
22 **Tanimizu N**, Kobayashi S, Ichinohe N, Mitaka T. Downregulation of miR122 by grainyhead-like 2 restricts the hepatocytic differentiation potential of adult liver progenitor cells. *Development* 2014; **141**: 4448-4456 [PMID: 25406394 DOI: 10.1242/dev.113654]
23 **Tanaka Y**, Kanai F, Tada M, Tateishi R, Sanada M, Nannya Y, Ohta M, Asaoka Y, Seto M, Shiina S, Yoshida H, Kawabe T, Yokosuka O, Ogawa S, Omata M. Gain of GRHL2 is associated with early recurrence of hepatocellular carcinoma. *J Hepatol* 2008; **49**: 746-757 [PMID: 18752864 DOI: 10.1016/j.jhep.2008.06.019]
24 **Martínez C**, Juarranz Y, Abad C, Arranz A, Miguel BG, Rosignoli F, Leceta J, Gomariz RP. Analysis of the role of the PAC1 receptor in neutrophil recruitment, acute-phase response, and nitric oxide production in septic shock. *J Leukoc Biol* 2005; **77**: 729-738 [PMID: 15661828 DOI: 10.1189/jlb.0704432]
25 **Reubi JC**. In vitro evaluation of VIP/PACAP receptors in healthy and diseased human tissues. Clinical implications. *Ann N Y Acad Sci* 2000; **921**: 1-25 [PMID: 11193811 DOI: 10.1111/j.1749-6632.2000.tb06946.x]
26 **Jinawath N**, Chamgramol Y, Furukawa Y, Obama K, Tsunoda T, Sripa B, Pairojkul C, Nakamura Y. Comparison of gene expression profiles between Opisthorchis viverrini and non-Opisthorchis viverrini associated human intrahepatic cholangiocarcinoma. *Hepatology* 2006; **44**: 1025-1038 [PMID: 17006947 DOI: 10.1002/hep.21330]
27 **Zhang Y**, Zhang Y, Sun K, Meng Z, Chen L. The SLC transporter in nutrient and metabolic sensing, regulation, and drug development. *J Mol Cell Biol* 2019; **11**: 1-13 [PMID: 30239845 DOI: 10.1093/jmcb/mjy052]
28 **Floyd RV**, Wray S, Martín-Vasallo P, Mobasheri A. Differential cellular expression of FXYD1 (phospholemman) and FXYD2 (gamma subunit of Na, K-ATPase) in normal human tissues: A study using high density human tissue microarrays. *Ann Anat* 2010; **192**: 7-16 [PMID: 19879113 DOI: 10.1016/j.aanat.2009.09.003]
29 **Nico D**, Martins Almeida F, Maria Motta J, Soares Dos Santos Cardoso F, Freire-de-Lima CG, Freire-de-Lima L, de Luca PM, Maria Blanco Martinez A, Morrot A, Palatnik-de-Sousa CB. NH36 and F3 Antigen-Primed Dendritic Cells Show Preserved Migrating Capabilities and CCR7 Expression and F3 Is Effective in Immunotherapy of Visceral Leishmaniasis. *Front Immunol* 2018; **9**: 967 [PMID: 29867949 DOI: 10.3389/fimmu.2018.00967]
30 **Zhou S**, Chen L, Qin J, Li R, Tao H, Zhen Z, Chen H, Chen G, Yang Y, Liu B, She Z, Zhong C, Liang C. Depletion of CD4+ CD25+ regulatory T cells promotes CCL21-mediated antitumor immunity. *PLoS One* 2013; **8**: e73952 [PMID: 24023916 DOI: 10.1371/journal.pone.0073952]
31 **Liu Y**, Li L, Liu J, She WM, Shi JM, Li J, Wang JY, Jiang W. Activated hepatic stellate cells directly induce pathogenic Th17 cells in chronic hepatitis B virus infection. *Exp Cell Res* 2017; **359**: 129-137 [PMID: 28780305 DOI: 10.1016/j.yexcr.2017.08.001]

32 **Benkheil M**, Van Haele M, Roskams T, Laporte M, Noppen S, Abbasi K, Delang L, Neyts J, Liekens S. CCL20, a direct-acting pro-angiogenic chemokine induced by hepatitis C virus (HCV): Potential role in HCV-related liver cancer. *Exp Cell Res* 2018; **372**: 168-177 [PMID: 30287142 DOI: 10.1016/j.yexcr.2018.09.023]

33 **Viallat JR**, Rey F, Farisse P, Henric A, Gastaut JA. [The frequency of Kaposi's bronchial sarcoma in AIDS. Personal experience in 1987]. *Rev Mal Respir* 1989; **6**: 71-73 [PMID: 2928585]

34 **Yu L**, Gong X, Sun L, Zhou Q, Lu B, Zhu L. The Circular RNA Cdr1as Act as an Oncogene in Hepatocellular Carcinoma through Targeting miR-7 Expression. *PLoS One* 2016; **11**: e0158347 [PMID: 27391479 DOI: 10.1371/journal.pone.0158347]

35 **Xu G**, Han X, Yuan G, An L, Du P. Screening for the protective effect target of deproteinized extract of calf blood and its mechanisms in mice with CCl4-induced acute liver injury. *PLoS One* 2017; **12**: e0180899 [PMID: 28700704 DOI: 10.1371/journal.pone.0180899]

36 **Yoo YG**, Lee MO. Hepatitis B virus X protein induces expression of Fas ligand gene through enhancing transcriptional activity of early growth response factor. *J Biol Chem* 2004; **279**: 36242-36249 [PMID: 15173177 DOI: 10.1074/jbc.M401290200]

37 **Lu L**, Ye X, Yao Q, Lu A, Zhao Z, Ding Y, Meng C, Yu W, Du Y, Cheng J. Egr2 enhances insulin resistance via JAK2/STAT3/SOCS-1 pathway in HepG2 cells treated with palmitate. *Gen Comp Endocrinol* 2018; **260**: 25-31 [PMID: 28842216 DOI: 10.1016/j.ygcen.2017.08.023]

38 **Janovec V**, Aouar B, Font-Haro A, Hofman T, Trejbalova K, Weber J, Chaperot L, Plumas J, Olive D, Dubreuil P, Nunès JA, Stranska R, Hirsch I. The MEK1/2-ERK Pathway Inhibits Type I IFN Production in Plasmacytoid Dendritic Cells. *Front Immunol* 2018; **9**: 364 [PMID: 29535732 DOI: 10.3389/fimmu.2018.00364]

39 **Liu S**, Yao X, Zhang D, Sheng J, Wen X, Wang Q, Chen G, Li Z, Du Z, Zhang X. Analysis of Transcription Factor-Related Regulatory Networks Based on Bioinformatics Analysis and Validation in Hepatocellular Carcinoma. *Biomed Res Int* 2018; **2018**: 1431396 [PMID: 30228980 DOI: 10.1155/2018/1431396]

40 **Li B**, Sheng Z, Liu C, Qian L, Wu Y, Wu Y, Ma G, Yao Y. Kallistatin Inhibits Atherosclerotic Inflammation by Regulating Macrophage Polarization. *Hum Gene Ther* 2019; **30**: 339-351 [PMID: 30205711 DOI: 10.1089/hum.2018.084]

41 **Zhang Y**, Liu Z, Li JS. Identifying Biomarkers of Hepatocellular Carcinoma Based on Gene Co-Expression Network from High-Throughput Data. *Stud Health Technol Inform* 2017; **245**: 667-671 [PMID: 29295180]

42 **Nielsen KO**, Jacobsen KS, Mirza AH, Winther TN, Størling J, Glebe D, Pociot F, Hogh B. Hepatitis B virus upregulates host microRNAs that target apoptosis-regulatory genes in an in vitro cell model. *Exp Cell Res* 2018; **371**: 92-103 [PMID: 30059664 DOI: 10.1016/j.yexcr.2018.07.044]

43 **Mamdouh S**, Khorshed F, Aboushousha T, Hamdy H, Diab A, Seleem M, Saber M. Evaluation of Mir-224, Mir-215 and Mir-143 as Serum Biomarkers for HCV Associated Hepatocellular Carcinoma. *Asian Pac J Cancer Prev* 2017; **18**: 3167-3171 [PMID: 29172295 DOI: 10.22034/APJCP.2017.18.11.3167]

44 **Lopatina T**, Grange C, Fonsato V, Tapparo M, Brossa A, Fallo S, Pitino A, Herrera-Sanchez MB, Kholia S, Camussi G, Bussolati B. Extracellular vesicles from human liver stem cells inhibit tumor angiogenesis. *Int J Cancer* 2019; **144**: 322-333 [PMID: 30110127 DOI: 10.1002/ijc.31796]

45 **Leong KW**, Cheng CW, Wong CM, Ng IO, Kwong YL, Tse E. miR-874-3p is down-regulated in hepatocellular carcinoma and negatively regulates PIN1 expression. *Oncotarget* 2017; **8**: 11343-11355 [PMID: 28076852 DOI: 10.18632/oncotarget.14526]

46 **Lee EB**. A review of sarilumab for the treatment of rheumatoid arthritis. *Immunotherapy* 2018; **10**: 57-65 [PMID: 29043871 DOI: 10.2217/imt-2017-0075]

47 **Li YH**, Yang SL, Zhang GF, Wu JC, Gong LL, Ming-Zhong, Lin RX. Mefloquine targets β-catenin pathway and thus can play a role in the treatment of liver cancer. *Microb Pathog* 2018; **118**: 357-360 [PMID: 29578061 DOI: 10.1016/j.micpath.2018.03.042]

48 **Zhou X**, Ren L, Yu Z, Huang X, Li Y, Wang C. The antipsychotics sulpiride induces fatty liver in rats via phosphorylation of insulin receptor substrate-1 at Serine 307-mediated adipose tissue insulin resistance. *Toxicol Appl Pharmacol* 2018; **345**: 66-74 [PMID: 29551354 DOI: 10.1016/j.taap.2018.02.023]

World Journal of Gastroenterology

Submit a Manuscript: https://www.f6publishing.com

World J Gastroenterol 2019 September 7; 25(33): 4933-4944

DOI: 10.3748/wjg.v25.i33.4933

ISSN 1007-9327 (print) ISSN 2219-2840 (online)

ORIGINAL ARTICLE

Retrospective Cohort Study

Proton pump inhibitor use increases mortality and hepatic decompensation in liver cirrhosis

Marianne Anastasia De Roza, Lim Kai, Jia Wen Kam, Yiong Huak Chan, Andrew Kwek, Tiing Leong Ang, John Chen Hsiang

ORCID number: Marianne A De Roza (0000-0003-4247-8777); Lim Kai (0000-0003-0941-6291); Jiawen Kam (0000-0002-5201-7678); Yiong Huak Chan (0000-0002-5076-5269); Andrew Kwek (0000-0003-2870-8150); Tiing Leong Ang (0000-0001-9993-8549); John Chen Hsiang (0000-0002-7124-6396).

Author contributions: De Roza MA and Hsiang JC designed the study and methods, and contributed to data collection, data verification, data analysis, interpretation of data, manuscript preparation, final drafting, and final approval of the version to be published; Kai L assisted with data collection and data verification; Kam JW and Chan YK performed the statistical analysis and interpretation of data; Kwek A and Ang TL contributed to the critical review of the manuscript and final approval of the version to be published.

Institutional review board statement: This study was conducted after receiving approval from the Singhealth Centralized Institutional Review Board with waiver of informed consent.

Informed consent statement: This study was approved by the Singhealth IRB for waiver of informed consent.

Conflict-of-interest statement: All authors declare there are no conflicts of interest. None of the authors received financial support or grants for this study.

Data sharing statement: Statistical

Marianne Anastasia De Roza, Lim Kai, Andrew Kwek, Tiing Leong Ang, John Chen Hsiang, Department of Gastroenterology and Hepatology, Changi General Hospital, Singhealth 529889, Singapore

Jia Wen Kam, Clinical Trials and Research Unit, Changi General Hospital, Singhealth 529889, Singapore

Yiong Huak Chan, Biostatistics Unit, Yong Loo Lin School of Medicine, National University of Singapore, Singapore 160608, Singapore

Corresponding author: John Chen Hsiang, MBChB, Attending Doctor, Doctor, Senior Researcher, Department of Gastroenterology and Hepatology, Changi General Hospital, 2 Simei Street 3, Singhealth 529889, Singapore. jchsiang@gmail.com
Telephone: +65-69302923

Abstract

BACKGROUND

Proton pump inhibitors (PPIs) are widely prescribed, often without clear indications. There are conflicting data on its association with mortality risk and hepatic decompensation in cirrhotic patients. Furthermore, PPI users and PPI exposure in some studies have been poorly defined with many confounding factors.

AIM

To examine if PPI use increases mortality and hepatic decompensation and the impact of cumulative PPI dose exposure.

METHODS

Data from patients with decompensated liver cirrhosis were extracted from a hospital database between 2013 to 2017. PPI users were defined as cumulative defined daily dose (cDDD) ≥ 28 within a landmark period, after hospitalisation for hepatic decompensation. Cox regression analysis for comparison was done after propensity score adjustment. Further risk of hepatic decompensation was analysed by Poisson regression.

RESULTS

Among 295 decompensated cirrhosis patients, 238 were PPI users and 57 were non-users. PPI users had higher mortality compared to non-users [adjusted HR = 2.10, (1.20-3.67); P = 0.009]. Longer PPI use with cDDD > 90 was associated with

coding and dataset is available from the corresponding author at jchsiang@gmail.com.

STROBE statement: The authors have read the STROBE Statement-checklist of items, and the manuscript was prepared and revised according to the STROBE Statement-checklist of items

Manuscript source: Unsolicited manuscript

Received: March 25, 2019
Peer-review started: March 25, 2019
First decision: May 24, 2019
Revised: July 12, 2019
Accepted: July 19, 2019
Article in press: July 19, 2019
Published online: September 7, 2019

P-Reviewer: Cholongitas E, Spahr L
S-Editor: Ma RY
L-Editor: Filipodia
E-Editor: Ma YJ

higher mortality, compared to non-users [aHR = 2.27, (1.10-5.14); P = 0.038]. PPI users had a higher incidence of hospitalization for hepatic decompensation [aRR = 1.61, (1.30-2.11); P < 0.001].

CONCLUSION
PPI use in decompensated cirrhosis is associated with increased risk of mortality and hepatic decompensation. Longer PPI exposure with cDDD > 90 increases the risk of mortality.

Key words: Proton pump inhibitor; Liver cirrhosis; Mortality; Hospitalisation; Complications; Portal hypertension; Variceal bleeding; Ascites; Spontaneous bacterial peritonitis; Hepatic encephalopathy

Core tip: Most proton pump inhibitor (PPI) studies have issues with poorly defining PPI users and having baseline confounders. Also, studies on PPI use in liver cirrhosis have not been focused on decompensated cirrhosis. Using propensity score analysis, we adjusted for 43 variables including baseline characteristics, comorbidities, PPI indication, and medications (including antiplatelets). Landmark analysis was used to define PPI users to reduce bias. PPI use in patients with decompensated liver cirrhosis was associated with higher mortality and increased risk of hepatic decompensation requiring hospital admissions. Longer PPI exposure with > 90 defined daily doses further increased mortality risk.

Citation: De Roza MA, Kai L, Kam JW, Chan YH, Kwek A, Ang TL, Hsiang JC. Proton pump inhibitor use increases mortality and hepatic decompensation in liver cirrhosis. *World J Gastroenterol* 2019; 25(33): 4933-4944
URL: https://www.wjgnet.com/1007-9327/full/v25/i33/4933.htm
DOI: https://dx.doi.org/10.3748/wjg.v25.i33.4933

INTRODUCTION

Liver cirrhosis is associated with significant morbidity and mortality[1], especially when portal hypertension-related complications or hepatocellular carcinoma (HCC) develop. Several host factors are associated with increased risk of morbidity and mortality in cirrhotic patients including type 2 diabetes[2,3], older age, obesity, and alcohol consumption[4]. Recent studies have shed light on abnormal gut microbiota composition and dysbiosis playing an important role in the pathophysiology of cirrhosis complications such as hepatic encephalopathy (HE), spontaneous bacterial peritonitis (SBP) and acute on chronic liver failure[5,6].

Proton pump inhibitors (PPIs), a frequently prescribed medication worldwide, has been shown to promote alterations in gut microbiota[7,8], leading to dysbiosis and impaired gut barrier function[9]. Its use in cirrhosis patients is associated with increased risk of SBP and HE[9-11]. In addition, Bajaj *et al*[12] showed that gut microbiota is modulated by PPI and results in increased oral origin microbiota, which can reduce upon PPI withdrawal. They also showed that initiation of PPI was an independent risk factor for hospital readmissions among cirrhotic patients; the 30-d readmission for those discharged with PPI was 50% compared to 32% for those who were not on PPI (P = 0.02).

Despite the increasing concerns of PPI use, it is still widely prescribed in liver cirrhosis patients. One study showed 62.7% of hospitalised cirrhosis patients were prescribed PPIs with unclear indications[13]. It is particularly concerning as PPIs are metabolised in the liver by cytochrome CYP450[11,14], and as a result, their half-life increases by 4-8 h in cirrhotic patients[15]. There have been concerns that PPI use increases the risk of mortality in patients with decompensated liver disease[16], and those with HE[17], but other studies dispute the association of mortality with PPI use in decompensated cirrhosis or cirrhotic patients with SBP[13,18]. Of the published data on PPI use and mortality in cirrhotic patients[13,16,17], "PPI users" are often defined as patients with PPI prescriptions at the study inclusion, and PPI dose duration is not measured. These could potentially lead to guarantee-time bias and exposure

classification bias[19,20]. Furthermore, given that PPI is widely used as a gastroprotective agent in patients with cardiovascular disease taking aspirin and antithrombotic agents, these should be adjusted as confounders.

Currently, the evidence supporting PPI exposure and increased mortality in cirrhosis patients is still not clear, with potential biases as PPI user status and dose exposure not well defined. Furthermore, data are lacking on the dose-dependent effect of PPI on mortality risk and further hepatic decompensation among cirrhotic patients, especially when PPI metabolism is affected in this population[15]. Therefore, we assessed if long-term PPI use in decompensated liver cirrhosis patients would increase the risk of mortality after adjusting for potential biases and defining true dosage exposure. The secondary aim was to determine if PPI use increases the risk of hospital admissions for further hepatic decompensation in patients with decompensated liver cirrhosis.

MATERIALS AND METHODS

Patient selection

Patients with liver cirrhosis using ICD10 coding (Supplemental Table 1) were extracted from January 2013 to June 2017 from the Changi General Hospital electronic database. Patient demographics, medical comorbidities (based on ICD codings forming Charlson's comorbidity index; Supplementary Table 1), biochemical profile, baseline medication use (Supplementary Table 2), and history of prior hepatic decompensation were reviewed and verified by three investigators. Clinical ICD codings of United States Food and Drug Administration (FDA)-approved PPI indications were also extracted such as gastroesophageal reflux disease (GERD), esophagitis, and peptic ulcer disease. Patients over 18 years of age with liver cirrhosis confirmed by histology, imaging or transient elastography and hospital admissions for hepatic decompensation during this period were included. Patients without hepatic decompensation were excluded.

The codings of hospital admission diagnoses were regularly reviewed and audited by the hospital medical record department to maintain data integrity as expected of a restructured public hospital governed by the health ministry. Mortality data were obtained from the Singapore National Registry of Diseases Office, and the date of liver transplant, if any, was obtained from the National Organ Transplant of Singapore.

The study's protocol conformed to the ethical guidelines of the 1975 Declaration of Helsinki as reflected in a priori approval by our institution's human research committee.

Outcomes

The primary outcome of this study was overall mortality, defined as death or liver transplant, whichever came first. The secondary outcome was the rate of further hepatic decompensation-related hospital admissions after the index admission at baseline. For secondary outcomes, each patient's hospital admission notes were reviewed by three investigators to verify that coding diagnoses of hepatic decompensation admissions were accurate. Hospital admissions for elective procedures such as radiofrequency ablation or trans-arterial chemoembolisation of HCC and those with incomplete data were excluded from the study.

The hepatic decompensation events were ascites, SBP, HE, variceal bleeding, and hepatorenal syndrome, as defined by current guidelines[21]. Overall survival was calculated from the end of the designated landmark period until the census date of 31st December 2017. Patients who died within the landmark period were excluded from primary analysis to reduce biases.

Definition of PPI user status

In pharmacoepidemiologic studies, there are biases involved in comparing time-to-event data for different groups as classification to "event" or "event-free" groups are dependent on length of follow-up[22]. Therefore, by using the landmark method, a fixed time after the initiation of therapy was selected as a landmark for conducting the survival analysis, which would minimise immortal time, selection, and indication bias. Taking this into consideration, we used a landmark period of 3 mo before to 6 mo after index hepatic decompensation admission (-3 mo to +6 mo), to define PPI user status.

The period of 3 mo before index admission (-3 mo to time 0) was utilised as PPI use in hospitalised cirrhotic patients, as it has been found to increase the risk of 1-mo and 3-mo hospital readmission rates[12]. Exclusion of these patients who were on PPI just

Table 1 Baseline characteristics between non-users and proton pump inhibitor users for the 6-mo landmark period

Baseline characteristics	Non-user(*n* = 57)	PPI user(*n* = 238)	*P* value
Gender, *n* (%)			0.96
Male	39 (68.4)	162 (68.1)	
Female	18 (31.6)	76 (31.9)	
Age in yr, Mean (± SD)	60.0 ± 13.3	63.3 ± 12.4	0.07
Race, *n* (%)			0.95
Chinese	33 (57.9)	132 (55.5)	
Malay	10 (17.5)	50 (21.0)	
Indian	8 (14.0)	33 (13.9)	
Others	6 (10.5)	23 (9.7)	
Aetiology of cirrhosis, *n* (%)			0.07
Hepatitis B	11 (19.3	42 (17.6)	
Alcohol	16 (28.1)	42 (17.6)	
Hepatitis C	11 (19.3)	52 (21.8)	
NASH	9 (15.8)	74 (31.1)	
Autoimmune	4 (7.0)	4 (1.7)	
Others	6 (10.5)	24 (10.1)	
Index hepatic event, *n* (%)			
HCC	6 (10.5)	20 (8.4)	0.61
Ascites	37 (64.9)	121 (50.8)	0.06
SBP	4 (7.0)	15 (6.3)	0.77
HE	9 (15.8)	59 (24.8)	0.15
Variceal bleed	8 (14.0)	53 (22.3)	0.17
History of the following, *n* (%)			
HCC	0 (0.0)	9 (3.8)	0.21
Ascites	9 (15.8)	32 (13.4)	0.65
HE	1 (1.8)	10 (4.2)	0.70
Variceal bleed	9 (15.8)	42 (17.6)	0.74
SBP	2 (3.5)	6 (2.5)	0.65
Biochemical results at baseline;			
Mean (± SD) or median (IQR)			
Albumin in g/L	27.0 ± 4.7	28.1 ± 6.2	0.14
INR	1.12 (1.01-1.26)	1.13 (1.03-1.28)	0.73
Creatinine in μmol/L	79.0 (65.0-124.5)	86.0 (66.8-117.0)	0.58
Bilirubin in μmol/L	29.4 (17.0-56.8)	25.9 (16.3-74.0)	0.16
Platelet count as 10^9/L	105.5 (67.3-150.3)	104.0 (71.0-159.0)	0.82
Haemoglobin in g/dL	11.4 ± 2.3	10.8 ± 2.6	0.15
MELD, median (IQR)	11.0 (8.0-14.5)	10.5 (8.0-14.3)	0.56
Medical comorbidities, *n* (%)			
GERD	0 (0.0)	19 (8.0)	0.03
Esophagitis	4 (7.0)	17 (7.1)	1.00
Peptic ulcer disease	1 (1.8)	32 (13.4)	0.01
Type 2 diabetes[1]			0.16
None	33 (57.9)	105 (44.1)	
Uncomplicated	14 (24.6)	70 (29.4)	
End-organ damage	10 (17.5)	63 (26.5)	
Malignancy[1]			0.84
None	47 (82.5)	199 (83.6)	
Leukaemia/lymphoma/localised solid tumour	8 (14.0)	33 (13.9)	
Metastatic solid tumour	2 (3.5)	6 (2.5)	
HIV/AIDS[1]	1 (1.8)	2 (0.8)	
Renal impairment[1]	9 (15.8)	51 (21.4)	
Congestive heart failure[1]	4 (7.0)	21 (8.8)	

Myocardial infarct[1]	2 (3.5)	33 (13.9)	
COPD[1]	2 (3.5)	9 (3.8)	
PVD[1]	0 (0.0)	4 (1.7)	
CVA/TIA[1]	2 (3.5)	24 (10.1)	
Dementia[1]	1 (1.8)	9 (3.8)	
Hemiplegia[1]	0 (0.0)	3 (1.3)	
	2 (3.5)	4 (1.7)	
Connective tissue disease[1]			
Baseline medications:			
Antivirals for viral hepatitis:			
Chronic HBV on long-term antivirals	2/11 (18.2)	14/42 (33.3)	0.48
Chronic HCV treated with DAA[2]	0/11 (0.0)	3/52 (5.8)	1.00
Use of other concurrent medications, > 3 mo use			
Insulin	2 (3.5)	42 (17.6)	0.01
Sulphonylureas	8 (14.0)	51 (21.4)	0.21
Insulin sensitisers	2 (3.5)	24 (10.1)	0.11
Metformin	5 (8.8)	45 (18.9)	0.07
DPP4 inhibitors	4 (7.0)	2 (0.8)	0.01
Antiplatelet	5 (8.8)	45 (18.9)	0.067
Aspirin	5 (8.8)	38 (16.0)	0.17
Statins	2 (3.5)	29 (12.2)	0.06
ACE-I/ARB	4 (7.0)	43 (18.1)	0.04
Non-selective beta blockers	8 (14.0)	81 (34.0)	0.003
Selective beta blockers	2 (3.5)	22 (9.2)	0.19

[1]As defined by Charlson's comorbidity index;
[2]3 patients given 12 wk of sofosbuvir/daclatasvir/ribavirin for hepatitis C virus cirrhosis; direct acting antiviral only became fully funded in early 2017. NASH: Non-alcoholic steatohepatitis; MELD: Model of end-stage liver disease; GERD: Gastroesophageal reflux disease; HIV/AIDS: Human immunodeficiency virus/acquired immune deficiency syndrome; COPD-Chronic obstructive pulmonary disease; PVD: Peripheral vascular disease; CVA/TIA: Cerebrovascular accident/transient ischemic attack; DPP4: Dipeptidyl peptidase-4; ACE-I/ARB: Angiotensin converting enzyme inhibitor/angiotensin II receptor blocker; DAA: Direct acting antiviral; HE: Hepatic encephalopathy; SBP: Spontaneous bacterial peritonitis; HCC: Hepatocellular carcinoma; IQR: Interquartile range; PPI: Proton pump inhibitor.

prior to liver decompensation would be a bias. Two additional landmark periods were used to validate the primary outcome: -3 mo to +3 mo and -3 mo to +9 mo.

PPI doses were defined using the "defined daily dose (DDD)," which is recommended by the World Health Organization to objectively measure the prescribed amount of a drug[23]. The cumulative defined daily dose (cDDD) ≥ 28 (≥ 1 mo of use) of prescribed medication was chosen, as PPI exposure of 1 mo has been reported to significantly cause adverse outcomes[24]. For the current study, PPI users were defined as those with a cDDD ≥ 28 within the landmark period. Patients with a past history of PPI use more than 3 mo prior to index admission were excluded from the study. Non-users were defined as those with cDDD < 28 within the landmark period, those with no PPI prescribed during the landmark period, or those prescribed with PPI after the landmark period regardless of the cumulative dosage.

Other relevant medication use at baseline, which could influence primary and secondary outcomes were also considered. Long-term use of concurrent medication was defined by more than 3 mo of medication prescribed, and was adjusted for in the analysis (Supplementary Table 2).

Statistical analysis

Categorical data were presented as frequency (percentage). Numeric data were presented as mean [standard deviation (SD)] for parametric distribution and median [interquartile range (IQR)] for non-parametric distribution. The differences in characteristics between PPI users and non-users were examined using the Chi-Square test or Fisher's Exact test for categorical variables, and two-sample *t*-test or Mann Whitney *U*-test for numerical variables, where appropriate.

Propensity score (PS) was first generated using logistic regression to reduce the selection bias of treatment allocation by balancing the characteristics of patients between treatment and control groups. The characteristics of patients such as demographics, aetiology of liver cirrhosis, history of HCC, and previous

Table 2 Mortality risk of proton pump inhibitor users by landmark periods and cumulative dose exposure

Periods	Number of patients	Adjusted HR (95%CI)	*P* value
6-mo landmark: (-3 to +6 mo)	Non-user = 57 PPI user = 238	Ref 2.10 (1.20-3.67)	0.009
3-mo landmark: (-3 to +3 mo)	Non-user = 71 PPI user = 261	Ref 1.36 (0.90-2.06)	0.143
9-mo landmark: (-3 to +9 mo)	Non-user = 42 PPI user = 221	Ref 3.44 (1.50-7.85)	0.003
Variable Dose Exposure	Number of patients	Adjusted HR (95%CI)	*P* value
6-mo landmark: (-3 to +6 mo)			
Non-user	57	Ref	
cDDD 28-90	18	1.34 (0.48-3.73)	0.579
cDDD 91-180	27	2.27 (1.10-5.14)	0.038
cDDD > 180	193	2.08 (1.17-3.61)	0.011
3-mo landmark: (-3 to +3 mo)			
Non-user	71	Ref	
cDDD 28-90	24	1.49 (0.74-3.03)	0.266
cDDD 91-180	34	2.04 (1.13-3.07)	0.019
cDDD > 180	203	1.33 (0.87 – 2.03)	0.188
9-mo landmark : (-3 to + 9 mo)			
Non-user	42	Ref	
cDDD 28-90	20	4.02 (1.33-12.12)	0.013
cDDD 91-180	22	3.38 (1.17 – 9.82)	0.025
cDDD > 180	179	3.52 (1.53 – 8.09)	0.003

HR: Hazard ratio (with propensity score adjustment); CI: Confidence interval; cDDD: Cumulative defined daily dose; PPI: Proton pump inhibitor.

decompensation (ascites, variceal bleed, SBP, HE, hepatorenal syndrome), medical co-morbidities, baseline MELD score, and baseline medication use (Supplementary Table 2), which could potentially confound the results on mortality and hospitalisation risks were adjusted for. For any significant differences in PS between the two groups, PS was further categorised into four quartiles in the two groups separately for matching.

After PS adjustment for 43 clinically important confounding variables at baseline, which could influence mortality and recurrent hepatic decompensation (Table 1), the effect of PPI use on mortality was assessed using the Cox proportional hazards model. Further variable landmark periods and subgroup analyses were performed to determine subgroups with increased risk of mortality. For secondary outcome of hospital admission for hepatic decompensation, Poisson regression (loglinear) was used with adjustment for PS (similarly as for primary outcome) and overall survival or number of days of follow-up. Relative risk and its 95% confidence interval (CI) were presented. A two-tailed, P value < 0.05 was considered statistically significant. Statistical analysis was performed with SPSS statistical software, version 19.0 (IBM Corp., Armonk, NY, United States). Statistical analysis and review were performed by biomedical statisticians.

RESULTS

A total of 2318 patients with ICD codings for liver cirrhosis at inpatient admissions were identified. A final cohort of 511 patients was included for landmark analysis (Figure 1), with 295 patients in the chosen landmark period of 6 mo. A total of 238 patients were PPI users and 57 were non-users; their baseline characteristics are described in Table 1. There were no significant differences in history of SBP or HE, between the PPI users and non-users. There was a higher usage of aspirin, anti-platelet drugs, statins, and non-selective beta blockers in the PPI user group compared to non-users. The baseline characteristics described were before propensity adjustment.

Overall risk of mortality

In the 6-mo landmark cohort, 102 of 238 (42.9%) PPI users and 13 of 57 (22.8%) non-

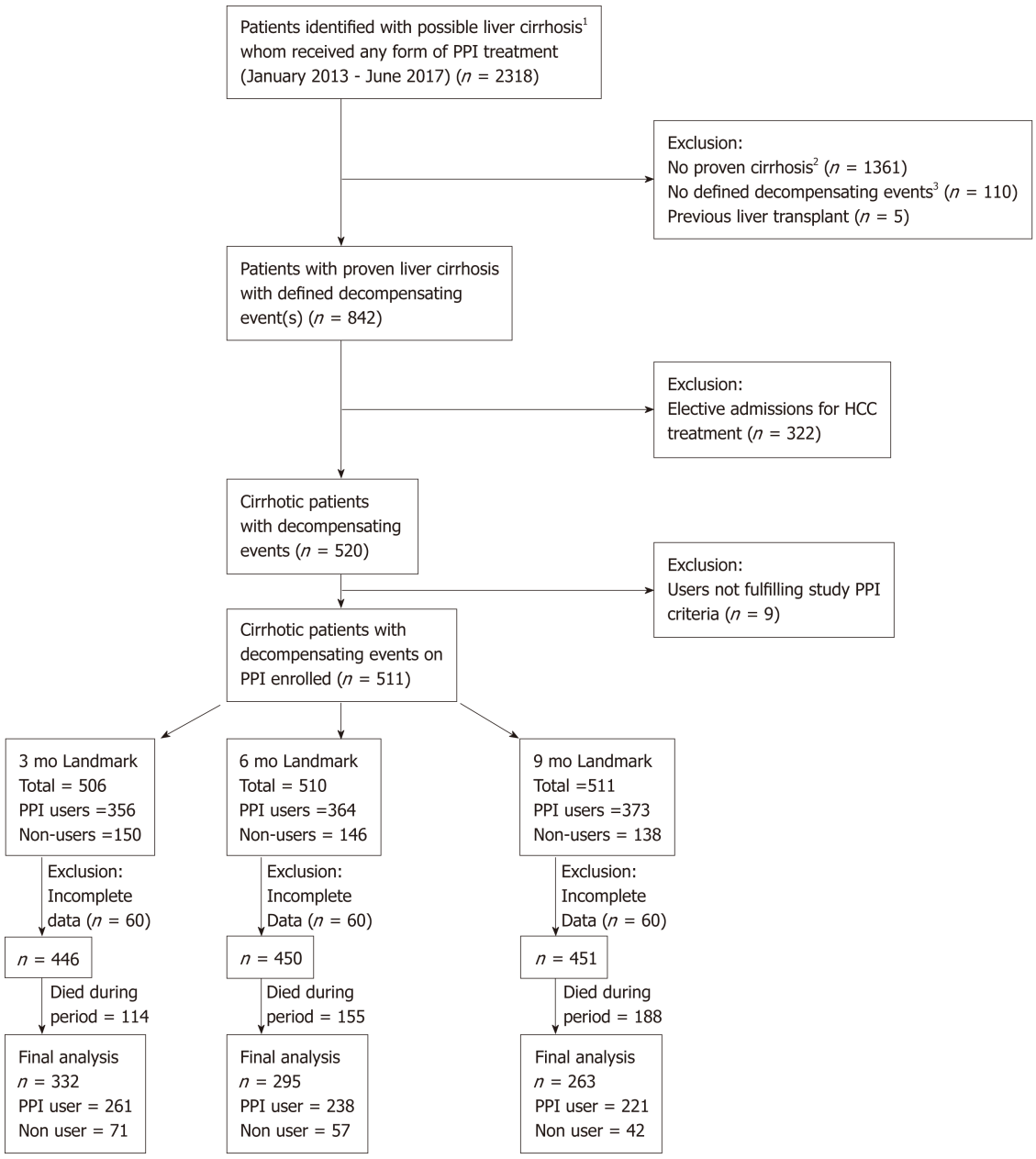

Figure 1 Consort diagram of landmark analysis. PPI: Proton pump inhibitor.

users died during the median follow-up period of 551 (IQR: 231-1017) and 584 (289-1152) d, respectively. Seven PPI users and one non-user underwent liver transplant during the follow-up period, before cox regression.

PPI users had a higher risk of overall mortality, compared to non-users with [adjusted HR (aHR) of 2.10, 95%CI (1.20-3.670); $P = 0.009$] (Table 2 and Figure 2). This was also observed in the 9-mo landmark cohort with aHR 3.44, (1.50-7.85); $P = 0.003$. In the 3-mo landmark cohort, the aHR was 1.36, but this was not statistically significant ($P = 0.143$). Longer PPI exposure with cDDD 91-180 was associated with higher mortality [aHR 2.27, (1.10-5.14); $P = 0.038$] compared to non-users in the 6-mo landmark cohort (Table 2). Long-term PPI exposure with cDDD > 180 was also associated with higher mortality in the 6-mo landmark cohort [aHR 2.08, (1.17-3.61); $P = 0.011$] (Table 2) and the 9-mo landmark cohort [aHR 3.52, (1.53-8.09); $P = 0.003$].

Subgroup and sensitivity analyses for mortality

In the subgroup analyses, PPI users with MELD15 was associated with increased mortality risk compared to non-users [aHR = 10.30, (1.41-75.58); $P = 0.022$] (Supplementary Table 3). There was a trend towards significance among patients with viral hepatitis aetiology [aHR 3.23, (0.99-10.52); $P = 0.052$], ascites [aHR 1.91, (0.96-3.78); $P = 0.063$], and those without prior decompensation at baseline [aHR 1.99, (0.98-4.00); $P = 0.057$] (Supplementary Table 3).

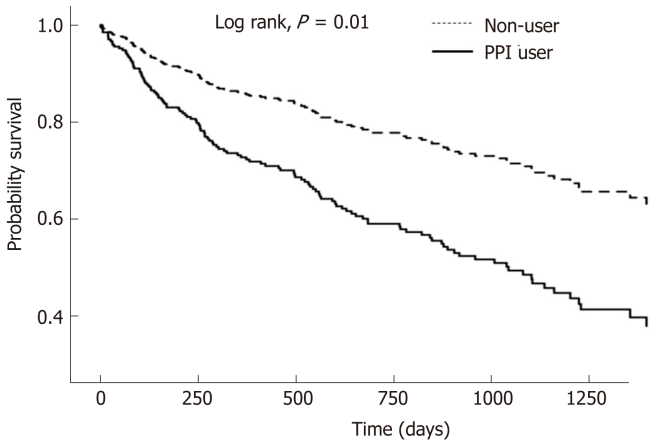

Time (d)	0	250	500	750	1000	1250
Non-user	57	50	46	45	44	44
PPI User	238	192	170	152	141	130

Figure 2 Survival analysis of PPI users and non-users for the 6-mo landmark period. PPI: Proton pump inhibitor.

Risk of hospitalisation for hepatic decompensation

The clinical characteristics of 335 PPI users and 116 non-users, for secondary outcome analysis, are described in Supplementary Table 4. There were 835 and 231 hospital admissions for PPI users and non-users respectively, for hepatic decompensation during the follow-up period. PPI users had a higher incidence of hospital admissions for hepatic decompensation with adjusted relative risk (aRR) of 1.61 [95%CI: 1.30-2.11, $P < 0.001$] (Table 3). Similar to the survival analysis for primary outcome, there was a dose-dependent effect of PPI on increased risk of hospitalisations for hepatic decompensation. Those with cDDD > 180 were more likely to have admissions for hepatic decompensation [aRR 1.91, (1.49-2.45); $P < 0.001$], compared to non-users (Figure 3).

DISCUSSION

In our study of patients with decompensated liver cirrhosis, PPI users had twice the risk of mortality [aHR 2.10, (1.20-3.67); $P = 0.009$] compared to non-users after adjusting for potential biases and confounders using landmark analysis, PS adjustment, and defined daily doses. We also found that PPI users were 61% more likely to have hospitalisation for hepatic decompensation than non-users [aRR = 1.61, (1.30-2.15); $P < 0.001$]. Longer exposure to PPI with cDDD 91-180 increased mortality risk [aHR = 2.27, (1.10-5.14); $P = 0.038$] and long-term PPI use with cDDD > 180 had a higher risk of admission for hepatic decompensation compared to non-users ($P < 0.001$).

Previous studies have suggested that PPI use may be associated with a higher risk of mortality. Dultz *et al*[16] reported PPI use to be an independent predictor of mortality in patients with compensated and decompensated liver cirrhosis [HR = 2.33, (1.26–4.29); $P = 0.007$], but another study performed on hospitalised cirrhotic patients did not show a difference in survival between PPI users and non-users[13]. Hung *et al*[17] studied the effect of inpatient PPI use on survival in cirrhotic patients admitted with HE and reported a higher 30-d mortality in the PPI group (HR = 1.360, (1.208-1.532); $P < 0.001$], but not in their separate study of patients with SBP[18]. These studies have not shown consistent results on the association of PPI use and mortality, which could potentially be related to issues with defining the duration of PPI exposure and the classification of PPI user status, leading to potential biases. As PPI use is prevalent particularly in patients with history of stroke or myocardial infarction, the mortality analysis in this population should be adjusted for underlying cardiovascular disease and the use of relevant medications. Our study showed that after correcting for these different potential biases and 43 relevant confounders for mortality, decompensated cirrhotic patients with PPI use, particularly with prolonged duration, have an increased risk of mortality.

The use of PPI has been shown to induce gut dysbiosis[7,8,25], which could increase the risk of hepatic decompensation with HE and SBP[9,10]. Our study found that PPI

Table 3 Hospital admissions for hepatic decompensation for proton pump inhibitor users and non-users with decompensated liver cirrhosis

	Number of patients	Hospital admissions for liver decompensation	
		Adjusted RR (95%CI)	*P* value
Entire cohort	PPI user = 335 Non-user = 116	1.61 (1.30-2.11)	< 0.001
Dose exposure			
Non-user	116	Ref	
cDDD 28-90	49	0.65 (0.39-1.08)	0.10
cDDD 91-180	61	1.08 (0.74-1.59)	0.69
cDDD > 180	225	1.91 (1.49-2.45)	< 0.001

cDDD: Cumulative defined daily dose; RR: Relative risk; CI: Confidence interval; PPI: Proton pump inhibitor.

users with decompensated cirrhosis had a higher risk of portal hypertension-related decompensations requiring hospital admission. Our study findings support the evidence from a recent study showing increased all-cause, 1-mo, and 3-mo hospital readmissions among cirrhotic patients[12].

There are several reasons that could explain higher mortality and increased occurrence of hepatic events with PPI use in patients with decompensated liver cirrhosis. First, pathological bacterial translocation increases with the severity of liver disease[26]. In decompensated cirrhosis, the secretion of antimicrobial peptides diminishes, intestinal permeability increases, and small intestinal bacterial overgrowth accelerates including enhanced transcellular epithelial crossing of viable bacteria[26], all of which lead to an increased risk of pathologic bacterial translocation. Second, gastric hydrochloric acid is bactericidal and is a defence mechanism from ingested microorganisms[27]. However, PPIs are strong gastric acid suppressants, thus limiting this defence[28]. Furthermore, in liver cirrhosis, there is reduced hepatic clearance of PPI[15], which thus increases the overall PPI exposure. Last and perhaps most importantly, PPIs also affect the gut microenvironment by modifying pH in the stomach and small intestine and is proven to cause gut dysbiosis. Dysbiosis in particular, can drive inflammasome-deficiency-associated changes through microbiome derived metabolites, which worsens hepatic inflammation and produces endotoxins that exacerbate intestinal permeability and inflammation[29,30]. These potentially explain why PPI use is a known risk factor for bacterial infections, HE, and SBP. Hence, PPI use, which diminishes the body's natural defence from microorganisms and causes dysbiosis, in combination with increased pathological bacterial translocation in decompensated cirrhosis could increase hepatic decompensation, infection risk, and ultimately mortality in patients with advanced liver cirrhosis. In our subgroup analysis, PPI users with MELD ≥ 15 were associated with a higher mortality risk compared to non-users. This suggests that patients with advanced cirrhosis are more prone to effects from dysbiosis, infections, and hepatic decompensation. Further studies are required to see if active cessation of PPI in advanced cirrhotic patients would improve survival.

In our study, we calculated PPI exposure using cumulative defined daily doses and used fixed landmark periods to define users, past users and non-users. This method reduces biases in selecting "users". In the landmark analysis, PPI use 3 mo prior to index admission was accounted for because PPI users with cirrhosis had increased 3-mo hospital readmission rates compared to non-users[12]. Exclusion of the group already exposed to PPI prior to decompensation would be a confounder and reduces the true effect of PPI on hepatic decompensation and mortality. Furthermore, there are significant baseline clinical characteristics, comorbidities, and concurrent medications that would be associated with hepatic decompensation, cardiovascular events, and ultimately overall mortality. Therefore, we considered PS adjustment for these variables (Supplementary Tables 1 and 2).

Our study had several limitations. First, PPI use was measured using physician prescriptions available in our electronic system. We do not have data on patient adherence to the PPI prescribed or data from private practitioners. However, only patients on follow-up at our hospital were included. Prescriptions from and admission to private hospitals were very minimal. To mitigate indication bias of PPI use, we included baseline comorbidities such as GERD, esophagitis, peptic ulcer disease, and those on anti-platelet agents such as aspirin and clopidogrel. We could

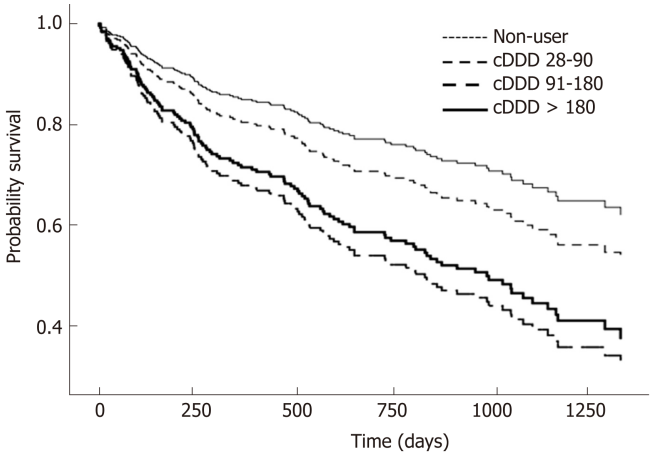

Figure 3 Survival analysis of PPI users and non-users with decompensated liver cirrhosis by cumulative dose exposure in the 6-mo landmark cohort. PPI: Proton pump inhibitor.

not adjust for PPI use in functional dyspepsia, but this should not require long-term PPI use. There are several residual confounders that could have impacted mortality and hepatic decompensation in our study such as obesity[4], sarcopenia[31,32], and smoking[33]. We adjusted for antibiotic use but did not include rifaximin, a non-aminoglycoside semi-synthetic antibacterial, as it was only publicly funded in Singapore towards the end of our study period and hence is not yet widely available. Our study did not analyse hospital admission for other reasons without hepatic decompensations such as pneumonia, *C. difficile* and enteric infections, which are known associations with PPI use[14]. However, most episodes of hepatic decompensation would be triggered as a result of infections and would hence be captured in our study. We used all-cause mortality as an objective measure of primary outcome. The exact cause of death was difficult to ascertain in this retrospective study. For example, when a decompensated patient was admitted for HE and passed on after developing aspiration pneumonia and SBP, it was unclear if the cause of death was pneumonia or a liver-related death. Analysing dichotomised outcomes for liver and non-liver related deaths would then introduce ambiguity and bias. Finally, our study only analysed episodes of decompensation severe enough for hospitalisation, but not those with mild decompensated cirrhosis managed as an outpatient.

In conclusion, PPI use in patients with decompensated liver cirrhosis is associated with higher mortality and severe hepatic decompensations requiring hospital admission. Further prospective studies are required to confirm these findings and determine causality. A cumulative defined daily dose > 90 has a higher risk of mortality and PPI should be limited to a shorter duration and dosage if needed, or stopped if there is no indication.

ARTICLE HIGHLIGHTS

Research background

Proton pump inhibitor (PPI) use is associated with an increased risk of mortality but is not well studied in patients with decompensated liver cirrhosis. The impact and definition of significant dose exposure are also not known. Although previous studies have looked into this relationship, there are several unaddressed issues such as PPI users not being well defined, the presence of many confounding factors, and indications for PPIs not being adjusted for. Also, this particular patient population of decompensated cirrhotic patients has not been well studied. Our study investigated if PPI use is independently associated with increased mortality risk in decompensated liver cirrhosis after adjustment for indications, medications, baseline variables and co-morbidities, and established the impact of dose exposure on mortality.

Research motivation

PPIs are prescribed widely and for long durations even in patients with liver cirrhosis. If a convincing relationship with increased mortality risk and dose exposure is established, stopping or shortening the duration of PPIs when possible should be strongly advocated.

Research objectives

This study confirms our main objective, that PPI usage in decompensated liver cirrhosis patients is an independent factor associated with an increased risk of mortality. In addition, a longer dose

exposure of more than 90 cumulative defined daily doses was found to significantly increase this risk. We hence advocate reviewing PPI use in patients with liver cirrhosis with a view to shorten or deprescribe when possible.

Research methods
This is a retrospective cohort study using a hospital database. PPI users were defined as those with more than 28 defined daily doses used within a study landmark period. Users and non-users were compared after adjusting for 43 variables including baseline characteristics, comorbidities, PPI indications, and medications.

Research results
A total of 295 patients were included for analysis in the study. PPI users had a higher mortality compared to non-users and longer PPI use with more than 90 cumulative defined daily doses was associated with higher mortality. PPI users also had a higher incidence of hospitalisation for hepatic decompensation.

Research conclusions
The impact of varying PPI dose exposure in decompensated cirrhotics has not been previously described. This study showed that a cumulative defined daily dose > 90 is associated with higher mortality in patients with decompensated liver cirrhosis. Patients with decompensated liver cirrhosis have increased intestinal permeability and decreased hepatic clearance of PPIs, which predispose to gut dysbiosis and increases the risk of severe hepatic decompensation and ultimately mortality. Higher dose exposure to PPI worsens this. PPIs can be harmful when given for long durations in patients with decompensated liver cirrhosis by increasing the risk of further decompensation and death. Longer PPI dose exposure, in particular more than 90 cumulative defined daily doses can be harmful in patients with decompensated liver cirrhosis. PPIs inhibit the bactericidal effect of gastric hydrochloric acid and predispose to gut dysbiosis. When used in patients with decompensated liver cirrhosis who have decreased hepatic clearance of PPI, there is increased dose exposure that can potentially cause more harm. PPI users were well defined in this study by using defined daily doses and a cumulative dose ≥ 28 within a landmark period. Also, users and non-users were compared after important adjustments such as indication for PPI use and medication use such as antiplatelets, which were not accounted for in prior studies. PPI use should be reviewed regularly especially in patients with liver cirrhosis. It should be stopped when there are no indications. If PPIs are indicated, dosage should be reduced to the lowest possible dose.

Research perspectives
There were potential confounding factors that could have affected the results. However, this represents real world data and the current difficulties faced. The differences were also minimised using statistical methods such as propensity adjustment or matching. Future research should be conducted to prove the mechanisms on how PPIs modulate gut microbiota causing dysbiosis and hepatic decompensations and also to determine if PPI withdrawal can reverse mortality risk. Larger cohort, prospective studies should be performed with a view on proving causality.

ACKNOWLEDGEMENTS
We would like to thank Dr. Prem Harichander Thurairajah for critically reviewing and proofreading the manuscript, and Dr. Zhenwei Teo for technical and language editing and proofreading the manuscript.

REFERENCES
1 **Maggio M**, Corsonello A, Ceda GP, Cattabiani C, Lauretani F, Buttò V, Ferrucci L, Bandinelli S, Abbatecola AM, Spazzafumo L, Lattanzio F. Proton pump inhibitors and risk of 1-year mortality and rehospitalization in older patients discharged from acute care hospitals. *JAMA Intern Med* 2013; **173**: 518-523 [PMID: 23460307 DOI: 10.1001/jamainternmed.2013.2851]
2 **Hsiang JC**, Gane EJ, Bai WW, Gerred SJ. Type 2 diabetes: a risk factor for liver mortality and complications in hepatitis B cirrhosis patients. *J Gastroenterol Hepatol* 2015; **30**: 591-599 [PMID: 25250942 DOI: 10.1111/jgh.12790]
3 **Pang Y**, Kartsonaki C, Turnbull I, Guo Y, Clarke R, Chen Y, Bragg F, Yang L, Bian Z, Millwood IY, Hao J, Han X, Zang Y, Chen J, Li L, Holmes MV, Chen Z. Diabetes, Plasma Glucose, and Incidence of Fatty Liver, Cirrhosis, and Liver Cancer: A Prospective Study of 0.5 Million People. *Hepatology* 2018; **68**: 1308-1318 [PMID: 29734463 DOI: 10.1002/hep.30083]
4 **Hart CL**, Morrison DS, Batty GD, Mitchell RJ, Davey Smith G. Effect of body mass index and alcohol consumption on liver disease: analysis of data from two prospective cohort studies. *BMJ* 2010; **340**: c1240 [PMID: 20223873 DOI: 10.1136/bmj.c1240]
5 **Acharya C**, Bajaj JS. Gut Microbiota and Complications of Liver Disease. *Gastroenterol Clin North Am* 2017; **46**: 155-169 [PMID: 28164848 DOI: 10.1016/j.gtc.2016.09.013]
6 **Bajaj JS**, Heuman DM, Hylemon PB, Sanyal AJ, White MB, Monteith P, Noble NA, Unser AB, Daita K, Fisher AR, Sikaroodi M, Gillevet PM. Altered profile of human gut microbiome is associated with cirrhosis and its complications. *J Hepatol* 2014; **60**: 940-947 [PMID: 24374295 DOI: 10.1016/j.jhep.2013.12.019]
7 **Imhann F**, Bonder MJ, Vich Vila A, Fu J, Mujagic Z, Vork L, Tigchelaar EF, Jankipersadsing SA, Cenit

MC, Harmsen HJ, Dijkstra G, Franke L, Xavier RJ, Jonkers D, Wijmenga C, Weersma RK, Zhernakova A. Proton pump inhibitors affect the gut microbiome. *Gut* 2016; **65**: 740-748 [PMID: 26657899 DOI: 10.1136/gutjnl-2015-310376]

8 **Freedberg DE**, Toussaint NC, Chen SP, Ratner AJ, Whittier S, Wang TC, Wang HH, Abrams JA. Proton Pump Inhibitors Alter Specific Taxa in the Human Gastrointestinal Microbiome: A Crossover Trial. *Gastroenterology* 2015; **149**: 883-885.e9 [PMID: 26164495 DOI: 10.1053/j.gastro.2015.06.043]

9 **Brandl K**, Schnabl B. Is intestinal inflammation linking dysbiosis to gut barrier dysfunction during liver disease? *Expert Rev Gastroenterol Hepatol* 2015; **9**: 1069-1076 [PMID: 26088524 DOI: 10.1586/17474124.2015.1057122]

10 **Dam G**, Vilstrup H, Watson H, Jepsen P. Proton pump inhibitors as a risk factor for hepatic encephalopathy and spontaneous bacterial peritonitis in patients with cirrhosis with ascites. *Hepatology* 2016; **64**: 1265-1272 [PMID: 27474889 DOI: 10.1002/hep.28737]

11 **Weersink RA**, Bouma M, Burger DM, Drenth JPH, Harkes-Idzinga SF, Hunfeld NGM, Metselaar HJ, Monster-Simons MH, van Putten SAW, Taxis K, Borgsteede SD. Safe use of proton pump inhibitors in patients with cirrhosis. *Br J Clin Pharmacol* 2018; **84**: 1806-1820 [PMID: 29688583 DOI: 10.1111/bcp.13615]

12 **Bajaj JS**, Acharya C, Fagan A, White MB, Gavis E, Heuman DM, Hylemon PB, Fuchs M, Puri P, Schubert ML, Sanyal AJ, Sterling RK, Stravitz TR, Siddiqui MS, Luketic V, Lee H, Sikaroodi M, Gillevet PM. Proton Pump Inhibitor Initiation and Withdrawal affects Gut Microbiota and Readmission Risk in Cirrhosis. *Am J Gastroenterol* 2018; **113**: 1177-1186 [PMID: 29872220 DOI: 10.1038/s41395-018-0085-9]

13 **Cole HL**, Pennycook S, Hayes PC. The impact of proton pump inhibitor therapy on patients with liver disease. *Aliment Pharmacol Ther* 2016; **44**: 1213-1223 [PMID: 27774677 DOI: 10.1111/apt.13827]

14 **Yang YX**, Metz DC. Safety of proton pump inhibitor exposure. *Gastroenterology* 2010; **139**: 1115-1127 [PMID: 20727892 DOI: 10.1053/j.gastro.2010.08.023]

15 **Lodato F**, Azzaroli F, Di Girolamo M, Feletti V, Cecinato P, Lisotti A, Festi D, Roda E, Mazzella G. Proton pump inhibitors in cirrhosis: tradition or evidence based practice? *World J Gastroenterol* 2008; **14**: 2980-2985 [PMID: 18494046 DOI: 10.3748/wjg.14.2980]

16 **Dultz G**, Piiper A, Zeuzem S, Kronenberger B, Waidmann O. Proton pump inhibitor treatment is associated with the severity of liver disease and increased mortality in patients with cirrhosis. *Aliment Pharmacol Ther* 2015; **41**: 459-466 [PMID: 25523381 DOI: 10.1111/apt.13061]

17 **Hung TH**, Lee HF, Tseng CW, Tsai CC, Tsai CC. Effect of proton pump inhibitors in hospitalization on mortality of patients with hepatic encephalopathy and cirrhosis but no active gastrointestinal bleeding. *Clin Res Hepatol Gastroenterol* 2018; **42**: 353-359 [PMID: 29551615 DOI: 10.1016/j.clinre.2017.11.011]

18 **Hung TH**, Tseng CW, Lee HF, Tsai CC, Tsai CC. Effect of Proton Pump Inhibitors on Mortality in Patients with Cirrhosis and Spontaneous Bacterial Peritonitis. *Ann Hepatol* 2018; **17**: 933-939 [DOI: 10.5604/01.3001.0012.7193]

19 **Giobbie-Hurder A**, Gelber RD, Regan MM. Challenges of guarantee-time bias. *J Clin Oncol* 2013; **31**: 2963-2969 [PMID: 23835712 DOI: 10.1200/JCO.2013.49.5283]

20 **Marshall RJ**. Assessment of exposure misclassification bias in case-control studies using validation data. *J Clin Epidemiol* 1997; **50**: 15-19 [DOI: 10.1016/S0895-4356(96)00315-0]

21 **European Association for the Study of the Liver**. European Association for the Study of the Liver, EASL Clinical Practice Guidelines for the management of patients with decompensated cirrhosis. *J Hepatol* 2018; **69**: 406-460 [PMID: 29653741 DOI: 10.1016/j.jhep.2018.03.024]

22 **Dafni U**. Landmark analysis at the 25-year landmark point. *Circ Cardiovasc Qual Outcomes* 2011; **4**: 363-371 [PMID: 21586725 DOI: 10.1161/CIRCOUTCOMES.110.957951]

23 **WHO Collaborating Centre for Drug Statistics Methodology**. Guidelines for ATC classification and DDD assignment, 2015. Oslo. 2014; Available from: http://www.whocc.no/filearchive/publications/2015_guidelines.pdf.

24 **Xie Y**, Bowe B, Li T, Xian H, Yan Y, Al-Aly Z. Risk of death among users of Proton Pump Inhibitors: a longitudinal observational cohort study of United States veterans. *BMJ Open* 2017; **7**: e015735 [PMID: 28676480 DOI: 10.1136/bmjopen-2016-015735]

25 **Wellhöner F**, Döscher N, Marius V, Plumeier I, Kahl S, Potthoff A, Manns MP, Dietmar P, Wedemeyer H, Cornberg M, Heidrich B. The Impact of proton pump inhibitors on the intestinal microbiota in chronic hepatitis C patients. *Journal of hepatology* [DOI: 10.1016/S0168-8278(18)31475-2]

26 **Wiest R**, Lawson M, Geuking M. Pathological bacterial translocation in liver cirrhosis. *J Hepatol* 2014; **60**: 197-209 [PMID: 23993913 DOI: 10.1016/j.jhep.2013.07.044]

27 **Freedberg DE**, Kim LS, Yang YX. The Risks and Benefits of Long-term Use of Proton Pump Inhibitors: Expert Review and Best Practice Advice From the American Gastroenterological Association. *Gastroenterology* 2017; **152**: 706-715 [PMID: 28257716 DOI: 10.1053/j.gastro.2017.01.031]

28 **Scarpignato C**, Gatta L, Zullo A, Blandizzi C; SIF-AIGO-FIMMG Group; Italian Society of Pharmacology, the Italian Association of Hospital Gastroenterologists, and the Italian Federation of General Practitioners. Effective and safe proton pump inhibitor therapy in acid-related diseases - A position paper addressing benefits and potential harms of acid suppression. *BMC Med* 2016; **14**: 179 [PMID: 27825371 DOI: 10.1186/s12916-016-0718-z]

29 **Henao-Mejia J**, Elinav E, Jin C, Hao L, Mehal WZ, Strowig T, Thaiss CA, Kau AL, Eisenbarth SC, Jurczak MJ, Camporez JP, Shulman GI, Gordon JI, Hoffman HM, Flavell RA. Inflammasome-mediated dysbiosis regulates progression of NAFLD and obesity. *Nature* 2012; **482**: 179-185 [PMID: 22297845 DOI: 10.1038/nature10809]

30 **Chen P**, Stärkel P, Turner JR, Ho SB, Schnabl B. Dysbiosis-induced intestinal inflammation activates tumor necrosis factor receptor I and mediates alcoholic liver disease in mice. *Hepatology* 2015; **61**: 883-894 [PMID: 25251280 DOI: 10.1002/hep.27489]

31 **Montano-Loza AJ**. Clinical relevance of sarcopenia in patients with cirrhosis. *World J Gastroenterol* 2014; **20**: 8061-8071 [PMID: 25009378 DOI: 10.3748/wjg.v20.i25.8061]

32 **European Association for the Study of the Liver**. European Association for the Study of the Liver. EASL Clinical Practice Guidelines on nutrition in chronic liver disease. *J Hepatol* 2019; **70**: 172-193 [PMID: 30144956 DOI: 10.1016/j.jhep.2018.06.024]

33 **Altamirano J**, Bataller R. Cigarette smoking and chronic liver diseases. *Gut* 2010; **59**: 1159-1162 [PMID: 20650922 DOI: 10.1136/gut.2008.162453]

World Journal of Gastroenterology

Submit a Manuscript: https://www.f6publishing.com

World J Gastroenterol 2019 September 7; 25(33): 4945-4958

DOI: 10.3748/wjg.v25.i33.4945

ISSN 1007-9327 (print) ISSN 2219-2840 (online)

ORIGINAL ARTICLE

Retrospective Cohort Study

Prognostic value of preoperative carcinoembryonic antigen/tumor size in rectal cancer

Du Cai, Zeng-Hong Huang, Hui-Chuan Yu, Xiao-Lin Wang, Liang-Liang Bai, Guan-Nan Tang, Shao-Yong Peng, Ying-Jie Li, Mei-Jin Huang, Guang-Wen Cao, Jian-Ping Wang, Yan-Xin Luo

ORCID number: Du Cai (0000-0002-8894-7973); Zeng-Hong Huang (0000-0003-3625-315X); Hui-Chuan Yu (0000-0001-8357-1615); Xiao-Lin Wang (0000-0002-3911-6911); Liang-Liang Bai (0000-0002-1547-7931); Guan-Nan Tang (0000-0001-6063-189X); Shao-Yong Peng (000-0002-5489-4869); Ying-Jie Li (0000-0003-3386-0210); Meijin Huang (0000-0002-5483-4591); Guang-Wen Cao (0000-0002-8094-1278); Jian-Ping Wang (0000-0003-4654-6722); Yan-Xin Luo (0000-0002-5200-3997).

Author contributions: Cai D and Huang ZH contributed equally to this paper. Luo YX, Wang JP, Cao GW, and Huang MJ designed the research; Cai D and Huang ZH analyzed the data and drafted the article; Yu HC and Luo YX revised the article; Bai LL, Tang GN, Peng SY, and Li YJ collected and collated the data.

Supported by the National Basic Research Program of China (973 Program) (No. 2015CB554001, JW), the National Natural Science Foundation of China (No. 81972245, YL; No. 81902877, HY), the Natural Science Fund for Distinguished Young Scholars of Guangdong Province (No. 2016A030306002, YL), the Tip-top Scientific and Technical Innovative Youth Talents of Guangdong special support program (No. 2015TQ01R454, YL), the Project 5010 of Clinical Medical Research of Sun Yat-sen University-5010 Cultivation Foundation (No. 2018026, YL), the Natural Science

Du Cai, Zeng-Hong Huang, Hui-Chuan Yu, Xiao-Lin Wang, Liang-Liang Bai, Guan-Nan Tang, Shao-Yong Peng, Ying-Jie Li, Jian-Ping Wang, Yan-Xin Luo, Guangdong Institute of Gastroenterology, Guangdong Provincial Key Laboratory of Colorectal and Pelvic Floor Disease (Supported by National Key Clinical Discipline), The Sixth Affiliated Hospital, Sun Yat-sen University, Guangzhou 510655, Guangdong Province, China

Du Cai, Zeng-Hong Huang, Shao-Yong Peng, Mei-Jin Huang, Jian-Ping Wang, Yan-Xin Luo, Department of Colorectal Surgery, The Sixth Affiliated Hospital, Sun Yat-sen University, Guangzhou 510655, Guangdong Province, China

Zeng-Hong Huang, Department of Biochemistry and Molecular Medicine, School of Medicine, University of California, Davis, Sacramento, CA 95817, United States

Guang-Wen Cao, Department of Epidemiology, Second Military Medical University, Shanghai 200433, China

Corresponding author: Yan-Xin Luo, MA, MD, PhD, Associate Professor, Chief Doctor, Doctor, Surgical Oncologist, Department of Colorectal Surgery, Guangdong Institute of Gastroenterology, Guangdong Provincial Key Laboratory of Colorectal and Pelvic Floor Disease, The Sixth Affiliated Hospital, Sun Yat-sen University, 26 Yuancun Erheng Road, Guangzhou 510655, Guangdong Province, China. luoyx25@mail.sysu.edu.cn
Telephone: +86-13826190263
Fax: +86-20-38254221

Abstract

BACKGROUND

Carcinoembryonic antigen (CEA) is a commonly used biomarker in colorectal cancer. However, controversy exists regarding the insufficient prognostic value of preoperative serum CEA alone in rectal cancer. Here, we combined preoperative serum CEA and the maximum tumor diameter to correct the CEA level, which may better reflect the malignancy of rectal cancer.

AIM

To assess the prognostic impact of preoperative CEA/tumor size in rectal cancer.

METHODS

We retrospectively reviewed 696 stage I to III rectal cancer patients who underwent curative tumor resection from 2007 to 2012. These patients were randomly divided into two cohorts for cross-validation: training cohort and validation cohort. The training cohort was used to generate an optimal cutoff

Foundation of Guangdong Province (No. 2016A030310222, HY; No. 2018A0303130303, HY), the Program of Introducing Talents of Discipline to Universities, and National Key Clinical Discipline (2012).

Institutional review board statement: This study was reviewed and approved by the Ethics Committee of the Sixth Affiliated Hospital, Sun Yat-sen University.

Informed consent statement: Patients were not required to provide informed consent for the study because the analysis used anonymous clinical data.

Conflict-of-interest statement: The authors declare that they have no conflict of interest.

Data sharing statement: No additional data are available.

STROBE statement: The authors have read the STROBE Statement-checklist of items, and the manuscript was prepared and revised according to the STROBE Statement-checklist of items.

Manuscript source: Invited manuscript

Received: March 12, 2019
Peer-review started: March 12, 2019
First decision: March 27, 2019
Revised: April 4, 2019
Accepted: May 18, 2019
Article in press: May 18, 2019
Published online: September 7, 2019

P-Reviewer: Alkan A, Ziogas DE
S-Editor: Ma RY
L-Editor: Wang TQ
E-Editor: Ma YJ

point and the validation cohort was used to further validate the model. Maximally selected rank statistics were used to identify the optimum cutoff for CEA/tumor size. The Kaplan-Meier method and log-rank test were used to plot the survival curve and to compare the survival data. Univariate and multivariate Cox regression analyses were used to determine the prognostic value of CEA/tumor size. The primary and secondary outcomes were overall survival (OS) and disease-free survival (DFS), respectively.

RESULTS

In all, 556 patients who satisfied both the inclusion and exclusion criteria were included and randomly divided into the training cohort (2/3 of 556, n = 371) and the validation cohort (1/3 of 556, n = 185). The cutoff was 2.429 ng/mL per cm. Comparison of the baseline data showed that high CEA/tumor size was correlated with older age, high TNM stage, the presence of perineural invasion, high CEA, and high carbohydrate antigen 19-9 (CA 19-9). Kaplan-Meier curves showed a manifest reduction in 5-year OS (training cohort: 56.7% *vs* 81.1%, P < 0.001; validation cohort: 58.8% *vs* 85.6%, P < 0.001) and DFS (training cohort: 52.5% *vs* 71.9%, P = 0.02; validation cohort: 50.3% *vs* 79.3%, P = 0.002) in the high CEA/tumor size group compared with the low CEA/tumor size group. Univariate and multivariate analyses identified CEA/tumor size as an independent prognostic factor for OS (training cohort: hazard ratio (HR) = 2.18, 95% confidence interval (CI): 1.28-3.73, P = 0.004; validation cohort: HR = 4.83, 95%CI: 2.21-10.52, P < 0.001) as well as DFS (training cohort: HR = 1.47, 95%CI: 0.93-2.33, P = 0.096; validation cohort: HR = 2.61, 95%CI: 1.38-4.95, P = 0.003).

CONCLUSION

Preoperative CEA/tumor size is an independent prognostic factor for patients with stage I-III rectal cancer. Higher CEA/tumor size is associated with worse OS and DFS.

Key words: Carcinoembryonic antigen; Carcinoembryonic antigen/tumor size; Rectal cancer; Prognosis; Survival analysis

Core tip: This is a retrospective study that sought to evaluate the prognostic value of carcinoembryonic antigen (CEA)/tumor size in rectal cancer, which may better reflect the tumor malignancy. Maximally selected rank statistics identified an optimal cutoff point of 2.429 ng/mL per cm for CEA/tumor size. Kaplan-Meier curves showed a significant reduction in the 5-year overall survival and disease-free survival in the high CEA/tumor size group. Univariate and multivariate analyses identified CEA/tumor size as an independent prognostic factor for stage I to III rectal cancer.

Citation: Cai D, Huang ZH, Yu HC, Wang XL, Bai LL, Tang GN, Peng SY, Li YJ, Huang MJ, Cao GW, Wang JP, Luo YX. Prognostic value of preoperative carcinoembryonic antigen/tumor size in rectal cancer. *World J Gastroenterol* 2019; 25(33): 4945-4958
URL: https://www.wjgnet.com/1007-9327/full/v25/i33/4945.htm
DOI: https://dx.doi.org/10.3748/wjg.v25.i33.4945

INTRODUCTION

Colorectal cancer (CRC) is the third most frequently diagnosed malignancy and one of the leading causes of cancer-related mortality worldwide[1]. Although Western developed countries show a steady or slightly declining trend, the morbidity and mortality of CRC in developing countries like China are still on the rise[2]. Unlike Western countries, the incidence of rectal cancer is higher than that of colon cancer in China and the prognosis of rectal cancer still needs to be improved[3]. Therapy options for CRC have been developed rapidly in the past decade, but selecting optimal treatments for individuals remains a great challenge for clinicians due to the lack of effective markers[4]. In recent years, biomarkers have played an increasingly vital role

in the detection and management of CRC[5]. Among the biomarkers, carcinoembryonic antigen (CEA) is one of the most common and most convenient preoperative detecting indexes in patients with colorectal cancer[6].

CEA, a large glycoprotein, has been recommended by the American Society of Clinical Oncology (ASCO) and the European Group on Tumor Markers (EGTM) as a prognostic biomarker that can be used to determine the prognosis and stage of CRC[5,7]. However, controversy still exists regarding the prognostic value of the absolute preoperative serum CEA level in colorectal cancer. Recent studies have noted that CEA is insufficiently sensitive to be used alone, and some researchers have sought new ways to improve its prognostic value by the addition of another factor, such as CD44v6, carbohydrate antigen (CA) 19-9, neutrophil-to-lymphocyte ratio (NLR), or peritoneal carcinomatosis index ratio (PCI)[6,8-11]. Intriguingly, a recent study indicated that postoperative tissue CEA (t-CEA) rather than serum CEA (s-CEA) is an independent prognostic factor in stage I to III CRC[12]. This indicated that we should pay more attention to the local CEA produced by tumor cells rather than the overall serum CEA level. Considering that detecting the CEA produced and secreted by all tumor cells is not realistic, using the ratio of CEA to tumor size may somehow reflect the ability of tumor cells to secrete CEA. Another research group demonstrated that CEA density is a prognostic factor for percutaneous ablation of pulmonary colorectal metastases[13]. Using tumor size to adjust and improve the prognostic value of tumor marker is not uncommon, such as prostate specific antigen density and tumor-infiltrating CD8+ T-cell density[14,15]. Maximum tumor diameter is also a prognostic indicator for some solid tumors including prostate cancer and colorectal liver metastases[16,17]. While the volume-adjusted prostate-specific antigen has been widely studied as a useful marker in prostate cancer[18,19], whether the combination of CEA level and tumor size serves as a novel prognostic factor for rectal cancer remains unresolved.

In this study, we considered both the preoperative serum CEA level and the rectal tumor size and devised the CEA/tumor size, which represents the CEA level adjusted by tumor size, to better reflect the malignancy of rectal cancer. We also refined the insufficient prognostic value of serum CEA. We aimed to apply this new approach to investigate the prognostic impact of the preoperative CEA/tumor size in patients with rectal cancer.

MATERIALS AND METHODS

Patients

Patients who were diagnosed with stage I to III rectal cancer and underwent a radical excision at the Sixth Affiliated Hospital of Sun Yat-Sen University from 2007 to 2012 were studied. This study was approved by the Medical Ethics Committee of the Sixth Affiliated Hospital of Sun Yat-sen University and did not cause any harm to the patients. All retrospective data were obtained from a database maintained by the Sixth Affiliated Hospital of Sun Yat-sen University. The inclusion criteria were as follows: (1) Histologically confirmed adenocarcinoma; (2) Stage I to III according to the 8th edition of the American Joint Committee on Cancer (AJCC); and (3) Radical resection. The following patients were excluded: (1) Those with nonprimary cancers; (2) Patients who received neoadjuvant chemotherapy and/or radiotherapy; and (3) Patients with missing data on preoperative CEA or tumor size. Patients who satisfied both the inclusion and exclusion criteria were randomly divided into two cohorts for cross-validation: Training cohort and validation cohort. The training cohort was used to generate an optimal cutoff point and the validation cohort was used to test the applicability of this cutoff point and the model.

Data collection

The following data were collected using the Electronic Medical Record System: Age, sex, histological features, TNM stage (AJCC), differentiation degree, presence of lymphovascular invasion, presence of perineural invasion, preoperative serum CA 19-9 and CEA levels, maximum tumor diameter, recurrence, and survival time. Follow-up was conducted every three months during the first year after resection, every six months during the next two years, and once a year thereafter. Routine physical examination, serum CEA test, and radiographic examinations including chest radiography, abdominopelvic computed tomographic scanning, or ultrasonography, whole-body bone scanning, double-contrast barium enema, and colonoscopy were performed and recorded six months after resection and yearly thereafter. The follow-up time ended in June 2016, and the follow-up interval varied from three to ten years.

Statistical analysis

In our study, we used the maximum diameter in the maximum cross section to represent the tumor size, which was measured by radiologists and pathologists (pathological data are preferred). We defined the CEA/tumor size as the ratio of preoperative CEA level to the maximum tumor diameter. The primary outcome was overall survival (OS), which was defined as the time in months from surgery to death. The secondary endpoint was disease-free survival (DFS), which was defined as the time in months from surgery to disease recurrence, whether radiological or histological. Maximally selected rank statistics were used to identify the optimal discriminator value for the CEA/tumor size, which was conducted in the training cohort. For every potential cutoff point, the absolute value of the standardized log-rank statistic was computed. The cutoff that provided the best separation of the survival outcome into two groups, where the standardized statistics reached their maximum, was selected as the cutoff point. Based on this cutoff, we divided the validation cohort into two groups: High CEA/tumor size group and low CEA/tumor size group. The intergroup comparisons of the clinicopathological variables were performed using the two independent samples *t*-test or Mann-Whitney *U* test for continuous variables, and the chi-square test or two-tailed Fisher's exact test for discrete variables. The Kaplan-Meier method and log-rank test were used to plot the survival curve and to compare the survival data. Univariate analysis of potential risk factors for each variable was performed using the Cox proportional hazards regression model. Variables with a *P*-value < 0.10 in the univariate analysis were selected to fit the multivariate Cox model. Multivariate analysis using the Cox proportional hazards regression model was used to identify independent risk factors. Variable selection methods, including forward, backward, and stepwise algorithms, as determined by the Akaike information criterion (AIC), were used to construct the appropriate model. The proportional hazards assumption of the Cox regression models was tested by Schoenfeld residuals. All tests were bilateral, and *P*-values < 0.05 were considered statistically significant. All analyses were performed using the R Language for Statistical Computing (version 3.5.1).

RESULTS

Baseline characteristics

Of the 696 patients diagnosed with rectal cancer who underwent surgical resection from 2007 to 2012, 11 were not histologically confirmed to have adenocarcinoma, 70 received neoadjuvant chemotherapy and/or radiotherapy, and 59 had missing data. Excluding these patients left 566 patients who satisfied both the inclusion and exclusion criteria (Figure 1). These patients were randomly divided into two cohorts: The training cohort (n = 371, 2/3 of 566) and the validation cohort (n = 185, 1/3 of 566).

Maximally selected rank statistics were performed to determine the optimal value with maximal standardized log-rank statistics. For all 371 rectal cancer patients in the training cohort, the CEA/tumor size of 2.429 ng/mL per cm (P = 0.016) provided the best separation of the survival outcomes of the two groups (Figure 2). Based on this cutoff value, 371 patients from the training cohort and 185 patients from the validation cohort were divided into the high CEA/tumor size group and the low CEA/ tumor size group, respectively. As shown in Table 1, high CEA/tumor size was correlated with older age, high TNM stage, the presence of perineural invasion, and high CEA and CA 19-9 levels in the training cohort. Somewhat differently, in the validation cohort, patients with a higher CEA/tumor size only tended to have higher preoperative CEA and CA 19-9 levels. Tumor size, sex, differentiation, and lymphovascular invasion did not differ significantly between the two groups in both cohorts.

Kaplan-Meier curves

Kaplan-Meier curves showed a manifest reduction in the 5-year OS (56.7% *vs* 81.1%, P < 0.001) and DFS (52.5% *vs* 71.9%, P = 0.02) in the high CEA/tumor size group compared with the low CEA/tumor size group in the training cohort (Figures 3A and 4A). The worse outcome of those with high CEA/tumor size was confirmed in the validation cohort, as those patients exhibited a lower 5-year OS (58.8% *vs* 85.6%, P < 0.001) and DFS (50.3% *vs* 79.3%, P = 0.002) (Figures 3B and 4B).

Univariate and multivariate analyses

According to the univariate analysis, age, TNM stage, differentiation, lymphovascular invasion, preoperative CEA and CA 19-9 levels, and CEA/tumor size were selected

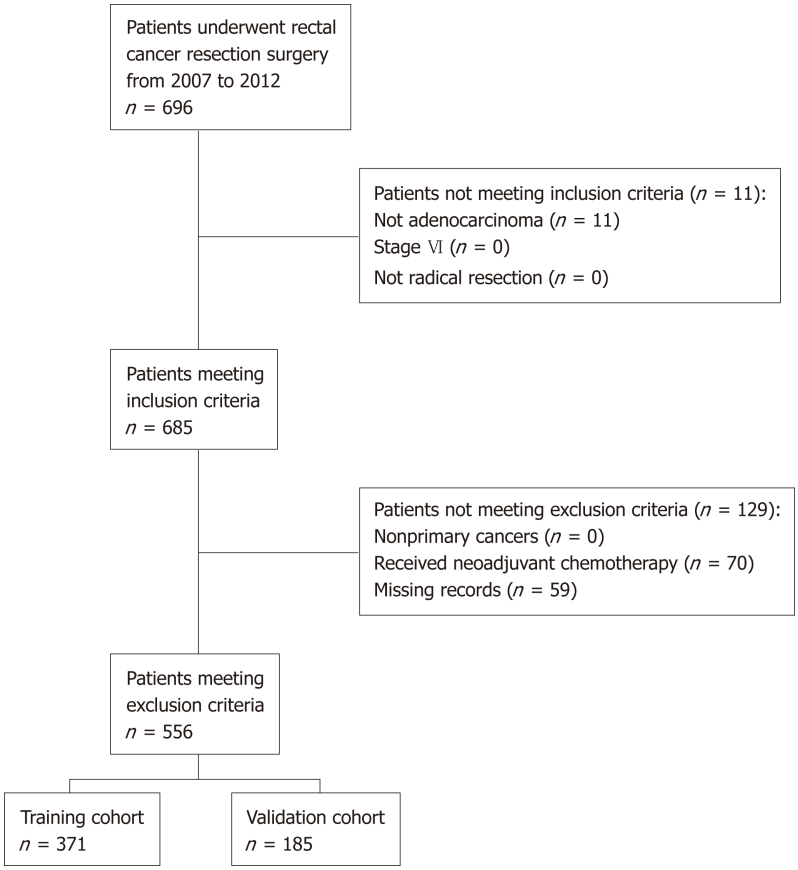

Figure 1 Flowchart of patient selection.

for the multivariate analysis for OS in both cohorts. As for DFS, the univariate analysis indicated that advanced TNM stage, the presence of lymphovascular invasion, high CEA level, and high CEA/tumor size might be associated with a poor outcome in both cohorts. However, the presence of perineural invasion only showed a significant association with DFS in the training cohort, while poor differentiation and high CA 19-9 level were associated with poor DFS only in the validation cohort (Tables 2 and 3).

To adjust for the influence of potential confounders, the prognostic impact of CEA/tumor size on OS and DFS was further explored by constructing a multivariate Cox proportional hazards model. Forward, backward, and stepwise algorithms determined by the AIC were used to construct the optimum model. All of the above methods generated identical models, and the results were similar in both cohorts. According to the multivariate analysis, older age, poor differentiation, advanced TNM stage, and higher CEA/tumor size were all significantly correlated with a worse OS. With respect to DFS, the significance of TNM stage, lymphovascular invasion, and CEA/tumor size was retained in the final model in both cohorts (Table 4). As a result, CEA/tumor size was significantly associated with OS in both the training cohort [hazard ratio (HR) = 2.18, 95%CI: 1.28-3.73] and in the validation cohort (HR = 4.83, 95%CI: 2.21-10.51). However, CEA/tumor size showed a critical association with DFS in the training cohort (HR = 1.47, 95%CI: 0.93-2.33) and a significant association in the validation cohort (HR = 2.61, 95%CI: 1.38-4.95). Plotting the Schoenfeld residuals against time showed that all the covariates in the Cox proportional hazards model for OS and DFS met the proportional hazard assumption ($P > 0.05$, Figures 5 and 6).

DISCUSSION

CEA is reliable for the detection of rectal cancer recurrence and is recommended by the ASCO and EGTM as a prognostic biomarker during routine follow-up for CRC after surgical resection[5,7]. Despite many published studies that have demonstrated the prognostic impact of CEA among CRC patients, no agreement concerning the cutoff values has been established[20-24]. Moreover, Tong *et al*[12] found that postoperative tissue CEA is significantly associated with the prognosis of CRC, and

Table 1 Association of carcinoembryonic antigen/tumor size with baseline characteristics of rectal cancer patients *n* (%)

	Training cohort (*n* = 371)				Validation cohort (*n* = 185)			
	Cases	Low	High	*P*-value	Cases	Low	High	*P*-value
Age	371	58 (21-89)	65 (32-86)	< 0.001[a]	185	61 (25-87)	57 (35-79)	0.149
Tumor size	371	4.3 (0.8-13)	4.3 (0.8-13.5)	0.773	185	4.5 (1-13)	4.3 (0.8-10)	0.472
Sex				0.419				0.199
Male	218	177 (58)	41 (64)		103	82 (53)	21 (68)	
Female	153	130 (42)	23 (36)		82	72 (47)	10 (32)	
TNM stage				0.008[a]				0.350
I	104	96 (31)	8 (12)		48	43 (28)	5 (16)	
II	127	99 (32)	28 (44)		74	61 (40)	13 (42)	
III	140	112 (36)	28 (44)		63	50 (32)	13 (42)	
Differentiation				0.395				0.826
Poor	60	51 (17)	9 (14)		24	19 (12)	5 (16)	
Moderate	209	176 (57)	33 (52)		102	85 (55)	17 (55)	
High	102	80 (26)	22 (34)		59	50 (32)	9 (29)	
Lymphovascular invasion				0.697				0.683
Negative	338	281 (92)	57 (89)		173	143 (93)	30 (97)	
Positive	33	26 (8)	7 (11)		12	11 (7)	1 (3)	
Perineural invasion				0.039[a]				0.073
Negative	340	286 (93)	54 (84)		172	146 (95)	26 (84)	
Positive	31	21 (7)	10 (16)		13	8 (5)	5 (16)	
CEA				< 0.001[a]				< 0.001[a]
0-5 ng/mL	263	262 (85)	1 (2)		127	126 (82)	1 (3)	
> 5 ng/mL	108	45 (15)	63 (98)		58	28 (18)	30 (97)	
CA 19-9				0.006[a]				0.027[a]
0-37 ng/mL	325	276 (90)	49 (77)		158	136 (88)	22 (71)	
> 37 ng/mL	46	31 (10)	15 (23)		27	18 (12)	9 (29)	

[a]*P* < 0.05; CEA: Carcinoembryonic antigen; CA 19-9: Carbohydrate antigen 19-9.

Huo *et al*[13] illustrated that serum CEA density was an independent prognostic factor in patients with colorectal pulmonary metastasis. CEA, as a classic tumor marker, is used to evaluate the biological activity of malignancies, but biological activity will also be affected by tumor quantity. When tumors grow, no matter how clumsily or aggressively, serum CEA level will increase as the expression of CEA increases in proliferating adenocarcinoma cells. Therefore, tumor size is a confounding factor that should be minimized. A new prognostic factor that better reflects the intra-tumor CEA concentration without omission of the tumor volume will be much more accurate than a classic serum CEA test. A comprehensive study stated that tumor size, especially the maximum horizontal tumor diameter, represented a valuable prognosticator in gastric cancer[25]. Another study found a direct relationship between tumor volume in rectal cancer and overall survival[26]. Therefore, we decided to use CEA/tumor size, which is a simple parameter that could reduce the confounding effect of tumor size. Taken together, these results indicate that the ratio of serum CEA to the maximum tumor diameter might be a better marker to assess the tumor's biological activity and to refine the insufficient prognostic value of serum CEA for rectal cancer.

This is the first study to evaluate the prognostic value of CEA/tumor size for stage I to III rectal cancer. We found that patients with a high CEA/tumor size (over 2.429 ng/mL per cm) had a significantly worse 5-year OS and DFS. Therefore, a correlation exists between the preoperative CEA/tumor size and the prognosis of rectal cancer patients after resection. Patients with high CEA/tumor size tended to have a worse outcome. In our study, no correlation was found between tumor size and survival outcome. Univariate and multivariate analyses showed that CEA/tumor size was independently associated with OS and DFS, while absolute serum CEA was not. This implied that adjusting the confounding effect of tumor size may improve the prognostic value of CEA. Thus, preoperative CEA/tumor size can be used as an

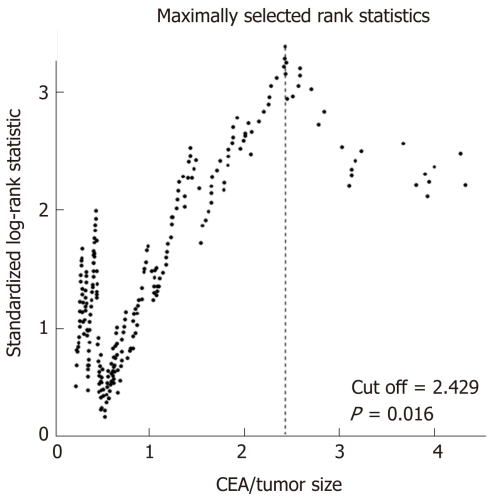

Figure 2 Maximally selected rank statistics for carcinoembryonic antigen/tumor size. Maximally selected rank statistics were used to identify the optimal discriminator value for the carcinoembryonic antigen/tumor size, which was conducted in the training cohort. For every potential cutoff point, the absolute value of the standardized log-rank statistic was computed. The cutoff point that provided the best separation of the survival outcome into two groups, where the standardized statistics reached their maximum, was selected as the cutoff point. CEA: Carcinoembryonic antigen.

independent prognostic factor for patients with stage I-III rectal cancer.

Notably, this study highlights the important relationship between serum CEA and tumor volume, which is in agreement with previous studies. With respect to the prevalence of serum CEA in clinical applications, additional improvement in the accuracy of estimating 5-year outcomes will benefit more patients. In addition, a growing tumor with little change in biological activity will exhibit an increased CEA level and a relatively unchangeable CEA/tumor size. Therefore, CEA/tumor size is not only more accurate but more stable than serum CEA. In patients with identical serum CEA levels, it is necessary to make a decision regarding clinical intervention for patients with smaller maximum tumor diameter. In contrast, a low CEA/tumor size may indicate less aggressive and malignant tumors.

However, we admit that our study has some inherent limitations. First, maximum tumor diameter as an indication of tumor volume is not so precise. Huo *et al*[13] used the spherical formula $(4 \times \pi \times \text{radius}^3)/3$ to represent the tumor volume since they assumed that pulmonary tumors were spherical. Nevertheless, unlike pulmonary metastases, rectal tumors are not a fixed geometric shape, which means this method is unreliable[26]. Alternatively, the careful delineation of the tumor boundary combined with specific software may provide a more accurate estimation of tumor size. However, maximum tumor diameter represents a quick and convenient method that can be used to roughly estimate tumor volume, and as a result, has more prospects for clinical application. Second, CEA/tumor size cannot be used as part of a routine follow-up index to dynamically monitor the recurrence and metastasis of rectal cancer after surgery. Surgical resection will remove the local tumor, and therefore CEA/tumor size will be unable to be continually calculated. For patients with new-found relapse and metastasis, the value of CEA/tumor size requires further investigation. Beyond that, we also noticed a newly published research study suggesting that postoperative CEA is a better prognostic marker for survival than preoperative CEA in colon cancer[27]. However, postoperative CEA indicates complete resection of the tumor, while CEA/tumor size is focused on tumor malignancy. Third, we did not include patients with neoadjuvant chemotherapy and/or radiotherapy because both of them can influence preoperative CEA and tumor size and may bias our result. Finally, in both cohorts, CEA/tumor size was included in the final Cox model for DFS, which means that CEA/tumor size is an essential factor for DFS. But the *P*-value was 0.003 in the validation cohort and 0.096 in the training cohort, which may result from the insufficient sample size or discrepancy between the two cohorts. Whether CEA/tumor size is really associated with DFS still needs further study.

Preoperative CEA/tumor size is a new method that can be used to predict the outcomes of patients with stage I-III rectal cancer, which may influence the decision-making process for a specific treatment regimen and patient counselling. Since both CEA level and tumor size are routinely measured before surgery, the data of CEA/tumor size can be obtained by simple calculation. This will facilitate the

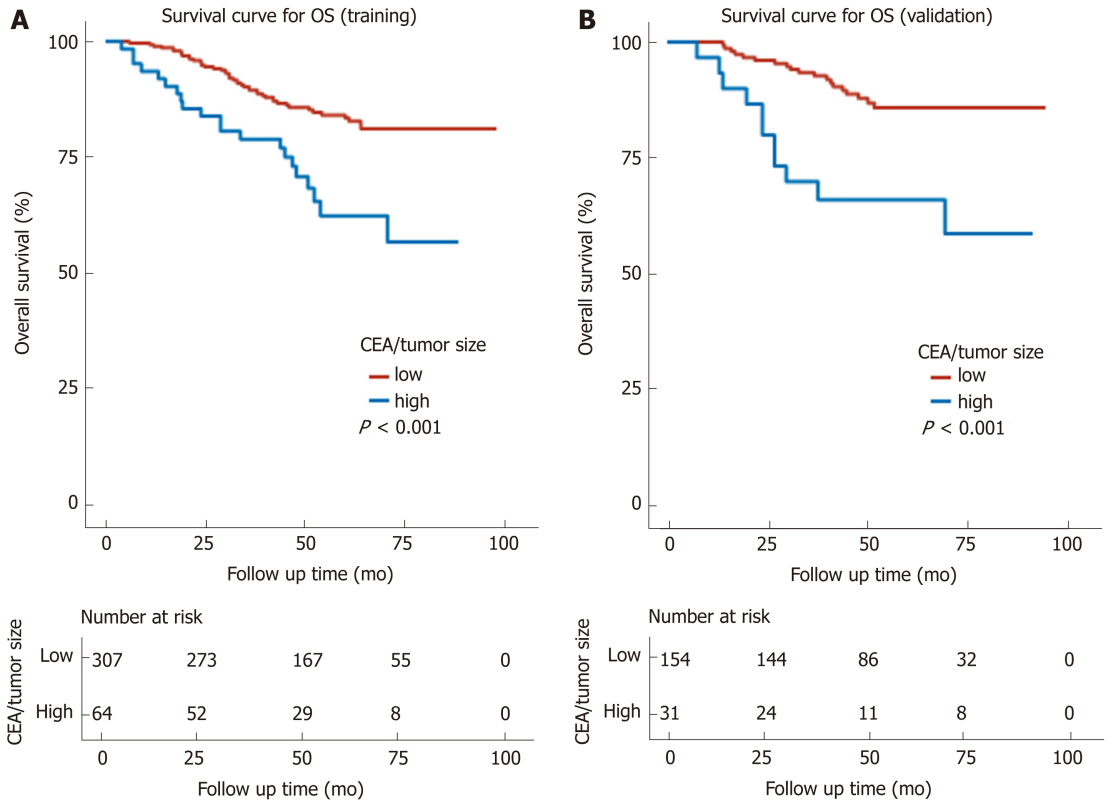

Figure 3 Kaplan-Meier survival curves and risk tables for overall survival. A: Kaplan-Meier survival curves and risk table for overall survival in the training cohort. The 5-year overall survival (OS) of the high and low carcinoembryonic antigen (CEA)/tumor size groups were 56.7% and 81.1% ($P < 0.001$), respectively. B: Kaplan-Meier survival curves and risk table for overall survival in the validation cohort. The 5-year OS of the high and low CEA/tumor size groups were 58.8% and 85.6% ($P < 0.001$), respectively. The log-rank test was used to calculate the *P*-value. OS: Overall survival; CEA: Carcinoembryonic antigen.

application of CEA/tumor size in clinical practice. Compared with CEA, a great advantage of CEA/tumor size is the ability to figure out those patients with higher CEA but relatively small tumor size. The result of our study suggests that these easily neglected tumors may represent higher malignancy and worse outcome. With the optimization of risk stratification, clinicians can choose individualized treatment options and the outcome of rectal cancer patients can be improved accordingly.

Of course, some limitations of our study design still need to be discussed. As a retrospective study, we were not able to obtain high-level clinical evidence. We also found that some patients did not reach an enough follow-up time, which may influence the accuracy of our result. Since the estimated cutoff point was relatively high, the high-risk group and low-risk group accounted for 20% and 80%, respectively. Although the number of events per variable > 10 in our Cox model, a larger sample size would be better to obtain more reliable results[28]. Therefore, a large-scale prospective study and longer follow-up time are needed and we will try our best to validate our conclusion in future studies. It is also worthwhile for other researchers to further validate our study with new evidence, as we are looking forward to a more accurate prognostic factor for rectal cancer.

In summary, patients with a high preoperative CEA/tumor size have a worse outcome than those with a low CEA/tumor size. Preoperative CEA/tumor size may play an important role in prognosis and treatment decisions of rectal cancer patients after surgery.

Table 2 Univariate analysis of prognostic factors for overall survival

Variable	Training cohort (*n* = 371)			Validation cohort (*n* = 185)		
	Hazard ratio	95%CI	*P*-value	Hazard ratio	95%CI	*P*-value
Age	1.02	1.00-1.04	0.024[a]	1.03	1.00-1.06	0.070
Tumor size	1.04	0.92-1.18	0.506	1.14	0.95-1.37	0.164
Sex (ref = male)	1.43	0.88-2.31	0.145	0.85	0.41-1.77	0.665
TNM[1] (ref = stage I)	1.74	1.26-2.41	0.001[a]	1.93	1.15-3.22	0.012[a]
Differentiation[1] (ref = poor)	0.58	0.40-0.84	0.004[a]	0.53	0.30-0.94	0.030[a]
Lymphovascular invasion (ref = negative)	1.88	0.96-3.68	0.066	3.11	1.19-8.13	0.021[a]
Perineural invasion (ref = negative)	1.03	0.41-2.56	0.954	1.29	0.31-5.46	0.729
CEA (ref = CEA < 5)	1.81	1.11-2.94	0.017[a]	2.72	1.33-5.59	0.006[a]
CA 19-9 (ref = CA 19-9 < 37)	1.88	1.04-3.39	0.036[a]	2.14	0.92-4.99	0.078
CEA/tumor size (ref = low)	2.45	1.46-4.11	0.001[a]	3.57	1.70-7.52	0.001[a]

[1]These variables were treated as ordinal categorical data;
[a]*P* < 0.05. CEA: Carcinoembryonic antigen; CA 19-9: Carbohydrate antigen 19-9; CI: Confidence interval; ref: Reference.

Table 3 Univariate analysis of prognostic factors for disease-free survival

Variable	Training cohort (*n* = 371)			Validation cohort (*n* = 185)		
	Hazard ratio	95%CI	*P*-value	Hazard ratio	95%CI	*P*-value
Age	1	0.99-1.02	0.572	1.02	0.99-1.04	0.173
Tumor size	1.01	0.91-1.12	0.828	1.12	0.97-1.30	0.128
Sex (ref = male)	1.26	0.85-1.87	0.247	0.75	0.41-1.37	0.353
TNM[1] (ref = stage I)	1.9	1.45-2.50	<0.001[a]	1.6	1.07-2.39	0.023[a]
Differentiation[1] (ref = poor)	0.78	0.58-1.06	0.113	0.6	0.38-0.95	0.031[a]
Lymphovascular invasion (ref = negative)	2.44	1.45-4.12	0.001[a]	2.63	1.11-6.22	0.028[a]
Perineural invasion (ref = negative)	2.17	1.23-3.82	0.008[a]	1.98	0.78-5.03	0.151
CEA (ref = CEA < 5)	1.55	1.03-2.32	0.034[a]	1.9	1.05-3.41	0.033[a]
CA 19-9 (ref = CA 19-9 < 37)	1.43	0.85-2.42	0.177	1.96	0.97-3.96	0.061
CEA/tumor size (ref = low)	1.72	1.10-2.71	0.018[a]	2.58	1.37-4.85	0.003[a]

[1]These variables were treated as ordinal categorical data;
[a]*P* < 0.05. CEA: Carcinoembryonic antigen; CA 19-9: Carbohydrate antigen 19-9; CI: Confidence interval; ref: Reference.

Table 4 Multivariate analysis of prognostic factors for overall survival and disease-free survival

	Training cohort (*n* = 371)			Validation cohort (*n* = 185)		
OS	Hazard radio	95%CI	*P*-value	Hazard radio	95%CI	*P*-value
Age	1.02	1.00-1.04	0.023[a]	1.05	1.02-1.09	0.003[a]
TNM[1] (ref = stage I)	1.47	1.04-2.07	0.031[a]	1.84	1.04-3.24	0.035[a]
Differentiation[1] (ref = poor)	0.57	0.39-0.85	0.006[a]	0.50	0.28-0.90	0.021[a]
CEA/tumor size (ref = low)	2.18	1.28-3.73	0.004[a]	4.83	2.21-10.52	<0.001[a]
DFS						
TNM[1] (ref = stage I)	1.75	1.32-2.32	<0.001[a]	1.43	0.94-2.17	0.091
Lymphovascular invasion (ref = negative)	1.85	1.08-3.16	0.024[a]	2.45	1.00-6.03	0.05
CEA/tumor size (ref = low)	1.47	0.93-2.33	0.096	2.61	1.38-4.95	0.003[a]

[1]These variables were treated as ordinal categorical data;
[a]*P* < 0.05. CEA: Carcinoembryonic antigen; CI: Confidence interval; ref: Reference; OS: Overall survival; DFS: Disease-free survival.

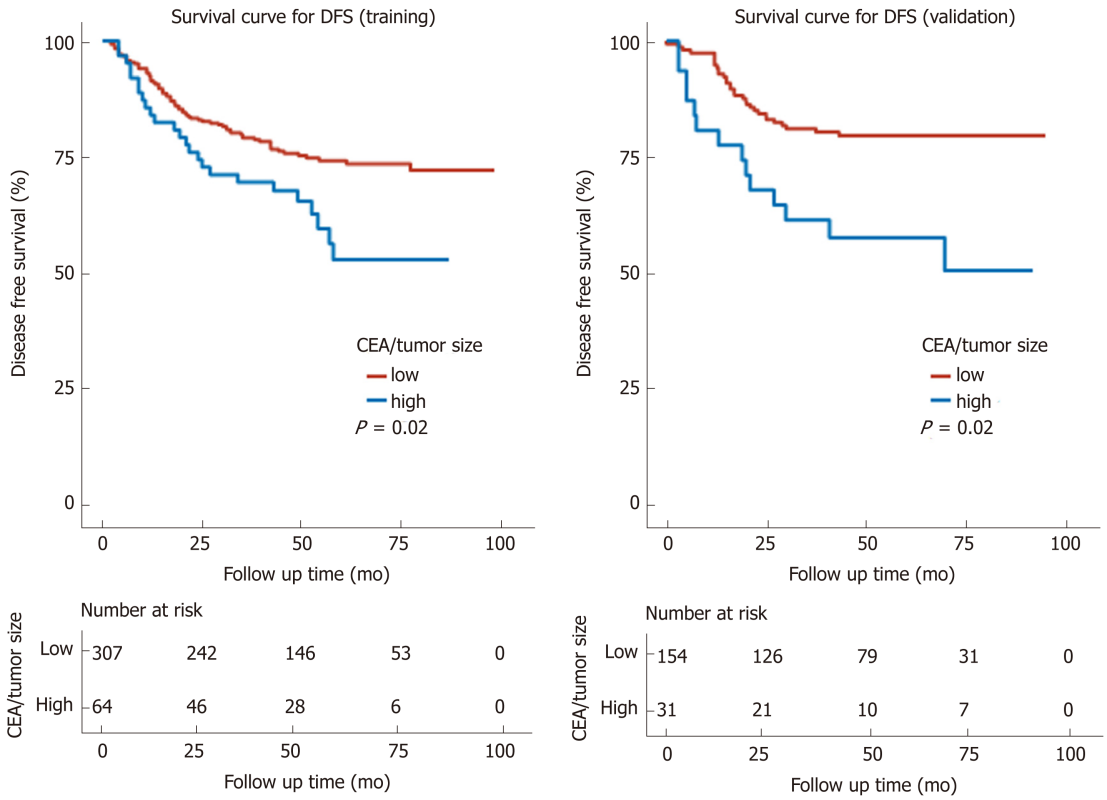

Figure 4 Kaplan-Meier survival curves and risk tables for disease-free survival. A: Kaplan-Meier survival curves and risk table for disease-free survival (DFS) in the training cohort. The 5-year DFS of the high and low CEA/tumor size groups were 52.5% and 71.9% (P = 0.02), respectively. B: Kaplan-Meier survival curves and risk table for DFS in the validation cohort. The 5-year DFS of the high and low CEA/tumor size groups were 50.3% *vs* 79.3% (P = 0.002), respectively. The log-rank test was used to calculate the P-value. DFS: Disease-free survival; CEA: Carcinoembryonic antigen.

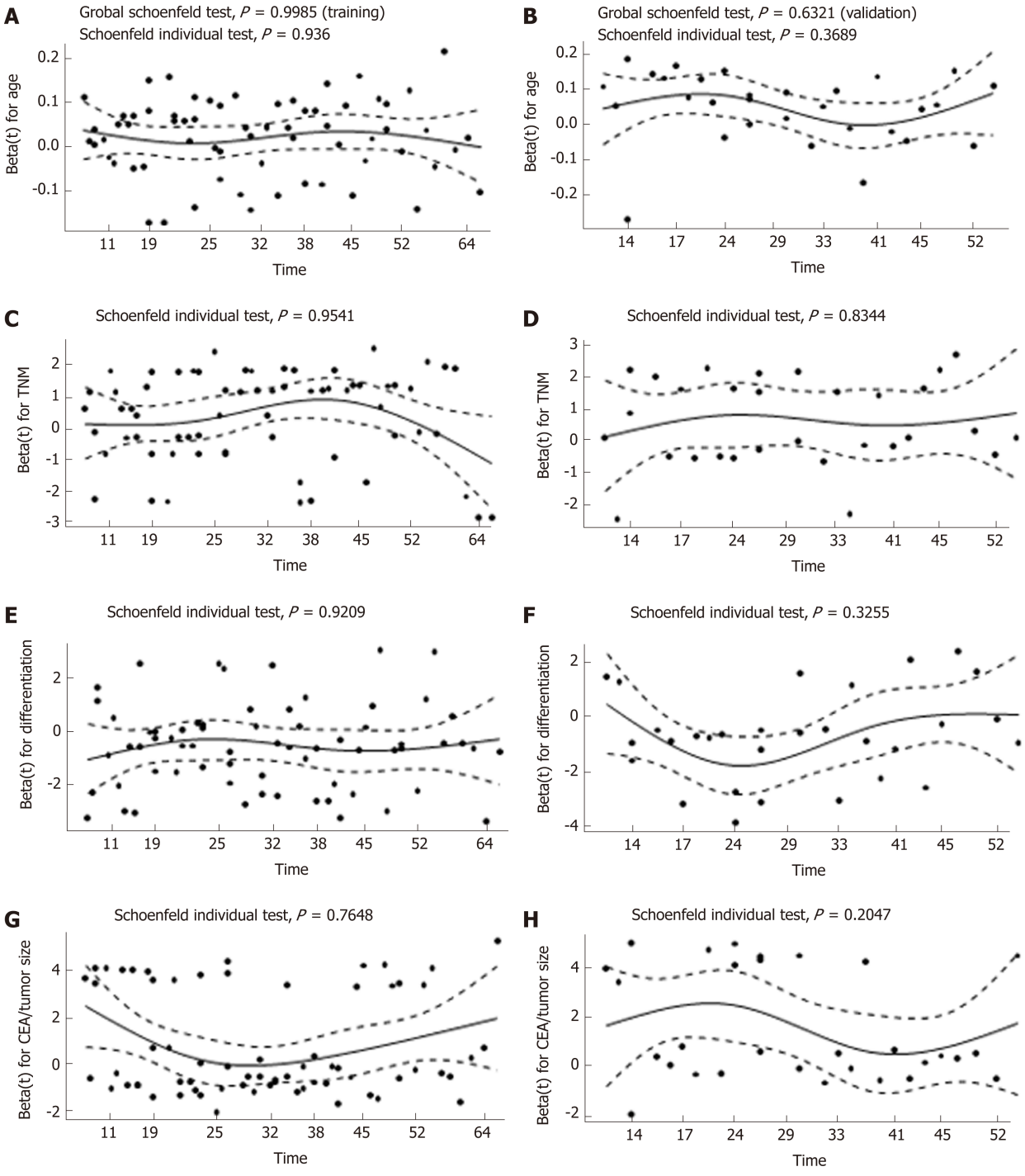

Figure 5 Proportional hazards assumption test for overall survival by plotting the Schoenfeld residuals against time in the training cohort (A, C, E, and G) and the validation cohort (B, D, F, and H). The X-axis represents the survival time, while the Beta values referring to age, TNM stage, differentiation, and carcinoembryonic antigen/tumor size are shown on the Y-axis. The constant mean of residuals across time confirms that the proportional hazard assumption holds for these covariate with all of the *P*-values > 0.05. CEA: Carcinoembryonic antigen.

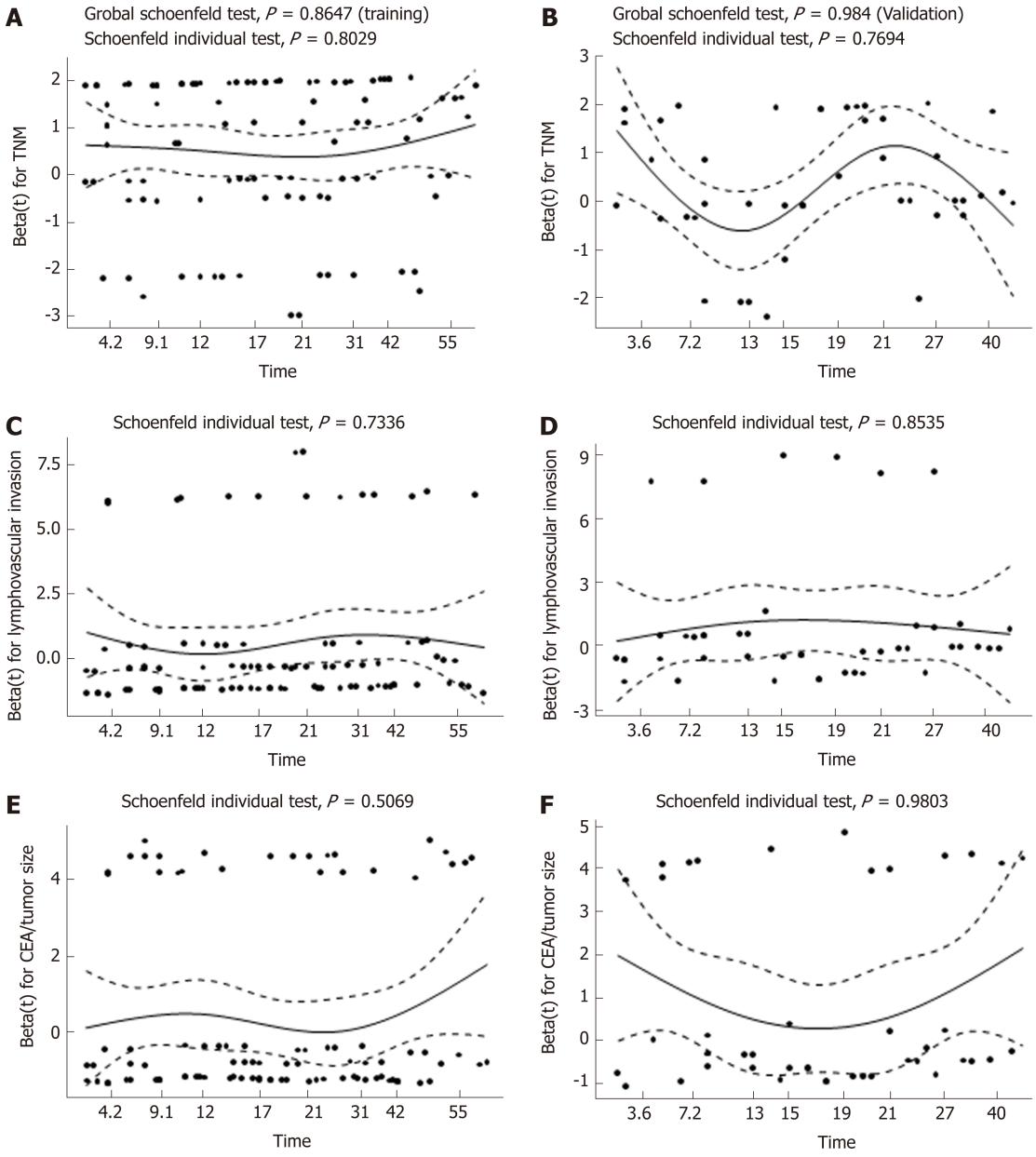

Figure 6 Proportional hazards assumption test for disease-free survival by plotting the Schoenfeld residuals against time in the training cohort (A, C, and E) and the validation cohort (B, D, and F). The X-axis represents the survival time, while the Beta values referring to TNM stage, lymphovascular invasion, and carcinoembryonic antigen/tumor size are shown on the Y-axis. The constant mean of residuals across time confirms that the proportional hazard assumption holds for these covariate with all of the *P*-values > 0.05. CEA: Carcinoembryonic antigen.

ARTICLE HIGHLIGHTS

Research background

Colorectal cancer (CRC) is the third most frequently diagnosed malignancy and one of the leading causes of cancer-related mortality worldwide. Therapy options for CRC have been developed rapidly in the past decade, but selecting optimal treatments for individuals remains a great challenge for clinicians due to the lack of effective markers.

Research motivation

Controversy exists regarding the insufficient prognostic value of preoperative serum CEA alone, which is a widely used biomarker in rectal cancer. Recent studies have found that local CEA may play a more important role in the prognosis of CRC than overall serum CEA. Some studies have tried to add another factor like tumor size to improve the prognostic value of biomarker, such as prostate specific antigen density and tumor-infiltrating CD8+ T-cell density. Here, we combined preoperative serum CEA and the maximum tumor diameter to correct the CEA level, which may better reflect the malignancy of rectal cancer and improve the risk stratification system.

Research objectives

We aimed to investigate the prognostic impact of the preoperative CEA/tumor size in patients with rectal cancer, which may influence the decision-making process for a specific treatment regimen and patient counselling.

Research methods

We retrospectively reviewed 696 stage I to III rectal cancer patients who underwent curative tumor resection from 2007 to 2012. These patients were randomly divided into two cohorts for cross-validation: Training cohort and validation cohort. The training cohort was used to generate an optimal cutoff point and the validation cohort was used to further validate the model. Maximally selected rank statistics were used to identify the optimum cutoff for CEA/tumor size. The Kaplan-Meier method and log-rank test were used to plot the survival curve and to compare the survival data. Univariate and multivariate Cox regression analyses were used to determine the prognostic value of CEA/tumor size. The primary and secondary outcomes were overall survival (OS) and disease-free survival (DFS), respectively.

Research results

In all, 556 patients who satisfied both the inclusion and exclusion criteria were included and randomly divided into a training cohort (2/3 of 556, n = 371) and a validation cohort (1/3 of 556, n = 185). The cutoff was 2.429 ng/mL per cm. Comparison of the baseline data showed that high CEA/tumor size was correlated with older age, high TNM stage, presence of perineural invasion, high CEA, and high carbohydrate antigen 19-9 (CA 19-9). Kaplan-Meier curves showed a manifest reduction in 5-year OS (training cohort: 56.7% *vs* 81.1%, P < 0.001; validation cohort: 58.8% *vs* 85.6%, P <0.001) and DFS (training cohort: 52.5% *vs* 71.9%, P = 0.02; validation cohort: 50.3% *vs* 79.3%, P = 0.002) in the high CEA/tumor size group compared with the low CEA/tumor size group. Univariate and multivariate analyses identified CEA/tumor size as an independent prognostic factor for OS (training cohort: hazard ratio (HR) = 2.18 95% confidence interval (CI): 1.28-3.73, P = 0.004; validation cohort: HR = 4.83, 95%CI: 2.21-10.52, P < 0.001) as well as DFS (training cohort: HR = 1.47, 95% CI: 0.93-2.33, P = 0.096; validation cohort: HR: 2.61, 95%CI = 1.38-4.95, P = 0.003).

Research conclusions

This is the first study to evaluate the prognostic value of CEA/tumor size for stage I to III rectal cancer. We found that patients with high CEA/tumor size tended to have a worse outcome. Adjusting the confounding effect of tumor size can improve the prognostic value of CEA. Compared with CEA, another great advantage of CEA/tumor size is the ability to figure out those patients with higher CEA but relatively small tumor size. The results of our study suggest that these easily neglected tumors may represent higher malignancy and worse outcome, which may challenge the conventional risk stratification system. Since both CEA level and tumor size are routinely measured before surgery, the data of CEA/tumor size can be obtained by simple calculation. Therefore, CEA/tumor size can be easily applied in clinical practice.

Research perspectives

As a retrospective study, we were not able to obtain high-level clinical evidence, but the current retrospective study will provide an important basis for us to carry out a prospective study. A large-scale prospective study and longer follow-up time are needed in future study.

REFERENCES

1 **Bray F**, Ferlay J, Soerjomataram I, Siegel RL, Torre LA, Jemal A. Global Cancer Statistics 2018: GLOBOCAN Estimates of Incidence and Mortality Worldwide for 36 Cancers in 185 Countries. *CA Cancer J Clin* 2018; **68**: 394-424 [PMID: 30207593 DOI: 10.3322/caac.21492]

2 **Arnold M**, Sierra MS, Laversanne M, Soerjomataram I, Jemal A, Bray F. Global patterns and trends in colorectal cancer incidence and mortality. *Gut* 2017; **66**: 683-691 [PMID: 26818619 DOI: 10.1136/gutjnl-2015-310912]

3 **Deng Y**. Rectal Cancer in Asian vs. Western Countries: Why the Variation in Incidence? *Curr Treat Options Oncol* 2017; **18**: 64 [PMID: 28948490 DOI: 10.1007/s11864-017-0500-2]

4 **Dienstmann R**, Salazar R, Tabernero J. Personalizing colon cancer adjuvant therapy: selecting optimal treatments for individual patients. *J Clin Oncol* 2015; **33**: 1787-1796 [PMID: 25918287 DOI: 10.1200/JCO.2014.60.0213]

5 **Duffy MJ**, Lamerz R, Haglund C, Nicolini A, Kalousová M, Holubec L, Sturgeon C. Tumor markers in colorectal cancer, gastric cancer and gastrointestinal stromal cancers: European group on tumor markers 2014 guidelines update. *Int J Cancer* 2014; **134**: 2513-2522 [PMID: 23852704 DOI: 10.1002/ijc.28384]

6 **Stiksma J**, Grootendorst DC, van der Linden PW. CA 19-9 as a marker in addition to CEA to monitor colorectal cancer. *Clin Colorectal Cancer* 2014; **13**: 239-244 [PMID: 25442815 DOI: 10.1016/j.clcc.2014.09.004]

7 **Locker GY**, Hamilton S, Harris J, Jessup JM, Kemeny N, Macdonald JS, Somerfield MR, Hayes DF, Bast RC; ASCO. ASCO 2006 update of recommendations for the use of tumor markers in gastrointestinal cancer. *J Clin Oncol* 2006; **24**: 5313-5327 [PMID: 17060676 DOI: 10.1200/JCO.2006.08.2644]

8 **Nicholson BD**, Shinkins B, Pathiraja I, Roberts NW, James TJ, Mallett S, Perera R, Primrose JN, Mant D. Blood CEA levels for detecting recurrent colorectal cancer. *Cochrane Database Syst Rev* 2015; CD011134 [PMID: 26661580 DOI: 10.1002/14651858.CD011134.pub2]

9 **Chen L**, Jiang B, Wang Z, Liu M, Yang H, Xing J, Zhang C, Yao Z, Zhang N, Cui M, Su X. Combined preoperative CEA and CD44v6 improves prognostic value in patients with stage I and stage II colorectal cancer. *Clin Transl Oncol* 2014; **16**: 285-292 [PMID: 23860725 DOI: 10.1007/s12094-013-1069-2]

10 **Zhan X**, Sun X, Hong Y, Wang Y, Ding K. Combined Detection of Preoperative Neutrophil-to-

Lymphocyte Ratio and CEA as an Independent Prognostic Factor in Nonmetastatic Patients Undergoing Colorectal Cancer Resection Is Superior to NLR or CEA Alone. *Biomed Res Int* 2017; **2017**: 3809464 [PMID: 28685148 DOI: 10.1155/2017/3809464]

11 **Kozman MA**, Fisher OM, Rebolledo BJ, Parikh R, Valle SJ, Arrowaili A, Alzahrani N, Liauw W, Morris DL. CEA to peritoneal carcinomatosis index (PCI) ratio is prognostic in patients with colorectal cancer peritoneal carcinomatosis undergoing cytoreduction surgery and intraperitoneal chemotherapy: A retrospective cohort study. *J Surg Oncol* 2018; **117**: 725-736 [PMID: 29266235 DOI: 10.1002/jso.24911]

12 **Tong G**, Xu W, Zhang G, Liu J, Zheng Z, Chen Y, Niu P, Xu X. The role of tissue and serum carcinoembryonic antigen in stages I to III of colorectal cancer-A retrospective cohort study. *Cancer Med* 2018; **7**: 5327-5338 [PMID: 30302946 DOI: 10.1002/cam4.1814]

13 **Huo YR**, Glenn D, Liauw W, Power M, Zhao J, Morris DL. Evaluation of carcinoembryonic antigen (CEA) density as a prognostic factor for percutaneous ablation of pulmonary colorectal metastases. *Eur Radiol* 2017; **27**: 128-137 [PMID: 27165139 DOI: 10.1007/s00330-016-4352-0]

14 **Aminsharifi A**, Howard L, Wu Y, De Hoedt A, Bailey C, Freedland SJ, Polascik TJ. Prostate Specific Antigen Density as a Predictor of Clinically Significant Prostate Cancer When the Prostate Specific Antigen is in the Diagnostic Gray Zone: Defining the Optimum Cutoff Point Stratified by Race and Body Mass Index. *J Urol* 2018; **200**: 758-766 [PMID: 29758219 DOI: 10.1016/j.juro.2018.05.016]

15 **Shimizu S**, Hiratsuka H, Koike K, Tsuchihashi K, Sonoda T, Ogi K, Miyakawa A, Kobayashi J, Kaneko T, Igarashi T, Hasegawa T, Miyazaki A. Tumor-infiltrating CD8⁺ T-cell density is an independent prognostic marker for oral squamous cell carcinoma. *Cancer Med* 2019; **8**: 80-93 [PMID: 30600646 DOI: 10.1002/cam4.1889]

16 **Eichelberger LE**, Koch MO, Eble JN, Ulbright TM, Juliar BE, Cheng L. Maximum tumor diameter is an independent predictor of prostate-specific antigen recurrence in prostate cancer. *Mod Pathol* 2005; **18**: 886-890 [PMID: 15803186 DOI: 10.1038/modpathol.3800405]

17 **Yoshimoto T**, Morine Y, Imura S, Ikemoto T, Iwahashi S, Saito YU, Yamada S, Ishikawa D, Teraoku H, Yoshikawa M, Higashijima J, Takasu C, Shimada M. Maximum Diameter and Number of Tumors as a New Prognostic Indicator of Colorectal Liver Metastases. *In Vivo* 2017; **31**: 419-423 [PMID: 28438872 DOI: 10.21873/invivo.11076]

18 **Tanaka N**, Fujimoto K, Chihara Y, Torimoto M, Hirao Y, Konishi N, Saito I. Prostatic volume and volume-adjusted prostate-specific antigen as predictive parameters for prostate cancer patients with intermediate PSA levels. *Prostate Cancer Prostatic Dis* 2007; **10**: 274-278 [PMID: 17339878 DOI: 10.1038/sj.pcan.4500957]

19 **Peng Y**, Shen D, Liao S, Turkbey B, Rais-Bahrami S, Wood B, Karademir I, Antic T, Yousef A, Jiang Y, Pinto PA, Choyke PL, Oto A. MRI-based prostate volume-adjusted prostate-specific antigen in the diagnosis of prostate cancer. *J Magn Reson Imaging* 2015; **42**: 1733-1739 [PMID: 25946664 DOI: 10.1002/jmri.24944]

20 **Becerra AZ**, Probst CP, Tejani MA, Aquina CT, González MG, Hensley BJ, Noyes K, Monson JR, Fleming FJ. Evaluating the Prognostic Role of Elevated Preoperative Carcinoembryonic Antigen Levels in Colon Cancer Patients: Results from the National Cancer Database. *Ann Surg Oncol* 2016; **23**: 1554-1561 [PMID: 26759308 DOI: 10.1245/s10434-015-5014-1]

21 **Huh JW**, Oh BR, Kim HR, Kim YJ. Preoperative carcinoembryonic antigen level as an independent prognostic factor in potentially curative colon cancer. *J Surg Oncol* 2010; **101**: 396-400 [PMID: 20119979 DOI: 10.1002/jso.21495]

22 **Park IJ**, Choi GS, Lim KH, Kang BM, Jun SH. Serum carcinoembryonic antigen monitoring after curative resection for colorectal cancer: clinical significance of the preoperative level. *Ann Surg Oncol* 2009; **16**: 3087-3093 [PMID: 19629600 DOI: 10.1245/s10434-009-0625-z]

23 **Peng Y**, Wang L, Gu J. Elevated preoperative carcinoembryonic antigen (CEA) and Ki67 is predictor of decreased survival in IIA stage colon cancer. *World J Surg* 2013; **37**: 208-213 [PMID: 23052808 DOI: 10.1007/s00268-012-1814-7]

24 **Thirunavukarasu P**, Sukumar S, Sathaiah M, Mahan M, Pragatheeshwar KD, Pingpank JF, Zeh H, Bartels CJ, Lee KK, Bartlett DL. C-stage in colon cancer: implications of carcinoembryonic antigen biomarker in staging, prognosis, and management. *J Natl Cancer Inst* 2011; **103**: 689-697 [PMID: 21421861 DOI: 10.1093/jnci/djr078]

25 **Jun KH**, Jung H, Baek JM, Chin HM, Park WB. Does tumor size have an impact on gastric cancer? A single institute experience. *Langenbecks Arch Surg* 2009; **394**: 631-635 [PMID: 18791731 DOI: 10.1007/s00423-008-0417-0]

26 **Tayyab M**, Razack A, Sharma A, Gunn J, Hartley JE. Correlation of rectal tumor volumes with oncological outcomes for low rectal cancers: does tumor size matter? *Surg Today* 2015; **45**: 826-833 [PMID: 25377268 DOI: 10.1007/s00595-014-1068-0]

27 **Konishi T**, Shimada Y, Hsu M, Tufts L, Jimenez-Rodriguez R, Cercek A, Yaeger R, Saltz L, Smith JJ, Nash GM, Guillem JG, Paty PB, Garcia-Aguilar J, Gonen M, Weiser MR. Association of Preoperative and Postoperative Serum Carcinoembryonic Antigen and Colon Cancer Outcome. *JAMA Oncol* 2018; **4**: 309-315 [PMID: 29270608 DOI: 10.1001/jamaoncol.2017.4420]

28 **Austin PC**, Allignol A, Fine JP. The number of primary events per variable affects estimation of the subdistribution hazard competing risks model. *J Clin Epidemiol* 2017; **83**: 75-84 [PMID: 28088594 DOI: 10.1016/j.jclinepi.2016.11.017]

World Journal of Gastroenterology

Submit a Manuscript: https://www.f6publishing.com

World J Gastroenterol 2019 September 7; 25(33): 4959-4969

DOI: 10.3748/wjg.v25.i33.4959

ISSN 1007-9327 (print) ISSN 2219-2840 (online)

ORIGINAL ARTICLE

Retrospective Study

Value of controlled attenuation parameter in fibrosis prediction in nonalcoholic steatohepatitis

Jung Il Lee, Hyun Woong Lee, Kwan Sik Lee

ORCID number: Jung Il Lee (0000-0002-0142-1398); Hyun Woong Lee (0000-0002-6958-3035); Kwan Sik Lee (0000-0002-3672-1198).

Author contributions: All authors helped to perform research; Lee JI and Lee KS drafted the concept, design the study; Lee HW collected the data and wrote the manuscript; Lee JI and Lee HW analyzed the data.

Supported by Basic Science Research Program through the National Research Foundation of Korea (NRF) funded by the Ministry of Science, ICT and Future Planning (NRF-2016R1A2B4015192).

Institutional review board statement: This study was reviewed and approved by the Institutional review board of Gangnam Severance Hospital (Permit No: 3-2019-0010).

Informed consent statement: Written informed consent of the patients was exempted by the institutional review board since the researchers only accessed the database for the analysis purposes and the personal information was blinded by coding.

Conflict-of-interest statement: Jung Il Lee has served as a speaker for Echosens; the other authors have nothing to disclose.

Data sharing statement: No additional data are available.

Jung Il Lee, Hyun Woong Lee, Kwan Sik Lee, Department of Internal Medicine, Gangnam Severance Hospital, Yonsei University College of Medicine, Seoul 06273, South Korea

Corresponding author: Jung Il Lee, MD, PhD, Associate Professor, Department of Internal Medicine, Gangnam Severance Hospital, Yonsei University College of Medicine, 211 Eonju-ro, Gangnam-gu, Seoul 06273, South Korea. mdflorence@yuhs.ac
Telephone: +82-2-20194365
Fax: +82-2-34633882

Abstract

BACKGROUND

Liver stiffness measurement (LSM) tends to overestimate fibrosis stage in nonalcoholic fatty liver disease (NAFLD). Controlled attenuation parameter (CAP), provided by LSM device, has been introduced for noninvasive quantification of hepatic steatosis.

AIM

To determine the role of CAP values in predicting liver fibrosis stage by LSM in nonalcoholic steatohepatitis (NASH).

METHODS

One hundred eighty-four patients with biopsy proven NASH had LSM and CAP evaluated at baseline. Among them, 130 patients had 1-year follow up LSM and analyzed for the changes of LSM after pioglitazone or ursodeoxycholic acid (UDCA) treatment.

RESULTS

In Kleiner fibrosis stage F0-1, LSM values increased at higher CAP tertile (P = 0.001), and in F2, at middle and higher tertiles (P = 0.027). No difference across CAP tertiles was noticed in F3-4 (P = 0.752). Receiver operating characteristic curve for LSM cutoff in diagnosis of F ≥ 2 identified 8.05 kPa for lower CAP tertile, 9.35 kPa for middle, and 10.55 kPa for high tertile. When changes in proportion of significant fibrosis (F ≥ 2) were assessed among pioglitazone and UDCA treated patients considering CAP values, pioglitazone treated patients demonstrated decrease in proportion of high LSM.

CONCLUSION

In patient with NAFLD, interpretation of LSM in association with CAP scores may provide helpful information sparing unnecessary liver biopsy.

Manuscript source: Unsolicited manuscript

Received: April 24, 2019
Peer-review started: April 24, 2019
First decision: July 22, 2019
Revised: July 29, 2019
Accepted: August 7, 2019
Article in press: August 7, 2019
Published online: September 7, 2019

P-Reviewer: Guo JS, Serrano-Luna J, Sherif Z
S-Editor: Yan JP
L-Editor: A
E-Editor: Ma YJ

Key words: Fibroscan; Controlled attenuation parameter; Liver stiffness; Nonalcoholic steatohepatitis; Liver fibrosis

Core tip: Liver stiffness measurement (LSM) is said to be exaggerated in nonalcoholic fatty liver disease (NAFLD). We investigated the role of controlled attenuation parameter (CAP), a means of measuring steatosis noninvasively, in predicting liver fibrosis by LSM in 184 biopsy proven nonalcoholic steatohepatitis patients. The optimum LSM cutoff for Kleiner fibrosis stage (F) ≥ 2 reflecting CAP values showed higher cutoff with increased CAP tertile (LSM, 8.05 kPa for lower CAP tertile, 9.35 kPa for middle, 10.45 kPa for high CAP tertile). Therefore, we suggest that interpretation of LSM in patients with NAFLD should take CAP scores into account in order to avoid unnecessary liver biopsy.

Citation: Lee JI, Lee HW, Lee KS. Value of controlled attenuation parameter in fibrosis prediction in nonalcoholic steatohepatitis. *World J Gastroenterol* 2019; 25(33): 4959-4969
URL: https://www.wjgnet.com/1007-9327/full/v25/i33/4959.htm
DOI: https://dx.doi.org/10.3748/wjg.v25.i33.4959

INTRODUCTION

Nonalcoholic fatty liver disease (NAFLD) is the most common cause of chronic liver disease around worldwide. The spectrum of NAFLD ranges from simple steatosis without evidence of liver injury to nonalcoholic steatohepatitis (NASH) with or without liver fibrosis[1]. Although the natural history of NAFLD requires further investigation, studies demonstrate that the severity of liver fibrosis is the most important determinant of mortality and morbidity in patients with NAFLD[2-4]. Patients with significant liver fibrosis [Kleiner classification fibrosis stage (F) ≥ 2] showed decreased survival compared to those with no or minimal fibrosis (F0-1)[4]. NAFLD may progress from simple steatosis to NASH with fibrosis, and estimation of severity of liver fibrosis is critical not only for the initial workup but also for follow-up[5].

Although liver biopsy is considered the gold standard for assessing the severity of fibrosis[6], it is an invasive procedure that might not be practical to perform sequentially. Instead, the liver stiffness measurement (LSM), obtained by transient elastograpy (TE) is a useful noninvasive means of assessing liver fibrosis. LSM values are well correlated with the biopsy determined severity of fibrosis[7-9]. However, the diagnostic performance of LSM is known to be affected by obesity and the severity of steatosis, which are closely associated with NAFLD, resulting in overestimation of the LSM in patients with NAFLD[10-12]. Recently, FibroScan, a type of TE, has been equipped with controlled attenuation parameter (CAP), software to enable noninvasive quantification of hepatic steatosis. The CAP value was strongly correlated with the histologically assessed percentage of liver fat in patients with NAFLD, but is susceptible to interference by liver fibrosis[13]. However, CAP may enhance the accuracy of TE measured LSM in patients with NAFLD[14]. We evaluated the role of the CAP value in predicting the liver fibrosis stage based on LSM in patients with biopsy proven NASH.

MATERIALS AND METHODS

Study design

This retrospective study involved patients with biopsy proven NASH evaluated at Gangnam Severance Hospital, Yonsei University College of Medicine, Seoul, Republic of Korea. Liver biopsy was performed to confirm the diagnosis of NASH in patients with ultrasound findings of fatty liver and persistent (> 6 mo) elevation of the alanine aminotransferase (ALT) or aspartate aminotransferase (AST) level without excessive alcohol consumption (30 g/day in men and 20 g/day in women). Patients in whom liver stiffness was evaluated within 1 mo before the liver biopsy were included in the analysis. The exclusion criteria were as follows: (1) Liver disease of other or mixed

etiology (such as hepatitis B infection, hepatitis C infection, alcohol abuse, autoimmune liver disease, Wilson's disease, or drug-induced liver disease); (2) LSM evaluated while the AST or ALT level was more than fivefold the upper limit of normal (ULN); (3) Hepatocellular carcinoma; (4) Advanced liver cirrhosis (Child-Turcotte-Pugh B and C); (5) Previous treatment with steatosis-inducing drugs such as tamoxifen, aromatase inhibitor, valproic acid, amiodarone or corticosteroid; (6) Human immunodeficiency virus infection; (7) Active intravenous drug addiction or use of cannabis; and (8) Insufficient clinical data.

This study was performed in accordance with the ethical guidelines of the 1975 Declaration of Helsinki and was approved by the Institutional Review Board (IRB) of Gangnam Severance Hospital (permit no: 3-2019-0010). The requirement for written informed consent was exempted by the IRB since the database was accessed only for analysis purposes and the patients' personal information was anonymized by coding.

Clinical assessment

Demographic, clinical and anthropometric data were collected at the time of liver biopsy. Hypertension was defined as use of antihypertensive medication and type 2 diabetes mellitus was considered present if the fasting glucose level was ≥ 126 mg/dL or antidiabetic agents were being used. Body mass index (BMI) was calculated as body weight in kilogram divided by the square of height in meters, and a BMI ≥ 25 kg/m^2 was considered to indicate obesity based on the criteria used in the Asian-Pacific region[15].

Liver stiffness measurement

TE was performed using a FibroScan (Echosens, Paris, France), medical device, with a standard probe. Only LS values with at least 10 valid measurements, a success rate of at least 60%, and an interquartile range-to-median ratio of < 30% were considered reliable, as suggested by previous studies[16,17]. In addition, patients in whom LS was measured while the AST or ALT > 5 × ULN was present, were excluded from the analysis due to possible exaggerated LSM values as previous studies demonstrated[18,19]. The baseline LSM was obtained within 1 month before liver biopsy. The follow-up LSM was performed after 12 mo of NASH treatment with daily dose of 15 mg pioglitazone, peroxisome proliferator-activated receptor (PPAR)-γ agonist, or 300 mg/day ursodeoxycholic acid (UDCA) following liver biopsy.

Histologic assessment

A single liver-dedicated expert pathologist, blinded to the patients' identity, performed the histologic analysis. A ≥ 15-mm-long biopsy specimen or the presence of at least 10 complete portal tracts was considered adequate for the analysis[20]. NASH was diagnosed according to the NASH Clinical Research Network System, and was defined as the presence of ≥ 5% hepatic steatosis and inflammation with hepatocyte injury such as ballooning with or without fibrosis[21].

Statistical analysis

All statistical tests were performed using IBM SPSS Statistics 22.0 (IBM, Armonk, NY, United States). Continuous variables are expressed as means ± standard deviation (SD) or medians (range). The area under the receiver-operating characteristic (ROC) curve was calculated to reflect the overall accuracy of LSM for diagnosing significant fibrosis (F2-4). Categorical variables were compared by using two-sided χ^2-test (or Fisher's exact test, or McNemar test, as appropriate) and continuous variables by independent or Mann-Whitney test as appropriate. A paired *t* test was performed to evaluate changes in LSM. A two-sided *P* value of < 0.05 was considered indicative of statistical significance.

RESULTS

Patients

From January 2010 to December 2017, 325 patients underwent liver biopsy and LSM assessed due to suspicion of NASH. Among them, 184 patients met the inclusion and exclusion criteria and were thus included in the analysis. The baseline characteristics of the 184 patients with NASH are listed in Table 1.

Assessment of steatosis using CAP

Among the 184 patients with biopsy proven NASH, the distribution of the histologically assessed steatosis grade (S) was as follows: S1, *n* = 44 (2.9%); S2, *n* = 81 (44.0%); S3, *n* = 59 (32.1%) (Figure 1). The CAP scores were significantly different between S1 and S2-S3 (*P* < 0.001). However, no significant difference was detected

Table 1 Demographic, clinical, biochemical and histological characteristics of 184 patients with nonalcoholic steatohepatitis

Variable	NAFLD (*n* = 184)
Age (yr)	44.6 ± 14.5
Male gender	127 (69.0%)
Body mass index, median (range, kg/m^2)	29.3 (19.8-44.5)
Body mass index ≥ 25 kg/m^2	156 (84.8%)
Diabetes	69 (37.5%)
Hypertension	54 (29.3%)
Hyperlipidemia	75 (40.8%)
Fasting glucose (mg/dL)	117.9 ± 32.9
HDL cholesterol (md/dL)	47.1 ± 11.8
Triglycerides (mg/dL)	193.8 ± 127.5
LDL cholesterol (mg/dL)	131.7 ± 31.3
Alanine aminotransferase (U/L)	92.4 ± 68.1
Aspartate aminotransferase (U/L)	67.3 ± 39.2
Gamma glutamyltransferase (U/L)	74.1 ± 86.7
Platelet (× 1000/mm^3)	244.8 ± 58.6
Albumin (g/dL)	4.5 ± 0.3
Liver stiffness (kPa)	10.9 ± 4.9
Stiffness IQR (kPa)	1.8 ± 3.3
CAP (dB/m)	320.9 ± 37.1
Lower tertile	223-310
Middle tertile	311-339
Higher tertile	340-400
CAP IQR (dB/m)	24.7 ± 9.5
Histology at biopsy	
Steatosis grade	
1 (5%-33%)	44 (23.9%)
2 (34%-66%)	81 (44.0%)
3 (> 66%)	59 (32.1%)
Stage of fibrosis (Kleiner)	
0	20 (10.9%)
1	84 (45.7%)
2	53 (28.8%)
3	21 (11.4%)
4	6 (3.3%)

Data are expressed as the mean ± standard deviation, median (range) or number (%). HDL: High-density lipoprotein; LDL: Low-density lipoprotein; CAP: Controlled attenuation parameter; IQR: Interquartile range; NAFLD: Nonalcoholic fatty liver disease.

between S2 and S3 (P = 0.075). The ROC curve showed the optimum CAP cutoff for ≥ S2 was 313.5 dB/m [area under the curve (AUC), 0.736; sensitivity, 72.9%; specificity, 63.6%]. On the other hands, the accuracy dropped to an AUC of 0.656 for S3, with a cutoff of 323.5 dB/m (sensitivity 64.4%; specificity 55.2%).

Factors associated with LSM

LSM significantly increased with the histologically detected fibrosis stage (F0, 7.5 ± 2.1; F1, 9.8 ± 2.7; F2, 11.8 ± 4.9; F3, 15.4 ± 6.9; and F4, 20.3 ± 8.8 kPa) (P < 0.001). The ROC curve showed that the optimum LSM cutoff for ≥ F2 was 8.95 kPa (AUC, 0.730; sensitivity, 72.5%; specificity, 65.4%). According to univariate and multivariate analyses, the CAP values and pathologically detected fibrosis stage was significantly associated with LSM (Table 2).

Although there were significant differences in CAP scores between S1 and S2-S3, no cutoff could differentiate S3 from S2. S2 and S3 accounted for the majority of the patients (76.1%, 140/184). Furthermore, in a multivariate analysis, the CAP value, but not the pathologically detected steatosis grade, was associated with LSM. Therefore,

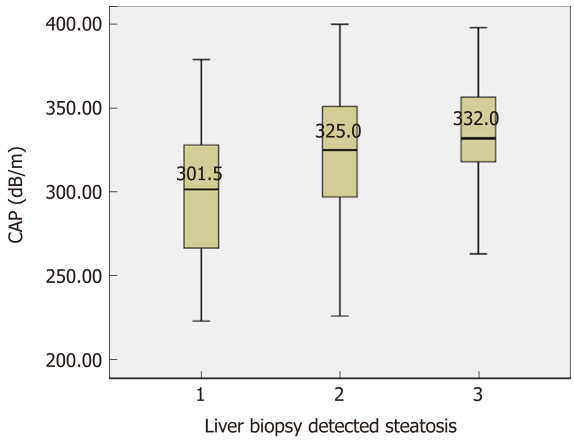

Figure 1 Distribution of controlled attenuation parameter scores according to histologically assessed steatosis grades (S). CAP: Controlled attenuation parameter.

the variations in the LSM value for each stage of liver fibrosis was evaluated according to arbitrary CAP tertiles (lower, 223-310; middle, 311-339; high 340-400 dB/m) (Figure 2). For F0-1, LSM values significantly increased at high CAP tertile (P = 0.001) (Figure 2A). For F2, LSM values were higher for the middle and high CAP tertiles (P = 0.027) (Figure 2B). However, the LSM values did not differ significantly according to CAP tertile in patients with NASH and advanced fibrosis (F3-4) (P = 0.752) (Figure 2C).

When cutoff of 8.95 kPa was used to diagnose significant fibrosis (F ≥ 2), positive predictive values in lower, middle and high CAP tertiles was 21/31 (67.7%), 19/32 (59.4%) and 23/49 (46.9%), respectively. False positive rates increased with increasing CAP tertile (Figure 3A). However, when different cutoffs were used for each CAP tertile, differences in false positive rates among different CAP tertile were reduced and the false positive rate in high CAP tertile decreased (Figure 3B). ROC curves showed that the optimum LSM cutoff for diagnosis of F ≥ 2 was 8.05 kPa (AUC, 0.682; sensitivity, 73.5%; specificity 51.7%) for the lower CAP tertile, LSM of 9.35 kPa (AUC, 0.843; sensitivity, 90.5%; specificity 71.8%) for the middle CAP tertile, and LSM of 10.55 kPa (AUC 0.682; sensitivity, 76.0%; specificity 52.8%) for high CAP tertile.

Effect of PPAR-γ agonist on follow up LSM

Among the 184 patients with biopsy proven NASH, 130 patients had LS measured 1 year after liver biopsy and were treated with PPAR-γ agonist (pioglitazone) 15 mg/day (n = 80) or UDCA 300 mg/day (n = 50). Regarding the baseline characteristics, there was no significant difference in BMI, LS value or CAP score between the two groups (Table 3). However, the pioglitazone group had higher rates of DM and hypertension (P = 0.048, P = 0.049, respectively).

The patients treated with pioglitazone demonstrated a decreased LSM value after 1- year of treatment (P < 0.001), when that in UDCA-treated patients did not change significantly (P = 0.068) (Figure 4). The CAP values did not show significant changes after treatment with pioglitazone (318.2 ± 37.9 *vs* 313.2 ± 41.5 dB/m, P = 0.197) or UDCA (319.3 ± 37.1 *vs* 309.2 ± 38.2 dB/m, P = 0.057). Changes in the proportion of patients with LSM suggesting significant fibrosis (F ≥ 2) were assessed separately in the pioglitazone and UDCA groups according to the LSM cutoffs for each CAP tertile, that were obtained from the analysis with 184 patients. Among the patient with lower CAP tertile (223-309 dB/m), those treated with pioglitazone showed a decreased proportion of high LSM values (F ≥ 2) but the proportion of high LSM values did not change significantly among the patients treated with UDCA (Figure 4A). Similar results were noted in patients with middle (310-332 dB/m) and high CAP tertile (333-400 dB/m) (Figure 4B and C).

DISCUSSION

This study of 184 patients with biopsy proven NASH demonstrated that high CAP scores are associated with increased LSM values at the same fibrosis stage, resulting in overestimation of liver fibrosis. Lower positive predictive values were noted in patients in the high CAP tertile, particularly those with F0-2. Therefore, higher LSM cutoffs might be useful for identifying significant fibrosis in patients with NAFLD and

Table 2 Univariate and multivariate analysis of factors associated with liver stiffness measurements as continuous variable in 184 patients with nonalcoholic steatohepatitis by linear regression analysis

	Univariate analysis			Multivariate analysis		
Variable	**β**	**SE**	***P***	**β**	**SE**	***P***
Age (yr)	0.053	0.025	0.037[a]	0.017	0.022	0.451
Male gender	0.957	0.792	0.228			
BMI (kg/m^2)	-0.032	0.083	0.700			
CAP (dB/m)	0.022	0.010	0.026[a]	0.041	0.009	< 0.001[b]
LS IQR (kPa)	0.329	0.109	0.003[b]	0.294	0.022	0.451
Histology at biopsy						
Steatosis	-0.895	0.490	0.069	-0.532	0.445	0.233
Lobular inflammation	1.134		0.082	0.152		0.776
	1.366	0.650	0.008[b]	0.638	0.532	0.131
Ballooning	2.769	0.509	< 0.001[b]	2.665	0.421	< 0.001[b]
Fibrosis		0.331			0.344	

[a]*P* < 0.05;
[b]*P* < 0.01. SE: Standard error; BMI: Body mass index; CAP: Controlled attenuated parameter; LS IQR: Liver stiffness interquartile range.

high CAP values. Although a "high CAP cutoff value" had yet to be defined, the cutoff for the high CAP tertile in this study was 330-340 dB/m.

Two prospective cohort studies on the natural history of NAFLD proposed that the severity of liver fibrosis is the most important predictor of liver-related complications as well as survival in patients with NAFLD[2,3]. In addition, recent studies suggested that only the severity of fibrosis is an important prognostic factor for NAFLD, and is independent of NASH and the severity of inflammation[4,22]. These studies investigated the prognostic value of the baseline liver fibrosis stage, and one also assessed the progression of liver fibrosis in patients with NAFLD[5]. Therefore, when sequential liver biopsy is not practical, accurate prediction of fibrosis stage using noninvasive methods is important. To reduce the effect of hepatic steatosis, as indicated by CAP scores, on the prediction of fibrosis based on LSM, we calculated the cutoff values for significant fibrosis in according to CAP tertile. We applied arbitrary CAP tertiles since the CAP score did not accurately differentiate S2 from S3 which accounted for the majority of the patients. Also, CAP reportedly cannot differentiate adjacent grades of steatosis with high precision[23]. As a noninvasive means of steatosis measurement, magnetic resonance imaging (MRI)-proton density fat traction (PDFF) is reported to be more accurate for predicting hepatic steatosis compared to CAP[24]. Magnetic resonance elastography (MRE) has the highest diagnostic accuracy for staging fibrosis in patients with NAFLD. However, both MRI-PDFF and MRE are MRI-based tools that require more space and more costly than FibroScan with CAP[25].

Cutoff values according to CAP tertile were applied to estimate the effect of pioglitazone and UDCA on the LSM values at the 1-year follow up. Treatment with pioglitazone reduced LSM-estimated proportion of significant fibrosis. However, the CAP score did not change significantly after pioglitazone or UDCA administration. In recent NAFLD practice guidance, pioglitazone and 800 IU/day vitamin E are recommended to improve liver histology in patients with NASH[26]. The 184 patients from which the LSM cutoff values for significant fibrosis were estimated included 130 patients treated with pioglitazone or UDCA. Although pioglitazone improved the LSM value, the utility of this result is limited by several factors. Ironically, the accuracy of LSM cutoff determined based on the CAP score cannot be validated without follow-up biopsy after pioglitazone or UDCA treatment in patients with NASH. Therefore, studies involving paired liver biopsies are needed, until more reliable LSM standards for NAFLD are established. Secondly, being a retrospective, observational study, the baseline demographic parameters of the pioglitazone and UDCA-treated groups were not matched. Patients treated with pioglitazone were more likely to be diabetic and hypertensive which are important elements of metabolic syndrome. Among NAFLD patients with fibrosis progression, 80% were diabetic, suggesting that diabetes promotes the progression of NASH[5]. Although it involved a larger number of patients with diabetes, our study showed that

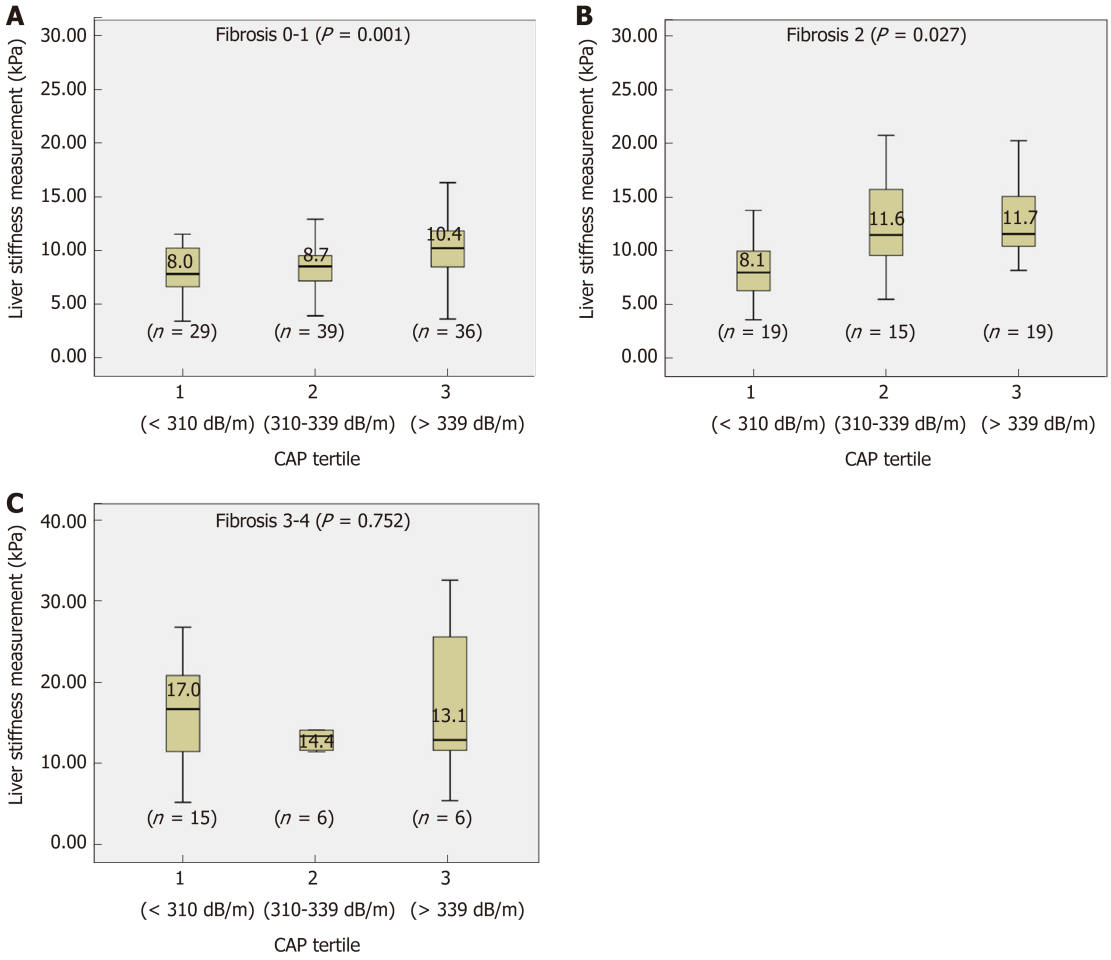

Figure 2 Distribution of liver stiffness values within the same Kleiner fibrosis stages (F0-4) in different controlled attenuation parameter tertiles. A: F0-1; B: F2; C: F3-4. CAP: Controlled attenuation parameter.

pioglitazone resulted in a reduced proportion of patients with high LSM values compared to UDCA. However, the sample size was too small to reach a definite conclusion. Finally, unlike previous investigations of the effect of pioglitazone on NASH, the patients in this study received low dose of pioglitazone (15 mg/day). Two randomized studies of the effect of pioglitazone on NASH prescribed pioglitazone 30 mg or 45 mg daily to patients with NASH[27,28]. The mean BMIs of the patients in these previous studies were about 33-35 kg/m^2, compare to 29.2 ± 4.5 kg/m^2 in this study, and the lower dose of pioglitazone may have been effective due to the lower BMI of our patients. Further studies investigating smaller doses of pioglitazone on patients with NASH are needed to verify our results.

In conclusion, LSM in patients with NASH may overestimate the liver fibrosis stage, particularly in those with high CAP values. Interpretation of LSM results taking into consideration the simultaneously measured CAP scores may prevent the performance of unnecessary liver biopsy in patients with NAFLD.

Table 3 Demographic, clinical, biochemical and histological characteristics of patients with nonalcoholic steatohepatitis under either pioglitazone or ursodeoxycholic acid

Variable	Pioglitazone group (*n* = 80)	UDCA group (*n* = 50)	*P* value
Age (yr)	47.6 ± 14.5	44.9 ± 14.5	0.303
Male gender	60 (75.0%)	30 (60.0)	0.071
Body mass index ≥ 25 kg/m^2	66 (82.5%)	41 (82.0%)	0.942
Diabetes	38 (47.5%)	15 (30.0)	0.048[a]
Hypertension	29 (36.2%)	10 (20.0%)	0.049[a]
Hyperlipidemia	36 (45.0%)	26 (52.0%)	0.437
Fasting glucose (mg/dL)	121.3 ± 34.5	112.5 ± 24.1	0.090
HDL cholesterol (md/dL)	47.9 ± 10.0	47.7 ± 14.1	0.923
Triglycerides (mg/dL)	199.5 ± 147.7	185.9 ± 105.2	0.590
LDL cholesterol (mg/dL)	130.5 ± 29.4	136.4 ± 34.8	0.435
Alanine aminotransferase (U/L)	103.0 ± 76.1	74.6 ± 48.7	0.011[a]
Aspartate aminotransferase (U/L)	70.2 ± 40.5	65.7 ± 42.8	0.554
Gamma glutamyltransferase (U/L)	63.9 ± 61.3	62.3 ± 41.8	0.856
Platelet (× 1000/mm^3)	229.8 ± 54.8	253.2 ± 54.4	0.019[a]
Albumin (g/dL)	4.5 ± 0.3	4.5 ± 0.3	0.866
Liver stiffness (kPa)	11.7 ± 4.8	10.5 ± 5.4	0.183
Stiffness IQR (kPa)	2.2 ± 4.7	1.4 ± 0.9	0.387
CAP (dB/m)	318.2 ± 37.9	319.3 ± 37.1	0.873
CAP IQR (dB/m)	25.2 ± 9.0	23.0 ± 10.1	0.216
Fibrosis score (Kleiner)			0.017[a]
F0	2 (2.5%)	9 (18.0%)	
F1	41 (51.2%)	21 (42.0%)	
F2	24 (30.0%)	15 (30.0%)	
F3-4	13 (16.3%)	5 (10.0%)	

Data are expressed as the mean ± standard deviation or median (range) or number (%),
[a]*P* < 0.05. UDCA: Ursodeoxycholic acid; HDL: High-density lipoprotein; LDL: Low-density lipoprotein; CAP: Controlled attenuation parameter; IQR: Interquartile range.

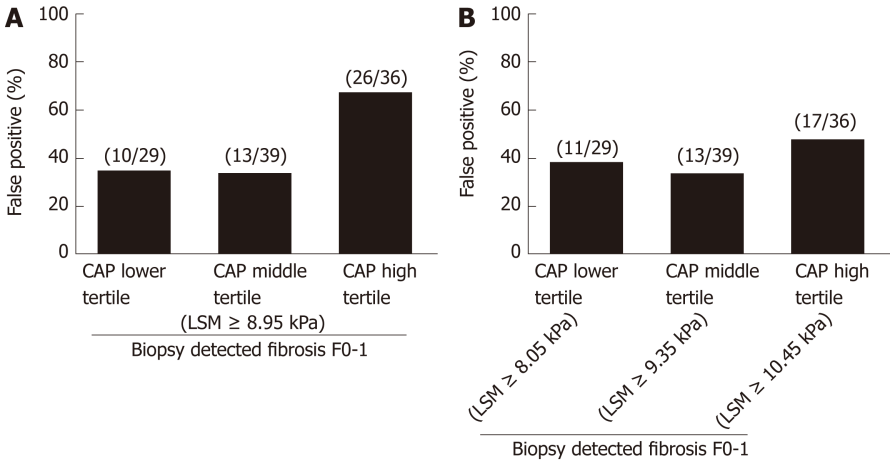

Figure 3 False-positive rates when evaluating liver fibrosis stages by liver stiffness measurements. A: The cutoff of 8.95 kPa for detecting Kleiner fibrosis stage (F) ≥ 2 was applied in all controlled attenuation parameter (CAP) tertiles; B: Different cutoffs were applied according to CAP tertiles. CAP: Controlled attenuation parameter; LSM: Liver stiffness measurements.

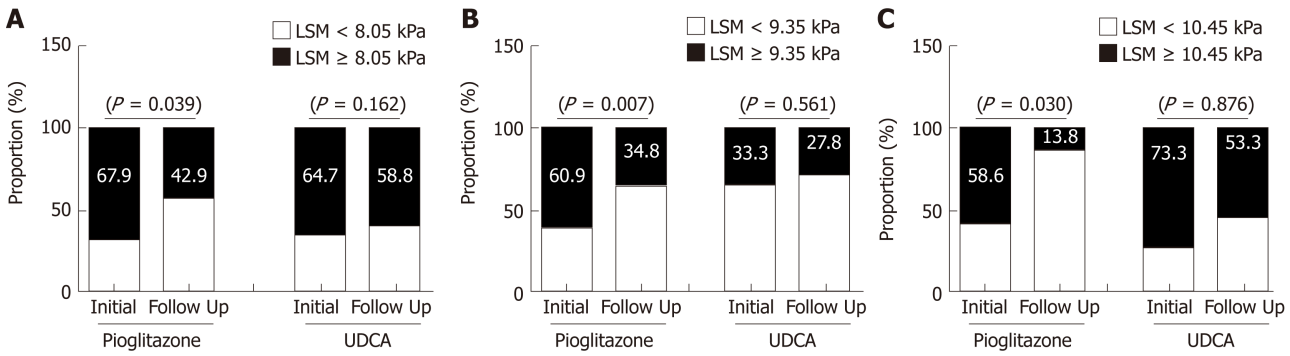

Figure 4 Change in the proportion of liver stiffness measurements predicting significant liver fibrosis, Kleiner fibrosis stage F ≥ 2, after 1-year of pioglitazone or ursodeoxycholic acid treatment. A: In the lower controlled attenuation parameter (CAP) tertile; B: In the middle CAP tertile; C: In the high CAP tertile. The liver stiffness measurements (LSM) cutoff values for F ≥ 2 are derived from the analysis 184 patients with biopsy proven nonalcoholic steatohepatitis after considering different CAP scores in tertiles. The changes in LSM values are compared by paired *t*-test. CAP: Controlled attenuation parameter; LSM: Liver stiffness measurements.

ARTICLE HIGHLIGHTS

Research background

In nonalcoholic fatty liver disease (NAFLD), studies demonstrate that the severity of liver fibrosis is the most important determinant of the disease prognosis. Although liver biopsy is considered the gold standard for identifying fibrosis stage, it is an invasive procedure, and liver stiffness measurement (LSM) is widely preformed as a noninvasive means. However, LSM tends to overestimate fibrosis stage in NAFLD.

Research motivation

Controlled attenuation parameter (CAP), provided by LSM device, has been introduced for noninvasive quantification of hepatic steatosis. It also has been suggested that CAP may contribute in enhancing the accuracy of transient elastography measured LSM in patients with NAFLD.

Research objectives

Our aim was to determine the role of CAP values in predicting liver fibrosis stages by LSM.

Research methods

This retrospective study involves 184 patients with biopsy proven nonalcoholic steatohepatitis (NASH), seen at a tertiary hospital in Seoul, Republic of Korea between 2010 and 2017. These patients had LSM and CAP evaluated within one month before the liver biopsy. Liver stiffness and CAP scores were measured by the FibroScan (Echosens, Paris, France), a medical device, using a standard probe. The patients in whom liver stiffness was measured when aspartate aminotransferase or alanine aminotransferase level was more than fivefold the upper limit of normal were excluded from the analysis due to the possibility of exacerbated LSM values. From 184 patients, 130 patients had 1-year follow-up LSM and analyzed for the changes of LSM after pioglitazone or ursodeoxycholic acid (UDCA) treatment.

Research results

Among 184 NASH patients with liver biopsy, histologically assessed steatosis grade (S) was distributed as follows: S1, n = 44 (2.9%); S2, n = 81 (44.0%); S3, n = 59 (32.1%). CAP scores were significantly different between S1 and S2-S3 (P < 0.001). However, no significant difference was found between S2 and S3 (P = 0.075). LSM significantly increased in accordance with the liver biopsy detected fibrosis stage (P < 0.001). After multivariate analysis, CAP value along with pathologically detected fibrosis stages was identified as a significant factor associated with LSM. Since our assessment showed that no reliable cutoff was demonstrated to differentiate S3 from S2 and 76.1% (140/184) of our study patients were either S2 or S3, variations of LSM within the same stage of liver fibrosis was evaluated according to the arbitrary CAP tertiles (lower 223-310, middle 311-339, high 340-400 dB/m). In Kleiner fibrosis stage F0 - 1, LSM values increased at high CAP tertile (P = 0.001), and in F2, at middle and high tertile (P = 0.027). No difference was noticed in F3-4 (P = 0.752) according to CAP tertile. Receiver operating characteristic curves for LSM cutoff in diagnosis of F ≥ 2 identified 8.05 kPa for lower CAP tertile, 9.35 kPa for middle, and 10.55 kPa for high tertile. The patients treated with pioglitozone demonstrated decreased LSM values after 1 year of the treatment (P < 0.001), when that in UDCA treated patients did not show significant changes (P = 0.068). CAP values did not show significant changes after pioglitazone (P = 0.197) or UDCA treatment (P = 0.057). When changes in proportion of significant fibrosis (F ≥ 2) were assessed among pioglitazone or UDCA treated patients reflecting CAP values, pioglitazone treated patients demonstrated decrease in proportion of high LSM.

Research conclusions

In conclusion, LSM in NASH may overestimate the liver fibrosis stage particularly in patients with high CAP values. Interpretation of LSM considering simultaneously measured CAP scores may provide more helpful information preventing unnecessary liver biopsy in patients with NAFLD.

Research perspectives

In patients with NAFLD with high CAP scores, LSM cutoff that leads to liver biopsy may need to be set higher than in those with other chronic liver diseases. Validation studies for more precise LSM cutoffs should be performed incorporating larger number of patients with biopsy proven NAFLD. With more reliable LSM cutoffs for noninvasive diagnosis of liver fibrosis in NAFLD, clinical studies evaluating efficacies of treatment would be more widely preformed in NAFLD.

REFERENCES

1 **Farrell GC**, Larter CZ. Nonalcoholic fatty liver disease: From steatosis to cirrhosis. *Hepatology* 2006; **43**: S99-S112 [PMID: 16447287 DOI: 10.1002/hep.20973]
2 **Ekstedt M**, Hagström H, Nasr P, Fredrikson M, Stål P, Kechagias S, Hultcrantz R. Fibrosis stage is the strongest predictor for disease-specific mortality in NAFLD after up to 33 years of follow-up. *Hepatology* 2015; **61**: 1547-1554 [PMID: 25125077 DOI: 10.1002/hep.27368]
3 **Angulo P**, Kleiner DE, Dam-Larsen S, Adams LA, Bjornsson ES, Charatcharoenwitthaya P, Mills PR, Keach JC, Lafferty HD, Stahler A, Haflidadottir S, Bendtsen F. Liver Fibrosis, but No Other Histologic Features, Is Associated With Long-term Outcomes of Patients With Nonalcoholic Fatty Liver Disease. *Gastroenterology* 2015; **149**: 389-97.e10 [PMID: 25935633 DOI: 10.1053/j.gastro.2015.04.043]
4 **Hagström H**, Nasr P, Ekstedt M, Hammar U, Stål P, Hultcrantz R, Kechagias S. Fibrosis stage but not NASH predicts mortality and time to development of severe liver disease in biopsy-proven NAFLD. *J Hepatol* 2017; **67**: 1265-1273 [PMID: 28803953 DOI: 10.1016/j.jhep.2017.07.027]
5 **McPherson S**, Hardy T, Henderson E, Burt AD, Day CP, Anstee QM. Evidence of NAFLD progression from steatosis to fibrosing-steatohepatitis using paired biopsies: Implications for prognosis and clinical management. *J Hepatol* 2015; **62**: 1148-1155 [PMID: 25477264 DOI: 10.1016/j.jhep.2014.11.034]
6 **Spinzi G**, Terruzzi V, Minoli G. Liver biopsy. *N Engl J Med* 2001; **344**: 2030 [PMID: 11430340 DOI: 10.1056/NEJM200102153440706]
7 **Marcellin P**, Ziol M, Bedossa P, Douvin C, Poupon R, de Lédinghen V, Beaugrand M. Non-invasive assessment of liver fibrosis by stiffness measurement in patients with chronic hepatitis B. *Liver Int* 2009; **29**: 242-247 [PMID: 18637064 DOI: 10.1111/j.1478-3231.2008.01802.x]
8 **Verveer C**, Zondervan PE, ten Kate FJ, Hansen BE, Janssen HL, de Knegt RJ. Evaluation of transient elastography for fibrosis assessment compared with large biopsies in chronic hepatitis B and C. *Liver Int* 2012; **32**: 622-628 [PMID: 22098684 DOI: 10.1111/j.1478-3231.2011.02663.x]
9 **Li Y**, Huang YS, Wang ZZ, Yang ZR, Sun F, Zhan SY, Liu XE, Zhuang H. Systematic review with meta-analysis: The diagnostic accuracy of transient elastography for the staging of liver fibrosis in patients with chronic hepatitis B. *Aliment Pharmacol Ther* 2016; **43**: 458-469 [PMID: 26669632 DOI: 10.1111/apt.13488]
10 **Petta S**, Di Marco V, Cammà C, Butera G, Cabibi D, Craxì A. Reliability of liver stiffness measurement in non-alcoholic fatty liver disease: The effects of body mass index. *Aliment Pharmacol Ther* 2011; **33**: 1350-1360 [PMID: 21517924 DOI: 10.1111/j.1365-2036.2011.04668.x]
11 **Wong GL**, Chan HL, Choi PC, Chan AW, Lo AO, Chim AM, Wong VW. Association between anthropometric parameters and measurements of liver stiffness by transient elastography. *Clin Gastroenterol Hepatol* 2013; **11**: 295-302.e1-3 [PMID: 23022698 DOI: 10.1016/j.cgh.2012.09.025]
12 **Petta S**, Maida M, Macaluso FS, Di Marco V, Cammà C, Cabibi D, Craxì A. The severity of steatosis influences liver stiffness measurement in patients with nonalcoholic fatty liver disease. *Hepatology* 2015; **62**: 1101-1110 [PMID: 25991038 DOI: 10.1002/hep.27844]
13 **Fujimori N**, Tanaka N, Shibata S, Sano K, Yamazaki T, Sekiguchi T, Kitabatake H, Ichikawa Y, Kimura T, Komatsu M, Umemura T, Matsumoto A, Tanaka E. Controlled attenuation parameter is correlated with actual hepatic fat content in patients with non-alcoholic fatty liver disease with none-to-mild obesity and liver fibrosis. *Hepatol Res* 2016; **46**: 1019-1027 [PMID: 27183219 DOI: 10.1111/hepr.12649]
14 **Petta S**, Wong VW, Cammà C, Hiriart JB, Wong GL, Marra F, Vergniol J, Chan AW, Di Marco V, Merrouche W, Chan HL, Barbara M, Le-Bail B, Arena U, Craxì A, de Ledinghen V. Improved noninvasive prediction of liver fibrosis by liver stiffness measurement in patients with nonalcoholic fatty liver disease accounting for controlled attenuation parameter values. *Hepatology* 2017; **65**: 1145-1155 [PMID: 27639088 DOI: 10.1002/hep.28843]
15 **Oh SW**. Obesity and metabolic syndrome in Korea. *Diabetes Metab J* 2011; **35**: 561-566 [PMID: 22247896 DOI: 10.4093/dmj.2011.35.6.561]
16 **Jung KS**, Kim SU, Ahn SH, Park YN, Kim DY, Park JY, Chon CY, Choi EH, Han KH. Risk assessment of hepatitis B virus-related hepatocellular carcinoma development using liver stiffness measurement (FibroScan). *Hepatology* 2011; **53**: 885-894 [PMID: 21319193 DOI: 10.1002/hep.24121]
17 **Kim MN**, Kim SU, Kim BK, Park JY, Kim DY, Ahn SH, Song KJ, Park YN, Han KH. Increased risk of hepatocellular carcinoma in chronic hepatitis B patients with transient elastography-defined subclinical cirrhosis. *Hepatology* 2015; **61**: 1851-1859 [PMID: 25643638 DOI: 10.1002/hep.27735]
18 **Fung J**, Lai CL, Cheng C, Wu R, Wong DK, Yuen MF. Mild-to-moderate elevation of alanine aminotransferase increases liver stiffness measurement by transient elastography in patients with chronic hepatitis B. *Am J Gastroenterol* 2011; **106**: 492-496 [PMID: 21157442 DOI: 10.1038/ajg.2010.463]
19 **Kim SU**, Kim JK, Park YN, Han KH. Discordance between liver biopsy and Fibroscan® in assessing liver fibrosis in chronic hepatitis B: Risk factors and influence of necroinflammation. *PLoS One* 2012; **7**: e32233 [PMID: 22384189 DOI: 10.1371/journal.pone.0032233]
20 **Colloredo G**, Guido M, Sonzogni A, Leandro G. Impact of liver biopsy size on histological evaluation of chronic viral hepatitis: The smaller the sample, the milder the disease. *J Hepatol* 2003; **39**: 239-244 [PMID: 12873821 DOI: 10.1016/S0168-8278(03)00191-0]
21 **Kleiner DE**, Brunt EM. Nonalcoholic fatty liver disease: Pathologic patterns and biopsy evaluation in clinical research. *Semin Liver Dis* 2012; **32**: 3-13 [PMID: 22418883 DOI: 10.1055/s-0032-1306421]

22 **Vilar-Gomez E**, Calzadilla-Bertot L, Wai-Sun Wong V, Castellanos M, Aller-de la Fuente R, Metwally M, Eslam M, Gonzalez-Fabian L, Alvarez-Quiñones Sanz M, Conde-Martin AF, De Boer B, McLeod D, Hung Chan AW, Chalasani N, George J, Adams LA, Romero-Gomez M. Fibrosis Severity as a Determinant of Cause-Specific Mortality in Patients With Advanced Nonalcoholic Fatty Liver Disease: A Multi-National Cohort Study. *Gastroenterology* 2018; **155**: 443-457.e17 [PMID: 29733831 DOI: 10.1053/j.gastro.2018.04.034]

23 **Sasso M**, Beaugrand M, de Ledinghen V, Douvin C, Marcellin P, Poupon R, Sandrin L, Miette V. Controlled attenuation parameter (CAP): A novel VCTE™ guided ultrasonic attenuation measurement for the evaluation of hepatic steatosis: Preliminary study and validation in a cohort of patients with chronic liver disease from various causes. *Ultrasound Med Biol* 2010; **36**: 1825-1835 [PMID: 20870345 DOI: 10.1016/j.ultrasmedbio.2010.07.005]

24 **Castera L**, Friedrich-Rust M, Loomba R. Noninvasive Assessment of Liver Disease in Patients With Nonalcoholic Fatty Liver Disease. *Gastroenterology* 2019; **156**: 1264-1281.e4 [PMID: 30660725 DOI: 10.1053/j.gastro.2018.12.036]

25 **Xiao G**, Zhu S, Xiao X, Yan L, Yang J, Wu G. Comparison of laboratory tests, ultrasound, or magnetic resonance elastography to detect fibrosis in patients with nonalcoholic fatty liver disease: A meta-analysis. *Hepatology* 2017; **66**: 1486-1501 [PMID: 28586172 DOI: 10.1002/hep.29302]

26 **Chalasani N**, Younossi Z, Lavine JE, Charlton M, Cusi K, Rinella M, Harrison SA, Brunt EM, Sanyal AJ. The diagnosis and management of nonalcoholic fatty liver disease: Practice guidance from the American Association for the Study of Liver Diseases. *Hepatology* 2018; **67**: 328-357 [PMID: 28714183 DOI: 10.1002/hep.29367]

27 **Belfort R**, Harrison SA, Brown K, Darland C, Finch J, Hardies J, Balas B, Gastaldelli A, Tio F, Pulcini J, Berria R, Ma JZ, Dwivedi S, Havranek R, Fincke C, DeFronzo R, Bannayan GA, Schenker S, Cusi K. A placebo-controlled trial of pioglitazone in subjects with nonalcoholic steatohepatitis. *N Engl J Med* 2006; **355**: 2297-2307 [PMID: 17135584 DOI: 10.1056/NEJMoa060326]

28 **Cusi K**, Orsak B, Bril F, Lomonaco R, Hecht J, Ortiz-Lopez C, Tio F, Hardies J, Darland C, Musi N, Webb A, Portillo-Sanchez P. Long-Term Pioglitazone Treatment for Patients With Nonalcoholic Steatohepatitis and Prediabetes or Type 2 Diabetes Mellitus: A Randomized Trial. *Ann Intern Med* 2016; **165**: 305-315 [PMID: 27322798 DOI: 10.7326/M15-1774]

World Journal of Gastroenterology

Submit a Manuscript: https://www.f6publishing.com

World J Gastroenterol 2019 September 7; 25(33): 4970-4984

DOI: 10.3748/wjg.v25.i33.4970

ISSN 1007-9327 (print) ISSN 2219-2840 (online)

ORIGINAL ARTICLE

Retrospective Study

Lymphocyte-to-monocyte ratio effectively predicts survival outcome of patients with obstructive colorectal cancer

Xian-Qiang Chen, Chao-Rong Xue, Ping Hou, Bing-Qiang Lin, Jun-Rong Zhang

ORCID number: Xian-Qiang Chen (0000-0001-5503-9840); Chao-Rong Xue (0000-0001-9543-4909); Ping Hou (0000-0001-6110-8080); Bing-Qiang Lin (0000-0001-7882-4235); Jun-Rong Zhang (0000-0001-8073-7405).

Author contributions: Chen XQ and Xue CR contributed equally to this work; Zhang JR, Hou P, and Chen XQ conceived the study, analyzed the data, and drafted the manuscript; Lin BQ helped revise the manuscript critically for important intellectual content; Xue CR helped collect the data and design the study.

Supported by Qihang Project of Fujian Medical University, No. 2017XQ1050.

Institutional review board statement: The study protocol was approved by the Institutional Review Board of Fujian Medical University Union Hospital.

Conflict-of-interest statement: All authors read and approved the final manuscript and declared no conflicts of interest.

Data sharing statement: No additional data are available.

STROBE statement: All the study design and drafting comply with the guidelines of the STROBE statement.

Xian-Qiang Chen, Chao-Rong Xue, Bing-Qiang Lin, Jun-Rong Zhang, Department of General Surgery (Emergency Surgery), Fujian Medical University Union Hospital, Fuzhou 350001, Fujian Province, China

Ping Hou, Immunotherapy Institute, Fujian Medical University, Fuzhou 350122, Fujian Province, China

Corresponding author: Jun-Rong Zhang, MD, Attending Doctor, Chief Doctor, Surgeon, Surgical Oncologist, Department of General Surgery (Emergency Surgery), Fujian Medical University Union Hospital, No. 29, Xin Quan Road, Fuzhou 350001, Fujian Province, China.
junrongzhang@fjmu.edu.cn
Telephone: +86-13705955083

Abstract

BACKGROUND

Obstructive colorectal cancer (OCC) is always accompanied by severe complications, and the optimal strategy for patients with OCC remains undetermined. Different from emergency surgery (ES), self-expandable metal stents (SEMS) as a bridge to surgery (BTS), could increase the likelihood of primary anastomosis. However, the stent failure and related complications might give rise to a high recurrence rate. Few studies have focused on the indications for either method, and the relationship between preoperative inflammation indexes and the prognosis of OCC is still underestimated.

AIM

To explore the indications for ES and BTS in OCCs based on preoperative inflammation indexes.

METHODS

One hundred and twenty-eight patients who underwent ES or BTS from 2008 to 2015 were enrolled. Receiver operating characteristic (ROC) curve analysis was used to define the optimal preoperative inflammation index and its cutoff point. Kaplan–Meier analyses and Cox proportional hazards models were applied to assess the association between the preoperative inflammation indexes and the survival outcomes [overall survival (OS) and disease-free survival (DFS)]. Stratification analysis was performed to identify the subgroups that would benefit from ES or BTS.

RESULTS

OS and DFS were comparable between the ES and BTS groups ($P > 0.05$). ROC

Manuscript source: Unsolicited manuscript

Received: April 29, 2019
Peer-review started: April 29, 2019
First decision: May 30, 2019
Revised: June 9, 2019
Accepted: July 19, 2019
Article in press: July 19, 2019
Published online: September 7, 2019

P-Reviewer: Chiba T, Watanabe T
S-Editor: Ma YJ
L-Editor: Wang TQ
E-Editor: Ma YJ

curve analysis showed derived neutrophil-to-lymphocyte ratio (dNLR) as the optimal biomarker for the prediction of DFS in ES ($P < 0.05$). Lymphocyte-to-monocyte ratio (LMR) was recommended for BTS with regard to OS and DFS ($P < 0.05$). dNLR was related to stoma construction ($P = 0.001$), pneumonia ($P = 0.054$), and DFS ($P = 0.009$) in ES. LMR was closely related to lymph node invasion (LVI) ($P = 0.009$), OS ($P = 0.020$), and DFS ($P = 0.046$) in the BTS group. dNLR was an independent risk factor for ES in both OS ($P = 0.032$) and DFS ($P = 0.016$). LMR affected OS ($P = 0.053$) and DFS ($P = 0.052$) in the BTS group. LMR could differentiate the OS between the ES and BTS groups ($P < 0.05$).

CONCLUSION
Preoperative dNLR and LMR could predict OS and DFS in patients undergoing ES and BTS, respectively. For OCC, as the potential benefit group, patients with a low LMR might be preferred for BTS *via* SEMS insertion.

Key words: Inflammation indexes; Emergency surgery; Self-expanding metal stent insertion as a bridge to surgery; Obstructive colorectal cancers

Core tip: As a supplement to recent guidelines, this manuscript demonstrates that lymphocyte-to-monocyte ratio could effectively differentiates the survival outcome between self-expanding metal stenting and emergency surgery in patients with obstructive colon cancer. Self-expanding metal stents might be preferred to the "potential benefit group" that with a low preoperative lymphocyte-to-monocyte ratio (<1.67).

Citation: Chen XQ, Xue CR, Hou P, Lin BQ, Zhang JR. Lymphocyte-to-monocyte ratio effectively predicts survival outcome of patients with obstructive colorectal cancer. *World J Gastroenterol* 2019; 25(33): 4970-4984
URL: https://www.wjgnet.com/1007-9327/full/v25/i33/4970.htm
DOI: https://dx.doi.org/10.3748/wjg.v25.i33.4970

INTRODUCTION

Although several studies have been implemented in the screening for colorectal cancer, approximately 8%-29% of patients are diagnosed with obstructive colorectal cancer (OCC) as the first symptom[1,2]. Emergency surgery (ES) with or without stoma construction and self-expandable metal stent (SEMS) insertion as a bridge to surgery (BTS) are the current methods for OCC[3]. A BTS is preferred for symptomatic OCC due to effective decompression, better preoperative nutritional preparation, an improvement in the immunological reaction, and a lower incidence of stoma creation[4,5]. However, the enhancement of tumor dissemination and early recurrence reported by some studies hinder the usage of a self-expandable metal stent in OCC[6,7]. Despite this, there is still no common consensus. Several predictive models on the prognostic outcome of OCC, including ASA, age, Duck's stage, and prognostic nutritional index, have been established[8,9], but few focus on the inflammation index[10].

The inflammatory response plays a dual role in the development of a tumor. On one hand, a chronic inflammatory response triggers the local accumulation of monocytes, platelets, and neutrophils, which secrete cytokines and inflammatory factors to induce tumor angiogenesis and metastasis. On the other hand, increasing monocytes and lymphatic cells would enhance the resistance against tumor invasion[11]. Increasing evidence shows that an elevated neutrophil-to-lymphocyte ratio (NLR) is closely related to a poor prognosis in ovarian cancer, cholangiocarcinoma, and elective colorectal cancer (CRC)[12-14]. The overexpression of circulating derived NLR, an effective biomarker for the diagnosis of early pancreatic cancer[15], was accompanied by increasing distal organ invasion in metastatic CRC[16]. An elevated preoperative lymphocyte-to-monocyte ratio (LMR), as a superior existing biomarker, was positively correlated with the survival outcomes of patients with resectable CRC and presented better overall survival[17]. Other inflammatory indexes, such as the platelet-to-lymphocyte ratio (PLR)[14] and systemic immune inflammation

index (SII)[18], have also been studied in the exploration of optimal predictive models for tumor recurrence.

Different from the acute inflammatory response in patients undergoing ES, the alleviation of bowel obstruction after successful SEMS insertion in patients undergoing BTS would elicit a better immunological reaction and nutritional support, which might change the predictive factors for prognosis between the two groups. Preoperative inflammation indexes might favor patient selection and the establishment of a valid predictive model for the prognosis of OCC. In this study, we compared different inflammation indexes and other clinicopathological factors to evaluate the potential indications for ES and BTS for OCC.

MATERIALS AND METHODS

Patient population

All patients (n = 128) who underwent surgery for OCC at the Department of Emergency Surgery of Fujian Medical University Union Hospital from January 2008 to October 2015 were included in this study. Data from the patients' records were retrospectively collected and evaluated. The Institutional Review Board of Fujian Medical Union Hospital approved the study protocol. All patients provided informed consent for surgery. Patients were divided into an ES group and a BTS group based on the grade of bowel obstruction and families' choices. For incomplete obstruction, ES was preferred as the first choice. For complete obstruction, once patients who refused to accept SEMS insertion or failed in SEMS insertion, they would accept ES with intraoperative decompression.

Classification criteria

Patients who manifested with bowel obstruction were enrolled in this study. All diagnoses of OCC were confirmed by both emergency abdominal computed tomography (CT) and a pathological examination. The exclusion criteria were as follows: (1) Patients who rejected surgery or were diagnosed with acute peritonitis or perforation; (2) Patients with severe infection, hematological diseases, or an immunological deficit; and (3) Patients who received preoperative adjuvant chemotherapy, radiotherapy, or immunotherapy.

Surgical protocols

For left-side OCC, we performed intraoperative lavage or manual decompression for better bowel preparation, and these protocols have been previously depicted. For right-side OCC, radical dissection with one-stage anastomosis was performed[19].

SEMS with BTS

Stent insertion was performed by an endoscopist who had experienced over 400 endoscopic retrograde cholangiopancreatography (ERCP) procedures. Bridge to elective surgery was performed, once the stent was so successfully inserted that the intestinal obstruction completely relieved. Otherwise, ES was immediately performed.

Definition of variants

The neutrophil, lymphocyte, monocyte, and platelet counts from the peripheral blood tests and the inflammation indexes dependent on these factors were performed before surgery (*e.g.*, NLR, dNLR, LMR, PLR, and SII) and stent insertion (*e.g.*, NLR-pre, dNLR-pre, LMR-pre, PLR-pre, and SII-pre). The methods for the calculation of NLR, dNLR, LMR, and PLR have been described in previous studies[13]. The SII was calculated as (platelet count × neutrophil count)/lymphocyte count[18]. The cutoff point and the area under the curve (AUC) value of each inflammation index for the prediction of OS and DFS were determined with X-tile 3.6.1 software (Yale University, New Haven, CT, United States)[20]. According to the cutoff point, patients were divided into low-ratio and high-ratio groups for further analysis.

According to the American Joint Committee on Cancer (AJCC) Cancer Staging Manual (7th edition)[21], we classified the tumor pathological stage. Comorbidities were defined as hypertension, diabetes mellitus, and single and multiple organ dysfunction. The degree of obstructive symptoms was divided into five grades, termed as The ColoRectal Obstruction Scoring System (CROSS)[22]. According to the Clavien-Dindo classification system[23,24], we classified the perioperative complications into five grades.

Statistical analysis

Qualitative variables were compared by the χ^2 test or Fisher's exact test, and quantitative variables were compared *via* *t*-tests. Through Kaplan-Meier analysis, the

3-year OS and 3-year DFS were calculated. A Cox proportional hazards regression model was built to identify the independent risk factors for 3-year DFS and 3-year OS. Stratification analysis was used to compare the differences between subgroups. All *P*-values less than 0.05 were considered statistically significant. All statistical analyses and graphs were generated using SPSS 23.0 software.

RESULTS

Baseline characteristics

There were 128 patients enrolled in this study, who were divided into an ES group (n = 90) and a BTS group (n = 38), with similar age and sex ratios between the groups (P > 0.05). The average tumor size was 6.88 ± 2.68 cm in the BTS group, with a higher proportion of tumors located on the left side of the colon (73.70% *vs* 41.10%, P = 0.005), and was much larger than the tumor size in the ES group (5.76 ± 2.12 cm, P = 0.015). Moreover, the obstructive symptoms were more severe in the BTS group than in the ES group (Grade 0-I, 97.40% *vs* 68.50%, P = 0.001), as presented in Table 1. The remaining characteristic factors, including BMI, abdominal surgery history, comorbidities, ASA grade, pTNM stage, histological features, and the ratio of chemotherapy were similar between the ES and BTS groups (P > 0.05).

Outcome comparison between the ES and BTS groups

The blood loss in the BTS group was lower than that in the ES group (133.68 ± 95.76 mL *vs* 177.30 ± 134.37 mL, P = 0.072), with similar gastrointestinal recovery and postoperative complications (P > 0.05) (Table 2). Analogical survival outcomes including 3-year OS (30.10 ± 9.64 mo *vs* 29.41 ± 11.33 mo, P = 0.732) and 3-year DFS (27.59 ± 12.19 mo *vs* 27.48 12.17 mo, P = 0.969) were compared between the ES and BTS groups, and are plotted in Figure 1.

Predictive values and cutoff points of different inflammation indexes

A decreasing tendency was observed for WBC ($8.56 \times 10^9 \pm 3.44 \times 10^9$), NLR (4.88 ± 3.02), and SII (1235.74 ± 849.53) in the BTS group after SEMS insertion, compared with the WBC ($7.57 \times 10^9 \pm 2.61 \times 10^9$), NLR (6.05 ± 3.03), and SII (1712.60 ± 1157. 32) before SEMS insertion (P < 0.05), as presented in Table 1. Different inflammation indexes were analyzed between the ES and BTS groups. As a result, dNLR was preferred as a prognostic biomarker for the ES group since it had the highest AUC for 3-year OS (0.679, 95%CI: 0.551-0.808) and 3-year DFS (0.679, 95%CI: 0.551-0.808); the cutoff point value was 1.57. Conversely, based on the highest AUC for 3-year OS (0.611, 95%CI: 0.424-0.798) and 3-year DFS (0.571, 95%CI: 0.366-0.776), the LMR was recommended as a prognostic biomarker for the BTS group, with 1.67 as its cutoff point. These data are depicted in Table 3 and plotted in Figure 2.

Clinical evaluation of different inflammation indexes

In Table 4, patients were divided into high-ratio and low-ratio grades based on the dNLR in the ES group and the LMR in the BTS group. A high-ratio grade of dNLR (≥ 1.57) was closely related to a higher proportion of tumors located on the left side of the colon and rectum (P = 0.007), and a higher incidence of stoma construction (P = 0.001) and postoperative pneumonia (P = 0.054), with a lower 3-year DFS (dNLR ≥ 1.57: 23.10 ± 13.85 mo *vs* dNLR < 1.57: 31.45 ± 9.35 mo, P = 0.009) in the ES group. Separately, a high-ratio grade of the LMR (≥ 1.67) in the BTS group showed more advanced lymphovascular metastasis (P = 0.072) and lymph node invasion (P = 0.009), with a lower 3-year OS (LMR ≥ 1.67: 25.26 ± 13.88 mo *vs* LMR < 1.67: 33.78 ± 5.35 mo, P = 0.020) and 3-year DFS (LMR ≥ 1.67: 22.67 ± 14.02 mo *vs* LMR < 1.67: 31.50 ± 8.89 mo, P = 0.046). The dNLR was the only independent risk factor in the ES group both for 3-year OS (HR = 2.34, 95%CI: 1.08-5.07, P = 0.032) and 3-year DFS (HR = 3.02, 95%CI: 1.23-7.42, P = 0.016). In contrast, the status of LVI (HR = 3.52, 95%CI: 1.03-12.02, P = 0.045) and the LMR (HR = 4.57, 95%CI: 0.98-21.38, P = 0.053) significantly affected the 3-year OS in the BTS group. Only the LMR was an independent risk factor for 3-year DFS (HR = 3.11, 95%CI: 1.13-8.54, P = 0.052) in the BTS group, as shown in Tables 5 and 6 and Figure 2.

Selective choices based on inflammatory biomarkers

By stratification analysis of 3-year OS and 3-year DFS in different grades of dNLR and LMR, we revealed that only the LMR obviously differentiated the oncological and survival outcomes between the ES and BTS groups. A lower LMR (<1.67), as a protective factor, indicated a lower rate of death (HR = 0.40, 95%CI: 0.18-0.92, P = 0.031) and tumor recurrence (HR = 0.42, 95%CI: 0.17-1.07, P = 0.068) in the BTS group. Conversely, a higher LMR (≥1.67), as a risk factor, showed a higher proportion of

Table 1 Comparison of clinicopathological characteristics between emergency surgery and bridge to surgery groups

Characteristic	ES group (*n* = 90)	BTS group (*n* = 38)	*P*-value
Age (yr)	61.58 ± 14.84	63.21 ± 13.55	0.561
Female/Male, (%)	31 (34.40)/59 (65.60)	15 (39.50)/23 (60.50)	0.588
Size, (cm)	5.76 ± 2.12	6.88 ± 2.68	**0.015**
BMI, (kg/m^2)	21.76 ± 2.42	22.20 ± 3.20	0.411
Cross score, (%)			**0.001**
0	21 (23.60)	21 (55.30)	
1	40 (44.90)	16 (42.10)	
2	17 (19.10)	1 (2.60)	
3	10 (11.20)	0 (0.00)	
4	1 (0.80)	0 (0.00)	
ASH (+)/(-), (%)	17 (18.90)/73 (81.10)	10 (26.30)/28 (73.70)	0.347
Comorbidities (+)/(-), (%)	37 (41.10)/53 (58.90)	21 (55.30)/17 (44.70)	0.142
ASA grade, (%)			0.299
I	2 (2.20)	3 (7.90)	
II	63 (70.00)	28 (73.70)	
≥ III	25 (27.80)	7 (18.40)	
Location, (%)			**0.005**
Right-side colon	13 (14.40)	1 (2.60)	
Transverse colon	30 (33.30)	5 (13.20)	
Left-side colon	37 (41.10)	28 (73.70)	
Rectum	10 (11.10)	4 (10.50)	
pTNM stage, (%)			0.186
I	4 (4.40)	0 (0.00)	
II	23 (25.60)	9 (23.70)	
III	44 (48.90)	25 (65.80)	
IV	19 (21.10)	4 (10.50)	
T stage, (%)			0.186
T1	4 (4.40)	0 (0.00)	
T2	23 (25.60)	9 (23.70)	
T3	44 (48.90)	25 (65.80)	
T4	19 (21.10)	4 (10.50)	
N stage, (%)			0.471
N0	31 (34.40)	9 (23.70)	
N1	35 (38.90)	18 (47.40)	
N2	24 (26.70)	11 (28.90)	
M stage, (%)			0.292
M0	71 (78.9)	33 (86.8)	
M1	19 (21.1)	5 (13.2)	
Histological features, (%)			0.308
Well differentiated	3 (2.30)	0 (0.00)	
Moderately differentiated	61 (67.80)	30 (78.90)	
Poorly differentiated	26 (28.90)	8 (21.10)	
LVI (+)/(-), (%)	15 (16.70)/75 (83.30)	14(36.80)/24(63.20)	**0.013**
WBC, (10^9)	8.99 ± 5.10	7.57 ± 2.61	**0.042**
NLR, (ratio)	7.11 ± 6.72	4.88 ± 3.02	**0.012**
dNLR, (ratio)	1.66 ± 0.41	1.67 ± 0.27	0.756
PLR, (ratio)	245.61 ± 144.17	229.98 ± 122.38	0.562
LMR, (ratio)	2.84 ± 2.43	2.34 ± 1.19	0.127
SII, (ratio)	1969.03 ± 2316.10	1235.74 ± 849.53	**0.011**
WBC-pre, (10^9)	9.18 ± 5.13	8.56 ± 3.44	0.434
NLR-pre, (ratio)	7.62 ± 6.97	6.05 ± 3.03	0.084
dNLR-pre, (ratio)	1.65 ± 0.41	1.68 ± 0.45	0.652

PLR-pre, (ratio)	263.98 ± 161.96	270.89 ± 171.35	0.830
LMR-pre, (ratio)	2.77 ± 2.32	2.38 ± 1.66	0.354
SII-pre, (ratio)	2186.46 ± 2474.96	1712.60 ± 1157.32	0.149
CEA, (ng/mL)	30.19 ± 120.54	17.88 ± 27.47	0.541
Chemotherapy (+)/(-), (%)	62 (68.90)/28 (31.10)	20 (52.60)/18 (47.40)	0.080

SEMS: Self-expanding metal stents; BTS: Bridge to surgery; ASH: Abdominal surgery history; WBC: White blood cells; dNLR: Derived neutrophil–to-lymphocyte ratio; PLR: Platelet-to-lymphocyte ratio; SII: Systemic immune inflammation index; LMR: Lymphocyte-to-monocyte ratio; Cross: Colorectal obstruction scoring system; LVI: Lymphovascular invasion. $P < 0.05$ was considered statistically significant.

death (HR = 4.32, 95%CI: 1.27-14.82, $P = 0.019$) and tumor recurrence (HR = 2.72, 95%CI: 0.97-7.65, $P = 0.058$) in the BTS group; these data are presented in Table 7 and Figure 3.

DISCUSSION

OCC is always accompanied by a severe local and systemic inflammatory response; some reasons, including the overgrowth of intestinal bacteria, their translocation through the distended colonic wall, and, moreover, septic shock, have been recognized. In this study, we found that the cutoff point for the NLR of 19.30 was much higher than that in elective CRC[14,24], supporting the existing severe systemic inflammation. Although ES and BTS *via* SEMS insertion have been widely performed, there is still not an objective indication for either. Weighing the balance between oncological outcomes and better preoperative nutritional support with the alleviation of systemic inflammation, BTS *via* SEMS insertion is only recommended for symptomatic and high surgical risk groups, especially left-side OCC, by the ESGE and World Society of Emergency Surgery (WSES)[1,3]. In this study, analogous with a previous study[25], the BTS group had a higher proportion of LVI (36.80%), though similar 3-year OS and 3-year DFS were observed between the ES and BTS groups. A decreasing tendency in the WBC, NLR, and SII levels was observed after SEMS insertion, which might explain the reason why different inflammation indexes were concluded from the ES (dNLR) and BTS (LMR) groups in our study.

Since 1970, a decreasing peripheral lymphocyte count has been recorded in advanced colon cancer[26], and the inflammation index has been investigated in several kinds of cancer, as it is cost-effective and convenient. The dysbiosis and outgrowth of intestinal microbial species, as a result of acute bowel obstruction and distention, triggers systemic inflammation, leading to the accumulation of neutrophils and monocytes that secrete cytokines and chemokines with the induction of reactive oxygen species (ROS) and reactive nitrogen intermediates (RNI), which might aggravate colonic injury and DNA damage[11]. OCC almost coexists with immunosuppression, which causes a deficiency in adaptive immunologic cells such as T lymphocytes and B lymphocytes, which play important roles in immune surveillance and pathogen depletion[27]. The mechanical stress of SEMS and chronic ablation to the colonic wall enhances local platelet adhesion and the mediation of tumor invasion into lymphovascular vessels[28], which was supported in the current study by a higher proportion of LVI in the BTS group. In this study, we compared different inflammation indexes, including the NLR, dNLR, PLR, LMR and SII, with the CEA level in terms of the predictive value for the prognosis between the ES and BTS groups. Finally, the dNLR was defined as the most efficient index in the ES group; a high dNLR (≥ 1.57) was closely related to low survival benefits, a high incidence of stoma construction, and postoperative pneumonia. Dissimilarly, the LMR was defined as the most efficient index in the BTS group; a high LMR (≥ 1.67) was closely related to low survival benefits and a high incidence of LVI and lymph node invasion.

The reason why different predictive models for the ES and BTS groups were observed in OCC is still unknown. This might be owing to the hypothesis that, as a result of bacterial outgrowth and translocation, OCC always has a severe systemic inflammatory response and immunological deficit, and for patients with a high surgical risk, a BTS *via* SEMS insertion is preferred. In this study, we found that the BTS group had more severe obstructive symptoms and a bigger tumor size than the ES group. Sufficient alleviation of bowel distention and preoperative nutritional support would improve systemic inflammation and enhance the immunological reaction in the BTS group. However, the mechanical stress of the metal stent might aggravate the local inflammatory response[29-31] and enhance tumor invasion. In our

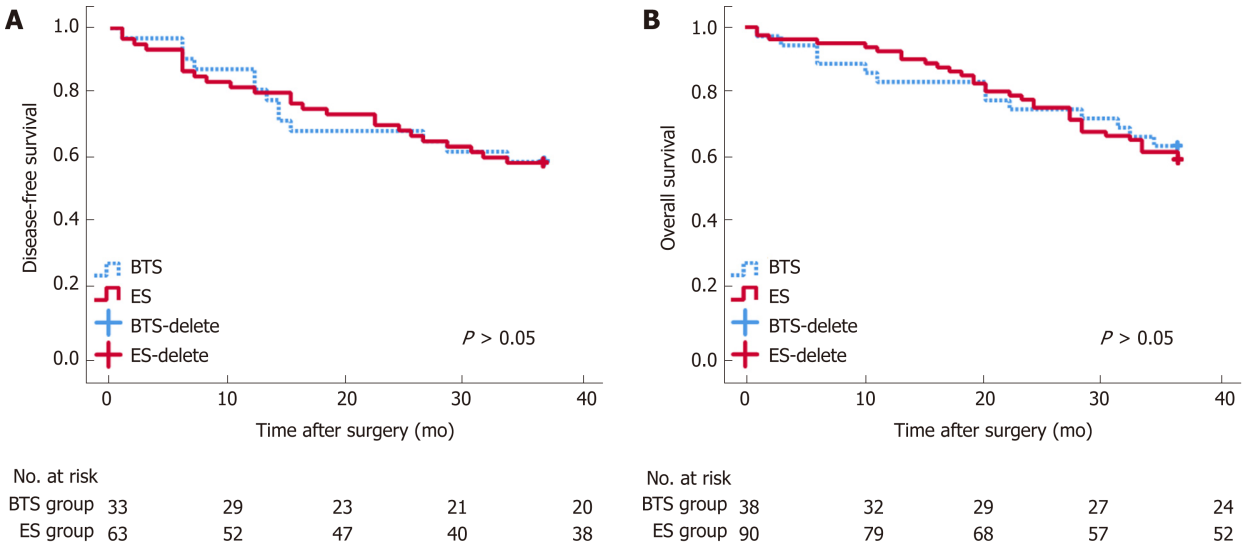

Figure 1 Long-term survival analysis between emergency surgery and bridge to surgery groups. Disease-free survival (DFS, A) and overall survival (OS, B) after surgery seemed similar between the bridge to surgery (BTS) and emergency surgery (ES) groups.

study, with the dramatic decrease of the systemic inflammatory response in the BTS group, the dNLR could not determine the benefit group for ES or BTS. Only the LMR could serve as an objective biomarker for the indication for OCC. A low LMR (< 1.67) was correlated with a low incidence of death and tumor recurrence in the BTS group. Conversely, a high LMR (≥ 1.67) showed a high proportion of death and tumor recurrence in the BTS group, and was preferred for ES.

There were some limitations existing in this study. First, this was a retrospective study in a single center; thus, we will initiate a prospective, multicenter study to confirm our findings. Second, the sample size was not so large that more patients are needed in future research. Furthermore, this study just analyzed the ratio of immune cell populations in the peripheral blood, instead of systematic immune responses including the production of cytokines or expression of PD-1 or CTLA-4. More efforts should be made on the investigation of immune responses occurring in the systemic circulation or tumor.

In conclusion, this study suggests a similar survival and oncological benefits for BTS and ES in patients with OCC. Even though different inflammation indexes for prediction of the prognosis were observed between the ES and BTS groups, they could serve as effective biomarkers. The dNLR was closely related to the prognosis in the ES group, while the LMR was closely related to the prognosis in the BTS group. Specifically, as the potential benefit group, patients with a low LMR might be preferred for BTS *via* SEMS insertion.

Table 2 Comparison of short-term and long-term outcomes between emergency surgery and bridge to surgery groups

Characteristic	ES group (*n* = 90)	BTS group (*n* = 38)	*P*-value
Surgical time, (min)	217.89 ± 60.69	204.64 ± 66.13	0.275
Blood loss, (mL)	177.30 ± 134.37	133.68 ± 95.76	**0.072**
Number of LNs	19.51 ± 9.47	21.45 ± 8.29	0.276
Time to flatus, (d)	3.88 ± 1.65	3.61 ± 1.15	0.359
Time to semi-fluid, (d)	8.62 ± 3.22	8.64 ± 3.96	0.738
Total hospital-stay, (d)	22.17 ± 12.48	22.34 ± 7.78	0.936
Stoma construction, *n* (%)	20 (22.20)	8 (21.10)	0.884
CD classification system, *n* (%)			0.547
Grade I	0 (0.00)	2 (2.20)	
Grade II	44 (48.90)	16 (42.10)	
Grade III	13 (14.40)	5 (13.20)	
Grade IV	9 (10.00)	2 (5.30)	
Grade V	1 (2.60)	1 (1.10)	
Pneumonia, *n* (%)	18 (20.00)	8 (21.10)	0.892
Incision infection, *n* (%)	16 (17.80)	5 (13.20)	0.519
ICU intervention, *n* (%)	8 (8.90)	1 (2.60)	0.192
Leakage, *n* (%)	3 (3.30)	1 (2.60)	0.658
Sepsis, *n* (%)	3 (3.30)	1 (2.60)	0.658
SAE, *n* (%)	23 (25.60)	8 (21.10)	0.587
30 d-mortality, *n* (%)	1 (1.10)	1 (2.60)	0.507
36-OS time, (mo)	30.10 ± 9.64	29.41 ± 11.33	0.732
36-DFS time, (mo)	27.59 ± 12.19	27.48 ± 12.17	0.969

LN: Lymph node; SEMS: Self-expanding metal stents; BTS: Bridge to surgery; SAE: Severe adverse effects. $P < 0.05$ was considered statistically significant.

Table 3 Receiver operating characteristic curve analysis of long-term survival of emergency surgery and bridge to surgery groups

Group	Characteristic	3-year OS			3-year DFS		
		Cutoff point	AUC	95%CI	Cutoff point	AUC	95%CI
ES	NLR	19.3	0.582	0.446-0.718	19.3	0.565	0.407-0.723
	dNLR	2.02	0.679	0.551-0.808	1.57	0.696	0.554-0.837
	PLR	155	0.550	0.414-0.686	317	0.549	0.392-0.707
	SII	3645	0.587	0.454-0.721	3645	0.564	0.403-0.726
	CEA	6.7	0.591	0.458-0.724	11.2	0.604	0.442-0.766
BTS	LMR	1.67	0.611	0.424-0.798	1.67	0.571	0.366-0.776
	CEA	7.6	0.549	0.350-0.747	5.5	0.552	0.348-0.756

SEMS: Self-expanding metal stents; BTS: Bridge to surgery; AUC: Area under the receiver operating characteristic curve; dNLR: Derived neutrophil-to-lymphocyte ratio; PLR: Platelet–to-lymphocyte ratio; SII: Systemic immune inflammation index; LMR: Lymphocyte-to-monocyte ratio; OS: Overall survival; DFS: Disease-free survival; CEA: Carcino-embryonic antigen. $P < 0.05$ was considered statistically significant.

Table 4 Comparison of clinicopathological features between high-ratio and low-ratio grades in both emergency surgery and bridge to surgery groups

Characteristic	ES group (*n* = 86)			BTS group (*n* = 38)		
	dNLR ≥ 1.57	dNLR < 1.57	*P*-value	LMR ≥ 1.67	LMR < 1.67	*P*-value
Cross score, (%)			0.738			0.378
0	11 (27.5)	10 (21.7)		10 (50.0)	11 (61.1)	
1	16 (40.0)	22 (47.8)		10 (50.0)	6 (33.3)	
2	8 (20.0)	8 (17.4)		0 (0.0)	1 (5.6)	
3	4 (10.0)	6 (13.0)				
4	1 (2.5)	0 (0.0)				
ASH (+)/(-), (%)	6 (15.0)/34 (85.0)	10 (21.7)/36 (78.3)		4 (20.0)/16 (80.0)	6 (33.3)/12 (66.7)	
Comorbidities (+)/(-), (%)	20 (50.0)/20 (50.0)	17 (37.0)/29 (63.0)		9 (45.0)/11 (55.0)	12 (66.7/)/6 (33.3)	
ASA grade, (%)			0.320			0.623
I	0 (0.0)	1 (1.6)		1 (5.0)	2 (11.1)	
II	13 (56.5)	47 (74.6)		16 (80.0)	12 (66.7)	
≥ III	10 (43.5)	15 (23.8)		3 (15.0)	4 (22.2)	
Location, (%)			**0.007**			0.523
Right-side colon	2 (5.0)	11 (23.9)		1 (5.0)	0 (0.00)	
Transverse colon	10 (25.0)	19 (41.3)		3 (15.0)	2 (11.1)	
Left-side colon	21 (52.5)	13 (28.3)		13 (65.0)	15 (83.3)	
Rectum	7 (17.5)	3 (6.5)		3 (15.0)	1 (5.6)	
pTNM stage, (%)			0.141			0.592
I	0 (0.0)	4 (8.7)		-	-	
II	12 (30.0)	10 (21.7)		4 (20.0)	5 (27.8)	
III	17 (42.5)	24 (52.2)		13 (65.0)	12 (66.7)	
IV	11 (27.5)	8 (17.4)		3 (15.0)	1 (5.6)	
T stage, (%)			0.141			0.592
T1	0 (0.0)	4 (8.7)		-	-	
T2	12 (30.0)	10 (21.7)		4 (20.0)	5 (27.8)	
T3	17 (42.5)	24 (52.2)		13 (65.0)	12 (66.7)	
T4	11 (27.5)	8 (17.4)		3 (15.0)	1 (5.6)	
N stage, (%)			0.648			**0.009**
N0	16 (40.0)	14 (30.4)		4 (20.0)	5 (27.8)	
N1	14 (35.0)	19 (41.3)		6 (30.0)	12 (66.7)	
N2	10 (25.0)	13 (28.3)		10 (50.0)	1 (5.6)	
M stage, (%)			0.260			0.552
M0	29 (72.5)	38 (82.6)		17 (85.0)	16 (88.9)	
M1	11 (27.5)	8 (17.4)		3 (15.0)	2 (11.1)	
Histological features, (%)			0.605			0.411
Well differentiated	1 (2.5)	2 (4.3)		-	-	
Moderately differentiated	30 (75.0)	30 (65.2)		15 (75.0)	15 (83.3)	
Poorly differentiated	9 (22.5)	14 (30.4)		5 (25.0)	3 (16.7)	
LVI (+)/(-), (%)	9 (22.5)/31 (77.5)	6 (13.0)/40 (87.0)	0.249	10 (50.0)/10 (50.0)	4 (22.2)/14 (77.8)	**0.076**
Stoma construction, (%)			**0.000**			0.589
Stoma	17 (42.5)	3 (6.5)		4 (20.0)	4 (22.2)	
None	23(57.5)	43 (93.5)		16 (80.0)	14 (77.8)	
Pneumonia, (+)/(-), (%)	12 (30.0)/28 (70.0)	6 (13.0)/40 (87.0)	**0.054**	2 (10.0)/18(90.0)	6 (33.3)/12 (66.7)	0.086
Incision infection, (+)/(-), (%)	8 (20.0)/32 (80.0)	8 (17.4)/38 (82.6)	0.486	2 (10.0)/18 (90.0)	3 (16.7)/15 (83.3)	0.448
ICU intervention, (+)/(-), (%)	5 (12.5)/35 (87.5)	3 (6.5)/43 (93.5)	0.281	1 (5.0)/19 (95.0)	0 (0.0)/18 (100.0)	0.526
Leakage, (+)/(-), (%)	1 (2.5)/39 (97.5)	2 (4.3)/44 (95.7)	0.553	0 (0.0)/20 (100.0)	1 (5.6)/17 (94.4)	0.474
Sepsis, (+)/(-), (%)	1 (2.5)/39 (97.5)	2 (4.3)/44 (95.7)	0.553	0 (0.0)/20 (100.0)	1 (5.6)/17 (94.4)	0.474
SAE, (+)/(-), (%)	10 (25.0)/30 (75.0)	11 (23.9)/35 (76.1)	0.907	5 (25.0)/15 (75.0)	3 (16.7)/15 (83.3)	0.411
30-day mortality, *n* (%)	1 (2.5)/39 (97.5)	0 (0.0)/46 (100.0)	0.465	1 (5.0)/19 (95.0)	0 (0.0)/18 (100.0)	0.526
36-OS time, (months)	28.05 ± 10.28	31.61 ± 9.16	0.106	25.26 ± 13.88	33.78 ± 5.35	0.020

36-DFS time, (months)	23.10 ± 13.85	31.45 ± 9.35	0.009	22.67 ± 14.02	31.50 ± 8.89	0.046

SEMS: Self-expanding metal stents; BTS: Bridge to surgery; Cross: Colorectal obstruction scoring system; ASH: Abdominal surgery history; dNLR: Derived neutrophil-to-lymphocyte ratio; PLR: Platelet-to-lymphocyte ratio; SII: Systemic immune inflammation index; LMR: Lymphocyte-to-monocyte ratio; LVI: Lymphovascular invasion; OS: Overall survival; DFS: Disease-free survival; ICU: Intense care unit; SAE: Severe adverse effects. $P < 0.05$ was considered statistically significant.

Table 5 Univariate and multivariate analyses of risk factors for survival outcomes in both emergency surgery and bridge to surgery groups

3-year overall survival	ES group (*n* = 90)				BTS group (*n* = 38)			
	Univariate		Multivariate		Univariate		Multivariate	
Characteristic	HR (95%CI)	*P*-value	HR (95%CI)	*P*-value	HR (95%CI)	*P*-value	HR (95%CI)	*P*-value
CEA (≥ 5 ng/mL *vs* < 5 ng/mL)	1.48 (0.70-3.11)	0.303			2.53 (0.68-9.35)	0.165		
ASA (Grade ≥ III *vs* Grade < III)	1.50 (0.72-3.11)	0.277			1.64 (0.45-5.96)	0.454		
pT stage (pT3-4 *vs* pT1-2)	1.66 (0.72-3.83)	0.238			4.17 (1.09-15.95)	**0.037**		
pN stage (pN+ *vs* pN0)	1.05 (0.51-2.19)	0.887			5.02 (0.65-38.66)	0.122		
LVI (+) *vs* LVI (-)	1.30 (0.53-3.15)	0.568			3.78 (1.23-11.64)	**0.020**	3.52 (1.03-12.02)	**0.045**
NLR ≥ 19.3 *vs* NLR < 19.3	2.98 (1.27-6.97)	**0.012**						
dNLR ≥ 1.57 *vs* dNLR < 1.57	2.40 (1.12-5.13)	**0.024**	2.34 (1.08-5.07)	**0.032**				
PLR ≥ 155 *vs* PLR < 155	1.83 (0.70-4.79)	0.217						
SII ≥ 3645 *vs* SII < 3645	1.61 (0.71-3.61)	0.252						
LMR ≥ 1.67 *vs* LMR < 1.67					4.09 (1.12-14.87)	**0.033**	4.57 (0.98-21.38)	**0.053**
Chemotherapy (+) *vs* (-)	0.74 (0.36-1.51)	0.402			1.43 (0.47-4.38)	0.529		

SEMS: Self-expanding metal stents; BTS: Bridge to surgery; dNLR: Derived neutrophil-to-lymphocyte ratio; PLR: Platelet–to-lymphocyte ratio; SII: Systemic immune inflammation index; LMR: Lymphocyte-to-monocyte ratio; LVI: Lymphovascular invasion. $P < 0.05$ was considered significant.

Table 6 Univariate and multivariate analyses of risk factors for oncological outcomes in both emergency surgery and bridge to surgery groups

3-year disease-free survival	ES group (*n* = 56)				BTS group (*n* = 32)			
	Univariate		Multivariate		Univariate		Multivariate	
Characteristic	HR (95%CI)	*P*-value	HR (95%CI)	*P*-value	HR (95%CI)	*P*-value	HR (95%CI)	*P*-value
CEA (≥ 5 ng/mL *vs* < 5 ng/mL)	1.71 (0.74-3.95)	0.209			2.67 (0.72-9.90)	0.141		
ASA (Grade ≥ III *vs* Grade < III)	0.890 (0.36-2.23)	0.803			1.49 (0.41-5.43)	0.542		
pT stage (pT3-4 *vs* pT1-2)	2.26 (0.85-6.02)	0.104			2.48 (0.55-11.18)	0.239		
pN stage (pN+ *vs* pN0)	1.48 (0.64-3.43)	0.361			2.48 (0.55-11.18)	0.239		
LVI (+) *vs* LVI (-)	2.92 (1.25-6.81)	**0.013**			1.97 (0.66-5.88)	0.224		
NLR ≥ 19.3 *vs* NLR < 19.3	2.76 (1.02-7.45)	**0.046**						
dNLR ≥ 1.57 *vs* dNLR < 1.57	2.85 (1.17-6.95)	**0.021**	3.02(1.23-7.42)	**0.016**				
PLR ≥ 317 *vs* PLR < 317	1.55 (0.66-3.67)	0.314						
SII ≥ 3645 *vs* SII < 3645	2.04 (0.86-4.83)	0.104						
LMR ≥ 1.67 *vs* LMR < 1.67					2.54 (0.83-7.80)	0.091	3.11 (1.13-8.54)	**0.052**
Chemotherapy (+) *vs* (-)	0.95 (0.41-2.19)	0.896			1.44 (0.47-4.41)	0.523		

SEMS: Self-expanding metal stents; BTS: Bridge to surgery; dNLR: Derived neutrophil-to-lymphocyte ratio; PLR: Platelet-to-lymphocyte ratio; SII: Systemic immune inflammation index; LMR: Lymphocyte-to-monocyte ratio; LVI: Lymphovascular invasion. Chemotherapy (+), accept chemotherapy lately. Chemotherapy (-), refuse to chemotherapy lately. $P < 0.05$ was considered significant.

Table 7 Stratification analysis of oncological and survival outcomes between high-ratio and low-ratio grades in both emergency surgery and bridge to surgery groups

Characteristic	3-year OS		3-year DFS	
	HR (95%CI)	*P*-value	HR (95%CI)	*P*-value
ES (dNLR < 1.57)	Reference	-	Reference	-
BTS (dNLR < 1.57)	0.51 (0.18-1.39)	0.185	0.42 (0.13-1.34)	0.144
ES (dNLR ≥ 1.57)	Reference	-	Reference	-
BTS (dNLR ≥ 1.57)	1.87 (0.79-4.43)	0.155	1.79 (0.77-4.20)	0.178
ES (LMR < 1.67)	Reference	-	Reference	-
BTS (LMR < 1.67)	4.34 (1.27-14.82)	0.019	2.72 (0.97-7.65)	0.058
ES (LMR ≥ 1.67)	Reference	-	Reference	-
BTS (LMR ≥ 1.67)	0.40 (0.18-0.92)	0.031	0.42 (0.17-1.07)	0.068

SEMS: Self-expanding metal stents; BTS: Bridge to surgery; dNLR: Derived neutrophil-to-lymphocyte ratio; OS: Overall survival; DFS: Disease-free survival; LMR: Lymphocyte-to-monocyte ratio. $P < 0.05$ was considered statistically significant.

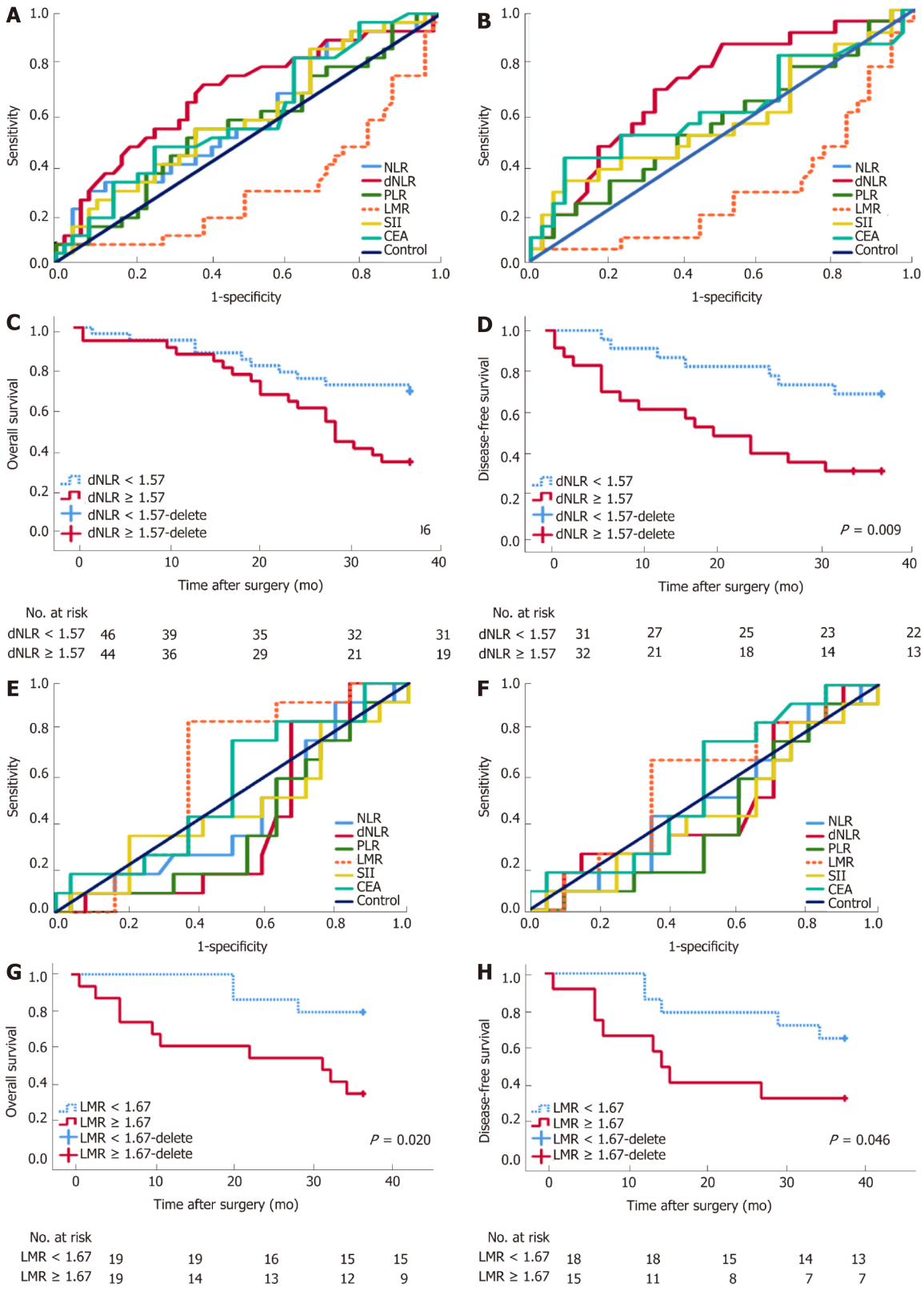

Figure 2 Receiver operating characteristic curve and long-term survival analysis of emergency surgery and bridge to surgery group. Derived neutrophil-to-lymphocyte ratio (dNLR) is preferred as a prognostic biomarker for the emergency surgery (ES) group with the highest area under receiver operating characteristic curve (AUC) for 3-year overall survival (OS) (0.679, 95%CI: 0.551-0.808) (A) and 3-year disease-free survival (DFS) (0.679, 95%CI: 0.551-0.808) (B), with a cutoff point value of 1.57. High-ratio grade of dNLR (≥ 1.57) was closely related to lower 3-year DFS (≥ 1.57 *vs* <1.57, 23.10 ± 13.85 mo *vs* 31.45 ± 9.35 mo, $P = 0.009$) in the ES group (D), but not with 3-year OS (C). Lymphocyte-to-monocyte ratio (LMR) was preferred as a prognostic biomarker for bridge to surgery (BTS) group with the highest AUC for 3-year OS (0.611, 95%CI: 0.424-0.798) (E) and 3-year DFS (0.571, 95%CI: 0.366-0.776) (F), with a cutoff point value of 1.67. High-ratio grade of LMR (≥ 1.67) was closely related to lower 3-year OS (≥ 1.67 *vs* <1.67, 23.10 ± 13.85 mo *vs* 33.78 ± 5.35 mo, $P = 0.020$) (G) and 3-year DFS (≥ 1.67 *vs* < 1.67, 22.67 ± 14.02 mo *vs* 31.50 ± 8.89 mo, $P = 0.046$) in the BTS group (H).

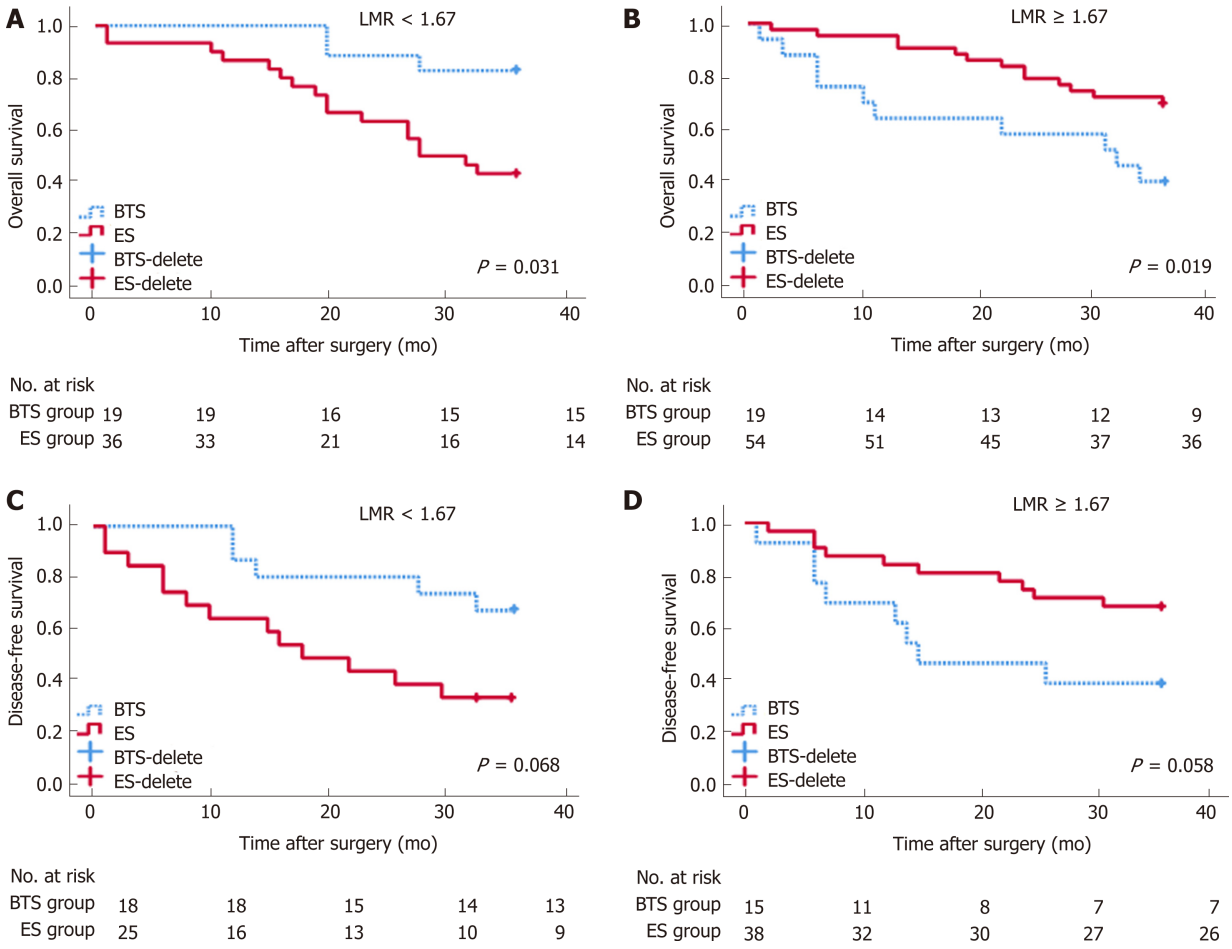

Figure 3 Analysis of 3-year overall survival and 3-year disease-free survival, by different lymphocyte-to-monocyte ratios between emergency surgery and bridge to surgery groups. $P < 0.05$ (log-rank test). Low lymphocyte-to-monocyte ratio (LMR) (LMR < 1.67) indicated higher rates of 3-year OS (A) (HR = 0.40, 95%CI: 0.18-0.92, $P = 0.031$) and 3-year disease-free survival (DFS) (C) (HR = 0.42, 95%CI: 0.17-1.07, $P = 0.068$) in the bridge to surgery (BTS) group. Conversely, high LMR (LMR ≥ 1.67) showed lower proportions of 3-year OS (B) (HR = 4.32, 95%CI: 1.27-14.82, $P = 0.019$) and 3-year DFS (D) (HR = 2.72, 95%CI: 0.97-7.65, $P = 0.058$) in the BTS group.

ARTICLE HIGHLIGHTS

Research background

Obstructive colorectal cancer (OCC) presenting with acute abdominal symptoms is always accompanied by severe complications, and the optimal strategy for patients with OCCs remains undetermined. Emergency surgery (ES) and self-expandable metal stents (SEMS) as a bridge to surgery (BTS) were the major treatments for OCCs, however, the indications remain debated. According to different status of immunology and nutrition, predictive factors for prognosis might be different between the two groups. Preoperative inflammation indexes might favor patient selection in terms of the prognosis of OCC.

Research motivation

Weighing the waxes and wanes of ES and BTS, both acute and chronic inflammation responses should be accounted for the selection of optimal patients.

Research objectives

This study was designed to build an inflammatory model for the surgical indications for ES and BTS in OCC.

Research methods

This was a retrospective study in which 128 patients who underwent surgery for OCC at the Department of Emergency Surgery of Fujian Medical University Union Hospital from January 2008 to October 2015 were included in this study. Patients were divided into an ES group and a BTS group according to the surgeon' advises and patients' selection. Inflammation indexes were fully evaluated in this study.

Research results

Comparable survival outcomes were observed between the ES and BTS groups. Receiver

operating characteristic curve analysis showed dNLR as the optimal biomarker for the prediction of DFS in ES, by contrast, LMR was recommended for BTS with regard to OS and DFS. dNLR was related to stoma construction, postoperative pneumonia, and DFS in the ES group. LMR was closely related to lymph nodes invasion, OS, and DFS in the BTS group. LMR could differentiate OS between the ES and BTS groups. A low LMR (< 1.67) was correlated with a low incidence of death and tumor recurrence in the BTS group.

Research conclusions

As a supplement for the latest ESGE guidelines, the indications for the use of SEMSs in OCC might elaborate to patients with low preoperative LMR, who would benefit from BTS *via* SEMS insertion.

REFERENCES

1 **van Hooft JE**, van Halsema EE, Vanbiervliet G, Beets-Tan RG, DeWitt JM, Donnellan F, Dumonceau JM, Glynne-Jones RG, Hassan C, Jiménez-Perez J, Meisner S, Muthusamy VR, Parker MC, Regimbeau JM, Sabbagh C, Sagar J, Tanis PJ, Vandervoort J, Webster GJ, Manes G, Barthet MA, Repici A; European Society of Gastrointestinal Endoscopy (ESGE). Self-expandable metal stents for obstructing colonic and extracolonic cancer: European Society of Gastrointestinal Endoscopy (ESGE) Clinical Guideline. *Gastrointest Endosc* 2014; **80**: 747-61.e1-75 [PMID: 25436393 DOI: 10.1016/j.gie.2014.09.018]

2 **Yeo HL**, Lee SW. Colorectal emergencies: review and controversies in the management of large bowel obstruction. *J Gastrointest Surg* 2013; **17**: 2007-2012 [PMID: 24048614 DOI: 10.1007/s11605-013-2343-x]

3 **Pisano M**, Zorcolo L, Merli C, Cimbanassi S, Poiasina E, Ceresoli M, Agresta F, Allievi N, Bellanova G, Coccolini F, Coy C, Fugazzola P, Martinez CA, Montori G, Paolillo C, Penachim TJ, Pereira B, Reis T, Restivo A, Rezende-Neto J, Sartelli M, Valentino M, Abu-Zidan FM, Ashkenazi I, Bala M, Chiara O, De' Angelis N, Deidda S, De Simone B, Di Saverio S, Finotti E, Kenji I, Moore E, Wexner S, Biffl W, Coimbra R, Guttadauro A, Leppäniemi A, Maier R, Magnone S, Mefire AC, Peitzmann A, Sakakushev B, Sugrue M, Viale P, Weber D, Kashuk J, Fraga GP, Kluger I, Catena F, Ansaloni L. 2017 WSES guidelines on colon and rectal cancer emergencies: obstruction and perforation. *World J Emerg Surg* 2018; **13**: 36 [PMID: 30123315 DOI: 10.1186/s13017-018-0192-3]

4 **Govindarajan A**, Naimark D, Coburn NG, Smith AJ, Law CH. Use of colonic stents in emergent malignant left colonic obstruction: a Markov chain Monte Carlo decision analysis. *Dis Colon Rectum* 2007; **50**: 1811-1824 [PMID: 17899279 DOI: 10.1007/s10350-007-9047-9]

5 **Martinez-Santos C**, Lobato RF, Fradejas JM, Pinto I, Ortega-Deballón P, Moreno-Azcoita M. Self-expandable stent before elective surgery vs. emergency surgery for the treatment of malignant colorectal obstructions: comparison of primary anastomosis and morbidity rates. *Dis Colon Rectum* 2002; **45**: 401-406 [PMID: 12068202]

6 **Takahashi G**, Yamada T, Iwai T, Takeda K, Koizumi M, Shinji S, Uchida E. Oncological Assessment of Stent Placement for Obstructive Colorectal Cancer from Circulating Cell-Free DNA and Circulating Tumor DNA Dynamics. *Ann Surg Oncol* 2018; **25**: 737-744 [PMID: 29235008 DOI: 10.1245/s10434-017-6300-x]

7 **Sloothaak DA**, van den Berg MW, Dijkgraaf MG, Fockens P, Tanis PJ, van Hooft JE, Bemelman WA; collaborative Dutch Stent-In study group. Oncological outcome of malignant colonic obstruction in the Dutch Stent-In 2 trial. *Br J Surg* 2014; **101**: 1751-1757 [PMID: 25298250 DOI: 10.1002/bjs.9645]

8 **Tekkis PP**, Kinsman R, Thompson MR, Stamatakis JD; Association of Coloproctology of Great Britain, Ireland. The Association of Coloproctology of Great Britain and Ireland study of large bowel obstruction caused by colorectal cancer. *Ann Surg* 2004; **240**: 76-81 [PMID: 15213621]

9 **Haraguchi N**, Ikeda M, Miyake M, Yamada T, Sakakibara Y, Mita E, Doki Y, Mori M, Sekimoto M. Colonic stenting as a bridge to surgery for obstructive colorectal cancer: advantages and disadvantages. *Surg Today* 2016; **46**: 1310-1317 [PMID: 27048552 DOI: 10.1007/s00595-016-1333-5]

10 **Palin RP**, Devine AT, Hicks G, Burke D. Association of pretreatment neutrophil-lymphocyte ratio and outcome in emergency colorectal cancer care. *Ann R Coll Surg Engl* 2018; **100**: 308-315 [PMID: 29364006 DOI: 10.1308/rcsann.2017.0232]

11 **Grivennikov SI**, Greten FR, Karin M. Immunity, inflammation, and cancer. *Cell* 2010; **140**: 883-899 [PMID: 20303878]

12 **Buettner S**, Spolverato G, Kimbrough CW, Alexandrescu S, Marques HP, Lamelas J, Aldrighetti L, Gamblin TC, Maithel SK, Pulitano C, Weiss M, Bauer TW, Shen F, Poultsides GA, Marsh JW, IJzermans JNM, Koerkamp BG, Pawlik TM. The impact of neutrophil-to-lymphocyte ratio and platelet-to-lymphocyte ratio among patients with intrahepatic cholangiocarcinoma. *Surgery* 2018; **164**: 411-418 [PMID: 29903509 DOI: 10.1016/j.surg.2018.05.002]

13 **Farolfi A**, Petrone M, Scarpi E, Gallà V, Greco F, Casanova C, Longo L, Cormio G, Orditura M, Bologna A, Zavallone L, Ventriglia J, Franzese E, Loizzi V, Giardina D, Pigozzi E, Cioffi R, Pignata S, Giorda G, De Giorgi U. Inflammatory Indexes as Prognostic and Predictive Factors in Ovarian Cancer Treated with Chemotherapy Alone or Together with Bevacizumab. A Multicenter, Retrospective Analysis by the MITO Group (MITO 24). *Target Oncol* 2018; **13**: 469-479 [PMID: 29948780 DOI: 10.1007/s11523-018-0574-1]

14 **Tao Y**, Ding L, Yang GG, Qiu JM, Wang D, Wang H, Fu C. Predictive impact of the inflammation-based indices in colorectal cancer patients with adjuvant chemotherapy. *Cancer Med* 2018; [Epub ahead of print] [PMID: 29761858]

15 **Liu JX**, Li A, Zhou LY, Liu XF, Wei ZH, Wang XZ, Ying HQ. Significance of combined preoperative serum Alb and dNLR for diagnosis of pancreatic cancer. *Future Oncol* 2018; **14**: 229-239 [PMID: 29338337 DOI: 10.2217/fon-2017-0339]

16 **Diakos CI**, Tu D, Gebski V, Yip S, Wilson K, Karapetis CS, O'Callaghan CJ, Shapiro J, Tebbutt N, Jonker DJ, Siu LL, Wong R, Doyle C, Strickland AH, Price TJ, Simes J, Clarke S. Is the derived neutrophil to lymphocyte ratio (dNLR) an independent prognostic marker in patients with metastatic colorectal cancer (mCRC)? Analysis of the CO.17 and CO.20 studies. *Ann Oncol* 2016; **27**: 588P [DOI: 10.1093/annonc/mdw370.136]

17 **Chan JC**, Chan DL, Diakos CI, Engel A, Pavlakis N, Gill A, Clarke SJ. The Lymphocyte-to-Monocyte

Ratio is a Superior Predictor of Overall Survival in Comparison to Established Biomarkers of Resectable Colorectal Cancer. *Ann Surg* 2017; **265**: 539-546 [PMID: 27070934]
18 **Hu B**, Yang XR, Xu Y, Sun YF, Sun C, Guo W, Zhang X, Wang WM, Qiu SJ, Zhou J, Fan J. Systemic immune-inflammation index predicts prognosis of patients after curative resection for hepatocellular carcinoma. *Clin Cancer Res* 2014; **20**: 6212-6222 [PMID: 25271081 DOI: 10.1158/1078-0432.CCR-14-0442]
19 **Lin BQ**, Wang RL, Li QX, Chen W, Huang ZY. Investigation of treatment methods in obstructive colorectal cancer. *J BUON* 2015; **20**: 756-761 [PMID: 26214627]
20 **Camp RL**, Dolled-Filhart M, Rimm DL. X-tile: a new bio-informatics tool for biomarker assessment and outcome-based cut-point optimization. *Clin Cancer Res* 2004; **10**: 7252-7259 [PMID: 15534099 DOI: 10.1158/1078-0432.CCR-04-0713]
21 **Wittekind C**. [2010 TNM system: on the 7th edition of TNM classification of malignant tumors]. *Pathologe* 2010; **31**: 331-332 [PMID: 20703480 DOI: 10.1007/s00292-010-1349-3]
22 **Saito S**, Yoshida S, Isayama H, Matsuzawa T, Kuwai T, Maetani I, Shimada M, Yamada T, Tomita M, Koizumi K, Hirata N, Kanazawa H, Enomoto T, Sekido H, Saida Y. A prospective multicenter study on self-expandable metallic stents as a bridge to surgery for malignant colorectal obstruction in Japan: efficacy and safety in 312 patients. *Surg Endosc* 2016; **30**: 3976-3986 [PMID: 26684205 DOI: 10.1007/s00464-015-4709-5]
23 **Dindo D**, Demartines N, Clavien PA. Classification of surgical complications: a new proposal with evaluation in a cohort of 6336 patients and results of a survey. *Ann Surg* 2004; **240**: 205-213 [PMID: 15273542]
24 **DeOliveira ML**, Winter JM, Schafer M, Cunningham SC, Cameron JL, Yeo CJ, Clavien PA. Assessment of complications after pancreatic surgery: A novel grading system applied to 633 patients undergoing pancreaticoduodenectomy. *Ann Surg* 2006; **244**: 931-7; discussion 937-9 [PMID: 17122618 DOI: 10.1097/01.sla.0000246856.03918.9a]
25 **Haram A**, Boland MR, Kelly ME, Bolger JC, Waldron RM, Kerin MJ. The prognostic value of neutrophil-to-lymphocyte ratio in colorectal cancer: A systematic review. *J Surg Oncol* 2017; **115**: 470-479 [PMID: 28105646 DOI: 10.1002/jso.24523]
26 **Sabbagh C**, Chatelain D, Trouillet N, Mauvais F, Bendjaballah S, Browet F, Regimbeau JM. Does use of a metallic colon stent as a bridge to surgery modify the pathology data in patients with colonic obstruction? A case-matched study. *Surg Endosc* 2013; **27**: 3622-3631 [PMID: 23572218 DOI: 10.1007/s00464-013-2934-3]
27 **Kim US**, Papatestas AE. Letter: Peripheral lymphocyte counts in colonic disease. *Lancet* 1974; **2**: 462-463 [PMID: 4136971]
28 **Menges T**, Engel J, Welters I, Wagner RM, Little S, Ruwoldt R, Wollbrueck M, Hempelmann G. Changes in blood lymphocyte populations after multiple trauma: association with posttraumatic complications. *Crit Care Med* 1999; **27**: 733-740 [PMID: 10321662]
29 **Gay LJ**, Felding-Habermann B. Contribution of platelets to tumour metastasis. *Nat Rev Cancer* 2011; **11**: 123-134 [PMID: 21258396 DOI: 10.1038/nrc3004]
30 **Tse JM**, Cheng G, Tyrrell JA, Wilcox-Adelman SA, Boucher Y, Jain RK, Munn LL. Mechanical compression drives cancer cells toward invasive phenotype. *Proc Natl Acad Sci U S A* 2012; **109**: 911-916 [PMID: 22203958 DOI: 10.1073/pnas.1118910109]
31 **Kim BG**, Gao MQ, Kang S, Choi YP, Lee JH, Kim JE, Han HH, Mun SG, Cho NH. Mechanical compression induces VEGFA overexpression in breast cancer via DNMT3A-dependent miR-9 downregulation. *Cell Death Dis* 2017; **8**: e2646 [PMID: 28252641 DOI: 10.1038/cddis.2017.73]

World Journal of Gastroenterology

Submit a Manuscript: https://www.f6publishing.com

World J Gastroenterol 2019 September 7; 25(33): 4985-4998

DOI: 10.3748/wjg.v25.i33.4985

ISSN 1007-9327 (print) ISSN 2219-2840 (online)

ORIGINAL ARTICLE

Observational Study

Tenofovir is a more suitable treatment than entecavir for chronic hepatitis B patients carrying naturally occurring rtM204I mutations

Won Hyeok Choe, Kijeong Kim, So-Young Lee, Yu-Min Choi, So Young Kwon, Jeong Han Kim, Bum-Joon Kim

ORCID number: Won Hyeok Choe (0000-0002-8019-5412); Ki Jeong Kim (0000-0002-5132-1774); So Young Lee (0000-0002-9638-893X); Yu Min Choi (0000-0003-4709-3155); So Young Kwon (0000-0003-4290-1950); Jeong Han Kim (0000-0002-8383-8524); Bum Joon Kim (0000-0003-0085-6709).

Author contributions: Choe WH and Kim K contributed equally to this work; Kim K and Kim BJ contributed to study conception and design, and designed and performed experiments; Choe WH, Kim JH, and Kwon SY contributed to collection of clinical data; Choe WH, Kim K, Lee SY, Choi YM, and Kim BJ contributed to data acquisition, data analysis and interpretation; Choe WH, Kim K, Lee SY, Choi YM, Kwon SY, Kim JH, and Kim BJ contributed to writing of article, editing, reviewing and final approval of article.

Institutional review board statement: Based on the Declaration of Helsinki, the Institutional Review Board of Konkuk University Hospital approved the retrospective use of the clinical, biochemical, and radiographic data for the present study.

Informed consent statement: The requirements for informed consent were waived due to the retrospective design.

Conflict-of-interest statement: The authors declare they have no potential conflicts of interest.

Data sharing statement: No

Won Hyeok Choe, So Young Kwon, Jeong Han Kim, Department of Internal Medicine, Konkuk University School of Medicine, Seoul 05030, South Korea

Kijeong Kim, Department of Microbiology, College of Medicine, Chung-Ang University, Seoul 06974, South Korea

So-Young Lee, Yu-Min Choi, Bum-Joon Kim, Department of Biomedical Sciences, Microbiology and Immunology, Liver Research Institute, Cancer Research Institute and SNUMRC, College of Medicine, Seoul National University, Seoul 03080, South Korea

Corresponding author: Bum Joon Kim, PhD, Professor, Department of Biomedical Sciences, Microbiology and Immunology, Liver Research Institute, Cancer Research Institute and SNUMRC, College of Medicine, Seoul National University, 103 Daehak-ro, Jongno-gu, Seoul 03080, South Korea. kbumjoon@snu.ac.kr
Telephone: +82-2-7408315
Fax: +82-2-7430881

Abstract

BACKGROUND

Hepatitis B virus (HBV) DNA polymerase mutations usually occur to long term use of nucleos(t)ide analogues (NAs), but they can occur spontaneously in treatment-naïve chronic hepatitis B (CHB) patients. The naturally occurring HBV DNA polymerase mutations might complicate antiviral therapy with NAs, leading to the generation of drug-resistant viral mutants and disease progression. The most common substitutions are known to be YMDD-motif mutations, but their prevalence and the influence on antiviral therapy is unclear.

AIM

To investigate prevalence of the naturally occurring rtM204I mutations in treatment-naïve CHB genotype C2 patients and their influence on antiviral therapy.

METHODS

A total of 410 treatment-naïve CHB patients infected with HBV genotype C2 strains were enrolled in this retrospective study. Among the 410 patients, 232 were treated with NAs for at least 12 mo. Significant fibrosis was defined as fibrosis-4 index > 3.25 or aspartate aminotransferase to platelet ratio index > 1.5. Complete viral response (CVR) during NAs was defined as undetectable serum HBV DNA (< 24 IU/mL). The rtM204I variants were analyzed by a newly developed locked nucleotide probe (LNA probe) based real-time PCR (LNA-RT-PCR) method.

additional data are available.

STROBE statement: The authors have read and checked the STROBE checklist.

Manuscript source: Unsolicited manuscript

Received: June 17, 2019
Peer-review started: June 17, 2019
First decision: July 21, 2019
Revised: July 30, 2019
Accepted: August 19, 2019
Article in press: August 19, 2019
Published online: September 7, 2019

P-Reviewer: Jain M, Komatsu H, Xu XY, Zheng SJ
S-Editor: Yan JP
L-Editor: A
E-Editor: Ma YJ

RESULTS

The LNA-RT-PCR could discriminate rtM204I mutant-type (17 patients, 4.2%) from rtM204 wild-type (386 patients, 95.8%) in 403 of 410 patients (98.3% sensitivity). Multivariate analysis showed that naturally occurring rtM204I variants were more frequently detected in patients with significant fibrosis [odd-ratio (OR) 3.397, 95% confidence-interval (CI) 1.119-10.319, $P = 0.031$]. Of 232 patients receiving NAs, multivariate analysis revealed that achievement of CVR was reversely associated with naturally occurring rtM204I variants prior to NAs treatment (OR 0.014, 95%CI 0.002-0.096, $P < 0.001$). Almost patients receiving tenofovir achieved CVR at 12 mo of tenofovir, irrespective of pre-existence of naturally occurring rtM204I mutations (CVR rates: patients with rtM204I, 100%; patients without rtM204I, 96.6%), whereas, pre-existence of naturally-occurring rtM204I-mutations prior to NAs significantly affects CVR rates in patients receiving entecavir (at 12 mo: Patients with rtM204I, 16.7%; patients without rtM204I, 95.6%, $P < 0.001$).

CONCLUSION

The newly developed LNA-RT-PCR method could detect naturally occurring rtM204I mutations with high-sensitivity. Theses mutations were more frequent in patients with liver fibrosis. Tenofovir is a more suitable treatment than entecavir for CHB patients carrying the naturally occurring rtM204I mutations.

Key words: Chronic hepatitis B; Entecavir; Hepatitis B virus; Liver fibrosis; Mutation; Tenofovir

Core tip: Hepatitis B virus (HBV) DNA polymerase mutations have been known to be prevalent in treatment-naïve chronic hepatitis B (CHB) patients infected with HBV genotype C2 strains. The newly developed locked nucleotide probe based real-time PCR method could discriminate the naturally-occurring rtM204I mutations from wild type with high sensitivity in treatment-naïve patients. Multivariate analyses showed that the naturally-occurring rtM204I variants were more frequently pre-existed in patients with liver fibrosis, and the pre-existence of the naturally-occurring rtM204I variants were significantly associated with incomplete viral response to nucleos(t)ide analogues. Tenofovir is a more suitable nucleos(t)ide analogues than entecavir for treatment-naïve CHB patients carrying the naturally occurring rtM204I mutations.

Citation: Choe WH, Kim K, Lee SY, Choi YM, Kwon SY, Kim JH, Kim BJ. Tenofovir is a more suitable treatment than entecavir for chronic hepatitis B patients carrying naturally occurring rtM204I mutations. *World J Gastroenterol* 2019; 25(33): 4985-4998
URL: https://www.wjgnet.com/1007-9327/full/v25/i33/4985.htm
DOI: https://dx.doi.org/10.3748/wjg.v25.i33.4985

INTRODUCTION

Hepatitis B virus (HBV) infection is a global health issue because of its worldwide distribution and is a potential leading cause of adverse outcomes, including liver cirrhosis (LC), hepatic decompensation, and hepatocellular carcinoma (HCC)[1,2]. Nucleos(t)ide analogues (NAs) are recommended by international guidelines for suppressing HBV replication and have been shown to decrease the rate of complications[3,4]. While NAs are well tolerated and effective in suppressing viral replication, long-term treatment with oral antiviral drugs can lead to the emergence of drug resistance mutations[5]. For instance, rtM204I is a classic mutation reducing susceptibility to mono-therapy by NAs with low genetic barriers, such as lamivudine (LAM), telbivudine (L-dT) and clevudine (CLV)[6].

HBV is an enveloped, partially double stranded DNA virus containing a genome that is approximately 3.2 kb in length and contains 4 overlapping open reading frames encoding the polymerase, core, surface antigen, and X protein[7]. The polymerase gene includes four domains, the terminal protein, spacer, ribonuclease H, and reverse

transcriptase (RT) regions. The RT region replicates the HBV genome through its DNA polymerase activity using RNA intermediates as a template. Since the RT lacks proofreading activity during viral replication, the error rate of HBV genome synthesis has been found to be 10^{-7} per nucleotide, which is 10-fold higher than those of other DNA viruses[8]. The high rate of mutations in the HBV genome complicates antiviral therapy with NAs, leading to the generation of drug-resistant viral strains and disease progression[9].

Previous studies have reported the existence of HBV DNA polymerase mutations in chronic hepatitis B (CHB) individuals prior to NA treatment; however, the prevalence varies from 0 to 30%[10-13]. This wide range might may be due to several factors including different study designs, regions, ethnicities, mutation detection methods, sample sizes, *etc*.[9,14,15]. Because of the high replication rate of HBV, viral mutations, including mixed wild-type and mutant populations in a single host, are commonly seen, but a low sensitivity assay could not enable the discrimination between wild and mutant types.

The purpose of this study was to determine the prevalence and clinical characteristics of naturally occurring rtM204I mutations in treatment-naïve patients infected with HBV genotype C2 strains by using a newly developed locked nucleotide probe (LNA probe) based real time PCR (LNA-RT-PCR) method, which can detect subspecies at 5% of the circulating HBV population.

MATERIALS AND METHODS

Primer and LNA probe design and real-time PCR

We designed two different LNA probes for the specific simultaneous detection in a single reaction of wild type (WT) and rtM204I variant of HBV. We used LC PDS (version 2.0) software for the probe design and referred to the design guidelines of LNA manufacturer (Integrated DNA technologies). We attached two different reporter dyes, FAM to probe for rtM204I variant, and Hex to probe for WT, respectively, to differentially identify rtM204I variant and WT HBV DNA. The primer and probe specificity for detection of rtM204I variant was further analyzed using Primer-Blast at NCBI (http://www.ncbi.nlm.nih.gov/tools/primer-blast/) and the Oligo software version 6.5. There were no PCR products formed by Primer-blast with the designed primer sequences in Homo sapiens, bacteria, and viruses other than HBV. Probe sequences were exclusively found in the amplicon sequence analyzed by the Oligo software with an HBV DNA sequence. The sequences of primers and LNA probes are shown in Figure 1 and Table 1. The LNA probes were purchased from Integrated DNA technologies, and primers from Macrogen.

A LightCycler Version 96 system (Roche) was used for LNA probe-based real-time PCR, and two channels were used for the experiment. Optimal reaction mixture was established for the sensitive and specific detection of target sequences. A 10-μL reaction mixture was prepared for each sample as follows: 1 μl PCR reaction buffer for Taq (Bioneer E-3150 buffer), 4.25 mM MgCl2, 0.425 mM deoxynucleoside triphosphate mixture (Takara), 0.3 μM forward primer, 1 μM reverse primer, 0.25 μM LNA FAM probe (rtM204I variant), 0.25 μM LNA Hex probe (rtM204I variant), 0.6 U Hot Start Taq (Bioneer E-3150), 1 mg/mL bovine serum albumin (Ambion, Lifetechnologies), 2 μL template DNA, and PCR-grade water (Roche). The cycling conditions were 300 s at 95 °C and 15 cycles of 10 s at 95 °C, 15 s at 58 °C, and 40 s at 75 °C, followed by 32 cycles of 10 s at 95 °C, 15 s at 47 °C (single acquisition of fluorescence signals), 15 s at 62 °C, and 40 s at 75 °C at a ramping speed of 1.1 °C/s. Melting curve analysis was subsequently continued without any pause by use of cycling for 10 s at 95 °C and 60 s at 43 °C, and the temperature was then increased from 43 °C to 85 °C at a temperature transition rate of 0.17 °C/s, during which the fluorescence signal was continuously acquired by three readings per degrees Celsius. All the following LNA real-time PCR experiments were done in quadruplicate with positive control DNAs and mixtures of WT and rtM204I at a variety of ratios and concentrations as aforementioned. The experiments were all repeated to examine inter-assay reliability.

Application of LNA real-time PCR to clinical samples

DNAs of a total of 410 human sera were tested for the identification of WT and rtM204I variant of HBV RT gene by LNA real-time PCR in duplicate. Tm, melting peak height, and quantification cycle (Cq) produced by WT- and rtM204I -targeting LNA probes with a sample DNA were measured. Identification of WT and rtM204I variant was determined by comparing their Tm s obtained from their specific channel (FAM for rtM204I, HEX for WT) with their diagnostic Tm ranges obtained from standard assays. Positive identification of WT and rtM204I variant was recorded only

Table 1 Primers and LNA probes developed for identification of hepatitis B virus wild type (YMDD) and rtM204I variants (YIDD) by real-time PCR

Primer/probe	Sequence (5'-3') [1]	*Tm* (°C)[2]	Target	Channel
Primers (product: 127 bp)				
Forward	TGGGCCTCAGTCCGTTTCT	65.4	HBV RT gene	
Reverse	TGTACAGACTTGGCCCCCAAWAC	65.2-66.1	HBV RT gene	
LNA Probes				
YMDD	5' HEX-TAT+A+T+G+G+AT+GAT- 3' IB®FQ	58	YMDD (wild type)	HEX
YIDD	5' 6-FAM-TAT+A+T+T+G+AT+GAT- 3' IB®FQ	53	YIDD	FAM

[1]LNA nucleotides are written +A, +C, +T or +G;
[2]Primer melting temperature was calculated by using LC PDS software V 2.0 and probe melting temperature by https://www.exiqon.com/ls/pages/exiqontmpredictiontool.aspx. *Tm*: Melting temperature; RT: Reverse transcriptase; HBV: Hepatitis B virus.

when distinct melting peak formation with their diagnostic Tm is recognized.

Throughout the real-time PCR assay, two rtM204I positive controls with high copies (2400000) and low copies (2400), two rtM204I positive controls with high copies (2400000) and low copies (2400), and two non-template controls were included in each run to monitor validity of Cqs, Tm s, and cross-contamination for inter-assays. Comparison of LNA real-time PCR and direct sequencing for identification of rtM204I variant and WT DNA.

Study patients

Data were collected retrospectively from a total of 410 treatment-naïve HBV patients who were followed in the Digestive Disease Center of Konkuk University Hospital, Korea, between March 2011 and February 2014. All of the patients were diagnosed with CHB and confirmed to have not taken any NAs or interferon. The inclusion criteria for the CBH patients included hepatitis B surface antigen (HBsAg) positive for more than 6 months and HBV-DNA viral loads were detectable, while the exclusion criteria included hepatitis C virus or human immunodeficiency virus coinfection, autoimmune liver disease, and alcohol or drug abuse. Prior to antiviral treatments, sera were collected from patients for analyses of the pre-existence of antiviral variants prior to NAs. This study was approved by the Institutional Review Board of Konkuk University Hospital.

Clinical and laboratory parameters

In all cases, demographic, clinical, biochemical and virologic data were collected. A diagnosis of LC was made clinically when a patient had at least two of the following three criteria: cirrhotic configuration of the liver (nodular liver surface or caudate lobe hypertrophy) and/or splenomegaly confirmed on imaging studies, thrombocytopenia (< 100000 platelets/mm^3), or the presence of varices detected by esophago-gastroduodenoscopy. Liver fibrosis was assessed using noninvasive biomarkers to calculate two composite scores The Fibrosis-4 index (FIB-4) score was calculated using age, aspartate aminotransferase (AST), alanine aminotransferase (ALT), and platelet count in the following formula: FIB-4 = [age (years) × AST (IU/L)] / [platelets (10^9/L) × ALT (IU/L)]. The AST to platelet ratio index (APRI) score was calculated using AST and platelet counts in the following formula: APRI = [AST level (IU/L) / AST upper limit of normal (IU/L) / platelet count (109/L)] × 100. Significant fibrosis of liver was defined as FIB-4 > 3.25 or APRI > 1.5[16]. The diagnosis of HCC was made based on histological evidence or typical radiological findings (the presence of arterial phase enhancement and portal venous phase wash-out of a nodule 1 cm or more in size)[17].

A complete viral response (CVR) was regarded as HBV-DNA levels being lower than detectable levels (24 IU/mL) at 12 mo of antiviral therapy, and incomplete (suboptimal) responders were defined as individuals having detectable HBV-DNA levels after at least 12 mo of treatment[18].

Statistical analysis

Data were mainly expressed as the mean and standard deviation (SD). Fisher's exact test was used to compare categorical variables. One-way ANOVA and Duncan's multiple comparison tests were used to compare continuous variables among the groups, and Student's *t*-test was for the analysis between the groups. Logistic regression analyses were performed to identify the independent factors for the presence of naturally occurring rtM204I mutations, or antiviral responsiveness. The Statistical Package for Social Science (SPSS Inc., Chicago, IL, United States), version

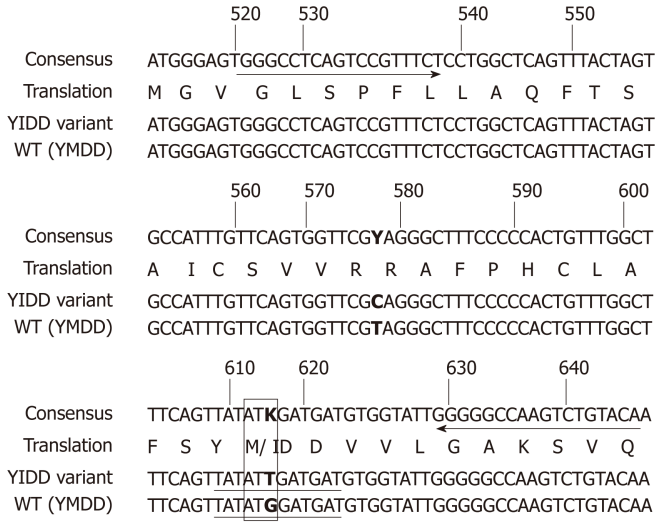

Figure 1 Primer and LNA-probe positions designed for the detection of hepatitis B virus rtM204I (YIDD) variant and rtM204 (YMDD) wild type. Arrows indicate the primer positions. Underlines indicate the probe positions. The numbers designate the nucleotide position on the hepatitis B virus reverse transcriptase gene sequence. Boldface bases denote the different bases. The box represents the codon and amino acid sequences of the rtM204 (YMDD) wild type and rtM204I (YIDD) variant. This single nucleotide difference is the basis of their discriminative identification by LNA probes in this study. The amino acid sequence is shown as the one-letter amino acid symbols. WT: Wild type.

15.0 was used for all analyses.

RESULTS

Determination of diagnostic Tm range for the identification of WT and rtM204I variants by LNA real-time PCR

Identification of WT and rtM204I variants was performed by LNA real-time PCR melting curve analysis by the observation of melting peak formation and specific Tm measurements in the specified channels (Figure 2, Table 2). LNA real-time PCR with samples of rtM204I positive control DNAs (n = 48) in amounts ranging from 24 to 2400000 copies resulted in a 100% positive detection rate and 100% specificity showing a distinct melting peak formation at the FAM channel in all of the rtM204I control DNA samples with Tms ranging from 51.3 to 52.2 °C (mean, 51.7 ± 0.2 °C) but no significant melting peak formation at the HEX channel (WT detection channel). LNA real-time PCR with samples of WT control DNAs (n = 48) in amounts ranging from 24 to 2400000 copies resulted in a 95.8% positive detection rate and 100% specificity showing a distinct melting peak formation at the HEX channel in all of the WT control DNA samples with Tms ranging from 61.9 to 63.3 °C (mean, 62.6 ± 0.4 °C) but no significant melting peak formation at the FAM channel (rtM204I detection channel). Two WT control DNA samples that had the lowest copy numbers were not detected. This suggests high sensitivity and specificity of our newly developed LNA RT-PCR assay.

Application of LNA real-time PCR to clinical samples

Of 410 clinical samples tested in duplicate by our LNA real-time PCR method, 403 samples (98.3%) were positively identified as WT and/or rtM204I variants, with two samples found to be mixed with presumably unknown variants with non-typable Tms. Of the seven unidentified samples, two samples were amplified but non-typable due to their non-diagnostic melting temperatures (50.4 °C, 57.9 °C) at the HEX channel and five samples did not show any positive signals. Thus, only four samples among all clinical samples tested carried non-typable Tms in this study.

Among the positively identified samples, all of the samples produced a distinct melting peak or peaks with a Tm or Tms being in the diagnostic Tm range for WT or rtM204I. Among all clinical samples, seventeen samples (4.1%) were identified as carrying rtM204I variants and among these samples, nine samples were rtM204I variant exclusively and eight samples were rtM204I variant coexistent with WT. Among these, in four samples, rtM204I was dominant over WT; in one sample, codominant; in three samples, WT was dominant over rtM204I (Table 3). Overall,

Table 2 Measurement of melting temperatures of hepatitis B virus wild type (YMDD) and rtM204I variants (YIDD) by LNA real-time PCR

Sample (copies, number of samples *n*)	Measured *Tm* (°C) at channel					
	FAM			HEX		
	Min	Max	Mean ± SD(number of positives)	Min	Max	Mean ± SD(number of positives)
YIDD positive control DNA (24-2400000, *n* = 48)	51.3	52.2	51.7 ± 0.2 (48, 100%)	(-)	(-)	(-)
WT positive control DNA (24-2400000, *n* = 48)	(-)	(-)	(-)	61.9	63.3	62.6 ± 0.4 (46, 95.8%)
YIDD and WT standard mixtures (24-2400000, *n* = 280)	50.1	52.6	51.5 ± 0.3 (280, 100%)	61.9	64.0	63.0 ± 0.4 (280, 100%)
YIDD and WT standard mixtures (24, *n* = 56)	49.9	51.9	51.2 ± 0.5 (45, 80.3%)	60.9	63.8	63.0 ± 0.5 (44, 78.6%)
YIDD of clinical samples in duplicate (82-180000, *n* = 17)	49.6	51.9	51.3 ± 0.5	(-)	(-)	(-)
YMDD of clinical samples in duplicate (65-13000000, *n* = 397)	(-)	(-)	(-)	61.1	64.0	62.8 ± 0.3

[1]The variants were identified by direct sequencing of PCR products. (-) indicates no significant melting temperature; SD: standard deviation; *Tm*: Melting temperature.

thirteen samples carried the rtM204I variant predominantly and one sample co-dominantly with WT. The majority of the clinical samples were WT.

Three of the four samples that showed Tms out of the WT-diagnostic Tm range were sequenced by direct sequencing of their PCR products. The one sample with a Tm of 50.4 °C was identified as a YVDD variant with a GTG codon and the other sample with a Tm of 57.9 °C was YMDD but had a TAC codon for the Y amino acid. The third sample that showed three melting peaks was revealed to have an additional codon for isoleucine of rtM204I. The results of direct PCR sequencing of thirty clinical samples randomly chosen among positively identified samples by LNA real-time PCR had results identical to those of our LNA real-time PCR assay, proving its reliability for screening for pre-existing rtM204I variants from treatment naïve CHB patients (Figure 3).

Baseline characteristics of enrolled 403 CHB patients typed by LNA real-time PCR

Four hundred and three treatment-naïve patients with chronic HBV infection that could be typed by LNA real-time PCR comprising 244 men and 159 women with a mean age of 43.9 ± 12.5 years were included. Baseline characteristics were shown in Table 4. Two hundred thirty-eight (59.1%) patients had HBeAg-positive CHB and 165 (40.9%) patients had HBeAg-negative CHB. Eighty-seven patients had LC, and fifty-one patients had HCC. One hundred fifty-seven had significant fibrosis (defined as FIB-4 score > 3.25, or APRI score > 1.5). Of the 403 treatment-naïve patients, 232 patients were treated with NAs over a period of 1 year. One-hundred ninety-two patients were treated with agents that had a high genetic barrier to resistance (95 patients were treated with tenofovir, and 97 patients were tread with entecavir), and 40 patients were treated with low genetic barrier agents [9, 19, and 12 patients were treated with LAM, adefovir (ADV), and LAM-ADV combination, respectively]. As it is well known that HBV genotype C is the universal type in almost all Korean chronic carriers, HBV genotyping is not routinely carried out in Korea. In our study, HBV genotyping was performed for 40 patients and all (100%) had genotype C2 strains.

Association between pre-existence of rtM204I variants and patient characteristics

The pre-existing rtM204I variants prior to NAs were detected in 17 of 403 treatment-naïve CHB patients (4.2%). The pre-existing rtM204I variants were more frequently detected in subjects with higher FIB-4 scores. These variants were more often detected in subjects with significant fibrosis, LC, and HCC (Table 4). Among the clinical factors (age, sex, HBeAg status, HBV-DNA titers, HBsAg quantitative levels, AST, ALT, total bilirubin, albumin, prothrombin time, platelet counts, presence of significant fibrosis, LC or HCC), univariate analysis showed that pre-existing rtM204I variants were more frequently detected in patients with significant fibrosis, or patients with HCC. Logistic multivariate analysis showed that pre-existing rtM204I variants were significantly more frequent in patients with significant fibrosis (odd ratio 3.397, 95% confidence interval 1.119-10.319, $P = 0.031$) (Table 5).

Association between the pre-existence of rtM204I variants and antiviral responsiveness

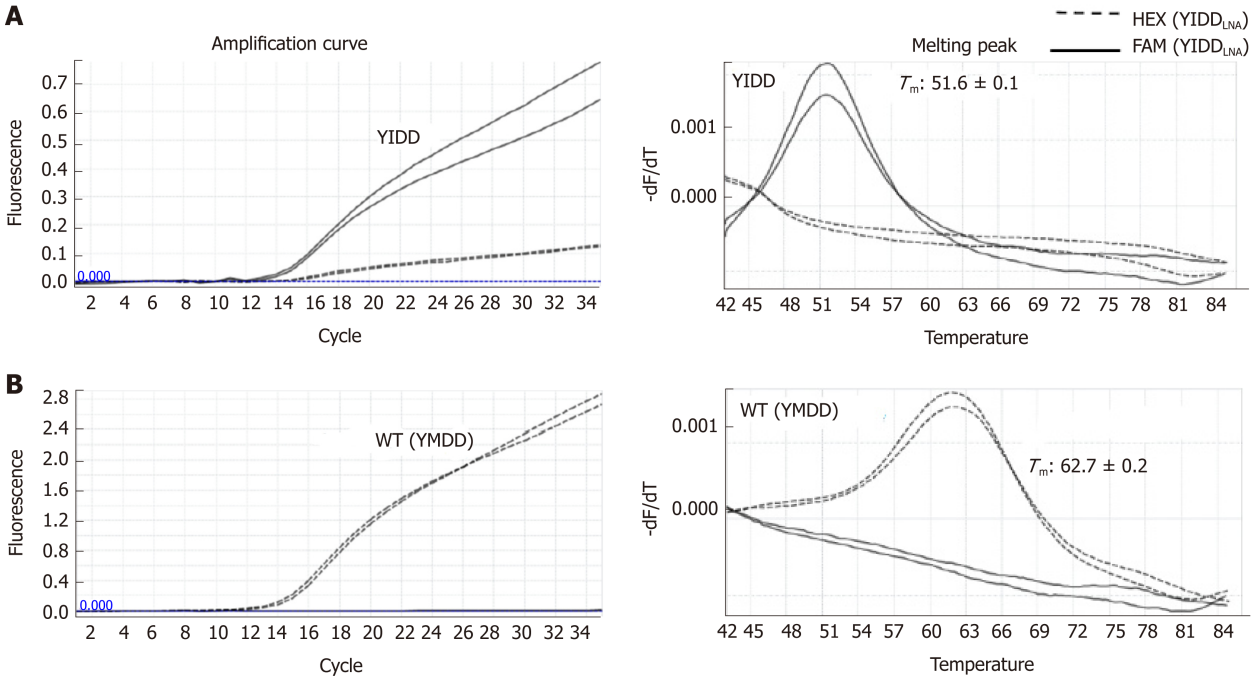

Figure 2 LNA real-time PCR for identification of hepatitis B virus rtM204I (YIDD) variant and rtM204 (YMDD) wild type. Amplification curves were shown on the left, melting peaks on the right. With YIDD variant DNA templates (A), YIDD specific signals at FAM channel (solid) were detected showing their dominant amplifications with minimal cross signals of amplification generated by a weak YMDD probe cross hybridization and distinct melting temperatures different from those of YMDD DNA with no significant cross signals on melting. For WT DNA templates (B), YMDD specific signals at HEX 6 channel (dashed) were detected showing their exclusive amplifications and distinct T_ms different from those of YIDD with no cross signals. WT: Wild type.

Two hundred and thirty-two patients were treated with oral NAs over a period of 12 mo, and their antiviral responsiveness to NAS was evaluated. One hundred and ninety-nine patients achieved a CVR at 12 months of anti-HBV therapy, whereas thirty-three patients had suboptimal (incomplete) responses. Logistic multivariate regression analysis revealed that achievement of CVR was reversely associated with higher HBV-DNA titers, treatment with low genetic barrier drugs, and, infection with pre-existing rtM204I variants prior to NAs (odds ratio 0.014, 95% confidence interval 0.002-0.096, $P < 0.001$; Table 6). Figure 4 shows the mean changes in the HBV-DNA level at each point. The decrease in HBV-DNA was significantly less prominent in patients infected with pre-existing rtM204I variants than in patients infected without pre-existing rtM204I variants, at 3, 6, 9, and 12 mo of antiviral treatments (all $P < 0.05$).

Among 95 patients treated with tenofovir, all seven patients with pre-existing rtM204I variants (7/7, 100%) as well as almost patients without pre-existing rtM204I variants (85/88, 96.6%) achieved CVR at 12 mo of tenofovir. Among 97 patients treated with entecavir, only one of six patients with pre-existing rtM204I variants (1/6, 16.7%) achieved CVR at 12 mo of entecavir, whereas almost patients without pre-existing rtM204I variants (87/91, 95.6%) achieved CVR at 12 mo entecavir (87/91, 95.6%). Among 40 patients treated with low genetic barriers, one of four patients with pre-existing rtM204I variants (1/4, 25.0%) and half of patients without pre-existing rtM204I variants (18/36, 50.0%) achieved CVR at 12 mo of low genetic barriers.

Table 7 shows the mean changes in the HBV-DNA levels and cumulative probabilities of CVR in 17 patients with pre-existing rtM204I variants. The cumulative probability of CVR at 12 mo of tenofovir was significantly higher than those of entecavir and low genetic barriers (the Fisher's exact test: tenofovir vs entecavir, $P = 0.005$; tenofovir vs low genetic barrier, $P = 0.024$).

DISCUSSION

Although antiviral resistance mutations occur secondarily to long term use of NAs, they can occur spontaneously in NAs-naïve patients. Since the HBV genome lacks a proofreading function on the RT region of the DNA polymerase, mutations can naturally occur due to random incorrect substitution of nucleos(t)ides. The most common substitutions are methionine at amino acid position 204 to either isoleucine (rtM204I, YIDD mutations) or valine (rtM204V, YVDD mutations)[19,20]. Many studies

Table 3 Rates of positive detection of hepatitis B virus wild type (YMDD) and rtM204I variant (YIDD) in 410 samples by LNA real-time PCR

Type of detection	No. of samples	Percentage
Clinical samples	410	100%
Identified	403	98.3%
YIDD	17	4.1%
YIDD exclusively	9	2.2%
YIDD + YMDD	3	0.7%
YIDD + YMDD + **YIDD with ATA codon**[1]	1	0.2%
YIDD + **YMDD**	1	0.5%
YIDD + **YMDD**	3	0.7%
YMDD	394	96.3%
YMDD exclusively	385	93.9%
YMDD + **unknown variant**	1	0.2%
Unidentified	7	1.7%
Non-target T_m	2	0.5%
HEX 50.4 °C; **YV**DD[1]	1	0.2%
HEX 57.9 °C; YMDD with Y of TA**C** codon[1]	1	0.2%
No positive signal	5	1.2%

Bold type indicates dominant form.
[1]The variants were identified by direct sequencing of PCR products. *Tm*: Melting temperature.

have revealed that YMDD-motif mutations can emerge naturally in treatment-naïve CHB patients, but their reported prevalence vary greatly (0% to approximately 30%) or are even contradictory[10-13].

Our group recently analyzed the RT region of the HBV polymerase by full-length HBV RT sequences in NAs-naive CHB patients, and we found that approximately 60% of them had antiviral resistant variants with substitutions at T184, M204, L180, or L80 prior to NAs therapy[14]. Among these variants, spontaneous rtM204I/V variants were detected in approximately 1.5% of NAs-native patients, and the rtM204I variant was the dominant type. Additionally, they were more frequently detected in patients with HCC than in patients without HCC. Thus, in this research, we focused on the spontaneous rtM204I variants, and they were evaluated using an LNA-RT-PCR method, which is a more sensitive method than sequence analysis. We also tripled the sample number of NAs-naïve patients with various phases of CHB genotype C infection.

In this study, we have confirmed that spontaneous rtM204I mutations exist in NAs-naïve patients with CHB genotype C infection, and their prevalence is approximately 4%. Spontaneous M204I mutations were more frequently detected in patients with higher scores on the FIB-4 index, which is considered to be a noninvasive marker of liver fibrosis, and multivariate analysis showed that pre-existing M204I mutations were more frequently detected in patients with significant fibrosis[21]. These data suggest that spontaneous rtM204I variants might be risk factors for the progression of liver fibrosis. Although the mechanism is unclear, a possible reason for the significant association between spontaneous rtM204I variants and liver fibrosis might also be related to HBV genotype C. Many studies have demonstrated that naturally occurring mutations, such as variants in the pre-S region, are associated with LC and HCC development in CHB patients, especially those infected with genotype C[22,23]. Hence, this study suggested that progression of fibrosis might be related to spontaneous occurrence of rtM204I mutations prior to NAs, as well as infection with naturally occurring pre-S variants, in treatment-naïve patients infected with HBV genotype C2 strains.

Another finding of this study is that spontaneous rtM204I variants could affect antiviral responsiveness in treatment-naïve patients when they are treated with NAs. Our data showed that CVR rate to antiviral therapy was significantly lower in patients infected with spontaneous rtM204I variants. Indeed, rtM204I variants are the predominant mutations causing resistance to NAs with low genetic barriers, such as LAM, L-dT, and CLV[6,24]. These variants can also reduce the susceptibility to entecavir therapy and induce entecavir resistance[25]. This study also revealed that all seven patients carrying pre-existing rtM204I mutations achieved CVR to tenofovir, which

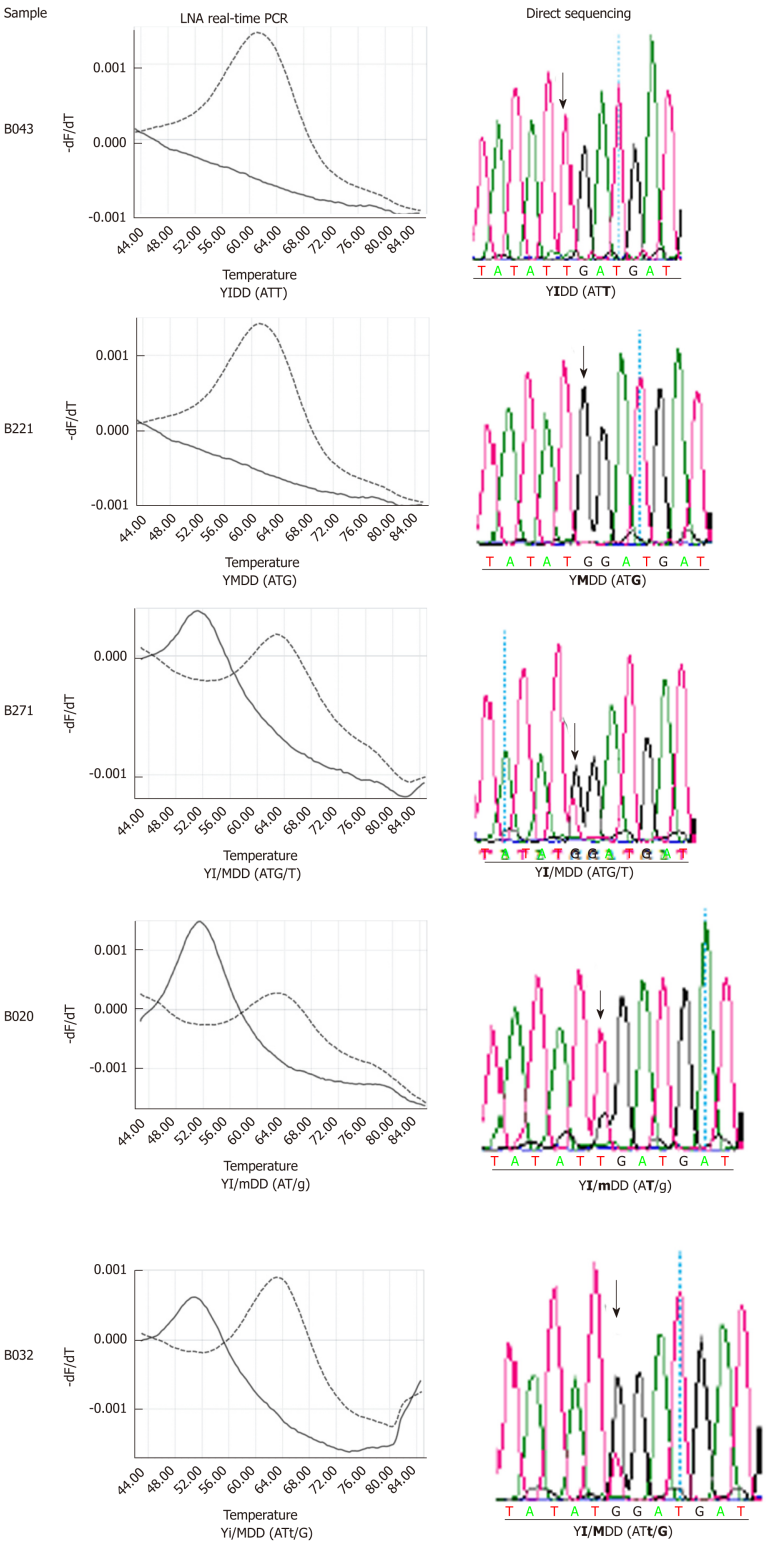

Figure 3 Confirmation of LNA real-time PCR identification results of hepatitis B virus rtM204I (YIDD) variant and rtM204 (YMDD) wild type by direct sequencing. Nucleotide bases are shown in the parenthesis. Lower case letters represent the base in a lower amount relative to the dominant variant. Bold indicates the target amino acid and bases.

can effectively suppress not only WT HBV strains but also rtM204I variants. In contrast, only one of six patients carrying pre-existing rtM204I mutations achieved CVR at 12 mo of entecavir treatment, and one of four patients achieved CVR at 12 mo of low genetic barrier agents. Therefore, tenofovir is the preferred treatment since its higher barrier to resistance provides the best chance for successful long-term therapy in treatment-naïve patients carrying spontaneous rtM204I variants.

Recently, a Korean population-based cohort study demonstrated that tenofovir

Table 4 Baseline characteristics of 403 treatment-naïve patients with chronic hepatitis B

Characteristics	Pre-existing rtM204I *n* = 17	Wild type rtM204 *n* = 386	*P* value
Gender (M/F)	14/3	230/156	0.060
Age (yr)	48.8 ± 9.3	43.7 ± 12.6	0.101
HBeAg (positive/negative)	10/7	228/158	0.984
HBV-DNA (log_{10} IU/mL)	6.33 ± 0.66	6.06 ± 1.77	0.519
qHBsAg (log_{10} IU/mL)	3.43 ± 0.30	3.59 ± 0.70	0.334
AST (IU/L)	104.7 ± 40.9	78.7 ± 65.2	0.103
ALT (IU/L)	77.8 ± 29.4	85.4 ± 84.1	0.709
Total bilirubin (mg/dL)	0.93 ± 0.33	0.88 ± 0.60	0.743
Albumin (g/dL)	4.02 ± 0.43	4.14 ± 0.52	0.338
Prothrombin time (INR)	1.07 ± 0.10	1.02 ± 0.16	0.246
Platelet count (× 10^3/mm^3)	155.7 ± 55.6	181.4 ± 64.4	0.106
FIB-4	4.38 ± 2.33	2.91 ± 2.92	0.041
APRI	1.94 ± 0.98	1.34 ± 1.35	0.068
Significant fibrosis[1] (presence/absence)	12/5	145/241	0.006
Liver cirrhosis (presence/absence)	7/10	80 / 306	0.045
HCC (presence/absence)	5/12	46 / 340	0.034

[1]Significant fibrosis was defined as aspartate aminotransferase to platelet ratio index > 1.5 or fibrosis-4 index > 3.25. ALT: Alanine aminotransferase; APRI: Aspartate aminotransferase to platelet ratio index; AST: Aspartate aminotransferase; FIB-4: Fibrosis-4 Index; HCC: Hepatocellular carcinoma; INR: International normalized ratio; qHBsAg: Quantitative hepatitis B surface antigen levels; HBV: Hepatitis B virus.

treatment was associated with a significantly lower risk of HCC compared with entecavir treatment[26]. This result might be related to the fact that tenofovir therapy can more effectively suppress HBV-DNA compared to entecavir therapy and consequently decrease the risk of LC progression or HCC development in Korean patients infected with HBV genotype C strains, some of whom have spontaneous rtM204I variants.

In conclusion, the LNA-RT-PCR method can detect pre-existing rtM204I variants with high sensitivity in NAs-naïve CHB patients. rtM204I mutations can occur spontaneously with a rate of approximately 4% in treatment-naïve patients infected with HBV genotype C2. The rtM204I variants more frequently pre-existed in patients with significant fibrosis, and the pre-existence of rtM204I variants was associated with incomplete responses to NAs. Therefore, the detection of pre-existing rtM204I variants with the newly developed LNA-RT-PCR method could play a relevant role in the clinical management of NA-naïve patients with CHB genotype C2 infection.

Table 5 Independent factors for pre-existing rtM204I variants in treatment-naïve chronic hepatitis B patients

	Pre-existing rtM204I (*n* = 17)	Wild type rtM204 (*n* = 386)	Univariate			Multivariate		
			OR	95%CI	*P* value	OR	95%CI	*P* value
Gender (male)	14 (82.4%)	230 (59.6%)	3.165	(0.895-11.197)	0.074			
Age, yr	48.8 ± 9.3	43.7 ± 12.6	1.033	(0.993-1.074)	0.105			
HBeAg status (positive)	10 (58.8%)	228 (59.1%)	0.990	(0.369-2.656)	0.984			
HBV-DNA, $\log_{10}$ IU/mL	6.33 ± 0.66	6.06 ± 1.77	1.098	(0.827-1.458)	0.519			
qHBsAg, $\log_{10}$ IU/mL	3.43 ± 0.30	3.59 ± 0.70	0.555	(0.336-0.916)	0.021			
AST, IU/L	104.7 ± 40.9	78.7 ± 65.2	1.005	(0.999-1.011)	0.109			
ALT, IU/L	77.8 ± 29.4	85.4 ± 84.1	0.999	(0.992-1.005)	0.709			
Total bilirubin, mg/dL	0.93 ± 0.33	0.88 ± 0.60	1.140	(0.522-2.487)	0.742			
Albumin, g/dL	4.02 ± 0.43	4.14 ± 0.52	0.655	(0.275-1.559)	0.339			
Prothrombin time, INR	1.07 ± 0.10	1.02 ± 0.16	4.625	(0.339-63.020)	0.250			
Platelet count, × 10^3/mm^3	155.7 ± 55.6	181.4 ± 64.4	0.993	(0.985-1.001)	0.108			
Significant fibrosis[1]	12 (70.6%)	145 (37.6%)	3.989	(1.377-11.553)	0.011	3.397	(1.119-10.319)	0.031
Liver cirrhosis	7 (41.2%)	80 (20.7%)	2.677	(0.988-7.255)	0.053			
HCC	5 (29.4%)	46 (11.9%)	3.080	(1.038-9.139)	0.043	1.961	(0.626-6.143)	0.248

[1]Significant fibrosis was defined as aspartate aminotransferase to platelet ratio index > 1.5 or fibrosis-4 index > 3.25. ALT: Alanine aminotransferase; APRI: Aspartate aminotransferase to platelet ratio index; AST: Aspartate aminotransferase; FIB-4: Fibrosis-4 Index; HCC: Hepatocellular carcinoma; INR: International normalized ratio; qHBsAg: Quantitative hepatitis B surface antigen levels; HBV: Hepatitis B virus.

Table 6 Independent factors for complete response at 12 mo of antiviral therapy in 232 patients who were treated with nucleos(t)ide analogues

	Complete response (*n* = 199)	Incomplete response (*n* = 33)	Univariate			Multivariate		
			OR	95%CI	*P* value	OR	95%CI	*P* value
Gender (male)	130 (65.3%)	20 (60.6%)	1.225	(0.575-2.610)	0.600			
Age, yr	47.3 ± 11.9	43.6 ± 10.9	1.028	(0.996-1.062)	0.087			
HBeAg status (positive)	106 (53.3%)	30 (90.9%)	0.114	(0.034-0.386)	< 0.001	0.438	(0.086-2.226)	0.320
HBV-DNA, $\log_{10}$ IU/mL	5.97 ± 1.40	7.69 ± 1.13	0.402	(0.290-0.559)	< 0.001	0.185	(0.083-0.412)	< 0.001
qHBsAg, $\log_{10}$ IU/mL	3.46 ± 0.57	3.89 ± 0.74	0.270	(0.134-0.544)	< 0.001	1.492	(0.501-4.447)	0.473
AST, IU/L	94.6 ± 69.5	83.0 ± 47.2	1.003	(0.997-1.009)	0.361			
ALT, IU/L	103.5 ± 92.7	91.6 ± 57.5	1.002	(0.997-1.006)	0.474			
Total bilirubin, mg/dL	0.95 ± 0.57	0.76 ± 0.30	2.201	(0.964-5.024)	0.061			
Albumin, g/dL	4.06 ± 0.53	4.14 ± 0.44	0.743	(0.351-1.573)	0.438			
Prothrombin time, INR	1.05 ± 0.16	1.01 ± 0.10	8.323	(0.444-155.931)	0.156			
Platelet count, × 10^3/mm^3	164.6 ± 63.8	182.6 ± 53.0	0.995	(0.990-1.001)	0.128			
Significant fibrosis	105 (52.8%)	13 (39.4%)	1.718	(0.810-3.644)	0.158			
Liver cirrhosis	58 (29.1%)	6 (18.2%)	1.851	(0.726-4.720)	0.197			
HCC	33 (16.6%)	3 (9.1%)	1.988	(0.573-6.899)	0.279			
High genetic barrier	180 (90.5%)	12 (36.4%)	16.579	(7.069-38.882)	< 0.001	82.076	(14.945-450.760)	< 0.001
Pre-existing rtM204I	9 (4.5%)	8 (24.2%)	0.148	(0.052-0.419)	< 0.001	0.014	(0.002-0.096)	< 0.001

ALT: Alanine aminotransferase; AST: Aspartate aminotransferase; INR: International normalized ratio; qHBsAg: Quantitative hepatitis B surface antigen levels; HBV: Hepatitis B virus; HCC: Hepatocellular carcinoma.

Table 7 Treatment responses during nucleos(t)ide analogues in patients with pre-existing rtM204I variants

Outcome	Tenofovir (*n* = 7)	Entecavir (*n* = 6)	Low genetic barriers[1] (*n* = 4)	*P* value
Reduction of HBV-DNA (log_{10} IU/mL), mean ± SD				
Mo 3	-3.22 ± 0.74	-2.12 ± 0.53[2]	-2.22 ± 0.40[2]	0.011
Mo 6	-3.97 ± 0.75	-2.71 ± 0.43[2]	-2.92 ± 0.51[2]	0.005
Mo 9	-4.44 ± 0.70	-3.33 ± 0.48[2]	-3.28 ± 0.35[2]	0.004
Mo 12	-4.75 ± 0.59	-3.65 ± 0.43[2]	-3.52 ± 0.60[2]	0.003
Complete virologic response, cumulative incidence				
Mo 12	100%	16.7%[2]	25%[2]	0.021

[1]The low genetic barriers include lamivudine, adefovir, or combination of lamivudine and adefovir;
[2]The same number of superscripted indicates non-specific difference between groups. The continuous variables were tested by one-way ANOVA among groups, and categorical variables were tested by Fisher's exact test. SD: standard deviation; HBV: Hepatitis B virus.

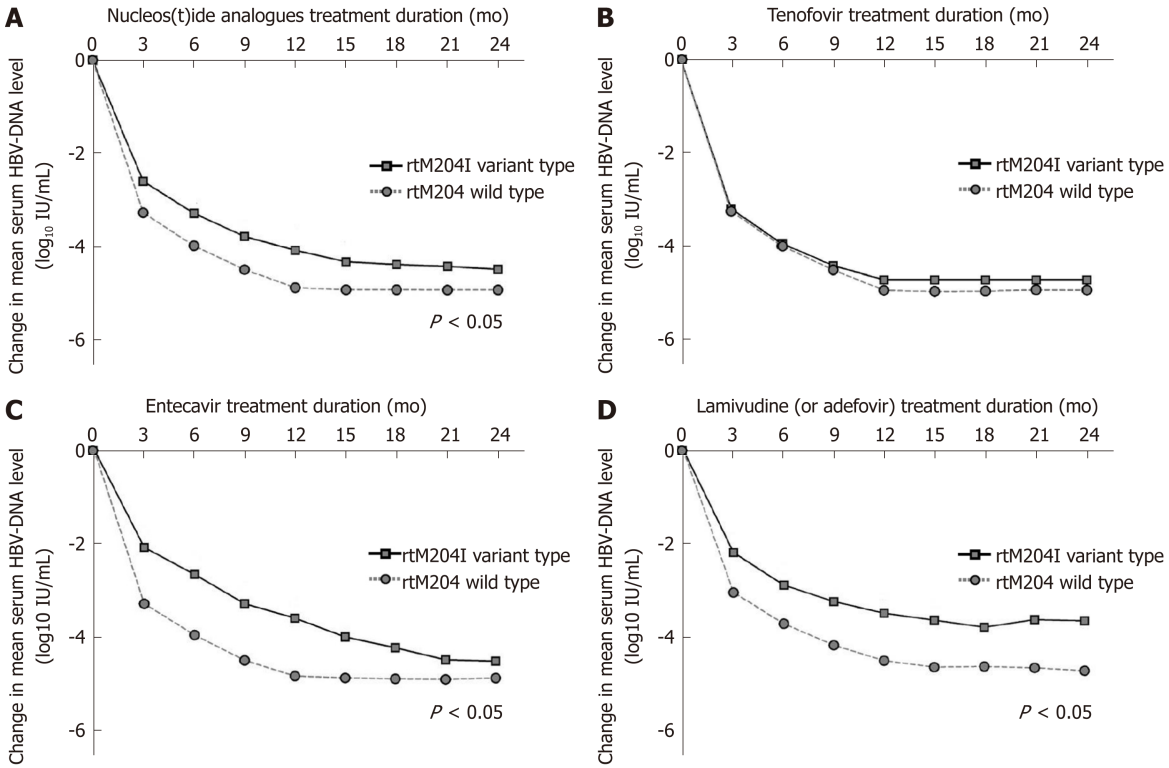

Figure 4 Changes in mean log values of the serum hepatitis B virus DNA levels from baseline during nucleos(t)ide analogues treatment. A: The decrease in hepatitis B virus (HBV) DNA was significantly less prominent in patients infected with naturally occurring rtM204I variants than in patients without pre-existing rtM204I variants at 3, 6, 9, 12, 15 mo of nucleos(t)ide analogues (all $P < 0.05$); B: There was no differences in HBV-DNA declines during tenofovir therapy between patients with and without naturally occurring rtM204I variants; C: The decrease in HBV DNA was significantly less prominent in patients infected with naturally occurring rtM204I variants than in patients without pre-existing rtM204I variants at 3, 6, 9, 12, 15 mo of entecavir (all $P < 0.05$); D: The decrease in HBV DNA was significantly less prominent in patients infected with naturally occurring rtM204I variants than in patients without pre-existing rtM204I variants at 3, 6, 9, 12, 15 mo of low genetic barriers (all $P < 0.05$). Student's *t*-test was used for the statistical analysis at each time point. HBV: Hepatitis B virus.

ARTICLE HIGHLIGHTS

Research background

Hepatitis B virus (HBV) DNA polymerase mutations usually occur to long term use of nucleos(t)ide analogues (NAs), but they can occur spontaneously in treatment-naïve chronic hepatitis B (CHB) patients. The naturally occurring HBV-DNA polymerase mutations might complicate antiviral therapy with NAs, leading to the generation of drug-resistant viral mutants and disease progression. The most common substitutions are known to be YMDD-motif mutations, but their prevalence and the influence on antiviral therapy is unclear.

Research motivation

HBV DNA polymerase mutations have been known to be prevalent in treatment-naïve CHB

patients infected with HBV genotype C2 strains. But there is still controversy regarding prevalence of the naturally occurring rtM204I mutations prior to antiviral treatments. Moreover, the clinical characteristics of the naturally occurring rtM204I mutations have not been fully elucidated.

Research objectives
The objective of this study was to determine the prevalence and clinical characteristics of naturally occurring rtM204I mutations in treatment-naïve patients infected with HBV genotype C2 strains by using a newly developed locked nucleotide probe (LNA probe) based real time PCR (LNA-RT-PCR) method, which can detect subspecies at 5% of the circulating HBV population.

Research methods
The retrospective study enrolled a total of 410 treatment-naïve CHB patients infected with HBV genotype C2 strains. Among the 410 patients, 232 were treated with NAs for at least 12 mo. Significant fibrosis was defined as fibrosis-4 index > 3.25 or aspartate aminotransferase to platelet ratio index > 1.5. Complete viral response (CVR) during NAs was defined as undetectable serum HBV DNA (< 24 IU/mL). The rtM204I variants were analyzed by a newly developed LNA RT-PCR method.

Research results
The LNA-RT-PCR could discriminate rtM204I mutant-type (17 patients, 4.2%) from rtM204 wild-type (386 patients, 95.8%) in 403 of 410 patients (98.3% sensitivity). Multivariate analysis showed that naturally occurring rtM204I variants were more frequently detected in patients with significant fibrosis [odd-ratio (OR) 3.397, 95% confidence-interval (CI) 1.119-10.319, $P = 0.031$]. Of 232 patients receiving NAs, multivariate analysis revealed that achievement of CVR was reversely associated with naturally occurring rtM204I variants prior to NAs treatment (OR 0.014, 95%CI 0.002-0.096, $P < 0.001$). Almost patients receiving tenofovir achieved CVR at 12 mo of tenofovir, irrespective of pre-existence of naturally occurring rtM204I mutations (CVR rates: patients with rtM204I, 100%; patients without rtM204I, 96.6%), whereas, pre-existence of naturally-occurring rtM204I-mutations prior to NAs significantly affects CVR rates in patients receiving entecavir (at 12 mo: Patients with rtM204I, 16.7%; patients without rtM204I, 95.6%, $P < 0.001$).

Research conclusions
The newly developed LNA-RT-PCR method can detect pre-existing rtM204I variants with high sensitivity in NAs-naïve CHB patients. rtM204I mutations can occur spontaneously with a rate of approximately 4% in treatment-naïve patients infected with HBV genotype C2. The rtM204I variants more frequently pre-existed in patients with significant fibrosis, and the pre-existence of rtM204I variants was associated with incomplete responses to NAs. Tenofovir is a more suitable treatment than entecavir for CHB patients carrying the naturally occurring rtM204I mutations.

Research perspectives
The detection of pre-existing rtM204I variants with the newly developed LNA-RT-PCR method could play a relevant role in the clinical management of NA-naïve patients with CHB genotype C2 infection. Further prospective studies should be performed to verify our conclusions.

ACKNOWLEDGEMENTS

This research was supported by the Basic Science Research Program through the National Research Foundation of Korea (NRF) funded by the Ministry of Education, Science and Technology (Grant No., 2016932422 and 2019R1A2C1084511).

REFERENCES

1 **Dienstag JL**. Hepatitis B virus infection. *N Engl J Med* 2008; **359**: 1486-1500 [PMID: 18832247 DOI: 10.1056/NEJMra0801644]
2 **Wong GL**. Management of chronic hepatitis B patients in immunetolerant phase: What latest guidelines recommend. *Clin Mol Hepatol* 2018; **24**: 108-113 [PMID: 29353469 DOI: 10.3350/cmh.2017.0068]
3 **European Association for the Study of the Liver**. EASL 2017 Clinical Practice Guidelines on the management of hepatitis B virus infection. *J Hepatol* 2017; **67**: 370-398 [PMID: 28427875 DOI: 10.1016/j.jhep.2017.03.021]
4 **Terrault NA**, Bzowej NH, Chang KM, Hwang JP, Jonas MM, Murad MH; American Association for the Study of Liver Diseases. AASLD guidelines for treatment of chronic hepatitis B. *Hepatology* 2016; **63**: 261-283 [PMID: 26566064 DOI: 10.1002/hep.28156]
5 **Pawlotsky JM**, Dusheiko G, Hatzakis A, Lau D, Lau G, Liang TJ, Locarnini S, Martin P, Richman DD, Zoulim F. Virologic monitoring of hepatitis B virus therapy in clinical trials and practice: Recommendations for a standardized approach. *Gastroenterology* 2008; **134**: 405-415 [PMID: 18242209 DOI: 10.1053/j.gastro.2007.11.036]
6 **Bartholomeusz A**, Locarnini SA. Antiviral drug resistance: Clinical consequences and molecular aspects. *Semin Liver Dis* 2006; **26**: 162-170 [PMID: 16673294 DOI: 10.1055/s-2006-939758]
7 **Glebe D**, Bremer CM. The molecular virology of hepatitis B virus. *Semin Liver Dis* 2013; **33**: 103-112

[PMID: 23749666 DOI: 10.1055/s-0033-1345717]
8 **Locarnini S**, Zoulim F. Molecular genetics of HBV infection. *Antivir Ther* 2010; **15** Suppl 3: 3-14 [PMID: 21041899 DOI: 10.3851/IMP1619]
9 **Kim BJ**. Hepatitis B virus mutations related to liver disease progression of Korean patients. *World J Gastroenterol* 2014; **20**: 460-467 [PMID: 24574714 DOI: 10.3748/wjg.v20.i2.460]
10 **Tan Y**, Ding K, Su J, Trinh X, Peng Z, Gong Y, Chen L, Cui Q, Lei N, Chen X, Yu R. The naturally occurring YMDD mutation among patients chronically infected HBV and untreated with lamivudine: A systematic review and meta-analysis. *PLoS One* 2012; **7**: e32789 [PMID: 22479339 DOI: 10.1371/journal.pone.0032789]
11 **Heo J**, Cho M, Kim HH, Shin YM, Jang HJ, Park HK, Kim CM, Kim GH, Kang DH, Song GA, Yang US. Detection of YMDD motif mutants by oligonucleotide chips in lamivudine-untreated patients with chronic hepatitis B virus infection. *J Korean Med Sci* 2004; **19**: 541-546 [PMID: 15308845 DOI: 10.3346/jkms.2004.19.4.541]
12 **Horgan M**, Brannigan E, Crowley B, Levis J, Fanning LJ. Hepatitis B genotype and YMDD profiles in an untreated Irish population. *J Clin Virol* 2006; **35**: 203-204 [PMID: 16213785 DOI: 10.1016/j.jcv.2005.08.004]
13 **Kirishima T**, Okanoue T, Daimon Y, Itoh Y, Nakamura H, Morita A, Toyama T, Minami M. Detection of YMDD mutant using a novel sensitive method in chronic liver disease type B patients before and during lamivudine treatment. *J Hepatol* 2002; **37**: 259-265 [PMID: 12127432 DOI: 10.1016/S0168-8278(02)00145-9]
14 **Choi YM**, Lee SY, Kim BJ. Naturally occurring hepatitis B virus reverse transcriptase mutations related to potential antiviral drug resistance and liver disease progression. *World J Gastroenterol* 2018; **24**: 1708-1724 [PMID: 29713126 DOI: 10.3748/wjg.v24.i16.1708]
15 **Kim H**, Jee YM, Song BC, Hyun JW, Mun HS, Kim HJ, Oh EJ, Yoon JH, Kim YJ, Lee HS, Hwang ES, Cha CY, Kook YH, Kim BJ. Analysis of hepatitis B virus quasispecies distribution in a Korean chronic patient based on the full genome sequences. *J Med Virol* 2007; **79**: 212-219 [PMID: 17245716 DOI: 10.1002/jmv.20789]
16 **Xiao G**, Yang J, Yan L. Comparison of diagnostic accuracy of aspartate aminotransferase to platelet ratio index and fibrosis-4 index for detecting liver fibrosis in adult patients with chronic hepatitis B virus infection: A systemic review and meta-analysis. *Hepatology* 2015; **61**: 292-302 [PMID: 25132233 DOI: 10.1002/hep.27382]
17 **Yu SJ**. A concise review of updated guidelines regarding the management of hepatocellular carcinoma around the world: 2010-2016. *Clin Mol Hepatol* 2016; **22**: 7-17 [PMID: 27044761 DOI: 10.3350/cmh.2016.22.1.7]
18 **Sarin SK**, Kumar M, Lau GK, Abbas Z, Chan HL, Chen CJ, Chen DS, Chen HL, Chen PJ, Chien RN, Dokmeci AK, Gane E, Hou JL, Jafri W, Jia J, Kim JH, Lai CL, Lee HC, Lim SG, Liu CJ, Locarnini S, Al Mahtab M, Mohamed R, Omata M, Park J, Piratvisuth T, Sharma BC, Sollano J, Wang FS, Wei L, Yuen MF, Zheng SS, Kao JH. Asian-Pacific clinical practice guidelines on the management of hepatitis B: A 2015 update. *Hepatol Int* 2016; **10**: 1-98 [PMID: 26563120 DOI: 10.1007/s12072-015-9675-4]
19 **Tsubota A**. How do naturally occurring YMDD-motif mutants influence the clinical course of lamivudine-naïve patients with chronic hepatitis B virus infection? *J Gastroenterol Hepatol* 2006; **21**: 1769-1771 [PMID: 17074012 DOI: 10.1111/j.1440-1746.2006.04768.x]
20 **Keeffe EB**, Dieterich DT, Pawlotsky JM, Benhamou Y. Chronic hepatitis B: Preventing, detecting, and managing viral resistance. *Clin Gastroenterol Hepatol* 2008; **6**: 268-274 [PMID: 18328434 DOI: 10.1016/j.cgh.2007.12.043]
21 **Houot M**, Ngo Y, Munteanu M, Marque S, Poynard T. Systematic review with meta-analysis: Direct comparisons of biomarkers for the diagnosis of fibrosis in chronic hepatitis C and B. *Aliment Pharmacol Ther* 2016; **43**: 16-29 [PMID: 26516104 DOI: 10.1111/apt.13446]
22 **Kim H**, Kim BJ. Association of preS/S Mutations with Occult Hepatitis B Virus (HBV) Infection in South Korea: Transmission Potential of Distinct Occult HBV Variants. *Int J Mol Sci* 2015; **16**: 13595-13609 [PMID: 26084041 DOI: 10.3390/ijms160613595]
23 **Kim H**, Lee SA, Do SY, Kim BJ. Precore/core region mutations of hepatitis B virus related to clinical severity. *World J Gastroenterol* 2016; **22**: 4287-4296 [PMID: 27158197 DOI: 10.3748/wjg.v22.i17.4287]
24 **Zeng Y**, Li D, Wang W, Su M, Lin J, Chen H, Jiang L, Chen J, Yang B, Ou Q. Establishment of real time allele specific locked nucleic acid quantitative PCR for detection of HBV YIDD (ATT) mutation and evaluation of its application. *PLoS One* 2014; **9**: e90029 [PMID: 24587198 DOI: 10.1371/journal.pone.0090029]
25 **Gish R**, Jia JD, Locarnini S, Zoulim F. Selection of chronic hepatitis B therapy with high barrier to resistance. *Lancet Infect Dis* 2012; **12**: 341-353 [PMID: 22326017 DOI: 10.1016/S1473-3099(11)70314-0]
26 **Choi J**, Kim HJ, Lee J, Cho S, Ko MJ, Lim YS. Risk of Hepatocellular Carcinoma in Patients Treated With Entecavir vs Tenofovir for Chronic Hepatitis B: A Korean Nationwide Cohort Study. *JAMA Oncol* 2019; **5**: 30-36 [PMID: 30267080 DOI: 10.1001/jamaoncol.2018.4070]

World Journal of Gastroenterology

Submit a Manuscript: https://www.f6publishing.com

World J Gastroenterol 2019 September 7; 25(33): 4999-5016

DOI: 10.3748/wjg.v25.i33.4999

ISSN 1007-9327 (print) ISSN 2219-2840 (online)

META-ANALYSIS

Efficacy of *Lactobacillus rhamnosus* GG in treatment of acute pediatric diarrhea: A systematic review with meta-analysis

Ya-Ting Li, Hong Xu, Jian-Zhong Ye, Wen-Rui Wu, Ding Shi, Dai-Qiong Fang, Yang Liu, Lan-Juan Li

ORCID number: Ya-Ting Li (0000-0002-0761-4967); Hong Xu (0000-0001-6453-4683); Jian-Zhong Ye (0000-0001-8174-2580); Wenrui Wu (0000-0002-8457-9675); Ding Shi (0000-0003-3988-9321); Dai-Qiong Fang (0000-0002-0758-3988); Yang Liu (0000-0003-0246-4418); Lan-Juan Li (0000-0001-6945-0593).

Author contributions: Li YT, Xu H, and Ye JZ contributed equally to this work; Li YT and Xu H identified eligible articles and extracted applicable data; Li YT, Xu H, and Ye JZ contributed to the design of the study; Wu WR contributed to the analysis and interpretation of the outcomes; Liu Y, Fang DQ, and Shi D participated in writing and editing the article; all authors approved the final draft of the manuscript.

Supported by the National Natural Science Foundation of China, No. 81330011.

Conflict-of-interest statement: None.

PRISMA 2009 Checklist statement: The guidelines of the PRISMA 2009 Statement have been adopted in this manuscript.

Ya-Ting Li, Jian-Zhong Ye, Wen-Rui Wu, Ding Shi, Dai-Qiong Fang, Lan-Juan Li, State Key Laboratory for the Diagnosis and Treatment of Infectious Diseases, The First Affiliated Hospital, School of Medicine, Zhejiang University, Hangzhou 310003, Zhejiang Province, China

Ya-Ting Li, Jian-Zhong Ye, Wen-Rui Wu, Ding Shi, Dai-Qiong Fang, Lan-Juan Li, Collaborative Innovation Center for the Diagnosis and Treatment of Infectious Diseases, School of Medicine, Zhejiang University, Hangzhou 310003, Zhejiang Province, China

Hong Xu, Department of Orthopedics, Xiaoshan Traditional Chinese Medical Hospital, Hangzhou 310003, Zhejiang Province, China

Yang Liu, Department of Orthopedics, Clinical Sciences, Lund, Lund University, Lund 22185, Sweden

Corresponding author: Lan-Juan Li, MD, PhD, Academic Research, Doctor, Professor, Senior Researcher, State Key Laboratory for the Diagnosis and Treatment of Infectious Diseases, The First Affiliated Hospital, School of Medicine, Zhejiang University, No. 79, Qingchun Road, Hangzhou 310003, Zhejiang Province, China. ljli@zju.edu.cn
Telephone: +86-571-87236759
Fax: +86-571-87236459

Abstract

BACKGROUND

Diarrhea is a major infectious cause of childhood morbidity and mortality worldwide. In clinical trials, *Lactobacillus rhamnosus* GG ATCC 53013 (LGG) has been used to treat diarrhea. However, recent randomized controlled trials (RCTs) found no evidence of a beneficial effect of LGG treatment.

AIM

To evaluate the efficacy of LGG in treating acute diarrhea in children.

METHODS

The EMBASE, MEDLINE, PubMed, Web of Science databases, and the Cochrane Central Register of Controlled Trials were searched up to April 2019 for meta-analyses and RCTs. The Cochrane Review Manager was used to analyze the relevant data.

RESULTS

Nineteen RCTs met the inclusion criteria and showed that compared with the control group, LGG administration notably reduced the diarrhea duration [mean difference (MD) -24.02 h, 95% confidence interval (CI) (-36.58, -11.45)]. More

Manuscript source: Unsolicited manuscript

Received: April 28, 2019
Peer-review started: April 28, 2019
First decision: May 30, 2019
Revised: July 4, 2019
Accepted: July 19, 2019
Article in press: July 19, 2019
Published online: September 7, 2019

P-Reviewer: Tuna Kirsacliogl CT, Reyes VEE, Rhoads JM
S-Editor: Yan JP
L-Editor: Wang TQ
E-Editor: Wu YXJ

effective results were detected at a high dose ≥ 10^{10} CFU per day [MD -22.56 h, 95%CI (-36.41, -8.72)] *vs* a lower dose. A similar reduction was found in Asian and European patients [MD -24.42 h, 95%CI (-47.01, -1.82); MD -32.02 h, 95%CI (-49.26, -14.79), respectively]. A reduced duration of diarrhea was confirmed in LGG participants with diarrhea for less than 3 d at enrollment [MD -15.83 h, 95%CI (-20.68, -10.98)]. High-dose LGG effectively reduced the duration of rotavirus-induced diarrhea [MD -31.05 h, 95%CI (-50.31, -11.80)] and the stool number per day [MD -1.08, 95%CI (-1.87, -0.28)].

CONCLUSION
High-dose LGG therapy reduces the duration of diarrhea and the stool number per day. Intervention at the early stage is recommended. Future trials are expected to verify the effectiveness of LGG treatment.

Key words:*Lactobacillus rhamnosus* GG; Acute diarrhea; Children; Rotavirus; Probiotics; Systematic review; Meta-analysis

Core tip: The treatment effectiveness of *Lactobacillus rhamnosus* GG (LGG) for acute diarrhea in children was assessed in our study. LGG was confirmed to effectively reduce the duration of diarrhea and the stool number per day. LGG was particularly efficacious in patients treated at a dose > 10^{10} CFU/day, those treated at an early stage of illness, and those diagnosed with rotavirus-positive diarrhea.

Citation: Li YT, Xu H, Ye JZ, Wu WR, Shi D, Fang DQ, Liu Y, Li LJ. Efficacy of *Lactobacillus rhamnosus* GG in treatment of acute pediatric diarrhea: A systematic review with meta-analysis. *World J Gastroenterol* 2019; 25(33): 4999-5016
URL: https://www.wjgnet.com/1007-9327/full/v25/i33/4999.htm
DOI: https://dx.doi.org/10.3748/wjg.v25.i33.4999

INTRODUCTION

The World Health Organization and United Nations International Children's Emergency Fund define diarrhea as more than three loose or watery stools during a 24-h period. A duration of 14 days is the proposed criterion for acute diarrhea or persistent diarrhea. Diarrhea is a major infectious cause of childhood morbidity and mortality worldwide, especially in developing countries[1]. As the second most common cause of death among children under 5 years of age[2], the frequency of acute diarrhea in one year is approximately two to three episodes per child[1]. Previous data showed that the incidence of diarrhea was 6 to 12 episodes in 12 months per child in developing countries[3].

The goals of treatment are prevention or resolution of dehydration and reduction of the diarrhea duration and infectious period[4]. Oral rehydration, gut motility inhibitors, and antibiotics are used to treat acute gastroenteritis[4]. Oral rehydration contributes to a reduced likelihood of dehydration but has no appreciable effects on bowel movements or the duration of diarrhea and is not utilized to its full extent[5]. Antibiotics should be considered if pathogenic bacteria are detected. Smectite and zinc remain under-utilized as adjuvant therapies[6,7].

Probiotic supplements have gained considerable popularity in the global market and are predicted to generate 64 billion United States dollars in revenue by 2023[8]. Probiotics have health benefits for hosts[9] and have been evaluated in the treatment of diarrhea, and multiple mechanisms of diarrhea improvement have been identified. Probiotics modulate the host immune response[10]. Furthermore, colonic bacterial metabolites such as short-chain fatty acids increase colonic Na and fluid absorption through a cyclic adenosine monophosphate-independent mechanism[5]. In clinical trials, the well-known probiotics *Saccharomyces boulardii*, *Lactobacillus reuteri* DSM 17938, and *Lactobacillus rhamnosus* GG ATCC 53013 (LGG) have been used to treat diarrhea[2,4]. Previously, rotavirus-induced diarrhea was considered an adaptation disease associated with LGG treatment[11]. Wolvers D revealed that the probiotic dose mediated the effectiveness of treatment, and 10^{10}-10^{11} CFU per day was

recommended[12]. In addition, a greater effect was observed in the early stage of illness, and a poorer effect on invasive bacterial diarrhea versus watery diarrhea was observed. LGG treatment has been endorsed by leading experts[13-15]. However, most recent randomized controlled trials (RCTs) conducted by Schnadower *et al*[8] yielded no evidence of a beneficial effect of LGG treatment. Therefore, we conducted a meta-analysis to evaluate the available validated data and update existing knowledge and thus provide guidance to patients.

MATERIALS AND METHODS

Literature search

Relevant studies published before April 2019 were retrieved from the EMBASE, MEDLINE, PubMed, Web of Science databases, and the Cochrane Central Register of Controlled Trials (CENTRAL, the Cochrane Library). The search strategy was conducted with medical subject headings and the search terms "diarrhoea, diarrhea, diarrh*, gastroenteritis, probiotic*, *Lactobacillus rhamnosus* GG, *Lactobacillus* GG, and LGG". No language restrictions were applied. Additional studies were identified by manually searching review articles.

Study selection

Nineteen RCTs describing LGG interventions for acute diarrhea were included. The PRISMA statement and the guidelines from the Cochrane Collaboration were followed for this evidence-based medicine study[16,17]. The participants were children aged less than 18 years. The dose of LGG was provided in various forms at different times. Antibiotic-associated diarrhea and persistent diarrhea were excluded. Other applications of LGG, such as preventive strategies, were not included. Some particular article types without complete data were excluded, such as abstracts and letters. We also excluded studies using mixtures of more than one probiotic strain. The primary outcomes were directly related to the development of persistent diarrhea, including the duration of diarrhea and diarrhea lasting ≥ 3 and ≥ 4 d. Secondary outcomes included the hospital stay duration, stool frequency, and improvement in stool consistency and vomiting.

Data extraction

Two investigators (Li YT and Xu H) independently identified eligible articles and extracted applicable data following the inclusion criteria. Quality control was assessed by another reviewer (Wu WR). The data set included the baseline characteristics of the participants, the duration of diarrhea, the hospital stay duration, the time to improvement in stool consistency, the mean number of stools per day during diarrhea episodes, the proportion of patients with vomiting, the duration of vomiting, stool frequency on days 2 and 3 after treatment, and the number of patients with diarrhea lasting ≥ 3 or 4 d. Cochrane Review Manager (Version 5.1. Copenhagen: The Nordic Cochrane Centre, The Cochrane Collaboration, 2011) and STATA version 12.0 (StataCorp LP, College Station, TX, United States) were used for data analyses. Any discrepancies were resolved by discussion.

Risk of bias

All included trials were evaluated following the Cochrane Collaboration's risk of bias tool. Seven domains were examined to identify the bias risk: selection bias, including random sequence generation and allocation concealment, performance bias, including blinding of participants and personnel, detection bias, including blinding of outcome assessments, attrition bias, including incomplete outcome data, reporting bias, including selective reporting, and other bias. Adequate allocation concealment was implemented to ensure blinding of the participants and investigators to avoid influences on the measures. Randomization was performed based on confirmed allocation concealment. Unclear allocation concealment was noted when no method was mentioned. The integrity of the data was evaluated, including the proportion of excluded participants (http://www.cochrane-handbook.org).

Statistical analysis

The Cochrane Review Manager was used to analyze the relevant data. The mean differences (MDs) in continuous data under LGG or placebo treatment were measured. Dichotomous results are pooled and presented as risk ratios. Additionally, 95% confidence intervals (CIs) are reported for all types of outcomes. I^2 and χ^2 values were calculated to quantify and reflect heterogeneity. A P-value < 0.05 indicates that heterogeneity should not be ignored; thus, a random-effects model was used. A fixed-effects model was employed when no statistically significant inconsistency was

detected. Publication bias was assessed by funnel plot asymmetry[18]. Sensitivity analyses were conducted to detect the robustness of results by assessing randomization, missing data, blinding, and allocation concealment. Each individual study was systematically removed from the meta-analysis, and the effect was recalculated and estimated from the remaining studies (Supporting information Figure S1). Regression analysis was conducted, and the relationships between the duration of diarrhea and other covariates, including publication year, participant age, the duration of diarrhea before study enrollment, and the LGG dosage, were examined. Subgroup analyses were performed to diminish significant inconsistency. Preplanned subgroup analyses were performed according to the following clinical characteristics and results from sensitivity or regression analysis: (1) The dosage of LGG per day. A dosage of 10^{10} CFU/day was observed to be a critical element of effective treatment in the study by Szajewska *et al*[13]. In addition, a larger dose was suggested in other studies[19,20]; (2) The etiology of diarrhea. Diarrhea mortality and severe diarrhea were most frequently caused by rotavirus in children[21]. Compared to control children, several rotavirus-positive children with watery stools in a probiotic group were reported to exhibit a marked reduction in diarrhea symptoms after 24 h[22]. A meta-analysis performed by Szajewska *et al*[23] in 2007 concluded that the duration of rotavirus-induced diarrhea was significantly attenuated by LGG supplementation; (3) The site of treatment (inpatient *vs* outpatient); (4) Vaccination status; (5) Geography of the clinical trials. The location of the study affected the sanitary habits, exposure to various pathogens, and nutrient status of the participants. All studied environmental factors contribute to various outcomes; (6) Early probiotic administration. A beneficial effect of probiotics was reported in the course of disease when initiated early[12]; and (7) Publication date.

RESULTS

Study selection

A total of 349 potentially relevant studies were identified. The process of screening was carried out according to the flow diagram shown in Figure S2 (Supporting information). The characteristics of each included study are summarized in Table 1. With 988 participants in a 2007 meta-analysis and 2683 participants in a 2013 meta-analysis, a total of 4073 participants in 19 RCTs were identified in the literature. Two experimental arms in the study of Basu *et al*[24] were listed separately to exhibit different doses of probiotics, which were marked as Basu 2009a and Basu 2009b. Therefore, the figures, tables, and full texts of 18 articles were reviewed[8,24-40]. A large number of trials were conducted in Europe and Asia. Patients were recruited from outpatient, inpatient, and emergency departments. Inconsistency existed in the daily doses and routes of LGG supplementation during the treatment period. Different criteria were used to define diarrhea in the included studies. Diarrhea resolution was commonly defined as passage of the first normal stool or the last watery stool.

Antibiotic treatment before recruitment was assessed, and different studies varied regarding the use of antibiotics. Similarly, the duration of treatment varied. Studies of moderate to high quality were adequately assessed and are summarized in Figure S3 (Supporting information).

Evaluation before enrollment (days)

Before enrollment, age was assessed in 16 studies, and the duration of diarrhea was reported in nine studies (Supporting information Figures S4 and S5). No obvious difference in age was found. The statistical differences and high heterogeneity resulting from the duration of diarrhea [MD -6.21 h, 95%CI (-9.04, -3.38)] could be reduced by subgrouping according to the outcomes of the sensitivity analysis (Supporting information Figure S1). The subgroup excluding the study of Ritchie *et al*[37] performed in 2010 showed acceptable heterogeneity, and no statistical significance was observed for the duration of diarrhea before study enrollment [MD -0.9 h, 95%CI (-4.02, 2.22)] (I^2 = 10%). Sensitivity analysis revealed differences in the duration of diarrhea before study enrollment between the two groups in the study of Ritchie *et al*[37], which recruited aboriginal children in the Northern Territory of Australia. Social disadvantages and poverty contributed to malnutrition in these children[4]. However, no significant differences in the primary and secondary outcomes were found by sensitivity analysis, which is inconsistent with the findings reported in previous meta-analyses[4,13] (Supporting information Figure S1).

Duration of diarrhea

A reduced duration of diarrhea was found in the LGG group compared to that in the

Table 1 Characteristics of the included trials

Article	Type of article	Age group	Country	Patient source	n (exp/control)	Inclusion criteria	Exclusion criteria	LGG (dosage)	Control group	Duration of intervention	Etiology
Basu *et al*[25], 2007	RCT; 1 center; Duration: 1 yr	Children	India	Inpatients	323/323	≥ 3 watery stools/day without visible blood or mucus; <10 white blood cells/high-power field and no red cells, mucus flakes, or bacteria on stool microscopy; negative hanging drop preparation; negative bacterial stool culture	Systemic illness other than diarrhea on admission; systemic complications of diarrhea during hospitalization; failure to provide informed consent	120×10^6; CFU/day	ORF	7 d	Bacterial diarrhea excluded; Rotavirus-induced diarrhea 75.8%
Basu *et al*[24], 2009a	RCT; 1 center; Duration: 1 yr	Children	India	Inpatients	188/185	≥ 3 watery stools/day without macroscopic blood or mucus, <10 white blood cells/high-power field, and no red blood cells, mucus flakes, or bacteria on stool microscopy; negative hanging drop preparation; negative bacterial stool culture	Symptoms of illness other than diarrhea; development of any systemic complication of diarrhea during hospitalization; failure to provide informed consent	2×10^{10}; CFU/day	ORF	7 d or until diarrhea stopped	Bacterial diarrhea excluded; Rotavirus diarrhea 57.1%
Basu *et al*[24] 2009b	RCT; 1 center; Duration: 1 yr	Children	India	Inpatients	186/185	≥ 3 watery stools/day without macroscopic blood or mucus, <10 white blood cells/high-power field, and no red blood cells, mucus flakes, or bacteria on stool microscopy; negative hanging drop preparation; negative bacterial stool culture	Symptoms of illness other than diarrhea; development of any systemic complication of diarrhea during hospitalization; failure to provide informed consent	2×10^{12}; CFU/day	ORF	7 d or until diarrhea stopped	Bacterial diarrhea excluded; Rotavirus-induced diarrhea 56.06%
Canani *et al*[26], 2007	RCT; 6 centers; Duration: 12 mo	3-36 mo	Italy	Outpatients	100/92	> 2 loose or liquid stools/day for <48 h	Malnutrition; severe dehydration; coexisting acute systemic illness; immunodeficiency; underlying severe chronic disease; cystic fibrosis; food allergy or other chronic GI diseases; use of probiotics in the previous 3 wk; antibiotics or any other antidiarrheal medication in the previous 3 wk; poor compliance	12×10^9; CFU/day	No details given	5 d	Stool culture in only a few participants and no data presented
Costa *et al*[27] 2003	RCT; 1 center	Boys, 1-24 mo	Brazil	Inpatients	61/63	Acute diarrhea (3 or more watery or loose stools per 24 h during at least one 24-h period in the 72 h before admission) with moderate or severe dehydration after correction with rapid IV fluids	Systemic infections requiring antibiotics; severe malnutrition (weight for age < 65% of NCHS standards; bloody diarrhea	10^{10}; CFU/day	Inulin 320 mg/day	Unclear	Rotavirus-induced diarrhea 50%; Bloody diarrhea excluded
Czerwionka-Szaflarska *et al*[28], 2009	RCT; 1 center	Unclear	Poland	Inpatients	50/50	Infants and children with acute infectious diarrhea and failed oral rehydration	Bloody stools; coexisting disease that may influence the course of diarrhea	50 ml/kg/day	Unclear	Unclear	Bloody diarrhea excluded; Rotavirus-induced diarrhea 58%

Schnadower *et al*[8] 2018	RCT	3-48 mo	United States	University-affiliated PED	483/488	≥ 3 watery stools per day, with or without vomiting, for fewer than 7 d	Pancreatitis, bilious emesis, or hematochezia; a known allergy to L. rhamnosus GG or to microcrystalline cellulose or a known allergy to erythromycin, clindamycin, and beta-lactam antibiotic agents; caregiver did not speak English or Spanish; children receiving antibiotics	1×10^{10}; CFU twice daily	Matching placebo	5 d	Norovirus GI or GII 19.6%; Rotavirus 17.7%; Adenovirus 9.1%; Clostridium difficile 7.4%; Shigella 5.0%
Guandalini *et al*[29], 2000	RCT; multicenter; Duration: 1 yr	1-36 mo	Listed as follows	Inpatients and outpatients	147/140	Infants and children with > 4 liquid or	Previous probiotic usage; untreated underlying chronic small bowel disease; inflammatory bowel disease; any underlying chronic disease or immunosuppressive disease or treatment	$\geq 10 \times 10^{9}$; CFU/250 mL/day with ORF	ORF	As tolerated for 4-6 h, then ad libitum	Rotavirus 35%; Bacteria 24%; Parasites 4.5%; No pathogens 34.5%; Bloody diarrhea 8.7%
Guarino *et al*[30], 1997	RCT; 1 center Duration: 3 mo	3-36 mo	Italy	Outpatients	52/48	semiliquid stools/day for 1 to 5 d Infants and children with ≥ 3 watery stools/day for < 48 h	Antibiotic treatment in the last 3 wk, breastfeeding; a weight: height ratio < the 5th percentile	6×10^{9}; CFU/day with ORF	ORF	≤ 5 d	Rotavirus-induced diarrhea 61%
Isolauri *et al*[31], 1994	RCT; 1 center Duration: not stated	≤ 36 mo	Finland	Inpatients	21/21	Infants and children with > 3 watery stools/day for < 7 d and stools positive for rotavirus; average dehydration of approximately 5% in both groups	Not stated	2×10^{10}; CFU/day	No probiotic	5 d	Rotavirus-induced diarrhea 100%
Jasinski *et al*[32], 2002	RCT; 12 centers; Duration: not stated	1-36 mo	Africa	Inpatients and outpatients	45/52	> 3 watery stools in 12 h or 1 liquid or semiliquid stool with mucus, pus, or blood; < 5 d	Antibiotic or probiotic use in the last 5 d; chronic diseases of the small or large intestine; immunosuppression; phenylketonuria	ORS + LGG 10^{10} CFU/day	ORS with no LGG	Unclear	Bacterial pathogens 68%; Rotavirus 40.0%; parasites 6%; No pathogens identified: probiotic group 25%
Misra *et al*[33], 2009	RCT; 1 center; Duration: not stated	≤ 36 mo	Egypt Europe America India	Inpatients	105/105	> 3 stools per day (watery or assuming the shape of the container)	Parents refused consent; children living outside the municipal area; bloody diarrhea; severe dehydration; shock, inability to take and retain oral foods; suspected systemic infection	$1 \times 10^{6-9}$ CFU/day	Crystalline micro cellulose	Unclear	Rotavirus 25.6%; Bloody diarrhea excluded; White blood cells in stools 14.3%; Bacterial diarrhea 4.7%
Nixon *et al*[34], 2012	RCT	6-72 mo	United States	PED	77/78	More than 2 loose stools in the last 24 h	Risk factors for non-viral diarrhea (prolonged diarrhea lasting more than 7 d, gross blood, antibiotic exposure, or inflammatory bowel disease); immune compromise; risk factors for probiotic-associated systemic illness or an allergy to milk products	LGG powder twice daily	Inulin	5 d	Unclear
Pant *et al*[35], 1996	RCT; 1 center; Duration: 6 wk	1-24 mo	Thailand	Inpatients	20/19	Infants and children with > 3 watery stools in last 24 h and diarrhea for < 14 d	Exclusive breastfeeding; septicemia	10^{9-10} CFU twice daily	Placebo	2 d	Bloody stools 33.3%;

Raza *et al*[36], 1995	RCT; 1 center Duration: 2 mo	1-24 mo	Pakistan	Inpatients	21/19	Undernourished infants and children with > 3 watery stools in the last 24 h for < 14 d and at least moderate dehydration	Severe malnutrition; septicemia	$2 \times 10^{11-12}$ CFU/day	Placebo	2 d	Rotavirus 17.9%; Astrovirus 2.5% Bloody diarrhea
Ritchie *et al*[37], 2010	RCT; 1 center; Duration: 21 mo	4-24 mo	Australia	Unclear	33/31	Aboriginal children with acute diarrhea defined as ≥ 3 loose stools during 24 h before presentation for < 7 d and able to tolerate ORF	Oxygen required during the study period; chronic cardiac, renal, or respiratory disease; previous gastrointestinal surgery; proven sucrose intolerance; suspected on known immunodeficiency; probiotic use before enrollment; younger than 4 mo of age	$> 15 \times 10^{9}$ CFU/day	Identical placebo	3 d	Bacterial pathogens 12.5%; Rotavirus 8.5%; Parasites 6%
Shornikova *et al*[38], 1997	RCT; 1 center; Duration: 1 yr	1-36 mo	Russia	Inpatients	59/64	≥ 1 watery stool in the last 24 h and diarrhea for < 5 d	Not stated	10^{10} CFU/day	Placebo	5 d	Rotavirus 27.4%; Bacterial diarrhea 21%
Sindhu *et al*[39], 2014	RCT	6-60 mo	India	Unclear	65/59	Diarrhea was defined as ≥ 3 loose watery stools within a 24-h period	Coinfections (the presence of both rotavirus and Cryptosporidium); severe malnutrition; probiotic consumption in the preceding month; allergy to probiotics; acute abdomen or colitis	10^{10} CFU and 170 mg of microcrystalline / day cellulose	170 mg of cellulose	4 wk	Rotavirus 52.4%; Cryptosporidium species 47.6%
Sunny *et al*[40] 2014	Open-label; RCT	6-60 mo	India	OPD or PED	100/100	Passage of three or more loose stools in the last 24 h	Severe malnutrition; dysentery; clinical evidence of coexisting acute systemic illnesses; clinical evidence of chronic disease; probiotic use in the preceding three weeks; antibiotic use	1×10^{10} CFU per day	ORS and zinc 20 mg/d	5 d	Rotavirus 24.1%

The study of Guandalini *et al*[29] was conducted in Poland, Pakistan, Egypt, Croatia, Italy, Slovenia, Netherlands, Greece, Israel, the United Kindom, and Portugal. RCT: Randomized controlled trial; PED: Pediatric emergency department; OPD: Outpatient department; LGG: Lactobacillus rhamnosus GG.

matched group according to 15 RCTs submitted to meta-analysis, which included 3721 participants [MD -24.02 h, 95%CI (-36.58, -11.45)] (Figure 1A). Significantly heterogeneous results were detected among the included trials ($I2$ = 98%). Our data support the results of the prior meta-analyses[4] indicating that LGG treatment reduced participants' duration of diarrhea.

Subgroup analyses were conducted based on clinical features such as age, geographical location, treatment time, outpatient or inpatient settings, the time of enrollment, and literature quality scores. Differences in methodological quality could not explain the statistically significant heterogeneity (Supporting information Figure S6). Regression analysis between the duration of diarrhea and LGG dose revealed that different doses of LGG contributed to the heterogeneity (P = 0.009, adjusted R-squared = 40.21%), suggesting that subgroups according to a high or low dose of LGG should be assessed. A reduced duration of diarrhea was noted in the studies applying > 10^{10} CFU/day of LGG [MD -22.56 h, 95%CI (-36.41, -8.72)] (Figure 1A). In contrast, although only three studies used lower dosages, no statistically significant differences were detected in the groups receiving lower dosages [MD -30.95 h, 95%CI (-83.28, -21.39)] (Figure 1A). A reduced duration of diarrhea was supported in the studies with participants who received LGG treatment before the second day of diarrhea symptoms [MD -1.58 h, 95%CI (-3.05, -0.11)] and during the second to third days of diarrhea symptoms [MD -15.83 h, 95%CI (-20.06, -10.98)] (Figure 1B). However, Ritchie *et al*[37] enrolled participants with diarrhea for more than 3 d, and no statistically significant differences were found in the duration of diarrhea [MD 1.2 h, 95%CI (-21.42, 23.82)] (Figure 1B). A reduced diarrhea duration was reported in studies performed in both Asia and Europe [MD -24.42 h, 95%CI (-47.10, -1.82); MD -32.02 h, 95%CI (-49.26, -14.79), respectively]. Paradoxically, the reduction in the diarrhea duration in other regions was not statistically significant [MD -9.35 h, 95%CI (-20.77, 2.07)] (Figure 1C). In the etiological analysis, the effectiveness of LGG was clearly demonstrated in rotavirus-induced diarrhea cases [seven RCTs; MD -31.05 h, 95%CI (-50.31, -11.80)] (Figure 2). Analysis with the studies carried out in the 1990s and 2000s revealed a clear reduction in the diarrhea duration [MD -36.32 h, 95%CI (-62.20, -10.45); MD -29.40 h, 95%CI (-50.56, -8.25), respectively] (Supporting information Figure S7). In contrast, no reduction in the diarrhea duration was observed in the analysis with studies carried out in the 2010s [MD -3.43 h, 95%CI (-13.25, 6.39)] (Supporting information Figure S7). No studies evaluated the effectiveness of LGG in children vaccinated against rotavirus.

Diarrhea ≥ 3 d

A meta-analysis of four RCTs was performed using a fixed-effects model. The risk of experiencing diarrhea for 3 or more days was reduced when patients received LGG [odds ratio (OR) 0.54, 95%CI (0.38, 0.77)] (Figure 3A).

Diarrhea ≥ 4 d

Three studies were pooled (n = 479) and showed a reduction in the risk of diarrhea lasting for 4 or more days for participants treated with LGG [OR 0.58, 95%CI (0.4, 0.84)] (Figure 3B).

Stool number and consistency

Stool number and consistency were evaluated in most trials. Eight trials reported the mean number of stools in one day during diarrhea episodes. A notable decrease in the stool number per day was noted in the LGG group [MD -0.9, 95%CI (-1.56, -0.23)] (Figure 4A). However, a significantly reduced stool number was observed in the high-dose LGG groups receiving no less than 10^{10} CFU/day [MD -1.08, 95%CI (-1.87, -0.28)], while the lower-dose groups showed no significant reduction [MD -0.25 d, 95%CI (-1.43, 0.93)] (Figure 4A). After the intervention, stool frequency was evaluated on days 2 and 3. Seven trials provided data on day 2, and the overall effect did not differ between the two groups [MD -0.46, 95%CI (-1.06, 0.15)] (Figure 4B). In addition, similar frequencies were observed in the two groups on day 3, with no differences between them [MD 0.34, 95%CI (-0.29, 0.97)] (Figure 4C). Three trials calculated the mean time to improvement in stool consistency, and an obvious reduction was reported [MD -5.65, 95%CI (-7.49, -3.80)] (Figure 4D).

Hospital stay duration

A total of 1823 participants from six RCTs were analyzed. Due to statistically significant heterogeneity, a random-effects model was used, which revealed a significant reduction in the hospital stay duration in the two groups [MD -39.16 h, 95%CI (-72.24, -6.07)] (Figure 5A). A reduction in the hospital stay duration was found in rotavirus-positive children [MD -21.12 h, 95%CI (-26.96, -15.28)] (Figure 5B).

A

Study or subgroup	LGG Mean	LGG SD	LGG Total	Placebo Mean	Placebo SD	Placebo Total	Weight	Mean difference IV, Random, 95%CI
1.1 ≥ 10^{10} CFU/day								
Basu, S. 2009 a	120.5	31.7	188	173.5	30.5	185	7.2%	-53.00 [-59.31, -46.69]
Basu, S. 2009 b	122.9	27.8	186	173.5	30.5	185	7.2%	-50.60 [-56.54, -44.66]
Canani, R. B. 2007	78.5	35.52	100	115.5	23.53	92	7.1%	-37.00 [-45.46, -28.54]
Costa, R.H. 2003	38.3	3.78	61	39.1	4.6	63	7.3%	-0.80 [-2.28, 0.68]
David, S. 2018	54.3	41.3	472	52.4	37.7	480	7.2%	1.90 [-3.13, 6.93]
Guandalini, S. 2000	58.3	27.6	147	71.9	35.8	140	7.1%	-13.60 [-21.02, -6.18]
Isolauri, E.1994	36.0	16.8	21	55.2	19.2	21	6.9%	-19.20 [-30.11, -8.29]
Jasinski.C. 2002	74.64	47.76	45	133.44	53.76	52	6.1%	-58.80 [-79.00, -38.60]
Ritchie, B. K. 2010	52.4	49.8	33	51.2	42.4	31	5.9%	1.20 [-21.42, 23.82]
Shornikova, A. V. 1997	64.8	52.8	59	91.2	67.2	64	6.0%	-26.40 [-47.67, -5.13]
Sindhu, K. N. 2014	96.0	53.3	65	96.0	53.3	59	6.3%	0.00 [-18.78, 18.78]
Sunny, A. 2014	58.3	27.6	100	71.9	35.8	100	7.0%	-13.60 [-22.46, -4.74]
Subtotal (95%CI)			**1477**			**1472**	**81.3%**	**-22.56 [-36.41, -8.72]**
Heterogeneity: Tau² = 555.67; Chi² = 578.18, *df* = 11 (*P* < 0.00001); I^2 = 98%								
Test for overall effect: *Z* = 3.19 (*P* = 0.001)								
1.2 < 10^{10} CFU/day								
Basu, S. 2007	163.2	50.4	323	158.4	55.2	323	7.1%	4.80 [-3.35, 12.95]
Guarino, A. 1997	76.8	34.61	52	141.6	33.26	48	6.7%	-64.80 [-78.10, -51.50]
Pant, A. R.1996	45.6	14.4	14	79.2	55.2	12	4.9%	-33.60 [-65.73, -1.47]
Subtotal (95%CI)			**389**			**383**	**18.7%**	**-30.95 [-83.28, 21.39]**
Heterogeneity: Tau² = 2033.82; Chi² = 77.77, *df* = 2 (*P* < 0.00001); I^2 = 97%								
Test for overall effect: *Z* = 1.16 (*P* = 0.25)								
Total (95%CI)			**1866**			**1855**	**100%**	**-24.02 [-36.58, -11.45]**
Heterogeneity: Tau² = 563.68; Chi² = 661.03, *df* = 14 (*P* < 0.00001); I^2 = 98%								
Test for overall effect: *Z* = 3.75 (*P* = 0.0002)								
Test for subgroup differences: Chi² = 0.09, *df* = 1 (*P* = 0.76), I^2 = 0%								

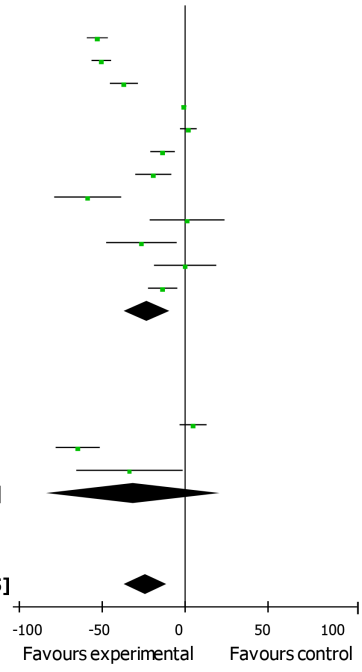

B

Study or subgroup	LGG Mean	LGG SD	LGG Total	Placebo Mean	Placebo SD	Placebo Total	Weight	Mean difference IV, Fixed, 95%CI
1.3 Duration of diarrhoea before LGG subjects' enrollment ≤ 2 d (> 1 d)								
Costa, R.H. 2003	38.3	3.78	61	39.1	4.6	63	90.1%	-0.80 [-2.28, 0.68]
Guarino, A. 1997	76.8	34.61	52	141.6	33.26	48	1.1%	-64.80 [-78.10, -51.50]
Subtotal (95%CI)			**113**			**111**	**91.2%**	**-1.58 [-3.05, -0.11]**
Heterogeneity: Chi² = 87.80, *df* = 1 (*P* < 0.00001); I^2 = 99%								
Test for overall effect: *Z* = 2.11 (*P* = 0.04)								
1.4 Duration of diarrhoea before LGG subjects' enrollment ≤ 3 d (> 2 d)								
Guandalini, S. 2000	58.3	27.6	147	71.9	35.8	140	3.6%	-13.60 [-21.02, -6.18]
Isolauri, E.1994	36.0	16.8	21	55.2	19.2	21	1.7%	-19.20 [-30.11, -8.29]
Pant, A. R.1996	45.6	14.4	14	79.2	55.2	12	0.2%	-33.60 [-65.73, -1.47]
Shornikova, A. V. 1997	64.8	52.8	59	91.2	67.2	64	0.4%	-26.40 [-47.67, -5.13]
Sunny, A. 2014	58.3	27.6	100	71.9	35.8	100	2.5%	-13.60 [-22.46, -4.74]
Subtotal (95%CI)			**341**			**337**	**8.4%**	**-15.83 [-20.68, -10.98]**
Heterogeneity: Chi² = 3.08, *df* = 4 (*P* = 0.54); I^2 = 0%								
Test for overall effect: *Z* = 6.39 (*P* < 0.00001)								
1.5 Duration of diarrhoea before LGG subjects' enrollment ≤ 4 d (> 3 d)								
Ritchie, B. K. 2010	52.4	49.8	33	51.2	42.4	31	0.4%	1.20 [-21.42, 23.82]
Subtotal (95%CI)			**33**			**31**	**0.4%**	**1.20 [-21.42, 23.82]**
Heterogeneity: Not applicable								
Test for overall effect: *Z* = 0.10 (*P* = 0.92)								
Total (95%CI)			**487**			**479**	**100%**	**-2.77 [-4.17, -1.36]**
Heterogeneity: Chi² = 121.33, *df* = 7 (*P* < 0.00001); I^2 = 94%								
Test for overall effect: *Z* = 3.86 (*P* = 0.0001)								
Test for subgroup differences: Chi² = 30.45, *df* = 2 (*P* < 0.00001), I^2 = 93.4%								

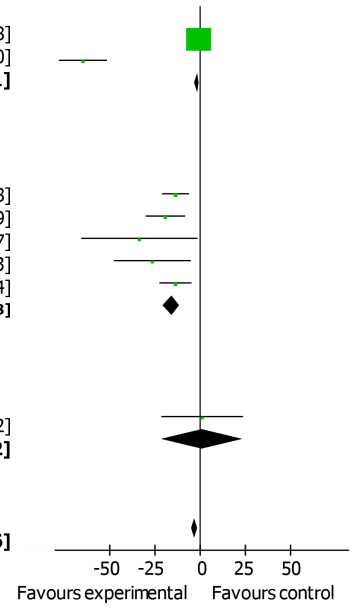

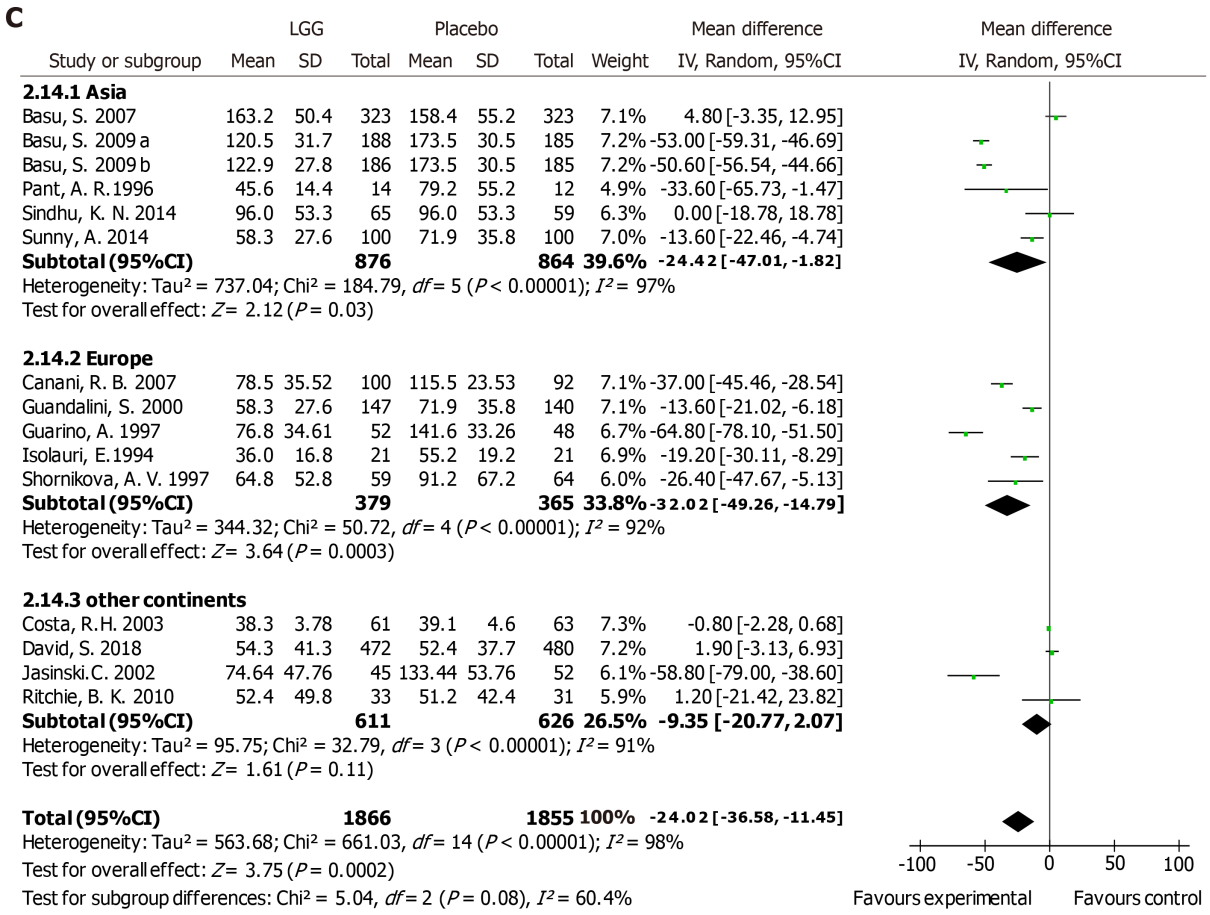

Figure 1 ***Lactobacillus* GG *vs* control with regard to the duration of diarrhea (hours).** A: High dose and low dose; B: The duration of diarrhea before *Lactobacillus rhamnosus* GG participants' enrollment: ≤2 d (>1 d), ≤3 d (>2 d), and ≤4 d (>3 d); C: Geography of the clinical trials: Asia, Europe, and other continents. LGG: *Lactobacillus rhamnosus* GG; CI: Confidence interval; SD: Standard deviation.

Vomiting

Vomiting in different trials was reported as the number of participants with vomiting [number (%)] or as the duration of vomiting (hours). Compared with the placebo group, no difference in the risk of vomiting was reported in the experimental group [OR 1.11, 95%CI (0.59, 2.12)] (Figure 6A). Furthermore, no reduction in the duration of vomiting was noted with LGG treatment [MD -2.02 h, 95%CI (-4.24, 0.21)] (Figure 6B).

Adverse effects

Probiotics have been proposed to be well-tolerated and safe therapeutic agents. Most authors did not report adverse effects. Raza *et al*[36] reported one case of myoclonic jerks in their trial. Lower rates of respiratory infection, wheezing, and even vulvar abscess were noted in Schnadower's trial[8,39], but these effects were not thought to be correlated with LGG use[40]. Aggarwal *et al*[40] reported no adverse effects, and a meta-analysis performed in 2013 showed comparable rates of adverse effects among study groups[13]. In our study, eight studies effectively evaluated the safety of LGG. Adverse effects were reported on a coded reporting form or during daily telephone calls[26,34]. In Schnadower's study, the caregivers completed a daily diary that was collected by telephone or through email[8]. However, the reporting methods were unclear in five articles[24,37,39-41]. In general, no adverse effects or similar rates of side effects were documented in the LGG and placebo groups.

Risk of bias in the included studies

The risk of bias in 18 articles was assessed according to the Cochrane Handbook for Systematic Reviews of Interventions. One trial employed alternating group allocation, and the random sequence generation method was not reported in five trials. Other RCTs provided detailed randomization methods, which mainly included computer-generated strategies, resulting in a low risk of selection bias. Allocation concealment was not applied in two trials and was not mentioned in seven. Nine trials used the sealed envelope technique for allocation concealment. Double blinding was strictly executed in 12 trials, while four trials allowed openness to patients or doctors, and

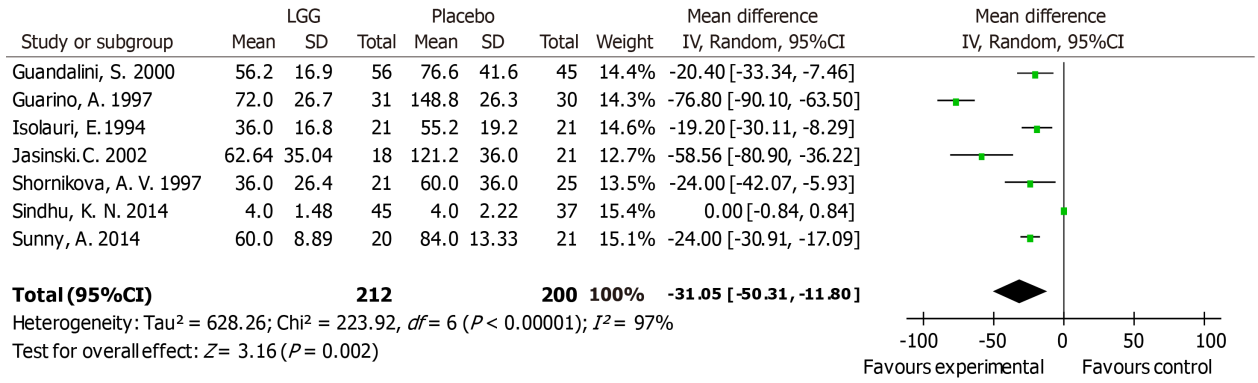

Figure 2 ***Lactobacillus* GG *vs* control with regard to mean duration of diarrhea (hours) in children with rotavirus diarrhea.** LGG: *Lactobacillus rhamnosus* GG; CI: Confidence interval; SD: Standard deviation.

two trials did not report a detailed blinding method. For detection bias, investigators were blinded to the group assignments in ten trials, while blinding assessments were not performed in three trials. Most trials provided complete data with a loss to follow-up rate less than 10%, although one trial had an unknown risk of incomplete outcome data, reflecting a low risk of attrition bias (Supporting information Figure S3).

Publication bias

According to Egger's[18] regression asymmetry test, no small sample or publication bias was found in a funnel plot [P = 0.10, 95%CI (-11.33, -1.14)] (Supporting information Figure S8).

DISCUSSION

Findings and agreement or disagreement with other studies

Nineteen trials comparing a control group with an experimental group treated with LGG were identified in this meta-analysis. In summary, the analysis revealed that treatment with LGG reduced both the duration of diarrhea and the hospital stay duration, especially in specific patient subsets. A striking finding was the time to improvement in stool consistency, which more investigators have confirmed since 2010[8,34,40]. In the whole range of diarrhea cases, the management of stools with this probiotic strain showed a modest beneficial effect on the number of stools per day and the time to improvement in stool consistency. However, no reduction in stool frequency was observed on days 2 and 3. Compared with the placebo group, the risk of diarrhea lasting more than 3 and 4 d was reduced by LGG administration. In both groups, similar rates of vomiting and adverse effects were observed.

Evidence from RCTs confirmed the beneficial effect of LGG on rotavirus-induced diarrhea[42]. In addition to interference with viral replication, most recent studies have shown that LGG prevented injuries to the epithelium and ameliorated rotavirus-induced diarrhea by modulating immune cells, such as dendritic cells and inflammatory cytokines[43,44]. The marked statistical difference in the diarrhea duration with a higher dosage of probiotics reflected greater effectiveness, which confirmed the dose dependence of dendritic cell activation. Treatment efficacy was related to the dose of LGG[45]. As confirmed in the study of Szajewska *et al*[13] in 2013, the importance of a daily LGG dose is high, and a dosage of 10^{10} CFU/day is needed for a positive effect. The statistical heterogeneity between studies can be explained by the timing of the LGG intervention, which was directly correlated with indicators such as the duration of diarrhea before study enrollment. Although the heterogeneity persisted in the subgroup with the shortest duration of diarrhea before study enrollment, probiotics should be applied early in the course of disease. Moreover, symptoms are usually mild at the early stage. Differences in prominent pathogens, sanitation conditions, and common comorbidities lead to dissimilarities between various study locations. Due to differences in the treatment effect among regions, the implications for clinical practice should be evaluated. The nutrient intake and dietary structure of humans have continuously changed in recent decades, which may have caused the reduced effectiveness of LGG reflected in the results of the trials conducted in the 2010s.

Probiotics manipulate and restore the gut microbiota, thus benefitting the

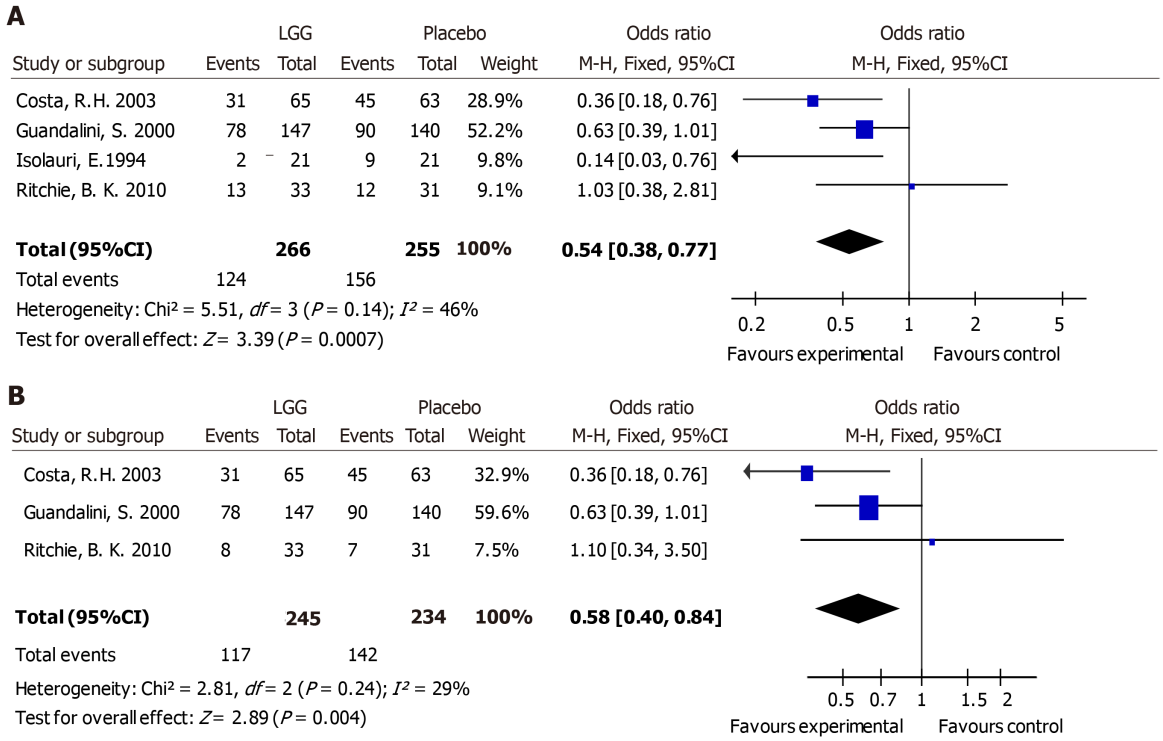

Figure 3 *Lactobacillus* GG *vs* control with regard to the presence of diarrhea. A: Diarrhea lasting > 3 d; B: Diarrhea lasting > 4 d. LGG: *Lactobacillus rhamnosus* GG; CI: Confidence interval.

prevention of diarrhea. Various therapeutic interventions designed to alter the microbiota range from probiotic administration to fecal microbiota transplantation[46,47]. However, due to the limited number of included studies and the self-limiting nature of disease, strategies should also be discussed in detail. Vomiting was reported as an adverse event in numerous studies[48,49], and it is one of the most common symptoms associated with diarrhea[50,51]. Additionally, less frequent clinical symptoms were observed in the probiotic groups[4], although our meta-analysis showed no improvement in the risk or duration of vomiting.

Safety

The safety of probiotic supplementation is generally certain. Nevertheless, pathologies correlated with the use of probiotic products to treat gastrointestinal disorders have been identified, such as endocarditis, sepsis, and bacteremia[52-54]. Unfortunately, the most prevalent strain implicated in the adverse effects was *Lactobacillus rhamnosus*. Conversely, most authors in our analysis did not report adverse effects or the adverse effects were not thought to be correlated with LGG treatment. In addition to the interventions, the primary illness contributed the most to the participant drop-out rate. A higher frequency of negative effects attributed to probiotics was found in catheterized (82.5%) and immunosuppressed (66%) participants[55]. Further safety evaluations of probiotics are necessary in the clinical setting, especially for susceptible individuals, such as those with immunodeficiency, immunosuppression, or malnourishment.

Application prospects

Preventing or correcting dehydration through treatment with zinc or 0.9% saline solution is the main approach used for diarrhea management[56]. However, during diarrhea episodes, infectious symptoms are not fully alleviated and the gut microbiota is not restored by rehydration measures[57]. Probiotics were investigated as therapeutic agents for diarrhea. The mechanisms by which probiotics alleviate diarrhea are described below. Host defenses are reinforced by enhanced antimicrobial peptide secretion. Probiotics prevent disruption of gut barrier integrity and stimulate the expression of junctional adhesion and tight junction molecules[58-61]. They produce short-chain fatty acids and induce the production of IgA to resist infections[62-64]. In epithelial cells and mucin, probiotics compete for binding sites to arrest pathogen colonization[65]. Probiotics can specifically and nonspecifically interfere with the viral cycle, thus impeding the progression of rotavirus-induced diarrhea[66-68]. The prevalence of diarrhea is seasonal, and almost all cases of rotavirus-induced diarrhea

A

Study or subgroup	LGG Mean	LGG SD	LGG Total	Placebo Mean	Placebo SD	Placebo Total	Weight	Mean difference IV, Random, 95%CI
2.5.1 ≥ 10^{10} CFU/day								
Basu, S. 2009 a	9.64	10.76	188	12.79	10.17	185	7.1%	-3.15 [-5.27, -1.03]
Basu, S. 2009 b	9.82	11.0	186	12.79	10.17	185	6.9%	-2.97 [-5.13, -0.81]
Canani, R. B. 2007	3.29	1.84	100	3.57	1.93	92	22.1%	-0.28 [-0.81, 0.25]
David, S. 2018	7.0	6.67	483	7.0	8.14	488	17.0%	0.00 [-0.94, 0.94]
Nixon, A. F. 2012	5.0	6.67	77	6.5	8.89	78	5.6%	-1.50 [-3.97, 0.97]
Sunny, A. 2014	9.17	1.88	100	10.36	1.87	100	22.2%	-1.19 [-1.71, -0.67]
Subtotal (95%CI)			**1134**			**1128**	**81.0%**	**-1.08 [-1.87, -0.28]**
Heterogeneity: Tau² = 0.55; Chi² = 17.49, *df* = 5 (*P* = 0.004); I^2 = 71%								
Test for overall effect: *Z* = 2.66 (*P* = 0.008)								
2.5.2 < 10^{10} CFU/day								
Basu, S. 2007	10.16	9.23	323	10.14	9.43	323	11.6%	0.02 [-1.42, 1.46]
Pant, A. R.1996	4.9	2.79	14	5.7	2.56	12	7.4%	-0.80 [-2.86, 1.26]
Subtotal (95%CI)			**337**			**335**	**19.0%**	**-0.25 [-1.43, 0.93]**
Heterogeneity: Tau² = 0.00; Chi² = 0.41, df = 1 (*P* = 0.52); I^2 = 0%								
Test for overall effect: Z = 0.41 (*P* = 0.68)								
Total (95%CI)			**1471**			**1463**	**100%**	**-0.90 [-1.56, -0.23]**
Heterogeneity: Tau² = 0.44; Chi² = 18.62, *df* = 7 (*P* = 0.009); I^2 = 62%								
Test for overall effect: *Z* = 2.65 (*P* = 0.008)								
Test for subgroup differences: Chi² = 1.30, *df* = 1 (*P* = 0.25), I^2 = 23.3%								

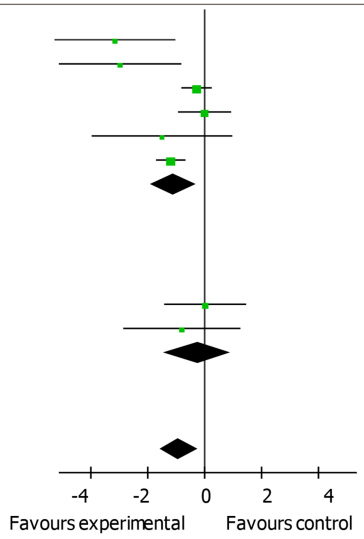

B

Study or subgroup	LGG Mean	LGG SD	LGG Total	Placebo Mean	Placebo SD	Placebo Total	Weight	Mean difference IV, Random, 95%CI
Basu, S. 2007	24.3	4.8	323	24.2	5.3	323	19.9%	0.10 [-0.68, 0.88]
Basu, S. 2009 a	22.8	6.12	188	23.5	6.1	185	13.2%	-0.70 [-1.94, 0.54]
Basu, S. 2009 b	23.2	6.05	186	23.5	6.1	185	13.3%	-0.30 [-1.54, 0.94]
Canani, R. B. 2007	4.0	1.48	100	3.7	1.7	92	25.4%	0.30 [-0.15, 0.75]
Pant, A. R.1996	3.5	1.3	14	5.2	2.8	12	8.7%	-1.70 [-3.42, 0.02]
Raza, S. 1995	5.8	3.1	19	7.0	3.3	17	6.5%	-1.20 [-3.30, 0.90]
Ritchie, B. K. 2010	3.2	2.54	33	4.7	2.59	31	13.0%	-1.50 [-2.76, -0.24]
Total (95%CI)			**863**			**845**	**100%**	**-0.46 [-1.06, 0.15]**
Heterogeneity: Tau² = 0.32; Chi² = 13.37, *df* = 6 (*P* = 0.04); I^2 = 55%								
Test for overall effect: *Z* = 1.48 (*P* = 0.14)								

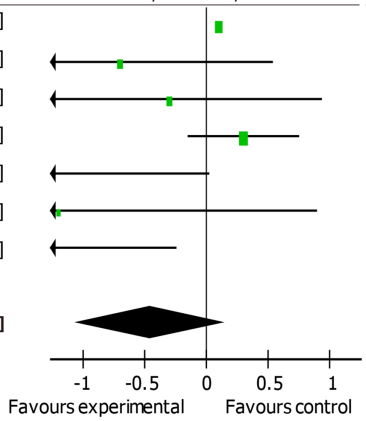

C

Study or subgroup	LGG Mean	LGG SD	LGG Total	Placebo Mean	Placebo SD	Placebo Total	Weight	Mean difference IV, Random, 95%CI
Basu, S. 2007	18.4	3.2	323	17.3	3.0	323	28.1%	1.10 [0.62, 1.58]
Basu, S. 2009 a	21.8	5.7	188	21.7	5.43	185	16.1%	0.10 [-1.03, 1.23]
Basu, S. 2009 b	22.1	6.03	186	21.7	5.43	185	15.6%	0.40 [-0.77, 1.57]
Canani, R. B. 2007	4.0	1.48	100	4.0	1.48	92	29.2%	0.00 [-0.42, 0.42]
Ritchie, B. K. 2010	2.9	2.54	33	3.3	3.68	31	11.0%	-0.40 [-1.96, 1.16]
Total (95%CI)			**830**			**816**	**100%**	**0.34 [-0.29, 0.97]**
Heterogeneity: Tau² = 0.31; Chi² = 12.99, *df* = 4 (*P* = 0.01); I^2 = 69%								
Test for overall effect: *Z* = 1.07 (*P* = 0.29)								

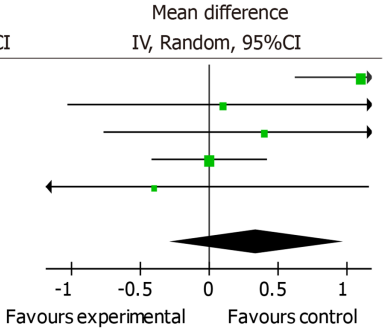

D

Study or subgroup	LGG Mean	LGG SD	LGG Total	Placebo Mean	Placebo SD	Placebo Total	Weight	Mean difference IV, Fixed, 95%CI
David, S. 2018	49.7	50.07	483	50.9	46.81	488	9.2%	-1.20 [-7.30, 4.90]
Nixon, A. F. 2012	60.0	54.81	77	74.0	57.04	78	1.1%	-14.00 [-31.61, 3.61]
Sunny, A. 2014	36.0	4.44	100	42.0	8.89	100	89.7%	-6.00 [-7.95, -4.05]
Total (95%CI)			**660**			**666**	**100%**	**-5.65 [-7.49, -3.80]**
Heterogeneity: Chi² = 3.03, *df* = 2 (*P* = 0.22); I^2 = 34%								
Test for overall effect: *Z* = 6.00 (*P* < 0.00001)								

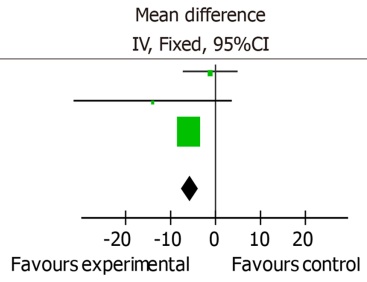

Figure 4 ***Lactobacillus*** **GG** ***vs*** **control with regard to stool number and consistency.** A: The average stool number per day (high dose and low dose); B: Stool frequency on day 2; C: Stool frequency on day 3; D: The mean time to improvement in stool consistency. LGG: *Lactobacillus rhamnosus* GG; CI: Confidence interval; SD: Standard deviation.

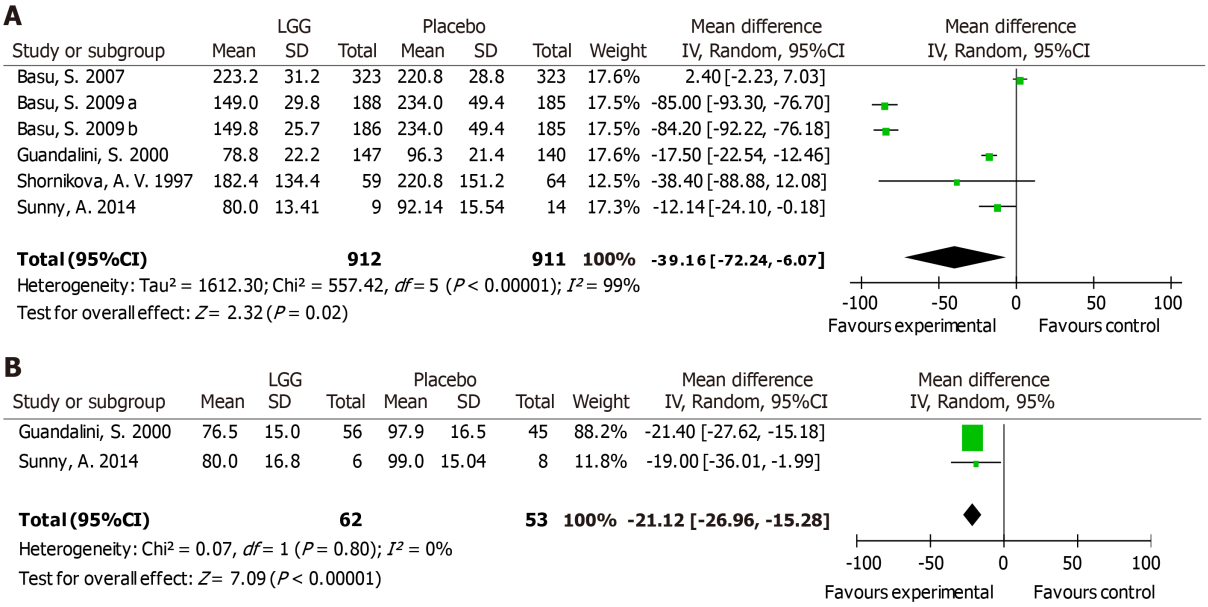

Figure 5 ***Lactobacillus* GG *vs* control.** A: The duration of hospital stay (hours); B: The hospital stay duration of rotavirus-positive children (hours). LGG: *Lactobacillus rhamnosus* GG; CI: Confidence interval; SD: Standard deviation.

occur from January to May in Russia[38]. By contrast, in regions where rotavirus is not prevalent, bacterial diarrhea commonly occurs from June to October[38]. Influenza seasons, dietary habits, and antibiotic use must be considered when evaluating heterogeneity in further studies. The efficacy of probiotic treatment was altered based on host and environmental factors[12]. Overall, our study supported the previous systematic reviews which concluded that LGG is an effective treatment for children with acute diarrhea.

Conclusions and limitations

Although most studies have suggested that LGG is efficacious, limited identification of pathogens, small sample sizes, varying therapeutic strategies, and methodological limitations such as articles without a strictly blinded design, including a lack of a standard clinical parameter format, weakened the conclusions and precluded further analyses across studies[69]. For example, Czerwionka-Szaflarska *et al*[28] did not specifically define the treatment applied, although a significantly reduced duration of diarrhea was detected. Salazar-Lindo *et al*[41] partially depicted the duration of diarrhea in children with or without LGG treatment. Although factors varied in the trials, according to the same criterion for both groups, no evidence suggests that a poor study design leads to overestimation of probiotic efficacy[4]. Appropriate subgroups, such as those stratified by etiology and nutritional status, are indispensable. In 2016, approximately 8.4% of children (480000) presenting with diarrhea ultimately died due to the condition worldwide (https://data.unicef.org/topic/child-health/diarrhoeal-disease/). Assessments of the availability of vaccines, the applicability of probiotics, and the effectiveness of current treatments under severe conditions and cost-effect analyses must be performed to optimize therapeutic strategies for acute diarrhea management in children.

In summary, the following conclusions were cautiously established: LGG reduces the duration of diarrhea, particularly in patients with rotavirus-positive diarrhea receiving a dosage no less than 10^{10} CFU per day and in patients treated at the early stage. In addition, studies conducted in Asia and Europe showed greater treatment efficacy. The therapeutic effect of LGG supplementation on the stool number per day and hospital stay duration associated with rotavirus-induced diarrhea is high.

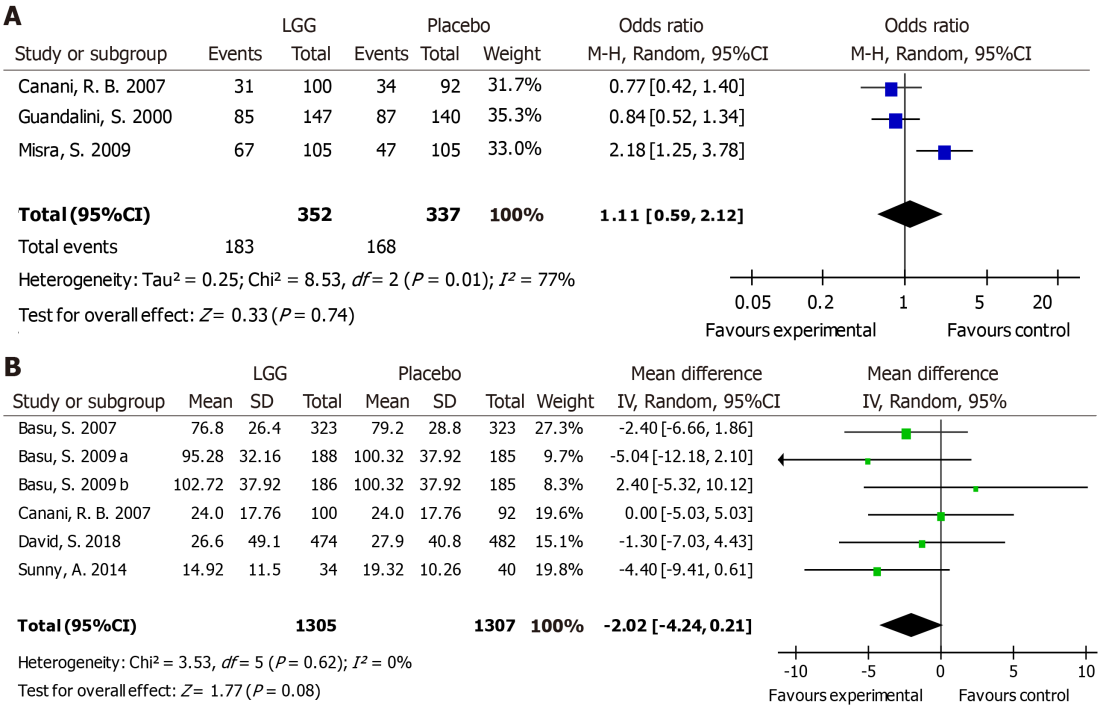

Figure 6 ***Lactobacillus* GG *vs* control with regard to vomiting.** A: The number of participants with vomiting [number (%)]; B: The duration of vomiting (hours). LGG: *Lactobacillus rhamnosus* GG; CI: Confidence interval; SD: Standard deviation.

ARTICLE HIGHLIGHTS

Research background

Diarrhea is a major infectious cause of childhood morbidity and mortality worldwide. Preventing or correcting dehydration through treatment with zinc or 0.9% saline solution is the main approach for diarrhea management; however, during diarrhea episodes, infectious symptoms are not fully alleviated by rehydration measures. Probiotics restore the gut microbiota and have been reported to reduce the duration of diarrhea.

Research motivation

Although previous studies have reported that *Lactobacillus rhamnosus* GG (LGG) is an effective therapeutic agent for acute diarrhea in children, a recent large, high-quality RCT found no adequate evidence of a beneficial effect of LGG treatment.

Research objectives

To evaluate the efficacy of LGG in treating acute diarrhea in children and provide some reference for future trials of treatments for diarrhea.

Research methods

The EMBASE, MEDLINE, PubMed, Web of Science databases, and the Cochrane Central Register of Controlled Trials were searched up to April 2019 for meta-analyses and randomized controlled trials (RCTs). Cochrane Review Manager was used to analyze the relevant data and primary outcomes, including the duration of diarrhea and diarrhea lasting ≥ 3 and ≥ 4 d. Secondary outcomes included the hospital stay duration, stool frequency, and improvement in stool consistency and vomiting.

Research results

The systematic review identified 19 RCTs that met the inclusion criteria and indicated that compared with the control group, LGG administration notably reduced the diarrhea duration [mean difference (MD) -24.02 h, 95% confidence interval (CI) (-36.58, -11.45)]. Greater reductions were detected at a high dose of ≥ 10^{10} CFU per day [MD -22.56 h, 95%CI (-36.41, -8.72)] and in LGG participants with diarrhea for less than 3 days at study enrollment [MD -15.83 h, 95%CI (-20.68, -10.98)]. The study locations contributed to differences in the reduction in the diarrhea duration in Asia and Europe [MD -24.42 h, 95%CI (-47.01, -1.82); MD -32.02 h, 95%CI (-49.26, -14.79), respectively]. High-dose LGG treatment was confirmed to effectively reduce the duration of rotavirus-induced diarrhea [MD -31.05 h, 95%CI (-50.31, -11.80)] and stool number [MD -1.08, 95%CI (-1.87, -0.28)].

Research conclusions

The following conclusions were cautiously established: compared to control children, children

who received a course of LGG had better outcomes, including a markedly reduced duration of diarrhea, especially those with rotavirus-positive diarrhea, those who received no less than 10^{10} CFU per day, and those treated at the early stage. Furthermore, studies conducted in Asia and Europe reported greater treatment efficacy. The therapeutic effect of LGG supplementation on the stool number per day and hospital stay duration associated with rotavirus-induced diarrhea was high.

Research perspectives

Our study found better outcomes among children with acute diarrhea who were treated by LGG supplementation. Limited identification of pathogens, small sample sizes, and a lack of a standard clinical parameter format precluded further analyses across studies, thus weakening the evidence required to guide clinical practice. Investigations are required to assess the cost-effectiveness of treating diarrhea with probiotics.

REFERENCES

1 **Walker CLF**, Rudan I, Liu L, Nair H, Theodoratou E, Bhutta ZA, O'Brien KL, Campbell H, Black RE. Global burden of childhood pneumonia and diarrhoea. *Lancet* 2013; **381**: 1405-1416 [PMID: 23582727 DOI: 10.1016/S0140-6736(13)60222-6]

2 **do Carmo MS**, Santos CID, Araújo MC, Girón JA, Fernandes ES, Monteiro-Neto V. Probiotics, mechanisms of action, and clinical perspectives for diarrhea management in children. *Food Funct* 2018; **9**: 5074-5095 [PMID: 30183037 DOI: 10.1039/c8fo00376a]

3 **Savarino SJ**, Bourgeois AL. Diarrhoeal disease: Current concepts and future challenges. Epidemiology of diarrhoeal diseases in developed countries. *Trans R Soc Trop Med Hyg* 1993; **87** Suppl 3: 7-11 [PMID: 8108853 DOI: 10.1016/0035-9203(93)90529-y]

4 **Allen SJ**, Martinez EG, Gregorio GV, Dans LF. Probiotics for treating acute infectious diarrhoea. *Cochrane Database Syst Rev* 2010; CD003048 [PMID: 21069673 DOI: 10.1002/14651858.CD003048.pub3]

5 **Binder HJ**, Brown I, Ramakrishna BS, Young GP. Oral rehydration therapy in the second decade of the twenty-first century. *Curr Gastroenterol Rep* 2014; **16**: 376 [PMID: 24562469 DOI: 10.1007/s11894-014-0376-2]

6 **Bryce J**, Terreri N, Victora CG, Mason E, Daelmans B, Bhutta ZA, Bustreo F, Songane F, Salama P, Wardlaw T. Countdown to 2015: Tracking intervention coverage for child survival. *Lancet* 2006; **368**: 1067-1076 [PMID: 16997661 DOI: 10.1016/S0140-6736(06)69339-2]

7 **Pérez-Gaxiola G**, Cuello-García CA, Florez ID, Pérez-Pico VM. Smectite for acute infectious diarrhoea in children. *Cochrane Database Syst Rev* 2018; **4**: CD011526 [PMID: 29693719 DOI: 10.1002/14651858.CD011526.pub2]

8 **Schnadower D**, Tarr PI, Casper TC, Gorelick MH, Dean JM, O'Connell KJ, Mahajan P, Levine AC, Bhatt SR, Roskind CG, Powell EC, Rogers AJ, Vance C, Sapien RE, Olsen CS, Metheney M, Dickey VP, Hall-Moore C, Freedman SB. Lactobacillus rhamnosus GG versus Placebo for Acute Gastroenteritis in Children. *N Engl J Med* 2018; **379**: 2002-2014 [PMID: 30462938 DOI: 10.1056/NEJMoa1802598]

9 **Guarner F**, Schaafsma GJ. Probiotics. *Int J Food Microbiol* 1998; **39**: 237-238 [PMID: 9553803 DOI: 10.1016/S0168-1605(97)00136-0]

10 **Lomax AR**, Calder PC. Probiotics, immune function, infection and inflammation: A review of the evidence from studies conducted in humans. *Curr Pharm Des* 2009; **15**: 1428-1518 [PMID: 19442167 DOI: 10.2174/138161209788168155]

11 **Szajewska H**, Mrukowicz JZ. Probiotics in the treatment and prevention of acute infectious diarrhea in infants and children: A systematic review of published randomized, double-blind, placebo-controlled trials. *J Pediatr Gastroenterol Nutr* 2001; **33** Suppl 2: S17-S25 [PMID: 11698781 DOI: 10.1097/00005176-200110002-00004]

12 **Wolvers D**, Antoine JM, Myllyluoma E, Schrezenmeir J, Szajewska H, Rijkers GT. Guidance for substantiating the evidence for beneficial effects of probiotics: Prevention and management of infections by probiotics. *J Nutr* 2010; **140**: 698S-712S [PMID: 20107143 DOI: 10.3945/jn.109.113753]

13 **Szajewska H**, Skórka A, Ruszczyński M, Gieruszczak-Białek D. Meta-analysis: Lactobacillus GG for treating acute gastroenteritis in children--updated analysis of randomised controlled trials. *Aliment Pharmacol Ther* 2013; **38**: 467-476 [PMID: 23841880 DOI: 10.1111/apt.12403]

14 **Szajewska H**, Guarino A, Hojsak I, Indrio F, Kolacek S, Shamir R, Vandenplas Y, Weizman Z; European Society for Pediatric Gastroenterology, Hepatology, and Nutrition. Use of probiotics for management of acute gastroenteritis: A position paper by the ESPGHAN Working Group for Probiotics and Prebiotics. *J Pediatr Gastroenterol Nutr* 2014; **58**: 531-539 [PMID: 24614141 DOI: 10.1097/MPG.0000000000000320]

15 **Guarino A**, Guandalini S, Lo Vecchio A. Probiotics for Prevention and Treatment of Diarrhea. *J Clin Gastroenterol* 2015; **49** Suppl 1: S37-S45 [PMID: 26447963 DOI: 10.1097/MCG.0000000000000349]

16 **Cipriani A**, Furukawa TA, Salanti G, Chaimani A, Atkinson LZ, Ogawa Y, Leucht S, Ruhe HG, Turner EH, Higgins JPT, Egger M, Takeshima N, Hayasaka Y, Imai H, Shinohara K, Tajika A, Ioannidis JPA, Geddes JR. Comparative efficacy and acceptability of 21 antidepressant drugs for the acute treatment of adults with major depressive disorder: A systematic review and network meta-analysis. *Lancet* 2018; **391**: 1357-1366 [PMID: 29477251 DOI: 10.1016/S0140-6736(17)32802-7]

17 **Liberati A**, Altman DG, Tetzlaff J, Mulrow C, Gøtzsche PC, Ioannidis JP, Clarke M, Devereaux PJ, Kleijnen J, Moher D. The PRISMA statement for reporting systematic reviews and meta-analyses of studies that evaluate healthcare interventions: Explanation and elaboration. *BMJ* 2009; **339**: b2700 [PMID: 19622552 DOI: 10.1136/bmj.b2700]

18 **Egger M**, Davey Smith G, Schneider M, Minder C. Bias in meta-analysis detected by a simple, graphical test. *BMJ* 1997; **315**: 629-634 [PMID: 9310563 DOI: 10.1136/bmj.315.7109.629]

19 **Johnston BC**, Goldenberg JZ, Vandvik PO, Sun X, Guyatt GH. Probiotics for the prevention of pediatric antibiotic-associated diarrhea. *Cochrane Database Syst Rev* 2011; CD004827 [PMID: 22071814 DOI: 10.1002/14651858.CD004827.pub3]

20 **Johnston BC**, Ma SS, Goldenberg JZ, Thorlund K, Vandvik PO, Loeb M, Guyatt GH. Probiotics for the

prevention of Clostridium difficile-associated diarrhea: A systematic review and meta-analysis. *Ann Intern Med* 2012; **157**: 878-888 [PMID: 23362517 DOI: 10.7326/0003-4819-157-12-201212180-00563]
21 **Cunliffe NA**, Kilgore PE, Bresee JS, Steele AD, Luo N, Hart CA, Glass RI. Epidemiology of rotavirus diarrhoea in Africa: A review to assess the need for rotavirus immunization. *Bull World Health Organ* 1998; **76**: 525-537 [PMID: 9868844 DOI: 10.1146/annurev.publhealth.19.1.527]
22 **Simakachorn N**, Pichaipat V, Rithipornpaisarn P, Kongkaew C, Tongpradit P, Varavithya W. Clinical evaluation of the addition of lyophilized, heat-killed Lactobacillus acidophilus LB to oral rehydration therapy in the treatment of acute diarrhea in children. *J Pediatr Gastroenterol Nutr* 2000; **30**: 68-72 [PMID: 10630442 DOI: 10.1097/00005176-200001000-00020]
23 **Szajewska H**, Skórka A, Ruszczyński M, Gieruszczak-Białek D. Meta-analysis: Lactobacillus GG for treating acute diarrhoea in children. *Aliment Pharmacol Ther* 2007; **25**: 871-881 [PMID: 17402990 DOI: 10.1111/j.1365-2036.2007.03282.x]
24 **Basu S**, Paul DK, Ganguly S, Chatterjee M, Chandra PK. Efficacy of high-dose Lactobacillus rhamnosus GG in controlling acute watery diarrhea in Indian children: A randomized controlled trial. *J Clin Gastroenterol* 2009; **43**: 208-213 [PMID: 18813028 DOI: 10.1097/MCG.0b013e31815a5780]
25 **Basu S**, Chatterjee M, Ganguly S, Chandra PK. Efficacy of Lactobacillus rhamnosus GG in acute watery diarrhoea of Indian children: A randomised controlled trial. *J Paediatr Child Health* 2007; **43**: 837-842 [PMID: 17803667 DOI: 10.1111/j.1440-1754.2007.01201.x]
26 **Canani RB**, Cirillo P, Terrin G, Cesarano L, Spagnuolo MI, De Vincenzo A, Albano F, Passariello A, De Marco G, Manguso F, Guarino A. Probiotics for treatment of acute diarrhoea in children: Randomised clinical trial of five different preparations. *BMJ* 2007; **335**: 340 [PMID: 17690340 DOI: 10.1136/bmj.39272.581736.55]
27 **Costa-Ribeiro H**, Ribeiro TC, Mattos AP, Valois SS, Neri DA, Almeida P, Cerqueira CM, Ramos E, Young RJ, Vanderhoof JA. Limitations of probiotic therapy in acute, severe dehydrating diarrhea. *J Pediatr Gastroenterol Nutr* 2003; **36**: 112-115 [PMID: 12500005 DOI: 10.1097/00005176-200301000-00021]
28 **Czerwionka-Szaflarska M**, Murawska S, Swincow G. Evaluation of influence of oral treatment with probiotic and/or oral rehydration solution on course of acute diarrhoea in children. *Przegl Gastroenterol* 2009; **4**: 166-172
29 **Guandalini S**, Pensabene L, Zikri MA, Dias JA, Casali LG, Hoekstra H, Kolacek S, Massar K, Micetic-Turk D, Papadopoulou A, de Sousa JS, Sandhu B, Szajewska H, Weizman Z. Lactobacillus GG administered in oral rehydration solution to children with acute diarrhea: A multicenter European trial. *J Pediatr Gastroenterol Nutr* 2000; **30**: 54-60 [PMID: 10630440 DOI: 10.1097/00005176-200001000-00018]
30 **Guarino A**, Canani RB, Spagnuolo MI, Albano F, Di Benedetto L. Oral bacterial therapy reduces the duration of symptoms and of viral excretion in children with mild diarrhea. *J Pediatr Gastroenterol Nutr* 1997; **25**: 516-519 [PMID: 9360205 DOI: 10.1097/00005176-199711000-00005]
31 **Isolauri E**, Kaila M, Mykkänen H, Ling WH, Salminen S. Oral bacteriotherapy for viral gastroenteritis. *Dig Dis Sci* 1994; **39**: 2595-2600 [PMID: 7995184 DOI: 10.1007/BF02087695]
32 **Jasinski C TM**, Tanzi MN, Schelotto F, Varela G, Zanetta E, Acuña A, and Arenas C, del Pilar Gadea M, Sirok A, Betancor L, Grotiuz G, Sandín D, Combol A, Xavier B, Vignoli R, Nairac A. Efficacy of Lactobacillus GG in oral rehydration solution. *Pediatrica* 2002; **22**: 231-243
33 **Misra S**, Sabui TK, Pal NK. A randomized controlled trial to evaluate the efficacy of lactobacillus GG in infantile diarrhea. *J Pediatr* 2009; **155**: 129-132 [PMID: 19559297 DOI: 10.1016/j.jpeds.2009.01.060]
34 **Nixon AF**, Cunningham SJ, Cohen HW, Crain EF. The effect of Lactobacillus GG on acute diarrheal illness in the pediatric emergency department. *Pediatr Emerg Care* 2012; **28**: 1048-1051 [PMID: 23023475 DOI: 10.1097/PEC.0b013e31826cad9f]
35 **Pant AR**, Graham SM, Allen SJ, Harikul S, Sabchareon A, Cuevas L, Hart CA. Lactobacillus GG and acute diarrhoea in young children in the tropics. *J Trop Pediatr* 1996; **42**: 162-165 [PMID: 8699584 DOI: 10.1093/tropej/42.3.162]
36 **Raza S**, Graham SM, Allen SJ, Sultana S, Cuevas L, Hart CA. Lactobacillus GG promotes recovery from acute nonbloody diarrhea in Pakistan. *Pediatr Infect Dis J* 1995; **14**: 107-111 [PMID: 7746691 DOI: 10.1097/00006454-199502000-00005]
37 **Ritchie BK**, Brewster DR, Tran CD, Davidson GP, McNeil Y, Butler RN. Efficacy of Lactobacillus GG in aboriginal children with acute diarrhoeal disease: A randomised clinical trial. *J Pediatr Gastroenterol Nutr* 2010; **50**: 619-624 [PMID: 20400916 DOI: 10.1097/MPG.0b013e3181bbf53d]
38 **Shornikova AV**, Isolauri E, Burkanova L, Lukovnikova S, Vesikari T. A trial in the Karelian Republic of oral rehydration and Lactobacillus GG for treatment of acute diarrhoea. *Acta Paediatr* 1997; **86**: 460-465 [PMID: 9183482 DOI: 10.1111/j.1651-2227.1997.tb08913.x]
39 **Sindhu KN**, Sowmyanarayanan TV, Paul A, Babji S, Ajjampur SS, Priyadarshini S, Sarkar R, Balasubramanian KA, Wanke CA, Ward HD, Kang G. Immune response and intestinal permeability in children with acute gastroenteritis treated with Lactobacillus rhamnosus GG: A randomized, double-blind, placebo-controlled trial. *Clin Infect Dis* 2014; **58**: 1107-1115 [PMID: 24501384 DOI: 10.1093/cid/ciu065]
40 **Aggarwal S**, Upadhyay A, Shah D, Teotia N, Agarwal A, Jaiswal V. Lactobacillus GG for treatment of acute childhood diarrhoea: An open labelled, randomized controlled trial. *Indian J Med Res* 2014; **139**: 379-385 [PMID: 24820831]
41 **Salazar-Lindo E**, Miranda-Langschwager P, Campos-Sanchez M, Chea-Woo E, Sack RB. Lactobacillus casei strain GG in the treatment of infants with acute watery diarrhea: A randomized, double-blind, placebo controlled clinical trial [ISRCTN67363048]. *BMC Pediatr* 2004; **4**: 18 [PMID: 15345099 DOI: 10.1186/1471-2431-4-18]
42 **Ahmadi E**, Alizadeh-Navaei R, Rezai MS. Efficacy of probiotic use in acute rotavirus diarrhea in children: A systematic review and meta-analysis. *Caspian J Intern Med* 2015; **6**: 187-195 [PMID: 26644891]
43 **Liu F**, Li G, Wen K, Wu S, Zhang Y, Bui T, Yang X, Kocher J, Sun J, Jortner B, Yuan L. Lactobacillus rhamnosus GG on rotavirus-induced injury of ileal epithelium in gnotobiotic pigs. *J Pediatr Gastroenterol Nutr* 2013; **57**: 750-758 [PMID: 24280990 DOI: 10.1097/MPG.0b013e3182a356e1]
44 **Jiang Y**, Ye L, Cui Y, Yang G, Yang W, Wang J, Hu J, Gu W, Shi C, Huang H, Wang C. Effects of Lactobacillus rhamnosus GG on the maturation and differentiation of dendritic cells in rotavirus-infected mice. *Benef Microbes* 2017; **8**: 645-656 [PMID: 28670908 DOI: 10.3920/BM2016.0157]
45 **Cai S**, Kandasamy M, Rahmat JN, Tham SM, Bay BH, Lee YK, Mahendran R. Lactobacillus rhamnosus GG Activation of Dendritic Cells and Neutrophils Depends on the Dose and Time of Exposure. *J Immunol*

Res 2016; **2016**: 7402760 [PMID: 27525288 DOI: 10.1155/2016/7402760]
46 **Khoruts A**. Targeting the microbiome: From probiotics to fecal microbiota transplantation. *Genome Med* 2018; **10**: 80 [PMID: 30376869 DOI: 10.1186/s13073-018-0592-8]
47 **Vemuri RC**, Gundamaraju R, Shinde T, Eri R. Therapeutic interventions for gut dysbiosis and related disorders in the elderly: Antibiotics, probiotics or faecal microbiota transplantation? *Benef Microbes* 2017; **8**: 179-192 [PMID: 28008784 DOI: 10.3920/BM2016.0115]
48 **Boudraa G**, Benbouabdellah M, Hachelaf W, Boisset M, Desjeux JF, Touhami M. Effect of feeding yogurt versus milk in children with acute diarrhea and carbohydrate malabsorption. *J Pediatr Gastroenterol Nutr* 2001; **33**: 307-313 [PMID: 11593127 DOI: 10.1097/00005176-200109000-00015]
49 **Kurugöl Z**, Koturoğlu G. Effects of Saccharomyces boulardii in children with acute diarrhoea. *Acta Paediatr* 2005; **94**: 44-47 [PMID: 15858959 DOI: 10.1111/j.1651-2227.2005.tb01786.x]
50 **Henriksson R**, Bergström P, Franzén L, Lewin F, Wagenius G. Aspects on reducing gastrointestinal adverse effects associated with radiotherapy. *Acta Oncol* 1999; **38**: 159-164 [PMID: 10227436 DOI: 10.1080/028418699431564]
51 **Uhnoo I**, Svensson L, Wadell G. Enteric adenoviruses. *Baillieres Clin Gastroenterol* 1990; **4**: 627-642 [PMID: 1962727 DOI: 10.1016/0950-3528(90)90053-J]
52 **Cannon JP**, Lee TA, Bolanos JT, Danziger LH. Pathogenic relevance of Lactobacillus: A retrospective review of over 200 cases. *Eur J Clin Microbiol Infect Dis* 2005; **24**: 31-40 [PMID: 15599646 DOI: 10.1007/s10096-004-1253-y]
53 **De Groote MA**, Frank DN, Dowell E, Glode MP, Pace NR. Lactobacillus rhamnosus GG bacteremia associated with probiotic use in a child with short gut syndrome. *Pediatr Infect Dis J* 2005; **24**: 278-280 [PMID: 15750472 DOI: 10.1097/01.inf.0000154588.79356.e6]
54 **Molinaro M**, Aiazzi M, La Torre A, Cini E, Banfi R. [Lactobacillus Rhamnosus sepsis in a preterm infant associated with probiotic integrator use: A case report.]. *Recenti Prog Med* 2016; **107**: 485-486 [PMID: 27727257 DOI: 10.1701/2354.25230]
55 **Gouriet F**, Million M, Henri M, Fournier PE, Raoult D. Lactobacillus rhamnosus bacteremia: An emerging clinical entity. *Eur J Clin Microbiol Infect Dis* 2012; **31**: 2469-2480 [PMID: 22544343 DOI: 10.1007/s10096-012-1599-5]
56 **World Health Organization**. *The Treatment of Diarrhea: A Manual for Physicians and other Senior Health Workers*. Geneva: World Health Organization 2005;
57 **Das RR**. Zinc in acute childhood diarrhea: Is it universally effective? *Indian J Pharmacol* 2012; **44**: 140; author reply 140-140; author reply 141 [PMID: 22345893 DOI: 10.4103/0253-7613.91891]
58 **Karczewski J**, Troost FJ, Konings I, Dekker J, Kleerebezem M, Brummer RJ, Wells JM. Regulation of human epithelial tight junction proteins by Lactobacillus plantarum in vivo and protective effects on the epithelial barrier. *Am J Physiol Gastrointest Liver Physiol* 2010; **298**: G851-G859 [PMID: 20224007 DOI: 10.1152/ajpgi.00327.2009]
59 **Mennigen R**, Nolte K, Rijcken E, Utech M, Loeffler B, Senninger N, Bruewer M. Probiotic mixture VSL#3 protects the epithelial barrier by maintaining tight junction protein expression and preventing apoptosis in a murine model of colitis. *Am J Physiol Gastrointest Liver Physiol* 2009; **296**: G1140-G1149 [PMID: 19221015 DOI: 10.1152/ajpgi.90534.2008]
60 **Yang F**, Wang A, Zeng X, Hou C, Liu H, Qiao S. Lactobacillus reuteri I5007 modulates tight junction protein expression in IPEC-J2 cells with LPS stimulation and in newborn piglets under normal conditions. *BMC Microbiol* 2015; **15**: 32 [PMID: 25888437 DOI: 10.1186/s12866-015-0372-1]
61 **Zyrek AA**, Cichon C, Helms S, Enders C, Sonnenborn U, Schmidt MA. Molecular mechanisms underlying the probiotic effects of Escherichia coli Nissle 1917 involve ZO-2 and PKCzeta redistribution resulting in tight junction and epithelial barrier repair. *Cell Microbiol* 2007; **9**: 804-816 [PMID: 17087734 DOI: 10.1111/j.1462-5822.2006.00836.x]
62 **Fukushima Y**, Kawata Y, Hara H, Terada A, Mitsuoka T. Effect of a probiotic formula on intestinal immunoglobulin A production in healthy children. *Int J Food Microbiol* 1998; **42**: 39-44 [PMID: 9706796 DOI: 10.1016/S0168-1605(98)00056-7]
63 **Rautava S**, Arvilommi H, Isolauri E. Specific probiotics in enhancing maturation of IgA responses in formula-fed infants. *Pediatr Res* 2006; **60**: 221-224 [PMID: 16864708 DOI: 10.1203/01.pdr.0000228317.72933.db]
64 **Naidu AS**, Bidlack WR, Clemens RA. Probiotic spectra of lactic acid bacteria (LAB). *Crit Rev Food Sci Nutr* 1999; **39**: 13-126 [PMID: 10028126 DOI: 10.1080/10408699991279187]
65 **Bujňáková D**, Kmeť V. Inhibitory potential of lactobacilli against Escherichia coli internalization by HT 29 cells. *Folia Microbiol (Praha)* 2012; **57**: 269-272 [PMID: 22528301 DOI: 10.1007/s12223-012-0122-9]
66 **Gonzalez-Ochoa G**, Flores-Mendoza LK, Icedo-Garcia R, Gomez-Flores R, Tamez-Guerra P. Modulation of rotavirus severe gastroenteritis by the combination of probiotics and prebiotics. *Arch Microbiol* 2017; **199**: 953-961 [PMID: 28634691 DOI: 10.1007/s00203-017-1400-3]
67 **Kang JY**, Lee DK, Ha NJ, Shin HS. Antiviral effects of Lactobacillus ruminis SPM0211 and Bifidobacterium longum SPM1205 and SPM1206 on rotavirus-infected Caco-2 cells and a neonatal mouse model. *J Microbiol* 2015; **53**: 796-803 [PMID: 26502964 DOI: 10.1007/s12275-015-5302-2]
68 **Paim FC**, Langel SN, Fischer DD, Kandasamy S, Shao L, Alhamo MA, Huang HC, Kumar A, Rajashekara G, Saif LJ, Vlasova AN. Effects of Escherichia coli Nissle 1917 and Ciprofloxacin on small intestinal epithelial cell mRNA expression in the neonatal piglet model of human rotavirus infection. *Gut Pathog* 2016; **8**: 66 [PMID: 27999620 DOI: 10.1186/s13099-016-0148-7]
69 **Kolaček S**, Hojsak I, Berni Canani R, Guarino A, Indrio F, Orel R, Pot B, Shamir R, Szajewska H, Vandenplas Y, van Goudoever J, Weizman Z; ESPGHAN Working Group for Probiotics and Prebiotics. Commercial Probiotic Products: A Call for Improved Quality Control. A Position Paper by the ESPGHAN Working Group for Probiotics and Prebiotics. *J Pediatr Gastroenterol Nutr* 2017; **65**: 117-124 [PMID: 28644359 DOI: 10.1097/MPG.0000000000001603]

Published By Baishideng Publishing Group Inc
7041 Koll Center Parkway, Suite 160, Pleasanton, CA 94566, USA
Telephone: +1-925-2238242
Fax: +1-925-2238243
E-mail: bpgoffice@wjgnet.com
Help Desk:http://www.f6publishing.com/helpdesk
http://www.wjgnet.com